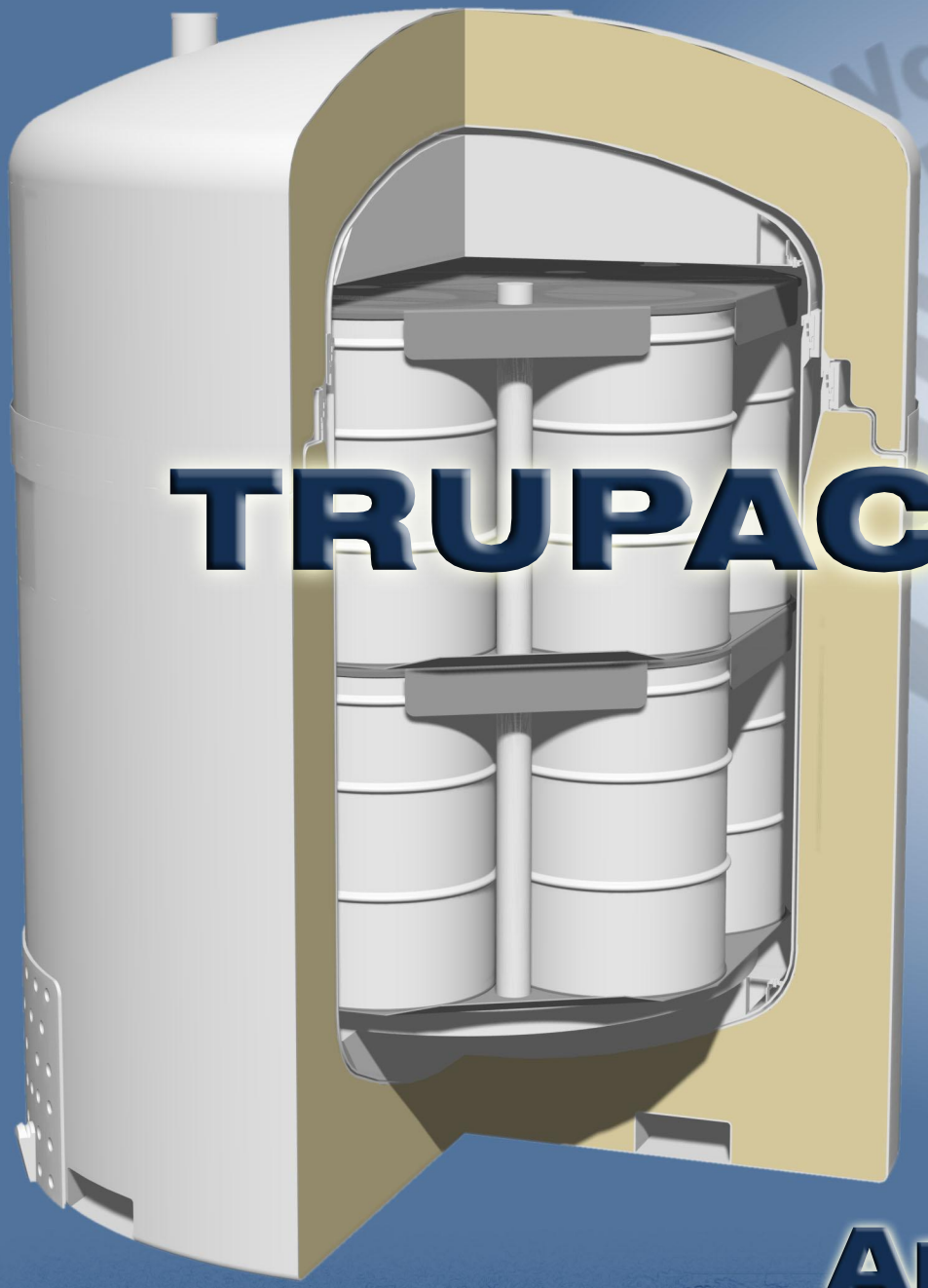

TRUPACT-II

Safety Analysis Report

Revision 23
December 2007

This page intentionally left blank to facilitate duplex printing.

TABLE OF CONTENTS

1.0 GENERAL INFORMATION 1.1-1

1.1 Introduction 1.1-1

1.2 Package Description 1.2-1

1.2.1 Packaging 1.2-1

1.2.1.1 Packaging Description 1.2-1

1.2.1.2 Gross Weight 1.2-5

1.2.1.3 Neutron Moderation and Absorption 1.2-5

1.2.1.4 Receptacles, Valves, Testing, and Sampling Ports 1.2-5

1.2.1.5 Heat Dissipation 1.2-6

1.2.1.6 Coolants 1.2-6

1.2.1.7 Protrusions 1.2-6

1.2.1.8 Lifting and Tie-down Devices 1.2-6

1.2.1.9 Pressure Relief System 1.2-7

1.2.1.10 Shielding 1.2-7

1.2.2 Operational Features 1.2-7

1.2.3 Contents of Packaging 1.2-8

1.3 Appendices 1.3-1

1.3.1 Packaging General Arrangement Drawings 1.3.1-1

1.3.2 Glossary of Terms and Acronyms 1.3.2-1

2.0 STRUCTURAL EVALUATION 2.1-1

2.1 Structural Design 2.1-1

2.1.1 Discussion 2.1-1

2.1.1.1 Containment Vessel Structures 2.1-1

2.1.1.2 Non-Containment Vessel Structures 2.1-2

2.1.2 Design Criteria 2.1-3

2.1.2.1 Analytic Design Criteria (Allowable Stresses) 2.1-3

2.1.2.2 Miscellaneous Structural Failure Modes 2.1-4

2.2 Weights and Centers of Gravity 2.2-1

2.2.1 Effect of a Radial Payload Imbalance 2.2-1

2.2.2 Effect of an Axial Payload Imbalance 2.2-3

2.2.3 Significance of Package Center of Gravity Shifts 2.2-4

2.2.3.1 Lifting 2.2-4

2.2.3.2 Tie-down 2.2-4

2.2.3.3 Vibration 2.2-5

2.2.3.4 Free Drop and Puncture 2.2-5

2.3 Mechanical Properties of Materials 2.3-1

2.3.1 Mechanical Properties Applied to Analytic Evaluations 2.3-1

2.3.2 Mechanical Properties Applied to Certification Testing 2.3-2

2.4 General Standards for All Packages 2.4-1

2.4.1 Minimum Package Size 2.4-1

2.4.2 Tamper-indicating Feature 2.4-1

2.4.3 Positive Closure 2.4-1

2.4.4 Chemical and Galvanic Reactions 2.4-1

2.4.4.1 Packaging Materials of Construction 2.4-2

2.4.4.2 Payload Interaction with Packaging Materials of Construction .. 2.4-3

2.4.5 Valves 2.4-3

2.4.6 Package Design 2.4-3

2.4.7 External Temperatures 2.4-3

2.4.8 Venting 2.4-4

2.5 Lifting and Tie-down Standards for All Packages 2.5-1

2.5.1 Lifting Devices 2.5-1

2.5.2 Tie-down Devices 2.5-2

2.5.2.1 Tie-down Forces 2.5-2

2.5.2.2 Tie-down Stress Due to a Vertical Tensile Load 2.5-3

2.5.2.3 Tie-down Stress Due to a Vertical Compressive Load 2.5-7

2.5.2.4 Tie-down Stresses Due to a Horizontal Compressive Load 2.5-9

2.5.2.5 Response of the Package if Treated as a Fixed Cantilever Beam 2.5-11

2.5.2.6 Summary 2.5-11

2.6 Normal Conditions of Transport 2.6-1

2.6.1 Heat 2.6-2

2.6.1.1 Summary of Pressures and Temperatures 2.6-2

2.6.1.2 Differential Thermal Expansion 2.6-3

2.6.1.3 Stress Calculations 2.6-3

2.6.1.4 Comparison with Allowable Stresses 2.6-4

2.6.1.5 Range of Primary Plus Secondary Stress Intensities 2.6-5

2.6.2 Cold 2.6-6

2.6.2.1 Stress Calculations 2.6-6

2.6.2.2 Comparison with Allowable Stresses 2.6-7

2.6.3 Reduced External Pressure 2.6-7

2.6.4 Increased External Pressure 2.6-8

2.6.4.1 Stress Calculations 2.6-8

2.6.4.2 Comparison with Allowable Stresses 2.6-9

2.6.4.3 Buckling Assessment of the Torispherical Heads 2.6-9

2.6.4.4 Buckling Assessment of the Cylindrical Shells 2.6-10

2.6.5 Vibration 2.6-11

2.6.5.1 Vibratory Loads Determination 2.6-12

2.6.5.2 Calculation of Alternating Stresses 2.6-12

2.6.5.3 Stress Limits and Results 2.6-14
2.6.6 Water Spray 2.6-14
2.6.7 Free Drop 2.6-14
2.6.8 Corner Drop 2.6-14
2.6.9 Compression 2.6-14
2.6.10 Penetration 2.6-15
2.7 Hypothetical Accident Conditions 2.7-1
2.7.1 Free Drop 2.7-2
2.7.1.1 Technical Basis for the Free Drop Tests 2.7-2
2.7.1.2 Test Sequence for the Selected Tests 2.7-3
2.7.1.3 Summary of Results from the Free Drop Tests 2.7-3
2.7.1.4 End Drop Bucking Evaluation 2.7-4
2.7.2 Crush 2.7-4
2.7.3 Puncture 2.7-5
2.7.3.1 Technical Basis for the Puncture Drop Tests 2.7-5
2.7.3.2 Test Sequence for the Selected Tests 2.7-6
2.7.3.3 Summary of Results from the Puncture Drop Tests 2.7-6
2.7.4 Thermal 2.7-7
2.7.4.1 Summary of Pressures and Temperatures 2.7-8
2.7.4.2 Differential Thermal Expansion 2.7-8
2.7.4.3 Stress Calculations 2.7-8
2.7.4.4 Comparison with Allowable Stresses 2.7-9
2.7.5 Immersion – Fissile Material 2.7-9
2.7.6 Immersion – All Packages 2.7-9
2.7.6.1 Buckling Assessment of the Torispherical Heads 2.7-9
2.7.6.2 Buckling Assessment of the Cylindrical Shells 2.7-10
2.7.7 Deep Water Immersion Test 2.7-12
2.7.8 Summary of Damage 2.7-12
2.8 Special Form 2.8-1
2.9 Fuel Rods 2.9-1
2.10 Appendices 2.10-1
2.10.1 Finite Element Analysis (FEA) Models 2.10.1-1
2.10.1.1 Outer Containment Assembly (OCA) Structural Analysis 2.10.1-1
2.10.1.2 Inner Containment Assembly (ICV) Structural Analysis 2.10.1-5
2.10.2 Elastomer O-ring Seal Performance Tests 2.10.2-1
2.10.2.1 Introduction 2.10.2-1
2.10.2.2 Test Specimens and Equipment 2.10.2-1
2.10.2.3 Test Conditions 2.10.2-2
2.10.2.4 Test Procedure 2.10.2-2
2.10.2.5 Example O-ring Seal Compression Calculation 2.10.2-3
2.10.2.6 Test Results 2.10.2-4

2.10.2.7 Designating an Alternative Seal Material 2.10.2-5
2.10.3 Certification Tests 2.10.3-1
2.10.3.1 Introduction 2.10.3-1
2.10.3.2 Summary 2.10.3-1
2.10.3.3 Test Facilities 2.10.3-3
2.10.3.4 Description of the Certification Test Units 2.10.3-4
2.10.3.5 Technical Basis for Tests 2.10.3-9
2.10.3.6 Test Sequence for Selected Free Drop, Puncture Drop, and Fire Tests 2.10.3-13
2.10.3.7 Test Results 2.10.3-20

3.0 THERMAL EVALUATION 3.1-1

3.1 Discussion 3.1-1
3.1.1 Packaging 3.1-1
3.1.2 Payload Configuration 3.1-2
3.1.3 Boundary Conditions 3.1-3
3.1.4 Analysis Summary 3.1-4
3.2 Summary of Thermal Properties of Materials 3.2-1
3.3 Technical Specifications of Components 3.3-1
3.4 Thermal Evaluation for Normal Conditions of Transport 3.4-1
3.4.1 Thermal Model 3.4-1
3.4.1.1 Analytical Model 3.4-1
3.4.1.2 Test Model 3.4-3
3.4.2 Maximum Temperatures 3.4-3
3.4.3 Minimum Temperatures 3.4-3
3.4.4 Maximum Internal Pressure 3.4-3
3.4.4.1 Design Pressure 3.4-3
3.4.4.2 Maximum Pressure for Normal Conditions of Transport 3.4-3
3.4.4.3 Maximum Normal Operating Pressure 3.4-9
3.4.5 Maximum Thermal Stresses 3.4-10
3.4.6 Evaluation of Package Performance for Normal Conditions of Transport 3.4-11
3.5 Thermal Evaluation for Hypothetical Accident Conditions 3.5-1
3.5.1 Thermal Model 3.5-1
3.5.1.1 Analytical Model 3.5-1
3.5.1.2 Test Model 3.5-1
3.5.2 Package Conditions and Environment 3.5-2
3.5.2.1 CTU-1 Package Conditions and Environment 3.5-2
3.5.2.2 CTU-2 Package Conditions and Environment 3.5-3
3.5.3 Package Temperatures 3.5-3
3.5.4 Maximum Internal Pressure 3.5-3

3.5.5 Maximum Thermal Stresses 3.5-4
3.5.6 Evaluation of Package Performance for the Hypothetical Accident Thermal Conditions 3.5-4
3.6 Appendices 3.6-1
3.6.1 Computer Analysis Results 3.6.1-1
3.6.1.1 Fourteen 55-Gallon Drum Payload with 100 ºF Ambient and Full Solar, Uniformly Distributed Decay Heat Load in All Drums (Case 1) 3.6.1-1
3.6.1.2 Fourteen 55-Gallon Drum Payload with 100 ºF Ambient and Full Solar, Uniformly Distributed Decay Heat Load in Two Center Drums (Case 2) 3.6.1-4
3.6.1.3 Fourteen 55-Gallon Drum Payload with 100 ºF Ambient and Full Solar, Uniformly Distributed Decay Heat Load in Top Center Drum (Case 3) 3.6.1-7
3.6.1.4 Two Standard Waste Box Payload with 100 ºF Ambient and Full Solar, Uniformly Distributed Decay Heat Load in Both SWBs (Case 4) 3.6.1-10
3.6.1.5 Two Standard Waste Box Payload with 100 ºF Ambient and Full Solar, Uniformly Distributed Decay Heat Load in Top SWB (Case 5) 3.6.1-12
3.6.1.6 Fourteen 55-Gallon Drum Payload with 100 ºF Ambient and No Solar, 40 Watts Uniform Decay Heat Load 3.6.1-14
3.6.1.7 Two Standard Waste Box Payload with 100 ºF Ambient and No Solar, 40 Watts Uniform Decay Heat Load 3.6.1-16
3.6.2 Thermal Model Details 3.6.2-1
3.6.2.1 Convection Coefficient Calculation 3.6.2-1
3.6.2.2 Polyethylene Plastic Wrap Transmittance Calculation 3.6.2-2

4.0 CONTAINMENT 4.1-1

4.1 Containment Boundary 4.1-1
4.1.1 Containment Vessel 4.1-1
4.1.1.1 Outer Containment Assembly (Primary Level of Containment). 4.1-1
4.1.1.2 Inner Containment Vessel (Secondary Level of Containment)... 4.1-1
4.1.2 Containment Penetrations 4.1-1
4.1.3 Seals and Welds 4.1-2
4.1.3.1 Seals 4.1-2
4.1.3.2 Welds 4.1-2
4.1.4 Closure 4.1-3
4.1.4.1 Outer Containment Assembly (OCA) Closure 4.1-3
4.1.4.2 Inner Containment Vessel (ICV) Closure 4.1-3
4.2 Containment Requirements for Normal Conditions of Transport 4.2-1
4.2.1 Containment of Radioactive Material 4.2-1
4.2.2 Pressurization of Containment Vessel 4.2-1

4.2.3 Containment Criterion 4.2-1
4.3 Containment Requirements for Hypothetical Accident Conditions 4.3-1
4.3.1 Fission Gas Products 4.3-1
4.3.2 Containment of Radioactive Material 4.3-1
4.3.3 Containment Criterion 4.3-1
4.4 Special Requirements 4.4-1
4.4.1 Plutonium Shipments 4.4-1
4.4.2 Interchangeability 4.4-1

5.0 SHIELDING EVALUATION 5-1

6.0 CRITICALITY EVALUATION 6.1-1
6.1 Discussion and Results 6.1-1
6.2 Package Contents 6.2-1
6.2.1 Applicability of Case A Limit 6.2-2
6.2.2 Applicability of Case B Limit 6.2-3
6.2.3 Applicability of Case C Limit 6.2-3
6.2.4 Applicability of Case D Limit 6.2-4
6.2.5 Applicability of Case E Limit 6.2-5
6.2.6 Applicability of Case F Limit 6.2-5
6.3 Model Specification 6.3-1
6.3.1 Contents Model 6.3-1
6.3.1.1 Case A Contents Model 6.3-1
6.3.1.2 Case B Contents Model 6.3-2
6.3.1.3 Case C Contents Model 6.3-2
6.3.1.4 Case D Contents Model 6.3-2
6.3.2 Packaging Model 6.3-3
6.3.3 Single-Unit Models 6.3-5
6.3.4 Array Models 6.3-5
6.3.5 Package Regional Densities 6.3-6
6.4 Criticality Calculations 6.4-1
6.4.1 Calculational or Experimental Method 6.4-1
6.4.2 Fuel Loading or Other Contents Loading Optimization 6.4-1
6.4.3 Criticality Results 6.4-2
6.4.3.1 Criticality Results for a Single TRUPACT-II Package 6.4-3
6.4.3.2 Criticality Results for Infinite Arrays of TRUPACT-II Packages 6.4-4
6.4.3.3 Special Reflectors in CH-TRU Waste 6.4-7
6.4.3.4 Machine Compacted CH-TRU Waste 6.4-8

6.4.3.5 Applicable Criticality Limits for CH-TRU Waste 6.4-9
6.5 Critical Benchmark Experiments 6.5-1
6.5.1 Benchmark Experiments and Applicability 6.5-1
6.5.2 Details of Benchmark Calculations 6.5-2
6.5.3 Results of Benchmark Calculations 6.5-2

7.0 OPERATING PROCEDURES 7.1-1
7.1 Procedures for Loading the Package 7.1-1
7.1.1 Removal of the TRUPACT-II Package from the Transport Trailer/Railcar 7.1-1
7.1.2 Outer Containment Assembly (OCA) Lid Removal 7.1-1
7.1.3 Inner Containment Vessel (ICV) Lid Removal 7.1-2
7.1.4 Loading the Payload into the TRUPACT-II Package 7.1-2
7.1.5 Inner Containment Vessel (ICV) Lid Installation 7.1-3
7.1.6 Outer Containment Assembly (OCA) Lid Installation 7.1-4
7.1.7 Final Package Preparations for Transport (Loaded) 7.1-6
7.2 Procedures for Unloading the Package 7.2-1
7.2.1 Removal of the TRUPACT-II Package from the Transport Trailer/Railcar 7.2-1
7.2.2 Outer Containment Assembly (OCA) Lid Removal 7.2-1
7.2.3 Inner Containment Vessel (ICV) Lid Removal 7.2-2
7.2.4 Unloading the Payload from the TRUPACT-II Package 7.2-2
7.2.5 Inner Containment Vessel (ICV) Lid Installation 7.2-2
7.2.6 Outer Containment Assembly (OCA) Lid Installation 7.2-3
7.2.7 Final Package Preparations for Transport (Unloaded) 7.2-4
7.3 Preparation of an Empty Package for Transport 7.3-1
7.4 Preshipment Leakage Rate Test 7.4-1
7.4.1 Gas Pressure Rise Leakage Rate Test Acceptance Criteria 7.4-1
7.4.2 Determining the Test Volume and Test Time 7.4-1
7.4.3 Performing the Gas Pressure Rise Leakage Rate Test 7.4-2
7.4.4 Optional Preshipment Leakage Rate Test 7.4-2

8.0 ACCEPTANCE TESTS AND MAINTENANCE PROGRAM 8.1-1
8.1 Acceptance Tests 8.1-1
8.1.1 Visual Inspection 8.1-1
8.1.2 Structural and Pressure Tests 8.1-1
8.1.2.1 Lifting Device Load Testing 8.1-1
8.1.2.2 Containment Vessel Pressure Testing 8.1-1

8.1.3 Fabrication Leakage Rate Tests 8.1-2
8.1.3.1 Fabrication Leakage Rate Test Acceptance Criteria 8.1-2
8.1.3.2 Helium Leakage Rate Testing the ICV Structure Integrity 8.1-2
8.1.3.3 Helium Leakage Rate Testing the ICV Main O-ring Seal 8.1-3
8.1.3.4 Helium Leakage Rate Testing the ICV Outer Vent Port Plug O-ring Seal 8.1-4
8.1.3.5 Helium Leakage Rate Testing the OCV Structure Integrity 8.1-4
8.1.3.6 Helium Leakage Rate Testing the OCV Main O-ring Seal Integrity 8.1-5
8.1.3.7 Helium Leakage Rate Testing the OCV Vent Port Plug O-ring Seal Integrity 8.1-5
8.1.4 Component Tests 8.1-6
8.1.4.1 Polyurethane Foam 8.1-6
8.1.5 Tests for Shielding Integrity 8.1-19
8.1.6 Thermal Acceptance Test 8.1-19
8.2 Maintenance Program 8.2-1
8.2.1 Structural and Pressure Tests 8.2-1
8.2.1.1 Containment Vessel Pressure Testing 8.2-1
8.2.1.2 ICV Interior Surfaces Inspection 8.2-1
8.2.2 Maintenance/Periodic Leakage Rate Tests 8.2-1
8.2.2.1 Maintenance/Periodic Leakage Rate Test Acceptance Criteria .. 8.2-2
8.2.2.2 Helium Leakage Rate Testing the ICV Main O-ring Seal 8.2-2
8.2.2.3 Helium Leakage Rate Testing the ICV Outer Vent Port Plug O-ring Seal 8.2-2
8.2.3 Subsystems Maintenance 8.2-3
8.2.3.1 Fasteners 8.2-3
8.2.3.2 Locking Rings 8.2-3
8.2.3.3 Seal Areas and Grooves 8.2-3
8.2.4 Valves, Rupture Discs, and Gaskets on the Containment Vessel 8.2-7
8.2.4.1 Valves 8.2-7
8.2.4.2 Rupture Discs 8.2-7
8.2.4.3 Gaskets 8.2-7
8.2.5 Shielding 8.2-7
8.2.6 Thermal 8.2-7

9.0 QUALITY ASSURANCE 9.1-1
9.1 Introduction 9.1-1
9.2 Quality Assurance Requirements 9.2-1
9.2.1 U.S. Nuclear Regulatory Commission 9.2-1
9.2.2 U.S. Department of Energy 9.2-1
9.2.3 Transportation to or from WIPP 9.2-1
9.3 Quality Assurance Program 9.3-1

9.3.1 NRC Regulatory Guide 7.10 ..... 9.3-1
9.3.2 Design 9.3-1
9.3.3 Fabrication, Assembly, and Testing 9.3-1
9.3.4 Procurement 9.3-1
9.3.5 Use 9.3-1
9.3.5.1 DOE Shipments: To/From WIPP 9.3-1
9.3.5.2 Other DOE Shipments: Non-WIPP 9.3-2
9.3.5.3 Non-DOE Users of TRUPACT-II 9.3-2
9.3.6 Maintenance and Repair 9.3-2

LIST OF TABLES

Table 2.1-1 – Containment Structure Allowable Stress Limits 2.1-7
Table 2.1-2 – Non-Containment Structure Allowable Stress Limits 2.1-7
Table 2.2-1 – TRUPACT-II Weight and Center of Gravity 2.2-6
Table 2.3-1 – Mechanical Properties of Type 304 Stainless Steel Components (for Analysis) 2.3-5
Table 2.3-2 – Mechanical Properties of Polyurethane Foam (for Analysis) 2.3-7
Table 2.3-3 – Mechanical Properties of Metallic Materials (for Testing) 2.3-7
Table 2.6-1 – Summary of Stress Intensity Results for OCA Load Case 1① 2.6-16
Table 2.6-2 – Summary of Stress Intensity Results for OCA Load Case 2① 2.6-17
Table 2.6-3 – Summary of Stress Intensity Results for OCA Load Case 3① 2.6-18
Table 2.6-4 – Summary of Stress Intensity Results for OCA Load Case 4① 2.6-19
Table 2.6-5 – Summary of Stress Intensity Results for ICV Load Case 1① 2.6-20
Table 2.6-6 – Summary of Stress Intensity Results for ICV Load Case 2① 2.6-21
Table 2.6-7 – Buckling Geometry Parameters per Code Case N-284 ..... 2.6-22
Table 2.6-8 – Stress Results for 14.7 psig External Pressure 2.6-23
Table 2.6-9 – Shell Buckling Summary for 14.7 psig External Pressure 2.6-23
Table 2.6-10 – Tie-Down Lug Weld Shear Stresses 2.6-24
Table 2.6-11 – OCA Outer Shell Compressive Membrane Stresses 2.6-24
Table 2.6-12 – OCA Tie-down Weldment Compressive Membrane Stresses 2.6-24
Table 2.6-13 – Maximum Unit Alternating Stress Intensities 2.6-24
Table 2.7-1 – Summary of Tests for TRUPACT-II CTU-1 ..... 2.7-13
Table 2.7-2 – Summary of Tests for TRUPACT-II CTU-2 ..... 2.7-14
Table 2.7-3 – Summary of Tests for TRUPACT-II CTU-3 ..... 2.7-15

Table 2.7-4 – Buckling Geometry Parameters for a 385*g* HAC End Drop 2.7-17
Table 2.7-5 – Shell Buckling Summary for a 385*g* HAC End Drop 2.7-18
Table 2.7-6 – Buckling Geometry Parameters per Code Case N-284 ..... 2.7-19
Table 2.7-7 – Stress Results for 21 psig External Pressure 2.7-20
Table 2.7-8 – Shell Buckling Summary for 21 psig External Pressure 2.7-20
Table 2.10.1-1 – ANSYS® Input Listing for OCA Load Case 1 ..... 2.10.1-7
Table 2.10.1-2 – ANSYS® Input Listing for OCA Load Case 2 ..... 2.10.1-11
Table 2.10.1-3 – ANSYS® Input Listing for OCA Load Case 3 ..... 2.10.1-15
Table 2.10.1-4 – ANSYS® Input Listing for OCA Load Case 4 ..... 2.10.1-19
Table 2.10.1-5 – ANSYS® Input Listing for ICV Load Case 1 ..... 2.10.1-23
Table 2.10.1-6 – ANSYS® Input Listing for ICV Load Case 2 ..... 2.10.1-25
Table 2.10.2-1 – O-ring Seal Performance Test Results 2.10.2-9
Table 2.10.3-1 – Summary of CTU-1 Test Results in Sequential Order 2.10.3-33
Table 2.10.3-2 – Summary of CTU-2 Test Results in Sequential Order 2.10.3-34
Table 2.10.3-3 – Summary of CTU-3 Test Results in Sequential Order 2.10.3-35
Table 2.10.3-4 – CTU-1 Temperature Indicating Label Locations and Results 2.10.3-37
Table 2.10.3-5 – CTU-2 Temperature Indicating Label Locations and Results 2.10.3-39
Table 3.1-1 – NCT Steady-State Temperatures with 40 Watts Decay Heat Load and Insolation; Fourteen 55-Gallon Drums 3.1-6
Table 3.1-2 – NCT Steady-State Temperatures with 40 Watts Decay Heat Load and No Insolation; Fourteen 55-Gallon Drums 3.1-7
Table 3.1-3 – NCT Steady-State Temperatures with 40 Watts Decay Heat Load and Insolation; Two Standard Waste Boxes 3.1-8
Table 3.1-4 – NCT Steady-State Temperatures with 40 Watts Decay Heat Load and No Insolation; Two Standard Waste Boxes 3.1-9
Table 3.2-1 – Thermal Properties of Materials 3.2-2
Table 3.2-2 – Thermal Properties of Air 3.2-2
Table 3.2-3 – Thermal Radiative Properties 3.2-3
Table 3.4-1 – NCT Steady-State Temperatures with Insolation, Payload Configuration 1 - Fourteen 55-Gallon Drums, Thermal Case 1 ..... 3.4-12
Table 3.4-2 – NCT Steady-State Temperatures with Insolation, Payload Configuration 1 - Fourteen 55-Gallon Drums, Thermal Case 2 ..... 3.4-13
Table 3.4-3 – NCT Steady-State Temperatures with Insolation, Payload Configuration 1 - Fourteen 55-Gallon Drums, Thermal Case 3 ..... 3.4-14

Table 3.4-4 – NCT Steady-State Temperatures with Insolation, Payload Configuration 2 - Two Standard Waste Boxes, Thermal Case 4 ..... 3.4-15

Table 3.4-5 – NCT Steady-State Temperatures with Insolation, Payload Configuration 2 - Two Standard Waste Boxes, Thermal Case 5 ..... 3.4-16

Table 3.4-6 – TRUPACT-II Pressure Increase with a 14-Drum Payload, 60-Day Duration* 3.4-17

Table 3.4-7 – TRUPACT-II Pressure Increase with a 2 SWB Payload, 60-Day Duration* 3.4-17

Table 3.4-8 – TRUPACT-II Pressure Increase with 8 Drums Overpacked in 2 SWBs, 60-Day Duration* 3.4-17

Table 3.4-9 – TRUPACT-II Pressure Increase with 8 85-Gallon Drums or 8 55-Gallon Drums Overpacked in 8 85-Gallon Drums, 60-Day Duration* 3.4-18

Table 3.4-10 – TRUPACT-II Pressure Increase with 6 100-Gallon Drums, 60-Day Duration*. 3.4-18

Table 3.4-11 – TRUPACT-II Pressure Increase with a 1 TDOP Payload, 60-Day Duration* ... 3.4-18

Table 3.5-1 – HAC Pre-Fire Steady-State Temperatures with 40 Watts Decay Heat Load and No Insolation; Fourteen 55-Gallon Drums 3.5-5

Table 3.5-2 – HAC Pre-Fire Steady-State Temperatures with 40 Watts Decay Heat Load and No Insolation; Two Standard Waste Boxes 3.5-6

Table 3.5-3 – CTU-1 Temperature Indicating Label Locations and Results..... 3.5-7

Table 3.5-4 – CTU-2 Temperature Indicating Label Locations and Results..... 3.5-9

Table 3.5-5 – HAC Fire Temperature Readings; Fourteen 55-Gallon Drums 3.5-11

Table 6.1-1 – Fissile Material Limit per Payload Container 6.1-4

Table 6.1-2 – Fissile Material Limit per TRUPACT-II Package 6.1-4

Table 6.1-3 – Summary of Criticality Analysis Results 6.1-5

Table 6.2-1 – Special Reflector Material Parameters that Achieve the Reactivity of a 25%/75% Polyethylene/Water Mixture Reflector 6.2-6

Table 6.3-1 – Description of Contents Displacement in Array Models 6.3-6

Table 6.3-2 – Fissile Contents Model Properties for Various H/Pu Ratios..... 6.3-7

Table 6.3-3 – Composition of Modeled Steels 6.3-8

Table 6.3-4 – Composition of the Polyethylene/Water/Beryllium Reflector 6.3-8

Table 6.4-1 – Single-Unit, NCT, Case A, 325 FGE; k_s vs. H/Pu Ratio with Different Moderator and Reflector Compositions..... 6.4-10

Table 6.4-2 – Single Unit, NCT, Case A, 325 FGE; Variation of Reflector Volume Fraction (VF) at Near-Optimal H/Pu Ratio 6.4-11

Table 6.4-3 – Single-Unit, HAC, Case A, 325 FGE; k_s vs. H/Pu at Maximum Reflection Conditions 6.4-11

Table 6.4-4 – Infinite Array Variation 0, HAC, Case A, 325 FGE; k_s vs. H/Pu at Extremes of Reflection Conditions 6.4-12

Table 6.4-5 – Infinite Array Variation 0, HAC, Case A, 325 FGE; Variation of Reflector Volume Fraction at Near-Optimal H/Pu Ratios 6.4-13

Table 6.4-6 – Infinite Array Variation 1, HAC, Case A, 325 FGE; Variation of H/Pu Ratio at Extremes of Reflection Conditions 6.4-14

Table 6.4-7 – Infinite Array Variation 0, HAC, Case A; Variation of H/Pu Ratio for Various Gram Quantities of Pu-240 at Maximum Reflection Conditions 6.4-15

Table 6.4-8 – Infinite Array Variation 0, HAC, Case A, 5 g Pu-240, 340 FGE; k_s vs. H/Pu for Various Combinations of U-235 and Pu-239 under Maximum Reflection Conditions 6.4-16

Table 6.4-9 – Infinite Array Variation 0, HAC, Case B, 100 FGE; k_s vs. H/Pu at Maximum Reflection Conditions 6.4-17

Table 6.4-10 – Infinite Array Variation 0, HAC, Case B, 100 FGE; k_s vs. H/Pu for Various Moderator Volume Fractions of Beryllium under Maximum Reflection Conditions 6.4-18

Table 6.4-11 – Infinite Array Variation 0, HAC, Case B, 100 FGE; Variation of Reflector Volume Fraction at Near-Optimal H/Pu Ratio 6.4-19

Table 6.4-12 – Infinite Array Variation 1, HAC, Case B, 100 FGE; Variation of H/Pu Ratio at Reflector Volume Fraction to Maximize Interaction while Maintaining Beryllium Reflection 6.4-19

Table 6.4-13 – Infinite Array Variation 0, HAC, Case C, 250 FGE; k_s vs. H/Pu at Maximum Reflection Conditions 6.4-20

Table 6.4-14 – Infinite Array Variation 0, HAC, Case C, 250 FGE; Variation of Reflector Volume Fraction at Near-Optimal H/Pu Ratio 6.4-20

Table 6.4-15 – Infinite Array Variation 1, HAC, Case C, 250 FGE; Variation of H/Pu Ratio at Reflector Volume Fraction to Maximize Interaction while Maintaining Reflection 6.4-21

Table 6.4-16 – Infinite Array Variation 0, HAC, Case D, 325 FGE; k_s vs. H/Pu at Maximum Reflection Conditions 6.4-22

Table 6.4-17 – Infinite Array Variation 0, HAC, Case D, 325 FGE; Variation of Reflector Volume Fraction at Near-Optimal H/Pu Ratio 6.4-23

Table 6.4-18 – Infinite Array Variation 1, HAC, Case D, 325 FGE; Variation of H/Pu Ratio at Reflector Volume Fraction to Maximize Interaction while Maintaining Reflection 6.4-23

Table 6.5-1 – Benchmark Experiment Description with Experimental Uncertainties 6.5-4

Table 6.5-2 – Benchmark Case Parameters and Computed Results 6.5-5

Table 6.5-3 – Calculation of USL 6.5-13

Table 8.1-1 – Acceptable Compressive Stress Ranges for Foam (psi) 8.1-19
Table 8.2-1 – Calculation of Minimum O-ring Compression 8.2-4

LIST OF FIGURES

Figure 1.1-1 – TRUPACT-II Package Assembly 1.1-3
Figure 1.1-2 – TRUPACT-II Packaging Closure/Seal Region Details 1.1-4
Figure 1.2-1 – OCV Closure Design (ICV closure is Similar) 1.2-9
Figure 2.2-1 – TRUPACT-II Package Components 2.2-7
Figure 2.2-2 – Radial CG Shift for a 14 55-Gallon Drum Payload 2.2-8
Figure 2.2-3 – Radial Shift of CG for Eight 85-Gallon Drum Payload 2.2-9
Figure 2.2-4 – Radial Shift of CG for Six 100-Gallon Drum Payload 2.2-10
Figure 2.2-5 – Radial Shift of CG for SWB Payload 2.2-11
Figure 2.2-6 – Radial Shift of CG for TDOP Payload 2.2-12
Figure 2.5-1 – Tie-down Device Layout 2.5-12
Figure 2.5-2 – Tie-down Device Detail 2.5-13
Figure 2.5-3 – Tie-down Plan View and Reaction Force Diagram 2.5-14
Figure 2.5-4 – Tie-down Tensile/Shear Failure Modes 2.5-15
Figure 2.5-5 – Tie-down Lug Dimensions and Load Diagram 2.5-16
Figure 2.5-6 – Horizontal Doubler and Tripler Plate Details 2.5-17
Figure 2.6-1 – OCA Load Case 1, Overall Model 2.6-25
Figure 2.6-2 – OCA Load Case 1, Seal Region Detail 2.6-26
Figure 2.6-3 – OCA Load Case 2, Overall Model 2.6-27
Figure 2.6-4 – OCA Load Case 2, Seal Region Detail 2.6-28
Figure 2.6-5 – OCA Load Case 3, Overall Model 2.6-29
Figure 2.6-6 – OCA Load Case 3, Seal Region Detail 2.6-30
Figure 2.6-7 – OCA Load Case 4, Overall Model 2.6-31
Figure 2.6-8 – OCA Load Case 4, Seal Region Detail 2.6-32
Figure 2.6-9 – ICV Load Case 1, Overall Model 2.6-33
Figure 2.6-10 – ICV Load Case 1, Seal Region Detail 2.6-34
Figure 2.6-11 – ICV Load Case 2, Overall Model 2.6-35
Figure 2.6-12 – ICV Load Case 2, Seal Region Detail 2.6-36
Figure 2.7-1 – CTU-2 Free Drop Test No. 2 Accelerometer Data (Gage 1) 2.7-21

Figure 2.7-2 – CTU-2 Free Drop Test No. 2 Accelerometer Data (Gage 2) 2.7-21
Figure 2.7-3 – CTU-3 Free Drop Test No. 2 Accelerometer Data (Gage 1) 2.7-22
Figure 2.7-4 – CTU-3 Free Drop Test No. 2 Accelerometer Data (Gage 2) 2.7-22
Figure 2.10.1-1 – OCA Finite Element Analysis Model Element Plot 2.10.1-27
Figure 2.10.1-2 – ICV Finite Element Analysis Model Element Plot 2.10.1-28
Figure 2.10.2-1 – Test Fixture for O-ring Seal Performance Testing..... 2.10.2-11
Figure 2.10.3-1 – Drop Pad at the Coyote Canyon Aerial Cable Facility 2.10.3-41
Figure 2.10.3-2 – CTU OCV and ICV Pressurization Port Detail 2.10.3-42
Figure 2.10.3-3 – CTU Payload Representation (Concrete-Filled 55-Gallon Drums).... 2.10.3-43
Figure 2.10.3-4 – Schematic of the CTU-1 Test Orientations..... 2.10.3-44
Figure 2.10.3-5 – Schematic of the CTU-2 Test Orientations..... 2.10.3-45
Figure 2.10.3-6 – Schematic of the CTU-3 Test Orientations..... 2.10.3-46
Figure 2.10.3-7 – CTU-1 and CTU-2 ICV Temperature Indicating Label Locations..... 2.10.3-47
Figure 2.10.3-8 – CTU-1 OCV Temperature Indicating Label Locations 2.10.3-48
Figure 2.10.3-9 – CTU-2 OCV Temperature Indicating Label Locations 2.10.3-49
Figure 2.10.3-10 – CTU-1 OCV Thermocouple Locations..... 2.10.3-50
Figure 2.10.3-11 – CTU-2 OCV Thermocouple Locations..... 2.10.3-51
Figure 2.10.3-12 – CTU-1 OCV Thermocouple Data
(TH-1, TH-2, TH-3, TH-4) 2.10.3-52
Figure 2.10.3-13 – CTU-1 OCV Thermocouple Data
(TH-1A, TH-2A, TH-3A, TH-4A)..... 2.10.3-52
Figure 2.10.3-14 – CTU-1 OCV Thermocouple Data
(TH-1C, TH-2C, TH-3C, TH-4C)..... 2.10.3-53
Figure 2.10.3-15 – CTU-1 OCV Thermocouple Data
(TH-1D, TH-2D, TH-3D, TH-4D)..... 2.10.3-53
Figure 2.10.3-16 – CTU-2 OCV Thermocouple Data
(TH-1, TH-2, TH-3, TH-4) 2.10.3-54
Figure 2.10.3-17 – CTU-2 OCV Thermocouple Data
(TH-1A, TH-2A, TH-3A, TH-4A)..... 2.10.3-54
Figure 2.10.3-18 – CTU-2 Free Drop Test No. 2 Accelerometer Data (Gage 1) 2.10.3-55
Figure 2.10.3-19 – CTU-2 Free Drop Test No. 2 Accelerometer Data (Gage 2) 2.10.3-55
Figure 2.10.3-20 – CTU-2 Free Drop Test No. 3 Accelerometer Data (Gage 1) 2.10.3-56
Figure 2.10.3-21 – CTU-2 Free Drop Test No. 3 Accelerometer Data (Gage 2) 2.10.3-56
Figure 2.10.3-22 – CTU-3 Free Drop Test No. 2 Accelerometer Data (Gage 1) 2.10.3-57

Figure 2.10.3-23 – CTU-3 Free Drop Test No. 2 Accelerometer Data (Gage 2) 2.10.3-57
Figure 2.10.3-24 – CTU-1 Pressure Transducer Data During Fire Test No. 10 ..... 2.10.3-58
Figure 2.10.3-25 – CTU-2 Pressure Transducer Data During Fire Test No. 9 ..... 2.10.3-58
Figure 2.10.3-26 – CTU-1 Free Drop No. 1; Initial Preparation for Testing 2.10.3-59
Figure 2.10.3-27 – CTU-1 Free Drop No. 1; Pre-Drop Positioning 2.10.3-59
Figure 2.10.3-28 – CTU-1 Free Drop No. 1; Post-Drop Damage at Top (Lid) 2.10.3-60
Figure 2.10.3-29 – CTU-1 Free Drop No. 1; Post-Drop Damage at Bottom (Body) 2.10.3-60
Figure 2.10.3-30 – CTU-1 Free Drop No. 2; Pre-Drop Positioning 2.10.3-61
Figure 2.10.3-31 – CTU-1 Free Drop No. 2; Post-Drop Damage 2.10.3-61
Figure 2.10.3-32 – CTU-1 Free Drop No. 3; Pre-Drop Positioning 2.10.3-62
Figure 2.10.3-33 – CTU-1 Free Drop No. 3; Post-Drop Damage 2.10.3-62
Figure 2.10.3-34 – CTU-1 Free Drop No. 4; Pre-Drop Positioning 2.10.3-63
Figure 2.10.3-35 – CTU-1 Free Drop No. 4; Post-Drop Damage 2.10.3-63
Figure 2.10.3-36 – CTU-1 Puncture Drop No. 5; Pre-Drop Positioning 2.10.3-64
Figure 2.10.3-37 – CTU-1 Puncture Drop No. 5; Post-Drop Damage 2.10.3-64
Figure 2.10.3-38 – CTU-1 Puncture Drop No. 6; Pre-Drop Positioning 2.10.3-65
Figure 2.10.3-39 – CTU-1 Puncture Drop No. 6; Post-Drop Damage 2.10.3-65
Figure 2.10.3-40 – CTU-1 Puncture Drop No. 7; Pre-Drop Positioning 2.10.3-66
Figure 2.10.3-41 – CTU-1 Puncture Drop No. 7; Post-Drop Damage 2.10.3-66
Figure 2.10.3-42 – CTU-1 Puncture Drop No. 8; Pre-Drop Positioning 2.10.3-67
Figure 2.10.3-43 – CTU-1 Puncture Drop No. 8; Moment of Impact 2.10.3-67
Figure 2.10.3-44 – CTU-1 Puncture Drop No. 9; Pre-Drop Positioning 2.10.3-68
Figure 2.10.3-45 – CTU-1 Puncture Drop No. 9; Post-Drop Damage 2.10.3-68
Figure 2.10.3-46 – CTU-1 Fire No. 10; Pre-Fire Positioning, Side View 2.10.3-69
Figure 2.10.3-47 – CTU-1 Fire No. 10; Pre- Fire Positioning, Top End View 2.10.3-69
Figure 2.10.3-48 – CTU-1 Fire No. 10; Fully Engulfing Fire 2.10.3-70
Figure 2.10.3-49 – CTU-1 Fire No. 10; Post-Fire Cool-Down 2.10.3-70
Figure 2.10.3-50 – CTU-1 Disassembly; OCA Lid Unburned Foam 2.10.3-71
Figure 2.10.3-51 – CTU-1 Disassembly; OCA Lid Unburned Foam Thickness 2.10.3-71
Figure 2.10.3-52 – CTU-1 Disassembly; Payload Drum Removal 2.10.3-72
Figure 2.10.3-53 – CTU-1 Disassembly; Loose Debris on Pallet in ICV Body 2.10.3-72
Figure 2.10.3-54 – CTU-2 Free Drop No. 1; Initial Preparation for Testing 2.10.3-73

Figure 2.10.3-55 – CTU-2 Free Drop No. 1; Pre-Drop Positioning 2.10.3-73
Figure 2.10.3-56 – CTU-2 Free Drop No. 1; Post-Drop Damage 2.10.3-74
Figure 2.10.3-57 – CTU-2 Free Drop No. 1; Post-Drop Damage 2.10.3-74
Figure 2.10.3-58 – CTU-2 Free Drop No. 2; Pre-Drop Positioning 2.10.3-75
Figure 2.10.3-59 – CTU-2 Free Drop No. 2; Post-Drop Damage 2.10.3-75
Figure 2.10.3-60 – CTU-2 Free Drop No. 3; Pre-Drop Positioning 2.10.3-76
Figure 2.10.3-61 – CTU-2 Free Drop No. 3; Post-Drop Damage 2.10.3-76
Figure 2.10.3-62 – CTU-2 Puncture Drop No. R; Pre-Drop Positioning 2.10.3-77
Figure 2.10.3-63 – CTU-2 Puncture Drop R; Post-Drop Damage 2.10.3-77
Figure 2.10.3-64 – CTU-2 Puncture Drop No. 4; Pre-Drop Positioning 2.10.3-78
Figure 2.10.3-65 – CTU-2 Puncture Drop 4; Post-Drop Damage 2.10.3-78
Figure 2.10.3-66 – CTU-2 Puncture Drop No. 5; Pre-Drop Positioning 2.10.3-79
Figure 2.10.3-67 – CTU-2 Puncture Drop 5; Post-Drop Damage 2.10.3-79
Figure 2.10.3-68 – CTU-2 Puncture Drop No. 6; Pre-Drop Positioning 2.10.3-80
Figure 2.10.3-69 – CTU-2 Puncture Drop 6; Post-Drop Damage 2.10.3-80
Figure 2.10.3-70 – CTU-2 Puncture Drop No. 7; Pre-Drop Positioning 2.10.3-81
Figure 2.10.3-71 – CTU-2 Puncture Drop 7; Post-Drop Damage 2.10.3-81
Figure 2.10.3-72 – CTU-2 Puncture Drop No. 8; Pre-Drop Positioning 2.10.3-82
Figure 2.10.3-73 – CTU-2 Puncture Drop 8; Post-Drop Damage 2.10.3-82
Figure 2.10.3-74 – CTU-2 Fire No. 9; Pre-Fire Positioning 2.10.3-83
Figure 2.10.3-75 – CTU-2 Fire No. 9; Pre-Fire Positioning 2.10.3-83
Figure 2.10.3-76 – CTU-2 Fire No. 9; Starting Fire 2.10.3-84
Figure 2.10.3-77 – CTU-2 Fire No. 9; Post-Fire Cool-Down 2.10.3-84
Figure 2.10.3-78 – CTU-2 Disassembly; Loose Debris in ICV Lid 2.10.3-85
Figure 2.10.3-79 – CTU-2 Disassembly; Debris Contaminating the ICV Main O-ring Seals 2.10.3-85
Figure 2.10.3-80 – CTU-3 Free Drop No. 1; Pre-Drop Positioning 2.10.3-86
Figure 2.10.3-81 – CTU-3 Free Drop No. 1; Post-Drop Damage 2.10.3-86
Figure 2.10.3-82 – CTU-3 Free Drop No. 2; Pre-Drop Positioning 2.10.3-87
Figure 2.10.3-83 – CTU-3 Free Drop No. 2; Post-Drop Damage 2.10.3-87
Figure 2.10.3-84 – CTU-3 Free Drop No. 3; Pre-Drop Positioning 2.10.3-88
Figure 2.10.3-85 – CTU-3 Free Drop No. 3; Post-Drop Damage 2.10.3-88
Figure 2.10.3-86 – CTU-3 Puncture Drop No. 4; Pre-Drop Positioning 2.10.3-89

Figure 2.10.3-87 – CTU-3 Puncture Drop 4; Post-Drop Damage 2.10.3-89
Figure 2.10.3-88 – CTU-3 Puncture Drop No. 5; Pre-Drop Positioning..... 2.10.3-90
Figure 2.10.3-89 – CTU-3 Puncture Drop 5; Post-Drop Damage 2.10.3-90
Figure 2.10.3-90 – CTU-3 Puncture Drop No. 6; Pre-Drop Positioning..... 2.10.3-91
Figure 2.10.3-91 – CTU-3 Puncture Drop 6; Post-Drop Damage 2.10.3-91
Figure 2.10.3-92 – CTU-3 Puncture Drop No. 7; Pre-Drop Positioning..... 2.10.3-92
Figure 2.10.3-93 – CTU-3 Puncture Drop 7; Post-Drop Damage 2.10.3-92
Figure 2.10.3-94 – CTU-3 Puncture Drop No. 8; Pre-Drop Positioning..... 2.10.3-93
Figure 2.10.3-95 – CTU-3 Puncture Drop 8; Post-Drop Damage 2.10.3-93
Figure 2.10.3-96 – CTU-3 Disassembly; OCA Lid..... 2.10.3-94
Figure 2.10.3-97 – CTU-3 Disassembly; OCA Body..... 2.10.3-94
Figure 2.10.3-98 – CTU-3 Disassembly; ICV Lid Removal 2.10.3-95
Figure 2.10.3-99 – CTU-3 Disassembly; Loose Debris on Pallet in ICV Body 2.10.3-95
Figure 3.4-1 – TRUPACT-II Packaging Thermal Model Node Layout..... 3.4-19
Figure 3.4-2 – Seal Region Thermal Model Node Layout 3.4-20
Figure 3.4-3 – Fourteen 55-Gallon Drum Payload Thermal Node Layout 3.4-21
Figure 3.4-4 – Two Standard Waste Boxes Thermal Model Node Layout 3.4-22
Figure 3.5-1 – CTU-1 and CTU-2 ICV Temperature Indicating Label Locations..... 3.5-12
Figure 3.5-2 – CTU-1 OCV Temperature Indicating Label Locations 3.5-13
Figure 3.5-3 – CTU-2 OCV Temperature Indicating Label Locations 3.5-14
Figure 3.5-4 – CTU-1 OCV Thermocouple Locations..... 3.5-15
Figure 3.5-5 – CTU-2 OCV Thermocouple Locations..... 3.5-16
Figure 3.5-6 – CTU-1 OCV Thermocouple Data (TH-1, TH-2, TH-3, TH-4)..... 3.5-17
Figure 3.5-7 – CTU-1 OCV Thermocouple Data (TH-1A, TH-2A, TH-3A, TH-4A) 3.5-17
Figure 3.5-8 – CTU-1 OCV Thermocouple Data (TH-1B, TH-2B, TH-3B, TH-4B) 3.5-18
Figure 3.5-9 – CTU-1 OCV Thermocouple Data (TH-1C, TH-2C, TH-3C, TH-4C) 3.5-18
Figure 3.5-10 – CTU-2 OCV Thermocouple Data (TH-1, TH-2, TH-3, TH-4)..... 3.5-19
Figure 3.5-11 – CTU-2 OCV Thermocouple Data (TH-1A, TH-2A, TH-3A, TH-4A) 3.5-19
Figure 3.5-12 – CTU-1 Pressure Transducer Data During Fire Test No. 10 ..... 3.5-20
Figure 3.5-13 – CTU-2 Pressure Transducer Data During Fire Test No. 9..... 3.5-20
Figure 6.3-1 – Case A Contents Model 6.3-9
Figure 6.3-2 – Case B Contents Model..... 6.3-10

Figure 6.3-3 – Case C Contents Model 6.3-11
Figure 6.3-4 – Case D Contents Model 6.3-12
Figure 6.3-5 – NCT, Single-Unit Model; R-Z Slice 6.3-13
Figure 6.3-6 – HAC, Single-Unit Model; R-Z Slice 6.3-14
Figure 6.3-7 – Array Model Variation 0 (Reflective Boundary Conditions Imposed) 6.3-15
Figure 6.3-8 – Array Model Variation 1; X-Y Slice Through Top Axial Layer 6.3-16
Figure 7.4-1 – Pressure Rise Leakage Rate Test Schematic 7.4-2
Figure 8.2-1 – Method of Measuring Upper Seal Flange Groove Widths 8.2-8
Figure 8.2-2 – Method of Measuring Lower Seal Flange Groove Widths 8.2-9
Figure 8.2-3 – Method of Measuring Upper Seal Flange Tab Widths 8.2-10
Figure 8.2-4 – Method of Measuring Lower Seal Flange Tab Widths 8.2-11

1.0 GENERAL INFORMATION

This chapter of the Safety Analysis Report (SAR) presents a general introduction and description of the TRUPACT-II contact-handled transuranic waste (CH-TRU) package. The major components comprising the TRUPACT-II package are presented as Figure 1.1-1 and Figure 1.1-2, where Figure 1.1-1 presents an exploded view of all major TRUPACT-II packaging components, and Figure 1.1-2 presents a detailed view of the closure and seal region. Detailed drawings presenting the TRUPACT-II packaging design are presented in Appendix 1.3.1, *Packaging General Arrangement Drawings*. All details relating to payloads and payload preparation for shipment in a TRUPACT-II package are presented in the *Contact-Handled Transuranic Waste Authorized Methods for Payload Control* (CH-TRAMPAC)[1]. Descriptions of the standard, S100, S200, and S300 pipe overpack payload configurations are provided in Appendices 4.1, 4.2, 4.3, and 4.4 respectively, of the *CH-TRU Payload Appendices*[2]. Terminology and acronyms used throughout this document are presented as Appendix 1.3.2, *Glossary of Terms and Acronyms*.

1.1 Introduction

The model TRUPACT-II package has been developed for the U. S. Department of Energy (DOE) as a safe means for the transportation of CH-TRU materials and other authorized payloads.

The TRUPACT-II package is designed for truck transport. As many as three, loaded TRUPACT-II packages can be transported on a single semi-trailer. The rugged, lightweight design of the TRUPACT-II package allows the efficient transport of a maximum payload, thereby reducing the total number of radioactive shipments. The TRUPACT-II package is also suitable for rail transport. As many as seven loaded TRUPACT-II packages can be transported per railcar.

The goals of maintaining public safety while achieving a lightweight design are satisfied by use of a deformable sealing region that can absorb both normal conditions of transport (NCT) and hypothetical accident condition (HAC) deformations without loss of leaktight capability[3]. A variety of scaled and full-scale engineering development tests were included as part of the design process. Ultimately, three full-scale certification test units (CTUs) were subjected to a series of free drops and puncture drops. Following free drops and puncture tests, two CTUs were exposed to a fully engulfing pool fire test. These tests conclusively demonstrated containment integrity of the TRUPACT-II package.

The payload within each TRUPACT-II package will be within 55-gallon drums, 85-gallon drums, 100-gallon drums, standard waste boxes (SWBs), or a ten drum overpack (TDOP). Hereafter, the term “85-gallon drum” is used to refer to 75- to 88-gallon drums that may, with the appropriate dimensions, overpack a single 55-gallon drum. Pipe overpacks utilize 55-gallon drums as

---

[1] U.S. Department of Energy (DOE), *Contact-Handled Transuranic Waste Authorized Methods for Payload Control* (CH-TRAMPAC), U.S. Department of Energy, Carlsbad Field Office, Carlsbad, New Mexico.

[2] U.S. Department of Energy (DOE), *CH-TRU Payload Appendices*, U.S. Department of Energy, Carlsbad Field Office, Carlsbad, New Mexico.

[3] Leaktight is defined as 1×10^{-7} standard cubic centimeters per second (scc/s), or less, air leakage per the definition in ANSI N14.5-1997, *American National Standard for Radioactive Materials - Leakage Tests on Packages for Shipment,* American National Standards Institute, (ANSI), Inc.

overpacks. A single TRUPACT-II package can transport fourteen 55-gallon drums (with or without pipe components), eight 85-gallon drums, six 100-gallon drums, two SWBs, or one TDOP. Specifications for payload containers are provided in Section 2.0, *Container and Physical Properties Requirements*, of CH-TRAMPAC.

The TRUPACT-II packaging provides two leakage rate testable levels of containment for the payload during both normal conditions of transport (NCT) and hypothetical accident conditions (HAC).

Based on the shielding and criticality assessments provided in Chapter 5.0, *Shielding Evaluation*, and Chapter 6.0, *Criticality Evaluation*, the Criticality Safety Index (CSI) for the TRUPACT-II package is zero (0.0), and the shielding Transport Index (TI) is determined at the time of shipment.

Authorization is sought for shipment of the TRUPACT-II package by truck or railcar as a Type B(U)F-96 package per the definition delineated in 10 CFR §71.4[4].

[4] Title 10, Code of Federal Regulations, Part 71 (10 CFR 71), *Packaging and Transportation of Radioactive Material*, 01-01-07 Edition.

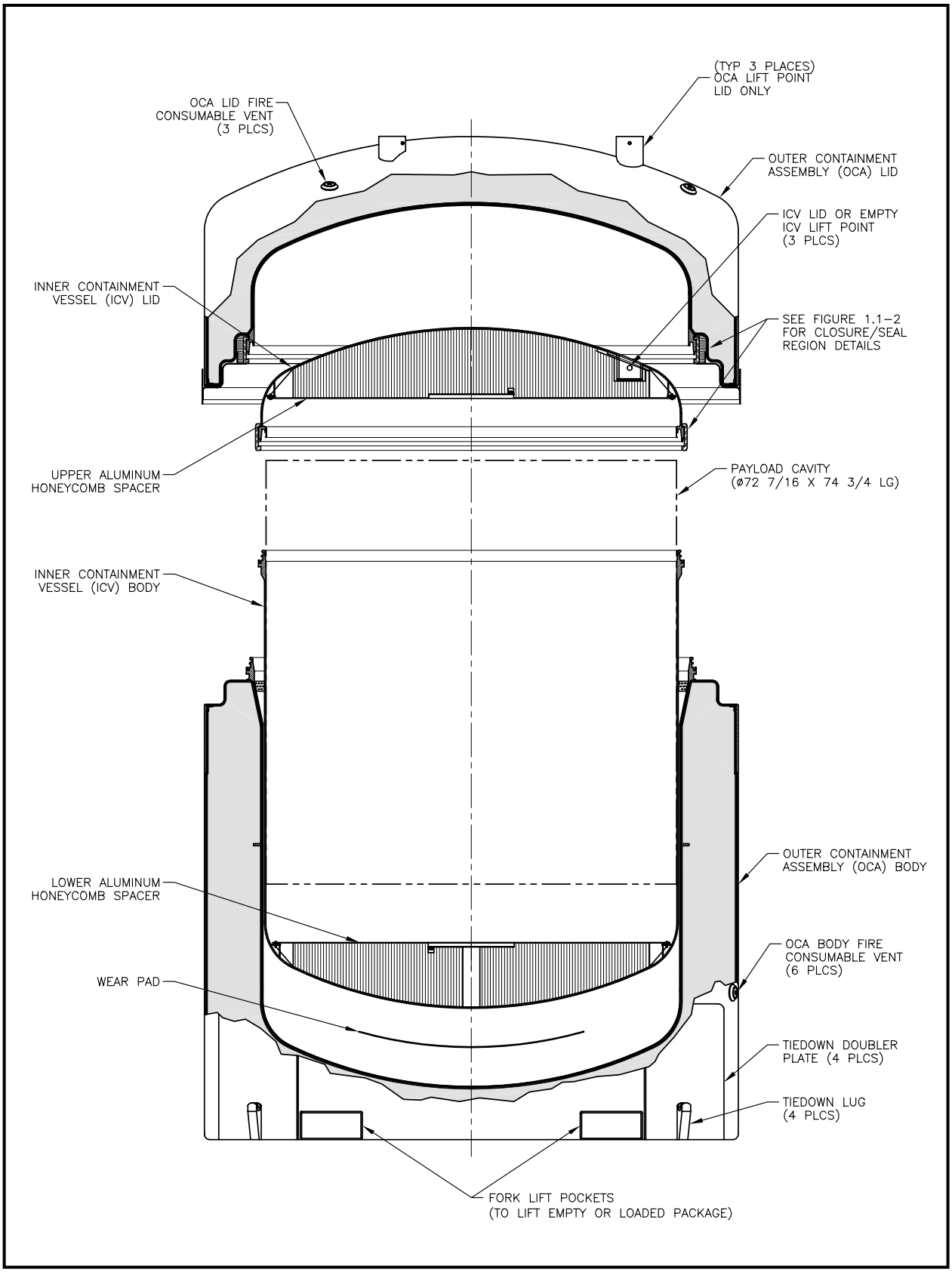

Figure 1.1-1 – TRUPACT-II Package Assembly

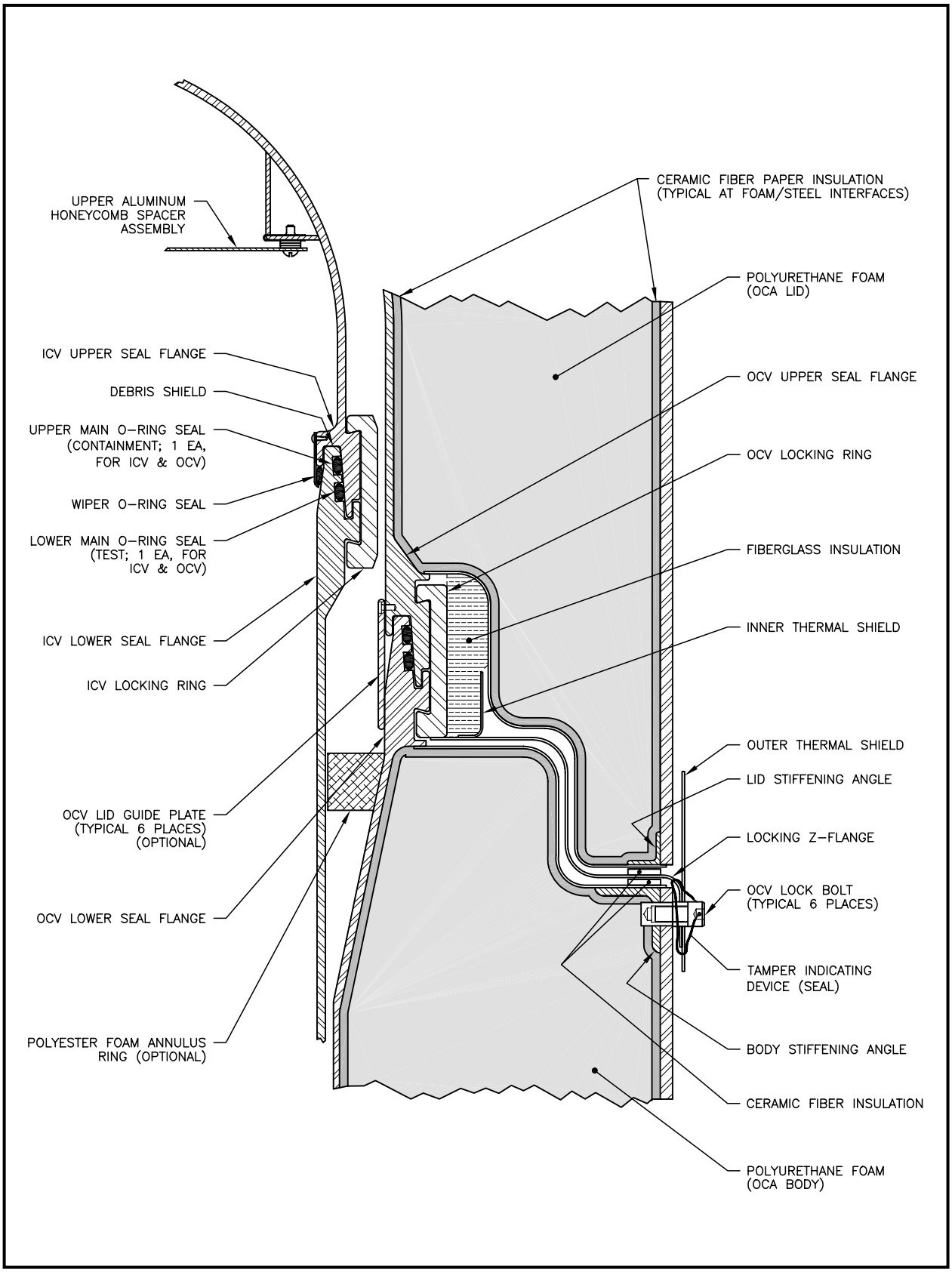

Figure 1.1-2 – TRUPACT-II Packaging Closure/Seal Region Details

1.2 Package Description

This section presents a basic description of the TRUPACT-II package. General arrangement drawings of the TRUPACT-II packaging are presented in Appendix 1.3.1, *Packaging General Arrangement Drawings*. Drawings illustrating payload assembly details are presented in the CH-TRAMPAC[1].

1.2.1 Packaging

1.2.1.1 Packaging Description

The TRUPACT-II packaging is comprised of an outer containment assembly (OCA) that provides the primary containment boundary, and an inner containment vessel (ICV) that provides the secondary containment boundary. Two aluminum honeycomb spacer assemblies are used within the ICV, one inside each ICV torispherical head. A silicone wear pad is utilized at the interface between the bottom exterior of the ICV and the bottom interior of the OCA. An optional polyester foam annulus ring may be used in the annulus between the ICV and OCV, just below the OCV lower seal flange, to prevent debris from becoming entrapped between the vessels.

Inside the ICV, the payload will be within 55-gallon drums, 85-gallon drums, 100-gallon drums, standard waste boxes (SWBs), or ten drum overpacks (TDOPs). The OCA, ICV, and the aluminum honeycomb spacer assemblies are fully described in the following subsections. The design details and overall arrangement of the TRUPACT-II packaging are presented in the Appendix 1.3.1, *Packaging General Arrangement Drawings*. Drawings illustrating payload assembly details are presented in the CH-TRAMPAC.

1.2.1.1.1 Outer Containment Assembly (OCA)

The outer containment assembly (OCA) consists of an OCA lid and OCA body, each primarily comprised of an inner stainless steel shell structure, a relatively thick layer of rigid polyurethane foam, and an external stainless steel shell structure. The inner OCA shell structure comprises the outer containment vessel (OCV).

Not considering the seal flange region, the OCA lid has a nominal external diameter of 94⅜ inches and a nominal internal diameter of 76¹³⁄₁₆ inches. Likewise, not considering the seal flange region, the OCA body has a nominal external diameter of 94⅜ inches and a nominal internal diameter of 73⅝ inches, tapering outward to a nominal inside diameter of 76⅞ inches at the OCV lower seal flange. The nominal external diameter of the OCV seal region is 95 inches, and the nominal internal diameter of the OCV seal region is 76⁷⁄₁₆ inches. With the OCA lid installed onto the OCA body, the OCA has a nominal external length of 121½ inches, and a nominal internal height is 100 inches at the OCV cavity centerline.

The containment boundary provided by the OCA consists of the inner stainless steel vessel formed by a mating lid and body, plus the uppermost of two main O-ring seals enclosed between an upper and lower seal flange. The upper main O-ring seal (containment seal) is butyl rubber

[1] U.S. Department of Energy (DOE), *Contact-Handled Transuranic Waste Authorized Methods for Payload Control* (CH-TRAMPAC), U.S. Department of Energy, Carlsbad Field Office, Carlsbad, New Mexico.

with a nominal 0.400 inch diameter cross-section. The lower main O-ring seal (test seal) may be neoprene or ethylene propylene with a nominal 0.375 inch diameter cross-section. The purpose of the lower main O-ring seal is for establishing a vacuum on the exterior side of the upper main O-ring seal for helium and pressure rise leakage rate testing.

A vent port feature in the OCV body's lower seal flange is the only other containment boundary penetration. A vent port coupling, a seal welded threaded fitting, and an OCV vent port plug with an O-ring seal defines the containment boundary at the OCV vent port penetration. Access to the OCV vent port is gained through an external penetration in the OCA outer shell once an outer 1½ NPT plug and a foam or ceramic fiber material plug is removed. The connecting tube is fabricated of non-thermally conductive fiberglass.

Leakage rate testing of the OCV's upper main O-ring seal (containment seal) is performed through an OCV seal test port that is located in the OCA lid. Similar in design to the OCV vent port, access to the OCV seal test port is gained through an external penetration in the OCA outer shell once an outer 1½ NPT plug and a foam or ceramic fiber material plug is removed. The connecting tube is fabricated of thin-walled stainless steel.

The cylindrical portion of the OCV body is 3/16 inch nominal thickness, Type 304, stainless steel. All other shells comprising the OCV are 1/4 inch nominal thickness, Type 304, stainless steel, including the lower and upper torispherical heads. A single, 3/8 inch thick stiffening ring, extending radially out from the OCV shell, is included in the design. The OCA outer shell varies between 1/4 inch and 3/8 inch nominal thickness, Type 304, stainless steel. The 3/8 inch nominal thickness material is used adjacent to the closure interface to ensure protection from HAC puncture bar penetration near the sealing regions. All other shells comprising the OCA exterior are 1/4 inch nominal thickness, Type 304, stainless steel, including the lower flat head and upper torispherical head. As illustrated in Figure 1.1-2, the inner and outer shell structures for both the OCA lid and OCA body are connected together via 14 gauge (0.075 inch thick), Type 304, stainless steel Z-flanges. Secure attachment of the 14 gauge Z-flanges to the 3/8 inch thick OCA outer shell is assured by the use of rolled angle reinforcements (2 × 2 × 1/4 inch for the OCA body junction, and 1 × 1 × 1/8 inch for the OCA lid junction). A locking Z-flange between the upper and lower (i.e., OCA lid and OCA body) Z-flanges allows rotation of the OCV locking ring from the TRUPACT-II package exterior. The Z-flanges serve the purpose of precluding direct flame impingement on the OCV seal flanges during the hypothetical accident condition (HAC) thermal event (fire). To further preclude flame and hot gas entry into the Z-flange channel, inner and outer thermal shields are included as part of the locking Z-flange assembly.

The OCA lid is secured to the OCA body via the OCV locking ring located at the outer diameter of the OCV upper and lower seal flanges. Closure design and operation is illustrated in Figure 1.2-1. The lower end of the OCV locking ring has 18 tabs that mate with a corresponding set of 18 tabs on the OCV lower seal flange. To install the OCA lid, the OCV locking ring is rotated to the "unlocked" position, using alignment marks on the OCA exterior for reference. The unlocked position aligns the tabs on the OCV locking ring with the cutouts between the tabs on the OCV lower seal flange. Next, install the OCA lid onto the OCA body, optionally evacuating the OCV cavity through the OCV vent port sufficiently to allow free movement of the OCV locking ring. Positive closure is attained by rotating the OCV locking ring to the "locked" position, again using the alignment marks on the OCA exterior for reference. In order to allow rotation of the OCV locking ring from the TRUPACT-II packaging exterior, a locking Z-flange

extends radially outward to the OCA exterior. Six, 1/2 inch diameter stainless steel socket head cap screws secure the locking Z-flange in the locked position. A single, localized cutout in the OCV locking ring is provided for access to the OCV seal test port feature.

Within the annular void between the OCV and the OCA outer shell structure is a relatively thick layer of thermally insulating and energy absorbing, rigid, polyurethane foam. Surrounding the periphery of the polyurethane foam cavity is a layer of 1/4 inch nominal thickness, ceramic fiber paper capable of resisting temperatures in excess of 2,000 ºF. The combination of OCA exterior shell, fire resistant polyurethane foam, and insulating ceramic fiber paper is sufficient to protect the containment boundary from the consequences of all regulatory defined tests.

Two forklift pockets are incorporated into the base of the OCA body. These pockets provide the handling interface for lifting a TRUPACT-II package. Three sets of lifting straps are included in the OCA lid assembly for lifting of the OCA lid only, and are so appropriately identified. Four tie-down lugs with reinforcing doubler plates are also provided at the base of the OCA body.

Rubber materials used in the OCA include butyl, and ethylene propylene or neoprene, as applicable, for the main O-ring seals, silicone for the wear pad, and polyester foam for the optional annulus foam ring. Plastic is used for the polyurethane foam cavity, fire-consumable vent plugs. The OCA lid lift pockets, vent port access tube, and a portion of the seal test port access tube are made from fiberglass. Brass is used for the OCV vent and seal test port plugs. High alloy stainless steel is used for the OCV locking ring joint pins. Insulating materials such as ceramic fiber paper along the periphery of the polyurethane foam cavity, and fiberglass-type insulation for the inner thermal shield are also used. Finally, a variety of stainless steel fasteners, greases and lubricants, and adhesives are also utilized, as specified in Appendix 1.3.1, *Packaging General Arrangement Drawings*.

1.2.1.1.2 Inner Containment Vessel (ICV) Assembly

The inner containment vessel (ICV) assembly consists of an ICV lid and ICV body, each primarily comprised of a stainless steel shell structure. Not considering the seal flange region, the ICV lid has a nominal external diameter of 74⅜ inches and a nominal internal diameter of 73⅞ inches. Likewise, not considering the seal flange region, the ICV body has a nominal external diameter of 73⅛ inches and a nominal internal diameter of 72⅝ inches. The nominal external diameter of the ICV seal region is 76 5/16 inches, and the nominal internal diameter of the ICV seal region is 72 7/16 inches. With the ICV lid installed onto the ICV body, the ICV has a nominal external length of 99 inches, and a nominal internal height is 98½ inches at the ICV cavity centerline.

The containment boundary provided by the ICV consists of a stainless steel vessel formed by a mating lid and body, plus the uppermost of two main O-ring seals enclosed between an upper and lower seal flange. The upper main O-ring seal (containment) is butyl rubber with a nominal 0.400 inch diameter cross-section. The lower main O-ring seal (test) may be neoprene or ethylene propylene with a nominal 0.375 inch diameter cross-section. The purpose of the lower main O-ring seal is for establishing a vacuum on the exterior side of the upper main O-ring seal for helium and pressure rise leakage rate testing. To protect the main O-ring seals from debris that may be associated with some payloads, a wiper O-ring seal is used between the ICV upper and lower seal flanges. In addition to the wiper O-ring seal, a silicone debris shield, located at the top of the ICV lower seal flange, provides a secondary debris barrier to the upper main O-ring seal. To ensure that helium tracer gas reaches the region directly above the upper main

O-ring seal (containment) during helium leakage rate testing, a helium fill port is integral to the ICV vent port configuration (see Appendix 1.3.1, *Packaging General Arrangement Drawings*). In addition, to allow for pressure equalization across the silicone debris shield during ICV lid installation and removal, three, 1/8 inch nominal diameter holes are located in the top of the ICV lower seal flange.

A vent port feature in the ICV body's lower seal flange is the only other containment boundary penetration. A vent port insert and an outer ICV vent port plug with an O-ring seal define the containment boundary at the ICV vent port penetration.

Leakage rate testing of the ICV's upper main O-ring seal (containment seal) is performed through an ICV seal test port that is located in the ICV lid.

All shells comprising the ICV are 1/4 inch nominal thickness, Type 304, stainless steel, including the lower and upper torispherical heads.

Similar to the OCV, the ICV lid is secured to the ICV body via the ICV locking ring located at the outer diameter of the ICV upper and lower seal flanges. Closure design and operation is almost identical to the OCV, as illustrated in Figure 1.2-1. The lower end of the ICV locking ring has 18 tabs that mate with a corresponding set of 18 tabs on the ICV lower seal flange. To install the ICV lid, the ICV locking ring is rotated to the "unlocked" position, using alignment marks for reference. The unlocked position will align the tabs on the ICV locking ring with the cutouts between the tabs on the ICV lower seal flange. Next, the ICV lid is installed onto the ICV body, optionally evacuating the ICV cavity through the ICV vent port sufficiently to allow free movement of the ICV locking ring. Positive closure is attained by rotating the ICV locking ring to the "locked" position, using the alignment marks for reference. Three, 1/2 inch diameter stainless steel socket head cap screws secure the ICV locking ring in the locked position.

Three lift sockets, each containing a lift pin, are integrated into the ICV lid for lifting the ICV lid or an empty ICV assembly. Any lifting of the loaded ICV is performed using the OCA forklift pockets with the ICV located within the OCA.

Rubber materials used in the ICV include butyl, ethylene propylene, neoprene, buna-N, flourosilicone or flourocarbon, as applicable, for the main and wiper O-ring seals, and silicone for the debris shield. Brass is used for the ICV vent and seal test port plugs. High alloy stainless steel is used for the ICV locking ring joint pins. Finally, a variety of stainless steel fasteners, and greases and lubricants are also utilized, as specified in Appendix 1.3.1, *Packaging General Arrangement Drawings*.

1.2.1.1.3 Aluminum Honeycomb Spacer Assemblies

Aluminum honeycomb spacer assemblies are designed to fit within the torispherical heads at each end of the ICV cavity. Each aluminum honeycomb spacer assembly includes an optional, 18 inch nominal diameter by 1½ inch nominal depth pocket that may be used in the future to accommodate a catalyst assembly. The lower spacer assembly also includes a 3 inch nominal diameter hole at the center that serves as an inspection port to check for water accumulation in the ICV lower head. With the spacer assemblies in place, the nominal ICV cavity height becomes 74¾ inches.

1.2.1.2 Gross Weight

The gross shipping weight of a TRUPACT-II package is 19,250 pounds maximum. A summary of overall component weights is delineated in Table 2.2-1 of Section 2.2, *Weights and Centers of Gravity*.

1.2.1.3 Neutron Moderation and Absorption

The TRUPACT-II package does not require specific design features to provide neutron moderation and absorption for criticality control. Fissile materials in the payload are limited to amounts that ensure safely subcritical packages for both NCT and HAC. The fissile material limits for a single TRUPACT-II Package are based on optimally moderated and reflected fissile material. The structural materials in the TRUPACT-II packaging are sufficient to maintain reactivity between the fissile material in an infinite array of damaged TRUPACT-II packages at an acceptable level. Further discussion of neutron moderation and absorption is provided in Chapter 6.0, *Criticality Evaluation*.

1.2.1.4 Receptacles, Valves, Testing, and Sampling Ports

There are no receptacles or valves used on the TRUPACT-II packaging, however, the OCV and ICV each have a seal test port and a vent port (see Appendix 1.3.1, *Packaging General Arrangement Drawings*). For each containment vessel, a seal test port provides access to the region between the upper and lower (containment and test) main O-ring seals between the upper and lower (lid and body) seal flanges. The seal test ports are used to leakage rate test the seals to verify proper assembly of the TRUPACT-II package prior to shipment.

The vent port is used during loading and unloading to facilitate lid installation and removal, and to allow blowdown of internal vacuum or pressure prior to opening a loaded package. As an option, a low vacuum may be applied to the vent port to fully seat the lid and assure free rotation of the locking ring.

Two separate penetrations through the polyurethane foam within the OCA are provided to access the seal test port and vent port plugs. The access ports are capped at the OCA exterior surface with 1½ inch pipe plugs (NPT) within 3 inch diameter couplings. Reinforcing doubler plates are also included on the inner surface of the OCA exterior shell, adjacent to the couplings. In addition, removable foam or ceramic fiber plugs fill the region within the access hole tubes to provide a level of thermal protection from the HAC thermal event. The vent port access tube is comprised of a non-metallic fiberglass, and a fiberglass link is included with the stainless steel, seal test port access tube as a lining to reduce radial thermal conductivity. When the OCA lid is removed, the ICV vent and seal test port plugs are readily accessible.

The OCV seal test port and both the ICV seal test and vent port plugs are accessed through localized cutouts in the corresponding vessel locking rings. An elongated cutout in the ICV locking ring is utilized at the ICV vent port location to allow locking ring rotation while an optional vacuum pump is installed. Smaller cutouts are provided in the ICV and OCV locking rings at the seal test port locations since these ports are only used with the locking rings in the locked position. The OCV vent port feature is located in the OCA body, therefore a cutout in the OCV locking ring is not necessary.

Detailed drawings of the test and vent port features and the associated local cutouts in the locking rings are provided in Appendix 1.3.1, *Packaging General Arrangement Drawings*.

1.2.1.5 Heat Dissipation

The TRUPACT-II package design capacity is 40 thermal watts maximum. The TRUPACT-II package dissipates this relatively low internal heat load entirely by passive heat transfer for both NCT and HAC. No special devices or features are needed or utilized to enhance the dissipation of heat. Features are included in the design to enhance thermal performance in the HAC thermal event. These include the use of a high temperature insulating material (ceramic fiber paper) at polyurethane foam-to-steel interfaces and the presence of an inner and outer thermal shield at the OCA lid-to-body interface. A more detailed discussion of the package thermal characteristics is provided in Chapter 3.0, *Thermal Evaluation*.

1.2.1.6 Coolants

Due to the passive design of the TRUPACT-II package with regard to heat transfer, there are no coolants utilized within the TRUPACT-II package.

1.2.1.7 Protrusions

The only significant protrusions on the TRUPACT-II package exterior are those associated with the lifting and tie-down features on the OCA exterior. The only significant external protrusions from the OCA lid are lift straps and corresponding guide pockets that extend from three equally spaced locations at the lid top. These lift features protrude above the OCA upper torispherical head, but are radially located such that they remain below torispherical head's crown and do not affect overall package height. The guide pockets are made of a fiberglass material that is designed to break away for lid-end impacts. The only significant external protrusions from the OCA body are the tie-down features at the bottom end of the package. Four tie-down lugs, with associated doubler plates, are used at locations corresponding with the main beams of the trailer. These tie-down protrusions extend a maximum of 2⅛ inch radially from the OCA body exterior shell.

The only significant protrusion on the ICV exterior is the ICV locking ring. The ICV locking ring extends radially outward approximately one inch from the outside surface of the upper ICV torispherical head. With its 3⅞ inch axial length directly backed and supported by the OCV (the nominal radial gap is 1/4 inch), this external protrusion is of little consequence for the package. The only significant protrusions on the ICV interior are the three lift pockets that penetrate the upper ICV torispherical head. These lift pockets are equally spaced on a 56 inch diameter, extending into the ICV cavity a maximum of 4½ inches from the inner surface of the upper ICV torispherical head. The ICV lift pockets are of little consequence as they are protected by the surrounding aluminum honeycomb spacer assembly. There are no significant internal or external protrusions associated with the ICV body.

1.2.1.8 Lifting and Tie-down Devices

Three sets of lift pins, lift straps and associated doubler plates used in the OCA lid are designed to handle the OCA lid only (including overcoming any resistance to lid removal associated with the presence of the main O-ring seals). The OCA lid lifting devices are not designed to lift a loaded package or empty OCA. Under excessive load, failure occurs in the region of the OCA

lift pin locations (at the pin-to-strap welds), away from the OCA torispherical head. A loaded TRUPACT-II package or any portion thereof can be lifted via the pair of forklift pockets that are located at the base of the OCA body. These pockets are sized to accommodate forks up to 10 inches wide and up to 4 inches thick. An overhead crane can also be used to lift the loaded package, utilizing lifting straps through the fork lift pockets.

Lifting of the ICV is via the three lift pockets inset into the upper ICV torispherical head. These lift pockets, with their associated lift pins and adjacent doubler plates, are sized to lift an empty ICV or handle the ICV lid (including overcoming any resistance to lid removal associated with the presence of the main O-ring seals). A loaded ICV must be fully supported with the OCA body and lifted via the OCA forklift pockets. Under excessive load, the ICV lift pins are designed to fail in shear prior to compromising the ICV containment boundary.

Both the OCA and ICV lifting points are appropriately labeled to limit their use to the intended manner.

Four tie-down lugs, with associated doubler plates, are used at locations corresponding with the main beams of the trailer. At each tie-down location, one doubler is used on the outside surface of the OCA side wall and one on the inside surface of the OCA lower flanged head. At each tie-down lug location, an internal gusset plate is also used between the inside of the OCA exterior shell and the doubler in the lower head to stiffen the tie-down regions. The doubler plates are sized to adequately distribute the regulatory-defined tie-down loads (10 *g*s longitudinal, 5 *g*s lateral, and 2 *g*s vertical, applied simultaneously) outwardly into the 1/4 inch thick OCA exterior shell. Each tie-down lug is welded directly to the adjacent side doubler plate. In an excessive load condition, these tie-down lug welds are sized to shear from the corresponding doubler plate.

A detailed discussion of lifting and tie-down designs, with corresponding structural analyses, is provided in Section 2.5, *Lifting and Tie-down Standards for All Packages*.

1.2.1.9 Pressure Relief System

There are no pressure relief systems included in the TRUPACT-II package design to relieve pressure from within the ICV or OCV. Fire-consumable vents in the form of plastic pipe plugs are employed on the exterior surface of the OCA. These vents are included to release any gases generated by charring polyurethane foam in the HAC thermal event (fire). During the HAC fire, the plastic pipe plugs melt allowing the release of gasses generated by the foam as it flashes to a char. Three vents are used on the OCA lid and six on the OCA body, located at the center of foam mass in each component. For optimum performance, the vents are located uniformly around the circumference of the OCA lid and body.

1.2.1.10 Shielding

Due to the nature of the contact-handled transuranic (CH-TRU) payload, no biological shielding is necessary or provided by the TRUPACT-II packaging.

1.2.2 Operational Features

The TRUPACT-II package is not considered to be operationally complex. All operational features are readily apparent from an inspection of the drawings provided in Appendix 1.3.1, *Packaging General Arrangement Drawings*, and the previous discussions presented in Section

1.2.1, *Packaging*. Operational procedures and instructions for loading, unloading, and preparing an empty TRUPACT-II package for transport are provided in Chapter 7.0, *Operating Procedures*.

1.2.3 Contents of Packaging

The TRUPACT-II packaging is designed to transport contact-handled transuranic (CH-TRU) and other authorized payloads such as tritium-contaminated materials that do not exceed 10^5 A_2 quantities. The *Contact-Handled Transuranic Waste Authorized Methods for Payload Control* (CH-TRAMPAC)[1] is the governing document for shipments of solid or solidified CH-TRU and tritium-contaminated wastes in the TRUPACT-II package. All users of the TRUPACT-II package shall comply with all payload requirements outlined in the CH-TRAMPAC, using one or more of the methods described in that document.

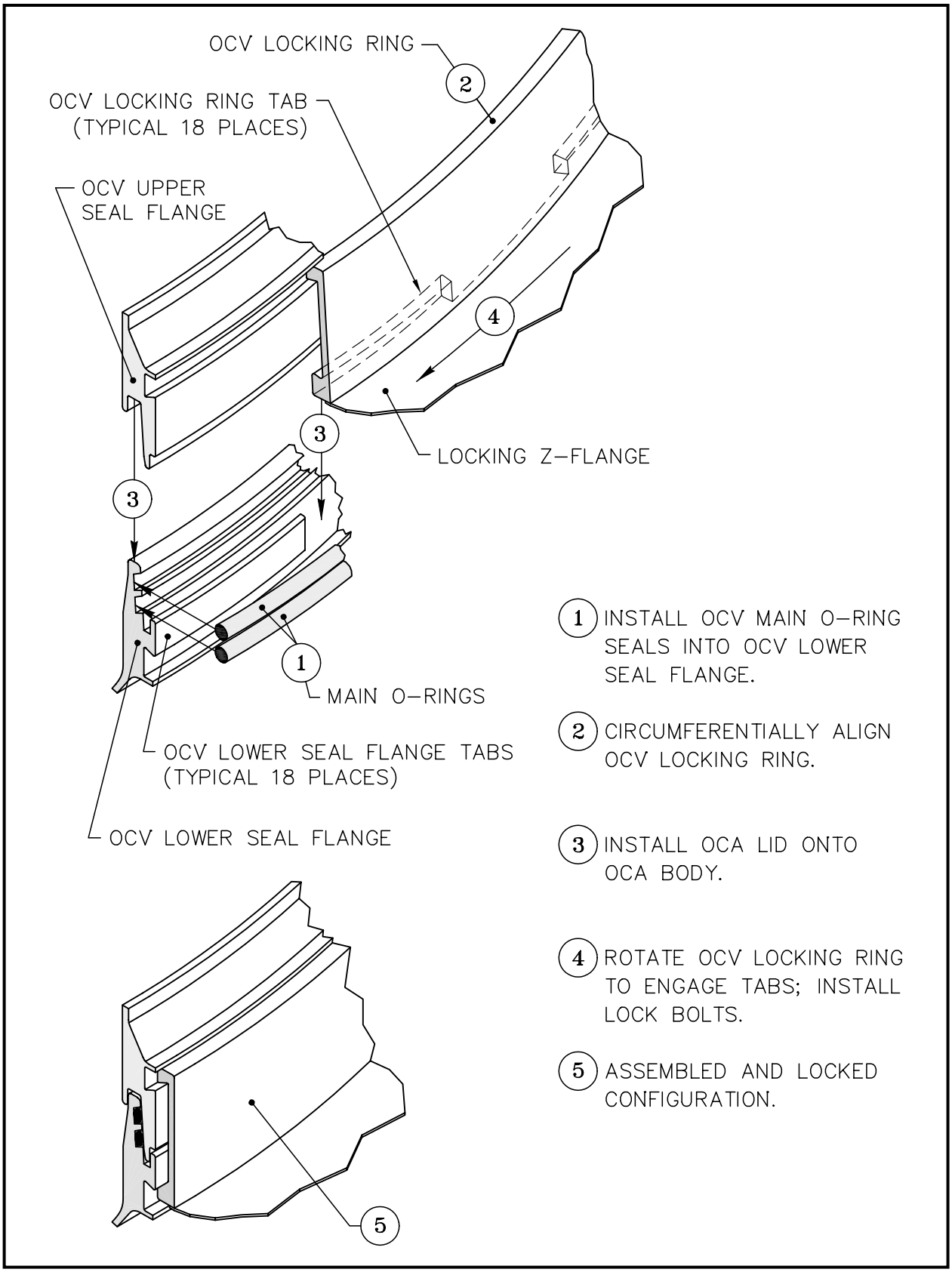

Figure 1.2-1 – OCV Closure Design (ICV closure is Similar)

This page intentionally left blank.

1.3 Appendices

1.3.1 *Packaging General Arrangement Drawings*

1.3.2 *Glossary of Terms and Acronyms*

This page intentionally left blank.

1.3.1 Packaging General Arrangement Drawings

This section presents the TRUPACT-II packaging general arrangement drawing[1], consisting of 11 sheets entitled, *TRUPACT-II Packaging SAR Drawing, Drawing Number 2077-500SNP*. In addition, the standard pipe overpack general arrangement drawing, consisting of 3 sheets entitled, *Standard Pipe Overpack, Drawing Number 163-001*, is presented in this section. The S100 pipe overpack, the S200 pipe overpack, and the S300 pipe overpack are depicted in *Drawing Numbers 163-002*, *163-003*, and *163-004*, respectively. The 55-gallon, 85-gallon, and 100-gallon compacted puck drum spacers are depicted in *Drawing Number 163-006*.

Within the packaging general arrangement drawing, dimensions important to the packaging's safety are dimensioned and toleranced (e.g., structural shell thicknesses, polyurethane foam thicknesses, and the sealing regions on the seal flanges). All other dimensions are provided as a reference dimension, and are toleranced in accordance with the general tolerance block.

[1] The TRUPACT-II packaging, pipe overpack, and compacted puck drum spacer general arrangement drawings utilize the uniform standard practices of ASME/ANSI Y14.5M, *Dimensioning and Tolerancing*, American National Standards Institute, Inc. (ANSI).

This page intentionally left blank.

Figure Withheld Under 10 CFR 2.390

Prepared for

U.S. Department of Energy

by PACKAGING TECHNOLOGY, INC.

TRUPACT–II PACKAGING
SAR DRAWING

A

WASTE ISOLATION PILOT PLANT WIPP

SCALE: NONE	WT. N/A
REV: W	SHEET 1 OF 11
DWG SIZE D	DWG NO. 2077–500SNP
	CADFILE: 500–01W.DWG

2 1

Figure Withheld Under 10 CFR 2.390

Prepared for

U.S. Department of Energy

by PACKAGING TECHNOLOGY, INC.

TRUPACT–II PACKAGING
SAR DRAWING

A

WASTE ISOLATION PILOT PLANT WIPP

SCALE: NOTED	WT. N/A
REV: W	SHEET 2 OF 11
DWG SIZE D	DWG NO. 2077–500SNP
	CADFILE: 500–02W.DWG

2 1

Figure Withheld Under 10 CFR 2.390

Prepared for

U.S. Department of Energy

by PACKAGING TECHNOLOGY, INC.

TRUPACT–II PACKAGING
SAR DRAWING

A

WASTE ISOLATION PILOT PLANT WIPP

SCALE: NOTED	WT. N/A
REV: W	SHEET 3 OF 11
DWG SIZE D	DWG NO. 2077–500SNP
	CADFILE: 500–03W.DWG

2 1

Figure Withheld Under 10 CFR 2.390

Prepared for

U.S. Department of Energy

by PACKAGING TECHNOLOGY, INC.

TRUPACT–II PACKAGING
SAR DRAWING

A

WASTE ISOLATION PILOT PLANT WIPP

SCALE: NOTED	WT. N/A
REV: W	SHEET 4 OF 11
DWG SIZE D	DWG NO. 2077–500SNP
	CADFILE: 500–04W.DWG

2 1

Figure Withheld Under 10 CFR 2.390

Prepared for

U.S. Department of Energy

by PACKAGING TECHNOLOGY, INC.

TRUPACT–II PACKAGING
SAR DRAWING

A

WASTE ISOLATION PILOT PLANT WIPP

SCALE: NOTED	WT. N/A
REV: W	SHEET 5 OF 11
DWG SIZE D	DWG NO. 2077–500SNP
	CADFILE: 500–05W.DWG

2 1

Figure Withheld Under 10 CFR 2.390

Prepared for

U.S. Department of Energy

by PACKAGING TECHNOLOGY, INC.

TRUPACT–II PACKAGING
SAR DRAWING

A

WASTE ISOLATION PILOT PLANT WIPP

SCALE: NOTED	WT. N/A
REV: W	SHEET 6 OF 11
DWG SIZE D	DWG NO. 2077–500SNP
	CADFILE: 500–06W.DWG

2 1

Figure Withheld Under 10 CFR 2.390

Prepared for

U.S. Department of Energy

by PACKAGING TECHNOLOGY, INC.

TRUPACT–II PACKAGING
SAR DRAWING

A

WASTE ISOLATION PILOT PLANT WIPP

SCALE: NOTED	WT. N/A
REV: W	SHEET 7 OF 11
DWG SIZE D	DWG NO. 2077–500SNP
	CADFILE: 500–07W.DWG

2 1

Figure Withheld Under 10 CFR 2.390

Prepared for

U.S. Department of Energy

by PACKAGING TECHNOLOGY, INC.

TRUPACT–II PACKAGING
SAR DRAWING

A

WASTE ISOLATION PILOT PLANT WIPP

SCALE: NOTED	WT. N/A
REV: W	SHEET 8 OF 11
DWG SIZE D	DWG NO. 2077–500SNP
	CADFILE: 500–08W.DWG

2 1

Figure Withheld Under 10 CFR 2.390

Prepared for

U.S. Department of Energy

by PACKAGING TECHNOLOGY, INC.

TRUPACT–II PACKAGING
SAR DRAWING

A

WASTE ISOLATION PILOT PLANT WIPP

SCALE: NOTED	WT. N/A
REV: W	SHEET 9 OF 11
DWG SIZE D	DWG NO. 2077–500SNP
	CADFILE: 500–09W.DWG

2 1

REVISION HISTORY

REV	DESCRIPTION	REL	DATE
V	GENERAL REVISION	BH	8/13/03
W	SEE DCR 4F.M2.01-01		

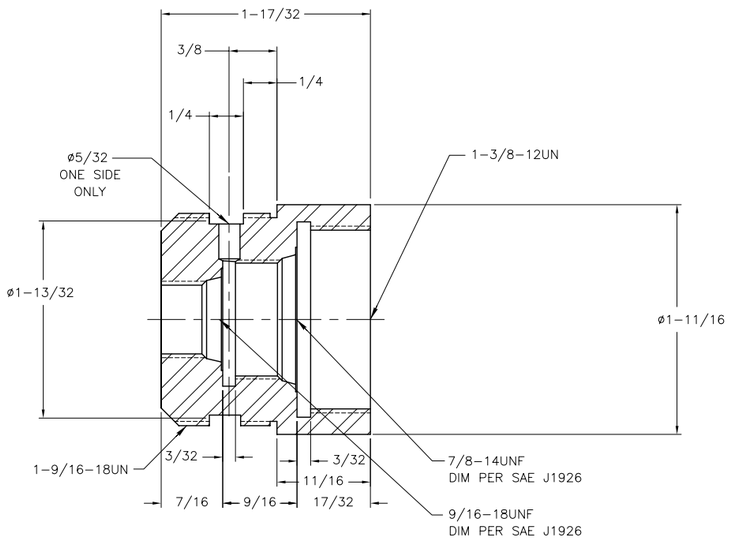

DETAIL
ICV VENT PORT INSERT 54
ASTM A479, TYPE 304 STAINLESS STEEL
(IN SECTION)

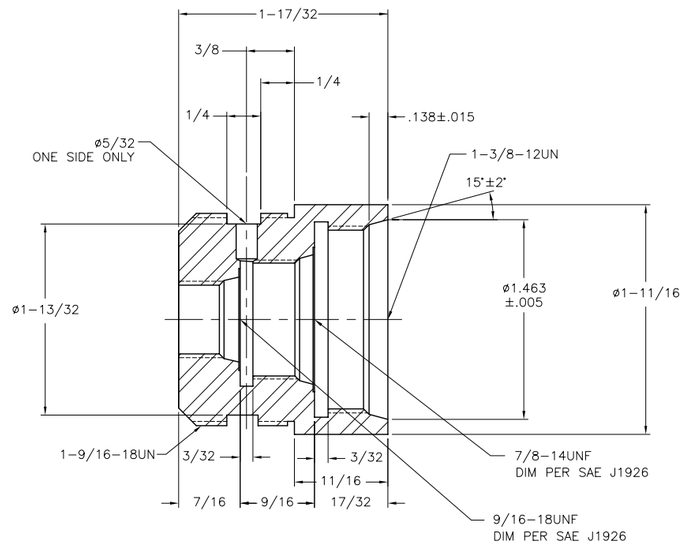

DETAIL
OPTIONAL ICV VENT PORT INSERT 54
ASTM-A479, TYPE 304 STAINLESS STEEL
(IN SECTION)

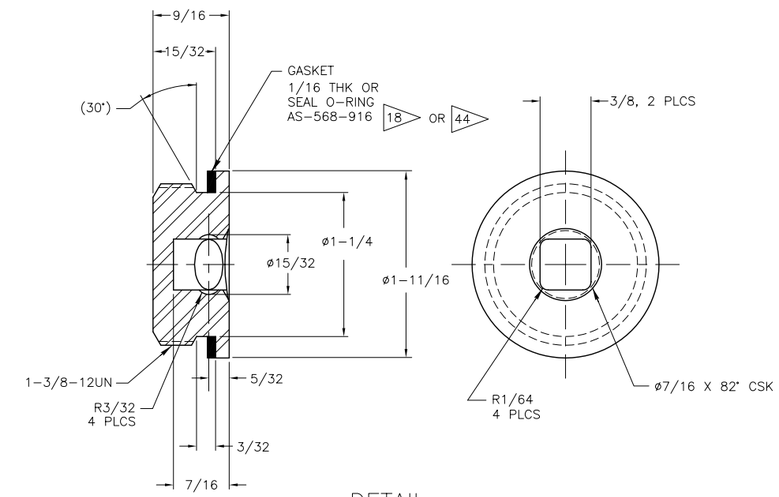

DETAIL
ICV VENT PORT COVER 54
ASTM B10, ALLOY 360 BRASS, 1/2 HARD TEMPER (OPTION: ASTM B16 ALLOY)
(IN SECTION)

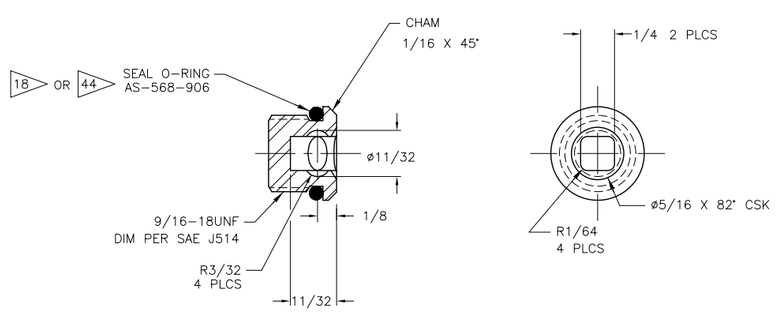

DETAIL
ICV INNER VENT PORT PLUG 54
ASTM B10, ALLOY 360 BRASS, 1/2 HARD TEMPER (OPTION: ASTM B16 ALLOY)
(IN SECTION)

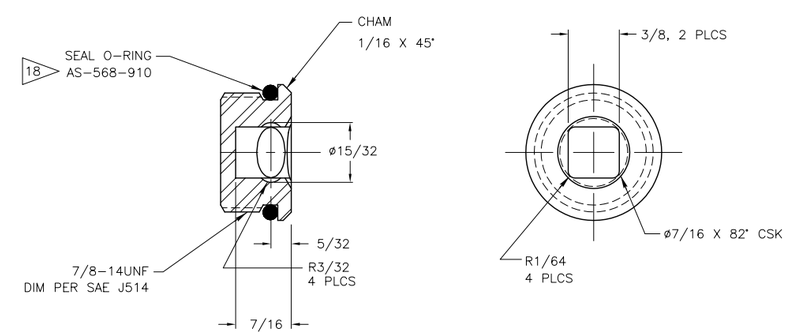

DETAIL
ICV OUTER VENT PORT PLUG 54
ASTM B10, ALLOY 360 BRASS, 1/2 HARD TEMPER (OPTION: ASTM B16 ALLOY)
(IN SECTION)

ITEM	QTY	NEXT ASSY

ORIGINAL SIGNATURES ON FILE

TOLERANCES, UNLESS OTHERWISE SPECIFIED:

LINEAL DIMENSION RANGE	DECIMAL 3 PLACE	DECIMAL 2 PLACE	DECIMAL 1 PLACE	FRACTIONAL	ANGULAR
0–6"	±0.020	±0.06	±0.2	±3/16	±2°
6"–24"	±0.030	±0.10	±0.3	±5/16	
24"–48"	±0.050	±0.20	±0.5	±1/2	
> 48"	±0.100	±0.30	±0.6	±5/8	

Prepared for
U.S. Department of Energy
by PACKAGING TECHNOLOGY, INC.

TRUPACT-II PACKAGING
SAR DRAWING

WASTE ISOLATION PILOT PLANT WIPP

SCALE: 2/1	WT. N/A
REV: W	SHEET 10 OF 11
DWG SIZE D	DWG NO. 2077-500SNP
	CADFILE: 500-10W.DWG

Figure Withheld Under 10 CFR 2.390

Prepared for

U.S. Department of Energy

by PACKAGING TECHNOLOGY, INC.

TRUPACT–II PACKAGING
SAR DRAWING

A

WASTE ISOLATION PILOT PLANT WIPP

SCALE: NOTED	WT. N/A
REV: W	SHEET 11 OF 11
DWG SIZE D	DWG NO. 2077–500SNP
	CADFILE: 500–11W.DWG

2 1

Figure Withheld Under 10 CFR 2.390

Y OPTIONALLY BE COATED
GREASE.

Prepared for

U.S. Department of Energy

by PACKAGING TECHNOLOGY, INC.

STANDARD PIPE OVERPACK
SAR DRAWING

A

WASTE ISOLATION PILOT PLANT WIPP

SCALE: 1/2	WT. N/A
REV: 6	SHEET 1 OF 3
DWG SIZE D	DWG NO. 163-001
	CADFILE: 163_0116.DWG

2 1

Figure Withheld Under 10 CFR 2.390

Prepared for

U.S. Department of Energy

by PACKAGING TECHNOLOGY, INC.

STANDARD PIPE OVERPACK
SAR DRAWING

A

WASTE ISOLATION PILOT PLANT WIPP

SCALE: 1/4	WT. N/A	
REV: 6	SHEET 2 OF 3	
DWG SIZE D	DWG NO. 163–001	
	CADFILE: 163_0126.DWG	

2 1

Figure Withheld Under 10 CFR 2.390

Prepared for

U.S. Department of Energy

by PACKAGING TECHNOLOGY, INC.

STANDARD PIPE OVERPACK
SAR DRAWING

A

WASTE ISOLATION PILOT PLANT WIPP

SCALE: 1/4	WT. N/A	
REV: 6	SHEET 3 OF 3	
DWG SIZE D	DWG NO. 163-001	
	CADFILE: 163_0136.DWG	

2 1

Figure Withheld Under 10 CFR 2.390

Prepared for

U.S. Department of Energy

by PACKAGING TECHNOLOGY, INC.

S100 PIPE OVERPACK
SAR DRAWING

A

WASTE ISOLATION PILOT PLANT WIPP

SCALE: 1/2	WT. N/A
REV: 4	SHEET 1 OF 2
DWG SIZE D	DWG NO. 163-002
	CADFILE: 163_0214.DWG

2 1

Figure Withheld Under 10 CFR 2.390

Prepared for

U.S. Department of Energy

by PACKAGING TECHNOLOGY, INC.

S100 PIPE OVERPACK
SAR DRAWING

A

WASTE ISOLATION PILOT PLANT WIPP

SCALE: 3/8	WT. N/A	
REV: 4	SHEET 2 OF 2	
DWG SIZE D	DWG NO. 163–002	
	CADFILE: 163_0224.DWG	

2 1

Figure Withheld Under 10 CFR 2.390

Prepared for

U.S. Department of Energy

by PACKAGING TECHNOLOGY, INC.

S200 PIPE OVERPACK
SAR DRAWING

A

WASTE ISOLATION PILOT PLANT WIPP

SCALE: 1/2	WT. N/A
REV: 3	SHEET 1 OF 2
DWG SIZE D	DWG NO. 163-003
	CADFILE: 163_0313.DWG

2 1

Figure Withheld Under 10 CFR 2.390

Prepared for

U.S. Department of Energy

by PACKAGING TECHNOLOGY, INC.

S200 PIPE OVERPACK
SAR DRAWING

A

WASTE ISOLATION PILOT PLANT WIPP

SCALE: 1/2	WT. N/A
REV: 3	SHEET 2 OF 2
DWG SIZE D	DWG NO. 163–003
	CADFILE: 163_0323.DWG

2 1

Figure Withheld Under 10 CFR 2.390

Prepared for

U.S. Department of Energy

by PACKAGING TECHNOLOGY, INC.

S300 PIPE OVERPACK
SAR DRAWING

A

WASTE ISOLATION PILOT PLANT WIPP

SCALE: 1/2	WT. N/A	
REV: 1	SHEET 1 OF 1	
DWG SIZE D	DWG NO. 163-004	
	CADFILE: 163_0411.DWG	

2 1

Figure Withheld Under 10 CFR 2.390

Prepared for

U.S. Department of Energy

by PACKAGING TECHNOLOGY, INC.

COMPACTED PUCK DRUM SPACERS
55–, 85–, & 100–GALLON
SAR DRAWING

A

WASTE ISOLATION PILOT PLANT WIPP

SCALE: 1/4	WT. N/A
REV: 0	SHEET 1 OF 1
DWG SIZE D	DWG NO. 163–006
	CADFILE: 163_0610.DWG

2 1

1.3.2 Glossary of Terms and Acronyms

55-Gallon Drum – A payload container yielding 55 gallons.

85-Gallon Drum – A payload container with a range of dimensions yielding 75 to 88 gallons.

85-Gallon Drum Overpacks – A payload container consisting of a 55-gallon drum overpacked within an 85-gallon drum of the appropriate dimensions.

100-Gallon Drum – A payload container yielding 100 gallons.

Aluminum Honeycomb Spacer Assembly – An assembly that is located within each end of the ICV. The aluminum honeycomb spacer assembly supplements the ICV void volume to accommodate gas generated by the payload material, and acts as an energy-absorbing barrier between the payload and the ICV torispherical heads for axial loads.

ASME – American Society of Mechanical Engineers.

ASME B&PVC – ASME Boiler and Pressure Vessel Code.

CTU – Certification Test Unit.

CH-TRAMPAC – Contact-Handled Transuranic Waste Authorized Methods for Payload Control.

CH-TRU Waste – Contact-Handled Transuranic Waste.

ICV – Inner Containment Vessel.

ICV Body – The assembly consisting of the ICV lower seal flange, the cylindrical vessel, and the ICV lower torispherical head.

ICV Inner Vent Port Plug – The brass plug and accompanying O-ring seal that provides the pressure boundary in the ICV vent port penetration.

ICV Lid – The assembly consisting of the ICV upper seal flange, the ICV locking ring, a short section of cylindrical vessel, and the ICV upper torispherical head.

ICV Lock Bolts – The three 1/2 inch, socket head cap screws used to secure the ICV locking ring in the locked position.

ICV Locking Ring – The component that connects and locks the ICV upper seal flange to the ICV lower seal flange; included as an ICV lid component.

ICV Lower Seal Flange – The ICV body's sealing interface containing two O-ring grooves, the ICV vent port access, and the ICV test port.

ICV Main O-ring Seal – The upper elastomeric O-ring seal in the ICV lower seal flange; forms the containment boundary.

ICV Main Test O-ring Seal – The lower elastomeric O-ring seal in the ICV lower seal flange; forms the test boundary for leakage rate testing.

ICV Outer Vent Port Plug – The brass plug and accompanying O-ring seal that provides the containment boundary in the ICV vent port penetration.

ICV Seal Test Port – The radial penetration between the ICV main O-ring seal and ICV main test O-ring seal to allow leakage rate testing of the ICV main O-ring seal.

ICV Seal Test Port Plug – The brass plug and accompanying O-ring seal for the ICV seal test port.

ICV Seal Test Port Insert – A welded-in, replaceable component within the ICV lower seal flange that interfaces with the ICV seal test port plug.

ICV Upper Seal Flange – The ICV lid's sealing interface containing a mating sealing surface for the ICV lower seal flange and location for a wiper O-ring seal.

ICV Vent Port – The radial penetration into the ICV cavity that is located in the ICV lower seal flange.

ICV Vent Port Cover – The outer brass cover that directly protects the ICV vent port plugs.

Inner Containment Vessel – The assembly (comprised of an ICV lid and ICV body) providing a secondary level of containment for the payload. Within each end of the inner containment vessel (ICV) is an aluminum honeycomb spacer assembly.

Locking Z-Flange – The z-shaped shell situated between the upper and lower Z-flanges that connects to the OCV locking ring; allows external operation of the OCV locking ring.

Lower Z-Flange – The z-shaped shell in the OCA body, connecting the OCA outer shell to the OCV lower seal flange.

OCA – Outer Containment Assembly.

OCA Body – The assembly consisting of the OCV lower seal flange, the OCV cylindrical and conical shells (including stiffening ring), the OCV lower torispherical head, the lower Z-flange, the OCA cylindrical shell, the OCA lower flat head, corner reinforcing angles, tie-down structures, ceramic fiber paper, and polyurethane foam.

OCA Inner Thermal Shield – The L-shaped, 16 gauge (0.060 inch thick), inner shield that holds fiberglass insulating material against the OCV locking ring thereby preventing hot gasses and flames from directly impinging on the OCV sealing region in the event of a HAC fire.

OCA Lid – The assembly consisting of the OCV upper seal flange, the OCV locking ring, a short section of cylindrical vessel, the OCV upper torispherical head, the upper and locking Z-flanges, the inner and outer thermal shields, a short section of cylindrical shell, the OCA upper torispherical head, corner reinforcing angles, ceramic fiber paper, and polyurethane foam.

OCA Lock Bolts – The six 1/2 inch, socket head cap screws used to secure the OCV locking ring in the locked position.

OCA Lower Head – The lower ASME flat head comprising the OCA outer shell.

OCA Outer Thermal Shield – The 14 gauge (0.075 inch thick) × 6⅛ inch wide outer shield surrounding the OCA lid-to-body joint that prevents hot gasses and flames from entering the joint in the event of a HAC fire.

OCA Upper Head – The upper ASME torispherical head comprising the OCA outer shell.

OCV – Outer Containment Vessel.

OCV Locking Ring – The component that connects and locks the OCV upper seal flange to the OCV lower seal flange; included as an OCA lid component.

OCV Lower Seal Flange – The OCA body's sealing interface containing two O-ring grooves.

OCV Main O-ring Seal – The upper O-ring seal in the OCV lower seal flange; forms the containment boundary.

OCV Main Test O-ring Seal – The lower O-ring seal in the OCV lower seal flange; forms the test boundary for leakage rate testing.

OCV Seal Test Port – The radial penetration between the OCV main O-ring seal and OCV main test O-ring seal to allow leakage rate testing of the OCV main O-ring seal.

OCV Seal Test Port Access Plug – The 1½ inch NPT plug located at the outside end of the OCV seal test port access tube (i.e., at the outside surface of the OCA lid outer shell).

OCV Seal Test Port Insert – A welded-in, replaceable component within the OCV lower seal flange that interfaces with the OCV seal test port plug.

OCV Seal Test Port Plug – The brass plug and accompanying O-ring seal for the OCV seal test port.

OCV Seal Test Port Thermal Plug – The foam or ceramic fiber plug located within the OCV seal test port access tube that thermally protects the OCV seal test port region.

OCV Upper Seal Flange – The OCA lid's sealing interface containing a mating sealing surface for the OCV lower seal flange.

OCV Vent Port – The radial penetration into the OCV cavity that is located in the OCV conical shell.

OCV Vent Port Access Plug – The 1½ NPT plug located at the outside end of the OCV vent port access tube (i.e., at the outside surface of the OCA body outer shell).

OCV Vent Port Access Tube – The fiberglass tube allowing external access to the OCV vent port.

OCV Vent Port Cover – The outer brass cover that directly protects the OCV vent port plug.

OCV Vent Port Plug – The brass plug and accompanying O-ring seal that provides the containment boundary in the OCV vent port penetration.

OCV Vent Port Thermal Plug – The foam or ceramic fiber plug located within the OCV vent port access tube that thermally protects the OCV vent port region.

Outer Containment Assembly – The assembly (comprised of an OCA lid and OCA body) providing a primary level of containment for the payload. The Outer Containment Assembly (OCA) completely surrounds the Inner Containment Vessel and consists of an exterior stainless steel shell, a relatively thick layer of polyurethane foam and an inner stainless steel boundary that forms the Outer Containment Vessel (OCV).

Outer Containment Vessel – The innermost boundary of the Outer Containment Assembly.

Packaging – The assembly of components necessary to ensure compliance with packaging requirements as defined in 10 CFR §71.4. Within this SAR, the packaging is denoted as the TRUPACT-II packaging.

Package – The packaging with its radioactive contents, or payload, as presented for transportation as defined in 10 CFR §71.4. Within this SAR, the package is denoted as the TRUPACT-II contact-handled transuranic waste package, or equivalently, the TRUPACT-II package.

Payload – Contact-handled transuranic (CH-TRU) waste or other authorized contents such as tritium-contaminated materials contained within approved payload containers. In this SAR, the payload includes a payload pallet for handling when drums are used. Any additional dunnage used that is external to the payload containers is also considered to be part of the payload. Payload requirements are defined by the CH-TRAMPAC.

Payload Container – Payload containers may be 55-gallon drums, pipe overpacks, 85-gallon drums (including overpacks), 100-gallon drums, standard waste boxes (SWBs), or ten drum overpacks (TDOPs).

Payload Pallet – A lightweight pallet, used for handling drum-type payload containers.

Pipe Component – A stainless steel container used for packaging specific waste forms within a 55-gallon drum. The pipe component is exclusively used as part of the pipe overpack.

Pipe Overpack – A payload container consisting of a pipe component positioned by dunnage within a 55-gallon drum with a rigid, polyethylene liner and lid. Fourteen pipe overpack assemblies will fit within the TRUPACT-II packaging.

RTV – Room Temperature Vulcanizing.

SAR – Safety Analysis Report (this document).

Standard Waste Box – A specialized payload container for use within the TRUPACT-II packaging.

SWB – Standard Waste Box.

Ten Drum Overpack – A specialized payload container for use within the TRUPACT-II packaging.

TDOP – Ten Drum Overpack.

TRUPACT-II Package – The package consisting of a TRUPACT-II packaging and the Payload.

TRUPACT-II Packaging – The packaging consisting of an outer containment assembly (OCA), an inner containment vessel (ICV), and two aluminum honeycomb spacer assemblies.

Upper Z-Flange – The z-shaped shell in the OCA lid, connecting the OCA outer shell to the OCV upper seal flange.

2.0 STRUCTURAL EVALUATION

This section presents evaluations demonstrating that the TRUPACT-II package meets all applicable structural criteria. The TRUPACT-II packaging, consisting of an outer containment assembly (OCA), with an integral outer containment vessel (OCV), and an inner containment vessel (ICV), with aluminum honeycomb spacer assemblies, is evaluated and shown to provide adequate protection for the payload. Normal conditions of transport (NCT) and hypothetical accident condition (HAC) evaluations, using analytic and empirical techniques, are performed to address 10 CFR 71[1] performance requirements. Analytic demonstration techniques comply with the methodology presented in NRC Regulatory Guides 7.6[2] and 7.8[3].

Numerous component and scale tests were successfully performed on the TRUPACT-II package during its development phase. Subsequent TRUPACT-II certification testing involved three, full-scale certification test units (CTUs). The TRUPACT-II CTUs were subjected to a series of free drop and puncture drop tests, and two of the three TRUPACT-II CTUs were subjected to fire testing. The TRUPACT-II CTUs remained leaktight[4] throughout certification testing. Details of the certification test program are provided in Appendix 2.10.3, *Certification Tests*.

2.1 Structural Design

2.1.1 Discussion

A comprehensive discussion on the TRUPACT-II package design and configuration is provided in Section 1.2, *Package Description*. Specific discussions relating to the aspects important to demonstrating the structural configuration and performance to design criteria for the TRUPACT-II package are provided in the following sections. Standard fabrication methods are utilized to fabricate the TRUPACT-II packaging.

2.1.1.1 Containment Vessel Structures

All containment vessel cylindrical and conical shell structures are fabricated in accordance with the tolerance requirements of the ASME Boiler and Pressure Vessel Code, Section III[5], Division 1, Subsection NE, Article NE-4220, as delineated on the drawings in Appendix 1.3.1, *Packaging General Arrangement Drawings*. All containment vessel shell-to-shell joints and transitions in thickness, such as from the 1/4 inch thick OCV lower head to the 3/16 inch thick

[1] Title 10, Code of Federal Regulations, Part 71 (10 CFR 71), *Packaging and Transportation of Radioactive Material*, 01-01-07 Edition.

[2] U. S. Nuclear Regulatory Commission, Regulatory Guide 7.6, *Design Criteria for the Structural Analysis of Shipping Cask Containment Vessels*, Revision 1, March 1978.

[3] U. S. Nuclear Regulatory Commission, Regulatory Guide 7.8, *Load Combinations for the Structural Analysis of Shipping Casks for Radioactive Material*, Revision 1, March 1989.

[4] Leaktight is defined as leakage of 1×10^{-7} standard cubic centimeters per second (scc/s), air, or less per ANSI N14.5-1997, *American National Standard for Radioactive Materials – Leakage Tests on Packages for Shipment,* American National Standards Institute, Inc. (ANSI).

[5] American Society of Mechanical Engineers (ASME) Boiler and Pressure Vessel Code, Section III, *Rules for Construction of Nuclear Power Plant Components*, 1986 Edition.

OCV shell, are fabricated in accordance with the ASME Boiler and Pressure Vessel Code, Section III, Division 1, Subsection NB, Article NB-4230, as delineated on the drawings in Appendix 1.3.1, *Packaging General Arrangement Drawings*.

All containment vessel heads are flanged torispherical heads, fabricated in accordance with the ASME Boiler and Pressure Vessel Code, Section VIII, Division 1[6], as delineated on the drawings in Appendix 1.3.1, *Packaging General Arrangement Drawings*.

All seal flange material is ultrasonically or radiographically test inspected in accordance with the ASME Boiler and Pressure Vessel Code, Section III, Division 1, Subsection NB, Article NB-2500 and Section V[7], Article 5 (ultrasonic) or Article 2 (radiograph), as delineated on the drawings in Appendix 1.3.1, *Packaging General Arrangement Drawings*.

Circumferential and longitudinal welds for the containment vessel shells, seal flanges, and locking rings are full penetration welds, subjected to visual and liquid penetrant examinations, and radiographically test inspected, as delineated on the drawings in Appendix 1.3.1, *Packaging General Arrangement Drawings*. Visual weld examinations are performed in accordance with AWS D1.1[8]. Liquid penetrant examinations are performed on the final pass in accordance with the ASME Boiler and Pressure Vessel Code, Section III, Division 1, Subsection NB, Article NB-5000 and Section V, Article 6. Radiograph test inspections are performed in accordance with the ASME Boiler and Pressure Vessel Code, Section III, Division 1, Subsection NB, Article NB-2500 and Section V, Article 2.

For both the OCV and ICV vent port penetrations, and the ICV lifting sockets, liquid penetrant examinations are performed on the final pass for single pass welds and on the root and final passes for multipass welds in accordance with the ASME Boiler and Pressure Vessel Code, Section III, Division 1, Subsection NB, Article NB-5000 and Section V, Article 6, as delineated on the drawings in Appendix 1.3.1, *Packaging General Arrangement Drawings*.

The maximum weld reinforcement for containment vessel welds shall be 3/32 inch in accordance with the ASME Boiler and Pressure Vessel Code, Section III, Division 1, Subsection NB, Article NB-4426, Paragraph NB-4426.1, as delineated on the drawings in Appendix 1.3.1, *Packaging General Arrangement Drawings*.

2.1.1.2 Non-Containment Vessel Structures

All non-containment vessel shell-to-shell joints and transitions in thickness, such as from the 3/8-to-1/4 inch thick OCA outer shell transition, are fabricated in accordance with the ASME Boiler and Pressure Vessel Code, Section III, Division 1, Subsection NF, Article NF-4230, as delineated on the drawings in Appendix 1.3.1, *Packaging General Arrangement Drawings*.

The OCA outer shell has a top, flanged torispherical head and bottom, flanged flat head that are fabricated in accordance with the ASME Boiler and Pressure Vessel Code, Section VIII, Division 1, as delineated on the drawings in Appendix 1.3.1, Packaging General Arrangement Drawings.

---

[6] American Society of Mechanical Engineers (ASME) Boiler and Pressure Vessel Code, Section VIII, Division 1, *Rules for Construction of Pressure Vessels*, 1986 Edition.

[7] American Society of Mechanical Engineers (ASME) Boiler and Pressure Vessel Code, Section V, *Nondestructive Examination*, 1986 Edition.

[8] ANSI/AWS D1.1, *Structural Welding Code–-Steel*, American Welding Society (AWS).

Circumferential and longitudinal welds for the non-containment vessel shells are full penetration welds, subjected to visual and liquid penetrant examinations, as delineated on the drawings in Appendix 1.3.1, *Packaging General Arrangement Drawings*. Visual weld examinations are performed in accordance with AWS D1.1. Liquid penetrant examinations are performed on the final pass in accordance with the ASME Boiler and Pressure Vessel Code, Section III, Division 1, Subsection NF, Article NF-5000.

The maximum weld reinforcement for non-containment vessel welds shall be 3/32 inch in accordance with the ASME Boiler and Pressure Vessel Code, Section III, Division 1, Subsection NF, Article NF-4400, as delineated on the drawings in Appendix 1.3.1, *Packaging General Arrangement Drawings*.

2.1.2 Design Criteria

Proof of performance for the TRUPACT-II package is achieved by a combination of analytic and empirical evaluations. The acceptance criteria for analytic assessments are in accordance with Regulatory Guide 7.6 and Section III of the ASME Boiler and Pressure Vessel Code. The acceptance criterion for empirical assessments is a demonstration that both containment boundaries remain leaktight throughout NCT and HAC certification testing. Additionally, package deformations obtained from certification testing must be such that deformed geometry assumptions used in subsequent thermal, shielding, and criticality evaluations are validated.

The remainder of this section presents the detailed acceptance criteria used for all analytic structural assessments of the TRUPACT-II package.

2.1.2.1 Analytic Design Criteria (Allowable Stresses)

This section defines the stress allowables for primary membrane, primary bending, secondary, shear, peak, and buckling stresses for containment and non-containment structures. These stress allowables are used for all analytic assessments of TRUPACT-II package structural performance. Regulatory Guide 7.6 is used in conjunction with Regulatory Guide 7.8 to evaluate the package integrity. Material yield strengths used in the analytic acceptance criteria, S_y, ultimate strengths, S_u, and design stress intensity values, S_m, are presented in Table 2.3-1 of Section 2.3, *Mechanical Properties of Materials*.

2.1.2.1.1 Containment Structures

A summary of allowable stresses used for containment structures is presented in Table 2.1-1. These data are consistent with Regulatory Guide 7.6, and the ASME Boiler and Pressure Vessel Code, Section III, Subsection NB-3000 and Appendix F.

2.1.2.1.2 Non-Containment Structures

A summary of allowable stresses used for non-containment structures is presented in Table 2.1-2.

For evaluation of lifting devices, the allowable stresses are limited to one-third of the material yield strength, consistent with the requirements of 10 CFR §71.45(a). For evaluation of tie-down devices, the allowable stresses are limited to the material yield strength, consistent with the requirements of 10 CFR §71.45(b).

For evaluations involving polyurethane foam, primary, load controlled compressive stresses are limited to two-thirds of the parallel-to-rise or perpendicular-to-rise compressive strength (as applicable) at 10% strain. Use of a two-thirds factor on compressive strength ensures elastic behavior of the polyurethane foam.

2.1.2.2 Miscellaneous Structural Failure Modes

2.1.2.2.1 Brittle Fracture

By avoiding the use of ferritic steels in the TRUPACT-II packaging, brittle fracture concerns are precluded. Specifically, most primary structural components are fabricated of Type 304 austenitic stainless steel. Since this material does not undergo a ductile-to-brittle transition in the temperature range of interest (down to -40 ºF), it is safe from brittle fracture.

The lock bolts used to secure the ICV and OCV locking rings in the locked position are stainless steel, socket head cap screws ensuring that brittle fracture is not of concern. Other fasteners used in the TRUPACT-II packaging assembly, such as the 36, 1/4 inch screws attaching the locking Z-flange to the OCV locking ring, provide redundancy and are made from stainless steel, again eliminating brittle fracture concerns.

2.1.2.2.2 Fatigue Assessment

2.1.2.2.2.1 Normal Operating Cycles

Normal operating cycles do not present a fatigue concern for the various TRUPACT-II packaging components. Most TRUPACT-II packaging components exhibit little-to-no stress concentrations, and by satisfying the allowable limit for range of primary plus secondary stress intensity for NCT ($3.0S_m$), the allowable fatigue stress limit for the expected number of operating cycles is satisfied. For TRUPACT-II packaging components that do exhibit stress concentrations, stresses are low enough that allowable fatigue stress limits are again satisfied.

The maximum number of operating cycles reasonably expected for the TRUPACT-II package is 3,640, and is based on two round trips per week for 35 years. Conservatively, 5,000 cycles (or in excess of 1 cycle every 3 days) is used in the following calculations. A cycle is defined as the process of the internal pressure within the OCV and ICV increasing gradually from zero psig at the time of loading, to 50 psig (the maximum normal operating pressure, MNOP, per Section 3.4.4, *Maximum Internal Pressure*) during transport and then returning to 0 psig when the containment vessel is vented prior to unloading the payload. This scenario is conservative because most shipments will never generate pressure to the magnitude of the MNOP, and the system could never achieve MNOP in less than the assumed transportation cycle of 3 days.

From Figure I-9.2.1 and Table I-9.1 of the ASME Boiler and Pressure Vessel Code[9], the fatigue allowable alternating stress intensity amplitude, S_a, for 5,000 cycles is 76,000 psi. This value, when multiplied by the ratio of elastic hot NCT modulus at 160 ºF (the package wall temperature from Section 2.6.1, *Heat*) to a modulus at 70 ºF, $27.8(10)^6/28.3(10)^6$, results in a fatigue

[9]American Society of Mechanical Engineers (ASME) Boiler and Pressure Vessel Code, Section III, *Rules for Construction of Nuclear Power Plant Components*, Appendix I, *Design Stress Intensity Values, Allowable Stresses, Material Properties, and Design Fatigue Curves*, 1986 Edition.

allowable alternating stress intensity amplitude at 160 ºF of 74,657 psi. The non-fatigue allowable stress intensity range, from the ASME Boiler and Pressure Vessel Code, Section III, Division 1, Subsection NB-3222.2, is 60,000 psi ($3.0S_m$, where S_m is 20,000 psi from Table 2.3-1 in Section 2.3, *Mechanical Properties of Materials*, at 160 ºF). The alternating stress intensity is one-half of this range, or 30,000 psi. Thus, in the absence of stress concentrations, the fatigue allowable alternating stress intensity will not govern the TRUPACT-II packaging design.

Regions of stress concentrations for the package occur in the ICV and OCV seal flanges and locking rings. The maximum range of primary plus secondary stress intensity occurs between the case of maximum internal pressure under NCT hot conditions (see Section 2.6.1.3, *Stress Calculations*) and the vacuum case. For the seal flanges and locking rings, the maximum primary plus secondary stress intensity of 30,810 + 2,688 = 33,498 psi occurs in the upper seal flange (see Table 2.6-1 and Table 2.6-4 for OCA Load Cases 1 and 4, respectively). The stress range is therefore 33,498 psi.

In accordance with Paragraph C.3 of Regulatory Guide 7.6, a stress concentration factor of four will conservatively be applied to the value of maximum stress intensity from above. The resultant range of peak stress intensity, correcting the modulus of elasticity for temperature, becomes:

$$S_{range} = (33{,}498)(4)\left(\frac{28.3(10)^6}{27.8(10)^6}\right) = 136{,}400 \text{ psi}$$

where the modulus of elasticity at 70 ºF is $28.3(10)^6$ psi, and the modulus of elasticity at 160 ºF is $27.8(10)^6$ psi, both from Table 2.3-1 in Section 2.3, *Mechanical Properties of Materials*. The alternating stress intensity is one-half of this range, or:

$$S_{alt} = \left(\frac{1}{2}\right)136{,}400 = 68{,}200 \text{ psi}$$

From Figure I-9.2.1 and Table I-9.1 of the ASME Boiler and Pressure Vessel Code, the allowable number of cycles for an alternating stress intensity amplitude of 68,200 psi is 7,740, or 55% more than the 5,000 cycles conservatively considered herein.

2.1.2.2.2.2 Normal Vibration Over the Road

Fatigue associated with normal vibration over the road is addressed in Section 2.6.5, *Vibration*.

2.1.2.2.2.3 Extreme Total Stress Intensity Range

Per paragraph C.7 of Regulatory Guide 7.6:

> The extreme total stress intensity range (including stress concentrations) between the initial state, the fabrication state, the normal operating conditions, and the accident conditions should be less than twice the adjusted value (adjusted to account for modulus of elasticity at the highest temperature) of S_a at 10 cycles given by the appropriate design fatigue curves.

Since the response of the TRUPACT-II package to accident conditions is typically evaluated empirically rather than analytically, the extreme total stress intensity range has not been quantified. However, full scale certification test units (see Appendix 2.10.3, *Certification Tests*) were tested at relatively low ambient temperatures during free drop and puncture testing, as well as exposure to

fully engulfing pool fire events. The CTUs were also fabricated in accordance with the drawings in Appendix 1.3.1, *Packaging General Arrangement Drawings*, thus incurring prototypic fabrication induced stresses, increased internal pressure equal to 150% of MNOP during fabrication pressure testing, and reduced internal pressure (i.e., a full vacuum during leak testing) conditions as part of initial acceptance. Exposure to these extreme conditions while demonstrating two levels of leaktight containment resulting from certification testing satisfy the intent of the previously defined extreme total stress intensity range requirement.

2.1.2.2.3 Buckling Assessment

Buckling, per Regulatory Guide 7.6, is an unacceptable failure mode for the containment vessels. The intent of this provision is to preclude large deformations that would compromise the validity of linear analysis assumptions and quasi-linear stress allowables, as given in Paragraph C.6 of Regulatory Guide 7.6.

Buckling prevention criteria are applicable to both the OCV and ICV containment boundaries within the TRUPACT-II packaging. Both containment vessel shells incorporate cylindrical midsections with torispherical heads at each end. The different geometric regions are considered separately to demonstrate that buckling will not occur for the two containment shells. The methodology of ASME Boiler and Pressure Vessel Code Case N-284[10] is applied for the cylindrical regions of the containment vessels (buckling analysis details are provided in Section 2.7.6, *Immersion – All Packages*). The methodology of the ASME Boiler and Pressure Vessel Code, Section III, Subsection NE, is applied for the torispherical heads.

Consistent with Regulatory Guide 7.6 philosophy, factors of safety corresponding to ASME Boiler and Pressure Vessel Code, Level A and Level D service conditions are employed for NCT and HAC loadings, respectively, with factors of safety of 2.00 and 1.34, respectively.

It is also noted that 30 foot drop tests performed on full scale models with the package in various orientations produced no evidence of buckling of any of the containment boundary shells (see Appendix 2.10.3, *Certification Tests*). Certification testing does not provide a specific determination of the margin of safety against buckling, but is considered as evidence that buckling will not occur.

[10] American Society of Mechanical Engineers (ASME) Boiler and Pressure Vessel Code, Section III, *Rules for Construction of Nuclear Power Plant Components*, Division 1, Class MC, Code Case N-284, *Metal Containment Shell Buckling Design Methods*, August 25, 1980 approval date.

Table 2.1-1 – Containment Structure Allowable Stress Limits

Stress Category	NCT	HAC
General Primary Membrane Stress Intensity	S_m	Lesser of: $2.4S_m$, $0.7S_u$
Local Primary Membrane Stress Intensity	$1.5S_m$	Lesser of: $3.6S_m$, S_u
Primary Membrane + Bending Stress Intensity	$1.5S_m$	Lesser of: $3.6S_m$, S_u
Range of Primary + Secondary Stress Intensity	$3.0S_m$	N/A
Pure Shear Stress	$0.6S_m$	$0.42S_u$
Peak	Per Section 2.1.2.2.2, *Fatigue Assessment*	
Buckling	Per Section 2.1.2.2.3, *Buckling Assessment*	

Table 2.1-2 – Non-Containment Structure Allowable Stress Limits

Stress Category	NCT	HAC
General Primary Membrane Stress Intensity	Greater of: S_m, S_y	$0.7S_u$
Local Primary Membrane Stress Intensity	Greater of: $1.5S_m$, S_y	S_u
Primary Membrane + Bending Stress Intensity	Greater of: $1.5S_m$, S_y	S_u
Range of Primary + Secondary Stress Intensity	Greater of: $3.0S_m$, S_y	N/A
Pure Shear Stress	Greater of: $0.6S_m$, $0.6S_y$	$0.42S_u$
Peak	Per Section 2.1.2.2.2, *Fatigue Assessment*	
Buckling	Per Section 2.1.2.2.3, *Buckling Assessment*	

This page intentionally left blank.

2.2 Weights and Centers of Gravity

The maximum gross weight of a TRUPACT-II package, including a maximum payload weight of 7,265 pounds, is 19,250 pounds. The maximum vertical center of gravity (CG) is located 59.0 inches above the bottom surface of the package for a fully loaded package. A conservative value of 60 inches is used in the lifting and tie-down calculations presented in Section 2.5, *Lifting and Tie-down Standards for All Packages*. These results are based on an assumption of a payload configuration consisting of uniformly loaded drums, standard waste boxes (SWBs), or a ten-drum overpack (TDOP). All other payload configurations result in a lower, package gross weight and CG than the uniformly loaded drum, SWB, or TDOP configurations. With reference to Figure 2.2-1, a detailed breakdown of the TRUPACT-II package component weights and CG is summarized in Table 2.2-1.

2.2.1 Effect of a Radial Payload Imbalance

A radial offset of the CG occurs when the individual payload containers do not have the same weight. The maximum offset of the radial CG is calculated in the following paragraphs.

Fourteen 55-Gallon Drum Payload Configuration:

The worst case CG offset occurs for an arrangement of four minimum weight (empty) 55-gallon drums, each having a weight of 60 pounds, together with three maximum weight (fully loaded) 55-gallon drums, each having a weight of 1,000 pounds, located in adjacent outside positions, as illustrated in Figure 2.2-2. A 55-gallon drum has a nominal outer diameter of 24 inches. For this case, the worst case radial location of the payload CG is:

$$\bar{r} = \frac{(24.0)(1{,}000) + 2(12.0)(1{,}000) + (0.0)(60) - 2(12.0)(60) - (24.0)(60)}{3(1{,}000) + 4(60)} = 13.93 \text{ inches}$$

The pipe overpack payload configurations, since they are enclosed and centered by dunnage within a 55-gallon drum, are enveloped by the foregoing considerations. For an empty package weight of 11,985 pounds, and a payload pallet weight of 350 pounds (see Table 2.2-1), the worst case radial offset of the CG of the entire TRUPACT-II package is:

$$\bar{R} = \frac{(13.93)(2)[3(1{,}000) + 4(60)]}{11{,}985 + 350 + 2[3(1{,}000) + 4(60)]} = 4.80 \text{ inches}$$

This radial offset equates to only 5.1% of the TRUPACT-II package's outer diameter of 94⅜ inches. The effect of this relatively small radial offset may be neglected.

Eight 85-Gallon Drum Payload Configuration:

The term "85-gallon drum" refers to drum overpacks of 75 to 88 gallons, as discussed in Section 1.1, *Introduction*. The worst case CG offset occurs for an arrangement of two minimum weight (empty), tall 85-gallon drums, each having a weight of approximately 81 pounds, together with two maximum weight (fully loaded), tall 85-gallon drums, each having a weight of 1,000 pounds, located adjacent, as illustrated in Figure 2.2-3. A tall 85-gallon drum has a nominal outer diameter of 28⅝ inches. For this case, the worst case radial location of the payload CG is:

$$\bar{r} = \frac{2(14.31)(1{,}000) - 2(14.31)(81)}{2(1{,}000) + 2(81)} = 12.17 \text{ inches}$$

For an empty package weight of 11,985 pounds, and a payload pallet weight of 350 pounds (see Table 2.2-1), the worst case radial offset of the CG of the entire TRUPACT-II package is:

$$\bar{R} = \frac{(12.17)(2)[2(1{,}000) + 2(81)]}{11{,}985 + 350 + 2[2(1{,}000) + 2(81)]} = 3.16 \text{ inches}$$

This radial offset equates to only 3.3% of the TRUPACT-II package's outer diameter of 94⅜ inches. The effect of this relatively small radial offset may be neglected

Six 100-Gallon Drum Payload Configuration:

The worst case CG offset occurs for an arrangement of two minimum weight (empty), 100-gallon drums, each having a weight of 95 pounds, together with one maximum weight (fully loaded), 100-gallon drum of 1,000 pounds, as illustrated in Figure 2.2-4. A 100-gallon drum has a nominal outer diameter of 32 inches. For this case, the worst case radial location of the payload CG is:

$$\bar{r} = \frac{(18.48)(1{,}000) - 2(9.24)(95)}{1{,}000 + 2(95)} = 14.05 \text{ inches}$$

For an empty package weight of 11,985 pounds, and a payload pallet weight of 350 pounds (see Table 2.2-1), the worst case radial offset of the CG of the entire TRUPACT-II package is:

$$\bar{R} = \frac{(14.05)(2)[1{,}000 + 2(95)]}{11{,}985 + 350 + 2[1{,}000 + 2(95)]} = 2.27 \text{ inches}$$

This radial offset equates to only 2.4% of the TRUPACT-II package's outer diameter of 94⅜ inches. The effect of this relatively small radial offset may be neglected.

Two Standard Waste Box (SWB) Payload Configuration:

For the maximum payload weight of 7,265 pounds, the maximum weight of a single loaded SWB is 7,265/2 = 3,633 pounds, where the weight of an empty SWB is 640 pounds. Therefore, the maximum weight of the contents is 3,633 - 640 = 2,993 pounds. The CG of the contents is conservatively located at a distance of 17.75 inches from the geometric center (i.e., one-quarter the SWB length), as illustrated in Figure 2.2-5. For this case, the worst case radial location of the payload CG is:

$$\bar{r} = \frac{(17.75)(2{,}993)}{3{,}633} = 14.6 \text{ inches}$$

For an empty package weight of 11,985 pounds (see Table 2.2-1), the worst case radial offset of the CG of the entire TRUPACT-II package is:

$$\bar{R} = \frac{(14.6)(7{,}265)}{11{,}985 + 7{,}265} = 5.51 \text{ inches}$$

This radial offset equates to only 5.8% of the TRUPACT-II package's outer diameter of 94⅜ inches. As before, the effect of this relatively small radial offset may be neglected.

One Ten-Drum Overpack (TDOP) Payload Configuration:

For the maximum payload weight of 6,700 pounds, the weight of an empty TDOP is 1,700 pounds. Therefore, the maximum weight of the contents is 6,700 – 1,700 = 5,000 pounds. Conservatively assume the CG of the contents is located at a distance of 18 inches from the geometric center (i.e., one-quarter the TDOP diameter), as illustrated in Figure 2.2-6. For this case, the worst-case radial location of the payload CG is:

$$\bar{r} = \frac{(18)(5{,}000)}{6{,}700} = 13.4 \text{ inches}$$

For an empty package weight of 11,985 pounds (see Table 2.2-1), the worst case radial offset of the CG of the entire TRUPACT-II package is:

$$\bar{R} = \frac{(13.4)(6{,}700)}{11{,}985 + 6{,}700} = 4.80 \text{ inches}$$

This radial offset equates to only 5.1% of the TRUPACT-II package's outer diameter of 94⅜ inches. As before, the effect of this relatively small radial offset may be neglected.

2.2.2 Effect of an Axial Payload Imbalance

The maximum height of the package CG is associated with a uniformly loaded payload, where the CG of the payload containers is located at their mid-height. Due to a payload of non-uniform density or possible settling of the payload contents, the CG height of the payload containers may decrease somewhat. The fourteen 55-gallon drum payload configuration, since it is the heaviest payload, will result in greatest potential shift in axial CG. The greatest shift in location of the CG of an individual drum is bounded by one-quarter of the drum height, i.e., a shift from the drum mid-height to the quarter height. Thus, for a total 55-gallon drum height of 35 inches, the drum centerline is 35/2 = 17.50 inches below the nominal centerline for all 14 drums and the axial shift is 35/4 = 8.75 inches downward from the drum centerline. Since the empty weight of a 55-gallon drum is 60 pounds, the maximum contents weight for one drum is 1,000 - 60 = 940 pounds. The greatest downward shift in CG location of the TRUPACT-II packaging, assuming all seven drums in the upper layer are empty and the CG location of all seven maximally loaded drums in the lower layer is at one quarter of the drum height instead of at mid-height, is:

$$\bar{H} = \frac{7(17.50 + 8.75)(940)}{19{,}250} = 8.97 \text{ inches}$$

The axial offset amounts to only 7.4% of the total TRUPACT-II package height of 121½ inches. The effect of this relatively small axial offset may be neglected. As an example, in the case of a hypothetical accident condition (HAC) puncture event where the puncture bar axis passes through the CG of the TRUPACT-II package, the variation in CG location of 9 inches is the same order of magnitude as the puncture bar diameter resulting in a variation of the puncture bar orientation of $TAN^{-1}[59.00/½(94.375)] - TAN^{-1}[(59.00 – 8.97)/½(94.375)] = 4.7°$. In addition,

vertical reduction of the CG would have no effect on lifting forces, and would serve to reduce tie-down forces. Therefore, the lifting and tie-down calculations, and the HAC free drop and puncture tests, are performed using a value that bounds the maximum CG height presented in Table 2.2-1, and the downward axial offset is conservatively neglected.

2.2.3 Significance of Package Center of Gravity Shifts

The 5.51 inch radial shift and 8.97 inch axial (downward) shift of the package CG associated with worst case non-uniform payload weight distributions are of little consequence for the TRUPACT-II package. The only load cases affected by such shifts are lifting, tie-down, vibration, free drop, and puncture. Each of these cases is discussed below.

2.2.3.1 Lifting

A radial package CG shift will affect the lifting load by increasing the compressive stress in the polyurethane foam directly above the forklift pockets. Per Section 2.5.1, *Lifting Devices*, the compressive stress in the polyurethane foam was determined to be 60 psi with the overall package CG centered between the forklift pockets. With a 49½ inch spacing between the forklift pocket centerlines, a 5.51 inch radial shift in the package CG increases the maximum stress in the polyurethane foam by a factor of:

$$f = \frac{49.5/2 + 5.51}{49.5/2} = 1.22$$

Using the polyurethane foam allowable crush strength of 100 psi per Section 2.5.1, *Lifting Devices*, the design margin becomes:

$$\frac{100}{1.22(60)} - 1 = +0.37$$

An axial package CG shift will have no effect on the lifting load cases since all lifting loads are applied along the axis of the package.

2.2.3.2 Tie-down

A radial package CG shift results in a slight increase in the vertical loads acting on the tie-down hardware since the four (4) tie-down locations no longer uniformly react the applied, vertical 2*g* tie-down load. With a 58.93 inch lateral distance between tie-down lugs, a 5.51 inch radial CG shift results in a maximum tie-down reaction load due to the vertical 2*g* tie-down load of:

$$\mathrm{F} = \left(\frac{1}{2}\right)\left[\frac{2(19{,}250)(58.93/2 + 5.51)}{58.93}\right] = 11{,}425\ \mathrm{lb}$$

or 1,800 pounds greater than the 9,625 pounds previously calculated in Section 2.5.2.1, *Tie-down Forces*. When added to the combined lateral and longitudinal tie-down load of 84,906 pounds from Section 2.5.2.1, *Tie-down Forces*, the maximum vertical tensile force on any single tie-down lug is 84,906 + 11,425 = 96,331 pounds, again 1,800 pounds greater than the 94,531 pounds previously calculated. This 1.9% increase in the tie-down force reduces the minimum design margin from +0.31 to +0.29.

An axial package CG shift is always downward, thus reducing the overturning moment resulting from the lateral and longitudinal tie-down loads. A reduction in overturning moment has the beneficial effect of directly reducing the vertical loads acting on the tie-down hardware.

2.2.3.3 Vibration

The vibration evaluation per Section 2.6.5, *Vibration*, utilized results available from the tie-down analysis to arrive at peak vibratory stress magnitudes. Repeating the Section 2.6.5, *Vibration*, calculations with the 11,425 pound vertical load determined in Section 2.2.3.2, *Tie-down*, in place of the previously used 9,625 pound load results in a maximum alternating stress intensity of 745 psi (as compared to the previous value of 628 psi per Section 2.6.5.2, *Calculation of Alternating Stresses*). Thus, the maximum alternating stress becomes 12,662 psi (as compared to the previous value of 11,726 psi per Section 2.6.5.2, *Calculation of Alternating Stresses*). With an allowable of 13,360 psi per Section 2.6.5.3, *Stress Limits and Results*, and the margin of safety becomes:

$$MS = \frac{S_a}{S_{alt}} - 1 = \frac{13{,}360}{12{,}662} - 1 = +0.06$$

2.2.3.4 Free Drop and Puncture

The free drop and puncture load conditions have been addressed by an extensive test program that utilized four full-scale TRUPACT-II package prototypes. For all test units, the payload weight was uniformly distributed within the payload cavity to achieve the highest possible CG for the loaded package. The high CG was selected for testing so that maximum damage to the closure/seal regions would occur.

Table 2.2-1 – TRUPACT-II Weight and Center of Gravity

Item	Weight, pounds		Height to CG, inches①	
	Component	Assembly	Component	Assembly
Outer Containment Assembly (OCA)		9,365		58.8
• Lid	3,600		97.2	
• Body	5,765		34.8	
Inner Containment Vessel (ICV)		2,620		64.7
• Lid	795		96.4	
• Body	1,625		49.8	
• Aluminum Honeycomb Spacers	200		60.4	
Total Empty Package		11,985		60.1
Payload and Payload Components		7,265		57.3
• Payload (14 55-Gallon Drums)	6,915		59.1	
• Payload Pallet	350		22.5	
Total Loaded Package (Maximum)		19,250		59.0

Notes:

① The reference datum is the bottom of the TRUPACT-II package.

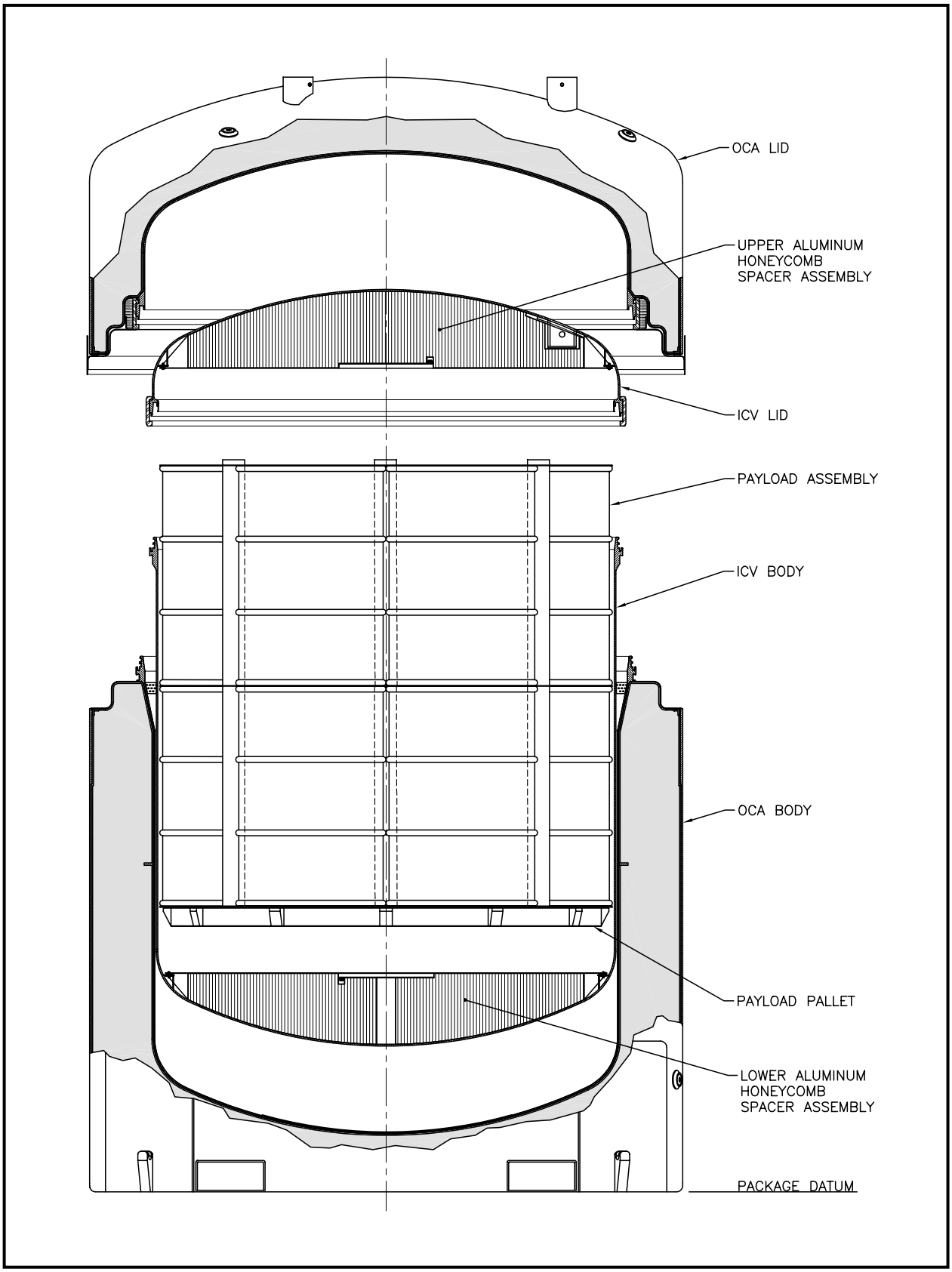

Figure 2.2-1 – TRUPACT-II Package Components

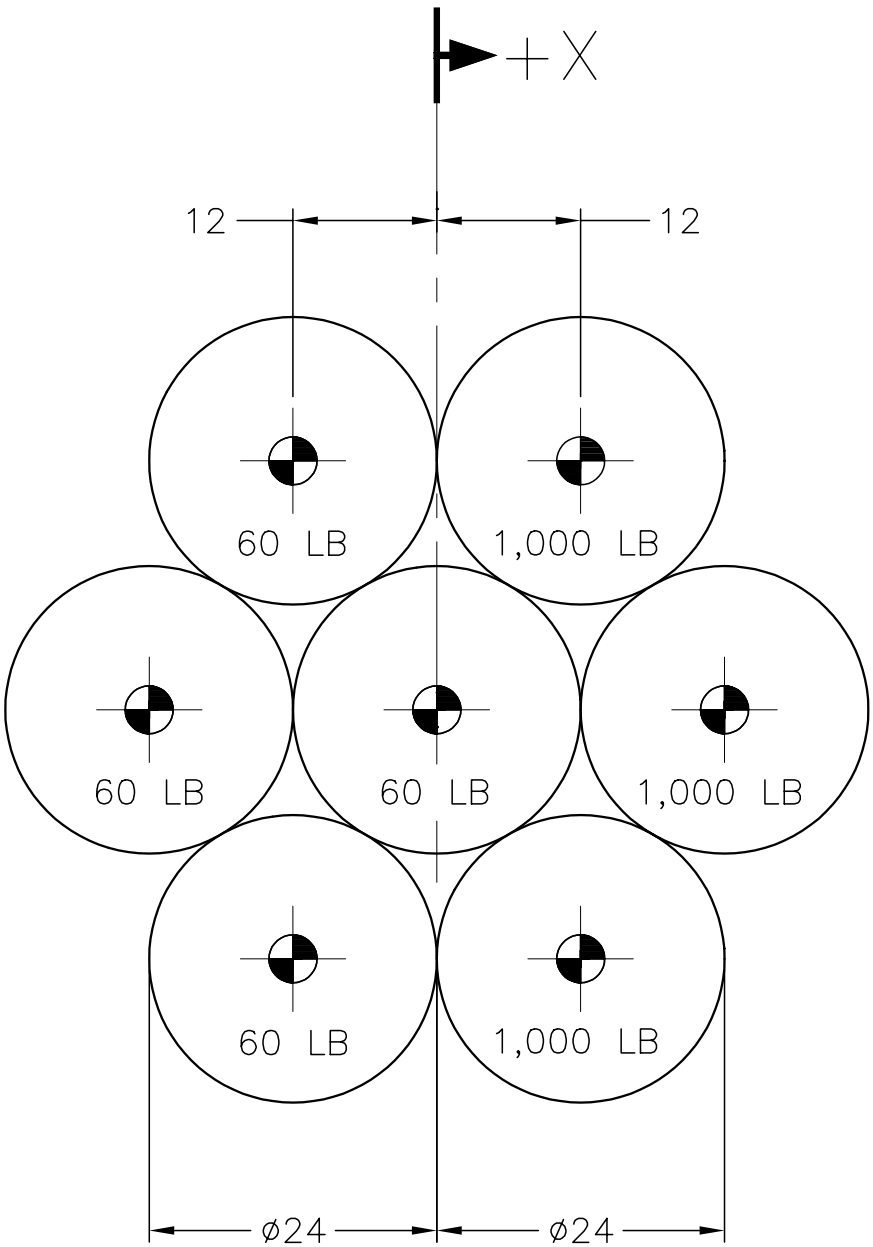

Figure 2.2-2 – Radial CG Shift for a 14 55-Gallon Drum Payload

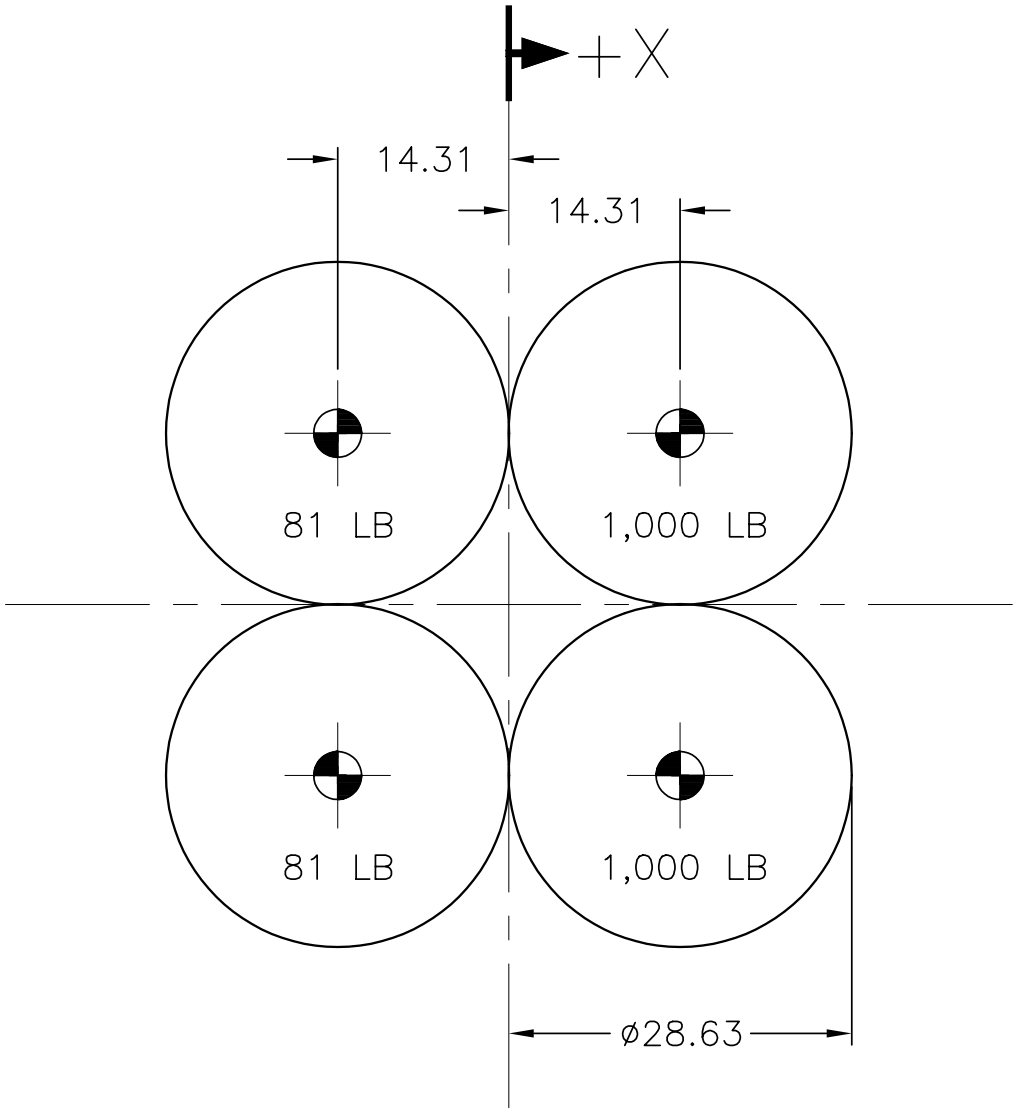

Figure 2.2-3 – Radial Shift of CG for Eight 85-Gallon Drum Payload

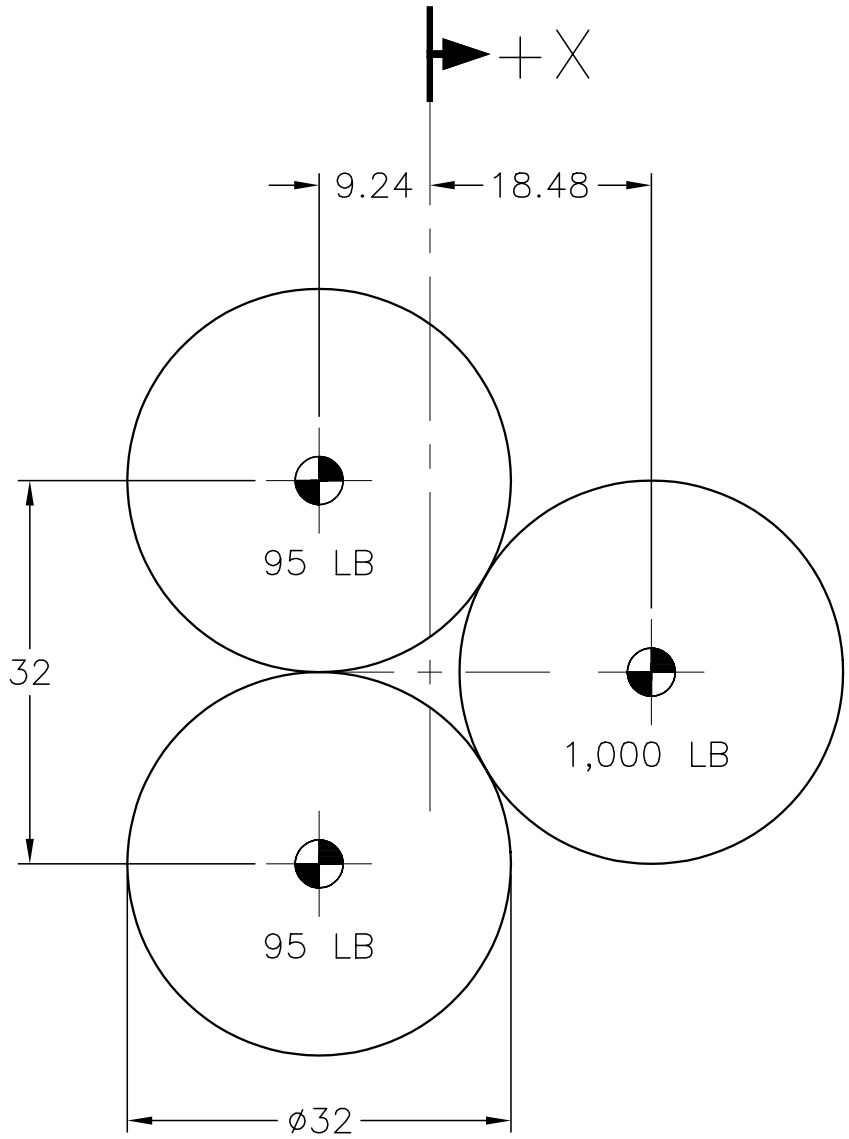

Figure 2.2-4 – Radial Shift of CG for Six 100-Gallon Drum Payload

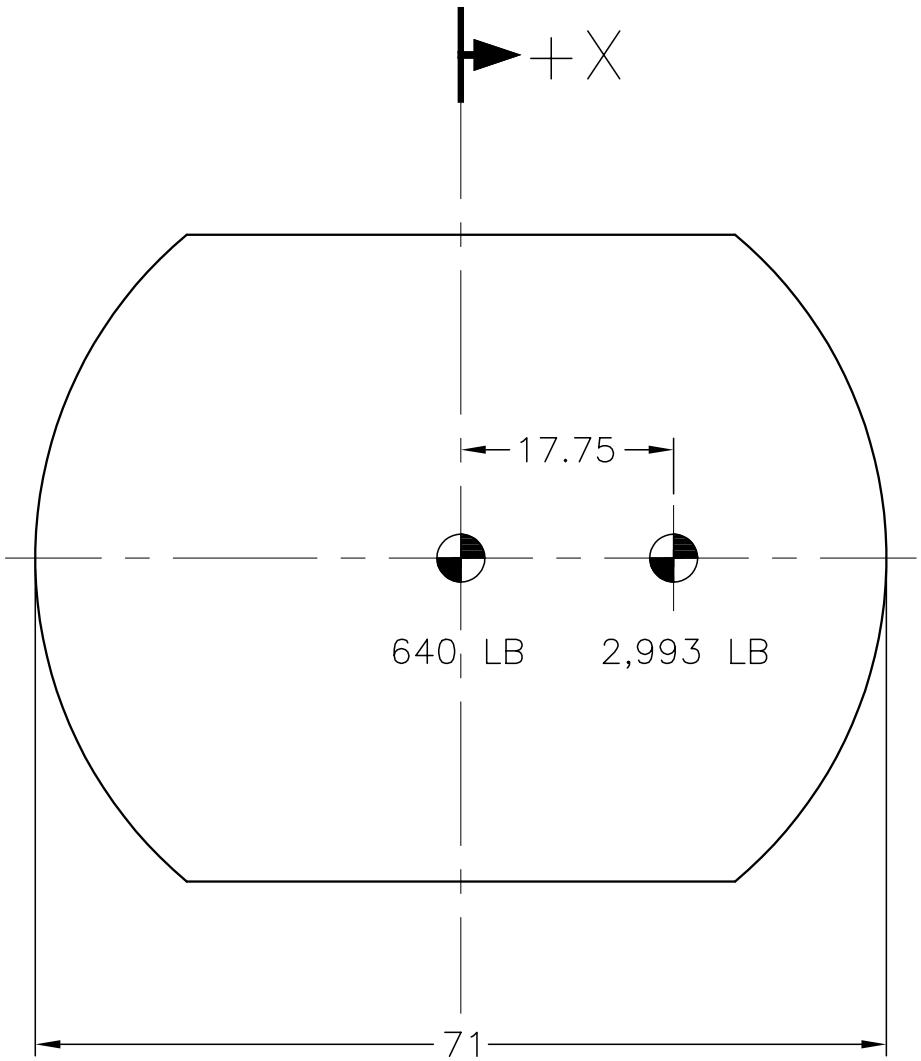

Figure 2.2-5 – Radial Shift of CG for SWB Payload

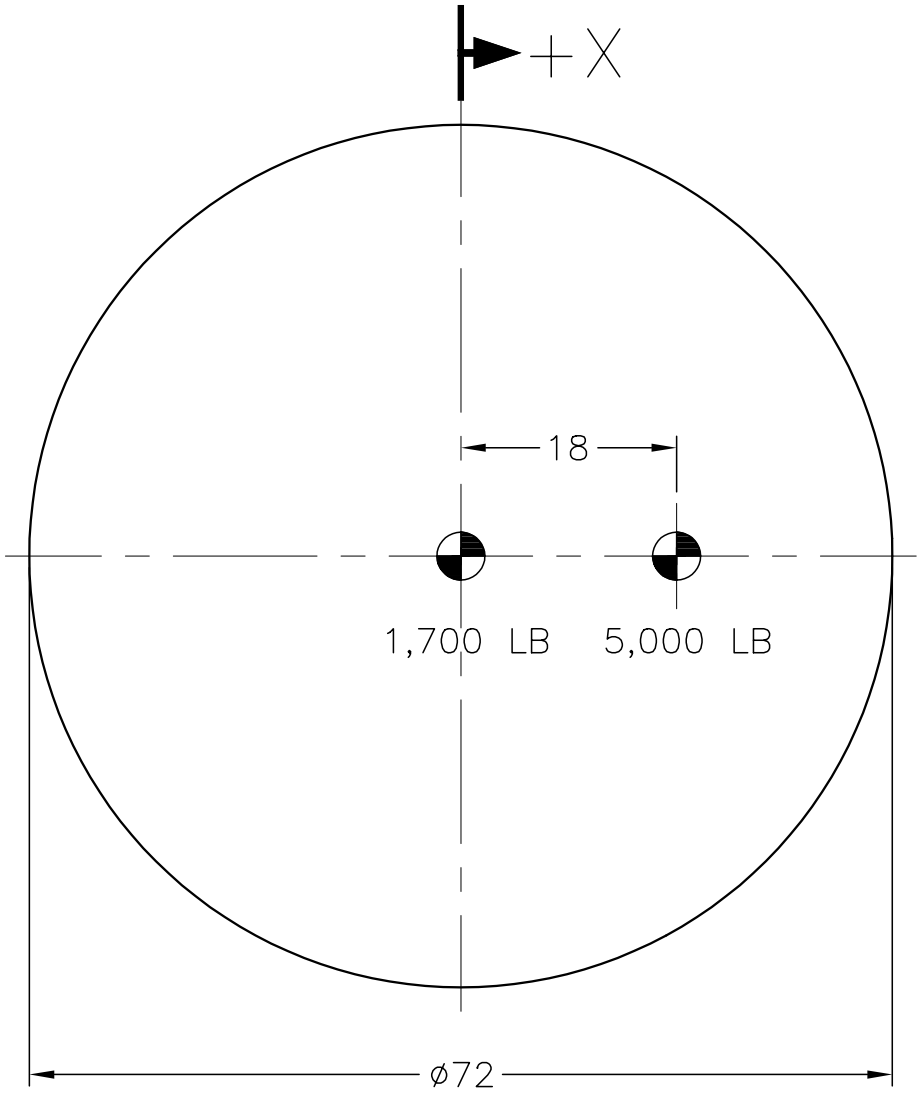

Figure 2.2-6 – Radial Shift of CG for TDOP Payload

2.3 Mechanical Properties of Materials

The major structural components, i.e., the outer containment assembly (OCA) outer shells, outer containment vessel (OCV), and inner containment vessel (ICV), of the TRUPACT-II packaging are fabricated of Type 304, austenitic stainless steel and 8¼ lb/ft^3 (nominal density) polyurethane foam. Other materials performing a structural function are ASTM B16 brass (for the ICV and OCV vent port and seal test port plugs and covers), aluminum honeycomb (for the ICV aluminum honeycomb spacer assemblies), 300 series stainless steel (for the ICV and OCV locking ring lock bolts, and for attaching the locking Z-flange to the OCV locking ring), and ASTM A564, Type 630, stainless steel (joint pins for the OCV and ICV locking rings). Several varieties of non-structural materials are also utilized. Representative non-structural materials include butyl rubber and other elastomeric O-ring seals, a silicone wear pad, aluminum guide tubes for the OCA lid lift operation, ceramic fiber paper, fiberglass insulation, and plastic fire consumable foam cavity vent plugs. The drawings presented in Appendix 1.3.1, *Packaging General Arrangement Drawings*, delineate the specific material(s) used for each TRUPACT-II packaging component.

The remainder of this section presents and discusses pertinent mechanical properties for the materials that perform a structural function. Section 2.3.1, *Mechanical Properties Applied to Analytic Evaluations*, presents all properties used in analytic structural evaluations of the TRUPACT-II package. Most normal conditions of transport (NCT) tests are demonstrated analytically. Section 2.3.2, *Mechanical Properties Applied to Certification Testing*, presents the mechanical properties associated with components whose performance is demonstrated via certification testing. With the exception of immersion, all hypothetical accident condition (HAC) tests are demonstrated via certification testing.

2.3.1 Mechanical Properties Applied to Analytic Evaluations

Analytic evaluations are performed for the basic OCA, OCV, and ICV shells, seal flanges, and locking rings, comprised of Type 304 stainless steel. Table 2.3-1 presents the mechanical properties for the Type 304 stainless steel used in the TRUPACT-II packaging. Each of the mechanical properties of Type 304 stainless steel is taken from Section III of the ASME Boiler and Pressure Vessel Code[1].

All analyses of the basic OCA, OCV, and ICV shells, seal flanges and locking rings utilize the properties presented for ASTM A240, Type 304, stainless steel. With the exception of elongation, which is not specifically used in the linear elastic analytic assessments, all materials presented in Table 2.3-1 exhibit equivalent or better properties than the ASTM A240 material. Minimum elongation values are important regarding testing and are therefore discussed in Section 2.3.2, *Mechanical Properties Applied to Certification Testing*. The density of stainless steel is taken as 0.29 lb/in^3, and Poisson's Ratio is 0.3.

Unlike the other ASTM materials specified in Table 2.3-1, ASTM A276 material does not have an identical ASME material specification. However, structural use of ASTM A276 is as an

[1] American Society of Mechanical Engineers (ASME) Boiler and Pressure Vessel Code, Section III, *Rules for Construction of Nuclear Power Plant Components*, 1986 Edition.

option for the OCA rolled angles used at the lid-to-body interface, the OCV stiffening ring, and the OCA lid lifting straps. As these components are not part of the containment boundary, the use of ASTM A276, whose chemical and mechanical properties are identical to ASTM A479, is justified. Thus, material properties of ASTM A276 versus temperature are taken to be the same as for ASTM A479.

The analytic assessments of the polyurethane foam used in the TRUPACT-II packaging are limited to the NCT internal pressure, differential thermal expansion, and lifting load cases. The data summarized in Table 2.3-2 are established according to the procedures outlined in Section 8.1.4.1, *Polyurethane Foam*. Detailed stress-strain relationships for the polyurethane foam are not required for analysis since analytic assessments for the NCT or HAC free drop or puncture events are not performed. However, as discussed in Section 2.3.2, *Mechanical Properties Applied to Certification Testing*, since TRUPACT-II package performance is demonstrated by certification testing, and performance is a function of foam properties, compressive stress-strain characteristics and installation techniques are carefully controlled.

Material properties are linearly interpolated between, or, if necessary, extrapolated beyond the temperature values shown. For example, when a temperature outside a tabulated range is of interest (e.g., low temperature properties to -40 ºF), data are extrapolated. When a particular analysis requires data extrapolation, it is identified within the applicable section of this chapter.

2.3.2 Mechanical Properties Applied to Certification Testing

The primary means of demonstrating the structural performance capabilities of the TRUPACT-II packaging under imposed NCT and HAC free drops, puncture, and thermal (fire) events is via certification testing. The overall response of the TRUPACT-II packaging to these events is dependent on the characteristics of several structural components. The characteristics of the polyurethane foam used in the OCA are of primary importance regarding TRUPACT-II package performance. For this reason, the method of installation of the foam material into the OCA, and the foam's compressive stress-strain characteristics are carefully controlled and monitored. Section 8.1.4.1, *Polyurethane Foam*, presents the details associated with foam installation and performance testing. Importantly, all TRUPACT-II packages will respond similarly to free drop, puncture, and thermal events. Thermal performance of the foam is discussed in Section 3.2, *Summary of Thermal Properties of Materials*.

At the time of polyurethane foam installation, test samples are retained from each foam pour, as discussed in Section 8.1.4.1, *Polyurethane Foam*. Using these samples, each foam pour is tested for compressive strength at strains of 10%, 40%, and 70%, both parallel and perpendicular to the direction of foam rise. To be acceptable, the average compressive strength of all tested samples from a single foamed component (i.e., the OCA lid or OCA body) for a particular rise direction is to fall within ±15% of the corresponding nominal compressive stress. Additionally, the stress value of any single test specimen from a single pour is to fall within ±20% of the corresponding nominal compressive stress.

In addition to controls on foam compressive stress, OCA foam thicknesses are controlled by the tolerances shown on the drawings provided in Appendix 1.3.1, *Packaging General Arrangement Drawings*. The foam thickness tolerance at the OCA top and sides is set at approximately ±5% of the nominal thickness. In regions where foam strains are very small (e.g., bottom end), a slightly greater thickness tolerance (approximately ±8%) is allowed. The thickness tolerance is

set at approximately one-third the magnitude of the compressive stress tolerance to minimize the effect on package performance in the unlikely event that both tolerances are simultaneously at their extreme values in a given TRUPACT-II packaging assembly. Importantly, in the unlikely event that compressive stress and thickness tolerances are simultaneously at their worst case extremes, the net effect of combining the two tolerances is nearly identical to the compressive stress tolerance acting alone. This is directly attributable to the fact that a long portion of the compressive stress-strain curve for foam (at strains of ~50% or less) exhibits a relatively shallow slope (i.e., "plateau"). Consequently, although small changes in foam thickness directly affect foam strains, small changes in strain while on the plateau portion of the stress-strain curve do not significantly affect stress. As demonstrated by testing (documented in Appendix 2.10.3, *Certification Tests*), the TRUPACT-II packaging deformations due to 30-foot free drops were relatively small, demonstrating that resultant foam strains remained within the "plateau" portion of the compressive stress-strain curve.

In addition to the polyurethane foam, the performance of other primary TRUPACT-II packaging structural components is addressed by certification testing rather than by analysis. These components include the ASTM B16, Alloy 360, half-hard temper, brass vent port plugs, the ICV upper and lower aluminum honeycomb spacer assemblies, the 300 series stainless steel socket head cap screws used to secure the locking rings in the locked position, the ASTM A564, Type 630, Condition 1150, stainless steel pins used in the locking ring joints, and the 1/4 inch, 300 series stainless steel pan head screws used to attach the locking Z-flange to the OCV locking ring. As indicated above, and on the drawings provided in Appendix 1.3.1, *Packaging General Arrangement Drawings*, each of these components has a specific material callout thereby providing a specific control on its mechanical properties. The structurally significant mechanical properties for these materials are presented in Table 2.3-3.

With the exception of the aluminum honeycomb spacer assemblies, the 1/4 inch stainless steel pan head screws, and the OCV lock bolts, all of the above components remained intact during certification testing, and showed essentially no evidence of distress. By design, the aluminum honeycomb spacer assemblies were partially crushed as a result of the certification test program, but still provided adequate protection for the ICV torispherical heads from the simulated payload of fourteen, rigid, concrete-filled, 55-gallon drums.

Many of the 1/4 inch pan head screws that attach the locking Z-flange to the OCV locking ring (or, in some cases, the Z-flange's sheet metal adjacent to the screws) failed in each of the first two certification test units: 19 of 24 for CTU No. 1, and 20 of 24 for CTU No. 2; the number of failed screws was not noted for CTU No. 3. Although failure of these fasteners does not directly unlatch the 18 interlocking seal flange/locking ring tabs, 36 fasteners are used for TRUPACT-II packaging production units instead of the 24 that were used for each of the test units. Failure of the fasteners for a particular test unit is not likely attributed to a single accident sequence (i.e., a single 30-foot free drop followed by a single 40 inch puncture event), but rather probably due to the multiple drops that were conservatively performed on each test unit.

The optional use of Type 304 stainless steel forgings or castings instead of ASTM A240 plate material for the OCV and ICV seal flanges and locking rings is stated on the drawings provided in Appendix 1.3.1, *Packaging General Arrangement Drawings*. As shown in Table 2.3-1, the ASTM A182 forging option and ASTM A351 casting option provide equivalent or improved strength, but a somewhat reduced elongation than does the ASTM A240. The reduced

elongation values (30% for ASTM A182 and 35% for ASTM A351 versus 40% for ASTM A240 material) are acceptable based on the results of the certification testing program. Relatively little permanent deformation was observed for the OCV or ICV seal flanges and locking rings as a result of certification testing, indicating that strains were well below the 30% minimum elongation provided by any of the specified materials. Any of the three material options are therefore acceptable for fabricating TRUPACT-II packagings.

Table 2.3-1 – Mechanical Properties of Type 304 Stainless Steel Components (for Analysis)

Material Specification	① Minimum Elongation (%)	Temperature (°F)	② Yield Strength, S_y ($\times 10^3$ psi)	③ Ultimate Strength, S_u ($\times 10^3$ psi)	④ Allowable Strength, S_m ($\times 10^3$ psi)	⑤ Elastic Modulus, E ($\times 10^6$ psi)	⑥⑦ Thermal Expansion Coefficient, α ($\times 10^{-6}$ in/in/°F)
ASTM A213	35	70	30.0	75.0	20.0	28.3	8.46
ASTM A240	40	100	30.0	75.0	20.0	-----	8.55
ASTM A312	35	200	25.0	71.0	20.0	27.6	8.79
ASTM A376	35	300	22.5	66.0	20.0	27.0	9.00
ASTM A479	30	400	20.7	64.4	18.7	26.5	9.19
Type 304		500	19.4	63.5	17.5	25.8	9.37
ASTM A182 Type F304 (<5 inch thick)	30	70	30.0	75.0	20.0	28.3	8.46
		100	30.0	75.0	20.0	-----	8.55
		200	25.0	71.0	20.0	27.6	8.79
		300	22.5	66.0	20.0	27.0	9.00
		400	20.7	64.4	18.7	26.5	9.19
		500	19.4	63.5	17.5	25.8	9.37
ASTM A351 Grade CF8A	35	70	35.0	77.0	23.3	28.3	8.46
		100	35.0	77.0	23.3	-----	8.55
		200	29.1	72.8	23.3	27.6	8.79
		300	26.3	67.8	22.6	27.0	9.00
		400	24.2	66.1	21.8	26.5	9.19
		500	22.8	65.2	20.5	25.8	9.37
ASTM A276⑧	30	70	30.0	75.0	20.0⑨	28.3⑨	8.46⑨

Notes: ① ASME Code, Section III, Part A, 1986.
② ASME Code, Section III, Table I-2.2, 1986.
③ ASME Code, Section III, Table I-3.2, 1986.
④ ASME Code, Section III, Table I-1.2, 1986.
⑤ ASME Code, Section III, Table I-6.0, 1986.
⑥ ASME Code, Section III, Table I-5.0, 1986.
⑦ Mean from 70 ºF.
⑧ ASTM Standards, A276, Type 304, 1988.
⑨ ASTM A479 material properties.

This page intentionally left blank.

Table 2.3-2 – Mechanical Properties of Polyurethane Foam (for Analysis)

Property	Direction	Nominal Room Temperature Value
Compressive Strength, S	Axial (Parallel-to-Rise)	235 psi
	Radial (Perpendicular-to-Rise)	195 psi
Compressive Modulus, E_c	Axial (Parallel-to-Rise)	6,810 psi
	Radial (Perpendicular-to-Rise)	4,773 psi
Tensile Modulus, E_t	Axial (Parallel-to-Rise)	10,767 psi
	Radial (Perpendicular-to-Rise)	6,935 psi
Shear Modulus, E_s	Axial (Parallel-to-Rise)	1,921 psi
	Radial (Perpendicular-to-Rise)	2,553 psi
Thermal Expansion Coefficient, α	-----	3.5×10^{-5} in/in/ºF
Poisson's Ratio, ν	-----	0.33
Density, ρ	-----	8.25 lb/ft^3

Table 2.3-3 – Mechanical Properties of Metallic Materials (for Testing)

Material	Minimum Mechanical Properties (unless otherwise specified)	Notes
ASTM B16, Alloy 360 Brass, Half-Hard Temper	σ_y = 25,000 psi σ_u = 55,000 psi	-----
Hexcel ACG-3/8-.003-3.6P Aluminum Honeycomb	σ_{bc} = 340 psi ±15% (Bare Compressive Strength) σ_c = 120 psi ±15% (Crush Strength)	①
300 Series Stainless Steel Socket Head Cap Screws	σ_y = 40,000 psi σ_u = 80,000 psi	②
ASTM A564, Type 630, Condition 1150, Stainless Steel	σ_y = 105,000 psi σ_u = 135,000 psi	③
1/4 inch, 300 Series Stainless Steel Pan Head Screws	σ_y = 30,000 psi σ_u = 75,000 psi	④

Notes:

① *Mechanical Properties of Hexcel Honeycomb Materials*, TSB-120 (Technical Service Bulletin 120), Hexcel, 1992. The term "Bare Compressive Strength" is defined as the maximum strength that is exhibited by the honeycomb material at the onset of crushing. The term "Crush Strength" is defined as the average compressive strength that is sustained as the honeycomb material undergoes crushing.

② UNBRAKO Socket Screw Products Catalog, Copyright 1988, SPS Technologies.

③ ASME Boiler and Pressure Vessel Code, Section III, 1986 Edition.

④ Industrial Fasteners Institute, *Fastener Standard*, Fifth Edition.

This page intentionally left blank.

2.4 General Standards for All Packages

This section defines the general standards for all packages. The TRUPACT-II package, with an outer containment vessel (OCV) that is integral to an outer containment assembly (OCA) for primary containment, and an inner containment vessel (ICV) for secondary containment, meets all requirements delineated for this section.

2.4.1 Minimum Package Size

The minimum transverse dimension (i.e., the diameter) of the TRUPACT-II package is 94⅜ inches, and the minimum longitudinal dimension (i.e., the height) is 121½ inches. Thus, the requirement of 10 CFR §71.43(a)[1] is satisfied.

2.4.2 Tamper-indicating Feature

Tamper-indicating seals are installed at one OCA lock bolt location and at the OCV vent port access plug, as delineated on the drawings in Appendix 1.3.1, *Packaging General Arrangement Drawings*. A lock wire device is used between two tie-points. For the OCV lock bolt, the tie-points are the bolt head and the locking Z-flange. The two tie-points for the OCV vent port access plug are the plug itself and a bolt tapped and welded to the OCA body outer shell. Failure of either tamper-indicating device provides evidence of possible unauthorized access. Thus, the requirement of 10 CFR §71.43(b) is satisfied.

2.4.3 Positive Closure

The TRUPACT-II package cannot be opened unintentionally. Both the OCA and ICV lids are attached to their respective bodies with locking rings. The OCV locking ring is secured with six, 1/2-13UNC, OCA lock bolts through the attached locking Z-flange. Similarly, the ICV locking ring is secured in the locked position with three, 1/2-13UNC, ICV lock bolts. For either lid, the presence of a single, lock bolt will prevent lid removal.

The OCV vent port has three levels of protection against inadvertent opening: 1) the OCV vent port access plug, 2) the OCV vent port cover, and 3) the OCV vent port plug. Each of these components are secured via threaded fittings. The ICV vent port has two levels of protection against inadvertent opening: 1) the ICV vent port cover, and 2) the ICV vent port plug. Thus, the requirements of 10 CFR §71.43(c) are satisfied.

2.4.4 Chemical and Galvanic Reactions

The major materials of construction of the TRUPACT-II packaging (i.e., austenitic stainless steel, aluminum, brass, polyurethane foam, ceramic fiber paper, fiberglass insulation, butyl rubber O-ring seals and other elastomeric materials) will not have significant chemical, galvanic or other reactions in air, inert gas or water environments, thereby satisfying the requirements of 10 CFR §71.43(d). These materials have been previously used, without incident, in radioactive material (RAM) packages for transport of similar payload materials. A successful RAM

[1] Title 10, Code of Federal Regulations, Part 71 (10 CFR 71), *Packaging and Transportation of Radioactive Material*, 01-01-07 Edition.

packaging history combined with successful use of these fabrication materials in similar industrial environments ensures that the integrity of the TRUPACT-II package will not be compromised by any chemical, galvanic or other reactions. The materials of construction and the payload are further evaluated below for potential reactions.

2.4.4.1 Packaging Materials of Construction

The TRUPACT-II packaging is primarily constructed of Type 304 stainless steel. This material is highly corrosion resistant to most environments. The metallic structure of the TRUPACT-II packaging is composed entirely of this material and compatible 300 series weld material. The weld material and processes have been selected in accordance with the ASME Boiler and Pressure Vessel Code[2] to provide as good or better material properties, including corrosion resistance, as the base material. Since both the base and weld materials are 300 series materials, they have nearly identical electrochemical potential thereby minimizing any galvanic corrosion that could occur.

The stainless steel within the OCA foam cavity is lined with a ceramic fiber paper, composed of alumina silica. This material is nonreactive with either the polyurethane foam or the stainless steel, both dry or in water. The ceramic fiber paper and the silicone adhesive are very low in free chlorides to minimize the potential for stress corrosion of the OCA structure.

The polyurethane foam that is used in the OCA is essentially identical to previously licensed transportation packagings, such as the NuPac 125B (Docket 71-9200), the NuPac 10-142 (71-9208), and the NuPac PAS-1 (Docket 71-9184). All of these packagings have had a long and successful record of performance demonstrating that the polyurethane foam does not cause any adverse conditions with the packaging. The polyurethane foam in the OCA is a rigid, closed-cell (non-water absorbent) foam that is very low in free halogens and chlorides, as discussed in Section 8.1.4.1, *Polyurethane Foam*. The polyurethane foam material cavity is sealed with plastic pipe plugs to preclude the entrance of moisture.

Aluminum honeycomb is used in the TRUPACT-II packaging for the two, ICV aluminum honeycomb spacer assemblies in the upper and lower ICV torispherical heads. Aluminum honeycomb material is used for dunnage only, and is not used as any part of the TRUPACT-II packaging's containment boundaries. The aluminum honeycomb is maintained at relatively low temperatures ensuring that no adverse reaction could occur at aluminum/steel interfaces that would compromise the packaging's containment integrity. Of final note, aluminum material is slightly anodic which serves to protect the stainless steel of the ICV.

The various brass fittings and plugs used in the TRUPACT-II packaging are very corrosion resistant. Like aluminum, brass material is slightly anodic to the stainless steel. Any damage that could occur to the brass is easily detectable since the fittings are all handled each time the TRUPACT-II package is loaded and unloaded.

The various elastomers (e.g., butyl rubber, polyester, silicone, etc.) that are used in the O-rings, annulus foam ring, debris shield, wear pad, etc., contain no corrosives that would react adversely affect the TRUPACT-II packaging. These materials are organic in nature and noncorrosive to the stainless steel containment boundaries of the TRUPACT-II packaging.

---

[2] American Society of Mechanical Engineers (ASME) Boiler and Pressure Vessel Code, Section III, *Rules for Construction of Nuclear Power Plant Components*, 1986 Edition.

2.4.4.2 Payload Interaction with Packaging Materials of Construction

The materials of construction of the TRUPACT-II packaging are checked for compatibility with the various payload chemistries when the payloads are evaluated for chemical compatibility. All payload materials are in approved payload containers delineated in the CH-TRAMPAC[3].

The payload is typically further confined within multiple layers of plastic for radiological health purposes. This configuration ensures that the payload material has an insignificant level of contact with the TRUPACT-II packaging materials of construction. However, the evaluation of compatibility is based on complete interaction of payload materials with the packaging.

The design of the TRUPACT-II package is for transport of CH-TRU materials and other authorized payloads that are limited in form to solid or solidified material. Corrosive materials, pressurized containers, explosives, non-radioactive pyrophorics, and liquid volumes greater than 1% are prohibited. These restrictions ensure that the waste in the payload is in a non-reactive form for safe transport in the TRUPACT-II package. For a comprehensive discussion defining acceptable payload properties, see the CH-TRAMPAC.

2.4.5 Valves

Neither the OCV nor the ICV have valves. However, beside their respective lids, the OCV and the ICV each have a vent port penetration into their containment cavities. These vent port penetrations are sealed using threaded vent port plugs comprised of brass material. Since the ICV is entirely contained within the OCV during transport, a tamper indicating device is not necessary. Access to the OCV vent port penetration is prevented by a lockwire that secures the OCV vent port access plug, as discussed in Section 2.4.2, *Tamper-indicating Feature*. Thus, the requirements of 10 CFR §71.43(e) are satisfied.

2.4.6 Package Design

As shown in Chapter 2.0, *Structural Evaluation*, Chapter 3.0, *Thermal Evaluation*, Chapter 5.0, *Shielding Evaluation*, and Chapter 6.0, *Criticality Evaluation*, the structural, thermal, shielding, and criticality requirements, respectively, of 10 CFR §71.43(f) are satisfied for the TRUPACT-II package.

2.4.7 External Temperatures

As shown in Table 3.5-1 and Table 3.5-2 from Section 3.5.3, *Package Temperatures*, the maximum accessible surface temperature with maximum internal decay heat load and no insolation is 102 ºF. Since the maximum external temperature does not exceed 122 ºF, the requirements of 10 CFR §71.43(g) are satisfied.

[3] U.S. Department of Energy (DOE), *Contact-Handled Transuranic Waste Authorized Methods for Payload Control* (CH-TRAMPAC), U.S. Department of Energy, Carlsbad Field Office, Carlsbad, New Mexico.

2.4.8 Venting

The TRUPACT-II package does not include any features intended to allow continuous venting during transport. Thus, the requirements of 10 CFR §71.43(h) are satisfied.

2.5 Lifting and Tie-down Standards for All Packages

For analysis of the lifting and tie-down components of the TRUPACT-II packaging, material properties from Section 2.3, *Mechanical Properties of Materials*, are taken at a bounding temperature of 160 ºF per Section 2.6.1.1, *Summary of Pressures and Temperatures*. The primary structural materials are Type 304 stainless steel, and polyurethane foam that is used in the outer containment assembly (OCA).

A loaded TRUPACT-II package is only lifted by forklift pockets, located at the bottom of the OCA body. For this case, TRUPACT-II package lifting loads act parallel to the direction of foam rise. The nominal compressive strength of the polyurethane foam, as delineated in Table 2.3-2 from Section 2.3.1, *Mechanical Properties Applied to Analytic Evaluations*, is reduced by 15% to account for manufacturing tolerance; polyurethane foam manufacturing tolerances are discussed in Section 8.1.4.1.2.3.2, *Parallel-to-Rise Compressive Stress*. The nominal compressive strength of the polyurethane foam is further reduced by 25% to account for elevated temperature effects, as discussed in Section 2.6.1.1, *Summary of Pressures and Temperatures*.

Properties of Type 304 stainless steel and polyurethane foam, parallel to the direction of foam rise accounting for manufacturing tolerances and elevated temperature, are summarized below.

Material Property	Value	Reference
Type 304 Stainless Steel at 160 ºF		
Elastic Modulus, E	27.8×10^6 psi	Table 2.3-1
Yield Strength, σ_y	27,000 psi	
Shear Stress, equal to $(0.6)\sigma_y$	16,200 psi	
Polyurethane Foam (parallel-to-rise) at 160 ºF		
Minimum compressive strength, σ_c	150 psi	Table 2.3-2
Bearing stress, assumed equal to $(2/3)\sigma_c$	100 psi	

2.5.1 Lifting Devices

This section demonstrates that the forklift pockets, the only attachments designed to lift the TRUPACT-II package, are designed with a minimum safety factor of three against yielding, per the requirements of 10 CFR §71.45(a). The lifting devices in the OCA lid are restricted to only lifting the OCA lid, and the lifting devices in the ICV lid are restricted to only lifting an ICV lid or empty ICV. Although these lifting devices are designed with a minimum safety factor of three against yielding, detailed analyses are not specifically included herein since these lifting devices are not intended for lifting a TRUPACT-II package.

When lifting the entire package, the applied lift force without yielding is simply three times the total package weight of 19,250 pounds, as given in Section 2.2, *Weights and Centers of Gravity*.

$$F_L = (3)(19{,}250) = 57{,}750 \text{ pounds}$$

The entire package is lifted via two forklift pockets located at the bottom of the OCA. Loads are considered to be concentrated at the forklift pocket interfaces and act parallel to the direction of foam rise. For the purposes of this analysis, the minimum assumed fork width is 8 inches, and the minimum assumed engagement length is 60 inches. The total bearing area for two forks is:

$$A = (2)(8)(60) = 960 \text{ in}^2$$

Assuming the entire lifted load is carried directly into the polyurethane foam, thereby ignoring any beneficial load carrying associated with the presence of the relatively stiff stainless steel forklift pocket and OCA outer shell, the compressive stress is:

$$\sigma_c = \frac{F_L}{A} = \frac{57{,}750}{960} = 60 \text{ psi}$$

The allowable compressive stress for the polyurethane foam is 100 psi. Therefore, the margin of safety is:

$$MS = \frac{100}{60} - 1 = +0.67$$

2.5.2 Tie-down Devices

The TRUPACT-II package is secured to its dedicated semi-trailer at four points, two on each trailer main beam. For railcar shipments, the TRUPACT-II package is secured to an adapter that mimics the trailer's four attachment points. Subsequent use of the term "trailer" or "trailer main beam(s)" encompass the railcar adapter and railcar frame. The attachment is made using trailer tie-down devices that pass over the tie-down lugs located at the bottom of the OCA body. The semi-trailer is also fitted with kick plates at the four tie-down points to provide horizontal restraint (blocking). The tie-down scheme utilized for the TRUPACT-II package is illustrated in Figure 2.5-1 and Figure 2.5-2.

Inertial loads of 10*g* longitudinally, 5*g* laterally, and 2*g* vertically, per 10 CFR §71.45(b)(1), are applied through the TRUPACT-II package center of gravity, conservatively assumed to be 60 inches above the package's base. The horizontal loads of 10*g* longitudinally and 5*g* laterally are reacted in compression against the kick plates. The resultant overturning moment is reacted in compression on a trailer main beam and in tension by the four tie-down lugs. The vertical load applied to the center of gravity (2*g*) is evenly reacted at the four tie-down points, and is assumed to act in the direction (up or down) that maximizes the total tie-down load (i.e., down for the compressive reaction point and up for the tensile reaction points).

2.5.2.1 Tie-down Forces

Tensile tie-down points are on a 48.4 inch radius circle (to the center of the tie-down lugs, in line with the tie-down fixture). The compressive reaction point is at the trailer main beam, occurring at the edge of the tie-down lug's doubler plate, a radius of 47.56 inches. A plan view of the tie-down geometry is depicted in Figure 2.5-3, including a corresponding free-body force diagram. If the TRUPACT-II package is treated as a rigid body, the reaction forces may be determined from the following set of equations:

$$F_1L_1 + F_2L_2 + F_3L_3 + F_4L_4 = HF_g$$

$$\frac{F_1}{L_1} = \frac{F_2}{L_2} = \frac{F_3}{L_3} = \frac{F_4}{L_4} = k$$

$$F_1 + F_2 + F_3 + F_4 = F_c$$

where, the height of the package center of gravity above its base, H = 60 inches, the horizontal inertia force, $F_g = 19{,}250 \times (10^2 + 5^2)^{1/2} = 215{,}222$ pounds, and the tie-down lug reaction lengths, $L_1 = 47.56 - 47.52 = 0.04$ inches, $L_2 = 47.56 - 21.16 = 26.40$ inches, $L_3 = 47.56 + 21.16 = 68.72$ inches, and $L_4 = 47.56 + 47.52 = 95.08$ inches. Solving for k:

$$k = \frac{HF_g}{L_1^2 + L_2^2 + L_3^2 + L_4^2} = \frac{(60)(215{,}222)}{(0.04)^2 + (26.40)^2 + (68.72)^2 + (95.08)^2} = 893 \text{ lb/in}$$

Therefore, $F_1 = k \times L_1 = 36$ pounds, $F_2 = k \times L_2 = 23{,}575$ pounds, $F_3 = k \times L_3 = 61{,}367$ pounds, $F_4 = k \times L_4 = 84{,}906$ pounds, and $F_c = 169{,}884$ pounds. The maximum vertical tensile force on any single tie-down lug, including the contribution of the vertical load of 2*g*, is then found as:

$$F_{t-max} = 84{,}906 + \frac{(2g)(19{,}250)}{4 \text{ lugs}} = 94{,}531 \text{ pounds}$$

Similarly, the maximum compressive force is found as:

$$F_{c-max} = 169{,}884 + \frac{(2g)(19{,}250)}{4 \text{ lugs}} = 179{,}509 \text{ pounds}$$

Since the line of action of the combined 10*g* longitudinal and the 5*g* lateral accelerations pass almost exactly over the centerline of the kickplate (27.6º for the kickplate centerline versus 26.6º for the line of action of the force), the total horizontal reaction force is conservatively assumed to be reacted against a single kickplate. This force is given by:

$$F_h = F_g = 215{,}222 \text{ pounds}$$

2.5.2.2 Tie-down Stress Due to a Vertical Tensile Load

Several failure modes are considered for the vertical tensile force on the tie-down lug. Shear failure of the tie-down lug itself is not an issue because the shear area of the lug is much greater than the lug attachment welds. The remaining failure modes, as illustrated in Figure 2.5-4, are:

(a) Shear and bending failure of the tie-down lug welds (shear + bending loads),

(b) Tearout of the tie-down lug doubler plate at the lug weld outline,

(c) Shear failure of the welds attaching the lug doubler plate to the OCA outer shell, and

(d) Tearout of the OCA outer shell at the doubler outline.

2.5.2.2.1 Failure of the Tie-down Lug Welds Due to Shear and Bending Loads

Figure 2.5-5 presents dimensional details of the tie-down, including an appropriate free-body diagram. The length of the tie-down lug weld along the two sides is 5.49 inches. The arc length

of the weld across the top of the lug is 3.38 inches. The groove weld at the bottom is 2.38 inches long. On three sides, the weld is a 3/8 inch fillet over a 3/8 inch groove. The minimum throat length for this weld is 0.375/(sin 45º) = 0.53 inches. For the 3/8 inch groove weld at the bottom, the minimum throat length is 0.375 inches. Thus, the total shear area for the weld is:

$$A_s = [(2)(5.49) + 3.38](0.53) + (2.38)(0.375) = 8.50 \text{ in}^2$$

The maximum shearing force, V, is the maximum tensile force, $F_{t\text{-}max}$ = 94,531 pounds from Section 2.5.2.1, *Tie-down Forces*, resulting in a corresponding shear stress of:

$$\tau_V = \frac{V}{A_s} = \frac{94{,}531}{8.50} = 11{,}121 \text{ psi}$$

The maximum weld shear stress due to bending is found using the standard beam bending formula, but by treating the weld as a line[1], or:

$$\tau_B = \frac{Mc}{I}$$

where M is the moment on weld group, c is the maximum weld distance from the weld group centroid, and I is the moment of inertia of weld group. The weld group centroid, relative to the bottom edge of the tie-down lug, is:

$$\bar{y} = \frac{(0.53)(3.38)(6.00) + 2(0.53)(5.49)(5.49/2)}{(0.53)(3.38) + 2(0.53)(5.49) + (0.375)(2.38)} = 3.143 \text{ inches}$$

where the centroid of the arc formed by the weld at the top of the tie-down lug is located 6.00 inches above the base of the lug. For the sides, the contribution to the moment of inertia is:

$$I_s = 2\left[\frac{tL^3}{12} + Ad^2\right] = 2\left[\frac{(0.53)(5.49)^3}{12} + (0.53)(5.49)\left(3.143 - \frac{5.49}{2}\right)^2\right] = 15.54 \text{ in}^4$$

For the top (arc-shaped) weld, conservatively ignoring the moment of inertia about its own centroid, the contribution to the moment of inertia is:

$$I_t = Ad^2 = (0.53)(3.38)(6.00 - 3.143)^2 = 14.62 \text{ in}^4$$

For the bottom weld, the contribution to the moment of inertia is:

$$I_b = Ad^2 = (0.375)(2.38)(3.143)^2 = 8.82 \text{ in}^4$$

Summing the contributions from each part of the weld group, the total moment of inertia of the weld group, treated as a line, is:

$$I = I_s + I_t + I_b = 15.54 + 14.62 + 8.82 = 38.98 \text{ in}^4$$

[1] Shigley, *Mechanical Engineering Design*, Third Edition, McGraw-Hill, Inc., 1977, Section 7-4, *Bending in Welded Joints*.

The distance from the centroid of the weld group to the extreme fiber is c = 3.143 inches. The line of action for the vertical force is 0.7 inches from the side of the tie-down doubler plate, as illustrated in Figure 2.5-5. Therefore, the shear stress on the weld group due to bending is:

$$\tau_B = \frac{Mc}{I} = \frac{(94{,}531)(0.7)(3.143)}{38.98} = 5{,}335 \text{ psi}$$

The maximum shear stress in the tie-down lug weld due to the shear and bending loads is:

$$\tau = \sqrt{\tau_V^2 + \tau_B^2} = \sqrt{(11{,}121)^2 + (5{,}335)^2} = 12{,}334 \text{ psi}$$

The allowable shear stress for the tie-down lug welds is 16,200 psi. Therefore, the margin of safety is:

$$MS = \frac{16{,}200}{12{,}334} - 1 = +0.31$$

2.5.2.2.2 Tearout of the Tie-down Doubler Plate at the Tie-Down Lug Weld Outline

Assume that a rectangular region equal to 2.88 + 2 × 0.375 = 3.63 inches wide by (6.25 + 0.375) = 6.63 inches high, tears out from the 3/8 inch thick doubler plate. Under the direct shear load of 94,531 pounds, the top edge will be in direct tension while the sides and bottom will be in direct shear. Conservatively assuming the top and sides are all in direct shear, the shear area in the 3/8 inch thick, tie-down doubler plate is:

$$A_p = [3.63 + 2(6.63)](0.375) = 6.33 \text{ in}^2$$

The shear area of the 1.0 inch groove weld attaching the bottom of the doubler plate to the OCA body flat head is:

$$A_w = (3.63)(1.0) = 3.63 \text{ in}^2$$

Thus, the total shear area is:

$$A_s = A_p + A_w = 6.33 + 3.63 = 9.96 \text{ in}^2$$

The maximum shearing force, V, is the maximum tensile force, $F_{t\text{-}max}$ = 94,531 pounds from Section 2.5.2.1, *Tie-down Forces*, resulting in a corresponding shear stress of:

$$\tau_V = \frac{V}{A_s} = \frac{94{,}531}{9.96} = 9{,}491 \text{ psi}$$

The maximum weld shear stress due to bending is found using the standard beam bending formula, but by treating the weld as a line, or:

$$\tau_B = \frac{Mc}{I}$$

where M is the moment on weld group, c is the maximum weld distance from the weld group centroid, and I is the moment of inertia of weld group. The weld group centroid, relative to the bottom edge of the tie-down lug, is:

$$\bar{y} = \frac{(0.375)(3.63)(6.63) + 2(0.375)(6.63)(6.63/2) + (1.0)(3.63)(1.0/2)}{(0.375)(3.63) + 2(0.375)(6.63) + (1.0)(3.63)} = 2.742 \text{ inches}$$

For the sides of the rectangular region, the contribution to the moment of inertia is:

$$I_s = 2\left[\frac{L^3 t}{12} + Ad^2\right] = 2\left[\frac{(6.63)^3(0.375)}{12} + (0.375)(6.63)\left(2.742 - \frac{6.63}{2}\right)^2\right] = 19.85 \text{ in}^4$$

For the top of the rectangular region, the contribution to the moment of inertia is:

$$I_t = \frac{Lt^3}{12} + Ad^2 = \frac{(3.63)(0.375)^3}{12} + (0.375)(3.63)(6.63 - 2.742)^2 = 20.59 \text{ in}^4$$

For the bottom groove weld, the contribution to the moment of inertia is:

$$I_b = \frac{Lt^3}{12} + Ad^2 = \frac{(3.63)(1.0)^3}{12} + (1.0)(3.63)\left(2.742 - \frac{1.0}{2}\right)^2 = 18.55 \text{ in}^4$$

Summing the contributions from each part of the rectangular region, the total moment of inertia of the weld group, treated as a line, is:

$$I = I_s + I_t + I_b = 19.85 + 20.59 + 18.55 = 58.99 \text{ in}^4$$

The distance from the centroid of the rectangular region to the extreme fiber is c = 6.63 – 2.742 = 3.888 inches. The line of action for the vertical force is 0.7 + 0.375/2 = 0.89 inches from the center of the tie-down doubler plate. Therefore, the shear stress due to bending is:

$$\tau_B = \frac{Mc}{I} = \frac{(94{,}531)(0.89)(3.888)}{58.99} = 5{,}545 \text{ psi}$$

The maximum shear stress in the tie-down doubler plate due to the shear and bending loads is:

$$\tau = \sqrt{\tau_V^2 + \tau_B^2} = \sqrt{(9{,}491)^2 + (5{,}545)^2} = 10{,}992 \text{ psi}$$

The allowable shear stress for the tie-down doubler plate is 16,200 psi. Therefore, the margin of safety is:

$$MS = \frac{16{,}200}{10{,}992} - 1 = +0.47$$

2.5.2.2.3 Shear Failure of the Tie-down Lug Doubler Plate to OCA Outer Shell Welds

The tie-down lug doubler plate is 24 inches square, and welded to the OCA outer shell on its top and sides with 1/4 inch fillet welds. Although the bottom weld is a groove weld, conservatively assume it acts as a 1/4 inch fillet weld, resulting in a total weld length of 96 inches. In addition, 30, 1½ inch diameter, 1/4 inch fillet welds supplement the peripheral fillet welds, providing an additional $30 \times \pi(1.5) = 141$ inches of weld. Thus, the total weld length is 237 inches, resulting in a weld shear area of:

$$A_s = (0.25)(\sin 45^\circ)(237) = 41.9 \text{ in}^2$$

The weld shear area is much greater than determined in both previous cases (i.e., $A_s = 8.50$ in^2 for Section 2.5.2.2.1, *Failure of the Tie-down Lug Welds Due to Shear and Bending Loads*, and $A_s = 9.96$ in^2 for Section 2.5.2.2.2, *Tearout of the Tie-down Doubler Plate at the Tie-Down Lug Weld Outline*). Thus, the weld shear stress for the same vertical load will be correspondingly less. Similarly, a much larger moment of inertia will be determined for a nearly identical bending moment, thereby resulting in a substantially reduced bending stress. In conclusion, by inspection the resulting margin of safety will correspondingly be much greater and does not need to be explicitly determined.

2.5.2.2.4 Tearout of the OCA Outer Shell at the Tie-Down Lug Doubler Plate Outline

A potential failure mode for the tie-down hardware is tearout of the 1/4 inch thick OCA outer shell just outboard of the 24.0 inch square doubler plate. The downward acting force puts the OCA shell adjacent to the top edge of the doubler plate in direct tension. The OCA outer shell immediately adjacent to the sides and bottom edge of the doubler plate is in direct shear.

Assume that the 24 × 24 inch tie-down lug doubler plate tears out from 1/4 inch thick OCA outer shell. Under the direct shear load of 94,531 pounds, the top edge will be in direct tension while the sides and bottom will be in direct shear. Conservatively assuming that all sides are all in direct shear, the shear area in the 1/4 inch thick OCA outer shell is:

$$A_s = 4(24)(0.25) = 24.0 \text{ in}^2$$

Once again, the shell shear area is much greater than determined in both previous cases (i.e., $A_s = 8.50$ in^2 for Section 2.5.2.2.1, *Failure of the Tie-down Lug Welds Due to Shear and Bending Loads*, and $A_s = 9.96$ in^2 for Section 2.5.2.2.2, *Tearout of the Tie-down Doubler Plate at the Tie-Down Lug Weld Outline*). Thus, the weld shear stress for the same vertical load will be correspondingly less. As before, a much larger moment of inertia will be determined for a nearly identical bending moment, thereby resulting in a substantially reduced bending stress. In conclusion, by inspection the resulting margin of safety will correspondingly be much greater and does not need to be explicitly determined.

2.5.2.3 Tie-down Stress Due to a Vertical Compressive Load

The stresses in the TRUPACT-II package due to a vertical compressive load may be analyzed by two bounding cases. First, the combination of overturning and vertical, 2*g* inertial compressive loads carried through the OCA outer shell and tie-down lug doubler plate, and second, the 2*g* inertial compressive load carried entirely by the polyurethane foam.

2.5.2.3.1 Bearing Stress in the OCA Outer Shell and Tie-down Lug Doubler Plate

The vertical compressive tie-down load is carried in bearing against the semi-trailer main beams. Conservatively assume that this load is carried only by the cylindrical portion of the OCA outer shell and doubler that is directly over the trailer main beams and tie-down support structure. With reference to Figure 2.5-3, the arc length, s, of the OCA that spans the trailer main beams is:

$$s = R\left(\frac{\pi}{180}\right)(\phi_1 - \phi_2) = (47.56)\left(\frac{\pi}{180}\right)\left[\sin^{-1}\left(\frac{32}{47.56}\right) - \sin^{-1}\left(\frac{18}{47.56}\right)\right] = 16.64 \text{ inches}$$

For an OCA outer shell thickness of 1/4 inch, and a tie-down lug doubler plate thickness of 3/8 inch, the area is:

$$A = (16.64)(0.25 + 0.375) = 10.40 \text{ in}^2$$

Thus, from Section 2.5.2.1, *Tie-down Forces*, the maximum compressive force, $F_{c\text{-}max}$ = 179,509 pounds, and the corresponding compressive stress is:

$$\sigma_c = \frac{F_{c-max}}{A} = \frac{179{,}509}{10.40} = 17{,}260 \text{ psi}$$

The allowable stress for the OCA outer shell and tie-down lug doubler plate is 27,000 psi. Therefore, the margin of safety is:

$$MS = \frac{27{,}000}{17{,}260} - 1 = +0.56$$

2.5.2.3.2 Compressive Stress in the Polyurethane Foam

The TRUPACT-II package is supported on the two main trailer beams during transport. With reference to Figure 2.5-3, the length, L, under the OCA that spans the trailer main beams is:

$$L = 2\sqrt{(47.56)^2 - (22)^2} = 84.3 \text{ inches}$$

For two, 8 inch wide, trailer main beams, the total compressive area is:

$$A = 2(8)(84.3) = 1{,}349 \text{ in}^2$$

Conservatively ignoring the load carrying capacity of the OCA outer shell and forklift pockets, the compressive stress in the polyurethane foam due to a 2*g* vertical (downward) inertial force is:

$$\sigma_c = \frac{2(19{,}250)}{A} = \frac{38{,}500}{1{,}349} = 29 \text{ psi}$$

The allowable stress for the polyurethane foam is 100 psi. Therefore, the margin of safety is:

$$MS = \frac{100}{29} - 1 = +2.45$$

2.5.2.4 Tie-down Stresses Due to a Horizontal Compressive Load

The horizontal load, F_h = 215,222 pounds, determined in Section 2.5.2.1, *Tie-down Forces*, is reacted by a single tie-down weldment. The following sections consider the bearing stress in the tie-down weldment, and the shear stresses in the welds holding the horizontal tripler plate to the doubler plate, and the doubler plate to the lower OCA flat head. Based on their relative thicknesses, assume that one-quarter the horizontal load is carried through the 1/4 inch thick OCA flat head, one-quarter is carried through the 1/4 inch thick doubler plate, and one-half is carried through the 1/2 inch thick tripler plate.

2.5.2.4.1 Bearing Stress in the Tie-down Weldment

The horizontal load, F_h = 215,222 pounds, is carried from the 8.0 inch wide, trailer kickplate through the horizontal doubler and tripler plates welded inside the lower OCA flat head, as illustrated in Figure 2.5-3. For a kickplate length, L = 8 inches, a bottom shell thickness, t_s = 1/4 inch, a doubler plate thickness, t_d = 1/4 inch, and a tripler plate thickness, t_t = 1/2 inch, the area available to carry the horizontal compressive load at the kickplate interface is:

$$A = L(t_s + t_d + t_t) = (8.0)(0.25 + 0.25 + 0.5) = 8.0 \text{ in}^2$$

The corresponding compressive (bearing) stress is:

$$\sigma_c = \frac{F_h}{A} = \frac{215{,}222}{8.0} = 26{,}903 \text{ psi}$$

The allowable bearing stress for the OCA outer shell, including the horizontal doubler and tripler plates, is 27,000 psi. Therefore, the margin of safety is:

$$MS = \frac{27{,}000}{26{,}903} - 1 = +0.004$$

2.5.2.4.2 Shear Stress in the Tripler Plate Welds

Based on the assumed load distribution in Section 2.5.2.4, *Tie-down Stresses Due to a Horizontal Compressive Load*, the force on the welds attaching the tripler plate to the doubler plate is then one-half of 215,222 pounds, or 107,611 pounds. The tripler plate is welded with 3/8 inch fillet welds along three of its edges, and a 1/2 inch groove weld along the outer edge. The two side welds are approximately 8 inches long, and the back weld is 7 inches long, for a total, 3/8 inch fillet weld length of 23 inches. Four, 1½ inch diameter, 3/8 inch fillet welds supplement the peripheral 3/8 inch fillet welds, providing an additional $4 \times \pi(1.5) = 18.85$ inches of 3/8 inch fillet weld. Thus, the total 3/8 inch fillet weld length is 41.85 inches. In addition, the 10 inch long outer edge is welded with a 1/2 inch groove weld. The resulting weld shear area is:

$$A_s = (0.375)(\sin 45^\circ)(41.85) + (0.5)(10) = 16.1 \text{ in}^2$$

Thus, the shear stress in the tripler plate fillet welds is:

$$\tau = \frac{107{,}611}{16.1} = 6{,}684 \text{ psi}$$

The allowable shear stress for the tripler plate welds is 16,200 psi. Therefore, the margin of safety is:

$$MS = \frac{16{,}200}{6{,}684} - 1 = +1.42$$

As an option, the tripler plate may be one inch thick, and welded into a cutout through the 1/4 inch thick, lower OCA flat head and 1/4 inch thick, doubler plate in the same orientation and location as shown in Figure 2.5-6. Full penetration groove welds are used around the periphery of the tripler plate (i.e., a one inch groove weld along the outside, 10 inch long edge, and 1/2 inch groove welds along the remaining three edges). The two side welds are approximately 8 inches long, and the back weld is 7 inches long, for a total weld length of 23 inches. The resulting weld shear area is:

$$A = (0.5)(23) + (1.0)(10) = 21.5 \text{ in}^2$$

Thus, the shear stress in the tripler plate groove welds is:

$$\tau = \frac{215{,}222}{21.5} = 10{,}010 \text{ psi}$$

The allowable shear stress for the tripler plate welds is 16,200 psi. Therefore, the margin of safety is:

$$MS = \frac{16{,}200}{10{,}010} - 1 = +0.62$$

2.5.2.4.3 Shear Stress in the Doubler Plate Welds

Based on the assumed load distribution in Section 2.5.2.4, *Tie-down Stresses Due to a Horizontal Compressive Load*, the force on the welds attaching the doubler plate to the OCA flat head is then one-half plus one-quarter of 215,222 pounds, or 161,417 pounds. The doubler plate is welded with 1/4 inch fillet welds along its four inner edges, for a total 1/4 inch fillet weld length of approximately 35 inches. Eighteen, 1 inch diameter, 1/4 inch fillet welds supplement the peripheral 1/4 inch fillet welds, providing an additional $18 \times \pi(1.0) = 56$ inches of 1/4 inch fillet weld. Thus, the total 1/4 inch fillet weld length is 91 inches. In addition, the 20 inch long outer edge is welded with a 1/4 inch groove weld. The resulting weld shear area is:

$$A_s = (0.25)(\sin 45^\circ)(91) + (0.25)(20) = 21.1 \text{ in}^2$$

Thus, the shear stress in the doubler plate fillet welds is:

$$\tau = \frac{161{,}417}{21.1} = 7{,}650 \text{ psi}$$

The allowable shear stress for the doubler plate welds is 16,200 psi. Therefore, the margin of safety is:

$$MS = \frac{16{,}200}{7{,}650} - 1 = +1.12$$

2.5.2.5 Response of the Package if Treated as a Fixed Cantilever Beam

The preceding sections considered stresses in a localized region in and around the tie-down components. This section demonstrates that a more global response of the TRUPACT-II package to tie-down loads is also acceptable. For this assessment, the TRUPACT-II package is treated as a cantilever beam, fixed at its base. The 1/4 inch thick, OCA outer shell is conservatively assumed to be the only structural member resisting the applied 10*g*, 5*g* and 2*g* inertia loads. Stress intensity, SI, in the OCA outer shell is determined as follows:

$$SI = 2\sqrt{\left(\frac{\sigma}{2}\right)^2 + \tau^2} = \sqrt{\left(\frac{P}{A} + \frac{Mc}{I}\right)^2 + \left(\frac{2V}{A}\right)^2}$$

where for 2*g* vertically, the axial force, P = (2)(19,250) = 38,500 pounds, the bending moment from Section 2.5.2.1, *Tie-down Forces*, $M = HF_g$ = (60)(215,222) = 12,913,320 in-lbs, the extreme fiber distance, c = ½(94⅜) = 47.2 inches, the horizontal shear force, $V = F_g$ = 215,222 pounds, the OCA outer shell cross-sectional area, $A = (\pi/4)[(94.375)^2 - (93.875)^2] = 74$ in^2, and the OCA outer shell moment of inertia, $I = (\pi/64)[(94.375)^4 - (93.875)^4] = 81{,}869$ in^4. The resulting stress intensity is:

$$SI = \sqrt{\left(\frac{38{,}500}{74} + \frac{(12{,}913{,}320)(47.2)}{81{,}869}\right)^2 + \left(\frac{2(215{,}222)}{74}\right)^2} = 9{,}863 \text{ psi}$$

The allowable stress intensity for the OCA outer shell is 27,000 psi. Therefore, the margin of safety is:

$$MS = \frac{27{,}000}{9{,}863} - 1 = +1.74$$

2.5.2.6 Summary

All margins of safety for tie-down loads, per 10 CFR §71.45(b)(1), are positive. The smallest tensile or shear margin of safety, MS = +0.31, is for failure of the welds attaching the tie-down lug to the doubler plate, indicating that this will be the mode of failure for the tie-downs under an excessive load condition. Note that compressive modes of failure are not considered relevant in the excessive load evaluation. In accordance with 10 CFR §71.45(b)(3), this failure mode does not compromise the performance capabilities of the TRUPACT-II package since no main shell is breached. Finally, it is noted that the forklift pockets and OCA lifting sockets are not intended to be used as tie-down devices, and are appropriately disabled to prevent inadvertent use. The forklift pockets and OCA lifting sockets are disabled by affixing a plate over each pocket and a cover over the each socket respectively (see the drawings in Appendix 1.3.1, *Packaging General Arrangement Drawings*).

Figure Withheld Under 10 CFR 2.390

Figure 2.5-1 – Tie-down Device Layout

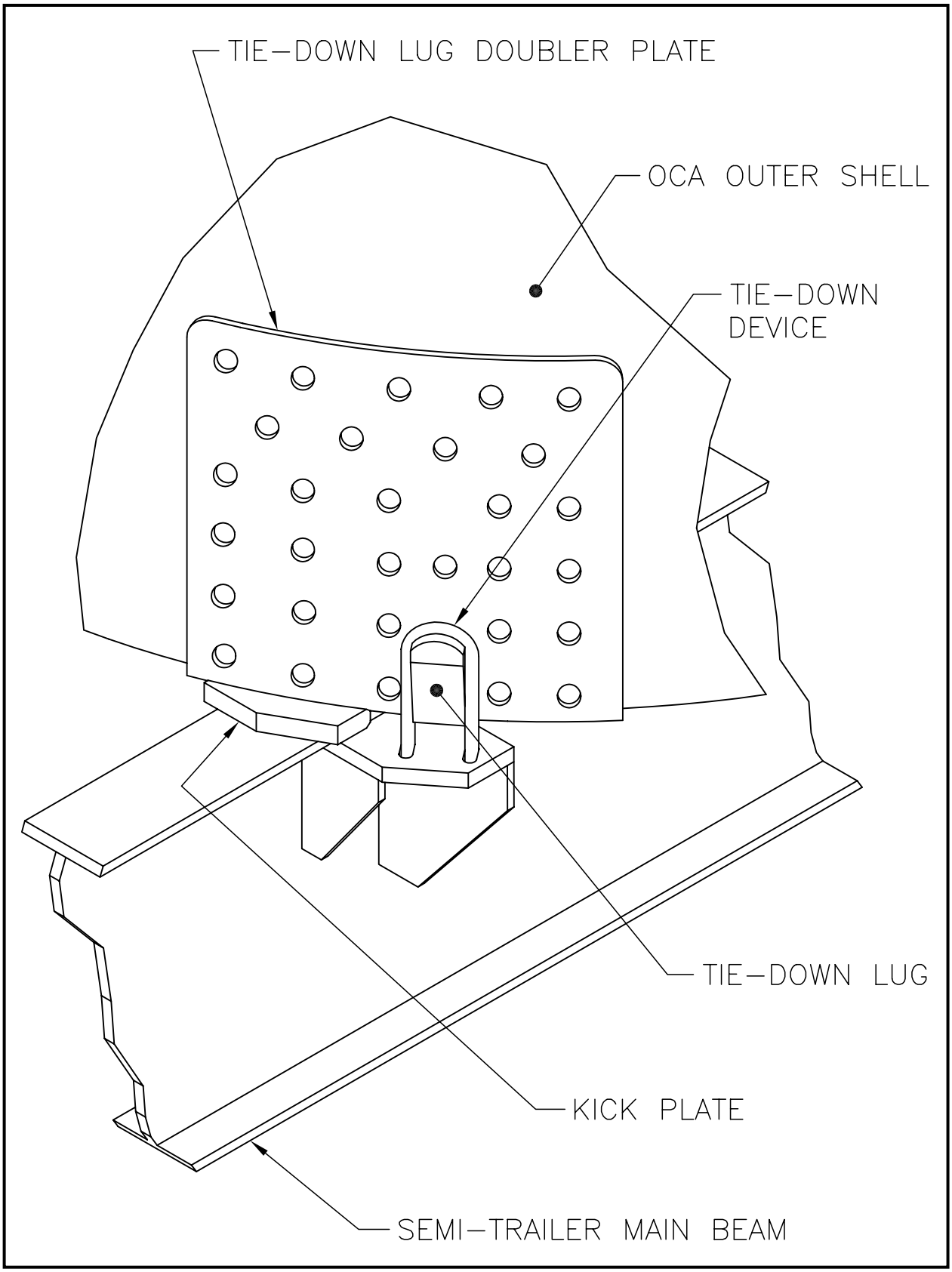

Figure 2.5-2 – Tie-down Device Detail

Figure Withheld Under 10 CFR 2.390

Figure 2.5-3 – Tie-down Plan View and Reaction Force Diagram

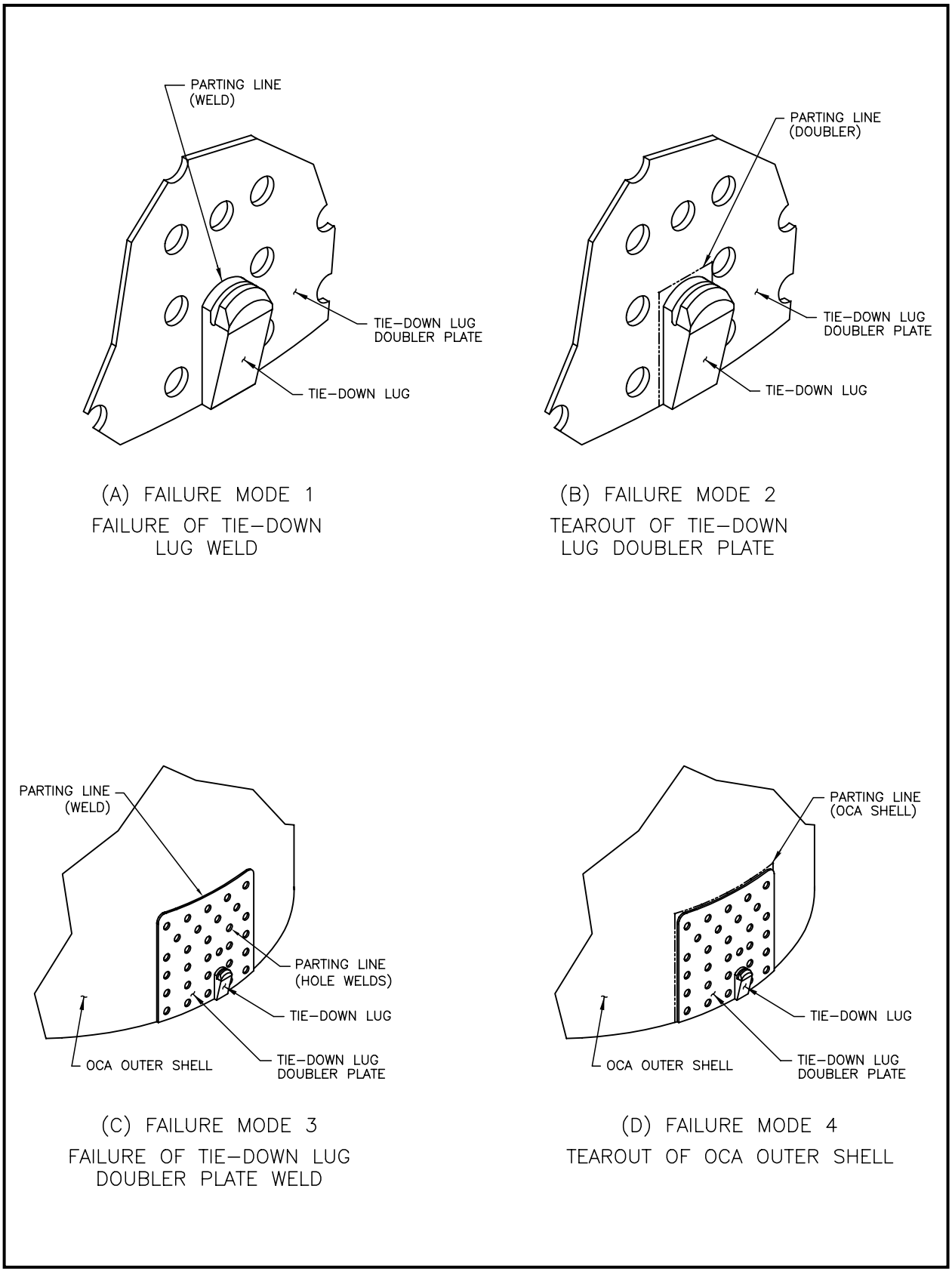

Figure 2.5-4 – Tie-down Tensile/Shear Failure Modes

Figure Withheld Under 10 CFR 2.390

Figure 2.5-5 – Tie-down Lug Dimensions and Load Diagram

Figure Withheld Under 10 CFR 2.390

Figure 2.5-6 – Horizontal Doubler and Tripler Plate Details

This page intentionally left blank.

2.6 Normal Conditions of Transport

The TRUPACT-II package, when subjected to the normal conditions of transport (NCT) specified in 10 CFR §71.71[1], is shown to meet the performance requirements specified in Subpart E of 10 CFR 71. As discussed in the introduction to this chapter, with the exception of the NCT free drop, the primary proof of NCT performance is via analytic methods. Regulatory Guide 7.6[2] criteria are demonstrated as acceptable for all NCT analytic evaluations presented in this section. Specific discussions regarding brittle fracture and fatigue are presented in Section 2.1.2.2, *Miscellaneous Structural Failure Modes*, and are shown not to be limiting cases for the TRUPACT-II package design. The ability of the butyl O-ring containment seals to remain leaktight is documented in Appendix 2.10.2, *Elastomer O-ring Seal Performance Tests*.

With the exception of the NCT free drop evaluation, analyses for heat, cold, reduced external pressure, increased external pressure, and vibration are performed in this section. Allowable stress limits are consistent with Table 2.1-1 and Table 2.1-2 in Section 2.1.2.1, *Analytic Design Criteria (Allowable Stresses)*, using temperature-adjusted material properties taken from Table 2.3-1 from Section 2.3.1, *Mechanical Properties Applied to Analytic Evaluations*.

For the analytic assessments performed within this section, properties for Type 304 stainless steel are based on data in Table 2.3-1 from Section 2.3.1, *Mechanical Properties Applied to Analytic Evaluations*. Similarly, the bounding values for polyurethane foam compressive strength are based on data in Table 2.3-2 from Section 2.3.1, *Mechanical Properties Applied to Analytic Evaluations*. Polyurethane foam compressive strength is further adjusted ±15% to account for manufacturing tolerance. At elevated NCT temperatures (i.e., 160 ºF), the nominal compressive strength is reduced 25% for elevated temperature effects and reduced 15% for manufacturing tolerance. At reduced NCT temperatures (i.e., -40 ºF), the nominal compressive strength is increased 50% for reduced temperature effects and increased 15% for manufacturing tolerance.

Properties of Type 304 stainless steel and polyurethane foam are summarized below.

Material Property	Material Property Value (psi)			Reference
	-40 ºF	70 ºF	160 ºF	
Type 304 Stainless Steel				
Elastic Modulus, E	28.8×10^6	28.3×10^6	27.8×10^6	Table 2.3-1
Design Stress Intensity, S_m	20,000	20,000	20,000	
Yield Strength, S_m	N/A	30,000	27,000	
Polyurethane Foam Compressive Strength				
Parallel-to-Rise Direction, σ_c	405	235	150	Table 2.3-2
Perpendicular-to-Rise Direction, σ_c	336	195	124	

[1] Title 10, Code of Federal Regulations, Part 71 (10 CFR 71), *Packaging and Transportation of Radioactive Material*, 01-01-07 Edition.

[2] U. S. Nuclear Regulatory Commission, Regulatory Guide 7.6, *Design Criteria for the Structural Analysis of Shipping Cask Containment Vessels*, Revision 1, March 1978.

Finite element analysis methods are utilized to determine stresses in the TRUPACT-II packaging structure at various temperature extremes, including the effects of differential thermal expansion, when appropriate, and internal (I) and external (E) pressure combinations, as summarized below.

Load Case Number	Reference Section	Differential Expansion?	Pressure Differential	Temperature		Table Number	Figure Numbers
				Uniform	Reference		
OCA Case 1	§2.6.1	No	61.2 psig (I)	160 ºF	160 ºF	2.6-1	2.6-1/-2
OCA Case 2	§2.6.1	Yes	61.2 psig (I)	160 ºF	70 ºF	2.6-2	2.6-3/-4
OCA Case 3	§2.6.2	Yes	0 psig	-40 ºF	70 ºF	2.6-3	2.6-5/-6
OCA Case 4	§2.6.4	No	14.7 psig (E)	70 ºF	70 ºF	2.6-4	2.6-7/-8
ICV Case 1	§2.6.1	No	61.2 psig (I)	160 ºF	160 ºF	2.6-5	2.6-9/-10
ICV Case 2	§2.6.4	No	14.7 psig (E)	70 ºF	70 ºF	2.6-6	2.6-11/-12

For the NCT free drop evaluation, a certification test program was undertaken using three TRUPACT-II certification test units (CTUs). Results from certification testing demonstrated that under NCT free drop conditions, two leaktight levels of containment were maintained. NCT certification testing also demonstrated the TRUPACT-II package's ability to survive subsequent HAC, 30 foot free drop, puncture, and fire tests was not compromised. Analyses are performed, when appropriate, to supplement or expand on the available test results. This combination of analytic and test, structural evaluations provides an initial configuration for NCT thermal, shielding and criticality performance. In accordance with 10 CFR §71.43(f), the evaluations performed herein successfully demonstrate that under NCT tests the TRUPACT-II package experiences "no substantial reduction in the effectiveness of the packaging". Summaries of the more significant aspects of the full scale free drop testing are included in Section 2.6.7, *Free Drop*, with details presented in Appendix 2.10.3, *Certification Tests*.

2.6.1 Heat

The NCT thermal analyses presented in Section 3.4, *Thermal Evaluation for Normal Conditions of Transport*, consists of exposing the TRUPACT-II package to direct sunlight and 100 ºF still air per the requirements of 10 CFR §71.71(b). Although the actual internal heat load is a function of the particular payload configuration being transported, this section utilizes the maximum internal heat allowed within a TRUPACT-II package, or 40 thermal watts. The 40-thermal watt case results in maximum temperature gradients throughout the TRUPACT-II package.

2.6.1.1 Summary of Pressures and Temperatures

The maximum normal operating pressure (MNOP) is 50 psig, as determined in Section 3.4.4, *Maximum Internal Pressure*. The pressure stress analyses within this section combine the internal pressure of 50 psig due to MNOP with a reduced external pressure, per 10 CFR §71.71(c)(3), of 3.5 psia (11.2 psig). The net resulting internal pressure utilized in all NCT structural analyses considering internal pressure is therefore 61.2 psig.

The NCT heat input results in modest temperatures and temperature gradients throughout the TRUPACT-II package. Maximum temperatures for the major packaging components are

summarized in Table 3.4-1 from Section 3.4.2, *Maximum Temperatures*. As shown in Table 3.4-1, all packaging temperatures remain at or below 156 ºF. For conservatism, structural analyses of the OCA and ICV utilize a uniform bounding temperature of 160 ºF. Use of a uniform bounding temperature is also conservative since material strengths are lowest at the highest temperatures. In addition, in the case of the OCA, the main contributor to thermal stress is the result of differential expansion of the polyurethane foam and the surrounding stainless steel. Also shown by the temperatures presented in Table 3.4-1, temperature gradients are modest for the NCT heat condition. Thus, temperature gradients are reasonably ignored in the analyses herein.

2.6.1.2 Differential Thermal Expansion

With NCT temperatures throughout the packaging being relatively uniform, (i.e., no significant temperature gradients), the concern with differential expansions is limited to regions of the TRUPACT-II packaging that employ adjacent materials with sufficiently different coefficients of thermal expansion. The OCA is a double-wall, composite construction of polyurethane foam between inner and outer shells of stainless steel. The polyurethane foam expands and contracts to a much greater degree than the surrounding stainless steel shells resulting in stresses due to differential thermal expansion. Finite element analyses presented in the following sections quantify these differential thermal expansion stresses. Differential thermal expansion stresses are negligible in the ICV for three reasons: 1) the temperature distribution throughout the entire ICV is relatively uniform, 2) the ICV is fabricated from only one type of structural material, and 3) the ICV is not radially or axially constrained within a tight-fitting structure (i.e., the OCV).

2.6.1.3 Stress Calculations

A finite element model of the OCA is used to determine the stresses due to the combined effects of pressure loads, and temperature loads due to differential thermal expansion. The details of this model are presented in Appendix 2.10.1.1, *Outer Containment Assembly (OCA) Structural Analysis*. The ICV is also analyzed for the combined effects of pressure and temperature using a finite element model that is described in Appendix 2.10.1.2, *Inner Containment Assembly (ICV) Structural Analysis*. For the NCT heat condition, evaluations include two load cases for the OCA and one load case for the ICV.

Maximum stress intensities are determined for each component, and classified according to primary or secondary, membrane or bending. Classification of stress intensities is per Table NB-3217-1 of the ASME Boiler and Pressure Vessel Code[3]. Maximum stress intensities are presented for the maximum general primary membrane stress intensity, P_m, the maximum local primary membrane stress intensity, P_L, the maximum primary membrane (general or local) plus primary bending stress intensity, $P_m + P_b$ or $P_L + P_b$, and the maximum primary plus secondary stress intensity, $P_m + P_b + Q$ or $P_L + P_b + Q$.

OCA Load Case 1 (see Table 2.6-1, and Figure 2.6-1 and Figure 2.6-2): This analysis is performed at a uniform temperature of 160 ºF, but with the reference temperature also set to 160 ºF thereby eliminating any differential thermal expansion stresses. The internal pressure considers the effects of a maximum normal operating pressure (MNOP) of 50 psig, internal,

[3] American Society of Mechanical Engineers (ASME) Boiler and Pressure Vessel Code, Section III, *Rules for Construction of Nuclear Power Plant Components*, 1986 Edition.

coupled with a reduced external pressure of 3.5 psia (i.e., 11.2 psig, internal). The net result is an internal pressure of 50.0 + 11.2 = 61.2 psig.

P_m = 16,170 psi, located in the OCV shell at the cylindrical/conical transition,

P_L = 27,990 psi, located in the knuckle region of the upper OCV torispherical head,

$P_L + P_b$ = 30,810 psi, located in the upper OCV seal flange/shell transition, and

$P_L + P_b + Q$ = 37,978 psi, located in the knuckle region of the upper OCV torispherical head.

OCA Load Case 2 (see Table 2.6-2, and Figure 2.6-3 and Figure 2.6-4): This analysis is performed at a uniform temperature of 160 ºF, but with the reference temperature set to 70 ºF thereby including any differential thermal expansion stresses. As with OCA Load Case 1, the MNOP is coupled with the reduced external pressure for a net internal pressure of 61.2 psig. The use of these two cases allows primary stress intensities (from pressure loads) to be considered independently of secondary stress intensities (from differential thermal expansion loads).

$P_L + P_b + Q$ = 39,520 psi, located in the knuckle region of the lower OCV torispherical head.

ICV Load Case 1 (see Table 2.6-5, and Figure 2.6-9 and Figure 2.6-10): This analysis is performed at a uniform temperature of 160 ºF, but with the reference temperature also set to 160 ºF thereby eliminating any differential thermal expansion stresses. As with OCA Load Cases 1 and 2, the MNOP is coupled with the reduced external pressure for a net internal pressure of 61.2 psig.

P_m = 15,236 psi, located in the crown region of the upper ICV torispherical head,

P_L = 26,935 psi, located in the knuckle region of the upper ICV torispherical head,

$P_L + P_b$ = 31,310 psi, located in the upper ICV seal flange/shell transition, and

$P_L + P_b + Q$ = 38,280 psi, located in the knuckle region of the upper ICV torispherical head.

Polyurethane foam stress intensities are insignificant for OCA Load Case 1 (maximum stress intensity is 16 psi) and reach a maximum value of 197 psi for OCA Load Case 2. This highly localized, secondary stress intensity results primarily from a compressive stress parallel to the direction of foam rise and occurs where the lower Z-flange joins the OCA body outer 3/8 inch thick shell. Adjacent nodes 528, 530, and 531 have stress intensities in the range 149 - 190 psi whereas stress intensity levels at all other nodes are less than 70 psi.

For the polyurethane foam at 160 ºF, the parallel-to-rise compressive strength is 150 psi and the perpendicular-to-rise compressive strength is 124 psi. Since the calculated compressive stress in the foam exceeds its crush strength, a minor amount of highly localized permanent crushing of the foam will occur. Such localized crushing will relieve the deformation controlled polyurethane foam stresses and will not affect the overall performance of the package. In addition, a beneficial effect results because stresses are also relieved in the adjacent stainless steel shell structures.

2.6.1.4 Comparison with Allowable Stresses

Section 2.1.2, *Design Criteria*, presents the design criteria for structural evaluation of the TRUPACT-II packaging. The containment vessel design criteria for NCT analyses are in accordance with Regulatory Guide 7.6, which uses as a basis the criteria defined for Level A

service limits in Section III of the ASME Boiler and Pressure Vessel Code[4]. Load combinations follow the guidelines of Regulatory Guide 7.8[5].

From Table 2.3-1 in Section 2.3.1, *Mechanical Properties Applied to Analytic Evaluations*, the design stress intensity for Type 304 stainless steel used in the ICV and OCV is S_m = 20,000 psi at 160 ºF. From Table 2.1-1 in Section 2.1.2.1.1, *Containment Structures*, the allowable stress intensities for the NCT hot condition is S_m for general primary membrane stress intensity (P_m), $1.5S_m$ for local primary membrane stress intensity (P_L), $1.5S_m$ for primary membrane (general or local) plus primary bending stress intensity ($P_m + P_b$ or $P_L + P_b$), and $3.0S_m$ for the range of primary plus secondary stress intensity ($P_m + P_b + Q$ or $P_L + P_b + Q$).

Maximum stress intensity, allowable stress intensity, and minimum margins of safety for each stress category and each load case are presented in Table 2.6-1, Table 2.6-2, and Table 2.6-5 for each of the cases discussed above. Since all margins of safety are positive, the design criteria are satisfied.

2.6.1.5 Range of Primary Plus Secondary Stress Intensities

Per Paragraph C.4 of Regulatory Guide 7.6, the maximum range of primary plus secondary stress intensity for NCT must be less than $3.0S_m$. This limitation on stress intensity range applies to the entire history of NCT loadings and not only to the stresses from each individual load transient.

2.6.1.5.1 Range of Primary Plus Secondary Stress Intensities for the OCA

The extreme ends of the stress range are determined from OCA Load Case 2 (from Section 2.6.1, *Heat*) and OCA Load Case 4 (from Section 2.6.4, *Increased External Pressure*). One extreme, OCA Load Case 2 represents the case of maximum internal pressure coupled with reduced external pressure, plus the effect of differential thermal expansion associated with heat-up from 70 ºF to 160 ºF. The other extreme, OCA Load Case 4, considers the effect of a minimum internal pressure at 70 ºF. Note that combinations of other OCA load cases such as increased external pressure (20 psia, 5.3 psig) plus cool-down from 70 ºF to -20 ºF were also considered and found not to be bounding for the stress intensity range calculation.

The maximum range of primary plus secondary stress intensity occurs in the knuckle region of the lower OCV torispherical head (element 320). The extreme values of stress intensity are 39,520 psi and 9,219 psi from Table 2.6-2 and Table 2.6-4 for OCA Load Cases 2 and 4, respectively. Since OCA Load Cases 2 and 4 have opposite loads, the maximum range of primary plus secondary stress intensity is simply 39,520 + 9,219 = 48,739 psi. The allowable stress intensity is $3.0S_m$, where S_m = 20,000 psi for Type 304 stainless steel at 160 ºF. The margin of safety is:

$$MS = \frac{3(20{,}000)}{48{,}739} - 1 = +0.23$$

The positive margin of safety indicates that the design criterion is satisfied.

[4] American Society of Mechanical Engineers (ASME) Boiler and Pressure Vessel Code, Section III, *Rules for Construction of Nuclear Power Plant Components*, 1986 Edition.

[5] U. S. Nuclear Regulatory Commission, Regulatory Guide 7.8, *Load Combinations for the Structural Analysis of Shipping Casks for Radioactive Material*, Revision 1, March 1989.

2.6.1.5.2 Range of Primary Plus Secondary Stress Intensities for the ICV

The extreme ends of the stress range are determined from ICV Load Case 1 (from Section 2.6.1, *Heat*) and ICV Load Case 2 (from Section 2.6.4, *Increased External Pressure*). One extreme, ICV Load Case 1 represents the case of maximum internal pressure coupled with reduced external pressure, plus the effect of differential thermal expansion associated with heat-up from 70 ºF to 160 ºF. The other extreme, ICV Load Case 2, considers the effect of a minimum internal pressure at 70 ºF.

The extreme values of stress intensity are 38,280 psi and 9,105 psi from Table 2.6-5 and Table 2.6-6 for ICV Load Cases 1 and 2, respectively, conservatively ignoring the fact that the extreme values occur at locations remote from each other. Since ICV Load Cases 1 and 2 have opposite loads, the maximum range of primary plus secondary stress intensity is simply 38,280 + 9,105 = 47,385 psi. The allowable stress intensity is $3.0S_m$, where S_m = 20,000 psi for Type 304 stainless steel at 160 ºF. The margin of safety is:

$$MS = \frac{3(20{,}000)}{47{,}385} - 1 = +0.27$$

The positive margin of safety indicates that the design criterion is satisfied.

2.6.2 Cold

The NCT cold condition consists of exposing the TRUPACT-II packaging to a steady-state ambient temperature of -40 ºF. Insolation and payload internal decay heat are assumed to be zero. These conditions will result in a uniform temperature throughout the package of -40 ºF. With no internal heat load (i.e., no contents to produce heat and, therefore, pressure), the net pressure differential is assumed to be zero (14.7 psia internal, 14.7 psia external).

For the OCA, the principal structural concern due to the NCT cold condition is the effect of the differential expansion of the polyurethane foam relative to the surrounding stainless steel shells. During the cool-down from 70 ºF to -40 ºF, the foam material shrinks onto the OCV because thermal expansion coefficient for foam is greater than stainless steel. The resulting stresses are discussed in Section 2.6.2.1, *Stress Calculations*.

Differential thermal expansion stresses are negligible in the ICV for three reasons: 1) the temperature distribution throughout the entire ICV is relatively uniform, 2) the ICV is fabricated from only one type of structural material, and 3) the ICV is not radially or axially constrained within a tight-fitting structure (i.e., the OCV).

Brittle fracture at -40 ºF is addressed in Section 2.1.2.2.1, *Brittle Fracture*. Performance of the O-ring seals at -40 ºF is discussed in Appendix 2.10.2, *Elastomer O-ring Seal Performance Tests*.

2.6.2.1 Stress Calculations

A finite element model of the OCA is used to determine the stresses due to the combined effects of pressure loads, and temperature loads due to differential thermal expansion. The details of this model are presented in Appendix 2.10.1.1, *Outer Containment Assembly (OCA) Structural Analysis*. For the NCT cold condition, evaluations include one load case for the OCA.

Maximum stress intensities are determined for each component, and classified according to primary or secondary, membrane or bending. Classification of stress intensities is per Table NB-3217-1 of the ASME Boiler and Pressure Vessel Code. Membrane and membrane plus bending stresses due to differential thermal expansion are classified as secondary stresses (Q). Since there are no pressure loads, primary stresses (P_m, P_L, and $P_m + P_b$ or $P_L + P_b$) are equal to zero.

OCA Load Case 3 (see Table 2.6-3, and Figure 2.6-5 and Figure 2.6-6): This analysis is performed at a uniform temperature of -40 ºF, but with the reference temperature set to 70 ºF thereby including differential thermal expansion stresses. For a uniform temperature cold case at -40 ºF, both payload decay heat and solar heat are assumed to be zero. These conditions result in an internal pressure of 14.7 psia balanced with an external pressure of 14.7 psia, for a net pressure differential of zero.

$P_L + P_b + Q$ = 14,746 psi, located in the lower OCV shell near the stiffening ring.

Polyurethane foam stress intensities are well below the allowable crush strength for OCA Load Case 3 (maximum stress intensity is 69 psi). For the polyurethane foam at -40 ºF (+50%) and applying the manufacturing tolerance (-15%), the minimum parallel-to-rise compressive strength is 300 psi and the minimum perpendicular-to-rise compressive strength is 249 psi.

2.6.2.2 Comparison with Allowable Stresses

Section 2.1.2, *Design Criteria*, presents the design criteria for structural evaluation of the TRUPACT-II packaging. The containment vessel design criteria for NCT analyses are in accordance with Regulatory Guide 7.6, which uses as a basis the criteria defined for Level A service limits in Section III of the ASME Boiler and Pressure Vessel Code. Load combinations follow the guidelines of Regulatory Guide 7.8.

In Table 2.3-1 from Section 2.3.1, *Mechanical Properties Applied to Analytic Evaluations*, the design stress intensity for Type 304 stainless steel used in the ICV and OCV is S_m = 20,000 psi at -40 ºF. In Table 2.1-1 from Section 2.1.2.1.1, *Containment Structures*, the allowable stress intensity for the NCT cold condition is $3.0S_m$ for the range of primary plus secondary stress intensity ($P_m + P_b + Q$ or $P_L + P_b + Q$).

Maximum stress intensity, allowable stress intensity, and minimum margins of safety for each stress category and each load case are presented in Table 2.6-3 for OCA Load Case 3. Since all margins of safety are positive, the design criteria are satisfied.

Since the NCT cold condition results in shrinking of the polyurethane foam onto the OCV shell, compressive stresses develop in the OCV shell. The buckling evaluation within Section 2.6.4, *Increased External Pressure*, demonstrates that the compressive stresses due to increased external pressure do not exceed the NCT allowable stresses. The compressive stresses generated during the NCT cold condition are bounded by the NCT increased external pressure condition, therefore no explicit buckling evaluation is required for the NCT cold condition.

2.6.3 Reduced External Pressure

The effect of a reduced external pressure of 3.5 psia (11.2 psig internal pressure), per 10 CFR §71.71(c)(3), is negligible for the TRUPACT-II packaging. This conclusion is based on the analyses presented in Section 2.6.1, *Heat*, addressing the ability of both containment vessels to independently withstand a maximum normal operating pressure (MNOP) of 50 psig, combined with a reduced external pressure of 3.5 psia, for a net effective internal pressure of 61.2 psig.

2.6.4 Increased External Pressure

The effect of an increased external pressure of 20 psia (5.3 psig external pressure), per 10 CFR §71.71(c)(4), is negligible for the TRUPACT-II packaging. Both containment vessels are designed to withstand a full vacuum equivalent to 14.7 psi external pressure during acceptance leakage rate testing of the TRUPACT-II package, as described in Section 8.1.3, *Fabrication Leakage Rate Tests*. Therefore, the worst case NCT external pressure loading is 14.7 psig.

The external pressure induces small compressive stresses in the containment boundaries that are limited by stability (buckling) requirements. Buckling assessments are performed for the OCV and ICV in Section 2.6.4.3, *Buckling Assessment of the Torispherical Heads*, and Section 2.6.4.4, *Buckling Assessment of the Cylindrical Shells*.

2.6.4.1 Stress Calculations

A finite element model of the OCA is used to determine the stresses due to the effect of a pressure load. The details of this model are presented in Appendix 2.10.1.1, *Outer Containment Assembly (OCA) Structural Analysis*. The ICV is also analyzed for the effects of a pressure using a finite element model that is described in Appendix 2.10.1.2, *Inner Containment Assembly (ICV) Structural Analysis*. For the NCT increased external pressure condition, evaluations include one load case for the OCA and one load case for the ICV.

Maximum stress intensities are determined for each component, and classified according to primary or secondary, membrane or bending. Classification of stress intensities is per Table NB-3217-1 of the ASME Boiler and Pressure Vessel Code. Maximum stress intensities are presented for the maximum general primary membrane stress intensity, P_m, the maximum local primary membrane stress intensity, P_L, the maximum primary membrane (general or local) plus primary bending stress intensity, $P_m + P_b$ or $P_L + P_b$, and the maximum primary plus secondary stress intensity, $P_m + P_b + Q$ or $P_L + P_b + Q$.

OCA Load Case 4 (see Table 2.6-4, and Figure 2.6-7 and Figure 2.6-8): This analysis is performed at a uniform temperature of 70 ºF, and the reference temperature also set to 70 ºF thereby eliminating any differential thermal expansion stresses. The external pressure is 14.7 psig.

P_m = 4,621 psi, located in the OCV shell at the cylindrical/conical transition,

P_L = 6,843 psi, located in the knuckle region of the upper OCV torispherical head,

$P_L + P_b$ = 4,880 psi, located in the OCV shell at the cylindrical/conical transition, and

$P_L + P_b + Q$ = 9,322 psi, located in the knuckle region of the upper OCV torispherical head.

ICV Load Case 2 (see Table 2.6-6, and Figure 2.6-11 and Figure 2.6-12): This analysis is performed at a uniform temperature of 70 ºF, but with the reference temperature also set to 70 ºF thereby eliminating any differential thermal expansion stresses. As with OCA Load Case 4, the external pressure is 14.7 psig.

P_m = 3,636 psi, located in the crown region of the upper ICV torispherical head,

P_L = 6,382 psi, located in the knuckle region of the upper ICV torispherical head,

$P_L + P_b$ = 4,650 psi, located in the crown region of the upper ICV torispherical head, and

$P_L + P_b + Q$ = 9,105 psi, located in the knuckle region of the upper ICV torispherical head.

Polyurethane foam stress intensities are insignificant for OCA Load Case 4.

2.6.4.2 Comparison with Allowable Stresses

Section 2.1.2, *Design Criteria*, presents the design criteria for structural evaluation of the TRUPACT-II packaging. The containment vessel design criteria for NCT analyses are in accordance with Regulatory Guide 7.6, which uses as a basis the criteria defined for Level A service limits in Section III of the ASME Boiler and Pressure Vessel Code. Load combinations follow the guidelines of Regulatory Guide 7.8.

In Table 2.3-1 from Section 2.3.1, *Mechanical Properties Applied to Analytic Evaluations*, the design stress intensity for Type 304 stainless steel used in the ICV and OCV is S_m = 20,000 psi at 160 ºF. In Table 2.1-1 from Section 2.1.2.1.1, *Containment Structures*, the allowable stress intensities for the NCT increased external pressure condition is S_m for general primary membrane stress intensity (P_m), 1.5S_m for local primary membrane stress intensity (P_L), 1.5S_m for primary membrane (general or local) plus primary bending stress intensity ($P_m + P_b$ or $P_L + P_b$), and 3.0S_m for the range of primary plus secondary stress intensity ($P_m + P_b + Q$ or $P_L + P_b + Q$).

Maximum stress intensity, allowable stress intensity, and minimum margins of safety for each stress category and each load case are presented in Table 2.6-4 and Table 2.6-6 for each of the cases discussed above. Since all margins of safety are positive, the design criteria are satisfied.

2.6.4.3 Buckling Assessment of the Torispherical Heads

The buckling analysis of the torispherical heads is based on the methodology outlined in Paragraph NE-3133.4(e), *Torispherical Heads*, of the ASME Boiler and Pressure Vessel Code, Section III, Subsection NE. The results from following this methodology are summarized below.

Parameter	OCV Torispherical Head		ICV Torispherical Head	
	Upper	Lower	Upper	Lower
R	77.3125	74.1250	74.3750	73.1250
T	0.25	0.25	0.25	0.25
$A = \frac{0.125}{(R/T)}$	0.00040	0.00042	0.00042	0.00043
B[6]	5,600	5,800	5,800	5,900
$P_a = \frac{B}{(R/T)}$	18.1	19.6	19.5	20.2

The smallest allowable pressure, P_a, is 18.1 psig for the OCV upper head. For an applied external pressure of 14.7 psig, the corresponding buckling margin of safety is:

[6] Factor B is found from American Society of Mechanical Engineers (ASME) Boiler and Pressure Vessel Code, Section III, *Rules for Construction of Nuclear Power Plant Components*, Figure VII-1102-4, *Chart for Determining Shell Thickness of Cylindrical and Spherical Components Under External Pressure When Constructed of Austenitic Steel (18Cr–8Ni, Type 304)*, 1986 Edition. The 100 ºF temperature curve is used for each case.

$$MS = \frac{18.1}{14.7} - 1 = +0.23$$

Since the margin of safety in the worst case is positive, it is concluded that none of the OCV or ICV torispherical heads will buckle for an external pressure of 14.7 psig.

2.6.4.4 Buckling Assessment of the Cylindrical Shells

The cylindrical portions of the OCV and ICV are evaluated using ASME Boiler and Pressure Vessel Code Case N-284[7]. Consistent with Regulatory Guide 7.6 philosophy, a factor of safety of 2.0 is applied for NCT buckling evaluations per ASME Code Case N-284, corresponding to ASME Code, Service Level A conditions.

Buckling analysis geometry parameters are summarized in Table 2.6-7, and loading parameters are summarized in Table 2.6-8. The cylindrical shell buckling analysis utilizes an OCV and ICV temperature of 70 ºF. The stresses are determined using an external pressure of 14.7 psig. The hoop stress, σ_θ, and axial stress, σ_ϕ, are found from:

$$\sigma_\theta = \frac{Pr}{t} \qquad \sigma_\phi = \frac{Pr}{2t}$$

where P is the applied external pressure of 14.7 psi, r is the mean radius, and t is the cylindrical shell thickness. As shown in Table 2.6-9, since all interaction check parameters are less than 1.0, as required, the design criteria are satisfied.

The OCV length is conservatively measured from the ring stiffener to an assumed support point located one-third of the depth of the lower OCV torispherical head below the head-to-shell interface (i.e., 32.67 inches).

OCV Shell Ring Stiffener Axial Compression Check:

Per Paragraph –1714.1(a) of ASME Boiler and Pressure Vessel Code Case N-284, the required ring stiffener cross-section area is the larger of:

$$A_\theta \geq \left(\frac{0.334}{M_s^{0.6}} - 0.063\right)\ell_{s\phi} t = 0.076\,\text{in}^2 \qquad \textit{or} \qquad A_\theta \geq (0.06)\ell_{s\phi} t = 0.350\,\text{in}^2$$

where, from Table 2.6-7, R = 36.91 inches and t = 0.188 inches, and $M_s = \ell_{si}/(Rt)^{1/2} = 11.77$, and the length, $\ell_{s\phi}$, is the average of the distance from the stiffening ring to the lower head (32.67 inches) and the distance from the stiffening ring to the upper seal flange (29.33 inches), or $\ell_{s\phi} = \ell_{si} = ½(32.67 + 29.33) = 31.00$ inches.

The cross-section area of the stiffening ring is $A = 0.375 \times 1.5 = 0.563\ \text{in}^2$. Since $A = 0.563\ \text{in}^2 > 0.350\ \text{in}^2 = A_\theta$, the size of the stiffening ring for axial compression is acceptable.

[7] American Society of Mechanical Engineers (ASME) Boiler and Pressure Vessel Code, Section III, *Rules for Construction of Nuclear Power Plant Components*, Division 1, Class MC, Code Case N-284, *Metal Containment Shell Buckling Design Methods*, August 25, 1980, approval date.

OCV Shell Ring Stiffener Hoop Compression Check:

Per Paragraph –1714.1(b)(1) of ASME Boiler and Pressure Vessel Code Case N-284, the required moment of inertia for an intermediate stiffening ring to resist hoop compression is:

$$I_{E\theta} = \frac{(1.2)\sigma_{\theta eL}\ell_{s\phi}R_c^2 t}{E(n^2-1)} = 0.264\,\text{in}^4$$

where $\sigma_{\theta eL}$ = 11,273 psi (Table 2.6-9), $\ell_{s\phi}$ = 31.00 inches, R_c = 36.91 + 0.356 = 37.27 inches, t = 0.188 inches, E = 28.3(10)^6 psi at 70 ºF, and n^2 is:

$$n^2 = \frac{(1.875)R^{3/2}}{L_B t^{1/2}} = 15.64$$

where R = 36.91 inches (Table 2.6-7), the effective length of the OCV shell between "bulkheads" is L_B = 62.0 inches, and t = 0.188 inches (Table 2.6-7).

The effective stiffness of the ring stiffener also includes a portion of the adjacent cylindrical shell whose length is determined from Paragraph –1200 of ASME Code Case N-284 as follows:

$$\ell_{ei} = 1.56\sqrt{Rt} = 4.11\,\text{in}$$

where, from Table 2.6-7, R = 36.91 inches and t = 0.188 inches.

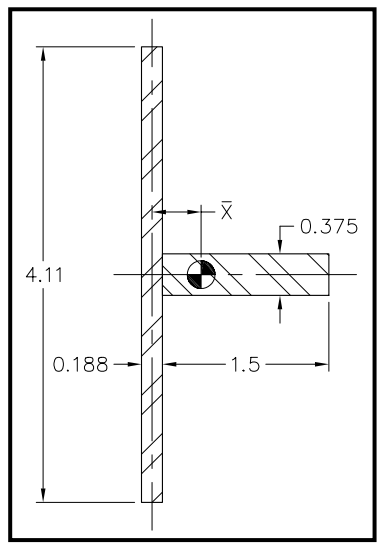

The distance to the composite stiffening ring neutral axis, $\overline{X}$, is:

$$\overline{X} = \frac{(0.375)(1.5)(0.188+1.5)}{2[(0.188)(4.11)+(0.375)(1.5)]} = 0.356\,\text{in}$$

Knowing the distance to the neutral axis of the composite stiffening ring, the ring stiffener in-plane moment of inertia is:

$$I_r = \frac{(0.375)(1.5)^3}{12} + (0.375)(1.5)\left(\frac{0.188+1.5}{2} - 0.356\right)^2 = 0.239\,\text{in}^4$$

Similarly, the shell out-of-plane moment of inertia is:

$$I_s = \frac{(4.11)(0.188)^3}{12} + (0.188)(4.11)(0.356)^2 = 0.100\,\text{in}^4$$

Combining both results, the effective moment of inertia is I_E = 0.239 + 0.100 = 0.339 in^4. Since I_E = 0.339 in^4 > 0.264 in^4 = $I_{E\theta}$, the size of the stiffening ring for hoop compression is acceptable.

2.6.5 Vibration

By comparing the alternating stresses arising during NCT with the established endurance limits of the TRUPACT-II packaging materials of construction, the effects of vibration normally incident to transport are shown to be acceptable. These comparisons apply the methodology and limits of

NRC Regulatory Guide 7.6. By conservatively comparing NCT stresses with endurance stress limits for an infinite service life, the development of accurate vibratory loading cycles is not required. The vibration evaluation is comprehensively addressed in the following sections.

2.6.5.1 Vibratory Loads Determination

ANSI N14.23[8] provides a basis for estimating peak truck trailer vibration inputs. A summary of peak vibratory accelerations for a truck semi-trailer bed with light loads (less than 15 tons) is provided in Table 2 of ANSI N14.23. The component accelerations are given in Table 2 as 1.3*g* longitudinally, 0.5*g* laterally, and 2.0*g* vertically. Three fully loaded TRUPACT-II packages on a single trailer will exceed the light load limit, but acceleration magnitudes associated with light loads are conservative for heavy loads per Table 2 of ANSI N14.23. The commentary provided within Section 4.2, *Package Response*, of ANSI N14.23 states that recent "tests conducted by Sandia National Laboratories have shown that the *truck bed* accelerations provide an upper bound on *cask* (response) accelerations." Based upon these data, conservatively assume the peak acceleration values from Table 2 are applied to the TRUPACT-II package in a continuously cycling fashion.

The compressive stress in the polyurethane foam for a 2g vertical acceleration is determined by conservatively ignoring the contributory effect of the OCA outer shell and dividing a maximum weight TRUPACT-II package (19,250 pounds) by the projected area of the package's bottom. The projected area of a TRUPACT-II package is simply $(\pi/4)(94.375)^2 = 6{,}995$ in^2. Therefore, the compressive stress is (2)(19,250)/6,995 = 6 psi. This stress is negligible compared to the parallel-to-rise compressive strength of 150 psi for polyurethane foam at 160 ºF, as discussed in Section 2.6.1, *Heat*. Therefore, the remainder of the NCT vibration evaluation addresses only the structural steel portions of the TRUPACT-II packaging.

2.6.5.2 Calculation of Alternating Stresses

The TRUPACT-II package is a compact right circular cylinder. As such, the stresses developed as a result of transportation vibration become significant only where concentrated in the vicinity of the tie-downs and package interfaces with the transport vehicle. This fact allows the stress analyses of Section 2.5.2, *Tie-down Devices*, to serve as the basis for derivation of alternating stress estimates.

The analyses of Section 2.5.2, *Tie-down Devices*, identify three maximum stress locations of importance in the immediate vicinity of the tie-down lugs:

1. **Tie-down lug weld shear stresses due to tensile tie-down forces.** Under a combined set of tie-down forces (i.e., 10*g* longitudinally, 5*g* laterally, and 2*g* vertically), the tie-down lug vertical tensile force is $F_{t\text{-}max} = 94{,}531$ pounds. The corresponding tie-down lug weld shear stress is $\tau = 12{,}334$ psi, from Section 2.5.2.2.1, *Failure of the Tie-down Lug Welds Due to Shear and Bending Loads*. Weld shear stresses associated with unit accelerations (i.e., 1*g*) are derived from these values, as presented in Table 2.6-10. Under unit horizontal and vertical accelerations, the maximum weld shear stresses are 991 psi and 628 psi, respectively, as shown in Table 2.6-10.

[8] ANSI N14.23, *Design Basis for Resistance to Shock and Vibration of Radioactive Material Packages Greater than One Ton in Truck Transport* (Draft), 1980, American National Standards Institute, Inc, (ANSI).

2. **OCA outer shell compressive membrane stresses due to vertical compressive loads.** Under a combined set of tie-down forces (i.e., 10*g* longitudinally, 5*g* laterally, and 2*g* vertically), the OCA outer shell and tie-down lug doubler plate vertical compressive load is $F_{c\text{-}max}$ = 179,509 pounds. The corresponding compressive membrane stress is σ_c = 17,260 psi, from Section 2.5.2.3.1, *Bearing Stress in the OCA Outer Shell and Tie-down Lug Doubler Plate*. Compressive membrane stresses associated with unit accelerations (i.e., 1*g*) are derived from these values, as presented in Table 2.6-11. Under unit horizontal and vertical accelerations, the maximum membrane compression stresses are 1,461 psi and 463 psi, respectively, as shown in Table 2.6-11.

3. **OCA tie-down weldment compressive membrane stresses due to horizontal compressive loads.** Under a combined set of tie-down forces (i.e., 10*g* longitudinally, 5*g* laterally, and 2*g* vertically), the OCA tie-down weldment horizontal compressive load is F_h = 215,222 pounds. The corresponding compressive membrane stress is σ_c = 26,903 psi, from Section 2.5.2.4.1, *Bearing Stress in the Tie-down Weldment*. Compressive membrane stresses associated with unit accelerations (i.e., 1*g*) are derived from these values, as presented in Table 2.6-12. Under unit horizontal accelerations, the maximum membrane compression stress is 2,406 psi, as shown in Table 2.6-12.

Alternating stress intensities, S_{alt}, due to 1*g* unit accelerations, are calculated directly from the above values since there are no other measurable stresses acting on the package at the locations considered. Unit alternating stress intensities at the three evaluated locations are found as shown in Table 2.6-13, making use of the definition of alternating stress intensity as one-half of the range of stress intensity at the location of interest, and the definition of stress intensity as twice the shear stress.

These maximum alternating stress intensity unit values correspond to the bearing stress in the tie-down weldment (horizontal component) and shear stress in the tie-down lug weld (vertical component). A stress concentration factor of four is conservatively applied in accordance with Paragraph C.3.d of Regulatory Guide 7.6. Normalizing the unit values to the peak acceleration estimates given in Section 2.6.5.1, *Vibratory Loads Determination*, and including the stress concentration factor of four and assuming these worst cases occur at the same location, results in the following conservative estimates of alternating stress intensity associated with the vibratory environments.

For the maximum horizontal alternating stress intensity of 1,203 psi from Table 2.6-13:

$$S_{alt} = 4(1{,}203)\sqrt{(1.3)^2 + (0.5)^2} = 6{,}702 \text{ psi}$$

and for the maximum vertical alternating stress intensity of 628 psi from Table 2.6-13:

$$S_{alt} = 4(628)(2.0) = 5{,}024 \text{ psi}$$

Assuming a simultaneous application of the above alternating stress intensities associated with horizontal and vertical loads yields a maximum alternating stress of 6,702 + 5,024 = 11,726 psi.

2.6.5.3 Stress Limits and Results

The permissible alternating stress intensity, S_a, is given by conservatively using the minimum asymptotic value from the design fatigue curves in Table I-9.2.2 of the ASME Boiler and Pressure Vessel Code[9]. For design fatigue curve C at 10^{11} cycles, S_a = 13,600 psi, based on an elastic modulus of $28.3(10)^6$ psi. This value, when multiplied by the ratio of the elastic modulus at 160 ºF of $27.8(10)^6$ psi to an elastic modulus at 70 ºF of $28.3(10)^6$ psi results in an allowable alternating stress intensity amplitude at 160 ºF of:

$$S_a = 13{,}600\left(\frac{27.8}{28.3}\right) = 13{,}360 \text{ psi}$$

Finally, a conservative estimate of the margin of safety for vibratory effects becomes:

$$MS = \frac{S_a}{S_{alt}} - 1 = \frac{13{,}360}{11{,}726} - 1 = +0.14$$

2.6.6 Water Spray

The materials of construction utilized for the TRUPACT-II package are such that the water spray test identified in 10 CFR §71.71(c)(6) will have a negligible effect on the package.

2.6.7 Free Drop

Since the maximum gross weight of the TRUPACT-II package is 19,250 pounds, a three-foot free drop is required per 10 CFR §71.71(c)(7). As discussed in Appendix 2.10.3, *Certification Tests*, a NCT, three-foot side drop, aligned over the OCV vent port, was performed on a TRUPACT-II package certification test unit (CTU) as an initial condition for subsequent hypothetical accident condition (HAC) tests. Leakage rate testing following certification testing demonstrated the ability of the TRUPACT-II package to maintain leaktight (i.e., 1.0×10^{-7} standard cubic centimeters per second (scc/sec), air) sealing integrity. Therefore, the requirements of 10 CFR §71.71(c)(7) are met.

2.6.8 Corner Drop

This test does not apply, since the package weight is in excess of 100 kg (220 pounds), and the materials do not include wood or fiberboard, as delineated in 10 CFR §71.71(c)(8).

2.6.9 Compression

This test does not apply, since the package weight is in excess of 5,000 kg (11,000 pounds), as delineated in 10 CFR §71.71(c)(9).

[9] American Society of Mechanical Engineers (ASME) Boiler and Pressure Vessel Code, Section III, *Rules for Construction of Nuclear Power Plant Components*, Appendix I, *Design Stress Intensity Values, Allowable Stresses, Material Properties, and Design Fatigue Curves*, 1986 Edition.

2.6.10 Penetration

The one-meter (40 inch) drop of a 13-pound, hemispherically-headed, 1¼ inch diameter, steel cylinder, as delineated in 10 CFR §71.71(c)(10), is of negligible consequence to the TRUPACT-II package. This is due to the fact that the TRUPACT-II package is designed to minimize the consequences associated with the much more limiting case of a 40 inch drop of the entire package onto a puncture bar as discussed in Section 2.7.3, *Puncture*. The 1/4 inch minimum thickness, OCA outer shell, the tie-down lugs and doubler plates, and the vent port and seal test port penetrations are not damaged by the penetration event.

Table 2.6-1 – Summary of Stress Intensity Results for OCA Load Case 1①

Component	Location	Stress Intensity (psi)			
		General Primary Membrane (P_m)	**Local Primary Membrane (P_L)**	**Primary Membrane + Bending ($P_{m/L} + P_b$)**	**Primary Plus Secondary ($P_{m/L} + P_b + Q$)**
OCV Shells	Cylindrical and Conical Shells	16,170 (Element 336)	-----	17,338 (Element 340)	-----
OCV Lower Torispherical Head	Crown	10,971 (Element 318)	-----	15,300 (Element 317)	-----
	Knuckle	-----	24,769 (Element 320)	-----	35,850 (Element 320)
OCV Upper Torispherical Head	Crown	13,360 (Element 347)	-----	18,672 (Element 348)	-----
	Knuckle	-----	27,990 (Element 345)	-----	37,978 (Element 345)
OCV Upper and Lower Seal Flanges	Shell side of the thickness transition	-----	-----	30,810 (Node 2010)	-----
	Flange side of the thickness transition	-----	-----	18,460 (Node 2016)	-----
OCV Locking Ring	Any location	-----	-----	23,040 (Node 3050)	-----
OCA Outer Shell and Z-flanges	Any location	7,986 (Element 414)	-----	13,642 (Element 414)	-----
Maximum Stress Intensity		16,170	27,990	30,810	37,978
Allowable Stress Intensity		20,000 (S_m)	30,000 ($1.5S_m$)	30,000 ($1.5S_m$)	60,000 ($3.0S_m$)
Minimum Design Margin		+0.24	+0.07	-0.03②	+0.58

Notes:

① 64.7 psia internal pressure, 3.5 psia external pressure; without differential thermal expansion (i.e., the uniform temperature is 160 ºF and the reference temperature is 160 ºF).

② Although slightly above the allowable stress intensity, this result is within the accuracy of the ANSYS® finite element model which itself is affected by element mesh size and element aspect ratio. In addition, actual pressure testing to 150% of the design pressure of 50 psig (75 psig) during the certification test program resulted in an acceptable nondestructive examination and no permanent dimensional changes to the OCV structure.

Table 2.6-2 – Summary of Stress Intensity Results for OCA Load Case 2①

Component	Location	Stress Intensity (psi)			
		General Primary Membrane (P_m)	Local Primary Membrane (P_L)	Primary Membrane + Bending ($P_{m/L} + P_b$)	Primary Plus Secondary ($P_{m/L} + P_b + Q$)
OCV Shells	Cylindrical and Conical Shells	-----	-----	-----	14,954 (Element 324)
OCV Lower Torispherical Head	Crown	-----	-----	-----	18,000 (Element 317)
	Knuckle	-----	-----	-----	39,520 (Element 320)
OCV Upper Torispherical Head	Crown	-----	-----	-----	18,514 (Element 348)
	Knuckle	-----	-----	-----	37,490 (Element 345)
OCV Upper and Lower Seal Flanges	Shell side of the thickness transition	-----	-----	-----	27,650 (Node 2010)
	Flange side of the thickness transition	-----	-----	-----	17,130 (Node 1025)
OCV Locking Ring	Any location	-----	-----	-----	22,740 (Node 3050)
OCA Outer Shell and Z-flanges	Any location	-----	-----	-----	20,581 (Element 406)
Maximum Stress Intensity		-----	-----	-----	39,520
Allowable Stress Intensity		20,000 (S_m)	30,000 ($1.5S_m$)	30,000 ($1.5S_m$)	60,000 ($3.0S_m$)
Minimum Design Margin		-----	-----	-----	+0.52

Notes:

① 64.7 psia internal pressure, 3.5 psia external pressure; with differential thermal expansion (i.e., the uniform temperature is 160 ºF and the reference temperature is 70 ºF).

Table 2.6-3 – Summary of Stress Intensity Results for OCA Load Case 3①

Component	Location	Stress Intensity (psi)			
		General Primary Membrane (P_m)	**Local Primary Membrane (P_L)**	**Primary Membrane + Bending ($P_{m/L} + P_b$)**	**Primary Plus Secondary ($P_{m/L} + P_b + Q$)**
OCV Shells	Cylindrical and Conical Shells	-----	-----	-----	14,746 (Element 331)
OCV Lower Torispherical Head	Crown	-----	-----	-----	3,048 (Element 317)
	Knuckle	-----	-----	-----	2,587 (Element 323)
OCV Upper Torispherical Head	Crown	-----	-----	-----	580 (Element 354)
	Knuckle	-----	-----	-----	3,677 (Element 342)
OCV Upper and Lower Seal Flanges	Shell side of the thickness transition	-----	-----	-----	682 (Node 2005)
	Flange side of the thickness transition	-----	-----	-----	543 (Node 2121)
OCV Locking Ring	Any location	-----	-----	-----	7 (Node 3006)
OCA Outer Shell and Z-flanges	Any location	-----	-----	-----	2,969 (Element 414)
Maximum Stress Intensity		-----	-----	-----	14,746
Allowable Stress Intensity		20,000 (S_m)	30,000 ($1.5S_m$)	30,000 ($1.5S_m$)	60,000 ($3.0S_m$)
Minimum Design Margin		-----	-----	-----	+3.07

Notes:

① 14.7 psia internal pressure, 14.7 psia external pressure; with differential thermal expansion (i.e., the uniform temperature is -40 ºF and the reference temperature is 70 ºF).

Table 2.6-4 – Summary of Stress Intensity Results for OCA Load Case 4①

Component	Location	Stress Intensity (psi)			
		General Primary Membrane (P_m)	**Local Primary Membrane (P_L)**	**Primary Membrane + Bending ($P_{m/L} + P_b$)**	**Primary Plus Secondary ($P_{m/L} + P_b + Q$)**
OCV Shells	Cylindrical and Conical Shells	4,621 (Element 336)	-----	4,880 (Element 336)	-----
OCV Lower Torispherical Head	Crown	2,780 (Element 318)	-----	4,283 (Element 317)	-----
	Knuckle	-----	6,330 (Element 320)	-----	9,219 (Element 320)
OCV Upper Torispherical Head	Crown	3,328 (Element 347)	-----	4,565 (Element 348)	-----
	Knuckle	-----	6,843 (Element 345)	-----	9,322 (Element 345)
OCV Upper and Lower Seal Flanges	Shell side of the thickness transition	-----	-----	-----	3,534 (Node 1016)
	Flange side of the thickness transition	-----	-----	4,103 (Node 1164)	-----
OCV Locking Ring	Any location	-----	-----	51 (Node 3148)	-----
OCA Outer Shell and Z-flanges	Any location	860 (Element 414)	-----	1,343 (Element 414)	-----
Maximum Stress Intensity		4,621	6,843	4,880	9,322
Allowable Stress Intensity		20,000 (S_m)	30,000 ($1.5S_m$)	30,000 ($1.5S_m$)	60,000 ($3.0S_m$)
Minimum Design Margin		+3.33	+3.38	+5.15	+5.44

Notes:

① 0.0 psia internal pressure, 14.7 psia external pressure; without differential thermal expansion (i.e., the uniform temperature is 70 ºF and the reference temperature is 70 ºF).

Table 2.6-5 – Summary of Stress Intensity Results for ICV Load Case 1①

Component	Location	Stress Intensity (psi)			
		General Primary Membrane (P_m)	**Local Primary Membrane (P_L)**	**Primary Membrane + Bending ($P_{m/L} + P_b$)**	**Primary Plus Secondary ($P_{m/L} + P_b + Q$)**
ICV Shells	Cylindrical Shells	14,827 (Element 364)	-----	21,441 (Element 365)	-----
ICV Lower Torispherical Head	Crown	14,712 (Element 299)	-----	18,910 (Element 298)	-----
	Knuckle	-----	25,853 (Element 302)	-----	36,741 (Element 301)
ICV Upper Torispherical Head	Crown	15,236 (Element 376)	-----	19,483 (Element 377)	-----
	Knuckle	-----	26,935 (Element 373)	-----	38,280 (Element 374)
ICV Upper and Lower Seal Flanges	Shell side of the thickness transition	-----	-----	31,310 (Node 2058)	-----
	Flange side of the thickness transition	-----	-----	25,930 (Node 2053)	-----
ICV Locking Ring	Any location	-----	-----	21,030 (Node 3046)	-----
Maximum Stress Intensity		15,236	26,935	31,310	38,280
Allowable Stress Intensity		20,000 (S_m)	30,000 ($1.5S_m$)	30,000 ($1.5S_m$)	60,000 ($3.0S_m$)
Minimum Design Margin		+0.31	+0.11	-0.04②	+0.57

Notes:

① 64.7 psia internal pressure, 3.5 psia external pressure; without differential thermal expansion (i.e., the uniform temperature is 160 ºF and the reference temperature is 160 ºF).

② Although slightly above the allowable stress intensity, this result is within the accuracy of the ANSYS® finite element model which itself is affected by element mesh size and element aspect ratio. In addition, actual pressure testing to 150% of the design pressure of 50 psig (75 psig) during the certification test program resulted in an acceptable nondestructive examination and no permanent dimensional changes to the ICV structure.

Table 2.6-6 – Summary of Stress Intensity Results for ICV Load Case 2①

Component	Location	Stress Intensity (psi)			
		General Primary Membrane (P_m)	**Local Primary Membrane (P_L)**	**Primary Membrane + Bending ($P_{m/L} + P_b$)**	**Primary Plus Secondary ($P_{m/L} + P_b + Q$)**
ICV Shells	Cylindrical Shells	2,354 (Element 363)	-----	2,532 (Element 364)	-----
ICV Lower Torispherical Head	Crown	3,534 (Element 299)	-----	4,542 (Element 298)	-----
	Knuckle	-----	6,210 (Element 302)	-----	8,825 (Element 301)
ICV Upper Torispherical Head	Crown	3,636 (Element 376)	-----	4,650 (Element 377)	-----
	Knuckle	-----	6,382 (Element 373)	-----	9,105 (Element 374)
ICV Upper and Lower Seal Flanges	Shell side of the thickness transition	-----	-----	-----	2,577 (Node 2054)
	Flange side of the thickness transition	-----	-----	3,561 (Node 1129)	-----
ICV Locking Ring	Any location	-----	-----	10 (Node 3141)	-----
Maximum Stress Intensity		3,636	6,382	4,650	9,105
Allowable Stress Intensity		20,000 (S_m)	30,000 ($1.5S_m$)	30,000 ($1.5S_m$)	60,000 ($3.0S_m$)
Minimum Design Margin		+4.50	+3.70	+5.45	+5.59

Notes:

① 0.0 psia internal pressure, 14.7 psia external pressure; without differential thermal expansion (i.e., the uniform temperature is 70 ºF and the reference temperature is 70 ºF).

Table 2.6-7 – Buckling Geometry Parameters per Code Case N-284

Geometry and Material Input		
	ICV	**OCV**
Mean Radius, inch	36.44	36.91
Shell Thickness, inch	0.25	0.188
Length, inch	65.70①	32.67②
Geometry Output (nomenclature consistent with ASME Code Case N-284)		
R =	36.44	36.91
t =	0.25	0.188
$(Rt)^{½}$ =	3.018	2.634
ℓ_ϕ =	65.70	32.67
ℓ_θ =	229.0	231.9
M_ϕ =	21.77	12.40
M_θ =	75.87	88.03
M =	21.77	12.40

Notes:

① The ICV length is conservatively measured from five inches below the top of the lower ICV seal flange (at the beginning of the 1/4 inch wall thickness) to an assumed support point located one-third of the depth of the lower ICV torispherical head below the head-to-shell interface.

② The OCV length is conservatively measured from the ring stiffener to an assumed support point located one-third of the depth of the lower OCV torispherical head below the head-to-shell interface. This length assumes that the ring stiffener is sized per the requirements in Paragraphs –1714.1(a) and –1714.1(b)(1) of ASME Code Case N-284.

Table 2.6-8 – Stress Results for 14.7 psig External Pressure

ICV		OCV	
Axial Stress, σ_ϕ	1,071	Axial Stress, σ_ϕ	1,443
Hoop Stress, σ_θ	2,143	Hoop Stress, σ_θ	2,886

Table 2.6-9 – Shell Buckling Summary for 14.7 psig External Pressure

Condition	ICV	OCV	Remarks
Capacity Reduction Factors (-1511)			
$\alpha_{\phi L}$ =	0.2670	0.2670	
$\alpha_{\theta L}$ =	0.8000	0.8000	
Plasticity Reduction Factors (-1610)			
η_ϕ =	1.0000	1.0000	
η_θ =	1.0000	1.0000	
Theoretical Buckling Values (-1712.1.1)			
C_ϕ =	0.6050	0.6050	
$\sigma_{\phi eL}$ =	117,464 psi	87,208 psi	
$C_{\theta h}$ =	0.0435	0.0782	
$\sigma_{\theta eL} = \sigma_{heL}$ =	8,452 psi	11,273 psi	
Elastic Interaction Equations (-1713.1.1)			
$\sigma_{\phi s}$ =	8,022 psi	10,809 psi	
$\sigma_{\theta s}$ =	5,358 psi	7,215 psi	
Axial + Hoop ⇨ Check (a):	*N/A*	*N/A*	
Axial + Hoop ⇨ Check (b):	0.435	0.473	<1 ∴ OK

Table 2.6-10 – Tie-Down Lug Weld Shear Stresses

Case and Orientation	Load Factors (*g*s)	Load (pounds)	Shear Stress (psi)
Combined	10(x), 5(y), 2(z)	94,531	12,334
Horizontal	$[10^2 + 5^2]^{1/2} = 11.18$ (unit horizontal of 1*g*)	84,906 (7,594)	11,079 (991)
Vertical	2.00 (unit vertical of 1*g*)	9,625 (4,813)	1,255 (628)

Table 2.6-11 – OCA Outer Shell Compressive Membrane Stresses

Case and Orientation	Load Factors (*g*s)	Load (pounds)	Membrane Stress (psi)
Combined	10(x), 5(y), 2(z)	179,509	17,260
Horizontal	$[10^2 + 5^2]^{1/2} = 11.18$ (unit horizontal of 1*g*)	169,884 (15,195)	16,334 (1,461)
Vertical	2.00 (unit vertical of 1*g*)	9,625 (4,813)	925 (463)

Table 2.6-12 – OCA Tie-down Weldment Compressive Membrane Stresses

Case and Orientation	Load Factors (*g*s)	Load (pounds)	Membrane Stress (psi)
Horizontal	$[10^2 + 5^2]^{1/2} = 11.18$ (unit horizontal of 1*g*)	215,222 (19,250)	26,903 (2,406)

Table 2.6-13 – Maximum Unit Alternating Stress Intensities

Case and Orientation	Alternating Stress Intensity
Lug Weld Shear	$S_{alt} = \frac{2\tau_{max}}{2}$ = 991 psi, Horizontal = 628 psi, Vertical
OCA Shell Compression	$S_{alt} = \frac{\sigma_{max}}{2}$ = 731 psi, Horizontal = 232 psi, Vertical
OCA Base Compression	$S_{alt} = \frac{\sigma_{max}}{2}$ = 1,203 psi, Horizontal
Maximum Unit Values	= 1,203 psi, Horizontal = 628 psi, Vertical

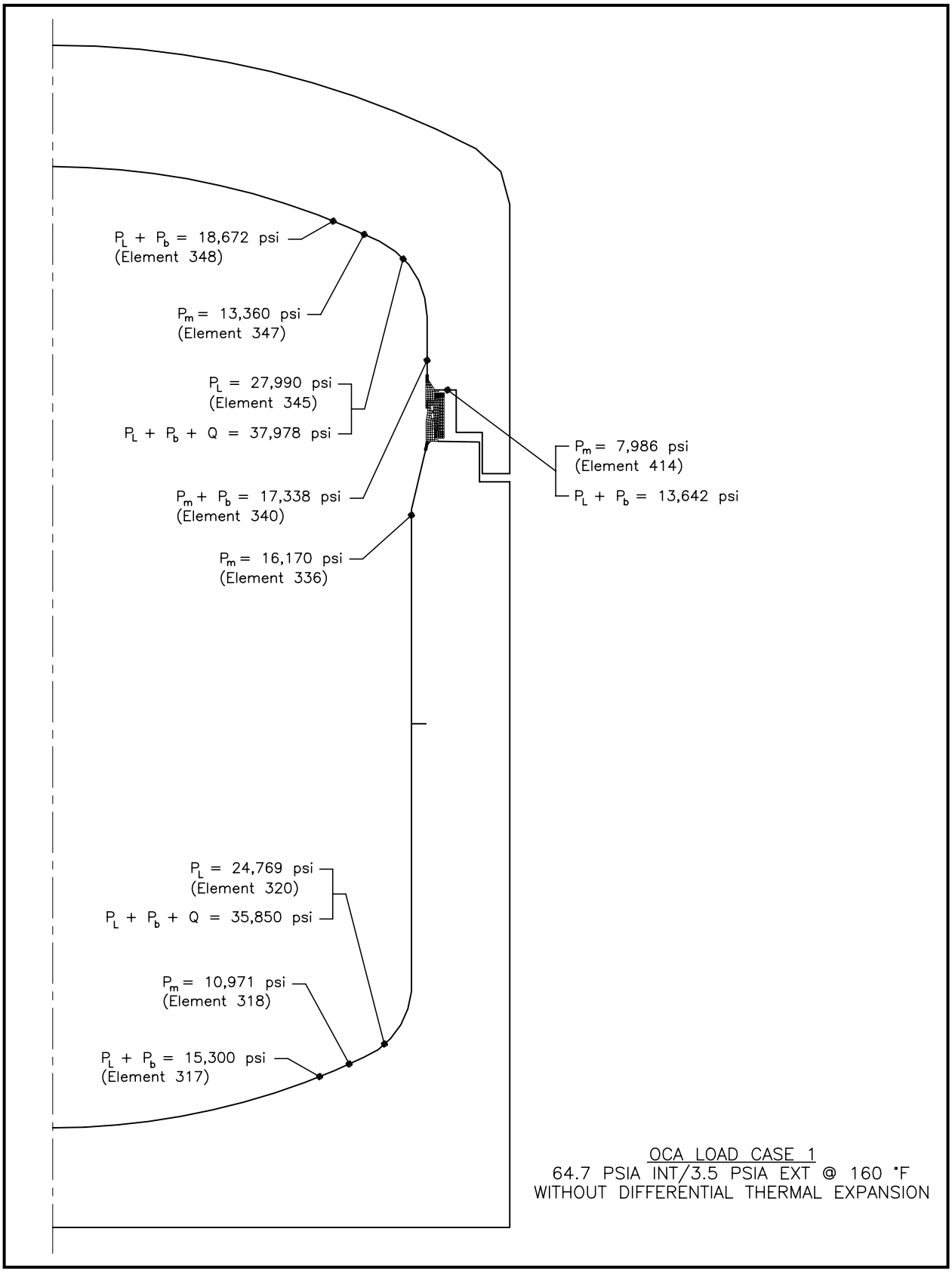

Figure 2.6-1 – OCA Load Case 1, Overall Model

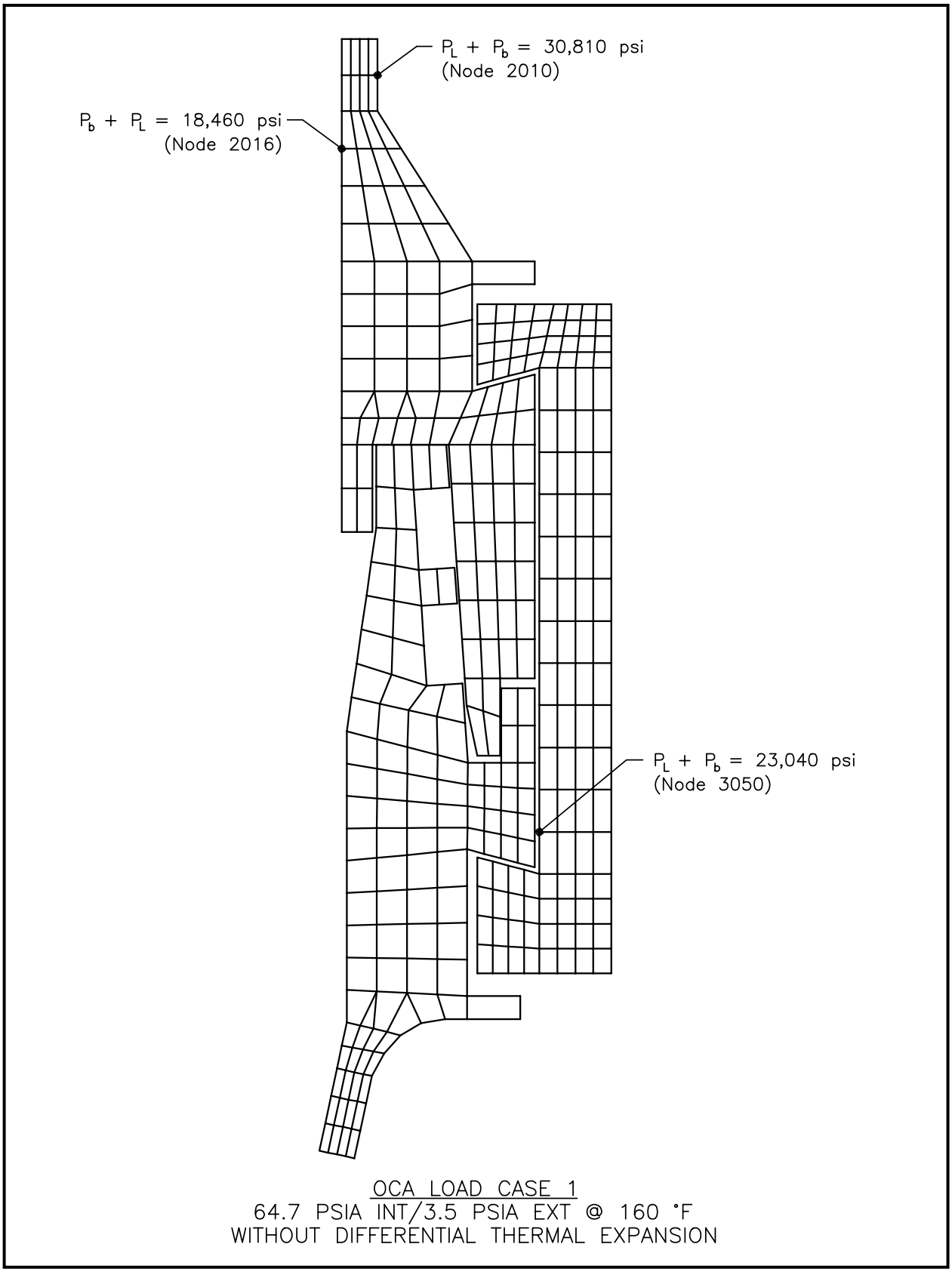

Figure 2.6-2 – OCA Load Case 1, Seal Region Detail

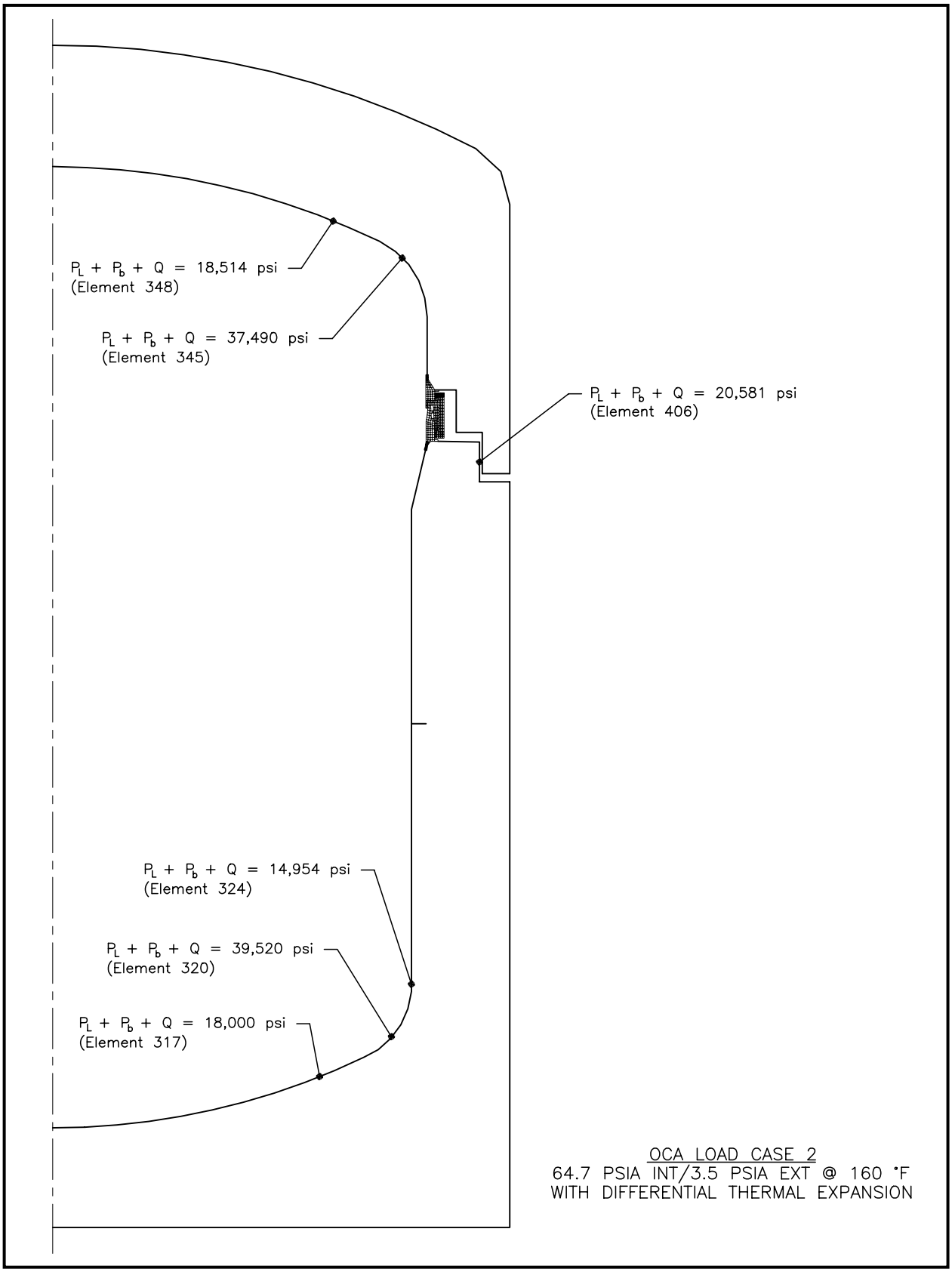

Figure 2.6-3 – OCA Load Case 2, Overall Model

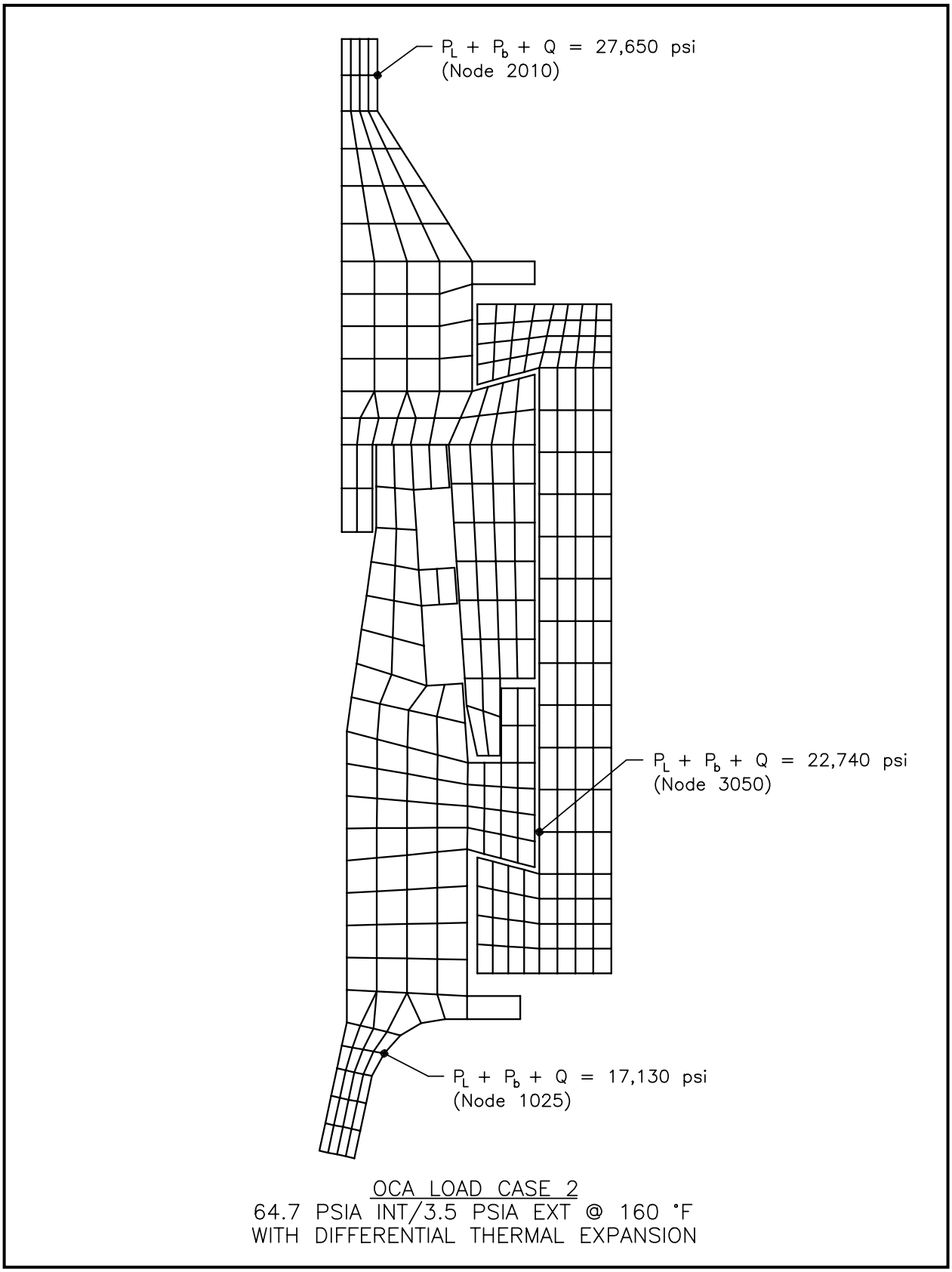

Figure 2.6-4 – OCA Load Case 2, Seal Region Detail

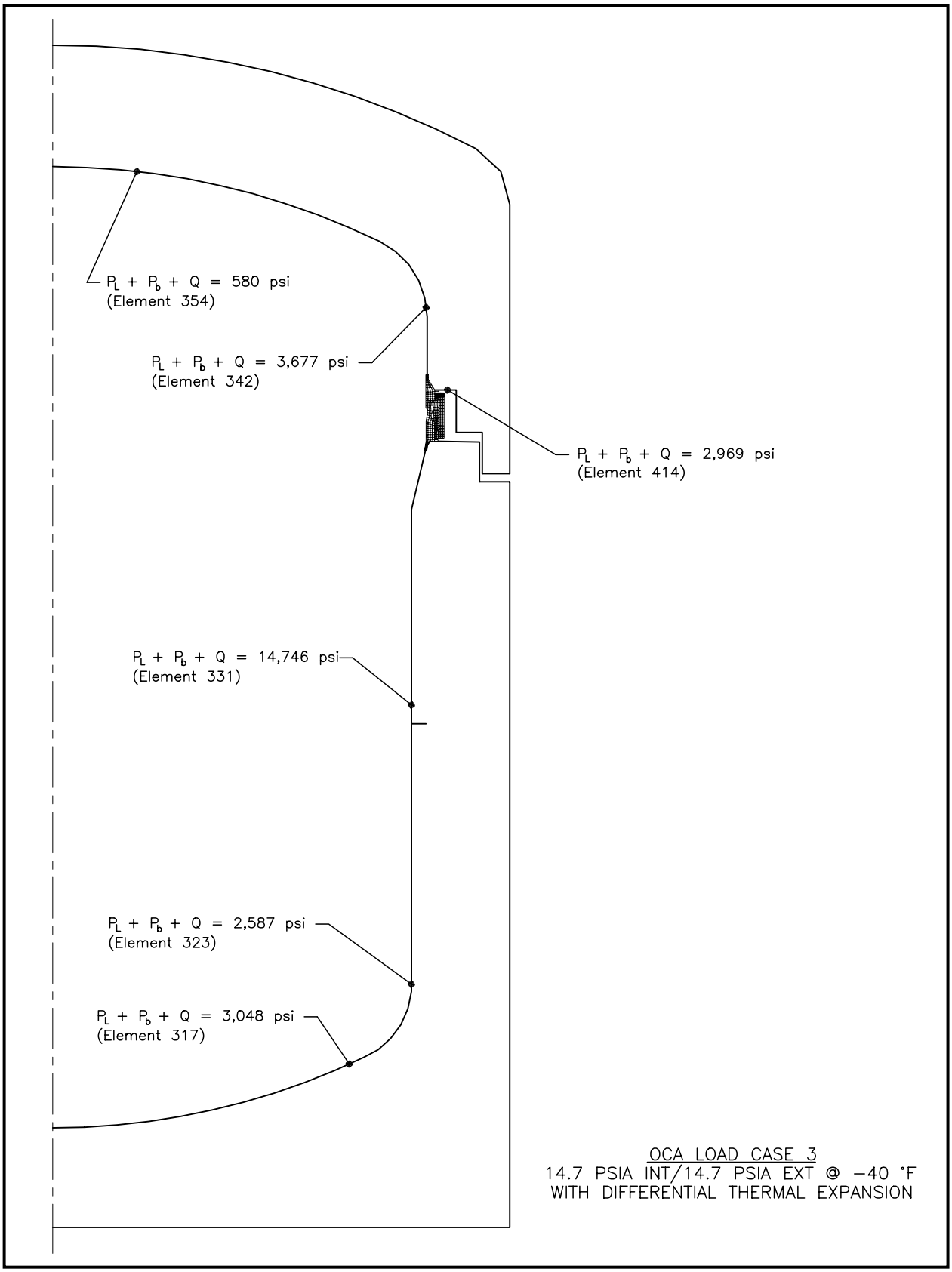

Figure 2.6-5 – OCA Load Case 3, Overall Model

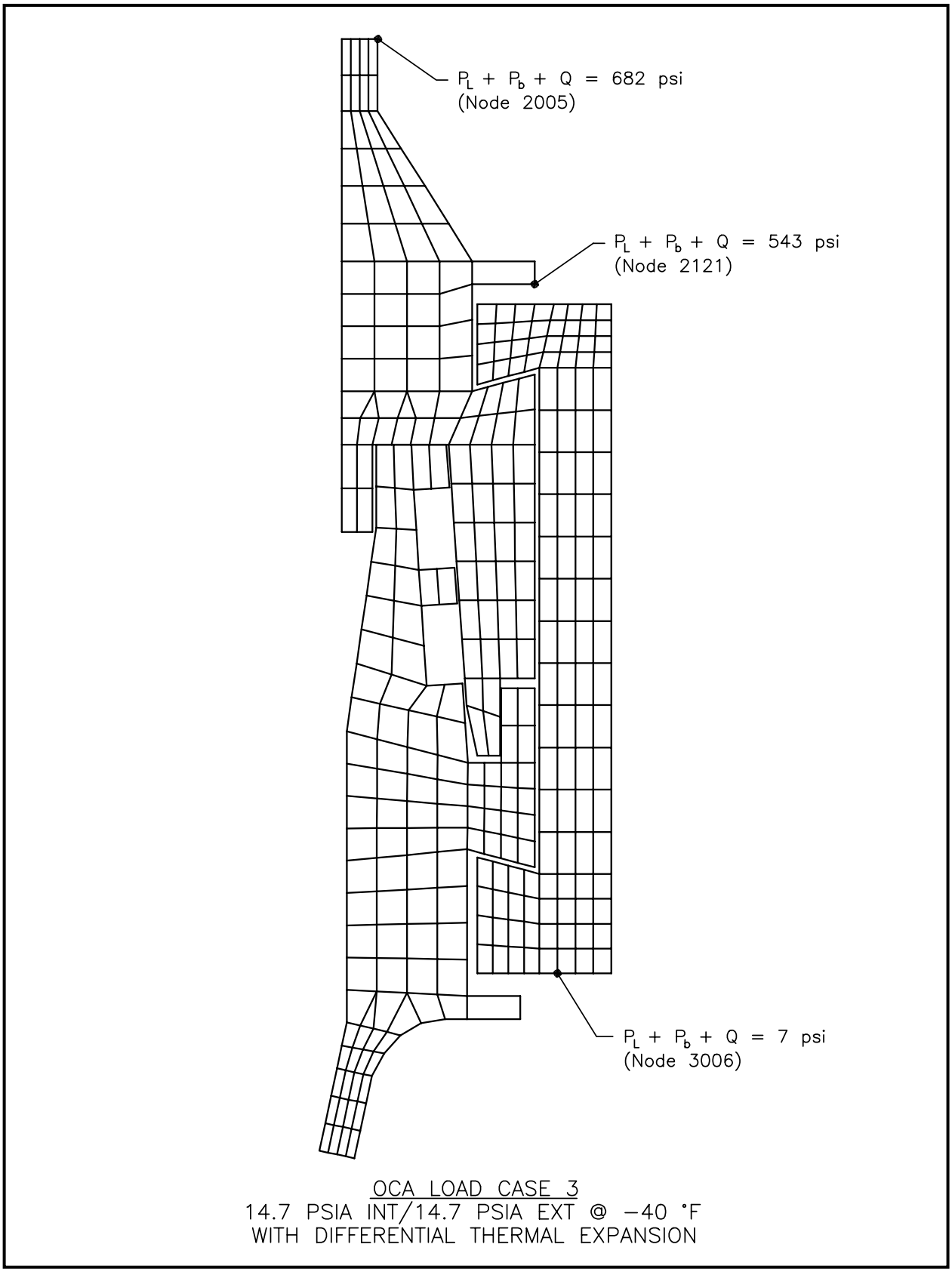

Figure 2.6-6 – OCA Load Case 3, Seal Region Detail

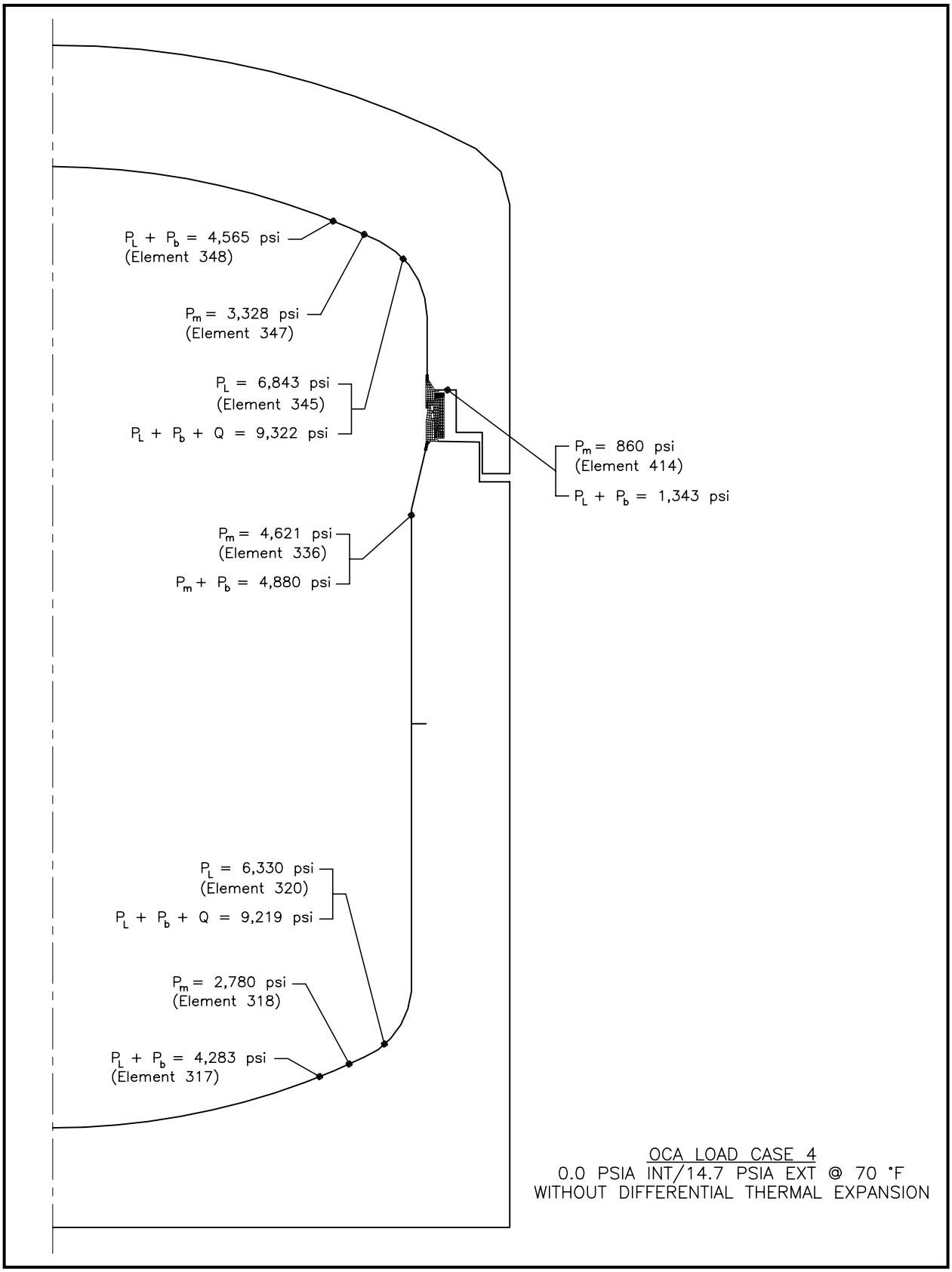

Figure 2.6-7 – OCA Load Case 4, Overall Model

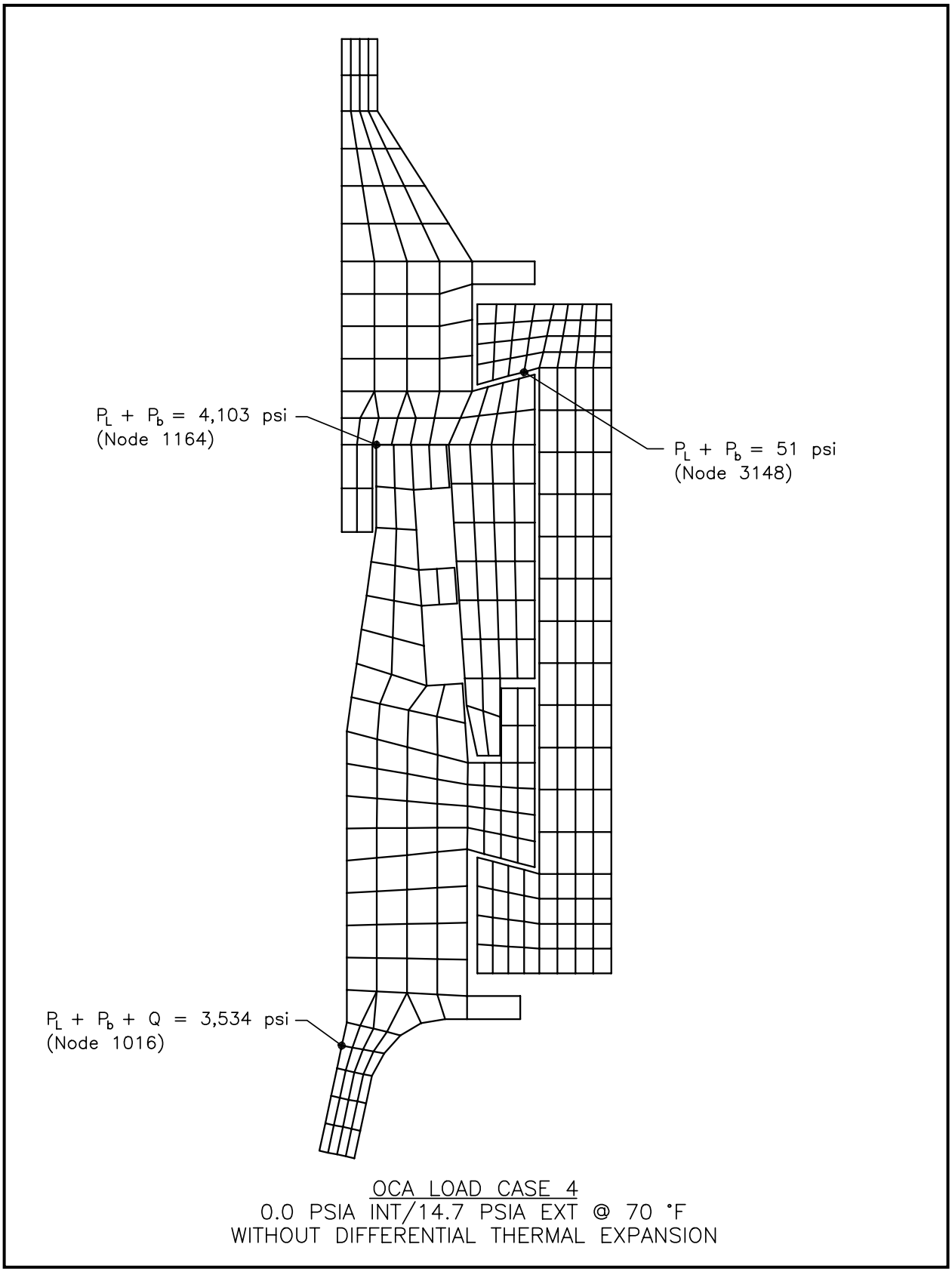

Figure 2.6-8 – OCA Load Case 4, Seal Region Detail

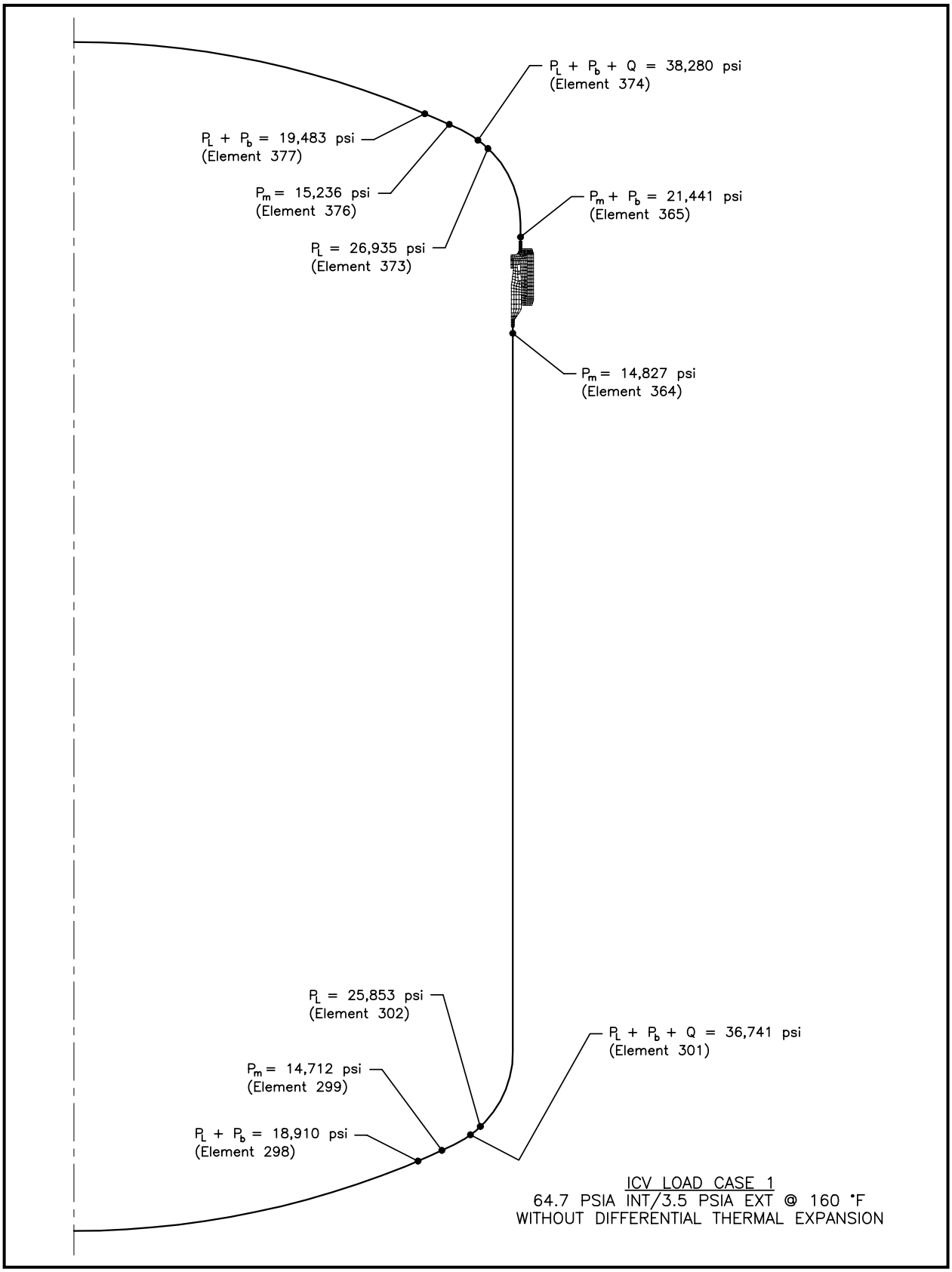

Figure 2.6-9 – ICV Load Case 1, Overall Model

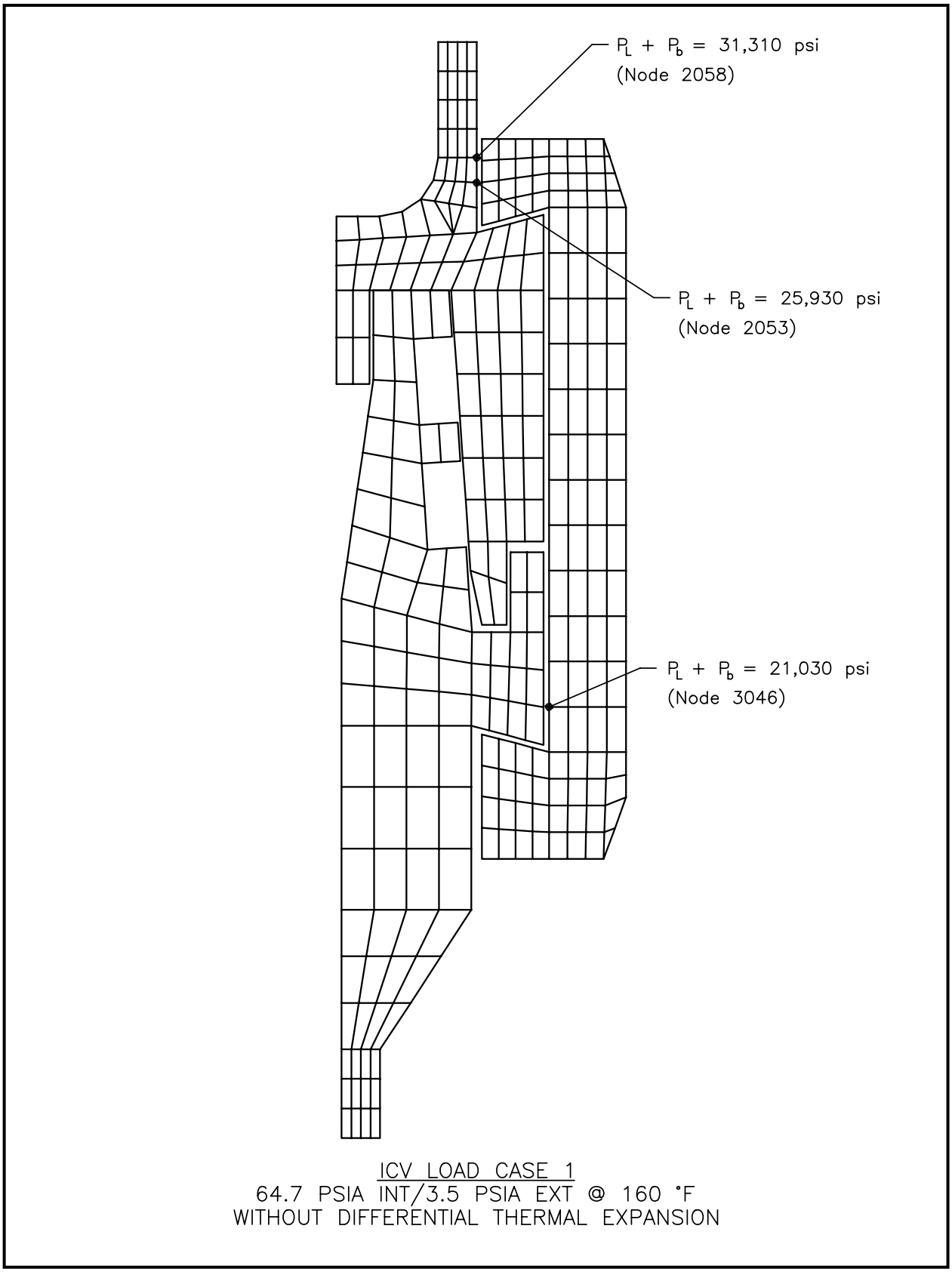

Figure 2.6-10 – ICV Load Case 1, Seal Region Detail

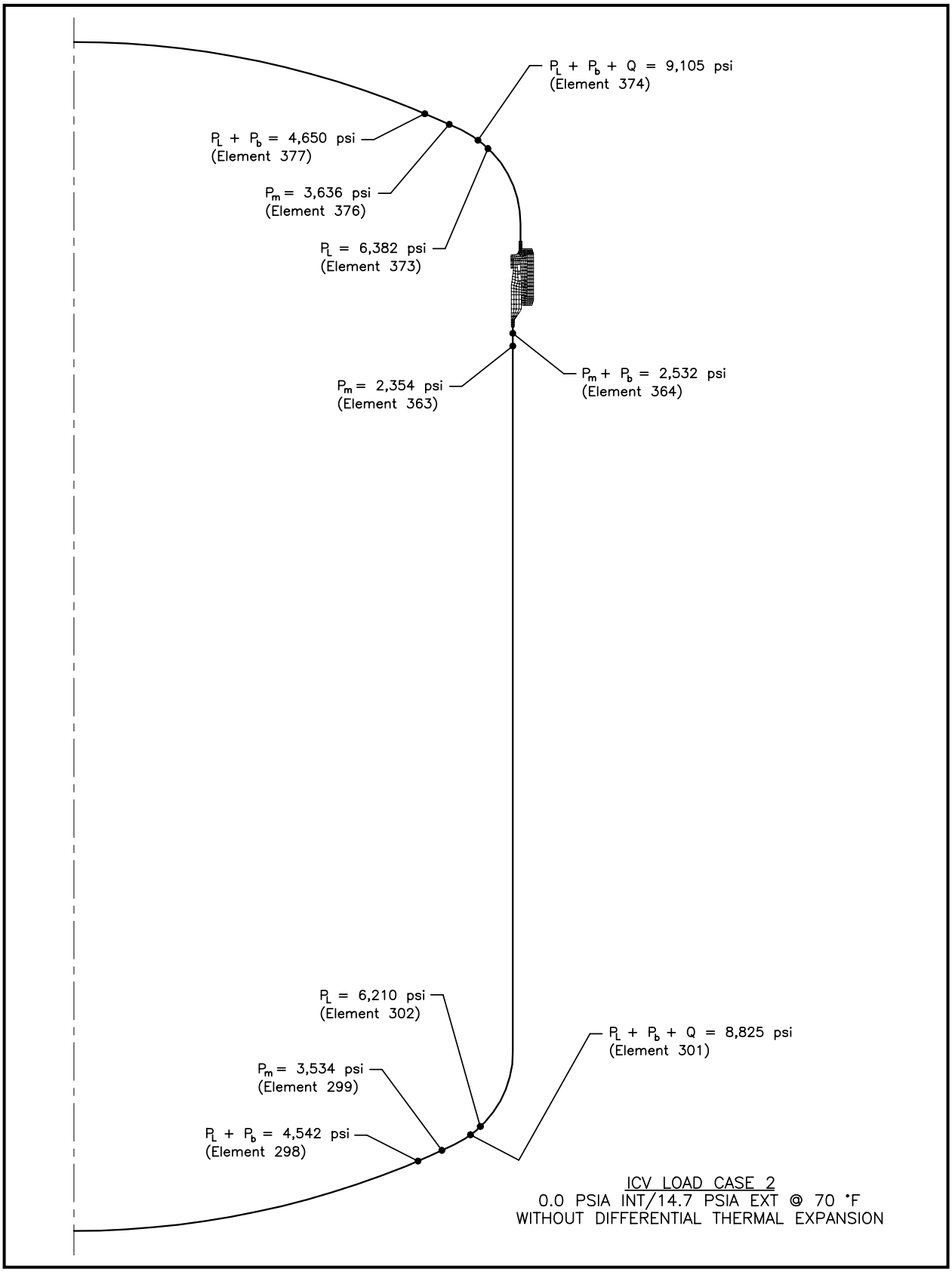

Figure 2.6-11 – ICV Load Case 2, Overall Model

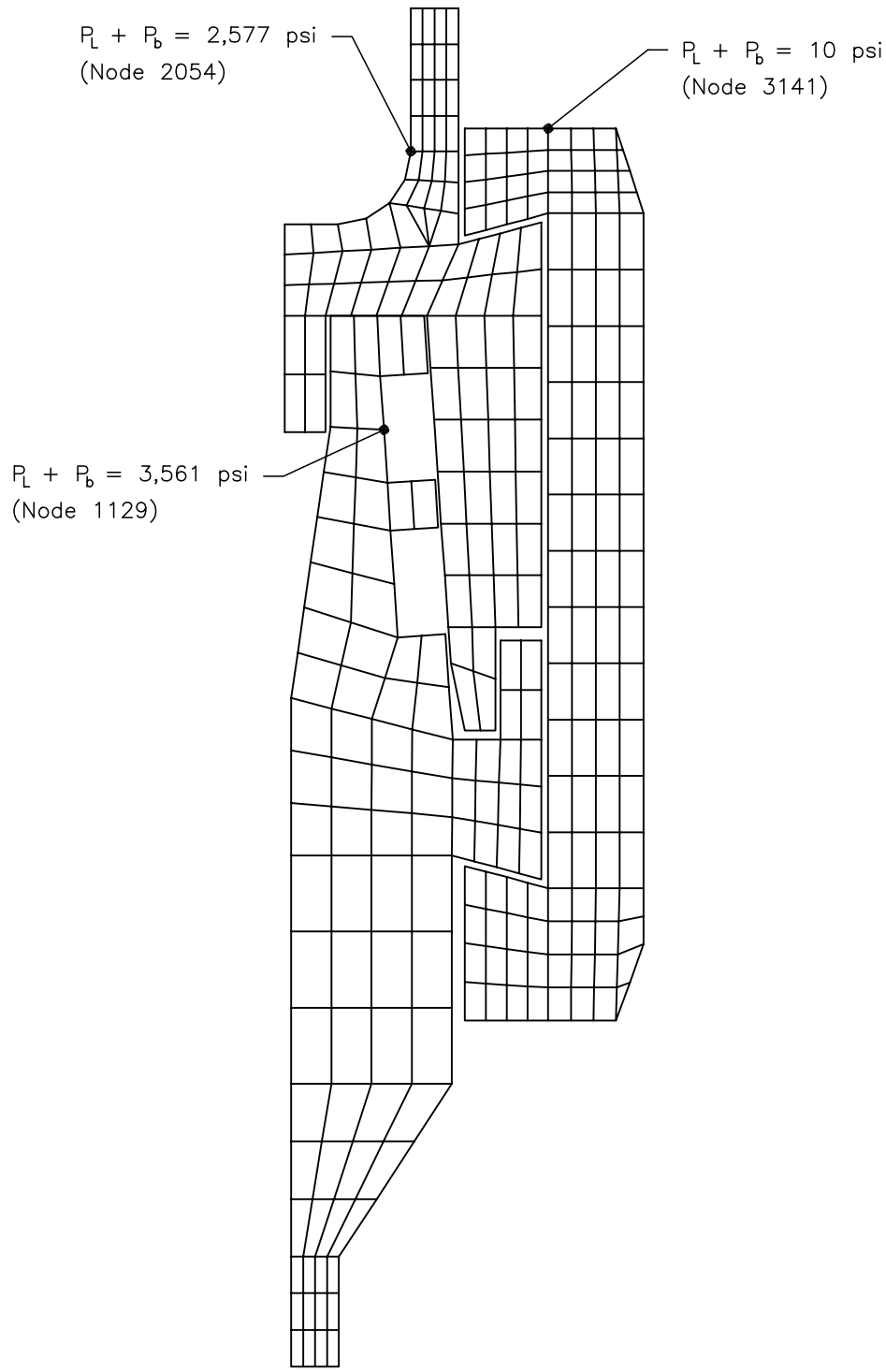

ICV LOAD CASE 2
0.0 PSIA INT/14.7 PSIA EXT @ 70 °F
WITHOUT DIFFERENTIAL THERMAL EXPANSION

Figure 2.6-12 – ICV Load Case 2, Seal Region Detail

2.7 Hypothetical Accident Conditions

The TRUPACT-II package, when subjected to the sequence of hypothetical accident condition (HAC) tests specified in 10 CFR §71.73[1], subsequent to the sequence of normal conditions of transport (NCT) tests specified in 10 CFR §71.71, is shown to meet the performance requirements specified in Subpart E of 10 CFR 71. As discussed in the introduction to Chapter 2.0, *Structural Evaluation*, with the exception of the immersion test, the primary proof of performance for the HAC tests is via the use of full-scale testing. Three certification test units (CTUs) were free drop, puncture, and fire tested (fire testing was not performed on the last CTU) to confirm that both the inner and outer containment boundaries remain leaktight after a worst-case HAC sequence. Observations from CTU testing confirm the conservative nature of the deformed geometry assumptions used in the criticality assessment provided in Chapter 6.0, *Criticality Evaluation*.

Test results are summarized in Section 2.7.8, *Summary of Damage*, with details provided in Appendix 2.10.3, *Certification Tests*. Immersion is addressed by analysis, employing acceptance criteria consistent with NRC Regulatory Guide 7.6[2].

For the analytic assessments performed within this section, properties for Type 304 stainless steel are based on data in Table 2.3-1 from Section 2.3.1, *Mechanical Properties Applied to Analytic Evaluations*. Similarly, the bounding values for the compressive strength of polyurethane foam are based on data in Table 2.3-2 from Section 2.3.1, *Mechanical Properties Applied to Analytic Evaluations*. Polyurethane foam compressive strength is further adjusted ±15% to account for manufacturing tolerance. At elevated HAC temperatures (i.e., 160 ºF), the nominal compressive strength is reduced 25% for elevated temperature effects and reduced 15% for manufacturing tolerance. At reduced HAC temperatures (i.e., -20 ºF), the nominal compressive strength is increased 40% for reduced temperature effects and increased 15% for manufacturing tolerance.

Properties of Type 304 stainless steel and polyurethane foam, as applied to analytic assessments within this section, are summarized below.

Material Property	Material Property Value (psi)			Reference
	-20 ºF	70 ºF	160 ºF	
Type 304 Stainless Steel				
Elastic Modulus, E	28.72×10^6	28.3×10^6	27.8×10^6	Table 2.3-1
Design Stress Intensity, S_m	20,000	20,000	20,000	
Yield Strength, S_m	35,000	30,000	27,000	
Polyurethane Foam Compressive Strength				
Parallel-to-Rise Direction, σ_c	378	235	150	Table 2.3-2
Perpendicular-to-Rise Direction, σ_c	314	195	124	

[1] Title 10, Code of Federal Regulations, Part 71 (10 CFR 71), *Packaging and Transportation of Radioactive Material*, 01-01-07 Edition.

[2] U. S. Nuclear Regulatory Commission, Regulatory Guide 7.6, *Design Criteria for the Structural Analysis of Shipping Cask Containment Vessels*, Revision 1, March 1978.

2.7.1 Free Drop

Subpart F of 10 CFR 71 requires performing a free drop test in accordance with the requirements of 10 CFR §71.73(c)(1). The free drop test involves performing a 30 foot, HAC free drop onto a flat, essentially unyielding, horizontal surface, with the package striking the surface in a position (orientation) for which maximum damage is expected. The ability of the TRUPACT-II package to adequately withstand this specified free drop condition is demonstrated via testing of three full-scale, TRUPACT-II CTUs.

2.7.1.1 Technical Basis for the Free Drop Tests

To properly select a worst-case package orientation for the 30-foot free drop event, items that could potentially compromise containment integrity, shielding integrity, and/or criticality safety of the TRUPACT-II package must be clearly identified. For the TRUPACT-II package design, the foremost item to be addressed is the ability of the containment seals to remain leaktight. Shielding integrity is not a controlling case for the reasons described in Chapter 5.0, *Shielding Evaluation*. Criticality safety is conservatively evaluated based on measured physical damage to the outer containment assembly (OCA) shells and polyurethane foam from certification testing, as described in Chapter 6.0, *Criticality Evaluation*.

The leaktight capability of the containment seals may be compromised by two methods: 1) as a result of excessive sealing surface deformation leading to reduced seal compression, and/or 2) as a result of thermal degradation of the seal material itself in a subsequent fire event. Importantly, these methods require significant impact damage to the surrounding polyurethane foam. In other words, a significant reduction in polyurethane foam thickness or a gross exposure of the foam through splits or punctures in the OCA outer shell would have to occur near the main O-ring seal or vent port seal region.

Additional items for consideration include the possibility of separating the OCA lid from the OCA body (or significantly opening up the nominal 1/2 inch gap which exists between the upper and lower z-flanges at the lid to body interface), and buckling of the outer containment vessel (OCV) or inner containment vessel (ICV) from a bottom end drop.

For the above reasons, testing must include impact orientations that affect the upper end of the TRUPACT-II package, with particularly emphasis in the closure region. Loads and resultant deformations occurring over the lower half of the package do not present a worst case regarding the leaktight capability of the seals or the separation of the OCA lid from the OCA body. However, as discussed above, a bottom end drop is of interest regarding the possibility of shell buckling because of the high axial acceleration forces imparted to the package.

In addition to package orientation, initial test conditions such as temperatures and pressures must be selected to complete the definition of the conditions existing at the time of a HAC free drop. In general, higher temperatures at the time of a drop test result in greater deformations and lesser acceleration loads than do lower temperatures. This is due primarily to the modest temperature sensitivity of the energy absorbing polyurethane foam used within the TRUPACT-II OCA.

Appendix 2.10.3, *Certification Tests*, provides a comprehensive report of the certification test process and results. Discussions specific to the configuration of the test units are provided in Appendix 2.10.3.4, *Description of the Certification Test Units*. Discussions specific to CTU test orientations for free drop, puncture, and fire tests, including initial test conditions, are provided

in Appendix 2.10.3.5, *Technical Basis for Tests*. Discussions specific to CTU test sequences for selected tests are provided in Appendix 2.10.3.6, *Test Sequence for Selected Free Drop, Puncture Drop, and Fire Tests*.

2.7.1.2 Test Sequence for the Selected Tests

Based on the above general discussions, the three CTUs were tested for various HAC 30-foot free drops. Although only a single "worst-case" 30-foot free drop is required by 10 CFR §71.73(c)(1), multiple 30-foot free drop tests were performed at different orientations to ensure that the most vulnerable package features were subjected to "worst-case" loads and deformations. The specific conditions selected for CTU free drop testing are summarized in Table 2.7-1, Table 2.7-2, and Table 2.7-3.

2.7.1.3 Summary of Results from the Free Drop Tests

Successful HAC free drop testing of the CTUs indicates that the various TRUPACT-II packaging design features are adequately designed to withstand the HAC 30-foot free drop event. The most important result of the testing program was the demonstrated ability of the OCV and ICV to remain leaktight[3]. Significant results of HAC free drop testing common to all test units are as follows:

- Buckling was not observed for either containment boundary shell. Additionally, accelerometers mounted directly on the OCV shell were utilized to determine the axial acceleration resulting from a 30-foot bottom end drop events on CTU Nos. 2 and 3 (see Section 2.7.1.4, *End Drop Bucking Evaluation*).
- No excessive distortion of the seal flange regions occurred for either containment vessel, although some permanent deformation was noted.
- All three (3) ICV and all six (6) OCV locking ring lock bolts remained intact and locking ring and lower seal flange tabs remained fully interlocked during and following the drop tests. Some OCA locking Z-flange-to-locking ring fasteners failed during the testing, but a sufficient number remained intact to securely retain the locking ring in the locked position. Additionally, for test purposes, only 24 fasteners were used whereas 36 are specified for the design.
- The containment boundaries were shown to be capable of maintaining pressure before, during, and after each 30-foot drop test. At the instant of impact, internal pressures in both the ICV and OCV would typically increase slightly (a few psi) for a moment and then return, within the accuracy of the instrumentation, to their initial, pre-drop test values.
- The aluminum honeycomb spacer assemblies used in the ICV upper and lower torispherical heads were shown to adequately protect the heads from damaging payload interactions.
- Rupture was not observed for the 3/8 inch thick, OCA outer shell.
- Internal pressures increased during the drops, but returned to pre-drop pressures afterward.
- Observed permanent deformations of the TRUPACT-II packaging were less than those assumed for the criticality evaluation.

[3] "Leaktight" is a leak rate not exceeding 1×10^{-7} standard cubic centimeters per second (scc/sec), air, as defined in ANSI N14.5-1997, *American National Standard for Radioactive Materials – Leakage Tests on Packages for Shipment,* American National Standards Institute, Inc. (ANSI).

A comprehensive summary of free drop test results is provided in Appendix 2.10.3.7, *Test Results*.

2.7.1.4 End Drop Bucking Evaluation

Figure 2.7-1 and Figure 2.7-2 present the axial acceleration time histories (filtered at 500 Hz) obtained from two axially oriented accelerometers located 180º apart on the OCV shell during bottom end drop event (Free Drop Test No. 2) for CTU-2. From Figure 2.7-1, a maximum acceleration of 385 *g*s results. The bottom end drop accelerations measured for CTU-3 are presented in Figure 2.7-3 and Figure 2.7-4, and show a lesser maximum impact acceleration of 335 *g*s. The CTU-2 value of 385 *g*s is therefore selected for analysis.

Although the ICV shell is slightly thicker than the OCV shell (1/4 inch versus 3/16 inch), it is the more buckling sensitive component. The OCV shell is less sensitive to buckling because it is surrounded by polyurethane foam and is reinforced by a stiffening ring located approximately at its mid-length. Under the action of 385 *g*s acceleration, the compressive stress in the 1/4 inch ICV shell at a location just above the lower torispherical head is:

$$\sigma_\phi = (385)\left(\frac{2{,}110}{2\pi(36.44)(0.25)}\right) = 14{,}192 \text{ psi}$$

where the axial ICV stress, σ_ϕ, is determined using a weight of 2,110 pounds consisting of the upper torispherical head (with honeycomb spacer), seal flanges and locking ring, and cylindrical shell. The ICV shell's cross-sectional area is $2\pi Rt$, where R = 36.44 inches, and t = 0.25 inches. Note that the hoop stress, σ_θ, and in-plane shear stress, $\sigma_{\phi\theta}$, are zero.

The cylindrical portion of the ICV is evaluated using ASME Boiler and Pressure Vessel Code Case N-284[4]. Consistent with Regulatory Guide 7.6 philosophy, a factor of safety of 1.34 is applied for HAC buckling evaluations per ASME Code Case N-284, corresponding to ASME Code, Service Level D conditions.

Buckling analysis geometry parameters are summarized in Table 2.7-4. The cylindrical shell buckling analysis utilizes an ICV temperature of -20 ºF, consistent with the temperature of the shells during the drop tests. At the -20 ºF temperature, the material's yield strength and elastic modulus are extrapolated from Table 2.3-1 in Section 2.3.1, *Mechanical Properties Applied to Analytic Evaluations*, and found to be 35,000 psi and $28.72(10)^6$ psi, respectively.

As shown in Table 2.7-5, since all interaction check parameters are less than 1.0, as required, the design criteria are satisfied.

2.7.2 Crush

Subpart F of 10 CFR 71 requires performing a dynamic crush test in accordance with the requirements of 10 CFR §71.73(c)(2). Since the TRUPACT-II package weight exceeds 1,100 pounds, the dynamic crush test is not required.

[4] American Society of Mechanical Engineers (ASME) Boiler and Pressure Vessel Code, Section III, *Rules for Construction of Nuclear Power Plant Components*, Division 1, Class MC, Code Case N-284, *Metal Containment Shell Buckling Design Methods*, August 25, 1980, approval date.

2.7.3 Puncture

Subpart F of 10 CFR 71 requires performing a puncture test in accordance with the requirements of 10 CFR §71.73(c)(3). The puncture test involves a 40 inch free drop of a package onto the upper end of a solid, vertical, cylindrical, mild steel bar mounted on an essentially unyielding, horizontal surface. The bar must be 6 inches in diameter, with the top surface horizontal and its edge rounded to a radius of not more than 1/4 inch. The package is to be oriented in a position for which maximum damage will occur. The minimum length of the bar is to be 8 inches. The ability of the TRUPACT-II package to adequately withstand this specified puncture drop condition is demonstrated via testing of three full-scale, TRUPACT-II CTUs.

2.7.3.1 Technical Basis for the Puncture Drop Tests

To properly select a worst-case package orientation for the puncture drop event, items that could potentially compromise containment integrity, shielding integrity, and/or criticality safety of the TRUPACT-II package must be clearly identified. For the TRUPACT-II package design, the foremost item to be addressed is the ability of the containment seals to remain leaktight. Shielding integrity is not a controlling case for the reasons described in Chapter 5.0, *Shielding Evaluation*. Criticality safety is conservatively evaluated based on measured physical damage to the outer containment assembly (OCA) shells and polyurethane foam from certification testing, as described in Chapter 6.0, *Criticality Evaluation*.

The leaktight capability of the O-ring seals would be most easily compromised by imposing gross deformations in the sealing region. These types of deformations are of concern from a mechanical viewpoint (i.e., leakage caused by excessive relative movement of the sealing surfaces). In addition, such deformations are of concern from a thermal viewpoint (i.e., leakage caused by thermal degradation of the butyl O-ring seals in a subsequent fire). Importantly, for mechanical damage to occur in the seal regions, the puncture event would have to result in a gross rupturing of the OCA outer shell near the O-ring seals. This could allow the puncture bar to reach and directly impact the OCA seal flanges or locking ring. Similarly, for thermal degradation of the butyl O-ring seals to occur in a subsequent fire, damage to the OCA outer shell near the O-ring seals would again have to occur as a result of the puncture event. Another item associated with the puncture event is the possibility of the puncture bar penetrating the OCA outer shell and rupturing the OCV containment boundary. Puncture is most likely to occur if the center of gravity of the package is directly in-line with the puncture bar, and the surface of the package is oriented at an angle to the bar axis. If the center of gravity of the package is not in-line with the puncture bar, puncture is less likely since package potential energy is transformed into rotational kinetic energy. Puncture is also more likely if the puncture bar impacts the package surface adjacent to a package shell weld seam. Observations from prior testing indicate that impacts with the package surface, normal to the axis of the puncture bar, will not lead to penetration of the OCA exterior shell. This is the primary reason for utilizing a torispherical head for the OCA lid. The torispherical head results in the puncture bar being oriented normal to the package surface when the center of gravity of the package is directly over the puncture bar. Further, a 3/8 inch thick, OCA outer shell is used near the closure region to ensure that no puncture will occur in this region, regardless of impact angle.

In addition to package orientation, initial test conditions such as temperatures and pressures must be selected to complete the definition of the conditions existing at the time of a HAC puncture

drop. In general, higher temperatures at the time of a puncture test result in greater deformations and lesser acceleration loads than do lower temperatures. This is due primarily to the modest temperature sensitivity of the polyurethane foam used within the TRUPACT-II OCA.

Appendix 2.10.3, *Certification Tests*, provides a comprehensive report of the certification test process and results. Discussions specific to the configuration of the test units are provided in Appendix 2.10.3.4, *Description of the Certification Test Units*. Discussions specific to orientations of the test units for free drop, puncture, and fire tests, including initial test conditions, are provided in Appendix 2.10.3.5, *Technical Basis for Tests*. Discussions specific to test sequences for selected tests for the test units is provided in Appendix 2.10.3.6, *Test Sequence for Selected Free Drop, Puncture Drop, and Fire Tests*.

2.7.3.2 Test Sequence for the Selected Tests

Based on the above general discussions, the three CTUs were tested for various HAC puncture drops. Although only a single "worst-case" puncture drop is required by 10 CFR §71.73(c)(3), multiple puncture drop tests were performed at different orientations to ensure that the most vulnerable package features were subjected to "worst-case" loads and deformations. The specific conditions selected for CTU puncture drop testing are summarized in Table 2.7-1, Table 2.7-2, and Table 2.7-3.

2.7.3.3 Summary of Results from the Puncture Drop Tests

Successful HAC puncture drop testing of the CTUs indicates that the various TRUPACT-II packaging design features are adequately designed to withstand the HAC puncture drop event. As with the free drop test, the most important result of the testing program was the demonstrated ability of the OCV and ICV to remain leaktight. Significant results of puncture drop testing common to all test units are as follows:

- With one exception, permanent deformations of the containment boundary are not attributed to the puncture event. The single exception occurred for a puncture impact onto the 1/4 inch thick OCA outer shell at a location 40 inches above the base of the package (Test No. 7 for CTU No. 1, and Test No. R for CTU No. 2). This puncture event resulted in a hole through the OCA outer shell. The permanent damage to the OCV and ICV shells was an inward bulge of approximately 1½ inches to the OCV and ICV sidewalls. Importantly, permanent deformations were limited to the cylindrical shell portions of the OCV and ICV lower bodies, with no significant deformation near the seal flanges.
- Rupture was not observed for the 3/8 inch thick, OCA outer shell. Penetrations of the OCA outer shell closest to the seal regions were 22 inches above and 37 inches below the closure interface. Minor tearing of the Z-flange-to-3/8 inch thick OCA interfaces was observed for some test orientations. These regions are covered by the outer thermal shield; therefore, such tears are of little consequence.
- Tearing of the OCA outer shell occurred at the 3/8-to-1/4 inch thick, OCA body outer shell transition (weld) during testing of CTU-2 and CTU-3 (Test 4).
- In the regions where a significant amount of polyurethane foam was exposed by a puncture event (i.e., 40 inches above the package base and near the OCA top knuckle), the intumescent (i.e., self-extinguishing) characteristics of the polyurethane foam were sufficient

to provide effective insulation from the effects of the subsequent HAC fire. Additional discussion regarding HAC fire testing is provided in Section 2.7.4, *Thermal*.

A comprehensive summary of test results is provided in Appendix 2.10.3.7, *Test Results*.

2.7.4 Thermal

Subpart F of 10 CFR 71 requires performing a thermal test in accordance with the requirements of 10 CFR §71.73(c)(4). To demonstrate the performance capabilities of the TRUPACT-II package when subjected to the HAC thermal test specified in 10 CFR §71.73(c)(4), two full-scale TRUPACT-II CTUs were burned in two, separate, fully engulfing pool fires. Each test unit was subjected to a variety of HAC, 30-foot free drop and puncture tests prior to being burned, as discussed in Section 2.7.1, *Free Drop*, and Section 2.7.3, *Puncture*, respectively. Active and passive temperature instrumentation was employed during CTU fire testing.

As discussed further in Appendix 2.10.3, *Certification Tests*, each CTU was oriented horizontally in a test stand a distance one-meter above the fuel per the requirements of 10 CFR §71.73(c)(4). The CTU was oriented circumferentially to position the worst-case damage from the various 30-foot free drops and puncture drops 1/2-meter above the lowest part of the package while on the stand (i.e., 1½ meters above the fuel[5]). This particular arrangement placed the maximum drop damage in the hottest section of the fire. Prior to fire testing, each CTU was preheated to the worst-case NCT steady-state temperature (i.e., 100 ºF still air without insolation).

Successful HAC fire testing of the CTUs indicates that the various TRUPACT-II packaging design features are adequately designed to withstand the HAC fire event. As with the free drop and puncture tests, the most important result of the testing program was the demonstrated ability of the OCV and ICV to remain leaktight. Significant results of fire testing common to both test units are as follows:

- The intumescent (i.e., self-extinguishing) characteristic of the polyurethane foam was sufficient to provide insulation from the effects of the HAC fire even in regions where the most significant amounts of foam were exposed.
- The maximum measured temperatures for the OCV and ICV elastomeric (butyl) O-ring seals were 260 ºF (thermocouple reading during the fire, 250 ºF by passive temperature indicating label) and 200 ºF, respectively. The maximum measured temperatures for the OCV and ICV structural components were 439 ºF and 270 ºF, respectively. The 270 ºF ICV temperature was most likely a result of the preheat operation used to heat the vessels prior to the fire test, rather than a result of the fire test itself. Air was pumped into the OCV/ICV annulus at 40 psi and 350 ºF, and within close proximity of the particular temperature indicating label that measured the 270 ºF temperature. The next highest ICV temperature reading was 220 ºF.

[5] M. E. Schneider and L. A. Kent, *Measurements of Gas Velocities and Temperatures in a Large Open Pool Fire*, Sandia National Laboratories (reprinted from *Heat and Mass Transfer in Fire*, A. K. Kulkarni and Y. Jaluria, Editors, HTD-Vol. 73 (Book No. H00392), American Society of Mechanical Engineers). Figure 3 shows that maximum temperatures occur at an elevation approximately 2.3 meters above the pool floor. The pool was initially filled with water and fuel to a level of 0.814 meters. The maximum temperatures therefore occur approximately 1½ meters above the level of the fuel, i.e., 1/2 meter above the lowest part of the package when set one meter above the fuel source per the requirements of 10 CFR §71.73(c)(4).

- Both containment boundaries demonstrated the capability of maintaining pressure before, during, and after the fire event. Note that pressure was lost in the CTU No. 1 OCV during fire testing. However, the loss of pressure was due to failure of a test-related pressure fitting, not to a packaging design feature. Post-test repair of the fitting and re-pressurization of the OCV indicated that the pressure retention capabilities of the OCV had not been compromised by the fire test.
- Following fire testing, disassembly of the OCA demonstrated that, except for the local area damaged by the puncture impacts 40 inches above the base of the package, a layer of unburned polyurethane foam remained around the entire OCV. For both CTUs, the average thickness of the layer was approximately 5 to 6 inches along the cylindrical sides and lower head of the OCV, and even greater adjacent to the OCV upper dished head. This residual polyurethane foam thickness is consistent with the shielding evaluation provided in Chapter 5.0, *Shielding Evaluation*, and the criticality evaluation presented in Chapter 6.0, *Criticality Evaluation*.

A comprehensive summary of test results is provided in Appendix 2.10.3.7, *Test Results*.

2.7.4.1 Summary of Pressures and Temperatures

Package pressures and temperatures due to the HAC fire test are presented in Appendix 2.10.3, *Certification Tests*. Detailed discussions regarding measured temperatures are provided in Section 3.5.3, *Package Temperatures*. Detailed discussions regarding calculated pressures are provided in Section 3.5.4, *Maximum Internal Pressure*.

2.7.4.1.1 Summary of Temperatures

Both active and passive temperature measuring devices were employed prior to, during, and following the HAC fire tests. As discussed in Section 2.7.4, *Thermal*, the maximum measured temperatures for the OCV and ICV O-ring seals were 260 ºF and 200 ºF, respectively.

2.7.4.1.2 Summary of Pressures

Even considering the test anomaly associated with CTU No. 1, the maximum measured internal pressures occurred for CTU No. 2. The maximum measured ICV pressure was 65.7 psia (53.7 psig internal pressure, plus 12 psia atmospheric pressure), with a 63.1 psia (51.1 psig) starting pressure. The maximum measured OCV pressure was 66.6 psia (54.6 psig), with a 62 psia (50 psig) starting pressure.

2.7.4.2 Differential Thermal Expansion

Fire testing of two, full scale TRUPACT-II prototypes indicate that the effects associated with differential thermal expansion of the various packaging components are negligible. Subsequent to all NCT and HAC free drop, puncture drop, and fire tests, comprehensive helium leak testing of both containment vessels demonstrated that differential thermal expansion does not affect the capability of the containment boundaries to remain leaktight.

2.7.4.3 Stress Calculations

As shown in Section 2.7.4.1.2, *Summary of Pressures*, the measured internal pressure within the ICV increases 2.6 psig (+5%), and within the OCV increases 4.6 psig (+9%) due to the HAC fire

test. Pressure stresses due to the HAC fire test correspondingly increase a maximum of 9%. With reference to Table 2.1-1 from Section 2.1.2.1.1, *Containment Structures*, the HAC allowable stress intensity for general primary membrane stresses (applicable to pressure loads) is 240% of the NCT allowable stress intensity. Therefore, a HAC pressure stress increase of 9% will not exceed the HAC allowable stresses. Further, the pressure stresses in conjunction with stresses associated with differential thermal expansion are limited to an acceptable level since both containment vessels were shown to be leaktight after all NCT and HAC free drop, puncture drop, and fire tests (see Appendix 2.10.3.7, *Test Results*).

2.7.4.4 Comparison with Allowable Stresses

As discussed in Section 2.7.4.3, *Stress Calculations*, further quantification of stresses in the various TRUPACT-II package components is not required.

2.7.5 Immersion – Fissile Material

Subpart F of 10 CFR 71 requires performing an immersion test for fissile material packages in accordance with the requirements of 10 CFR §71.73(c)(5). The criticality evaluation presented in Chapter 6.0, *Criticality Evaluation*, assumes optimum hydrogenous moderation of the contents, thereby conservatively addressing the effects and consequences of water in-leakage.

2.7.6 Immersion – All Packages

Subpart F of 10 CFR 71 requires performing an immersion test for all packages in accordance with the requirements of 10 CFR §71.73(c)(6). For the TRUPACT-II package design, the effect of a 21 psig external pressure due to immersion in 50 feet of water is applied to the OCV, since the OCA outer shell is not designed as a pressure boundary. For conservatism, a buckling evaluation of the ICV is also performed.

The external pressure induces small compressive stresses in the containment boundaries that are limited by stability (buckling) requirements. Buckling assessments are performed for the OCV and ICV in Section 2.7.6.1, *Buckling Assessment of the Torispherical Heads*, and Section 2.7.6.2, *Buckling Assessment of the Cylindrical Shells*.

2.7.6.1 Buckling Assessment of the Torispherical Heads

The buckling analysis of the torispherical heads is based on the methodology outlined in Paragraph NE-3133.4(e), *Torispherical Heads*, of the ASME Boiler and Pressure Vessel Code, Section III[6], Subsection NE. Since the external pressure loading due to immersion may be classified as Level D, the allowable buckling stress and, therefore, the allowable pressure, can be increased by 150% per paragraph NE-3222.2. The results from following this methodology are summarized below.

[6] American Society of Mechanical Engineers (ASME) Boiler and Pressure Vessel Code, Section III, *Rules for Construction of Nuclear Power Plant Components*, 1986 Edition.

Parameter	OCV Torispherical Head		ICV Torispherical Head	
	Upper	Lower	Upper	Lower
R	77.3125	74.1250	74.3750	73.1250
T	0.25	0.25	0.25	0.25
$A = \frac{0.125}{(R/T)}$	0.00040	0.00042	0.00042	0.00043
B[7]	5,600	5,800	5,800	5,900
$P_a = \frac{(1.5)B}{(R/T)}$	27.2	29.3	29.2	30.3

The smallest allowable pressure, P_a, is 27.2 psig for the OCV upper head. For an applied external pressure of 21 psig, the corresponding buckling margin of safety is:

$$MS = \frac{27.2}{21} - 1 = +0.30$$

Since the margin of safety in the worst case is positive, it is concluded that none of the OCV or ICV torispherical heads will buckle for an external pressure of 21 psig.

2.7.6.2 Buckling Assessment of the Cylindrical Shells

The cylindrical portions of the OCV and ICV are evaluated using ASME Boiler and Pressure Vessel Code Case N-284. Consistent with Regulatory Guide 7.6 philosophy, a factor of safety of 1.34 is applied for HAC buckling evaluations per ASME Code Case N-284, corresponding to ASME Code, Service Level D conditions.

Buckling analysis geometry parameters are summarized in Table 2.7-6, and loading parameters are summarized in Table 2.7-7. The cylindrical shell buckling analysis utilizes an OCV and ICV temperature of 70 ºF. The stresses are determined using an external pressure of 21.0 psig. The hoop stress, σ_θ, and axial stress, σ_ϕ, are found from:

$$\sigma_\theta = \frac{Pr}{t} \qquad \sigma_\phi = \frac{Pr}{2t}$$

where P is the applied external pressure of 21.0 psi, r is the mean radius, and t is the cylindrical shell thickness. As shown in Table 2.7-8, since all interaction check parameters are less than 1.0, as required, the design criteria are satisfied.

[7] Factor B is found from American Society of Mechanical Engineers (ASME) Boiler and Pressure Vessel Code, Section III, *Rules for Construction of Nuclear Power Plant Components*, Figure VII-1102-4, *Chart for Determining Shell Thickness of Cylindrical and Spherical Components Under External Pressure When Constructed of Austenitic Steel (18Cr–8Ni, Type 304)*, 1986 Edition. The 100 ºF temperature curve is used for each case.

The OCV length is conservatively measured from the ring stiffener to an assumed support point located one-third of the depth of the lower OCV torispherical head below the head-to-shell interface (i.e., 32.67 inches).

OCV Shell Ring Stiffener Axial Compression Check:

Per Paragraph –1714.1(a) of ASME Boiler and Pressure Vessel Code Case N-284, the required ring stiffener cross-section area is the larger of:

$$A_\theta \geq \left(\frac{0.334}{M_s^{0.6}} - 0.063\right)\ell_{s\phi} t = 0.076\,\text{in}^2 \qquad or \qquad A_\theta \geq (0.06)\ell_{s\phi} t = 0.350\,\text{in}^2$$

where, from Table 2.7-6, R = 36.91 inches and t = 0.188 inches, and $M_s = \ell_{si}/(Rt)^{1/2} = 11.77$, and the length, $\ell_{s\phi}$, is the average of the distance from the stiffening ring to the lower head (32.67 inches) and the distance from the stiffening ring to the upper seal flange (29.33 inches), or $\ell_{s\phi} = \ell_{si} = ½(32.67 + 29.33) = 31.00$ inches.

The cross-section area of the stiffening ring is $A = 0.375 \times 1.5 = 0.563\ \text{in}^2$. Since $A = 0.563\ \text{in}^2 > 0.350\ \text{in}^2 = A_\theta$, the size of the stiffening ring for axial compression is acceptable.

OCV Shell Ring Stiffener Hoop Compression Check:

Per Paragraph –1714.1(b)(1) of ASME Boiler and Pressure Vessel Code Case N-284, the required moment of inertia for an intermediate stiffening ring to resist hoop compression is:

$$I_{E\theta} = \frac{(1.2)\sigma_{\theta eL}\ell_{s\phi}R_c^2 t}{E(n^2 - 1)} = 0.264\,\text{in}^4$$

where $\sigma_{\theta eL}$ = 11,273 psi (Table 2.7-8), $\ell_{s\phi}$ = 31.00 inches, $R_c = 36.91 + 0.356 = 37.27$ inches, t = 0.188 inches, $E = 28.3(10)^6$ psi at 70 ºF, and n^2 is:

$$n^2 = \frac{(1.875)R^{3/2}}{L_B t^{1/2}} = 15.64$$

where R = 36.91 inches (Table 2.7-6), the effective length of the OCV shell between "bulkheads" is L_B = 62.0 inches, and t = 0.188 inches (Table 2.7-6).

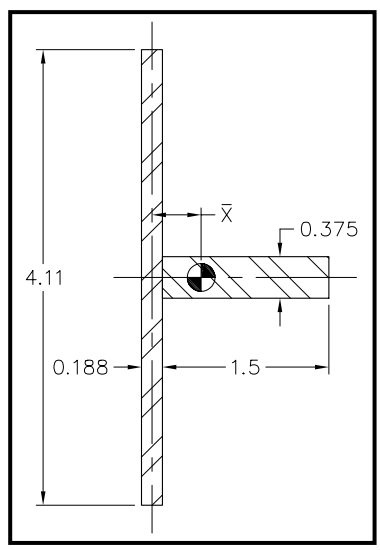

The effective stiffness of the ring stiffener also includes a portion of the adjacent cylindrical shell whose length is determined from Paragraph –1200 of ASME Code Case N-284 as follows:

$$\ell_{ei} = 1.56\sqrt{Rt} = 4.11\,\text{in}$$

where, from Table 2.7-6, R = 36.91 inches and t = 0.188 inches.

The distance to the composite stiffening ring neutral axis, $\bar{X}$, is:

$$\overline{X} = \frac{(0.375)(1.5)(0.188+1.5)}{2[(0.188)(4.11)+(0.375)(1.5)]} = 0.356\,\text{in}$$

Knowing the distance to the neutral axis of the composite stiffening ring, the ring stiffener in-plane moment of inertia is:

$$I_r = \frac{(0.375)(1.5)^3}{12} + (0.375)(1.5)\left(\frac{0.188+1.5}{2} - 0.356\right)^2 = 0.239\,\text{in}^4$$

Similarly, the shell out-of-plane moment of inertia is:

$$I_s = \frac{(4.11)(0.188)^3}{12} + (0.188)(4.11)(0.356)^2 = 0.100\,\text{in}^4$$

Combining both results, the effective moment of inertia is $I_E = 0.239 + 0.100 = 0.339$ in^4. Since $I_E = 0.339$ in$^4 > 0.264$ in$^4 = I_{E\theta}$, the size of the stiffening ring for hoop compression is acceptable.

2.7.7 Deep Water Immersion Test

Subpart E of 10 CFR 71 requires performing a deep water immersion test in accordance with 10 CFR §71.61. Since the TRUPACT–II does not transport payloads with an activity of greater than 10^5 A_2, this requirement does not apply.

2.7.8 Summary of Damage

As discussed in the previous sections, the cumulative damaging effects of free drop, puncture drop, and fire tests were satisfactorily withstood by the TRUPACT-II packaging during certification testing. Subsequent helium leak testing confirmed that containment integrity was maintained throughout the test series. Therefore, the requirements of 10 CFR §71.73 have been adequately met.

Table 2.7-1 – Summary of Tests for TRUPACT-II CTU-1

Test No.	Test Description	Test Unit Angular Orientation		Pressure (psig)		CTU Temperature	Remarks
		Axial①	Circumferential②	ICV	OCV		
1	NCT, 3-foot side drop onto OCV vent port	0º	110º	50	50	Ambient	Impact in region expected to produce worst-case cumulative damage to package.
2	HAC, 30-foot side drop onto OCV vent port	0º	110º	50	0	Ambient	Impact in region expected to produce worst-case cumulative damage to package.
3	HAC, 30-foot CG onto OCA lid knuckle near OCA lid lift pocket	-47º	-100º	50	50	Ambient	Payload drums centered over OCA lid lift pocket to produce maximum cumulative damage to lids.
4	HAC, 30-foot top drop	-90º	N/A	50	50	Ambient	Impact to produce maximum cumulative internal damage to lids.
5	HAC, puncture drop on OCA vent port fitting	-15º	110º	50	50	Ambient	Puncture in region expected to produce worst-case cumulative damage to package.
6	HAC, puncture drop onto OCA body below 1/4-to-3/8 shell weld	-3º	110º	50	50	Ambient	Puncture in region expected to produce worst-case cumulative damage to package.
7	HAC, puncture drop 40 inches above package bottom	28º	110º	50	0	Ambient	Puncture in region expected to produce worst-case cumulative damage to package.
8	HAC, puncture drop onto damaged OCA lid knuckle	-54º	110º	50	0	Ambient	Puncture in region expected to produce worst-case cumulative damage to package.
9	HAC, puncture drop on OCA seal test port fitting	-24º	20º	50	50	Ambient	Puncture in thinnest region of the package sidewall.
10	HAC, fire test	0º	145º	50	50	At HAC pre-fire temperature	Circumferential orientation places damage from most drop tests in hottest part of fire.

Notes:

① Axial angle, θ, is relative to horizontal (i.e., side drop orientation).

② Circumferential angle, ϕ, is relative to the forklift pockets when parallel to the ground.

Table 2.7-2 – Summary of Tests for TRUPACT-II CTU-2

Test No.	Test Description	Test Unit Angular Orientation		Pressure (psig)		CTU Temperature	Remarks
		Axial①	Circumferential②	ICV	OCV		
1	HAC, 30-foot top slapdown drop; initial impact on OCA lid knuckle	-20º	-5º	33	0	-20 ºF	Slapdown onto locking ring joints.
2	HAC, 30-foot bottom drop	90º	N/A	33	33	-20 ºF	Drop producing maximum axial acceleration.
3	HAC, 30-foot slapdown drop; initial impact on tie-down lug	18º	143º	50	50	Ambient	Slapdown in region expected to produce worst-case cumulative damage to package.
R	HAC, puncture drop 40 inches above package bottom	23º	143º	50	0	Ambient	Impact in region expected to produce worst-case cumulative damage to package; repeat of Test No. 7 for CTU-1.
4	HAC, puncture drop at the 1/4-to-3/8 lid shell interface	-42º	143º	50	50	Ambient	Puncture in region expected to produce worst-case cumulative damage to package.
5	HAC, puncture drop onto package bottom adjacent to forklift pocket	55º	-110º	50	0	Ambient	HAC impact at location not tested during previous TRUPACT-II certification tests.
6	HAC, puncture drop onto outer thermal shield	-67º	-67º	0	0	Ambient	Attempt to tear outer thermal shield away from OCA.
7	HAC, puncture drop onto OCA body at closure; 40º from OCA vent port fitting	-15º	110º	50	50	Ambient	Puncture at closure region at same elevation as OCA vent port fitting.
8	HAC, puncture drop onto OCA lid at closure; 180º from OCA seal test port fitting	-22º	-145º	50	50	Ambient	Puncture at closure region at same elevation as OCA seal test port fitting; thinnest region of the package sidewall.
9	HAC, fire test	0º	200º	50	50	At HAC pre-fire temperature	Circumferential orientation places damage from Tests 3, R, and 4 in hottest part of fire.

Notes:

① Axial angle, θ, is relative to horizontal (i.e., side drop orientation).

② Circumferential angle, ϕ, is relative to the forklift pockets when parallel to the ground.

Table 2.7-3 – Summary of Tests for TRUPACT-II CTU-3

Test No.	Test Description	Test Unit Angular Orientation		Pressure (psig)		CTU Temperature	Remarks
		Axial①	Circumferential②	ICV	OCV		
1	HAC, 30-foot top slapdown drop; initial impact on OCA lid knuckle	-20º	-5º	33	0	-20 ºF	Slapdown onto locking ring joints.
2	HAC, 30-foot bottom drop	90º	N/A	33	33	-20 ºF	Drop producing maximum axial acceleration.
3	HAC, 30-foot slapdown drop; initial impact on tie-down lug	18º	143º	50	50	Ambient	Slapdown in region expected to produce worst-case cumulative damage to package.
4	HAC, puncture drop at the 1/4-to-3/8 lid shell interface	-42º	143º	50	50	Ambient	Puncture in region expected to produce worst-case cumulative damage to package.
5	HAC, puncture drop onto package bottom adjacent to forklift pocket	55º	-110º	50	0	Ambient	HAC impact at location not tested during previous TRUPACT-II certification tests.
6	HAC, puncture drop onto outer thermal shield	-67º	-67º	0	0	Ambient	Attempt to tear outer thermal shield away from OCA.
7	HAC, puncture drop onto OCA body at closure; 40º from OCA vent port fitting	-15º	110º	50	50	Ambient	Puncture at closure region at same elevation as OCA vent port fitting.
8	HAC, puncture drop onto OCA lid at closure; 180º from OCA seal test port fitting	-22º	-145º	50	50	Ambient	Puncture at closure region at same elevation as OCA seal test port fitting; thinnest region of the package sidewall.

Notes:

① Axial angle, θ, is relative to horizontal (i.e., side drop orientation).

② Circumferential angle, ϕ, is relative to the forklift pockets when parallel to the ground.

This page intentionally left blank.

Table 2.7-4 – Buckling Geometry Parameters for a 385*g* HAC End Drop

Geometry and Material Input	
	ICV
Mean Radius, inch	36.44
Shell Thickness, inch	0.25
Length, inch	65.70①
Geometry Output (nomenclature consistent with ASME Code Case N-284)	
R =	36.44
t =	0.25
$(Rt)^{1/2}$ =	3.018
ℓ_ϕ =	65.70
ℓ_θ =	229.0
M_ϕ =	21.77
M_θ =	75.87
M =	21.77

Notes:

① The ICV length is conservatively measured from five inches below the top of the lower ICV seal flange (at the beginning of the 1/4 inch wall thickness) to an assumed support point located one-third of the depth of the lower ICV torispherical head below the head-to-shell interface.

Table 2.7-5 – Shell Buckling Summary for a 385*g* HAC End Drop

Condition	ICV	Remarks
Capacity Reduction Factors (-1511)		
$\alpha_{\phi L}$ =	0.3170	
$\alpha_{\theta L}$ =	0.8000	
Plasticity Reduction Factors (-1610)		
η_{ϕ} =	1.0000	
η_{θ} =	1.0000	
Theoretical Buckling Values (-1712.1.1)		
C_{ϕ} =	0.6050	
$\sigma_{\phi eL}$ =	119,207 psi	
$C_{\theta h}$ =	0.0435	
$\sigma_{\theta eL} = \sigma_{heL}$ =	8,577 psi	
Elastic Interaction Equations (-1713.1.1)		
$\sigma_{\phi s}$ =	59,991 psi	
$\sigma_{\theta s}$ =	0 psi	
Axial + Hoop ⇨ Check (a):	*N/A*	
Axial + Hoop ⇨ Check (b):	0.485	<1 ∴ OK

Table 2.7-6 – Buckling Geometry Parameters per Code Case N-284

Geometry and Material Input		
	ICV	**OCV**
Mean Radius, inch	36.44	36.91
Shell Thickness, inch	0.25	0.188
Length, inch	65.70①	32.67②
Geometry Output (nomenclature consistent with ASME Code Case N-284)		
R =	36.44	36.91
t =	0.25	0.188
$(Rt)^{½}$ =	3.018	2.634
ℓ_ϕ =	65.70	32.67
ℓ_θ =	229.0	231.9
M_ϕ =	21.77	12.40
M_θ =	75.87	88.03
M =	21.77	12.40

Notes:

① The ICV length is conservatively measured from five inches below the top of the lower ICV seal flange (at the beginning of the 1/4 inch wall thickness) to an assumed support point located one-third of the depth of the lower ICV torispherical head below the head-to-shell interface.

② The OCV length is conservatively measured from the ring stiffener to an assumed support point located one-third of the depth of the lower OCV torispherical head below the head-to-shell interface. This length assumes that the ring stiffener is sized per the requirements in Paragraphs –1714.1(a) and –1714.1(b)(1) of ASME Code Case N-284.

Table 2.7-7 – Stress Results for 21 psig External Pressure

ICV		OCV	
Axial Stress, σ_ϕ	1,530	Axial Stress, σ_ϕ	2,061
Hoop Stress, σ_θ	3,061	Hoop Stress, σ_θ	4,123

Table 2.7-8 – Shell Buckling Summary for 21 psig External Pressure

Condition	ICV	OCV	Remarks
Capacity Reduction Factors (-1511)			
$\alpha_{\phi L}$ =	0.2670	0.2670	
$\alpha_{\theta L}$ =	0.8000	0.8000	
Plasticity Reduction Factors (-1610)			
η_ϕ =	1.0000	1.0000	
η_θ =	1.0000	1.0000	
Theoretical Buckling Values (-1712.1.1)			
C_ϕ =	0.6050	0.6050	
$\sigma_{\phi eL}$ =	117,464 psi	87,208 psi	
$C_{\theta h}$ =	0.0435	0.0782	
$\sigma_{\theta eL} = \sigma_{heL}$ =	8,452 psi	11,273 psi	
Elastic Interaction Equations (-1713.1.1)			
$\sigma_{\phi s}$ =	7,679 psi	10,344 psi	
$\sigma_{\theta s}$ =	5,127 psi	6,906 psi	
Axial + Hoop ⇨ Check (a):	*N/A*	*N/A*	
Axial + Hoop ⇨ Check (b):	0.398	0.433	<1 ∴ OK

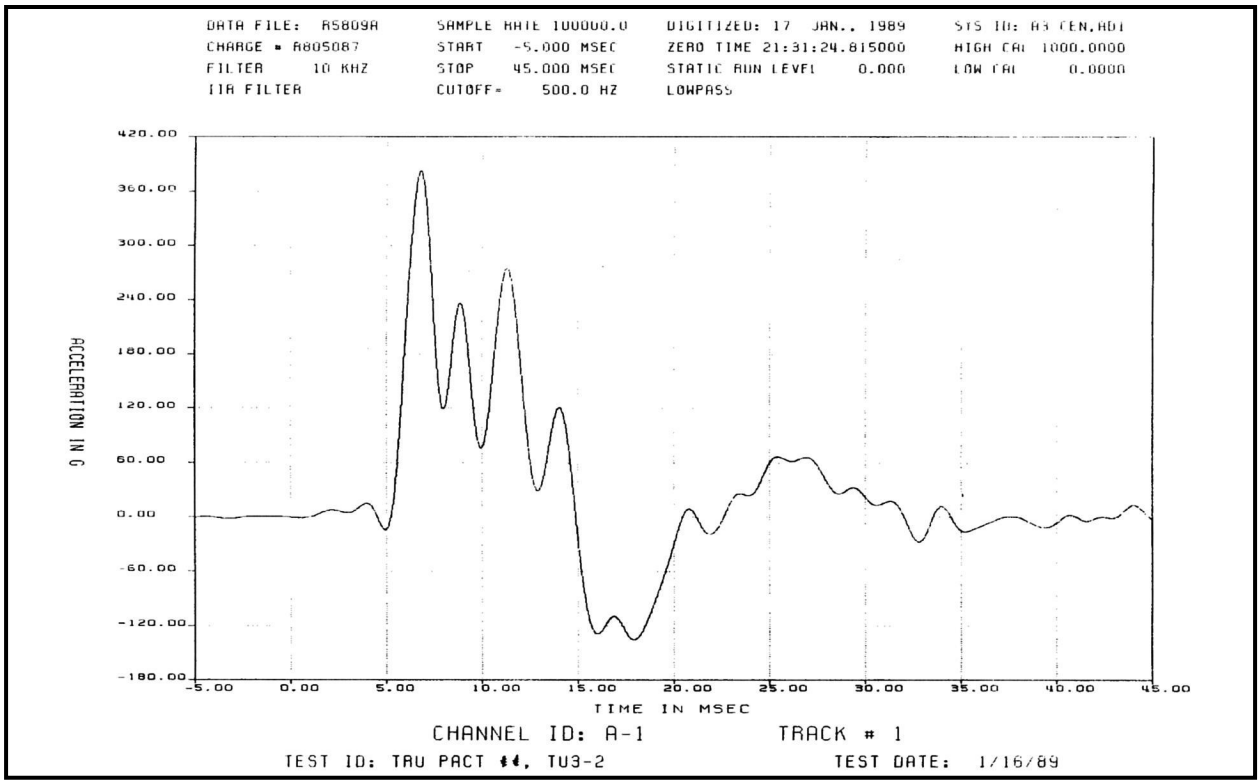

Figure 2.7-1 – CTU-2 Free Drop Test No. 2 Accelerometer Data (Gage 1)

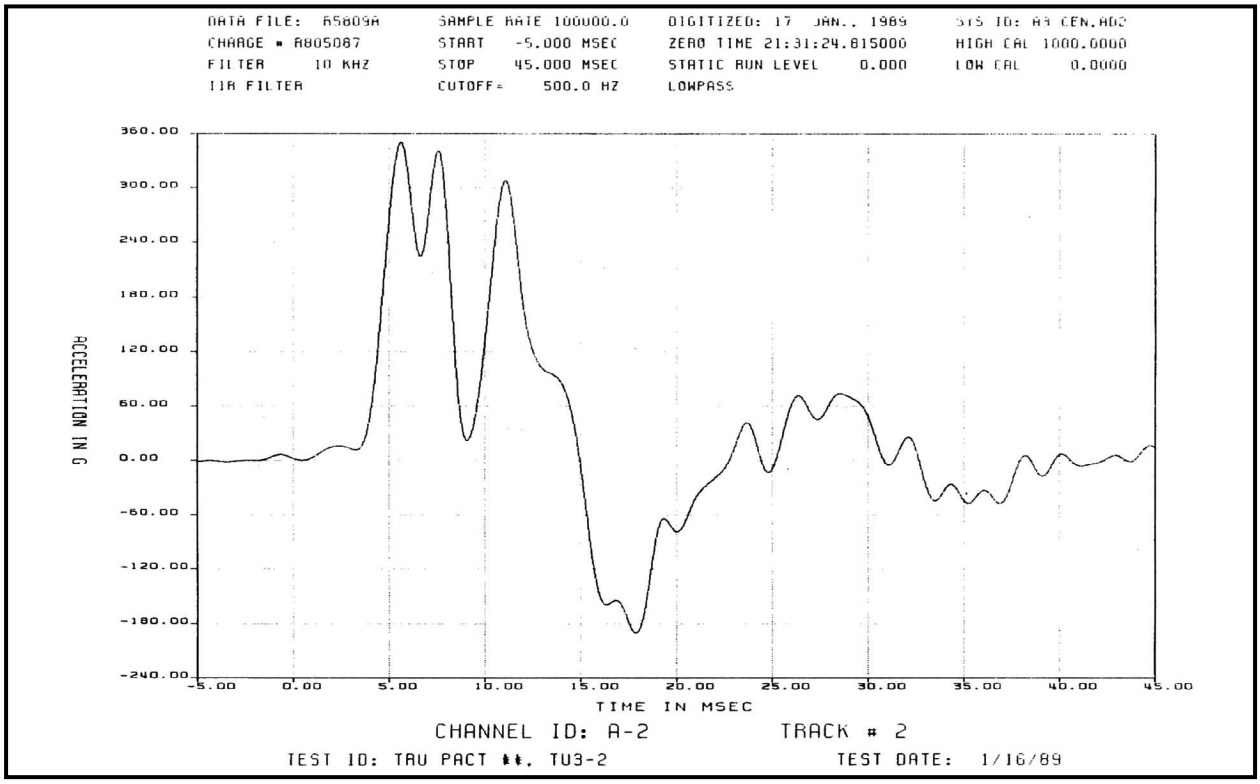

Figure 2.7-2 – CTU-2 Free Drop Test No. 2 Accelerometer Data (Gage 2)

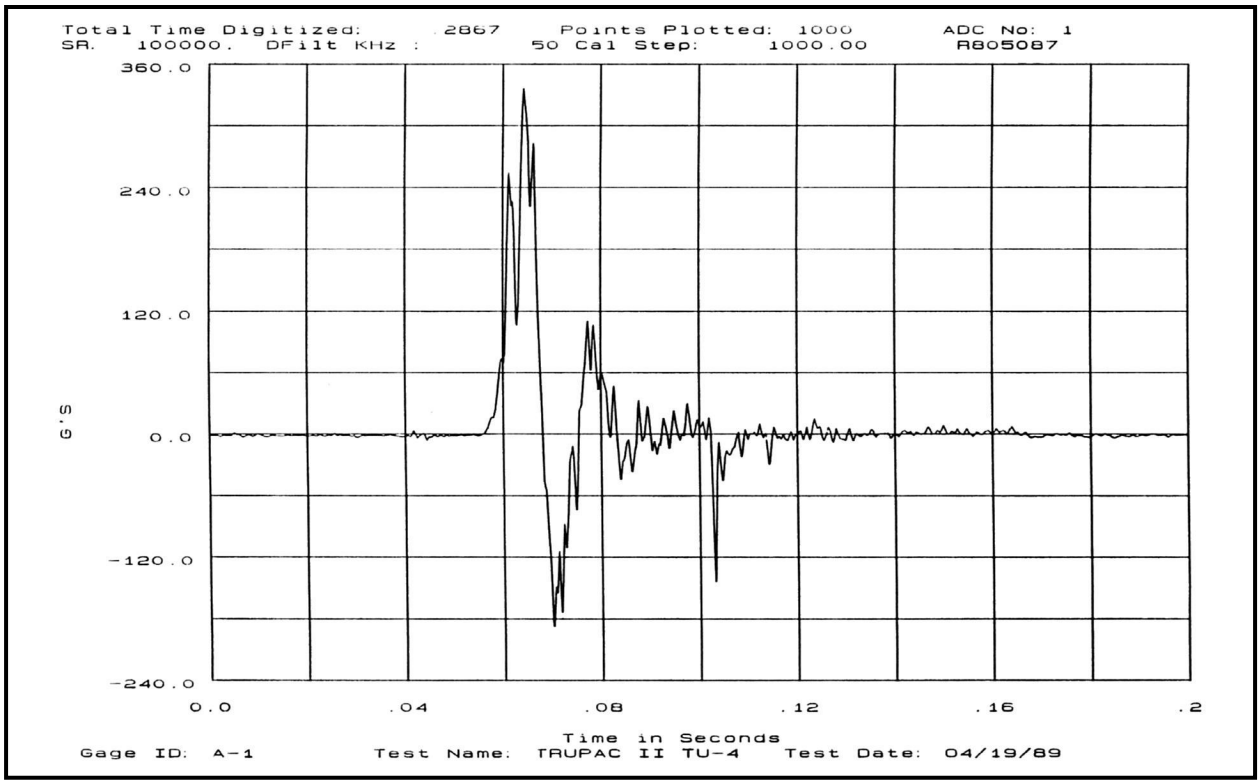

Figure 2.7-3 – CTU-3 Free Drop Test No. 2 Accelerometer Data (Gage 1)

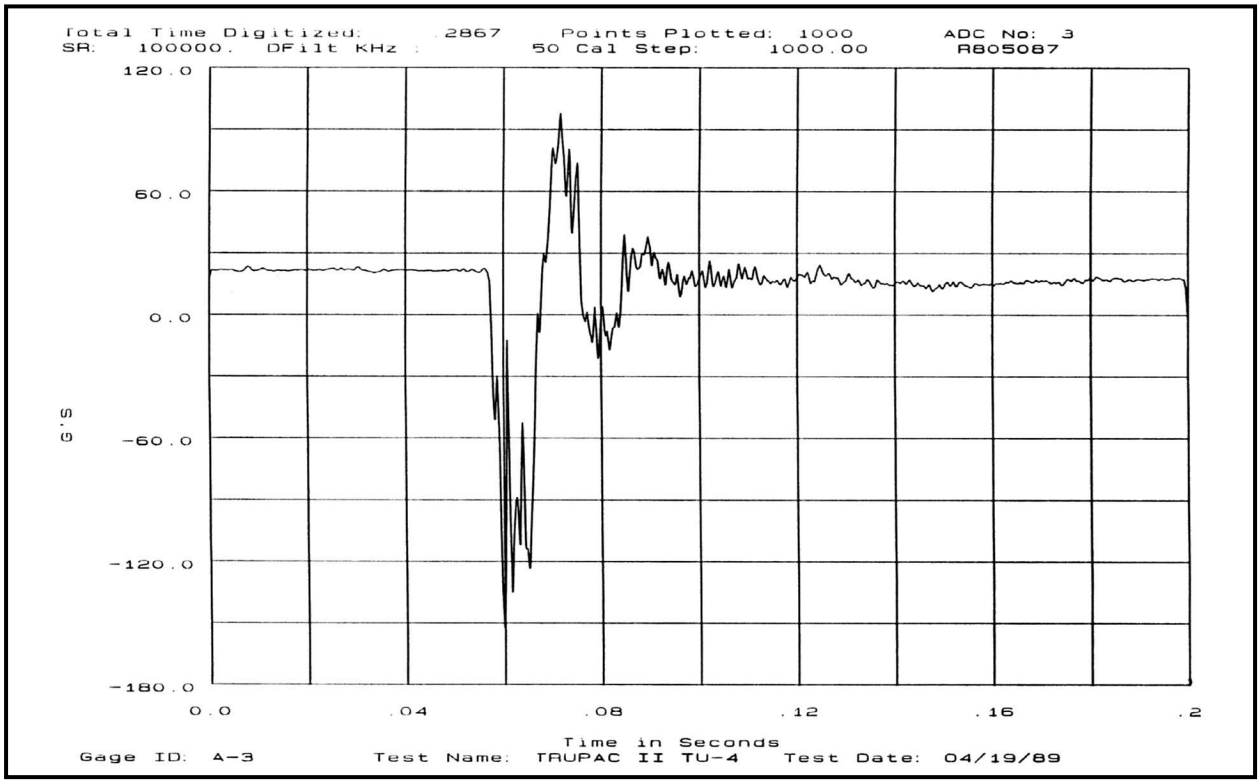

Figure 2.7-4 – CTU-3 Free Drop Test No. 2 Accelerometer Data (Gage 2)

2.8 Special Form

This section does not apply for the TRUPACT-II package, since special form is not claimed.

This page intentionally left blank.

2.9 Fuel Rods

This section does not apply for the TRUPACT-II package, since fuel rods are not included as an approved payload configuration.

This page intentionally left blank.

2.10 Appendices

2.10.1 *Finite Element Analysis (FEA) Models*

2.10.2 *Elastomer O-ring Seal Performance Tests*

2.10.3 *Certification Tests*

This page intentionally left blank.

2.10.1 Finite Element Analysis (FEA) Models

2.10.1.1 Outer Containment Assembly (OCA) Structural Analysis

Finite element analyses (FEA) are performed on the OCA structure to determine the stress states of the various components under normal conditions of transport (NCT) loads. The FEA analyses are performed using ANSYS® 4.3A2[1]. The OCA FEA model is comprised of six separate major structural components, modeled as shown in :

- upper OCV seal flange
- lower OCV seal flange
- OCV locking ring
- OCV shells
- OCA shells and z-flanges
- polyurethane foam

The lower and upper seal flanges, locking ring and polyurethane foam are modeled using 2-D, isoparametric solid elements (PLANE42). The quadrilateral elements are defined by four nodal points (a triangular element may be formed by defining duplicate the 3rd and 4th node numbers), each having two degrees of freedom: translations in the nodal x-direction (radial) and y-direction (axial).

The upper and lower OCA shells (OCA lid and body shells, respectively) are modeled using 2-D, axisymmetric conical shell elements (SHELL51). The lineal elements are defined by two nodal points, each having three degrees of freedom: translations in the nodal x-direction (radial) and y-direction (axial), and rotation about the nodal z-axis (hoop). In addition, the axisymmetric conical shell element is biaxial, with membrane and bending capabilities. The OCA inner shell defines the outer containment vessel (OCV).

Relatively stiff, 2-D elastic beams (BEAM3) are utilized to maintain bending continuity between the three degree of freedom conical shell elements and two degree of freedom, isoparametric solid elements. Specifically, for both the lower and upper OCV seal flanges, four stiff beams are placed at each junction between the shell elements and the solid elements of the seal flanges. These elements are included to transmit the moment (i.e., to maintain slope continuity) between the shell and flange portions of the model, and have a negligible effect on the stress results.

Three sets of 2-D interface elements (CONTAC12) are utilized to connect the lower and upper OCV seal flanges to each other and to the OCV locking ring. The interface element is capable of supporting a load only in the direction normal to the surfaces, and is frictionless in the tangential direction. The interface element has two degrees of freedom at each node: translations in the nodal x-direction (radial) and y-direction (axial). A stiffness of 2×10^{10} lb/in is chosen to reflect the relatively high contact stiffness when closed. Three sets of interface elements are used in these analyses: 1) between the lower OCV seal flange and the OCV locking ring, 2) between the upper OCV seal flange and the OCV locking ring, and 3) between the lower OCV seal flange and the upper OCV seal flange.

Interface elements are also located along the entire shell-to-foam periphery to allow relative motion between the steel shells and the polyurethane foam. This approach effectively models the ceramic fiber paper by allowing compression-only forces, and assumes no shear continuity or tension effects. A contact stiffness of 2×10^{10} lb/in is chosen to reflect the stiffness between the

[1] ANSYS®, Inc., *ANSYS Engineering Analysis System User's Manual for ANSYS® Revision 4.3A2*, Houston, PA.

shells, ceramic fiber paper, and polyurethane foam. Stress results in the package shells and OCV seal flanges exhibit a negligible dependence on the actual magnitude of the gap contact stiffness.

To account for the tangential (hoop) direction slotting for the lower OCV seal flange and OCV locking ring in the axisymmetric model, the material properties in the directly affected regions are modified. Specifically, material properties for the shaded elements in the lower OCV seal flange and OCV locking ring, illustrated in Figure 2.10.1-1, are modified to reflect only one-half the stainless steel being present for strength purposes. Specifically, the elastic modulus in the x- and y-directions is reduced to one-half their normal value (since only approximately one-half the material remains in the slotted regions), and the elastic modulus in the z-direction is set to set to a very low value to eliminate virtually all tangential (hoop) stiffness in the slotted regions. In addition, Poisson's ratio is set at the normal value of 0.3 for the x-y plane, but is set to zero in the x-z and y-z planes. In these ways, the analyses accurately depict the stress levels in all regions.

The global origin of the nodal coordinate system is located at the bottom center of the OCA body, as shown in Figure 2.10.1-1. As such, the nodal x-axis corresponds to the radial direction, the nodal y-axis corresponds to the axial direction, and the nodal z-axis corresponds to the tangential (or hoop) direction. The model is constrained from translating in the radial direction and rotating about the hoop axis at the y-z symmetry plane at x equal zero. The model is also constrained from translating in the axial direction at a single node on the OCV locking ring.

2.10.1.1.1 OCA Structural Analysis – Load Case 1

For OCA Load Case 1, the OCA structural analysis uses a 50 psig (64.7 psia) internal pressure, corresponding to the maximum normal operating pressure (MNOP) from Section 3.4.4, *Maximum Internal Pressure*, coupled with a reduced external pressure of 3.5 psia (equivalently an 11.2 psig internal pressure), per Section 2.6.3, *Reduced External Pressure*, and 10 CFR §71.51(c)(3)[2]. The net internal pressure for this case is 61.2 psig, applied throughout the inner periphery of the model. Relative to the upper and lower OCV seal flanges, the internal pressure does not extend beyond (below) the top of the upper main O-ring seal groove.

A uniform temperature of 160 ºF, per Section 2.6.1.1, *Summary of Pressures and Temperatures*, is utilized to determine the temperature-dependent, material property values. The only material properties affected by a temperature of 160 ºF are the elastic modulus and the thermal expansion coefficient for the stainless steel. Consistent with Table 2.3-1 from Section 2.3.1, *Mechanical Properties Applied to Analytic Evaluations*, the elastic modulus and thermal expansion coefficient for Type 304 stainless steel are $27.8(10)^6$ psi and $8.694(10)^{-6}$ inches/inch/ºF, respectively, at a temperature of 160 ºF.

The material properties for the polyurethane foam are consistent with those specified within Table 2.3-2 from Section 2.3.1, *Mechanical Properties Applied to Analytic Evaluations*. The elastic modulus in the x- (radial) and z- (hoop) directions is based on the average of the tensile and compressive, perpendicular-to-rise elastic modulus, or 5,854 psi. The elastic modulus in the y- (axial) direction is based on the average of the tensile and compressive, parallel-to-rise elastic modulus, or 8,789 psi. In addition, Poisson's ratio is 0.33, and the thermal expansion coefficient is $4.9(10)^{-5}$ inches/inch/ºF. Due to the relatively low stiffness of the polyurethane foam

[2] Title 10, Code of Federal Regulations, Part 71 (10 CFR 71), *Packaging and Transportation of Radioactive Material*, 01-01-07 Edition.

compared with the surrounding stainless steel structures, temperature adjusting the foam's elastic modulus will have a negligible effect on component stresses.

Both the reference and uniform temperature are set to 160 ºF, thereby excluding the effects of differential thermal expansion for this case. The effects of differential thermal expansion are considered in Section 2.10.1.1.2, *OCA Structural Analysis – Load Case 2*.

For analysis model review, the ANSYS® input file is listed in Table 2.10.1-1.

2.10.1.1.2 OCA Structural Analysis – Load Case 2

For OCA Load Case 2, the OCA structural analysis uses a 50 psig (64.7 psia) internal pressure, corresponding to the maximum normal operating pressure (MNOP) from Section 3.4.4, *Maximum Internal Pressure*, coupled with a reduced external pressure of 3.5 psia (equivalently an 11.2 psig internal pressure), per Section 2.6.3, *Reduced External Pressure*, and 10 CFR §71.51(c)(3). The net internal pressure for this case is 61.2 psig, applied throughout the inner periphery of the model. Relative to the upper and lower OCV seal flanges, the internal pressure does not extend beyond (below) the top of the upper main O-ring seal groove.

A uniform temperature of 160 ºF, per Section 2.6.1.1, *Summary of Pressures and Temperatures*, is utilized to determine the temperature-dependent, material property values. The only material properties affected by a temperature of 160 ºF are the elastic modulus and the thermal expansion coefficient for the stainless steel. Consistent with Table 2.3-1 from Section 2.3.1, *Mechanical Properties Applied to Analytic Evaluations*, the elastic modulus and thermal expansion coefficient for Type 304 stainless steel are $27.8(10)^6$ psi and $8.694(10)^{-6}$ inches/inch/ºF, respectively, at a temperature of 160 ºF.

The material properties for the polyurethane foam are consistent with those specified within Table 2.3-2 from Section 2.3.1, *Mechanical Properties Applied to Analytic Evaluations*. The elastic modulus in the x- (radial) and z- (hoop) directions is based on the average of the tensile and compressive, perpendicular-to-rise elastic modulus, or 5,854 psi. The elastic modulus in the y- (axial) direction is based on the average of the tensile and compressive, parallel-to-rise elastic modulus, or 8,789 psi. In addition, Poisson's ratio is 0.33, and the thermal expansion coefficient is $4.9(10)^{-5}$ inches/inch/ºF. Due to the relatively low stiffness of the polyurethane foam compared with the surrounding stainless steel structures, temperature adjusting the foam's elastic modulus will have a negligible effect on component stresses.

The reference temperature is set to 70 ºF, and the uniform temperature is set to 160 ºF, thereby including the effects of differential thermal expansion for this case.

For analysis model review, the ANSYS® input file is listed in Table 2.10.1-2.

2.10.1.1.3 OCA Structural Analysis – Load Case 3

For OCA Load Case 3, the OCA structural analysis uses a 0.0 psig (14.7 psia) internal pressure coupled with an external pressure of 0.0 psig (14.7 psia) for a net pressure differential of 0.0 psig.

A uniform temperature of -40 ºF, per Section 2.6.2, *Cold*, is utilized to determine the temperature-dependent, material property values. The only material properties affected by a temperature of -40 ºF are the elastic modulus and the thermal expansion coefficient for the stainless steel.

Consistent with Table 2.3-1 from Section 2.3.1, *Mechanical Properties Applied to Analytic Evaluations*, the elastic modulus and thermal expansion coefficient for Type 304 stainless steel are $28.8(10)^6$ psi and $8.08(10)^{-6}$ inches/inch/ºF, respectively, at a temperature of -40 ºF.

The material properties for the polyurethane foam are consistent with those specified within Table 2.3-2 from Section 2.3.1, *Mechanical Properties Applied to Analytic Evaluations*. The elastic modulus in the x- (radial) and z- (hoop) directions is based on the average of the tensile and compressive, perpendicular-to-rise elastic modulus, or 5,854 psi. The elastic modulus in the y- (axial) direction is based on the average of the tensile and compressive, parallel-to-rise elastic modulus, or 8,789 psi. In addition, Poisson's ratio is 0.33, and the thermal expansion coefficient is $4.3(10)^{-5}$ inches/inch/ºF. Due to the relatively low stiffness of the polyurethane foam compared with the surrounding stainless steel structures, temperature adjusting the foam's elastic modulus will have a negligible effect on component stresses.

The reference temperature is set to 70 ºF, and the uniform temperature is set to -40 ºF, thereby including the effects of differential thermal expansion for this case.

For analysis model review, the ANSYS® input file is listed in Table 2.10.1-3.

2.10.1.1.4 OCA Structural Analysis – Load Case 4

For OCA Load Case 4, the OCA structural analysis uses a -14.7 psig (0.0 psia) internal pressure (i.e., full vacuum) coupled with an increased external pressure of 0.0 psig (14.7 psia), per Section 2.6.4, *Increased External Pressure*. The net external pressure for this case is 14.7 psig, applied throughout the inner periphery of the model. Relative to the upper and lower OCV seal flanges, the internal pressure does not extend beyond (below) the top of the upper main O-ring seal groove.

A uniform temperature of 70 ºF is utilized to determine the temperature-dependent, material property values. The only material properties affected by a temperature of 70 ºF are the elastic modulus and the thermal expansion coefficient for the stainless steel. Consistent with Table 2.3-1 from Section 2.3.1, *Mechanical Properties Applied to Analytic Evaluations*, the elastic modulus and thermal expansion coefficient for Type 304 stainless steel are $28.3(10)^6$ psi and $8.46(10)^{-6}$ inches/inch/ºF, respectively, at a temperature of 70 ºF.

The material properties for the polyurethane foam are consistent with those specified within Table 2.3-2 from Section 2.3.1, *Mechanical Properties Applied to Analytic Evaluations*. The elastic modulus in the x- (radial) and z- (hoop) directions is based on the average of the tensile and compressive, perpendicular-to-rise elastic modulus, or 5,854 psi. The elastic modulus in the y- (axial) direction is based on the average of the tensile and compressive, parallel-to-rise elastic modulus, or 8,789 psi. In addition, Poisson's ratio is 0.33, and the thermal expansion coefficient is $4.6(10)^{-5}$ inches/inch/ºF.

Both the reference and uniform temperature are set to 70 ºF, thereby excluding the effects of differential thermal expansion for this case.

For analysis model review, the ANSYS® input file is listed in Table 2.10.1-4.

2.10.1.2 Inner Containment Assembly (ICV) Structural Analysis

Finite element analyses (FEA) are performed on the ICV structure to determine the stress states of the various components under normal conditions of transport (NCT) loads. The FEA analyses are performed using ANSYS® 4.3A2. The ICV FEA model is comprised of four separate major structural components, modeled as shown in Figure 2.10.1-2:

- upper ICV seal flange
- lower ICV seal flange
- ICV locking ring
- ICV shells

The lower and upper seal flanges, and locking ring are modeled using 2-D, isoparametric solid elements (PLANE42). The quadrilateral elements are defined by four nodal points (a triangular element may be formed by defining duplicate the 3rd and 4th node numbers), each having two degrees of freedom: translations in the nodal x-direction (radial) and y-direction (axial).

The upper and lower ICV shells (ICV lid and body shells, respectively) are modeled using 2-D, axisymmetric conical shell elements (SHELL51). The lineal elements are defined by two nodal points, each having three degrees of freedom: translations in the nodal x-direction (radial) and y-direction (axial), and rotation about the nodal z-axis (hoop). In addition, the axisymmetric conical shell element is biaxial, with membrane and bending capabilities.

Relatively stiff, 2-D elastic beams (BEAM3) are utilized to maintain bending continuity between the three degree of freedom conical shell elements and two degree of freedom, isoparametric solid elements. Specifically, for both the lower and upper ICV seal flanges, four stiff beams are placed at each junction between the shell elements and the solid elements of the seal flanges. These elements are included to transmit the moment (i.e., to maintain slope continuity) between the shell and flange portions of the model, and have a negligible effect on the stress results.

Three sets of 2-D gap elements (CONTAC12) are utilized to connect the lower and upper ICV seal flanges to each other and to the ICV locking ring. The gap element is capable of supporting a load only in the direction normal to the surfaces, and is frictionless in the tangential direction. The gap element has two degrees of freedom at each node: translations in the nodal x-direction (radial) and y-direction (axial). A stiffness of 2×10^{10} lb/in is chosen to reflect the relatively high contact stiffness when closed. Three sets of gap elements are used in these analyses: 1) between the lower ICV seal flange and the ICV locking ring, 2) between the upper ICV seal flange and the ICV locking ring, and 3) between the lower ICV seal flange and the upper ICV seal flange.

To account for the tangential (hoop) direction slotting for the lower ICV seal flange and ICV locking ring in the axisymmetric model, the material properties in the directly affected regions are modified. Specifically, material properties for the shaded elements in the lower ICV seal flange and ICV locking ring, illustrated in Figure 2.10.1-2, are modified to reflect only one-half the stainless steel being present for strength purposes. Specifically, the elastic modulus in the x- and y-directions is reduced to one-half their normal value (since only approximately one-half the material remains in the slotted regions), and the elastic modulus in the z-direction is set to set to a very low value to eliminate virtually all tangential (hoop) stiffness in the slotted regions. In addition, Poisson's ratio is set at the normal value of 0.3 for the x-y plane, but is set to zero in the y-z and x-z planes. In these ways, the analyses accurately depict the stress levels in all regions.

The global origin of the nodal coordinate system is located at the bottom center of the ICV body, as shown in Figure 2.10.1-2. As such, the nodal x-axis corresponds to the radial direction, the nodal y-axis corresponds to the axial direction, and the nodal z-axis corresponds to the tangential (or hoop) direction. The model is constrained from translating in the radial direction and rotating about the hoop axis at the y-z symmetry plane at x equal zero. The model is also constrained from translating in the axial direction at a single node on the ICV locking ring.

2.10.1.2.1 ICV Structural Analysis – Load Case 1

For ICV Load Case 1, the ICV structural analysis uses a 50 psig (64.7 psia) internal pressure, corresponding to the maximum normal operating pressure (MNOP) from Section 3.4.4, *Maximum Internal Pressure*, coupled with a reduced external pressure of 3.5 psia (equivalently an 11.2 psig internal pressure), per Section 2.6.3, *Reduced External Pressure*, and 10 CFR §71.51(c)(3). The net internal pressure for this case is 61.2 psig, applied throughout the inner periphery of the model. Relative to the upper and lower ICV seal flanges, the internal pressure does not extend beyond (below) the top of the upper main O-ring seal groove.

A uniform temperature of 160 ºF, per Section 2.6.1.1, *Summary of Pressures and Temperatures*, is utilized to determine the temperature-dependent, material property values. The only material properties affected by a temperature of 160 ºF are the elastic modulus and the thermal expansion coefficient for the stainless steel. Consistent with Table 2.3-1 from Section 2.3.1, *Mechanical Properties Applied to Analytic Evaluations*, the elastic modulus and thermal expansion coefficient for Type 304 stainless steel are $27.8(10)^6$ psi and $8.694(10)^{-6}$ inches/inch/ºF, respectively, at a temperature of 160 ºF.

Both the reference and uniform temperature are set to 160 ºF, thereby excluding the effects of differential thermal expansion for this case.

For analysis model review, the ANSYS® input file is listed in Table 2.10.1-5.

2.10.1.2.2 ICV Structural Analysis – Load Case 2

For ICV Load Case 2, the ICV structural analysis uses a -14.7 psig (0.0 psia) internal pressure (i.e., full vacuum) coupled with an increased external pressure of 0.0 psig (14.7 psia), per Section 2.6.4, *Increased External Pressure*. The net external pressure for this case is 14.7 psig, applied throughout the inner periphery of the model. Relative to the upper and lower ICV seal flanges, the internal pressure does not extend beyond (below) the top of the upper main O-ring seal groove.

A uniform temperature of 70 ºF is utilized to determine the temperature-dependent, material property values. The only material properties affected by a temperature of 70 ºF are the elastic modulus and the thermal expansion coefficient for the stainless steel. Consistent with Table 2.3-1 from Section 2.3.1, *Mechanical Properties Applied to Analytic Evaluations*, the elastic modulus and thermal expansion coefficient for Type 304 stainless steel are $28.3(10)^6$ psi and $8.46(10)^{-6}$ inches/inch/ºF, respectively, at a temperature of 70 ºF.

Both the reference and uniform temperature are set to 70 ºF, thereby excluding the effects of differential thermal expansion for this case.

For analysis model review, the ANSYS® input file is listed in Table 2.10.1-6.

Table 2.10.1-1 – ANSYS® Input Listing for OCA Load Case 1

```
/TITLE, OCV: PRES=64.7/3.5 PSIA; TEMP=160/160 DEG-F
C***   Define the element types
ET,1,42,,,1
ET,2,51
ET,3,42,,,1
ET,4,12,,,1
ET,5,12
ET,6,3
C***   Define the reference and uniform temperatures
TREF,160
TUNIF,160
C***   Define the material properties for non-slotted
steel regions
EX,1,27.8E+06
NUXY,1,.3
DENS,1,7.505E-04
ALPX,1,8.694E-06
C***   Define the material properties for slotted
steel regions
EX,2,13.9E+06
EY,2,13.9E+06
EZ,2,1
NUXY,2,.3
NUXZ,2,0
NUYZ,2,0
DENS,2,3.7525E-04
ALPX,2,8.694E-06
ALPY,2,8.694E-06
ALPZ,2,8.694E-06
C***   Define the material properties for the
polyurethane foam
EX,3,5854
EY,3,8789
EZ,3,5854
GXY,3,2553
GXZ,3,1921
GYZ,3,2553
NUXY,3,.33
DENS,3,1.198E-05
ALPX,3,4.9E-05
C***   Define the material properties for the rigid
coupling elements (STIF3 beams)
EX,4,27.8E+06
NUXY,4,.3
DENS,4,0
ALPX,4,8.694E-06
C***   Define the element real constants
R,1,.25
R,2,.1875
R,3,.375
R,4,.075
R,5,,2E+10,,1
R,6,-15,2E+10,-.036
R,7,15,2E+10,-.036
R,8,0,2E+10,,1
R,9,1,1,1
R,101,-180.000,2E+10,,1
R,102,-177.444,2E+10,,1
R,103,-174.888,2E+10,,1
R,104,-172.333,2E+10,,1
R,105,-169.777,2E+10,,1
R,106,-167.221,2E+10,,1
R,107,-164.665,2E+10,,1
R,108,-162.109,2E+10,,1
R,109,-159.553,2E+10,,1
R,110,-156.998,2E+10,,1
R,111,-154.442,2E+10,,1
R,112,-141.553,2E+10,,1
R,113,-128.665,2E+10,,1
R,114,-115.777,2E+10,,1
R,115,-102.888,2E+10,,1
R,116,-90.0000,2E+10,,1
R,130,-102.000,2E+10,,1
R,136,-77.1520,2E+10,,1
R,137,-64.3041,2E+10,,1
R,138,-51.4561,2E+10,,1
R,139,-38.6081,2E+10,,1
R,140,-25.7602,2E+10,,1
R,141,-23.1841,2E+10,,1
R,142,-20.6081,2E+10,,1
R,143,-18.0321,2E+10,,1
R,144,-15.4561,2E+10,,1
R,145,-12.8801,2E+10,,1
R,146,-10.3041,2E+10,,1
R,147,-7.72805,2E+10,,1
R,148,-5.15203,2E+10,,1
R,149,-2.57602,2E+10,,1
R,150,,2E+10,,1
R,639,-58.7238,2E+10,,1
R,640,-27.4476,2E+10,,1
R,641,-24.7029,2E+10,,1
R,642,-21.9581,2E+10,,1
R,643,-19.2133,2E+10,,1
R,644,-16.4686,2E+10,,1
R,645,-13.7238,2E+10,,1
R,646,-10.9790,2E+10,,1
R,647,-8.23429,2E+10,,1
R,648,-5.48952,2E+10,,1
R,649,-2.74476,2E+10,,1
C***   Define the nodes for the lower seal flange
LOCAL,11,,38.24941495,80.051977923,,-12
N,1001
N,1005,.25
FILL
N,1016,,.58677836
N,1020,.25,.58677836
FILL
FILL,1001,1016,2,1006,5,5,1
N,1026,,.896632635
LOCAL,12,,38.505,80
MOVE,1026,11,0,999,0,12,-.065,999,0
FILL,1016,1026,1,1021
LOCAL,11,1,39.12699808,80.47
N,1025,.5,148.5
N,1030,.5,129
N,1031,.5,109.5
N,1032,.5,90
CSYS,12
FILL,1021,1025,3,1022,1,2,5
N,1033,.775,.97
N,1034,1.145,.97
N,1076,-.065,2.98
FILL,1026,1076,8,1035,5
FILL,1035,1076,7,1041,5
N,1060,.775,2.15593612
NGEN,2,6,1033,1034,1,,.16
FILL,1039,1060,3,1045,5
FILL,1035,1039
FILL,1041,1045,3,1042,1,4,5
N,1064,1.245,2.03
FILL,1060,1064
N,1092,-.065,2.98
N,1096,.77960172,2.76
FILL
N,1100,1.245,2.76
FILL,1096,1100
FILL,1056,1092,3,1065,9,9,1
NGEN,3,9,1098,1100,1,,.26
N,1146,.14020351,4.4
FILL,1092,1146,5,1101,9
N,1164,.14020351,4.98
FILL,1146,1164,1,1155
LOCAL,11,,39.13520351,84.98,,-86.15
N,1168
N,1159,.3
NGEN,3,-1,1159,1159,,,-.125
N,1148,.58,-.25
NGEN,2,-18,1157,1159,1,.56
NGEN,2,-9,1139,1141,1,.25
NGEN,2,-27,1148,1148,,.81
NGEN,2,-18,1130,1132,1,.56
FILL,1096,1114,1,1105
CSYS,12
FILL,1101,1105
FILL,1110,1112,1,1111,,6,9
FILL,1164,1168
```

```
C***   Define the nodes for the upper seal flange

LOCAL,11,,38.405,82.81
N,2001,,5
N,2005,.25,5
FILL
NGEN,3,5,2001,2005,1,,-.25
N,2031,,3.45
N,2035,.91,3.45
FILL
FILL,2011,2031,3,2016,5,5,1
N,2051,,2.543442101
N,2055,.91,2.543442101
FILL
FILL,2031,2051,3,2036,5,4,1
N,2040,.91,3.29
FILL,2040,2055,2,2045,5
N,2059,1.345,2.66
FILL,2055,2059
N,2071,,2.17
N,2073,.21504507,2.17
FILL
N,2077,.74504507,2.17
FILL,2073,2077
FILL,2051,2071,1,2060
FILL,2054,2076,1,2065
FILL,2060,2065
N,2081,1.345,2.17
FILL,2077,2081
FILL,2055,2077,1,2066,,5,1
N,2107,.85759646,.54
N,2109,1.10488343,.54
FILL
N,2111,1.345,.54
FILL,2109,2111
FILL,2077,2107,5,2082,5,5,1
N,2117,.94488343
N,2119,1.10488343
FILL
FILL,2109,2119,1,2114
N,2112,.870715847,.35
FILL,2112,2114
N,2120,1.345,3.45
N,2121,1.345,3.29
NGEN,2,51,2071,2073,1,,-.305
NGEN,2,3,2122,2124,1,,-.305

C***   Define the nodes for the locking ring

LOCAL,11,,39.35,81.29
N,3001
N,3005,.435
FILL
N,3009,.935
FILL,3005,3009
N,3037,,.81
N,3041,.435,.693442101
FILL
N,3045,.935,.693442101
FILL,3041,3045
FILL,3001,3037,3,3010,9,9,1
N,3145,,4.11
N,3149,.435,4.226557899
FILL
N,3153,.935,4.226557899
FILL,3149,3153
FILL,3041,3149,11,3050,9,5,1
N,3181,,4.67
N,3185,.535,4.67
FILL
N,3189,.935,4.67
FILL,3185,3189
FILL,3145,3181,3,3154,9,9,1

C***   Define the nodes for the OCA inner shell (OCV)

LOCAL,11,1,,84.5
N,101,74.25,-90
N,111,74.25,-64.44174492
FILL
LOCAL,12,1,28.3125,24.29659664
N,116,8.625
FILL,111,116
CSYS
N,117,36.9375,25.79659664
N,123,36.9375,51.79659664
FILL
N,129,36.9375,73.95292590
FILL,123,129
NGEN,2,-872,1003,1003
FILL,129,131
NGEN,2,-1870,2003,2003
N,135,38.53,93.78649751
FILL,133,135
LOCAL,13,1,29.905,93.78649751
N,140,8.625,64.23984399
FILL,135,140
LOCAL,14,1,,31.8125
N,150,77.4375,90
FILL,140,150

C***   Define the nodes for the OCA outer shell

CSYS
N,601
N,613,47.0625
FILL
N,626,47.0625,64.7775
FILL,613,626
N,629,47.0625,76.7775
FILL,626,629
N,630,47.0625,77.6325
N,638,47.0625,105.3440689
FILL,630,638
LOCAL,15,1,40.5625,105.3440689
N,640,6.5,62.55238078
FILL,638,640
LOCAL,16,1,,27.25
N,650,94.5,90
FILL,640,650

C***   Define the nodes for the polyurethane foam
inner surface

CSYS
NGEN,2,100,101,150,1
N,132,38.58338729,80.97
N,232,38.53,86.26

C***   Define the nodes for the polyurethane foam
outer surface

NGEN,2,-100,601,650,1

C***   Define the intermediate polyurethane foam nodes

FILL,201,501,2,301,100,29,1
N,300,43.9375,80.9
N,331,41.5375,81.8825
N,332,41.5375,86.26
N,429,43.9375,76.7775
N,430,44.2375,77.6375
N,431,44.2375,81.8825
FILL,229,429,1,329,100,2,1
FILL,230,300,1,330
FILL,332,532,1,432
FILL,233,533,2,333,100,18,1
N,323,38.4375,51.79659664

C***   Define the nodes for the Z-flanges

NGEN,2,272,429,429,0
NGEN,2,402,300,300,0
NGEN,2,273,430,430,0
RP2,,,1,1
NGEN,2,374,331,331,0
RP2,,,1,1

C***   Define the elements for the lower seal flange

TYPE,1
MAT,1
REAL,1
E,1001,1002,1007,1006
RP4,1,1,1,1
EGEN,5,5,1,4,1
E,1026,1027,1036,1035
E,1027,1028,1036
E,1028,1029,1037,1036
E,1029,1030,1031,1037
E,1031,1032,1038,1037
RP3,1,1,1,1
E,1035,1036,1042,1041
RP4,1,1,1,1
E,1041,1042,1047,1046
RP4,1,1,1,1
EGEN,3,5,32,35,1
E,1056,1057,1066,1065
RP4,1,1,1,1
```

```
EGEN,4,9,44,47,1
MAT,2
E,1060,1061,1070,1069
RP4,1,1,1,1
EGEN,4,9,60,63,1
EGEN,3,9,74,75,1
EGEN,3,9,56,59,1
EGEN,7,9,84,85,1
EGEN,3,1,99,99
EGEN,3,1,93,93
C***   Define the elements for the upper seal flange
TYPE,1
MAT,1
REAL,1
E,2006,2007,2002,2001
RP4,1,1,1,1
EGEN,10,5,104,107,1
E,2040,2121,2120,2035
E,2060,2061,2052,2051
E,2061,2062,2052
E,2062,2063,2053,2052
E,2063,2064,2053
E,2064,2065,2054,2053
RP6,1,1,1,1
E,2071,2072,2061,2060
RP10,1,1,1,1
E,2122,2123,2072,2071
RP2,1,1,1,1
E,2125,2126,2123,2122
RP2,1,1,1,1
E,2082,2083,2078,2077
RP4,1,1,1,1
EGEN,6,5,169,172,1
EGEN,3,5,189,190,1
C***   Define the elements for the locking ring
TYPE,1
MAT,2
REAL,1
E,3001,3002,3011,3010
RP4,1,1,1,1
EGEN,4,9,197,200,1
MAT,1
E,3005,3006,3015,3014
RP4,1,1,1,1
EGEN,20,9,213,216,1
E,3145,3146,3155,3154
RP4,1,1,1,1
EGEN,4,9,293,296,1
C***   Define the elements for the OCA inner shell
(OCV)
TYPE,2
MAT,1
REAL,1
E,101,102
RP16,1,1
REAL,2
E,117,118
RP12,1,1
REAL,3
E,123,323
REAL,1
E,129,130
E,130,1003
E,2003,134
E,134,135
RP16,1,1
C***   Define the elements for the OCA outer shell
REAL,1
E,601,602
RP25,1,1
REAL,3
E,626,627
RP3,1,1
E,630,631
RP8,1,1
REAL,1
E,638,639
RP12,1,1
C***   Define the elements for the Z-flanges
REAL,4
E,629,701
E,701,702
E,702,1034
E,1034,1033
E,630,703
E,703,704
RP3,1,1
E,706,2120
E,2120,2035
C***   Define the polyurethane foam elements
TYPE,3
MAT,3
REAL,1
E,201,301,302,202
RP29,1,1,1,1
E,231,230,330
E,301,401,402,302
RP28,1,1,1,1
E,329,429,300,330
E,300,132,231,330
E,401,501,502,402
RP28,1,1,1,1
E,333,233,232,332
E,233,333,334,234
RP17,1,1,1,1
E,331,431,432,332
RP19,1,1,1,1
E,430,530,531,431
RP20,1,1,1,1
C***   Define the interface elements between the steel
shells and the polyurethane foam
TYPE,5
MAT,1
REAL,101
E,101,201
REAL,102
E,102,202
REAL,103
E,103,203
REAL,104
E,104,204
REAL,105
E,105,205
REAL,106
E,106,206
REAL,107
E,107,207
REAL,108
E,108,208
REAL,109
E,109,209
REAL,110
E,110,210
REAL,111
E,111,211
REAL,112
E,112,212
REAL,113
E,113,213
REAL,114
E,114,214
REAL,115
E,115,215
REAL,116
E,116,216
RP7,1,1
E,124,224
RP6,1,1
REAL,130
E,129,229
RP2,1,1
E,1003,231
REAL,101
E,702,300
E,701,429
E,622,529
REAL,150
E,706,332
E,705,331
E,704,431
E,703,430
E,630,530
REAL,116
E,300,702
E,429,701
```

```
E,706,332
E,705,331
E,704,431
E,703,430
E,2003,233
E,134,234
RP2,1,1
REAL,136
E,136,236
REAL,137
E,137,237
REAL,138
E,138,238
REAL,139
E,139,239
REAL,140
E,140,240
REAL,141
E,141,241
REAL,142
E,142,242
REAL,143
E,143,243
REAL,144
E,144,244
REAL,145
E,145,245
REAL,146
E,146,246
REAL,147
E,147,247
REAL,148
E,148,248
REAL,149
E,149,249
REAL,150
E,150,250
REAL,101
E,501,601
RP13,1,1
REAL,116
E,513,613
RP26,1,1
REAL,639
E,539,639
REAL,640
E,540,640
REAL,641
E,541,641
REAL,642
E,542,642
REAL,643
E,543,643
REAL,644
E,544,644
REAL,645
E,545,645
REAL,646
E,546,646
REAL,647
E,547,647
REAL,648
E,548,648
REAL,649
E,549,649
REAL,150
E,550,650
C***   Define the interface elements between the lower
seal flange and the locking ring
TYPE,4
MAT,1
REAL,6
E,3038,1061
RP3,1,1
C***   Define the interface elements between the upper
seal flange and the locking ring
TYPE,4
MAT,1
REAL,7
E,2056,3146
RP3,1,1
C***   Define the interface elements between the lower
seal flange and the upper seal flange
TYPE,5
MAT,1
REAL,8
E,1164,2073
RP5,1,1
C***   Couple the lower shell to the lower seal flange
TYPE,6
MAT,4
REAL,9
E,1001,1002
RP4,1,1
C***   Couple the upper shell to the upper seal flange
TYPE,6
MAT,4
REAL,9
E,2001,2002
RP4,1,1
C***   Define the displacement constraints
D,101,UX,0,,601,500,ROTZ
D,201,UX,0,,501,100
D,150,UX,0,,650,500,ROTZ
D,250,UX,0,,550,100
D,3099,UY,0
C***   Define the pressure loads
P,101,102,61.2,,129,1
P,130,1003,61.2
P,1001,1006,61.2,,1021,5
P,1026,1035,61.2
P,1035,1041,61.2
P,1041,1046,61.2,,1051,5
P,1056,1065,61.2,,1155,9
P,1164,1165,61.2,,1167,1
P,1168,1159,61.2
P,2077,2082,61.2
P,2073,2074,61.2,,2076,1
P,2127,2124,61.2
P,2124,2073,61.2
P,2125,2126,61.2,,2126,1
P,2122,2125,61.2
P,2071,2122,61.2
P,2001,2002,61.2,,2002,1
P,2001,2006,61.2,,2046,5
P,2051,2060,61.2
P,2060,2071,61.2
P,2003,134,61.2
P,134,135,61.2,,149,1
C***   Re-order the elements to reduce execution time
WSTART,101,601,100
WSTART,150,650,100
WSTART,1003
WSTART,1034
WSTART,2120
WSTART,2003
WAVES
C***   Set convergence criteria, write a solution
file, and exit
ITER,-20,20
AFWRITE
FINISH
```

Table 2.10.1-2 – ANSYS® Input Listing for OCA Load Case 2

```
/TITLE, OCV: PRES=64.7/3.5 PSIA; TEMP=70/160 DEG-F
C***   Define the element types
ET,1,42,,,1
ET,2,51
ET,3,42,,,1
ET,4,12,,,1
ET,5,12
ET,6,3
C***   Define the reference and uniform temperatures
TREF,70
TUNIF,160
C***   Define the material properties for non-slotted
steel regions
EX,1,27.8E+06
NUXY,1,.3
DENS,1,7.505E-04
ALPX,1,8.694E-06
C***   Define the material properties for slotted
steel regions
EX,2,13.9E+06
EY,2,13.9E+06
EZ,2,1
NUXY,2,.3
NUXZ,2,0
NUYZ,2,0
DENS,2,3.7525E-04
ALPX,2,8.694E-06
ALPY,2,8.694E-06
ALPZ,2,8.694E-06
C***   Define the material properties for the
polyurethane foam
EX,3,5854
EY,3,8789
EZ,3,5854
GXY,3,2553
GXZ,3,1921
GYZ,3,2553
NUXY,3,.33
DENS,3,1.198E-05
ALPX,3,4.9E-05
C***   Define the material properties for the rigid
coupling elements (STIF3 beams)
EX,4,27.8E+06
NUXY,4,.3
DENS,4,0
ALPX,4,8.694E-06
C***   Define the element real constants
R,1,.25
R,2,.1875
R,3,.375
R,4,.075
R,5,,2E+10,,1
R,6,-15,2E+10,-.036
R,7,15,2E+10,-.036
R,8,0,2E+10,,1
R,9,1,1,1
R,101,-180.000,2E+10,,1
R,102,-177.444,2E+10,,1
R,103,-174.888,2E+10,,1
R,104,-172.333,2E+10,,1
R,105,-169.777,2E+10,,1
R,106,-167.221,2E+10,,1
R,107,-164.665,2E+10,,1
R,108,-162.109,2E+10,,1
R,109,-159.553,2E+10,,1
R,110,-156.998,2E+10,,1
R,111,-154.442,2E+10,,1
R,112,-141.553,2E+10,,1
R,113,-128.665,2E+10,,1
R,114,-115.777,2E+10,,1
R,115,-102.888,2E+10,,1
R,116,-90.0000,2E+10,,1
R,130,-102.000,2E+10,,1
R,136,-77.1520,2E+10,,1
R,137,-64.3041,2E+10,,1
R,138,-51.4561,2E+10,,1
R,139,-38.6081,2E+10,,1
R,140,-25.7602,2E+10,,1
R,141,-23.1841,2E+10,,1
R,142,-20.6081,2E+10,,1
R,143,-18.0321,2E+10,,1
R,144,-15.4561,2E+10,,1
R,145,-12.8801,2E+10,,1
R,146,-10.3041,2E+10,,1
R,147,-7.72805,2E+10,,1
R,148,-5.15203,2E+10,,1
R,149,-2.57602,2E+10,,1
R,150,,2E+10,,1
R,639,-58.7238,2E+10,,1
R,640,-27.4476,2E+10,,1
R,641,-24.7029,2E+10,,1
R,642,-21.9581,2E+10,,1
R,643,-19.2133,2E+10,,1
R,644,-16.4686,2E+10,,1
R,645,-13.7238,2E+10,,1
R,646,-10.9790,2E+10,,1
R,647,-8.23429,2E+10,,1
R,648,-5.48952,2E+10,,1
R,649,-2.74476,2E+10,,1
C***   Define the nodes for the lower seal flange
LOCAL,11,,38.24941495,80.051977923,,-12
N,1001
N,1005,.25
FILL
N,1016,,.58677836
N,1020,.25,.58677836
FILL
FILL,1001,1016,2,1006,5,5,1
N,1026,,.896632635
LOCAL,12,,38.505,80
MOVE,1026,11,0,999,0,12,-.065,999,0
FILL,1016,1026,1,1021
LOCAL,11,1,39.12699808,80.47
N,1025,.5,148.5
N,1030,.5,129
N,1031,.5,109.5
N,1032,.5,90
CSYS,12
FILL,1021,1025,3,1022,1,2,5
N,1033,.775,.97
N,1034,1.145,.97
N,1076,-.065,2.98
FILL,1026,1076,8,1035,5
FILL,1035,1076,7,1041,5
N,1060,.775,2.15593612
NGEN,2,6,1033,1034,1,,.16
FILL,1039,1060,3,1045,5
FILL,1035,1039
FILL,1041,1045,3,1042,1,4,5
N,1064,1.245,2.03
FILL,1060,1064
N,1092,-.065,2.98
N,1096,.77960172,2.76
FILL
N,1100,1.245,2.76
FILL,1096,1100
FILL,1056,1092,3,1065,9,9,1
NGEN,3,9,1098,1100,1,,.26
N,1146,.14020351,4.4
FILL,1092,1146,5,1101,9
N,1164,.14020351,4.98
FILL,1146,1164,1,1155
LOCAL,11,,39.13520351,84.98,,-86.15
N,1168
N,1159,.3
NGEN,3,-1,1159,1159,,,-.125
N,1148,.58,-.25
NGEN,2,-18,1157,1159,1,.56
NGEN,2,-9,1139,1141,1,.25
NGEN,2,-27,1148,1148,,.81
NGEN,2,-18,1130,1132,1,.56
FILL,1096,1114,1,1105
CSYS,12
FILL,1101,1105
FILL,1110,1112,1,1111,,6,9
FILL,1164,1168
```

```
C***   Define the nodes for the upper seal flange

LOCAL,11,,38.405,82.81
N,2001,,5
N,2005,.25,5
FILL
NGEN,3,5,2001,2005,1,,-.25
N,2031,,3.45
N,2035,.91,3.45
FILL
FILL,2011,2031,3,2016,5,5,1
N,2051,,2.543442101
N,2055,.91,2.543442101
FILL
FILL,2031,2051,3,2036,5,4,1
N,2040,.91,3.29
FILL,2040,2055,2,2045,5
N,2059,1.345,2.66
FILL,2055,2059
N,2071,,2.17
N,2073,.21504507,2.17
FILL
N,2077,.74504507,2.17
FILL,2073,2077
FILL,2051,2071,1,2060
FILL,2054,2076,1,2065
FILL,2060,2065
N,2081,1.345,2.17
FILL,2077,2081
FILL,2055,2077,1,2066,,5,1
N,2107,.85759646,.54
N,2109,1.10488343,.54
FILL
N,2111,1.345,.54
FILL,2109,2111
FILL,2077,2107,5,2082,5,5,1
N,2117,.94488343
N,2119,1.10488343
FILL
FILL,2109,2119,1,2114
N,2112,.870715847,.35
FILL,2112,2114
N,2120,1.345,3.45
N,2121,1.345,3.29
NGEN,2,51,2071,2073,1,,-.305
NGEN,2,3,2122,2124,1,,-.305

C***   Define the nodes for the locking ring

LOCAL,11,,39.35,81.29
N,3001
N,3005,.435
FILL
N,3009,.935
FILL,3005,3009
N,3037,,.81
N,3041,.435,.693442101
FILL
N,3045,.935,.693442101
FILL,3041,3045
FILL,3001,3037,3,3010,9,9,1
N,3145,,4.11
N,3149,.435,4.226557899
FILL
N,3153,.935,4.226557899
FILL,3149,3153
FILL,3041,3149,11,3050,9,5,1
N,3181,,4.67
N,3185,.535,4.67
FILL
N,3189,.935,4.67
FILL,3185,3189
FILL,3145,3181,3,3154,9,9,1

C***   Define the nodes for the OCA inner shell (OCV)

LOCAL,11,1,,84.5
N,101,74.25,-90
N,111,74.25,-64.44174492
FILL
LOCAL,12,1,28.3125,24.29659664
N,116,8.625
FILL,111,116
CSYS
N,117,36.9375,25.79659664
N,123,36.9375,51.79659664
FILL
N,129,36.9375,73.95292590
FILL,123,129
NGEN,2,-872,1003,1003
FILL,129,131
NGEN,2,-1870,2003,2003
N,135,38.53,93.78649751
FILL,133,135
LOCAL,13,1,29.905,93.78649751
N,140,8.625,64.23984399
FILL,135,140
LOCAL,14,1,,31.8125
N,150,77.4375,90
FILL,140,150

C***   Define the nodes for the OCA outer shell

CSYS
N,601
N,613,47.0625
FILL
N,626,47.0625,64.7775
FILL,613,626
N,629,47.0625,76.7775
FILL,626,629
N,630,47.0625,77.6325
N,638,47.0625,105.3440689
FILL,630,638
LOCAL,15,1,40.5625,105.3440689
N,640,6.5,62.55238078
FILL,638,640
LOCAL,16,1,,27.25
N,650,94.5,90
FILL,640,650

C***   Define the nodes for the polyurethane foam
inner surface

CSYS
NGEN,2,100,101,150,1
N,132,38.58338729,80.97
N,232,38.53,86.26

C***   Define the nodes for the polyurethane foam
outer surface

NGEN,2,-100,601,650,1

C***   Define the intermediate polyurethane foam nodes

FILL,201,501,2,301,100,29,1
N,300,43.9375,80.9
N,331,41.5375,81.8825
N,332,41.5375,86.26
N,429,43.9375,76.7775
N,430,44.2375,77.6375
N,431,44.2375,81.8825
FILL,229,429,1,329,100,2,1
FILL,230,300,1,330
FILL,332,532,1,432
FILL,233,533,2,333,100,18,1
N,323,38.4375,51.79659664

C***   Define the nodes for the Z-flanges

NGEN,2,272,429,429,0
NGEN,2,402,300,300,0
NGEN,2,273,430,430,0
RP2,,,1,1
NGEN,2,374,331,331,0
RP2,,,1,1

C***   Define the elements for the lower seal flange

TYPE,1
MAT,1
REAL,1
E,1001,1002,1007,1006
RP4,1,1,1,1
EGEN,5,5,1,4,1
E,1026,1027,1036,1035
E,1027,1028,1036
E,1028,1029,1037,1036
E,1029,1030,1031,1037
E,1031,1032,1038,1037
RP3,1,1,1,1
E,1035,1036,1042,1041
RP4,1,1,1,1
E,1041,1042,1047,1046
RP4,1,1,1,1
EGEN,3,5,32,35,1
E,1056,1057,1066,1065
RP4,1,1,1,1
```

```
EGEN,4,9,44,47,1
MAT,2
E,1060,1061,1070,1069
RP4,1,1,1,1
EGEN,4,9,60,63,1
EGEN,3,9,74,75,1
EGEN,3,9,56,59,1
EGEN,7,9,84,85,1
EGEN,3,1,99,99
EGEN,3,1,93,93
C***   Define the elements for the upper seal flange
TYPE,1
MAT,1
REAL,1
E,2006,2007,2002,2001
RP4,1,1,1,1
EGEN,10,5,104,107,1
E,2040,2121,2120,2035
E,2060,2061,2052,2051
E,2061,2062,2052
E,2062,2063,2053,2052
E,2063,2064,2053
E,2064,2065,2054,2053
RP6,1,1,1,1
E,2071,2072,2061,2060
RP10,1,1,1,1
E,2122,2123,2072,2071
RP2,1,1,1,1
E,2125,2126,2123,2122
RP2,1,1,1,1
E,2082,2083,2078,2077
RP4,1,1,1,1
EGEN,6,5,169,172,1
EGEN,3,5,189,190,1
C***   Define the elements for the locking ring
TYPE,1
MAT,2
REAL,1
E,3001,3002,3011,3010
RP4,1,1,1,1
EGEN,4,9,197,200,1
MAT,1
E,3005,3006,3015,3014
RP4,1,1,1,1
EGEN,20,9,213,216,1
E,3145,3146,3155,3154
RP4,1,1,1,1
EGEN,4,9,293,296,1
C***   Define the elements for the OCA inner shell
(OCV)
TYPE,2
MAT,1
REAL,1
E,101,102
RP16,1,1
REAL,2
E,117,118
RP12,1,1
REAL,3
E,123,323
REAL,1
E,129,130
E,130,1003
E,2003,134
E,134,135
RP16,1,1
C***   Define the elements for the OCA outer shell
REAL,1
E,601,602
RP25,1,1
REAL,3
E,626,627
RP3,1,1
E,630,631
RP8,1,1
REAL,1
E,638,639
RP12,1,1
C***   Define the elements for the Z-flanges
REAL,4
E,629,701
E,701,702
E,702,1034
E,1034,1033
E,630,703
E,703,704
RP3,1,1
E,706,2120
E,2120,2035
C***   Define the polyurethane foam elements
TYPE,3
MAT,3
REAL,1
E,201,301,302,202
RP29,1,1,1,1
E,231,230,330
E,301,401,402,302
RP28,1,1,1,1
E,329,429,300,330
E,300,132,231,330
E,401,501,502,402
RP28,1,1,1,1
E,333,233,232,332
E,233,333,334,234
RP17,1,1,1,1
E,331,431,432,332
RP19,1,1,1,1
E,430,530,531,431
RP20,1,1,1,1
C***   Define the interface elements between the steel
shells and the polyurethane foam
TYPE,5
MAT,1
REAL,101
E,101,201
REAL,102
E,102,202
REAL,103
E,103,203
REAL,104
E,104,204
REAL,105
E,105,205
REAL,106
E,106,206
REAL,107
E,107,207
REAL,108
E,108,208
REAL,109
E,109,209
REAL,110
E,110,210
REAL,111
E,111,211
REAL,112
E,112,212
REAL,113
E,113,213
REAL,114
E,114,214
REAL,115
E,115,215
REAL,116
E,116,216
RP7,1,1
E,124,224
RP6,1,1
REAL,130
E,129,229
RP2,1,1
E,1003,231
REAL,101
E,702,300
E,701,429
E,622,529
REAL,150
E,706,332
E,705,331
E,704,431
E,703,430
E,630,530
REAL,116
E,300,702
E,429,701
```

```
E,706,332
E,705,331
E,704,431
E,703,430
E,2003,233
E,134,234
RP2,1,1
REAL,136
E,136,236
REAL,137
E,137,237
REAL,138
E,138,238
REAL,139
E,139,239
REAL,140
E,140,240
REAL,141
E,141,241
REAL,142
E,142,242
REAL,143
E,143,243
REAL,144
E,144,244
REAL,145
E,145,245
REAL,146
E,146,246
REAL,147
E,147,247
REAL,148
E,148,248
REAL,149
E,149,249
REAL,150
E,150,250
REAL,101
E,501,601
RP13,1,1
REAL,116
E,513,613
RP26,1,1
REAL,639
E,539,639
REAL,640
E,540,640
REAL,641
E,541,641
REAL,642
E,542,642
REAL,643
E,543,643
REAL,644
E,544,644
REAL,645
E,545,645
REAL,646
E,546,646
REAL,647
E,547,647
REAL,648
E,548,648
REAL,649
E,549,649
REAL,150
E,550,650
C***   Define the interface elements between the lower
seal flange and the locking ring
TYPE,4
MAT,1
REAL,6
E,3038,1061
RP3,1,1
C***   Define the interface elements between the upper
seal flange and the locking ring
TYPE,4
MAT,1
REAL,7
E,2056,3146
RP3,1,1
C***   Define the interface elements between the lower
seal flange and the upper seal flange
TYPE,5
MAT,1
REAL,8
E,1164,2073
RP5,1,1
C***   Couple the lower shell to the lower seal flange
TYPE,6
MAT,4
REAL,9
E,1001,1002
RP4,1,1
C***   Couple the upper shell to the upper seal flange
TYPE,6
MAT,4
REAL,9
E,2001,2002
RP4,1,1
C***   Define the displacement constraints
D,101,UX,0,,601,500,ROTZ
D,201,UX,0,,501,100
D,150,UX,0,,650,500,ROTZ
D,250,UX,0,,550,100
D,3099,UY,0
C***   Define the pressure loads
P,101,102,61.2,,129,1
P,130,1003,61.2
P,1001,1006,61.2,,1021,5
P,1026,1035,61.2
P,1035,1041,61.2
P,1041,1046,61.2,,1051,5
P,1056,1065,61.2,,1155,9
P,1164,1165,61.2,,1167,1
P,1168,1159,61.2
P,2077,2082,61.2
P,2073,2074,61.2,,2076,1
P,2127,2124,61.2
P,2124,2073,61.2
P,2125,2126,61.2,,2126,1
P,2122,2125,61.2
P,2071,2122,61.2
P,2001,2002,61.2,,2002,1
P,2001,2006,61.2,,2046,5
P,2051,2060,61.2
P,2060,2071,61.2
P,2003,134,61.2
P,134,135,61.2,,149,1
C***   Re-order the elements to reduce execution time
WSTART,101,601,100
WSTART,150,650,100
WSTART,1003
WSTART,1034
WSTART,2120
WSTART,2003
WAVES
C***   Set convergence criteria, write a solution
file, and exit
ITER,-20,20
AFWRITE
FINISH
```

Table 2.10.1-3 – ANSYS® Input Listing for OCA Load Case 3

```
/TITLE, OCV: PRES=14.7/14.7 PSIA; TEMP=70/-40 DEG-F
C***   Define the element types
ET,1,42,,,1
ET,2,51
ET,3,42,,,1
ET,4,12,,,1
ET,5,12
ET,6,3
C***   Define the reference and uniform temperatures
TREF,70
TUNIF,-40
C***   Define the material properties for non-slotted
steel regions
EX,1,28.8E+06
NUXY,1,.3
DENS,1,7.505E-04
ALPX,1,8.080E-06
C***   Define the material properties for slotted
steel regions
EX,2,14.4E+06
EY,2,14.4E+06
EZ,2,1
NUXY,2,.3
NUXZ,2,0
NUYZ,2,0
DENS,2,3.7525E-04
ALPX,2,8.080E-06
ALPY,2,8.080E-06
ALPZ,2,8.080E-06
C***   Define the material properties for the
polyurethane foam
EX,3,5854
EY,3,8789
EZ,3,5854
GXY,3,2553
GXZ,3,1921
GYZ,3,2553
NUXY,3,.33
DENS,3,1.198E-05
ALPX,3,4.3E-05
C***   Define the material properties for the rigid
coupling elements (STIF3 beams)
EX,4,28.8E+06
NUXY,4,.3
DENS,4,0
ALPX,4,8.080E-06
C***   Define the element real constants
R,1,.25
R,2,.1875
R,3,.375
R,4,.075
R,5,,2E+10,,1
R,6,-15,2E+10,-.036
R,7,15,2E+10,-.036
R,8,0,2E+10,,1
R,9,1,1,1
R,101,-180.000,2E+10,,1
R,102,-177.444,2E+10,,1
R,103,-174.888,2E+10,,1
R,104,-172.333,2E+10,,1
R,105,-169.777,2E+10,,1
R,106,-167.221,2E+10,,1
R,107,-164.665,2E+10,,1
R,108,-162.109,2E+10,,1
R,109,-159.553,2E+10,,1
R,110,-156.998,2E+10,,1
R,111,-154.442,2E+10,,1
R,112,-141.553,2E+10,,1
R,113,-128.665,2E+10,,1
R,114,-115.777,2E+10,,1
R,115,-102.888,2E+10,,1
R,116,-90.0000,2E+10,,1
R,130,-102.000,2E+10,,1
R,136,-77.1520,2E+10,,1
R,137,-64.3041,2E+10,,1
R,138,-51.4561,2E+10,,1
R,139,-38.6081,2E+10,,1
R,140,-25.7602,2E+10,,1
R,141,-23.1841,2E+10,,1
R,142,-20.6081,2E+10,,1
R,143,-18.0321,2E+10,,1
R,144,-15.4561,2E+10,,1
R,145,-12.8801,2E+10,,1
R,146,-10.3041,2E+10,,1
R,147,-7.72805,2E+10,,1
R,148,-5.15203,2E+10,,1
R,149,-2.57602,2E+10,,1
R,150,,2E+10,,1
R,639,-58.7238,2E+10,,1
R,640,-27.4476,2E+10,,1
R,641,-24.7029,2E+10,,1
R,642,-21.9581,2E+10,,1
R,643,-19.2133,2E+10,,1
R,644,-16.4686,2E+10,,1
R,645,-13.7238,2E+10,,1
R,646,-10.9790,2E+10,,1
R,647,-8.23429,2E+10,,1
R,648,-5.48952,2E+10,,1
R,649,-2.74476,2E+10,,1
C***   Define the nodes for the lower seal flange
LOCAL,11,,38.24941495,80.051977923,,-12
N,1001
N,1005,.25
FILL
N,1016,,.58677836
N,1020,.25,.58677836
FILL
FILL,1001,1016,2,1006,5,5,1
N,1026,,.896632635
LOCAL,12,,38.505,80
MOVE,1026,11,0,999,0,12,-.065,999,0
FILL,1016,1026,1,1021
LOCAL,11,1,39.12699808,80.47
N,1025,.5,148.5
N,1030,.5,129
N,1031,.5,109.5
N,1032,.5,90
CSYS,12
FILL,1021,1025,3,1022,1,2,5
N,1033,.775,.97
N,1034,1.145,.97
N,1076,-.065,2.98
FILL,1026,1076,8,1035,5
FILL,1035,1076,7,1041,5
N,1060,.775,2.15593612
NGEN,2,6,1033,1034,1,,.16
FILL,1039,1060,3,1045,5
FILL,1035,1039
FILL,1041,1045,3,1042,1,4,5
N,1064,1.245,2.03
FILL,1060,1064
N,1092,-.065,2.98
N,1096,.77960172,2.76
FILL
N,1100,1.245,2.76
FILL,1096,1100
FILL,1056,1092,3,1065,9,9,1
NGEN,3,9,1098,1100,1,,.26
N,1146,.14020351,4.4
FILL,1092,1146,5,1101,9
N,1164,.14020351,4.98
FILL,1146,1164,1,1155
LOCAL,11,,39.13520351,84.98,,-86.15
N,1168
N,1159,.3
NGEN,3,-1,1159,1159,,,-.125
N,1148,.58,-.25
NGEN,2,-18,1157,1159,1,.56
NGEN,2,-9,1139,1141,1,.25
NGEN,2,-27,1148,1148,,.81
NGEN,2,-18,1130,1132,1,.56
FILL,1096,1114,1,1105
CSYS,12
FILL,1101,1105
FILL,1110,1112,1,1111,,6,9
FILL,1164,1168
```

```
C***   Define the nodes for the upper seal flange

LOCAL,11,,38.405,82.81
N,2001,,5
N,2005,.25,5
FILL
NGEN,3,5,2001,2005,1,,-.25
N,2031,,3.45
N,2035,.91,3.45
FILL
FILL,2011,2031,3,2016,5,5,1
N,2051,,2.543442101
N,2055,.91,2.543442101
FILL
FILL,2031,2051,3,2036,5,4,1
N,2040,.91,3.29
FILL,2040,2055,2,2045,5
N,2059,1.345,2.66
FILL,2055,2059
N,2071,,2.17
N,2073,.21504507,2.17
FILL
N,2077,.74504507,2.17
FILL,2073,2077
FILL,2051,2071,1,2060
FILL,2054,2076,1,2065
FILL,2060,2065
N,2081,1.345,2.17
FILL,2077,2081
FILL,2055,2077,1,2066,,5,1
N,2107,.85759646,.54
N,2109,1.10488343,.54
FILL
N,2111,1.345,.54
FILL,2109,2111
FILL,2077,2107,5,2082,5,5,1
N,2117,.94488343
N,2119,1.10488343
FILL
FILL,2109,2119,1,2114
N,2112,.870715847,.35
FILL,2112,2114
N,2120,1.345,3.45
N,2121,1.345,3.29
NGEN,2,51,2071,2073,1,,-.305
NGEN,2,3,2122,2124,1,,-.305

C***   Define the nodes for the locking ring

LOCAL,11,,39.35,81.29
N,3001
N,3005,.435
FILL
N,3009,.935
FILL,3005,3009
N,3037,,.81
N,3041,.435,.693442101
FILL
N,3045,.935,.693442101
FILL,3041,3045
FILL,3001,3037,3,3010,9,9,1
N,3145,,4.11
N,3149,.435,4.226557899
FILL
N,3153,.935,4.226557899
FILL,3149,3153
FILL,3041,3149,11,3050,9,5,1
N,3181,,4.67
N,3185,.535,4.67
FILL
N,3189,.935,4.67
FILL,3185,3189
FILL,3145,3181,3,3154,9,9,1

C***   Define the nodes for the OCA inner shell (OCV)

LOCAL,11,1,,84.5
N,101,74.25,-90
N,111,74.25,-64.44174492
FILL
LOCAL,12,1,28.3125,24.29659664
N,116,8.625
FILL,111,116
CSYS
N,117,36.9375,25.79659664
N,123,36.9375,51.79659664
FILL
N,129,36.9375,73.95292590
FILL,123,129
NGEN,2,-872,1003,1003
FILL,129,131
NGEN,2,-1870,2003,2003
N,135,38.53,93.78649751
FILL,133,135
LOCAL,13,1,29.905,93.78649751
N,140,8.625,64.23984399
FILL,135,140
LOCAL,14,1,,31.8125
N,150,77.4375,90
FILL,140,150

C***   Define the nodes for the OCA outer shell

CSYS
N,601
N,613,47.0625
FILL
N,626,47.0625,64.7775
FILL,613,626
N,629,47.0625,76.7775
FILL,626,629
N,630,47.0625,77.6325
N,638,47.0625,105.3440689
FILL,630,638
LOCAL,15,1,40.5625,105.3440689
N,640,6.5,62.55238078
FILL,638,640
LOCAL,16,1,,27.25
N,650,94.5,90
FILL,640,650

C***   Define the nodes for the polyurethane foam
inner surface

CSYS
NGEN,2,100,101,150,1
N,132,38.58338729,80.97
N,232,38.53,86.26

C***   Define the nodes for the polyurethane foam
outer surface

NGEN,2,-100,601,650,1

C***   Define the intermediate polyurethane foam nodes

FILL,201,501,2,301,100,29,1
N,300,43.9375,80.9
N,331,41.5375,81.8825
N,332,41.5375,86.26
N,429,43.9375,76.7775
N,430,44.2375,77.6375
N,431,44.2375,81.8825
FILL,229,429,1,329,100,2,1
FILL,230,300,1,330
FILL,332,532,1,432
FILL,233,533,2,333,100,18,1
N,323,38.4375,51.79659664

C***   Define the nodes for the Z-flanges

NGEN,2,272,429,429,0
NGEN,2,402,300,300,0
NGEN,2,273,430,430,0
RP2,,,1,1
NGEN,2,374,331,331,0
RP2,,,1,1

C***   Define the elements for the lower seal flange

TYPE,1
MAT,1
REAL,1
E,1001,1002,1007,1006
RP4,1,1,1,1
EGEN,5,5,1,4,1
E,1026,1027,1036,1035
E,1027,1028,1036
E,1028,1029,1037,1036
E,1029,1030,1031,1037
E,1031,1032,1038,1037
RP3,1,1,1,1
E,1035,1036,1042,1041
RP4,1,1,1,1
E,1041,1042,1047,1046
RP4,1,1,1,1
EGEN,3,5,32,35,1
E,1056,1057,1066,1065
RP4,1,1,1,1
```

```
EGEN,4,9,44,47,1
MAT,2
E,1060,1061,1070,1069
RP4,1,1,1,1
EGEN,4,9,60,63,1
EGEN,3,9,74,75,1
EGEN,3,9,56,59,1
EGEN,7,9,84,85,1
EGEN,3,1,99,99
EGEN,3,1,93,93
C***   Define the elements for the upper seal flange
TYPE,1
MAT,1
REAL,1
E,2006,2007,2002,2001
RP4,1,1,1,1
EGEN,10,5,104,107,1
E,2040,2121,2120,2035
E,2060,2061,2052,2051
E,2061,2062,2052
E,2062,2063,2053,2052
E,2063,2064,2053
E,2064,2065,2054,2053
RP6,1,1,1,1
E,2071,2072,2061,2060
RP10,1,1,1,1
E,2122,2123,2072,2071
RP2,1,1,1,1
E,2125,2126,2123,2122
RP2,1,1,1,1
E,2082,2083,2078,2077
RP4,1,1,1,1
EGEN,6,5,169,172,1
EGEN,3,5,189,190,1
C***   Define the elements for the locking ring
TYPE,1
MAT,2
REAL,1
E,3001,3002,3011,3010
RP4,1,1,1,1
EGEN,4,9,197,200,1
MAT,1
E,3005,3006,3015,3014
RP4,1,1,1,1
EGEN,20,9,213,216,1
E,3145,3146,3155,3154
RP4,1,1,1,1
EGEN,4,9,293,296,1
C***   Define the elements for the OCA inner shell
(OCV)
TYPE,2
MAT,1
REAL,1
E,101,102
RP16,1,1
REAL,2
E,117,118
RP12,1,1
REAL,3
E,123,323
REAL,1
E,129,130
E,130,1003
E,2003,134
E,134,135
RP16,1,1
C***   Define the elements for the OCA outer shell
REAL,1
E,601,602
RP25,1,1
REAL,3
E,626,627
RP3,1,1
E,630,631
RP8,1,1
REAL,1
E,638,639
RP12,1,1
C***   Define the elements for the Z-flanges
REAL,4
E,629,701
E,701,702
E,702,1034
E,1034,1033
E,630,703
E,703,704
RP3,1,1
E,706,2120
E,2120,2035
C***   Define the polyurethane foam elements
TYPE,3
MAT,3
REAL,1
E,201,301,302,202
RP29,1,1,1,1
E,231,230,330
E,301,401,402,302
RP28,1,1,1,1
E,329,429,300,330
E,300,132,231,330
E,401,501,502,402
RP28,1,1,1,1
E,333,233,232,332
E,233,333,334,234
RP17,1,1,1,1
E,331,431,432,332
RP19,1,1,1,1
E,430,530,531,431
RP20,1,1,1,1
C***   Define the interface elements between the steel
shells and the polyurethane foam
TYPE,5
MAT,1
REAL,101
E,101,201
REAL,102
E,102,202
REAL,103
E,103,203
REAL,104
E,104,204
REAL,105
E,105,205
REAL,106
E,106,206
REAL,107
E,107,207
REAL,108
E,108,208
REAL,109
E,109,209
REAL,110
E,110,210
REAL,111
E,111,211
REAL,112
E,112,212
REAL,113
E,113,213
REAL,114
E,114,214
REAL,115
E,115,215
REAL,116
E,116,216
RP7,1,1
E,124,224
RP6,1,1
REAL,130
E,129,229
RP2,1,1
E,1003,231
REAL,101
E,702,300
E,701,429
E,622,529
REAL,150
E,706,332
E,705,331
E,704,431
E,703,430
E,630,530
REAL,116
E,300,702
E,429,701
```

```
E,706,332
E,705,331
E,704,431
E,703,430
E,2003,233
E,134,234
RP2,1,1
REAL,136
E,136,236
REAL,137
E,137,237
REAL,138
E,138,238
REAL,139
E,139,239
REAL,140
E,140,240
REAL,141
E,141,241
REAL,142
E,142,242
REAL,143
E,143,243
REAL,144
E,144,244
REAL,145
E,145,245
REAL,146
E,146,246
REAL,147
E,147,247
REAL,148
E,148,248
REAL,149
E,149,249
REAL,150
E,150,250
REAL,101
E,501,601
RP13,1,1
REAL,116
E,513,613
RP26,1,1
REAL,639
E,539,639
REAL,640
E,540,640
REAL,641
E,541,641
REAL,642
E,542,642
REAL,643
E,543,643
REAL,644
E,544,644
REAL,645
E,545,645
REAL,646
E,546,646
REAL,647
E,547,647
REAL,648
E,548,648
REAL,649
E,549,649
REAL,150
E,550,650

C***   Define the interface elements between the lower
seal flange and the locking ring

TYPE,4
MAT,1
REAL,6
E,3038,1061
RP3,1,1

C***   Define the interface elements between the upper
seal flange and the locking ring

TYPE,4
MAT,1
REAL,7
E,2056,3146
RP3,1,1

C***   Define the interface elements between the lower
seal flange and the upper seal flange

TYPE,5
MAT,1
REAL,8
E,1164,2073
RP5,1,1

C***   Couple the lower shell to the lower seal flange

TYPE,6
MAT,4
REAL,9
E,1001,1002
RP4,1,1

C***   Couple the upper shell to the upper seal flange

TYPE,6
MAT,4
REAL,9
E,2001,2002
RP4,1,1

C***   Define the displacement constraints

D,101,UX,0,,601,500,ROTZ
D,201,UX,0,,501,100
D,150,UX,0,,650,500,ROTZ
D,250,UX,0,,550,100
D,3099,UY,0

C***   Re-order the elements to reduce execution time

WSTART,101,601,100
WSTART,150,650,100
WSTART,1003
WSTART,1034
WSTART,2120
WSTART,2003
WAVES

C***   Set convergence criteria, write a solution
file, and exit

ITER,-20,20
AFWRITE
FINISH
```

Table 2.10.1-4 – ANSYS® Input Listing for OCA Load Case 4

```
/TITLE, OCV: PRES=0/14.7 PSIA; TEMP=70/70 DEG-F
C***   Define the element types
ET,1,42,,,1
ET,2,51
ET,3,42,,,1
ET,4,12,,,1
ET,5,12
ET,6,3
C***   Define the reference and uniform temperatures
TREF,70
TUNIF,70
C***   Define the material properties for non-slotted
steel regions
EX,1,28.3E+06
NUXY,1,.3
DENS,1,7.505E-04
ALPX,1,8.460E-06
C***   Define the material properties for slotted
steel regions
EX,2,14.15E+06
EY,2,14.15E+06
EZ,2,1
NUXY,2,.3
NUXZ,2,0
NUYZ,2,0
DENS,2,3.7525E-04
ALPX,2,8.460E-06
ALPY,2,8.460E-06
ALPZ,2,8.460E-06
C***   Define the material properties for the
polyurethane foam
EX,3,5854
EY,3,8789
EZ,3,5854
GXY,3,2553
GXZ,3,1921
GYZ,3,2553
NUXY,3,.33
DENS,3,1.198E-05
ALPX,3,4.6E-05
C***   Define the material properties for the rigid
coupling elements (STIF3 beams)
EX,4,28.3E+06
NUXY,4,.3
DENS,4,0
ALPX,4,8.460E-06
C***   Define the element real constants
R,1,.25
R,2,.1875
R,3,.375
R,4,.075
R,5,,2E+10,,1
R,6,-15,2E+10,-.036
R,7,15,2E+10,-.036
R,8,0,2E+10,,1
R,9,1,1,1
R,101,-180.000,2E+10,,1
R,102,-177.444,2E+10,,1
R,103,-174.888,2E+10,,1
R,104,-172.333,2E+10,,1
R,105,-169.777,2E+10,,1
R,106,-167.221,2E+10,,1
R,107,-164.665,2E+10,,1
R,108,-162.109,2E+10,,1
R,109,-159.553,2E+10,,1
R,110,-156.998,2E+10,,1
R,111,-154.442,2E+10,,1
R,112,-141.553,2E+10,,1
R,113,-128.665,2E+10,,1
R,114,-115.777,2E+10,,1
R,115,-102.888,2E+10,,1
R,116,-90.0000,2E+10,,1
R,130,-102.000,2E+10,,1
R,136,-77.1520,2E+10,,1
R,137,-64.3041,2E+10,,1
R,138,-51.4561,2E+10,,1
R,139,-38.6081,2E+10,,1
R,140,-25.7602,2E+10,,1
R,141,-23.1841,2E+10,,1
R,142,-20.6081,2E+10,,1
R,143,-18.0321,2E+10,,1
R,144,-15.4561,2E+10,,1
R,145,-12.8801,2E+10,,1
R,146,-10.3041,2E+10,,1
R,147,-7.72805,2E+10,,1
R,148,-5.15203,2E+10,,1
R,149,-2.57602,2E+10,,1
R,150,,2E+10,,1
R,639,-58.7238,2E+10,,1
R,640,-27.4476,2E+10,,1
R,641,-24.7029,2E+10,,1
R,642,-21.9581,2E+10,,1
R,643,-19.2133,2E+10,,1
R,644,-16.4686,2E+10,,1
R,645,-13.7238,2E+10,,1
R,646,-10.9790,2E+10,,1
R,647,-8.23429,2E+10,,1
R,648,-5.48952,2E+10,,1
R,649,-2.74476,2E+10,,1
C***   Define the nodes for the lower seal flange
LOCAL,11,,38.24941495,80.051977923,,-12
N,1001
N,1005,.25
FILL
N,1016,,.58677836
N,1020,.25,.58677836
FILL
FILL,1001,1016,2,1006,5,5,1
N,1026,,.896632635
LOCAL,12,,38.505,80
MOVE,1026,11,0,999,0,12,-.065,999,0
FILL,1016,1026,1,1021
LOCAL,11,1,39.12699808,80.47
N,1025,.5,148.5
N,1030,.5,129
N,1031,.5,109.5
N,1032,.5,90
CSYS,12
FILL,1021,1025,3,1022,1,2,5
N,1033,.775,.97
N,1034,1.145,.97
N,1076,-.065,2.98
FILL,1026,1076,8,1035,5
FILL,1035,1076,7,1041,5
N,1060,.775,2.15593612
NGEN,2,6,1033,1034,1,,.16
FILL,1039,1060,3,1045,5
FILL,1035,1039
FILL,1041,1045,3,1042,1,4,5
N,1064,1.245,2.03
FILL,1060,1064
N,1092,-.065,2.98
N,1096,.77960172,2.76
FILL
N,1100,1.245,2.76
FILL,1096,1100
FILL,1056,1092,3,1065,9,9,1
NGEN,3,9,1098,1100,1,,.26
N,1146,.14020351,4.4
FILL,1092,1146,5,1101,9
N,1164,.14020351,4.98
FILL,1146,1164,1,1155
LOCAL,11,,39.13520351,84.98,,-86.15
N,1168
N,1159,.3
NGEN,3,-1,1159,1159,,,-.125
N,1148,.58,-.25
NGEN,2,-18,1157,1159,1,.56
NGEN,2,-9,1139,1141,1,.25
NGEN,2,-27,1148,1148,,.81
NGEN,2,-18,1130,1132,1,.56
FILL,1096,1114,1,1105
CSYS,12
FILL,1101,1105
FILL,1110,1112,1,1111,,6,9
FILL,1164,1168
```

```
C***   Define the nodes for the upper seal flange

LOCAL,11,,38.405,82.81
N,2001,,5
N,2005,.25,5
FILL
NGEN,3,5,2001,2005,1,,-.25
N,2031,,3.45
N,2035,.91,3.45
FILL
FILL,2011,2031,3,2016,5,5,1
N,2051,,2.543442101
N,2055,.91,2.543442101
FILL
FILL,2031,2051,3,2036,5,4,1
N,2040,.91,3.29
FILL,2040,2055,2,2045,5
N,2059,1.345,2.66
FILL,2055,2059
N,2071,,2.17
N,2073,.21504507,2.17
FILL
N,2077,.74504507,2.17
FILL,2073,2077
FILL,2051,2071,1,2060
FILL,2054,2076,1,2065
FILL,2060,2065
N,2081,1.345,2.17
FILL,2077,2081
FILL,2055,2077,1,2066,,5,1
N,2107,.85759646,.54
N,2109,1.10488343,.54
FILL
N,2111,1.345,.54
FILL,2109,2111
FILL,2077,2107,5,2082,5,5,1
N,2117,.94488343
N,2119,1.10488343
FILL
FILL,2109,2119,1,2114
N,2112,.870715847,.35
FILL,2112,2114
N,2120,1.345,3.45
N,2121,1.345,3.29
NGEN,2,51,2071,2073,1,,-.305
NGEN,2,3,2122,2124,1,,-.305

C***   Define the nodes for the locking ring

LOCAL,11,,39.35,81.29
N,3001
N,3005,.435
FILL
N,3009,.935
FILL,3005,3009
N,3037,,.81
N,3041,.435,.693442101
FILL
N,3045,.935,.693442101
FILL,3041,3045
FILL,3001,3037,3,3010,9,9,1
N,3145,,4.11
N,3149,.435,4.226557899
FILL
N,3153,.935,4.226557899
FILL,3149,3153
FILL,3041,3149,11,3050,9,5,1
N,3181,,4.67
N,3185,.535,4.67
FILL
N,3189,.935,4.67
FILL,3185,3189
FILL,3145,3181,3,3154,9,9,1

C***   Define the nodes for the OCA inner shell (OCV)

LOCAL,11,1,,84.5
N,101,74.25,-90
N,111,74.25,-64.44174492
FILL
LOCAL,12,1,28.3125,24.29659664
N,116,8.625
FILL,111,116
CSYS
N,117,36.9375,25.79659664
N,123,36.9375,51.79659664
FILL
N,129,36.9375,73.95292590
FILL,123,129
NGEN,2,-872,1003,1003
FILL,129,131
NGEN,2,-1870,2003,2003
N,135,38.53,93.78649751
FILL,133,135
LOCAL,13,1,29.905,93.78649751
N,140,8.625,64.23984399
FILL,135,140
LOCAL,14,1,,31.8125
N,150,77.4375,90
FILL,140,150

C***   Define the nodes for the OCA outer shell

CSYS
N,601
N,613,47.0625
FILL
N,626,47.0625,64.7775
FILL,613,626
N,629,47.0625,76.7775
FILL,626,629
N,630,47.0625,77.6325
N,638,47.0625,105.3440689
FILL,630,638
LOCAL,15,1,40.5625,105.3440689
N,640,6.5,62.55238078
FILL,638,640
LOCAL,16,1,,27.25
N,650,94.5,90
FILL,640,650

C***   Define the nodes for the polyurethane foam
inner surface

CSYS
NGEN,2,100,101,150,1
N,132,38.58338729,80.97
N,232,38.53,86.26

C***   Define the nodes for the polyurethane foam
outer surface

NGEN,2,-100,601,650,1

C***   Define the intermediate polyurethane foam nodes

FILL,201,501,2,301,100,29,1
N,300,43.9375,80.9
N,331,41.5375,81.8825
N,332,41.5375,86.26
N,429,43.9375,76.7775
N,430,44.2375,77.6375
N,431,44.2375,81.8825
FILL,229,429,1,329,100,2,1
FILL,230,300,1,330
FILL,332,532,1,432
FILL,233,533,2,333,100,18,1
N,323,38.4375,51.79659664

C***   Define the nodes for the Z-flanges

NGEN,2,272,429,429,0
NGEN,2,402,300,300,0
NGEN,2,273,430,430,0
RP2,,,1,1
NGEN,2,374,331,331,0
RP2,,,1,1

C***   Define the elements for the lower seal flange

TYPE,1
MAT,1
REAL,1
E,1001,1002,1007,1006
RP4,1,1,1,1
EGEN,5,5,1,4,1
E,1026,1027,1036,1035
E,1027,1028,1036
E,1028,1029,1037,1036
E,1029,1030,1031,1037
E,1031,1032,1038,1037
RP3,1,1,1,1
E,1035,1036,1042,1041
RP4,1,1,1,1
E,1041,1042,1047,1046
RP4,1,1,1,1
EGEN,3,5,32,35,1
E,1056,1057,1066,1065
RP4,1,1,1,1
```

```
EGEN,4,9,44,47,1
MAT,2
E,1060,1061,1070,1069
RP4,1,1,1,1
EGEN,4,9,60,63,1
EGEN,3,9,74,75,1
EGEN,3,9,56,59,1
EGEN,7,9,84,85,1
EGEN,3,1,99,99
EGEN,3,1,93,93
C***   Define the elements for the upper seal flange
TYPE,1
MAT,1
REAL,1
E,2006,2007,2002,2001
RP4,1,1,1,1
EGEN,10,5,104,107,1
E,2040,2121,2120,2035
E,2060,2061,2052,2051
E,2061,2062,2052
E,2062,2063,2053,2052
E,2063,2064,2053
E,2064,2065,2054,2053
RP6,1,1,1,1
E,2071,2072,2061,2060
RP10,1,1,1,1
E,2122,2123,2072,2071
RP2,1,1,1,1
E,2125,2126,2123,2122
RP2,1,1,1,1
E,2082,2083,2078,2077
RP4,1,1,1,1
EGEN,6,5,169,172,1
EGEN,3,5,189,190,1
C***   Define the elements for the locking ring
TYPE,1
MAT,2
REAL,1
E,3001,3002,3011,3010
RP4,1,1,1,1
EGEN,4,9,197,200,1
MAT,1
E,3005,3006,3015,3014
RP4,1,1,1,1
EGEN,20,9,213,216,1
E,3145,3146,3155,3154
RP4,1,1,1,1
EGEN,4,9,293,296,1
C***   Define the elements for the OCA inner shell
(OCV)
TYPE,2
MAT,1
REAL,1
E,101,102
RP16,1,1
REAL,2
E,117,118
RP12,1,1
REAL,3
E,123,323
REAL,1
E,129,130
E,130,1003
E,2003,134
E,134,135
RP16,1,1
C***   Define the elements for the OCA outer shell
REAL,1
E,601,602
RP25,1,1
REAL,3
E,626,627
RP3,1,1
E,630,631
RP8,1,1
REAL,1
E,638,639
RP12,1,1
C***   Define the elements for the Z-flanges
REAL,4
E,629,701
E,701,702
E,702,1034
E,1034,1033
E,630,703
E,703,704
RP3,1,1
E,706,2120
E,2120,2035
C***   Define the polyurethane foam elements
TYPE,3
MAT,3
REAL,1
E,201,301,302,202
RP29,1,1,1,1
E,231,230,330
E,301,401,402,302
RP28,1,1,1,1
E,329,429,300,330
E,300,132,231,330
E,401,501,502,402
RP28,1,1,1,1
E,333,233,232,332
E,233,333,334,234
RP17,1,1,1,1
E,331,431,432,332
RP19,1,1,1,1
E,430,530,531,431
RP20,1,1,1,1
C***   Define the interface elements between the steel
shells and the polyurethane foam
TYPE,5
MAT,1
REAL,101
E,101,201
REAL,102
E,102,202
REAL,103
E,103,203
REAL,104
E,104,204
REAL,105
E,105,205
REAL,106
E,106,206
REAL,107
E,107,207
REAL,108
E,108,208
REAL,109
E,109,209
REAL,110
E,110,210
REAL,111
E,111,211
REAL,112
E,112,212
REAL,113
E,113,213
REAL,114
E,114,214
REAL,115
E,115,215
REAL,116
E,116,216
RP7,1,1
E,124,224
RP6,1,1
REAL,130
E,129,229
RP2,1,1
E,1003,231
REAL,101
E,702,300
E,701,429
E,622,529
REAL,150
E,706,332
E,705,331
E,704,431
E,703,430
E,630,530
REAL,116
E,300,702
E,429,701
```

```
E,706,332
E,705,331
E,704,431
E,703,430
E,2003,233
E,134,234
RP2,1,1
REAL,136
E,136,236
REAL,137
E,137,237
REAL,138
E,138,238
REAL,139
E,139,239
REAL,140
E,140,240
REAL,141
E,141,241
REAL,142
E,142,242
REAL,143
E,143,243
REAL,144
E,144,244
REAL,145
E,145,245
REAL,146
E,146,246
REAL,147
E,147,247
REAL,148
E,148,248
REAL,149
E,149,249
REAL,150
E,150,250
REAL,101
E,501,601
RP13,1,1
REAL,116
E,513,613
RP26,1,1
REAL,639
E,539,639
REAL,640
E,540,640
REAL,641
E,541,641
REAL,642
E,542,642
REAL,643
E,543,643
REAL,644
E,544,644
REAL,645
E,545,645
REAL,646
E,546,646
REAL,647
E,547,647
REAL,648
E,548,648
REAL,649
E,549,649
REAL,150
E,550,650
C***   Define the interface elements between the lower
seal flange and the locking ring
TYPE,4
MAT,1
REAL,6
E,3038,1061
RP3,1,1
C***   Define the interface elements between the upper
seal flange and the locking ring
TYPE,4
MAT,1
REAL,7
E,2056,3146
RP3,1,1
C***   Define the interface elements between the lower
seal flange and the upper seal flange
TYPE,5
MAT,1
REAL,8
E,1164,2073
RP5,1,1
C***   Couple the lower shell to the lower seal flange
TYPE,6
MAT,4
REAL,9
E,1001,1002
RP4,1,1
C***   Couple the upper shell to the upper seal flange
TYPE,6
MAT,4
REAL,9
E,2001,2002
RP4,1,1
C***   Define the displacement constraints
D,101,UX,0,,601,500,ROTZ
D,201,UX,0,,501,100
D,150,UX,0,,650,500,ROTZ
D,250,UX,0,,550,100
D,3099,UY,0
C***   Define the pressure loads
P,101,102,-14.7,,129,1
P,130,1003,-14.7
P,1001,1006,-14.7,,1021,5
P,1026,1035,-14.7
P,1035,1041,-14.7
P,1041,1046,-14.7,,1051,5
P,1056,1065,-14.7,,1155,9
P,1164,1165,-14.7,,1167,1
P,1168,1159,-14.7
P,2077,2082,-14.7
P,2073,2074,-14.7,,2076,1
P,2127,2124,-14.7
P,2124,2073,-14.7
P,2125,2126,-14.7,,2126,1
P,2122,2125,-14.7
P,2071,2122,-14.7
P,2001,2002,-14.7,,2002,1
P,2001,2006,-14.7,,2046,5
P,2051,2060,-14.7
P,2060,2071,-14.7
P,2003,134,-14.7
P,134,135,-14.7,,149,1
C***   Re-order the elements to reduce execution time
WSTART,101,601,100
WSTART,150,650,100
WSTART,1003
WSTART,1034
WSTART,2120
WSTART,2003
WAVES
C***   Set convergence criteria, write a solution
file, and exit
ITER,-20,20
AFWRITE
FINISH
```

Table 2.10.1-5 – ANSYS® Input Listing for ICV Load Case 1

```
/TITLE, ICV: PRES=64.7/3.5 PSIA; TEMP=160/160 DEG-F
C***   Define the element types
ET,1,42,,,1
ET,2,51
ET,3,12,,,1
ET,4,12
ET,5,3
C***   Define the reference and uniform temperatures
TREF,160
TUNIF,160
C***   Define the material properties for non-slotted
steel regions
EX,1,27.8E+06
NUXY,1,.3
DENS,1,7.505E-04
ALPX,1,8.694E-06
C***   Define the material properties for slotted
steel regions
EX,2,13.9E+06
EY,2,13.9E+06
EZ,2,1
NUXY,2,.3
NUYZ,2,0
NUXZ,2,0
DENS,2,3.7525E-04
ALPX,2,8.694E-06
ALPY,2,8.694E-06
ALPZ,2,8.694E-06
C***   Define the material properties for the rigid
coupling elements
EX,3,27.8E+06
NUXY,3,.3
DENS,3,0
ALPX,3,8.694E-06
C***   Define the element real constants
R,1,.25
R,2,-15,2E+10,-.036
R,3,15,2E+10,-.036
R,4,0,2E+10,-.01
R,5,1,1,1
C***   Define the nodes for the lower seal ring
LOCAL,11,0,36.315,75.08954245
N,1001
N,1005,.25
FILL
N,1016,,.575
N,1020,.25,.575
FILL
FILL,1001,1016,2,1006,5,5,1
N,1031,,1.48
N,1035,.84,1.48
FILL
FILL,1016,1031,2,1021,5,5,1
N,1046,,2.6759361
N,1050,.84,2.67593612
FILL
FILL,1031,1046,2,1036,5,5,1
N,1054,1.31,2.55
FILL,1050,1054
N,1073,,3.5
N,1077,.844601720,3.28
FILL
N,1079,1.095,3.28
FILL,1077,1079
N,1081,1.31,3.28
FILL,1079,1081
FILL,1046,1073,2,1055,9,9,1
N,1127,.205,4.92
FILL,1073,1127,5,1082,9
LOCAL,12,,37.01020351,80.58954246,,-86.15
N,1140,.3
N,1138,.3,-.25
FILL
N,1122,.86
N,1120,.86,-.25
FILL
N,1113,1.11
N,1111,1.11,-.25
FILL
N,1095,1.67
N,1093,1.67,-.25
FILL
CSYS,11
N,1145,.205,5.5
FILL,1127,1145,1,1136
N,1149,.695,5.5
FILL,1145,1149
FILL,1120,1138,1,1129
FILL,1093,1111,1,1102
FILL,1077,1095,1,1086
FILL,1091,1093,,,,6,9
FILL,1073,1091,1,1082,,5,1
NGEN,3,9,1079,1081,1,,.26
C***   Define the nodes for the upper seal ring
N,2001,-.035,4.89
N,2003,.180045070,4.89
FILL
N,2007,-0.035,5.5
N,2009,.180045070,5.5
FILL
FILL,2001,2007,1,2004,,3,1
N,2013,.710045070,5.5
FILL,2009,2013
N,2017,1.31,5.5
FILL,2013,2017
N,2040,-0.035,5.98
FILL,2007,2040,2,2018,11
N,2035,0.875,5.873442101
FILL,2029,2035
N,2039,1.31,5.99
FILL,2035,2039
FILL,2008,2030,1,2019,,10,1
N,2042,.245,5.98
FILL,2040,2042
N,2043,.390419704,6.008925778
N,2044,.513700577,6.091299423
N,2049,.596074222,6.214580296
N,2054,.625,6.36
N,2058,.875,6.36
FILL
FILL,2035,2058,2,2048,5
FILL,2044,2048
FILL,2049,2053
NGEN,5,5,2054,2058,1,,.1875
N,2104,.822596460,3.87
N,2106,1.07,3.87
FILL
N,2116,1.07,3.33
FILL,2106,2116,1,2111
N,2108,1.31,3.87
FILL,2106,2108
FILL,2013,2104,5,2079,5,5,1
N,2109,.835715950,3.68
FILL,2109,2111
N,2114,.909883430,3.33
FILL,2114,2116
C***   Define the nodes for the locking ring
LOCAL,13,0,37.225,76.89954245
N,3001
N,3005,.435
FILL
N,3008,.789412
FILL,3005,3008
N,3037,,.81
N,3041,.435,.693442101
FILL
N,3045,.935,.693442101
FILL,3041,3045
FILL,3001,3037,3,3010,9,8,1
N,3027,.935,.4
FILL,3008,3027,1,3018
FILL,3027,3045,1,3036
N,3101,,4.11
N,3105,.435,4.226557898
FILL
N,3109,.935,4.226557899
FILL,3105,3109
FILL,3041,3105,11,3046,5,5,1
N,3137,,4.67
N,3141,.435,4.67
FILL
N,3144,.789412,4.67
FILL,3141,3144
FILL,3101,3137,3,3110,9,8,1
FILL,3109,3144,3,3118,9
```

```
C***   Define the nodes for the lower shell

LOCAL,14,1,,73.25
N,4001,73.25,-90
N,4016,73.25,-64.50665929
FILL
LOCAL,15,1,27.815,14.9171927
N,4025,8.625
FILL,4016,4025
CSYS,0
N,4081,36.44,75.08954245
FILL,4025,4081
N,4001,0,0

C***   Define the nodes for the upper shell

LOCAL,16,1,,24.25
N,5001,74.5,90
N,5016,74.5,64.42280563
FILL
LOCAL,17,1,28.44,83.66954245
N,5025,8.625
FILL,5016,5025
CSYS,0
N,5027,37.065,82.16954245
FILL,5025,5027
N,5001,0,98.75

C***   Define the elements for the lower seal ring

TYPE,1
MAT,1
REAL,1
E,1001,1002,1007,1006
RP4,1,1,1,1
EGEN,9,5,1,4,1
E,1046,1047,1056,1055
RP4,1,1,1,1
EGEN,5,9,37,40,1
EGEN,7,9,53,54,1
EGEN,3,27,55,56,1
MAT,2
E,1050,1051,1060,1059
RP4,1,1,1,1
EGEN,3,9,73,76,1
EGEN,3,9,83,84,1

C***   Define the elements for the upper seal ring

TYPE,1
MAT,1
REAL,1
E,2001,2002,2005,2004
RP2,1,1,1,1
EGEN,2,3,89,90,1
E,2007,2008,2019,2018
RP10,1,1,1,1
EGEN,2,11,93,102,1
EGEN,2,11,103,107,1
E,2046,2045,2034
RP2,1,1,0
E,2034,2035,2048,2047
E,2044,2045,2050,2049
RP4,1,1,1,1
EGEN,6,5,121,124,1
E,2079,2080,2014,2013
RP4,1,1,1,1
E,2084,2085,2080,2079
RP4,1,1,1,1
EGEN,5,5,149,152,1
EGEN,3,5,165,166,1

C***   Define the elements for the locking ring

TYPE,1
MAT,2
REAL,1
E,3001,3002,3011,3010
RP4,1,1,1,1
EGEN,4,9,173,176,1
MAT,1
E,3005,3006,3015,3014
RP3,1,1,1,1
E,3018,3017,3008
E,3014,3015,3024,3023
RP4,1,1,1,1
EGEN,3,9,193,196,1
E,3041,3042,3047,3046
RP4,1,1,1,1
EGEN,11,5,205,208,1
E,3096,3097,3106,3105
RP4,1,1,1,1
E,3101,3102,3111,3110
RP8,1,1,1,1
EGEN,4,9,253,259,1
E,3117,3118,3127,3126
E,3126,3127,3136,3135
E,3135,3136,3144,3144

C***   Define the elements for the lower shell

TYPE,2
MAT,1
REAL,1
E,4001,4002
RP79,1,1
E,4080,1003

C***   Define the elements for the upper shell

TYPE,2
MAT,1
REAL,1
E,2076,5026
E,5026,5025
RP25,-1,-1

C***   Define the interface elements between the lower
seal flange and the locking ring

TYPE,3
MAT,1
REAL,2
E,3038,1051
RP3,1,1

C***   Define the interface elements between the upper
seal flange and the locking ring

TYPE,3
MAT,1
REAL,3
E,2036,3102
RP3,1,1

C***   Define the interface elements between the lower
seal flange and the upper seal flange

TYPE,4
MAT,1
REAL,4
E,1145,2009
RP5,1,1

C***   Couple the lower shell to the lower seal flange

TYPE,5
MAT,3
REAL,5
E,1001,1002
RP4,1,1

C***   Couple the upper shell to the upper seal flange

TYPE,5
MAT,3
REAL,5
E,2074,2075
RP4,1,1

C***   Define the displacement constraints

D,4001,UX,0,,5001,1000,ROTZ
D,3075,UY,0

C***   Define the pressure loads

P,4001,4002,61.2,,4079,1
P,4080,1003,61.2
P,1001,1006,61.2,,1041,5
P,1046,1055,61.2,,1136,9
P,1145,1146,61.2,,1148,9
P,1140,1149,61.2
P,2001,2002,61.2,,2002,1
P,2003,2006,61.2,,2006,3
P,2009,2010,61.2,,2012,1
P,2013,2079,61.2
P,2001,2004,61.2,,2004,3
P,2007,2018,61.2,,2029,11
P,2040,2041,61.2,,2043,1
P,2044,2049,61.2,,2069,5
P,5001,5002,61.2,,5025,1
P,5026,2076,61.2

C***   Re-order the elements to reduce execution time

WSTART,4001
WAVES

C***   Set convergence criteria, write a solution
file, and exit

ITER,-10,10
AFWRITE
FINISH
```

Table 2.10.1-6 – ANSYS® Input Listing for ICV Load Case 2

```
/TITLE, ICV: PRES=0/14.7 PSIA; TEMP=70/70 DEG-F
C***   Define the element types
ET,1,42,,,1
ET,2,51
ET,3,12,,,1
ET,4,12
ET,5,3
C***   Define the reference and uniform temperatures
TREF,70
TUNIF,70
C***   Define the material properties for non-slotted
steel regions
EX,1,28.3E+06
DENS,1,7.505E-04
NUXY,1,.3
ALPX,1,8.46E-06
C***   Define the material properties for slotted
steel regions
EX,2,14.15E+06
EY,2,14.15E+06
EZ,2,1
NUXY,2,.3
NUYZ,2,0
NUXZ,2,0
DENS,1,3.7525E-04
ALPX,2,8.46E-6
ALPY,2,8.46E-6
ALPZ,2,8.46E-6
C***   Define the material properties for the rigid
coupling elements
EX,3,28.3E+06
NUXY,3,.3
DENS,3,0
ALPX,3,8.46E-6
C***   Define the element real constants
R,1,.25
R,2,-15,2E+10,-.036
R,3,15,2E+10,-.036
R,4,0,2E+10,-.01
R,5,1,1,1
C***   Define the nodes for the lower seal ring
LOCAL,11,0,36.315,75.08954245
N,1001
N,1005,.25
FILL
N,1016,,.575
N,1020,.25,.575
FILL
FILL,1001,1016,2,1006,5,5,1
N,1031,,1.48
N,1035,.84,1.48
FILL
FILL,1016,1031,2,1021,5,5,1
N,1046,,2.6759361
N,1050,.84,2.67593612
FILL
FILL,1031,1046,2,1036,5,5,1
N,1054,1.31,2.55
FILL,1050,1054
N,1073,,3.5
N,1077,.844601720,3.28
FILL
N,1079,1.095,3.28
FILL,1077,1079
N,1081,1.31,3.28
FILL,1079,1081
FILL,1046,1073,2,1055,9,9,1
N,1127,.205,4.92
FILL,1073,1127,5,1082,9
LOCAL,12,,37.01020351,80.58954246,,-86.15
N,1140,.3
N,1138,.3,-.25
FILL
N,1122,.86
N,1120,.86,-.25
FILL
N,1113,1.11
N,1111,1.11,-.25
FILL
N,1095,1.67
N,1093,1.67,-.25
FILL
CSYS,11
N,1145,.205,5.5
FILL,1127,1145,1,1136
N,1149,.695,5.5
FILL,1145,1149
FILL,1120,1138,1,1129
FILL,1093,1111,1,1102
FILL,1077,1095,1,1086
FILL,1091,1093,,,,6,9
FILL,1073,1091,1,1082,,5,1
NGEN,3,9,1079,1081,1,,.26
C***   Define the nodes for the upper seal ring
N,2001,-.035,4.89
N,2003,.180045070,4.89
FILL
N,2007,-0.035,5.5
N,2009,.180045070,5.5
FILL
FILL,2001,2007,1,2004,,3,1
N,2013,.710045070,5.5
FILL,2009,2013
N,2017,1.31,5.5
FILL,2013,2017
N,2040,-0.035,5.98
FILL,2007,2040,2,2018,11
N,2035,0.875,5.873442101
FILL,2029,2035
N,2039,1.31,5.99
FILL,2035,2039
FILL,2008,2030,1,2019,,10,1
N,2042,.245,5.98
FILL,2040,2042
N,2043,.390419704,6.008925778
N,2044,.513700577,6.091299423
N,2049,.596074222,6.214580296
N,2054,.625,6.36
N,2058,.875,6.36
FILL
FILL,2035,2058,2,2048,5
FILL,2044,2048
FILL,2049,2053
NGEN,5,5,2054,2058,1,,.1875
N,2104,.822596460,3.87
N,2106,1.07,3.87
FILL
N,2116,1.07,3.33
FILL,2106,2116,1,2111
N,2108,1.31,3.87
FILL,2106,2108
FILL,2013,2104,5,2079,5,5,1
N,2109,.835715950,3.68
FILL,2109,2111
N,2114,.909883430,3.33
FILL,2114,2116
C***   Define the nodes for the locking ring
LOCAL,13,0,37.225,76.89954245
N,3001
N,3005,.435
FILL
N,3008,.789412
FILL,3005,3008
N,3037,,.81
N,3041,.435,.693442101
FILL
N,3045,.935,.693442101
FILL,3041,3045
FILL,3001,3037,3,3010,9,8,1
N,3027,.935,.4
FILL,3008,3027,1,3018
FILL,3027,3045,1,3036
N,3101,,4.11
N,3105,.435,4.226557898
FILL
N,3109,.935,4.226557899
FILL,3105,3109
FILL,3041,3105,11,3046,5,5,1
N,3137,,4.67
N,3141,.435,4.67
FILL
N,3144,.789412,4.67
FILL,3141,3144
FILL,3101,3137,3,3110,9,8,1
FILL,3109,3144,3,3118,9
```

```
C***   Define the nodes for the lower shell

LOCAL,14,1,,73.25
N,4001,73.25,-90
N,4016,73.25,-64.50665929
FILL
LOCAL,15,1,27.815,14.9171927
N,4025,8.625
FILL,4016,4025
CSYS,0
N,4081,36.44,75.08954245
FILL,4025,4081
N,4001,0,0

C***   Define the nodes for the upper shell

LOCAL,16,1,,24.25
N,5001,74.5,90
N,5016,74.5,64.42280563
FILL
LOCAL,17,1,28.44,83.66954245
N,5025,8.625
FILL,5016,5025
CSYS,0
N,5027,37.065,82.16954245
FILL,5025,5027
N,5001,0,98.75

C***   Define the elements for the lower seal ring

TYPE,1
MAT,1
REAL,1
E,1001,1002,1007,1006
RP4,1,1,1,1
EGEN,9,5,1,4,1
E,1046,1047,1056,1055
RP4,1,1,1,1
EGEN,5,9,37,40,1
EGEN,7,9,53,54,1
EGEN,3,27,55,56,1
MAT,2
E,1050,1051,1060,1059
RP4,1,1,1,1
EGEN,3,9,73,76,1
EGEN,3,9,83,84,1

C***   Define the elements for the upper seal ring

TYPE,1
MAT,1
REAL,1
E,2001,2002,2005,2004
RP2,1,1,1,1
EGEN,2,3,89,90,1
E,2007,2008,2019,2018
RP10,1,1,1,1
EGEN,2,11,93,102,1
EGEN,2,11,103,107,1
E,2046,2045,2034
RP2,1,1,0
E,2034,2035,2048,2047
E,2044,2045,2050,2049
RP4,1,1,1,1
EGEN,6,5,121,124,1
E,2079,2080,2014,2013
RP4,1,1,1,1
E,2084,2085,2080,2079
RP4,1,1,1,1
EGEN,5,5,149,152,1
EGEN,3,5,165,166,1

C***   Define the elements for the locking ring

TYPE,1
MAT,2
REAL,1
E,3001,3002,3011,3010
RP4,1,1,1,1
EGEN,4,9,173,176,1
MAT,1
E,3005,3006,3015,3014
RP3,1,1,1,1
E,3018,3017,3008
E,3014,3015,3024,3023
RP4,1,1,1,1
EGEN,3,9,193,196,1
E,3041,3042,3047,3046
RP4,1,1,1,1
EGEN,11,5,205,208,1
E,3096,3097,3106,3105
RP4,1,1,1,1
E,3101,3102,3111,3110
RP8,1,1,1,1
EGEN,4,9,253,259,1
E,3117,3118,3127,3126
E,3126,3127,3136,3135
E,3135,3136,3144,3144

C***   Define the elements for the lower shell

TYPE,2
MAT,1
REAL,1
E,4001,4002
RP79,1,1
E,4080,1003

C***   Define the elements for the upper shell

TYPE,2
MAT,1
REAL,1
E,2076,5026
E,5026,5025
RP25,-1,-1

C***   Define the interface elements between the lower
seal flange and the locking ring

TYPE,3
MAT,1
REAL,2
E,3038,1051
RP3,1,1

C***   Define the interface elements between the upper
seal flange and the locking ring

TYPE,3
MAT,1
REAL,3
E,2036,3102
RP3,1,1

C***   Define the interface elements between the lower
seal flange and the upper seal flange

TYPE,4
MAT,1
REAL,4
E,1145,2009
RP5,1,1

C***   Couple the lower shell to the lower seal flange

TYPE,5
MAT,3
REAL,5
E,1001,1002
RP4,1,1

C***   Couple the upper shell to the upper seal flange

TYPE,5
MAT,3
REAL,5
E,2074,2075
RP4,1,1

C***   Define the displacement constraints

D,4001,UX,0,,5001,1000,ROTZ
D,3075,UY,0

C***   Define the pressure loads

P,4001,4002,-14.7,,4079,1
P,4080,1003,-14.7
P,1001,1006,-14.7,,1041,5
P,1046,1055,-14.7,,1136,9
P,1145,1146,-14.7,,1148,9
P,1140,1149,-14.7
P,2001,2002,-14.7,,2002,1
P,2003,2006,-14.7,,2006,3
P,2009,2010,-14.7,,2012,1
P,2013,2079,-14.7
P,2001,2004,-14.7,,2004,3
P,2007,2018,-14.7,,2029,11
P,2040,2041,-14.7,,2043,1
P,2044,2049,-14.7,,2069,5
P,5001,5002,-14.7,,5025,1
P,5026,2076,-14.7

C***   Re-order the elements to reduce execution time

WSTART,4001
WAVES

C***   Set convergence criteria, write a solution
file, and exit

ITER,-10,10
AFWRITE
FINISH
```

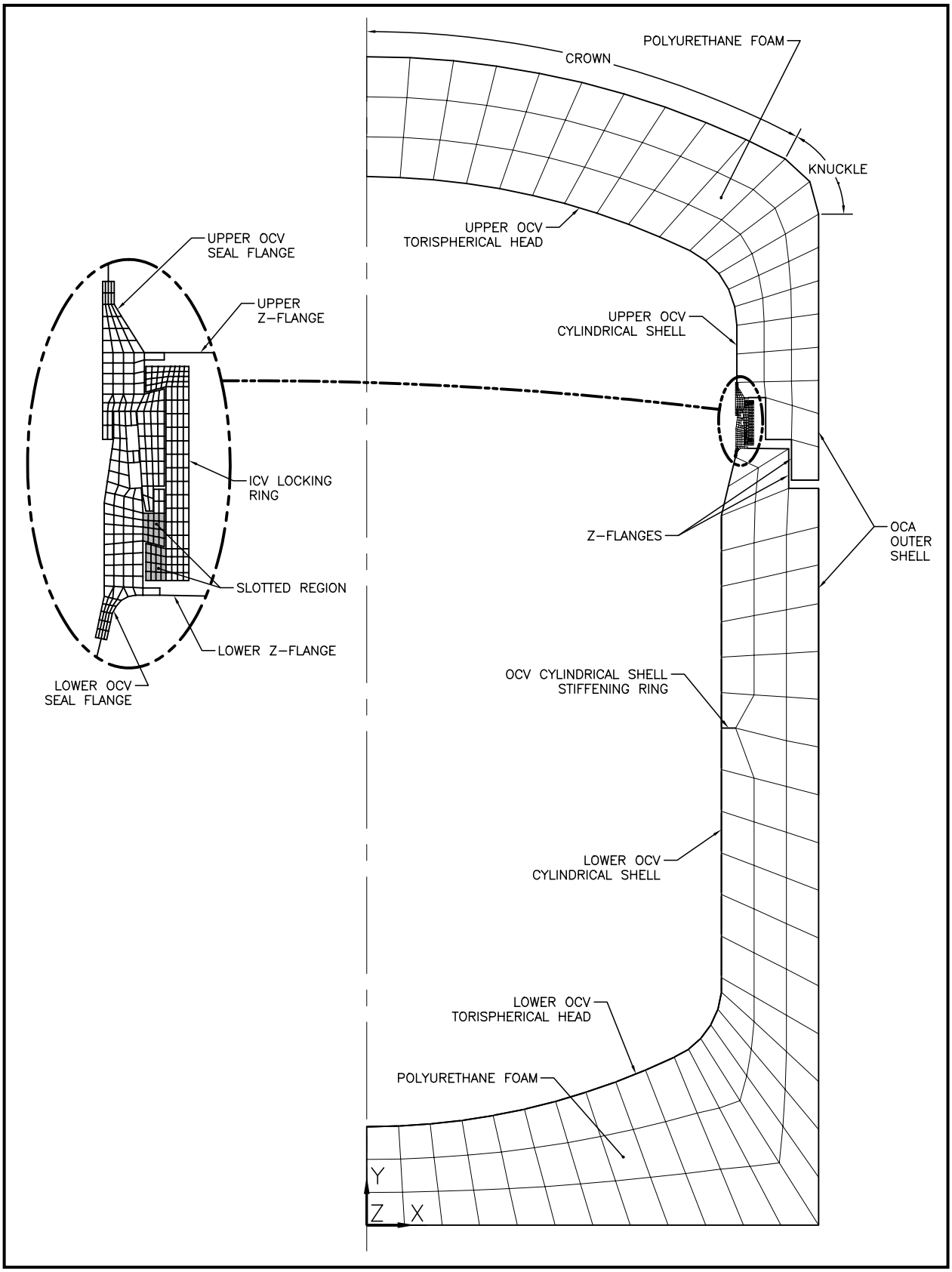

Figure 2.10.1-1 – OCA Finite Element Analysis Model Element Plot

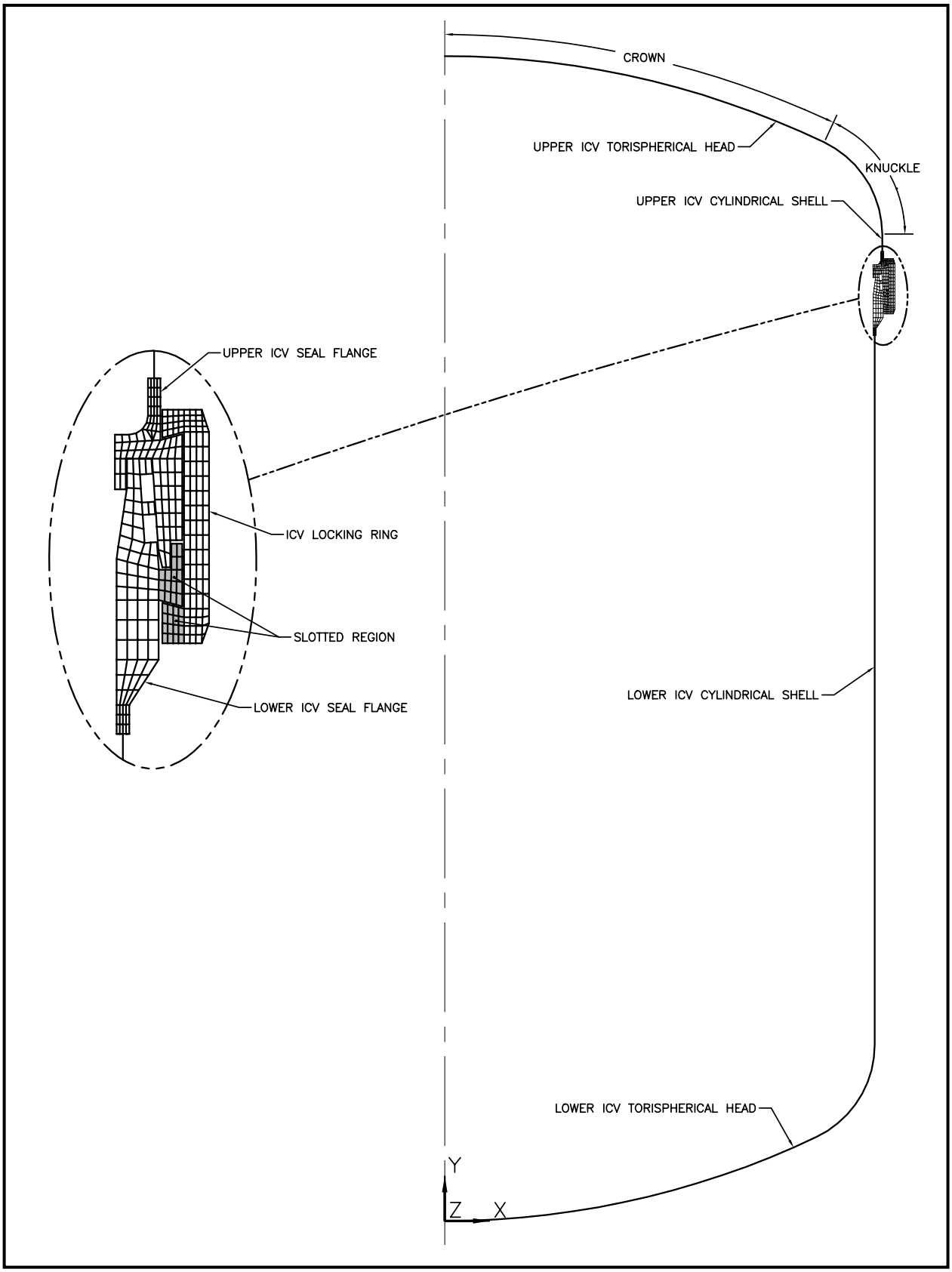

Figure 2.10.1-2 – ICV Finite Element Analysis Model Element Plot

2.10.2 Elastomer O-ring Seal Performance Tests

2.10.2.1 Introduction

Elastomer O-ring seal testing was performed in support of the certification of the TRUPACT-II package. The elastomer O-ring seal tests demonstrated the ability of Rainier Rubber's butyl compound RR0405-70[1], used for the main O-ring (containment) seal, to maintain a leaktight[2] containment boundary under the worst-case conditions of temperature, duration, and minimum compression. This appendix summarizes the information presented in the report *Design Development and Certification Testing of the TRUPACT-II Package*[3].

2.10.2.2 Test Specimens and Equipment

A bore-type test fixture was used to test the O-ring seals. The fixture included an inner disk containing two, side-by-side O-ring seal grooves. An O-ring seal of prototypic cross-section and butyl material, as delineated on the drawings in Appendix 1.3.1, *Packaging General Arrangement Drawings*, was placed into each seal groove, and the assembly was placed within a mating bore component. In this test fixture, the compression direction is radial and special jacking screws were utilized to displace the disk radially relative to the bore, resulting in decreased O-ring compression on one side of the test fixture. This decreased compression bounds the minimum compression that is possible in the TRUPACT-II package main O-ring seal under NCT or HAC. Therefore, the test fixture was capable of duplicating the worst-case conditions of minimum compression that could occur in a prototypic TRUPACT-II package. Figure 2.10.2-1 illustrates the O-ring seal test fixture.

The size and surface finish of the test fixture's O-ring seal grooves is prototypic of the main O-ring seal design used for the TRUPACT-II and HalfPACT packages. However, to ensure a worst-case O-ring seal compression for testing, the O-ring seal grooves and bore component were sized to ensure less compression than provided in a prototypic TRUPACT-II package. Worst-case compression of the O-ring seal in the test fixture occurs when the inner disk is radially displaced to achieve metal-to-metal contact on one side thereby resulting in minimum O-ring seal compression at the diametrically opposite location (180º away). As expected, the minimum O-ring seal compression in a TRUPACT-II package occurs when the upper and lower seal flanges are at their extreme dimensional tolerances.

The text fixture was designed with O-ring seal grooves to accommodate prototypically full-sized O-ring seals of 0.400 ±0.010 inch diameter, as delineated on the drawings in Appendix 1.3.1, *Packaging General Arrangement Drawings*. However, the test fixture's overall diameter was reduced relative to a full-scale TRUPACT-II/HalfPACT package to achieve a practical size for testing, with the gland having a bore diameter of 12.74 inches. A reduction in relative diameter is acceptable since the cross-sectional configuration and corresponding O-ring seal compression are

[1] Rainier Rubber Company, Seattle, WA.

[2] Leaktight is defined as leakage of 1×10^{-7} standard cubic centimeters per second (scc/sec), air, or less, per Section 5.4(3), *Reference Air Leakage Rate*, of ANSI N14.5-1997, *American National Standard for Radioactive Materials – Leakage Tests on Packages for Shipment,* American National Standards Institute, Inc. (ANSI).

[3] S. A. Porter, et al, *Design Development and Certification Testing of the TRUPACT-II Package*, 016-03-09, Portemus Engineering, Inc., Puyallup, Washington.

the parameters of primary importance relative to maintaining a leaktight seal. Additionally, the cross-sectional diameter of the actual test O-ring seals were on the low side of the tolerance range specified for TRUPACT-II O-ring seals of Ø0.400 ±0.010 inches. The test specimens were all in the range of Ø0.387 to Ø0.400 inches, thus minimizing the test compression. Actual minimum compressions are recorded in Appendix 2.10.2.6, *Test Results*. All test specimens were coated lightly with vacuum grease prior to installation into the test fixture. The fully assembled test fixture was placed within an environmental test chamber for both heating and cooling. Thermocouples attached to the fixture were used to confirm the O-ring seal temperature.

The region between the two O-ring seals, corresponding to the annulus between the upper main (containment) O-ring seal and lower main (test) O-ring seal on a TRUPACT-II packaging, constitutes a test volume. To perform a leak test, the test volume was connected to a helium mass spectrometer leak detector and the outside tented and flooded with helium gas, consistent with the guidelines of Section A3.10.2, *Helium Mass Spectrometer Envelope, Pressurized Envelope*, of ANSI N14.5[4]. An O-ring seal test was successful if the leakage between the seals was 1×10^{-7} standard cubic centimeters per second (scc/sec), air, or less (i.e., "leaktight").

2.10.2.3 Test Conditions

Test conditions were selected to simulate conditions of worst-case temperature and worst-case minimum compression for the prototypic O-ring seals. Tests were performed at -40 ºF, with the inner disk centered, to simulate NCT cold conditions. Tests were also performed at -20 ºF, with the inner disk fully offset, to simulate a cold temperature, HAC free drop or puncture event. Tests were further performed at elevated temperatures for 8-hour durations, with the inner disk fully offset, to simulate a HAC fire following the free drop and puncture events. A range of elevated temperatures was investigated to demonstrate the large margin of safety that exists for a leaktight seal in a prototypic TRUPACT-II package, based on temperatures measured from HAC fire testing as reported in Appendix 2.10.3, *Certification Tests*.

All helium leak tests were performed at cold temperatures, either at -40 ºF for the NCT cold condition case, or at -20 ºF for all other cases. No attempt was made to perform leak testing at elevated temperatures due to the rapid helium gas permeation and saturation of the elastomeric material at high temperatures. A fully saturated O-ring seal test specimen results in a measured leakage in excess of 1×10^{-7} scc/sec, air. The ability of the test fixture to establish a rapid, hard vacuum between the O-ring seals was used as the basis for acceptance at elevated temperatures, with leaktightness proven subsequent to the elevated temperature phase by leak testing at -20 ºF.

2.10.2.4 Test Procedure

The process of leak testing an O-ring seal is given below. Specific steps included for each test are provided in more detail in Table 2.10.2-1.

1. Assemble the test fixture, with O-ring seals, at ambient temperature conditions.
2. Perform a helium leak test with the disk centered in the bore.
3. Cool the test fixture to -40 ºF.

[4] ANSI N14.5-1997, *American National Standard for Radioactive Materials – Leakage Tests on Packages for Shipment,* American National Standards Institute, Inc. (ANSI).

4. Perform a helium leak test with the test fixture temperature at -40 ºF.
5. Warm the test fixture to -20 ºF.
6. Radially shift the disk inside the bore to establish metal-to-metal contact on one side, and minimum O-ring seal compression on the diametrically opposite side.
7. Perform a helium leak test with the test fixture temperature at -20 ºF.
8. Warm the test fixture to the elevated test temperature (i.e., 350 ºF, 400 ºF, or 450 ºF, according to the particular test), continuing to restrain the disk in the fully offset position relative to the bore.
9. Maintain the elevated temperature for an 8-hour duration.
10. At the end of the 8-hour period, confirm that a rapid, hard vacuum can be achieved and maintained in the test volume between the two, test O-ring seals at the elevated temperature.
11. Cool the test fixture to -20 ºF, continuing to restrain the disk in the fully offset position relative to the bore.
12. Perform a helium leak test with the test fixture temperature at -20 ºF.

2.10.2.5 Example O-ring Seal Compression Calculation

The minimum compression in the test specimens was calculated based on measured test fixture dimensions and the measured cross-sectional diameter of the test O-ring seal. The procedure for the calculation of minimum compression is now illustrated using Test No. 3 as an example (see Table 2.10.2-1 for applicable data). The same procedure was used for all tests.

Four quantities are needed for the compression calculation: 1) the cross-sectional diameter, W, of the O-ring seal, 2) stretch, S, of the O-ring seal, 3) groove depth, D, of the test fixture, and 4) the diametrical clearance or gap, G, between the test fixture gland and bore diameters. The minimum O-ring seal compression for Test No. 3 is found as follows:

1. **Extract Pertinent Data from Table 2.10.2-1.**

W_{min} = 0.387 inches, the minimum O-ring seal cross-sectional diameter

W_{max} = 0.399 inches, the maximum O-ring seal cross-sectional diameter

G = 0.052 inches, the maximum gap (offset) between the outside diameter of the disk and the inside diameter of the bore for the test fixture

D = 0.265 ±0.001, the test fixture groove depth

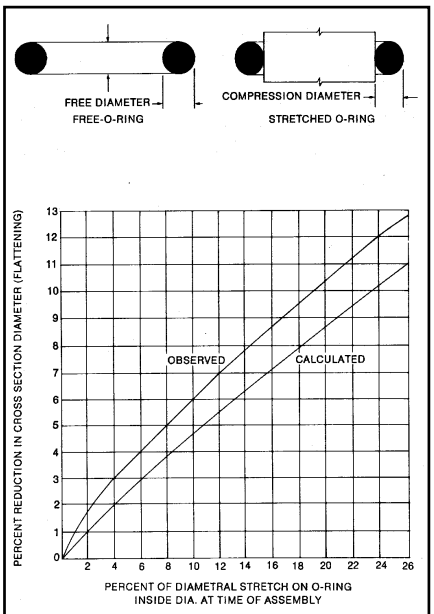

The "observed" curve is reproduced by courtesy of the Research Laboratories of General Motors Corporation at the General Motors Technical Center in Warren, Michigan. This curve is based on a statistical analysis of a much larger volume of experimental data than has been available previously.

In the stretched condition, an O-ring cross section is no longer circular. It is often necessary to compensate for the loss in squeeze resulting from the reduced "compression diameter." Dimensional changes in the "free diameter" do not affect the seal.

Empirical formulas for observed curve:

0 to 3% Inside Dia. Stretch: $Y = -0.005 + 1.19X - 0.19X^2 - 0.001X^3 + 0.008X^4$

3 to 25% Inside Dia. Stretch: $Y = .56 + .59X - .0046X^2$

Where X = percent stretch on centerline diameter (i.e. for 5% stretch, X = 5)
Y = percent reduction in cross section diameter

The calculated curve is based on the assumption that the O-ring section remains round and the volume does not change after stretching.

Formula: $Y = 100\left(1 - \frac{10}{\sqrt{100 + X}}\right)$

FIGURE A4-9 LOSS OF COMPRESSION DIAMETER (W) DUE TO STRETCH

2. Determine the Reduction in O-ring Seal Cross-Sectional Diameter Due to Stretch.

From Table 2.10.2-1, the stretch of the O-ring seal diameter over the groove diameter was from 2.0% to 4.1% for all tests. The resulting reduction in O-ring seal cross-sectional diameter is 1.7% and 3.1%, respectively, from Figure A4-9 of the Parker O-ring Handbook[5]. The reduced cross-sectional diameters, W_{Rmax} and W_{Rmin}, are thus 1.7% and 3.1%, respectively, less than the non-stretched diameters, W_{max} and W_{min}, or:

$$W_{Rmax} = (1 - 0.017)W_{max} = 0.392 \text{ inches}$$

$$W_{Rmin} = (1 - 0.031)W_{min} = 0.375 \text{ inches}$$

3. Calculate the O-ring Seal Compression.

Using the quantities that are determined in (1) and (2), above, the compression is calculated as:

$$C_{min} = W_{Rmin} - D_{max} - G = 0.057 \text{ inches}$$

$$C_{max} = W_{Rmax} - D_{min} - G = 0.076 \text{ inches}$$

Expressing these values as a percent of the cross-section gives:

$$\%C_{min} = \frac{C_{min}}{W_{R\,min}} \times 100 = \frac{0.057}{0.375} \times 100 = 15.2\%$$

$$\%C_{max} = \frac{C_{max}}{W_{R\,max}} \times 100 = \frac{0.076}{0.392} \times 100 = 19.4\%$$

Note that the minimum and maximum O-ring seal compression values determined above represent a range of minimum compression. Following the procedure used above, the minimum O-ring seal compressions are calculated for all tests. The results are summarized in Table 2.10.2-1. Corresponding minimum compression ranges for a prototypic TRUPACT-II packaging are 23.6% to 37.7% for the initially centered configuration, and 17.0% to 31.5% for the worst-case offset configuration.

2.10.2.6 Test Results

Test results are summarized in Table 2.10.2-1. As shown in the table, using worst-case, minimum O-ring seal compression at extreme operating temperatures, the butyl rubber material is capable of maintaining a leaktight seal when used for the TRUPACT-II package. These results confirm that the O-ring seals used in the TRUPACT-II package will remain leaktight if subjected to worst-case seal compressions over the range of NCT and HAC cold and hot temperatures. Additionally, following a HAC fire, the O-ring seals will remain leaktight when cooled to a temperature of -20 ºF.

An additional test using a maximum elevated temperature of 450 ºF was performed (see Test 2 in Table 2.10.2-1). In this case, the O-ring seals were not leaktight during the final, post-heat, -20 ºF leak test, a vacuum at the high temperature could not be rapidly achieved, and the seals evidenced

[5] ORD 5700, *Parker O-ring Handbook*, 1992, Parker Hannifin Corporation, Cleveland, OH.

loss of elasticity and visible cracking was evident. Such was not the case for tests where the maximum temperature was 400 ºF. It is therefore concluded that the upper limit for this butyl compound is somewhere between 400 ºF and 450 ºF, but an upper limit of 400 ºF is conservatively utilized.

Of final note, further developmental O-ring seal testing of Rainier Rubber's butyl compound RR0405-70 was conducted as part of the design effort for the Radioisotope Thermoelectric Generator (RTG) Transportation System Packaging[6]. This testing demonstrated that this specific butyl rubber compound has a peak temperature rating of 380 ºF, minimum, for durations of 24 hours or less. Continuous operation at temperatures between 350 ºF and 380 ºF may be allowed for longer durations, decreasing as a function of increasing temperature.

2.10.2.7 Designating an Alternative Seal Material

As discussed previously, Rainier Rubber RR0405-70 butyl rubber compound was selected for qualification testing that closely simulated the required performance characterized by package performance testing. The actual ability of the O-ring seals to meet these requirements is based on the seal material's basic characteristics.

Qualification testing identified certain key parameters that are important to seal performance. Of these, two important parameters for this application are resistance to helium permeation and acceptable resiliency at cold temperatures. Butyl rubber performs very well resisting helium permeation, and the TR-10 test in ASTM D1329[7] provides an acceptable method for determining cold temperature material resiliency, with the properties of the RR0405-70 acting as a baseline for the required resiliency.

The ability of the compound to withstand elevated temperatures while not having significant reduction in material properties is also required to maintain seal integrity after the hypothetical accident condition thermal event. Material properties in elastomers are reduced through the process of de-polymerization, an aging phenomenon. Elastomer aging can be accelerated by the application of energy (heat). The effect of aging can be quantified by measuring the reduction of physical properties after maintaining the seal material at an elevated temperature for a specific length of time. For the same amount of reduction in properties, a shorter time can be used at a higher temperature, or a longer time can be used at a lower temperature. ASTM D573[8] provides an acceptable method for determining the effects of temperature aging on elastomeric compounds.

---

[6] DOE Docket No. 94-6-9904, *Radioisotope Thermoelectric Generator Transportation System Safety Analysis Report for Packaging*, WHC-SD-RTG-SARP-001, prepared for the U.S. Department of Energy Office of Nuclear Energy under Contract No. DE-AC06-87RL10930 by Westinghouse Hanford Company, Richland, WA. Per Appendix 2.10.6, elevated temperature tests were performed on Rainier Rubber Company butyl rubber compound No. RR-0405-70 O-ring seals with seal compressions as low as 10%. The specific time-temperature test parameters evaluated were 380 ºF for 24 hours followed by 350 ºF for 144 hours, for a total of 168 hours (1 week). At these temperatures, all elastomeric compounds are susceptible to relatively high helium permeability; thus, helium leak testing was not performed. Instead, a hard vacuum of less than 0.0029 psia (20 Pa) was maintained on the test O-ring seals with no measurable pressure loss that would indicate leakage. At the end of the entire test sequence, the test O-ring seals were stabilized at -20 ºF and shown, via helium leak testing, to be leaktight (i.e., a leakage rate less than 1×10^{-7} standard cubic centimeters per second (scc/s), air leakage).

[7] ASTM D1329-88 (re-approved 1998), *Standard Test Method for Evaluating Rubber Property – Retraction at Lower Temperatures (TR Test),* American Society for Testing and Materials, Philadelphia, PA, Volume 09.01, 2001.

[8] ASTM D573-99, *Standard Test Method for Rubber – Deterioration in an Air Oven,* American Society for Testing and Materials, Philadelphia, PA, Volume 09.01, 2001.

ASTM D395[9] provides an acceptable method for determining the effects of compression set. RR0405-70 butyl rubber compound uses an acceptance criteria of less than 25% compression set for 22 hours at an elevated temperature of 70 ºC.

ASTM D2137[10] provides an acceptable method for determining an elastomeric material's ability to withstand cold temperatures and remain pliable. Although the TR-10 test in ASTM D1329 demonstrates the seal material's resiliency at a much lower temperature, this test verifies the seal material's lack of brittleness at the minimum regulatory temperature of -40 ºC.

Hardness or durometer along with tensile strength and elongation are defined and checked to ensure durability of the seal material during operation. ASTM D2240[11] provides an acceptable method for determining the required 70 ±5 durometer, and ASTM D412[12] provides an acceptable method for determining the required minimum 10 MPa (1,450 psi) tensile strength and minimum 250% elongation, with the properties of the RR0405-70 acting as a baseline for the required hardness, tensile strength, and elongation.

For proprietary seal materials that have fairly demanding requirements such as the RR0405-70 butyl rubber compound, the compound is commonly specified by a company designator and subsequently checked against exacting performance standards. Specifying an elastomeric compound by its chemistry alone is difficult considering the shear number of parameters that affect seal performance. However, by applying the above nationally recognized standards to a material batch, the important parameters are defined for verifying the performance of the seal material.

ASTM D1414[13] is the standard method for testing O-ring seals, and covers most, but not all, of the required testing delineated above. However, due to the overall size of the O-ring seals and the additional testing specified, ASTM D2000[14] provides a better standard classification system.

Each batch of compounded material requires testing, where a "batch" represents the chemical compounding of the material before vulcanizing and a "lot" refers to the quantity of finished product made at any one time.

Using the ASTM D2000 designator, O-ring seals with properties equivalent to RR0405-70 butyl rubber material are classified as follows; this designator callout is currently being specified for the RR0405-70 butyl rubber material, as discussed above, and summarized in the table below:

M4AA710 A13 B13 F17 F48 Z Trace Element

---

[9] ASTM D395-01, *Standard Test Methods for Rubber Property – Compression Set,* American Society for Testing and Materials, Philadelphia, PA, Volume 09.01, 2001.

[10] ASTM D2137-94 (re-approved 2000), *Standard Test Methods for Rubber Property – Brittleness Point of Flexible Polymers and Coated Fabrics,* American Society for Testing and Materials, Philadelphia, PA, Volume 09.02, 2001.

[11] ASTM D2240-00, *Standard Test Method for Rubber Property – Durometer Hardness,* American Society for Testing and Materials, Philadelphia, PA, Volume 09.01, 2002.

[12] ASTM D412-98a, *Standard Test Methods for Vulcanized Rubber and Thermoplastic Rubbers and Thermoplastic Elastomers – Tension,* American Society for Testing and Materials, Philadelphia, PA, Volume 09.01, 2001.

[13] ASTM D1414-94 (re-approved 1999), *Standard Test Methods for Rubber O-Rings,* American Society for Testing and Materials, Philadelphia, PA, Volume 09.02, 2001.

[14] ASTM D2000-01, *Standard Classification System for Rubber Products in Automotive Applications,* American Society for Testing and Materials, Philadelphia, PA, Volume 09.02, 2001.

Designator	Condition
M	Metric units designator (default condition)
4	Grade 4 acceptance criteria for the tests specified
AA	Butyl rubber compound
7	70 Shore A durometer hardness per ASTM D2240
10	Tensile strength and elongation per ASTM D 412; acceptance criteria are a minimum 10 MPa (1,450 psi) tensile strength and a minimum 250% elongation
A13	Heat resistance test per ASTM D573; the acceptance criteria are a maximum 10 Shore A durometer hardness increase, a maximum reduction in tensile strength of 25%, and a maximum reduction in ultimate elongation of 25% at 70 ºC
B13	Compression set per Method B of ASTM D395; acceptance criterion is a maximum 25% compression set after 22 hours at 70 ºC
F17	Cold temperature resistance specifying low temperature brittleness per Method A, 9.3.2, of ASTM D2137; non-brittle after 3 minutes at -40 ºC
F48	Cold temperature resiliency, where F is for cold temperature resistance, and 4 specifies testing to the TR-10 test of ASTM D1329; 8 indicates a TR-10 temperature of -50 ºC (-58 ºF), or less
Z Trace Element	Z designator allows specific notes to be added; "Z Trace Element" allows trace elements to be added to the elastomeric compound to meet the seal material requirements

Using the above seal material designator, the acceptable seal material for the TRUPACT-II package are O-ring seals meeting the SAR drawing requirements and specified as:

> "Butyl rubber material per Rainier Rubber RR0405-70, or equivalent meeting the requirements of ASTM D2000 M4AA710 A13 B13 F17 F48 Z Trace Element"

This page intentionally left blank.

Table 2.10.2-1 – O-ring Seal Performance Test Results

Test Number	O-ring Seal Cross-Sectional Diameter (inches)①				Stretch (%)		Maximum Gap (inches)		Minimum Compression (%)				Temperature for "Leaktight" Leak Test (Leakage ≤ 2.0 × 10^{-8} scc/sec, He)				
	O-ring Seal No. 1		O-ring Seal No. 2				Center Disk	Offset Disk	Center Disk		Offset Disk		Center Disk④		Offset Disk④		
	Min	Max	Min	Max	Min	Max			Min	Max	Min	Max	Ambient	-40 ºF	-20 ºF	8 hrs⑤	-20 ºF
1	0.387	0.397	0.387	0.396	2.0	4.1	0.026	③	22.1	25.6	14.9	20.0	Yes	Yes	Yes	350 ºF	Yes
2	0.388	0.398	0.387	0.398	2.0	4.1	0.029	0.050	21.3	25.1	15.7	19.7	Yes	Yes	⑥	450 ºF	No
3	0.387	0.397	0.387	0.399	2.0	4.1	0.027	0.052	21.9	25.8	15.2	19.4	Yes	Yes	Yes	400 ºF	Yes
4	②	②	②	②	2.0	4.1	0.027	0.053	21.9	25.8	14.9	19.1	Yes	Yes	Yes	400 ºF	Yes
5	②	②	②	②	2.0	4.1	0.026	0.050	22.1	26.0	15.7	19.9	Yes	Yes	Yes	400 ºF	Yes

Notes:

① Material for all O-ring seal test specimens is butyl rubber compound RR-0405-70, Rainier Rubber Co., Seattle, WA.

② Not measured; calculations assume the worst-case range as taken from Tests Numbers 1 - 3 (i.e., Ø0.387 inch minimum to Ø0.399 inch maximum).

③ Range of values is 0.048 inch minimum to 0.053 inch maximum due to an indirect method of gap measurement (used for this test only).

④ A "Yes" response indicates that helium leakage testing demonstrated that the leakage rate was ≤ 1.0 × 10^{-7} scc/sec, air (i.e., "leaktight" per ANSI N14.5). In all cases, measured leakage rates were ≤ 2.0 × 10^{-8} scc/sec, helium, for tests with a "Yes" response.

⑤ No helium leak tests were performed at elevated temperatures due to O-ring seal permeation and saturation by helium gas. The ability of the test fixture to establish a rapid, hard vacuum between the O-ring seals was used as the basis for leak test acceptance at elevated temperatures. All tests rapidly developed a hard vacuum, with the exception of Test Number 2 at an elevated temperature of 450 ºF, which slowly developed a vacuum.

⑥ Initial leakage of 1.0 × 10^{-5} scc/sec, helium; became leaktight (≤ 2.0 × 10^{-8} scc/sec, He) approximately one minute later.

This page intentionally left blank.

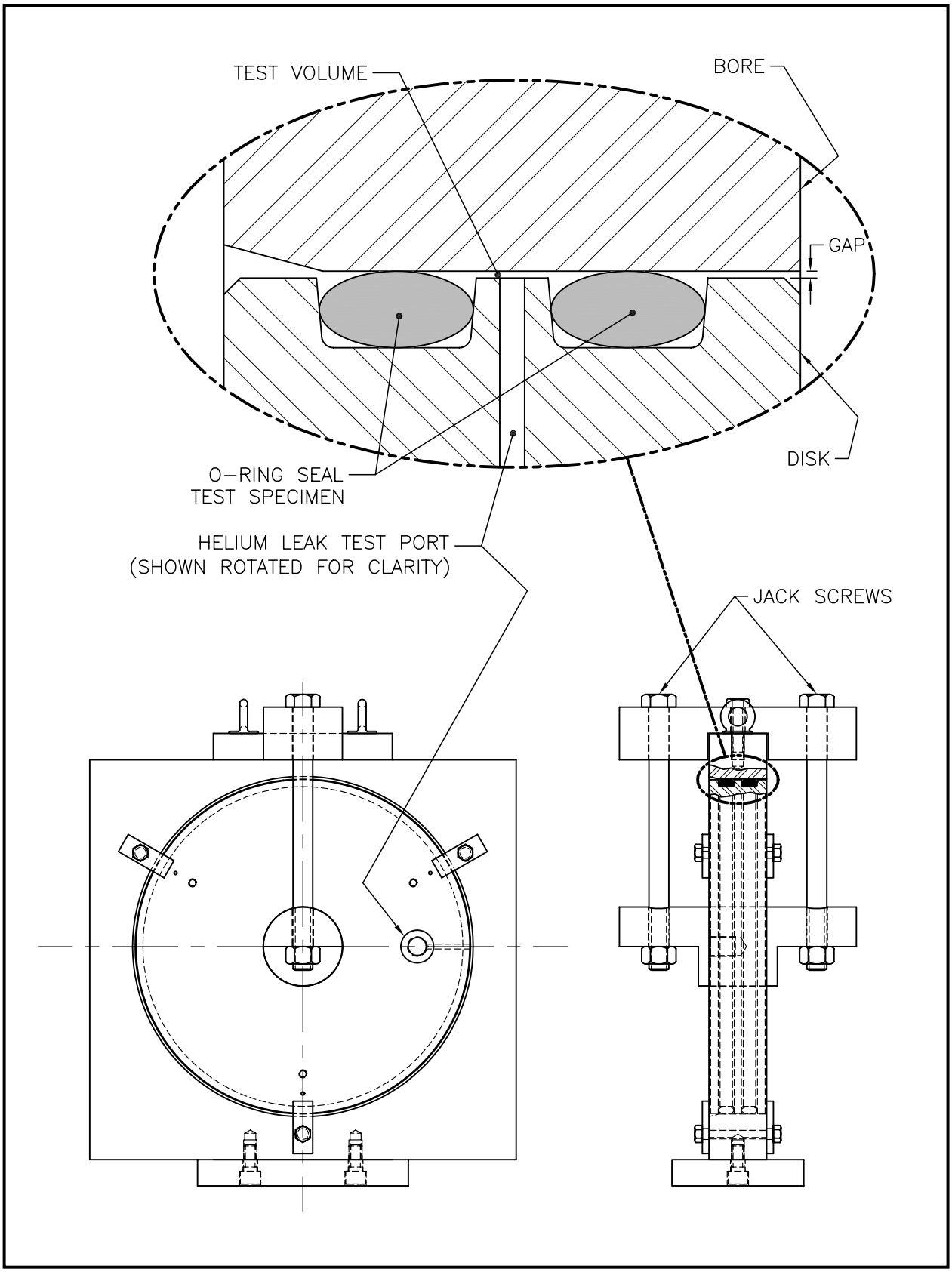

Figure 2.10.2-1 – Test Fixture for O-ring Seal Performance Testing

This page intentionally left blank.

2.10.3 Certification Tests

Presented herein are the results of normal conditions of transport (NCT) and hypothetical accident condition (HAC) tests that address the free drop, puncture, and fire test performance requirements of 10 CFR 71[1]. This appendix summarizes the information presented in the report *Design Development and Certification Testing of the TRUPACT-II Package*[2].

2.10.3.1 Introduction

The TRUPACT-II package, when subjected to the sequence of hypothetical accident condition (HAC) tests specified in 10 CFR §71.73, subsequent to the sequence of normal conditions of transport (NCT) tests specified in 10 CFR §71.71, is shown to meet the performance requirements specified in Subpart E of 10 CFR 71. As indicated in the introduction to Chapter 2.0, *Structural Evaluation*, with the exception of the immersion test, the primary proof of performance for the HAC tests is via the use of full-scale testing. In particular, free drop, puncture, and fire testing of three TRUPACT-II certification test units (CTUs) confirms that both the outer and inner containment boundaries will remain leaktight after a worst case HAC sequence. Observations from testing of the CTUs also confirm the conservative nature of deformed geometry assumptions used in the criticality assessment provided in Chapter 6.0, *Criticality Evaluation*.

2.10.3.2 Summary

Three CTUs (hereafter referred to as CTU-1, CTU-2, and CTU-3) were used to demonstrate compliance with the HAC structural and thermal requirements of 10 CFR 71. CTU-1 was subjected to ten tests: one NCT 3-foot free drop, three HAC 30-foot free drops, five HAC 40 inch puncture drops, and one HAC 30-minute fire. CTU-2 was subjected to nine separate tests and one repeat test: three HAC 30-foot free drops, six HAC 40 inch puncture drops (one being a repeat test for CTU-1), and one HAC 30-minute fire. CTU-3, using the same ICV and OCV as CTU-2 but modified to prevent debris encroachment into the ICV seals, was subjected to eight repeat tests for CTU-2: three HAC 30-foot free drops and five HAC 40 inch puncture drops; the HAC 30-minute fire test was not repeated.

As seen in the figures presented in Section 2.10.3.6.3, *Test Sequence for Selected Free Drop, Puncture Drop, and Fire Tests*, successful testing of the CTUs indicates that the various TRUPACT-II packaging design features are adequately designed to withstand the HAC tests specified in 10 CFR §71.73. The most important result of the testing program was the demonstrated ability of the outer containment vessel (OCV) and inner containment vessel (ICV) to remain leaktight[3].

---

[1] Title 10, Code of Federal Regulations, Part 71 (10 CFR 71), *Packaging and Transportation of Radioactive Material*, 01-01-07 Edition.

[2] S. A. Porter, et al, *Design Development and Certification Testing of the TRUPACT-II Package*, 016-03-09, Portemus Engineering, Inc., Puyallup, Washington.

[3] "Leaktight" is a leak rate not exceeding 1×10^{-7} standard cubic centimeters per second (scc/sec), air, as defined in ANSI N14.5-1997, *American National Standard for Radioactive Materials – Leakage Tests on Packages for Shipment,* American National Standards Institute, Inc. (ANSI).

Significant results of HAC free drop testing common to all CTUs are as follows:

- Buckling was not observed for either containment boundary shell. Additionally, accelerometers mounted directly on the OCV shell were utilized to determine the axial acceleration resulting from a 30-foot bottom end drop events on CTU-2 and CTU-3.
- No excessive distortion of the seal flange regions occurred for either containment vessel, although some permanent deformation was noted.
- All three (3) ICV and all six (6) OCV locking ring lock bolts remained intact and locking ring and lower seal flange tabs remained fully interlocked during and following the drop tests. Some OCA locking Z-flange-to-locking ring fasteners failed during the testing, but a sufficient number remained intact to securely retain the locking ring in the locked position. Additionally, for test purposes, only 24 fasteners were used whereas 36 are specified for the design.
- The containment boundaries were shown to be capable of maintaining pressure before, during, and after each 30-foot drop test. At the instant of impact, internal pressures in both the ICV and OCV would typically increase slightly (a few psi) for a moment and then return, within the accuracy of the instrumentation, to their initial, pre-drop test values.
- The aluminum honeycomb spacer assemblies used in the ICV upper and lower torispherical heads were shown to adequately protect the heads from damaging payload interactions.
- Rupture was not observed for the 3/8 inch thick, OCA outer shell.
- Internal pressures increased during the drops, but returned to pre-drop pressures afterward.
- Observed permanent deformations of the TRUPACT-II packaging were less than those assumed for the criticality evaluation.

Significant results of puncture drop testing common to all CTUs are as follows:

- With one exception, permanent deformations of the containment boundary are not attributed to the puncture event. The single exception occurred for a puncture impact onto the 1/4 inch thick OCA outer shell at a location 40 inches above the base of the package (Test No. 7 for CTU-1, and Test No. R for CTU-2). This puncture event resulted in a hole through the OCA outer shell. The permanent damage to the OCV and ICV shells was an inward bulge of approximately 1½ inches to the OCV and ICV sidewalls. Importantly, permanent deformations were limited to the cylindrical shell portions of the OCV and ICV lower bodies, with no significant deformation near the seal flanges.
- Rupture was not observed for the 3/8 inch thick, OCA outer shell. Penetrations of the OCA outer shell closest to the seal regions were 22 inches above and 37 inches below the closure interface. Minor tearing of the Z-flange-to-3/8 inch thick OCA interfaces was observed for some test orientations. These regions are covered by the outer thermal shield; therefore, such tears are of little consequence.
- Tearing of the OCA outer shell occurred at the 3/8-to-1/4 inch thick, OCA body outer shell transition (weld) during testing of CTU-2 and CTU-3 (Test 4).
- In the regions where a significant amount of polyurethane foam was exposed by a puncture event (i.e., 40 inches above the package base and near the OCA top knuckle), the intumescent (i.e., self-extinguishing) characteristics of the polyurethane foam were sufficient to provide effective insulation from the effects of the subsequent HAC fire.

Significant results of fire testing common to the first two CTUs are as follows:

- The intumescent (i.e., self-extinguishing) characteristic of the polyurethane foam was sufficient to provide insulation from the effects of the HAC fire even in regions where the most significant amounts of foam were exposed.
- The maximum measured temperatures for the OCV and ICV elastomeric (butyl) O-ring seals were 260 ºF (thermocouple reading during the fire, 250 ºF by passive temperature indicating label) and 200 ºF, respectively. The maximum measured temperatures for the OCV and ICV structural components were 439 ºF and 270 ºF, respectively. The 270 ºF ICV temperature was most likely a result of the preheat operation used to heat the vessels prior to the fire test, rather than a result of the fire test itself. Air was pumped into the OCV/ICV annulus at 40 psi and 350 ºF, and within close proximity of the corresponding temperature indicating label that measured the 270 ºF temperature. The next highest ICV temperature reading was 220 ºF.
- Both containment boundaries demonstrated the capability of maintaining pressure before, during, and after the fire event. Note that pressure was lost in the CTU-1 OCV during fire testing. However, the loss of pressure was due to failure of a test-related pressure fitting, not to a packaging design feature. Post-test repair of the fitting and re-pressurization of the OCV indicated that the pressure retention capabilities of the OCV had not been compromised by the fire test.
- Following fire testing, disassembly of the OCA demonstrated that, except for the local area damaged by the puncture impacts 40 inches above the base of the package, a layer of unburned polyurethane foam remained around the entire OCV. For both CTUs, the average thickness of the layer was approximately 5 to 6 inches along the cylindrical sides and lower head of the OCV, and even greater adjacent to the OCV upper dished head. This residual polyurethane foam thickness is consistent with the shielding evaluation provided in Chapter 5.0, *Shielding Evaluation*, and the criticality evaluation presented in Chapter 6.0, *Criticality Evaluation*.

2.10.3.3 Test Facilities

Drop testing of the TRUPACT-II package prototype test unit was performed at Sandia National Laboratories' Coyote Canyon Aerial Cable Facility in Albuquerque, New Mexico. The drop test facility utilizes free fall and, if needed, rocket power to attain closely controlled impact velocities as defined by a particular testing program. The drop test facility consists of a 5,000-foot long wire cable suspended across a mountain canyon. The cable can support proportionally heavier package weights at lower elevations, with a package weight in excess of 50,000 pounds for the regulatory defined, hypothetical accident condition 30-foot free drop test. The "unyielding" target consists of a highly reinforced, armor steel plated concrete block as illustrated in Figure 2.10.3-1. The target is designed to accommodate test packages weighing up to 100 tons.

In accordance with the requirements of 10 CFR §71.73(c)(3), the puncture bar was fabricated from solid, 6.0 inch diameter mild steel, and of sufficient length to perform the necessary test. The puncture bar was welded perpendicularly to a 1½ inch thick, mild steel plate having an outside diameter of approximately 24 inches. The top edge of the puncture bar was finished to a 1/4 inch radius. When utilized, the puncture bar was securely welded (mounted) to the impact surface.

Fire testing of the TRUPACT-II package prototype test unit was performed at Sandia National Laboratories' Lurance Canyon Burn Site in Albuquerque, New Mexico. The open pool fire

facility can be adjusted to a maximum size of 30-by-60 feet for performing free-burning fires for a duration of 2 hours, maximum. Packages weighing up to 149 tons can be supported at heights up to a few meters above the pool surface. During fire testing, thermocouples and calorimeters that are strategically placed measure and record fire temperatures and heat flux, respectively.

2.10.3.4 Description of the Certification Test Units

Three prototypic TRUPACT-II packages were built for certification testing, using prototypic fabrication processes and inspection techniques. Each CTU was built according to the design requirements delineated in Appendix 1.3.1, *Packaging General Arrangement Drawings*, with additions, omissions, differences from the general arrangement drawing requirements, measured as-built configurations, and selection of component options are described as follows. Payload representation is also described.

2.10.3.4.1 Additions, Omissions, Differences from Drawing Requirements, As-Built Configurations, and Component Options

2.10.3.4.1.1 Additions

- Painted external reference grid for photographic documentation; red for CTU-1, blue for CTU-2, and orange for CTU-3.
- External lifting devices for lifting and handling during certification testing.
- Internal lifting cables for lifting and handling the payload within the ICV.
- Secondary test vent port located circumferentially 180º from the prototypic vent port.
- Thermocouples (16 internal and 10 external for CTU-1, 8 internal and 8 external for CTU-2, and 5 internal for CTU-3).
- Temperature indicating labels.
- Axial-only accelerometers (two for CTU-2, and four for CTU-3).
- Remote pressurization port through the OCA/OCV/ICV bottom (see Figure 2.10.3-2)

2.10.3.4.1.2 Omissions

- Tapered lead-ins on the OCV and ICV upper seal flanges.
- Tamper-indicating devices.
- Warning/informational stenciling.
- OCV and ICV lock ring stop plates.
- OCA lid lift pocket fiberglass guide tubes (removed for tests 1 and 2 on CTU-1; removed for all tests on CTU-3).
- ICV lid lift pin diameter reduction grooves.
- Nameplates.

2.10.3.4.1.3 Differences from Drawing Requirements

- The relative locations of the OCA seal test port, vent port, and locking ring joint are different than delineated in Appendix 1.3.1, *Packaging General Arrangement Drawings*; fabrication of the CTUs occurred before operational considerations defined the final locations.

- The relative locations of the OCA lid lifting pockets are different than delineated in Appendix 1.3.1, *Packaging General Arrangement Drawings*; fabrication of the CTUs occurred before operational considerations defined the final locations.
- A 10 inch inside diameter (rather than a 3 inch inside diameter) was used for the silicone wear pad to prevent interference with the bottom test pressurization port.
- A 10 inch width (rather than the optional 18 inch width) was used for the neoprene weather seal for CTU-1.
- The OCV locking Z-flange was secured to the OCV lock ring via 24 (rather than 36), 1/4-20 UNC screws.
- The thickness of the ceramic fiber industrial textile (woven tape) between the upper/lower Z-flanges and the locking Z-flange was 1/4 inch thick (rather than 1/8 inch thick) for CTU-1 and CTU-2.
- The OCV lock bolt attachments in the OCA outer shell used inset Rivnuts with a 0.34 inch lock bolt thread engagement (rather than internal thread inserts inside cylindrical blocks with a 0.59 inch lock bolt thread engagement).
- The OCA lid top centerline thickness was 12½ inches (rather than 12¼ inches).
- The OCA body bottom centerline thickness was 9½ inches (rather than 9¼ inches).
- The outer thermal shield is located 3/8 inch above the location shown in Appendix 1.3.1, *Packaging General Arrangement Drawings*; the outer thermal shield was located 3/8 inch downward to enhance interchangeability of lids and bodies between different TRUPACT-II packages; a 3/4 inch × 10½ inch relief, not present in the CTUs, was added along the bottom edge of the outer thermal shield for OCA vent port tool clearance.
- The ICV vent port configuration included a polyurethane filter in the inner vent port plug to facilitate post-test helium leak testing (rather than a solid inner vent port plug).
- An ICV wiper O-ring seal and holder were not included for CTU-1 or CTU-2.
- ICV lid guide plates were used to facilitate assembly for CTU-1 and CTU-2; the addition of the ICV wiper O-ring seal configuration eliminated the need for the ICV lid guide plates.
- Some detailed dimensions for the tie-down lugs are slightly different from those delineated in Appendix 1.3.1, *Packaging General Arrangement Drawings*; fabrication of the CTUs occurred before operational considerations defined the final dimensions.
- The cross-sectional diameter of the lower main ICV and OCV O-ring seals was 0.393 inches and the material was butyl rubber (rather than a cross-section diameter of 0.375 inches and a material of either neoprene or ethylene propylene); these are non-containment seals.
- The CTUs were fabricated with a minimum main containment O-ring seal compression of 15%, whereas a minimum main containment O-ring seal compression of 12% is attainable by the dimensions delineated in Appendix 1.3.1, *Packaging General Arrangement Drawings*. Additional bench testing was performed after fabrication and testing of the CTUs that demonstrated the acceptability of the lower compression.
- The maximum reinforcement for the OCA external welds was 1/32 inch for the CTUs; a maximum reinforcement of 3/32 inch is delineated in Appendix 1.3.1, *Packaging General Arrangement Drawings*.

- The CTUs used an ICV silicone sponge debris shield with a nominally 1/4 inch thickness; a minimum 1/8 inch thickness is delineated in Appendix 1.3.1, *Packaging General Arrangement Drawings*.
- Some detailed dimensions for the recesses in the ICV and OCV seal test port plugs, ICV inner and outer vent port plugs, and the ICV vent port cover are slightly different from those delineated in Appendix 1.3.1, *Packaging General Arrangement Drawings*.

2.10.3.4.1.4 As-Built Measurements

2.10.3.4.1.4.1 Component Weights

The following table summarizes the major component weights for the three CTUs, and includes the calculated weights from Section 2.2, *Weights and Centers of Gravity*, for comparison:

Packaging Component	CTU-1	CTU-2	CTU-3	Calculated
Empty Package:				
• ICV Lid (without Spacer)	750	890	760	795
• ICV Body (without Spacer)	1,650	1,718	1,620	1,625
• ICV Upper Honeycomb Spacer	105	83	95	100
• ICV Lower Honeycomb Spacer	109	82	95	100
• OCA Lid	3,550	3,600	3,466	3,600
• OCA Body	5,900	5,800	5,730	5,765
• *Total*	12,064	12,173	11,766	11,985
Payload:				
• Drums	7,000	7,000	7,000	6,915
• Pallet	156	130	187	200
• Guide Tubes	20	21	20	20
• Slipsheets, Plates, and Cables	139	118	108	130
• *Total*	7,315	7,269	7,375①	7,265
Package Total:				
• Summing Above Components	19,379	19,442	19,141	19,250
• Truck Scale	19,360	19,260	- - -	- - -

Notes:

① Assembled payload weight using a Sandia National Laboratory load cell, and does not equal the sum of the individual components.

2.10.3.4.1.4.2 Polyurethane Foam Properties

The average parallel-to-rise and perpendicular-to-rise compressive strengths for the polyurethane foam in the OCA lids and bodies, including the nominal ±15% limits that are defined in Table 8.1-1 from Section 8.1.4.1, *Polyurethane Foam*, are summarized in the following table:

Compressive Strength (psi)	Parallel-to-Rise at Strain, $\varepsilon_{//}$			Perpendicular-to-Rise at Strain, $\varepsilon_{\perp}$		
	ε=10%	ε=40%	ε=70%	ε=10%	ε=40%	ε=70%
Nominal +15%	270	311	782	224	270	771
• CTU-1, Lid	231	266	667	190	234	667
• CTU-1, Body	233	267	674	194	239	670
• CTU-2, Lid	249	289	739	214	265	745
• CTU-2, Body	242	276	709	207	254	716
• CTU-3, Lid	222	258	666	194	237	678
• CTU-3, Body	230	261	673	201	245	676
Nominal –15%	200	230	578	166	200	570

In addition to the polyurethane foam compressive strength properties, the measured thicknesses of the OCA, including the minimum and maximum thicknesses specified in Appendix 1.3.1, *Packaging General Arrangement Drawings*, are summarized in the following table:

Polyurethane Foam Thickness (inches)	OCA Lid		OCA Body	
	Top	Side	Side	Bottom
Maximum Thickness	12⅞	9 3/16	11	10
CTUs	12½	8¾	10 7/16	9½
Minimum Thickness	11⅝	8 5/16	9⅞	8½

2.10.3.4.1.4.3 Upper Main O-ring Seal Compression (Containment)

The range of percent compression in the upper main O-ring seals is calculated via a set of direct measurements (O-ring seal cross-section, O-ring seal inside diameter, upper groove depth, upper groove inside diameter, and initial perpendicular gap between the lower and upper seal flanges at the upper groove). The following table summarizes the maximum and minimum percent O-ring compression for a "production" package based on the dimensions specified in Appendix 1.3.1, *Packaging General Arrangement Drawings*, and measurements taken for each CTU:

Percent O-ring Compression	Production		CTU-1		CTU-2		CTU-3	
	ICV	OCV	ICV	OCV	ICV	OCV	ICV	OCV
Maximum	31.5	31.5	18.0	17.5	17.1	18.0	18.3	17.5
Minimum	16.8	16.8	13.6	14.1	12.8	15.3	12.6	13.6

2.10.3.4.1.5 Component Options

- Z-flanges may be a welded construction of discs and cylinders or a spun construction; CTU-1 and CTU-2 used the welded option whereas CTU-3 used the spun option.
- Upper seal flanges, lower seal flanges, and locking rings may be fabricated using rolled and welded plate, forgings, or castings; all CTUs used the rolled and welded plate option.
- Attachment of the inner thermal shield to the locking Z-flange may be via pop rivets or spot welds; CTU-1 used the rivet option whereas CTU-2 and CTU-3 used the spot weld option.
- Vacuum grease may be applied to the seal flanges as well as the O-ring seals; only the O-ring seals were greased for CTU-1, whereas CTU-2 and CTU-3 used grease on the seal flanges as well.
- Vacuum grease may be applied to the vent port plug O-ring seals and covers; the CTU vent port plug O-ring seals and covers were greased.
- The upper inside taper on the ICV lower seal flange may have a length of 2.0 or 2.2 inches; all CTUs used a length of 2.0 inches.
- The wiper O-ring seal holder may be integrated into the ICV upper seal flange or fabricated from rolled sheet metal and attached with drive screws; CTU-3 used the rolled sheet metal/drive screw option.
- The 55-gallon drums used in the payload representation may be steel banded or wrapped with stretch plastic; all CTUs used the steel banding option.
- The 14-gauge aluminum sheet used for the aluminum honeycomb spacer assembly may be fabricated using a single sheet or two sheets with a full-penetration weld; all CTU spacers used a single sheet.
- The OCA outer shell welds may be inspected on the final pass using the liquid penetrant method; all CTU outer shell welds were inspected using the radiograph method.
- The exposed surfaces of the OCA may be unpainted or painted with a low-halogen paint; with the exception of painting colored reference grids, all CTUs were unpainted.
- Ceramic fiber paper is used on the inner surfaces of the OCA and OCV; all CTUs used Lytherm ceramic fiber paper.
- The wear pad may be plain or self-adhesive for securing to the bottom of the lower OCV torispherical head; all CTU wear pads were adhered to the lower OCV torispherical head.
- The maximum reinforcement for the OCA shell welds is 3/32 inch; the maximum reinforcement for the OCA shell welds for all CTUs was 1/32 inch.
- The ICV and OCV locking rings may be unplated or electroless nickel plated; all CTU locking rings were unplated.
- The ICV upper and lower spacer assembly bracket configurations may be a cantilever bracket or angle section; all CTUs used cantilever brackets.
- The insulating material for OCV vent and seal test port access plugs may be fabricated using polyurethane foam or ceramic fiber material; all CTUs used polyurethane foam plugs.
- The round tubing for the OCA lid lifting covers may be equivalent material to fiberglass; all CTUs used round fiberglass tubing.
- The OCA fire consumable vent plugs may use any plastic material; all CTUs used ABS plastic plugs.

- The OCA thread inserts may use an equivalent to Tridair inserts; all CTUs used Tridair KeenSerts.
- Butyl, neoprene, or ethylene propylene elastomers may be used for the OCV vent port plug and cover handling O-ring seal, the OCV vent port cover O-ring seal, the ICV inner vent port plug O-ring seal, and the ICV and OCV seal test port plug O-ring seals; all CTUs used butyl rubber for these non-containment O-ring seals.
- The OCA lock bolts may use either the OCA or OCA/ICV lock bolt configuration; all CTUs used the OCA lock bolt configuration.
- The material for the ICV inner and outer vent port plugs and cover may be ASTM B10 or B16 brass; all CTUs used ASTM B10 brass for the ICV inner and outer vent port plugs and cover.
- The ICV vent port insert has an optional configuration; all CTUs used the non-optional ICV vent port insert.
- The OCV and ICV seal test port inserts may be a threaded or slip-in configuration; all CTUs used the threaded configuration for the OCV and ICV seal test port inserts.

2.10.3.4.2 Payload Representation

Payloads for the all CTUs are essentially identical. Fourteen concrete filled 55-gallon drums are used to represent the worst-case payload configuration since they place the highest concentrated loading on the ICV. For conservatism, a 12 inch diameter tube was centered within each drum and the annulus filled with concrete to a weight near, but not over 500 pounds. Sand-filled bags were used to provide the remaining weight for precisely meeting the weight limit of 500 pounds. Figure 2.10.3-3 illustrates the payload representation.

In addition to the 500-pound 55-gallon drums, approximately nine (9) pounds of Portland cement and sand were added to the ICV cavity to represent loose debris that could move freely within the ICV and contaminate the sealing regions.

2.10.3.5 Technical Basis for Tests

The following sections supply the technical basis for the chosen test orientations and sequences for the TRUPACT-II CTUs as presented in Section 2.10.3.6, *Test Sequence for Selected Free Drop, Puncture Drop, and Fire Tests*.

2.10.3.5.1 Initial Test Conditions

2.10.3.5.1.1 Internal Pressure

The maximum normal operating pressure as well as the design pressure for both the ICV and the OCV is 50 psig. This pressure corresponds to a normal operating average ICV air temperature of 148 ºF (from Table 3.1-1 in Section 3.1, *Discussion*). Because of a constant internal volume, the corresponding pressure at -20 ºF is 33 psig, as found using Ideal Gas Law equations as follows:

$$P_{-20} = (50+12)\left(\frac{-20+460}{148+460}\right) = 45 \text{ psia} = 33 \text{ psig}$$

where the ambient pressure at the Sandia National Laboratory test site is 12 psia.

For drop test purposes, pressurizing the ICV to its maximum pressure consistent with the temperature selected for the particular drop is reasonable. The OCV may be either unpressurized or pressurized to its maximum design pressure consistent with the temperature selected for the drop. Note that with the exception of a slight pressure change associated with normal heat-up of the ICV/OCV annulus air or due to barometric changes, an unpressurized OCV is the expected condition during transport since the OCV can only become pressurized if the ICV fails. By pressurizing the OCV in some tests and not in others, pressure can be eliminated as a primary factor in demonstrating the package's ability to meet the applicable regulatory performance requirements. This conclusion is proven by showing that at the instant of impact, pressures within the vessels only increase by a few psig and immediately return to their initial values, and subsequent leak testing demonstrated containment integrity.

2.10.3.5.1.2 Temperature

In general, higher temperatures result in greater deformations and lesser acceleration loads than lower temperatures. This result is due primarily to the temperature sensitivity of the energy absorbing polyurethane foam used within the TRUPACT-II OCA. Linearly interpolating the polyurethane foam data shown in Section 2.6, *Normal Conditions of Transport*, the compressive strength at -20 ºF is approximately 40% greater than the compressive strength at 70 ºF, and the compressive strength at 160 ºF is approximately 25% less than the compressive strength at 70 ºF. The strength of the Type 304 stainless steel used in the TRUPACT-II packaging similarly varies as a function of temperature, but to a much lesser extent (e.g., yield strength decreases from 30,000 psi at 70 ºF to 27,000 psi at 160 ºF, per Table 2.3-1 in Section 2.3.1, *Mechanical Properties Applied to Analytic Evaluations*). Thus, for drop orientations where stresses in structural steel members are of concern (e.g., containment shell buckling), the worst-case temperature is -20 ºF, since this temperature results in the greatest ratio of the impact induced acceleration load-to-steel strength.

In contrast, for drop orientations where deformations are of concern, a higher temperature would result in a worst-case condition. Free drop tests at maximum temperatures are not necessary; parametric analyses[2] demonstrate an increase in polyurethane foam permanent deformation of 1/2 inches to 1⅛ inches, depending on the particular orientation. For this reason, free and puncture drops are performed at the prevailing ambient temperature at the time of the test.

2.10.3.5.2 Free Drop Tests

Properly selecting a worst-case TRUPACT-II package orientation for the 30-foot free drop event requires investigating parameters that may compromise package integrity. For the TRUPACT-II packaging design, the primary regulatory requirement is demonstration of containment integrity (i.e., the containment boundary remaining leaktight).

For the 30-foot free drop event, leaktightness of the O-ring seals may be compromised due to mechanical degradation caused by relative movement of the sealing surfaces (resulting in reduced O-ring seal compression), or thermal degradation of the butyl rubber material from the hypothetical accident condition fire event. Importantly, for mechanical or thermal degradation to occur, significant reduction in polyurethane foam thickness or significant direct exposure of the polyurethane foam to the fire would have to occur in the vicinity of the O-ring seals due to a 30-foot free drop event.

Another possibility is separation of the OCA lid from the OCA body (or significantly opening up the nominal 1/2 inch gap that exists between the upper and lower Z-flanges at the OCA lid-to-body interface), and buckling of the ICV or OCV in a bottom end drop orientation. Separation of the OCA lid from the OCA body is most likely to occur from a drop that imposes a significant lateral load on the knuckle portion of the OCA exterior torispherical head. Therefore, free drop testing includes impact orientations that affect the upper end of the package in general and the seal/closure area in particular. Loads and resultant deformations occurring over the lower half of the package do not present a worst-case regarding separation of the OCA lid from the OCA body.

As discussed earlier, a bottom end drop orientation is of interest because of the possibility of containment shell buckling due to the high acceleration forces imparted to the package in this orientation. These potential failure modes are worst when the ratio of applied load-to-steel strength is at its maximum value. Therefore, these free drop cases will be the worst-case if performed at cold temperatures.

2.10.3.5.3 Puncture Drop Tests

Properly selecting a worst-case TRUPACT-II package orientation for the puncture drop event requires investigating parameters that may compromise package integrity. For the TRUPACT-II packaging design, the primary regulatory requirement is demonstration of containment integrity (i.e., the containment boundary remaining leaktight).

For the puncture drop event, leaktightness of the O-ring seals may be compromised due to mechanical degradation caused by relative movement of the sealing surfaces (resulting in reduced O-ring seal compression), gross deformations of the sealing region, or thermal degradation of the butyl rubber material from the hypothetical accident condition fire event. Importantly, for mechanical degradation to occur, the puncture event would require gross rupturing of the OCA outer shell near the O-ring seals, thereby allowing the puncture bar to impact directly on the OCV seal flanges or locking ring. Similarly, for thermal degradation to occur, the puncture event would require gross rupturing of the OCA outer shell near the O-ring seals, thereby allowing direct flame impingement on the underlying polyurethane foam. For these reasons, puncture events are mostly directed at the seal regions.

Another possibility is the puncture bar penetrating the OCA outer shell and breaching the OCV containment boundary in a region removed from the seal regions. Based on the results of 1/2- and 3/4-scale design development testing and the full-scale engineering development testing, the puncture events most likely to lead to a penetration of the OCA exterior shell are those that have the package center of gravity directly above the puncture bar and, importantly, have the surface of the package at the point of contact with the puncture bar at an oblique angle with respect to the puncture bar. Specifically, if the impacting package surface is at an angle equal to or greater than approximately 20º relative to the top horizontal surface of the puncture bar, penetration is much more likely than if the package surface is normal to the axis of the puncture bar. The following table summarizes observations from the aforementioned development test programs. These results tested the package with the center of gravity directly over the puncture bar. If the center of gravity is not directly over the puncture bar, penetration becomes less likely since some of the available impact energy is transformed into rotational kinetic energy.

Full Scale Shell Thickness (in)	Orientation Relative to Puncture Bar	
	0º (normal)	≥20º
3/16	no penetration	penetration
1/4	no penetration	penetration
3/8	no penetration	no penetration

Observations from testing concluded that impacting the puncture bar with the package surface normal to the axis of the puncture bar will not lead to penetration of the OCA exterior shell. This was the primary reason for utilizing a torispherical (dished) upper head for the OCA lid. With a dished head, orientations with the package center of gravity directly over the puncture bar tend to be such that the package surface is also normal to the axis of the bar. Furthermore, observations concluded that a 3/8 inch thick shell could not be penetrated by the puncture bar, even under the worst-case conditions described earlier. Thus, 3/8 inch thick material was selected for use adjacent to the OCA closure joint (sealing regions) and as backup to the OCA vent and seal test ports to prevent puncture bar encroachment under all conditions.

Puncture drop tests were also selected to investigate regions containing stiffness discontinuities: 1/4 inch to 3/8 inch outer shell transitions, vent port and seal test port penetrations, and the forklift pocket structure. Finally, discontinuities in the OCA outer shell such as at the lid-to-body interface were tested to firmly establish the puncture resistant capability of that region.

Puncture drop events that do not significantly penetrate the OCA outer shell to expose significant amounts of foam are not of concern as packaging deformations and resultant acceleration loads associated with these events will be much less significant than the deformations and acceleration loads associated with the preceding 30-foot free drop tests. Additionally, differing temperatures and pressures during puncture drop testing will not significantly affect performance of the package. For this reason, although a variety of initial pressure conditions were included in the drop sequences, all puncture tests were performed at the prevailing ambient temperature.

2.10.3.5.4 Fire Test

At the conclusion of free drop and puncture drop testing, the CTU-1 and CTU-2 were subjected to a fully engulfing pool fire test in accordance with 10 CFR §71.73(c)(4). The package was oriented horizontally in the flames and minimally supported to least impede the heat flow into the package. The combined worst-case damage due to the drop tests was located in the hottest portion of the fire, i.e., 1½ meters above the fuel surface and 1/2 meter above the lowest part of the package[4]. Prior to fire testing, each CTU was preheated to the worst-case NCT steady-state temperature (i.e., 100 ºF still air without insolation).

[4] M. E. Schneider and L. A. Kent, *Measurements of Gas Velocities and Temperatures in a Large Open Pool Fire*, Sandia National Laboratories (reprinted from *Heat and Mass Transfer in Fire*, A. K. Kulkarni and Y. Jaluria, Editors, HTD-Vol. 73 (Book No. H00392), American Society of Mechanical Engineers). Figure 3 shows that maximum temperatures occur at an elevation approximately 2.3 meters above the pool floor. The pool was initially filled with water and fuel to a level of 0.814 meters. The maximum temperatures therefore occur approximately 1½ meters above the level of the fuel, i.e., 1/2 meter above the lowest part of the package when set one meter above the fuel source per the requirements of 10 CFR §71.73(c)(4).

2.10.3.6 Test Sequence for Selected Free Drop, Puncture Drop, and Fire Tests

The following sections establish the selected free drop, puncture drop, and fire test sequence for the TRUPACT-II CTUs based on the discussions provided in Section 2.10.3.5, *Technical Basis for Tests*. Test sequences are summarized in Table 2.10.3-2, Table 2.10.3-3, and Table 2.10.3-3, and correspondingly illustrated in Figure 2.10.3-4, Figure 2.10.3-5, and Figure 2.10.3-6, for CTU-1, CTU-2, and CTU-3, respectively.

2.10.3.6.1 Test Sequence for CTU-1

CTU-1 Free Drop No. 1 is an NCT free drop from a height of 3 feet, impacting horizontally on the CTU side, aligned with the OCV vent port. The 3-foot free drop height is based on the requirements of 10 CFR §71.71(c)(7). The purpose of this test is to demonstrate that the NCT free drop does not compromise the ability of the TRUPACT-II package to successfully sustain subsequent HAC test events in the same or other orientations.

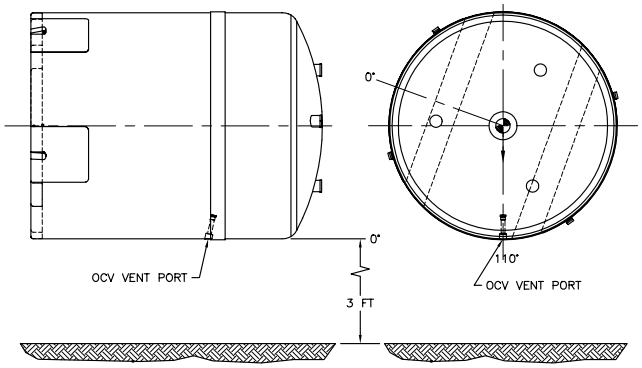

CTU-1 Free Drop No. 2 is a HAC free drop from a height of 30 feet, impacting horizontally on the CTU side, aligned with the OCV vent port. The 30-foot drop height is based on the requirements of 10 CFR §71.73(c)(1). The purpose of Free Drop Nos. 1 and 2, combined with Puncture Drop Nos. 5, 6, 7, and 8, is to create the greatest possible cumulative damage (i.e., the greatest reduction in foam thickness) in a region punctured through the OCA outer shell.

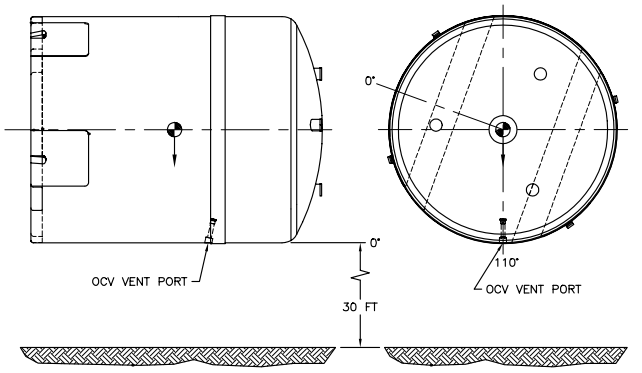

CTU-1 Free Drop No. 3 is a HAC free drop from a height of 30 feet, impacting near an OCA lid lift pocket and almost opposite the cumulative damage created by Free Drop Nos. 1 and 2, and Puncture Drop Nos. 5, 6, 7, and 8. The 30-foot drop height is based on the requirements of 10 CFR §71.73(c)(1). This drop orientation aligns the centerline of the 55-gallon drums with the point of impact. The purpose of this test is to produce maximum concentrated damage to the OCA lid.

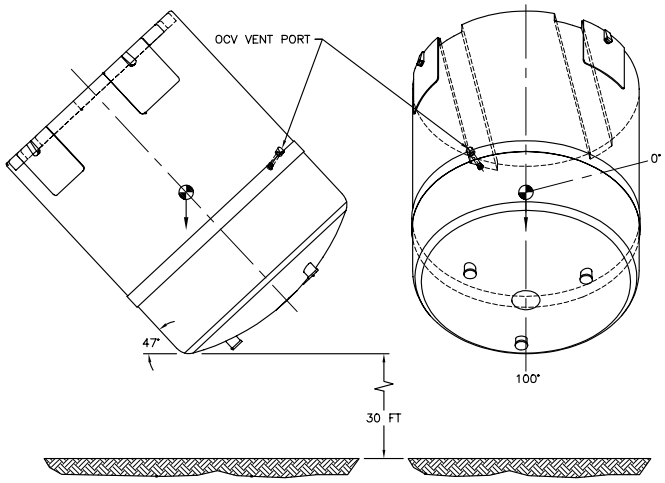

CTU-1 Free Drop No. 4 is a HAC free drop from a height of 30 feet, impacting vertically on the CTU top. The 30-foot drop height is based on the requirements of 10 CFR §71.73(c)(1). This top-down drop aligns the 55-gallon drums directly over the three lift pockets. The purpose of this test is to create the greatest possible damage (i.e., the greatest reduction in foam thickness) to the OCA lid top, and to drive the OCA lift pocket steel straps inward against the OCV lid's torispherical (i.e., dished) head.

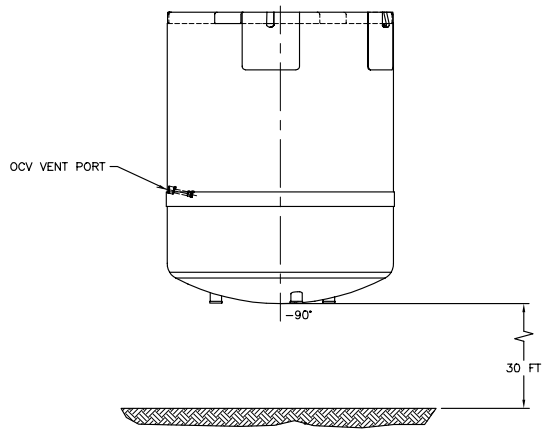

CTU-1 Puncture Drop No. 5 impacts directly onto the OCV vent port fitting, compounding the cumulative damage created by Free Drop Nos. 1 and 2. The puncture drop height is based on the requirements of 10 CFR §71.73(c)(3). The purpose of this test is to create the greatest cumulative damage (i.e., greatest reduction in foam thickness) over the OCV vent port region. Cumulative testing of this package region demonstrates that containment integrity is maintained.

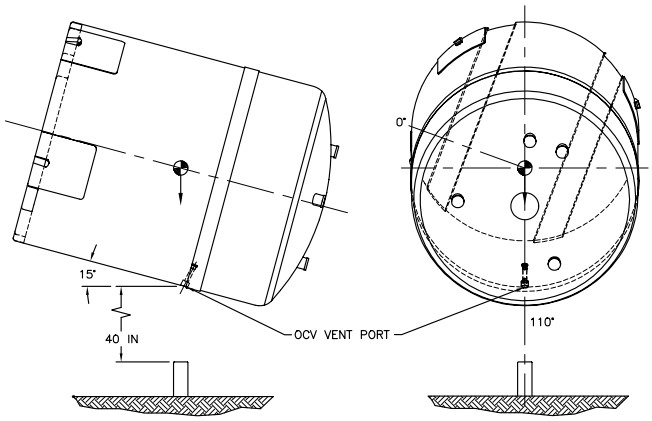

CTU-1 Puncture Drop No. 6 impacts directly onto the damage created by Free Drop Nos. 1 and 2, and onto the 3/8-to-1/4 inch, OCA body's outer shell transition. The puncture drop height is based on the requirements of 10 CFR §71.73(c)(3). The purpose this test is to penetrate the outer shell. Cumulative testing of this package region demonstrates that containment integrity is maintained.

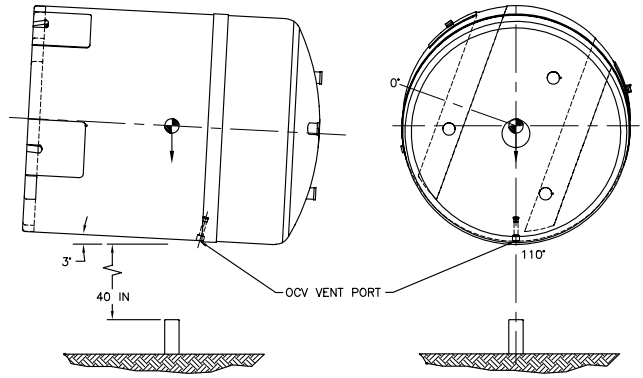

CTU-1 Puncture Drop No. 7 impacts directly onto the damage created by Free Drop Nos. 1 and 2, at a distance 40 inches above the package bottom. The puncture drop height is based on the requirements of 10 CFR §71.73(c)(3). The purpose of this test is to penetrate the 1/4 inch thick OCA body outer shell; this impact angle will ensure penetration occurs. Cumulative testing of this package region demonstrates that containment integrity is maintained.

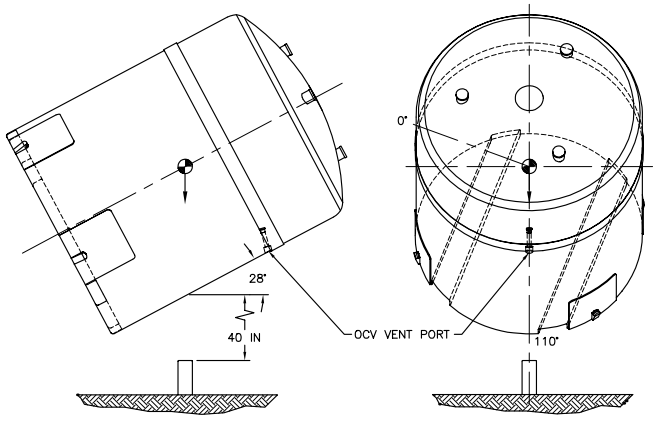

CTU-1 Puncture Drop No. 8 impacts directly onto the OCA's torispherical (i.e., dished) head, compounding the cumulative damage created by Free Drop Nos. 1 and 2. The puncture drop height is based on the requirements of 10 CFR §71.73(c)(3). The purpose of this test is to penetrate the region most weakened by Free Drop Nos. 1 and 2 (i.e., side drops). Cumulative testing of this package region demonstrates that containment integrity is maintained.

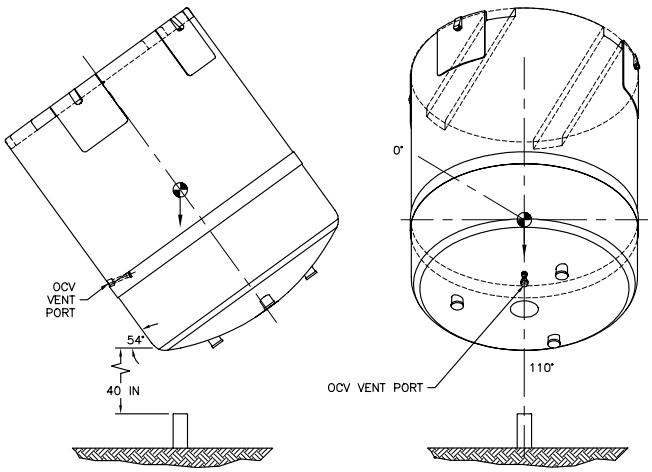

CTU-1 Puncture Drop No. 9 impacts directly onto the OCV seal test port fitting. The puncture drop height is based on the requirements of 10 CFR §71.73(c)(3). The purpose of this test is to create the greatest cumulative damage (i.e., greatest reduction in foam thickness) over the OCV seal test port region, and to demonstrate reliability of the underlying doubler support structure. Testing of this package region demonstrates that containment integrity is maintained.

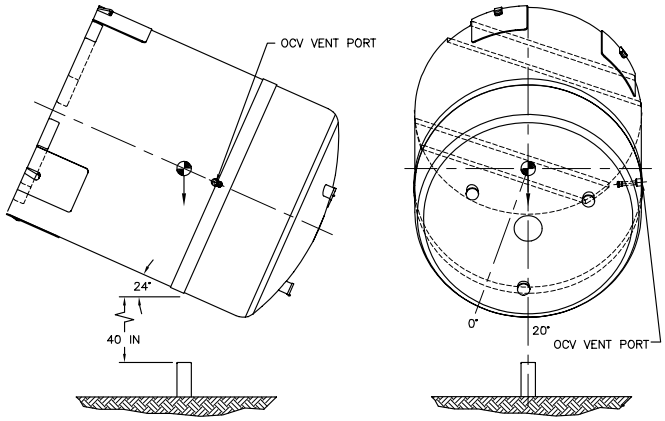

CTU-1 Fire No. 10 is performed by orienting the cumulative damage from Free Drop Nos. 1 and 2, and Puncture Drop Nos. 5, 6, 7, and 8 at the hottest location in the fire (i.e., 1½ meters above the fuel surface). The purpose of this test is to demonstrate that the reduction in sidewall thickness and puncture drop damage do not inhibit the package's containment integrity.

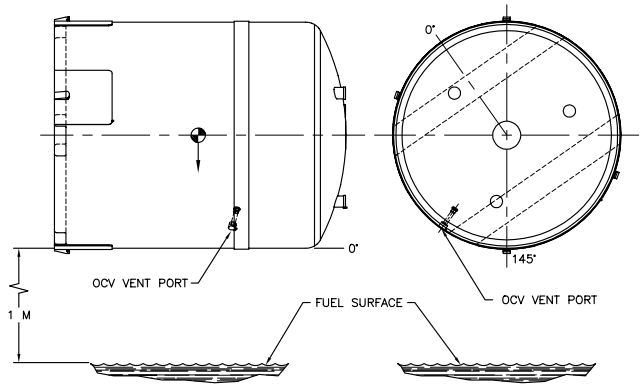

2.10.3.6.2 Test Sequence for CTU-2

CTU-2 Free Drop No. 1 is a HAC free drop from a height of 30 feet. This slapdown drop initially impacts on the OCA top knuckle. The 30-foot drop height is based on the requirements of 10 CFR §71.73(c)(1). The impact point is aligned with both the ICV and OCV pinned locking ring joints and underlying 55-gallon drum payload. The purpose of Free Drop No. 1 is to cause the most damage to the locking rings.

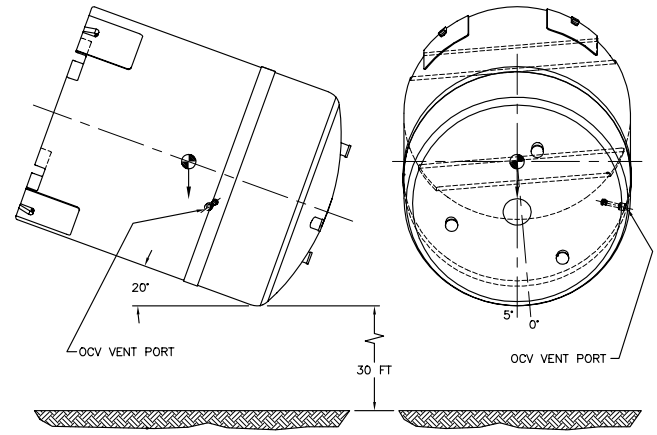

CTU-2 Free Drop No. 2 is a HAC free drop from a height of 30 feet, impacting vertically on the CTU bottom. The 30-foot drop height is based on the requirements of 10 CFR §71.73(c)(1). The purpose of this test is to create the greatest axial acceleration on the cylindrical containment vessels. This test will demonstrate that both the ICV and OCV cylindrical shells will not buckle or collapse.

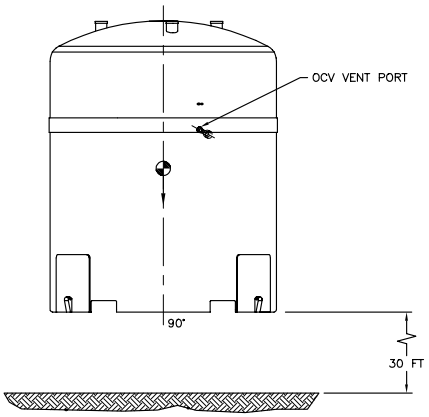

CTU-2 Free Drop No. 3 is a HAC free drop from a height of 30 feet. This slapdown drop initially impacts on the tie-down lug and its relatively rigid underlying structure, with secondary impact on the OCA top knuckle. The 30-foot drop height is based on the requirements of 10 CFR §71.73(c)(1). The purpose of this test is to create the maximum bending moment in the closure region by maximizing the slapdown drop accelerations.

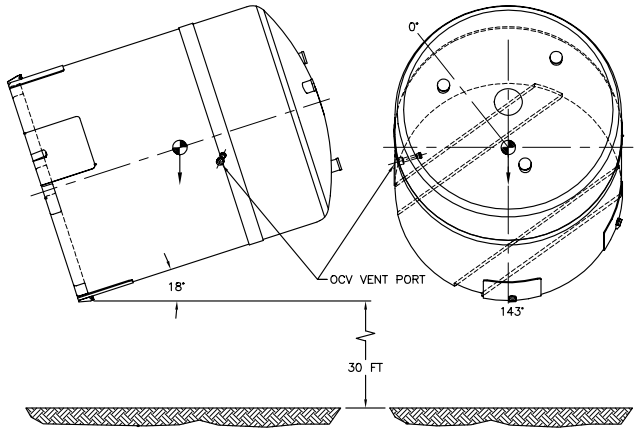

CTU-2 Puncture Drop No. R impacts at a distance 40 inches above the package bottom; this puncture drop test repeats Puncture Drop No. 7 on CTU-1. The puncture drop height is based on the requirements of 10 CFR §71.73(c)(3). The purpose of this test is to penetrate the 1/4 inch thick OCA body outer shell; this impact angle will assure that penetration occurs.

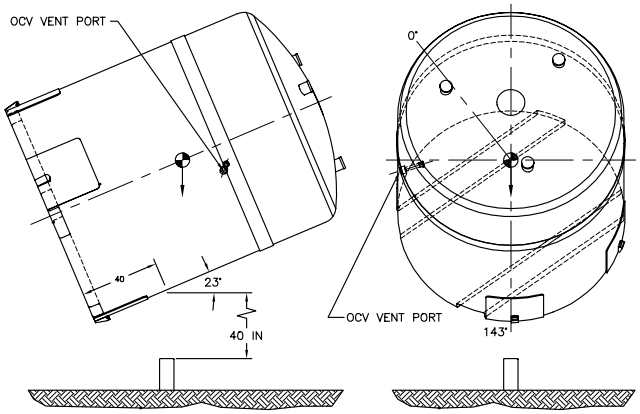

CTU-2 Puncture Drop No. 4 impacts directly onto the damage created by Free Drop No. 3, and onto the 3/8-to-1/4 inch, OCA lid's outer shell transition. The puncture drop height is based on the requirements of 10 CFR §71.73(c)(3). The purpose of this test is to attempt to penetrate the outer shell at the 3/8-to-1/4 inch transition between the OCA lid cylindrical shell and the relatively stiff upper torispherical (i.e., dished) head's knuckle. Cumulative testing of this package region demonstrates that containment integrity is maintained.

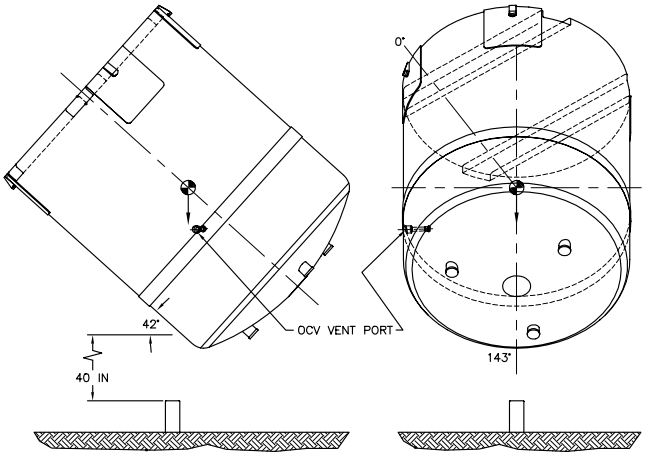

CTU-2 Puncture Drop No. 5 impacts directly onto the package bottom corner, adjacent to a forklift pocket. The puncture drop height is based on the requirements of 10 CFR §71.73(c)(3). The purpose of this test is to penetrate the 1/4 inch thick OCA flat bottom at a location where structural discontinuities will more easily induce tearing. Should tearing occur, this location could create a possible "chimney" for the HAC fire test by allowing free flow of air from the penetration due to Puncture Drop No. R.

CTU-2 Puncture Drop No. 6 impacts directly onto the inverted package's OCA lid side, adjacent to the outer thermal shield. The puncture drop height is based on the requirements of 10 CFR §71.73(c)(3). The purpose of this test is to attempt a tearing dislocation of the outer thermal shield by getting the pin to slide into and "snag" the protruding sheet metal. Sufficient removal of the outer thermal shield could expose the OCA closure joint gap to direct flame impingement during the HAC fire test.

CTU-2 Puncture Drop No. 7 impacts directly onto the OCA body at the same elevation as the OCV vent port fitting. The puncture drop height is based on the requirements of 10 CFR §71.73(c)(3). The purpose of this test is to demonstrate that the 3/8 inch thick OCA body cylindrical shell adjacent to the closure will not deform inward to the extent that the HAC fire test damages the O-ring seal region.

CTU-2 Puncture Drop No. 8 impacts directly onto the OCA body at the same elevation as the OCV seal test port fitting. The puncture drop height is based on the requirements of 10 CFR §71.73(c)(3). The purpose of this test is to demonstrate that the 3/8 inch thick OCA lid cylindrical shell adjacent to the closure will not deform inward to the extent that the HAC fire test damages the O-ring seal region.

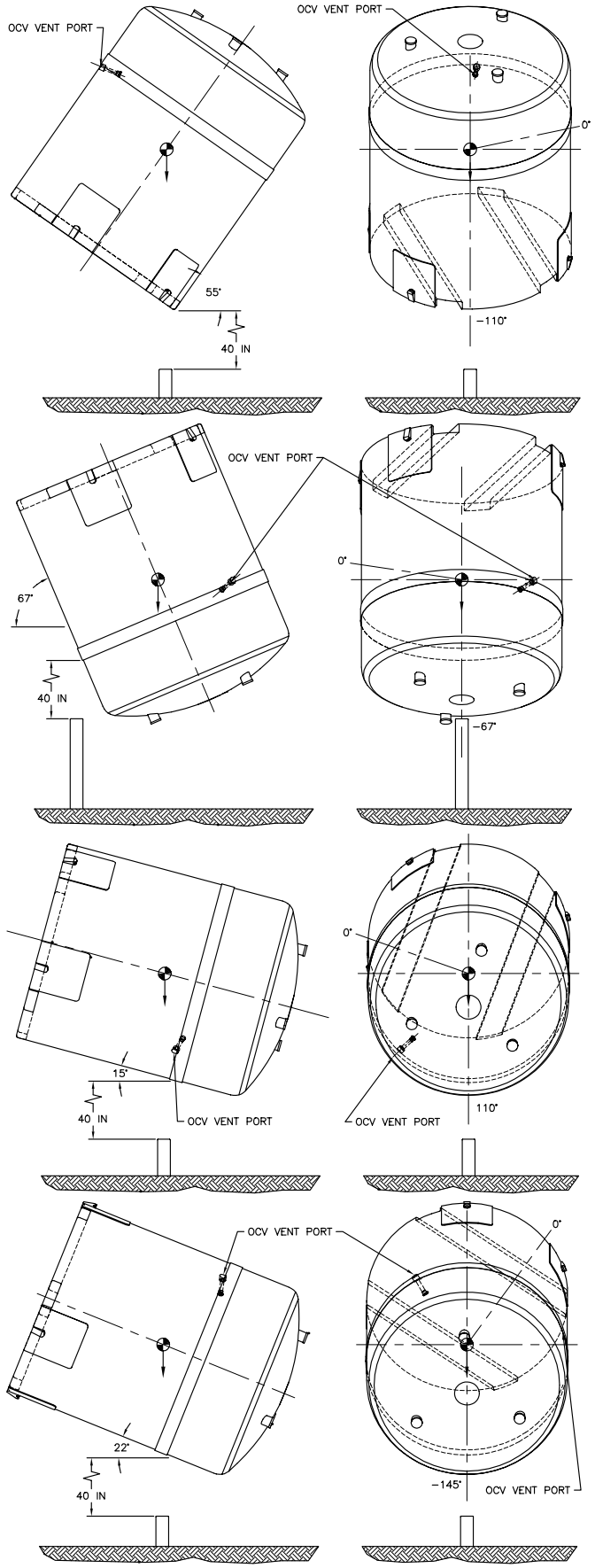

CTU-2 Fire No. 9 is performed by orienting the cumulative damage from Free Drop No. 3, and Puncture Drop Nos. 4, R, and 5 at the hottest location in the fire (i.e., 1½ meters above the fuel surface). The purpose of this test is to demonstrate that the reduction in sidewall thickness and puncture drop damage do not inhibit the package's containment integrity.

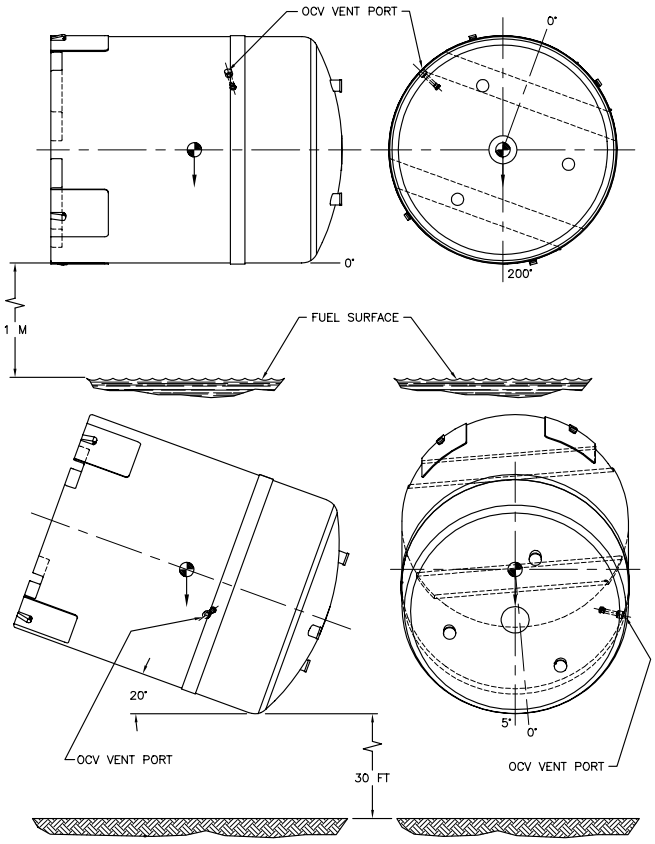

2.10.3.6.3 Test Sequence for CTU-3

CTU-3 Free Drop No. 1 is a HAC free drop from a height of 30 feet. This slapdown drop initially impacts on the OCA top knuckle. The 30-foot drop height is based on the requirements of 10 CFR §71.73(c)(1). The impact point is aligned with both the ICV and OCV pinned locking ring joints and underlying 55-gallon drum payload. The purpose of Free Drop No. 1 is to cause the most damage to the locking rings.

CTU-3 Free Drop No. 2 is a HAC free drop from a height of 30 feet, impacting vertically on the CTU bottom. The 30-foot drop height is based on the requirements of 10 CFR §71.73(c)(1). The purpose of this test is to create the greatest axial acceleration on the cylindrical containment vessels. This test will demonstrate that both the ICV and OCV cylindrical shells will not buckle or collapse.

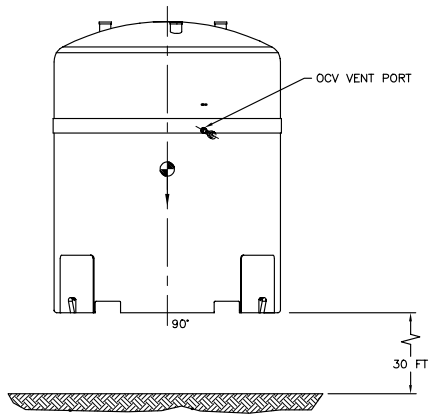

CTU-3 Free Drop No. 3 is a HAC free drop from a height of 30 feet. This slapdown drop initially impacts on the tie-down lug and its relatively rigid underlying structure, with secondary impact on the OCA top knuckle. The 30-foot drop height is based on the requirements of 10 CFR §71.73(c)(1). The purpose of this test is to create the maximum bending moment in the closure region by maximizing the slapdown drop accelerations.

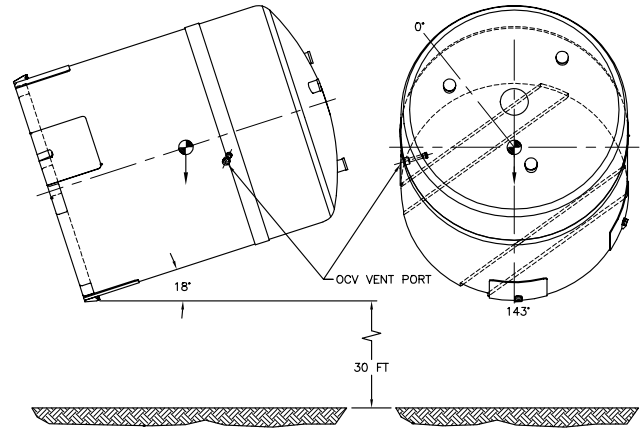

CTU-3 Puncture Drop No. 4 impacts directly onto the damage created by Free Drop No. 3, and onto the 3/8-to-1/4 inch, OCA lid's outer shell transition. The puncture drop height is based on the requirements of 10 CFR §71.73(c)(3). The purpose of this test is to attempt to penetrate the outer shell at the 3/8-to-1/4 inch transition between the OCA lid cylindrical shell and the relatively stiff upper torispherical (i.e., dished) head's knuckle. Cumulative testing of this package region demonstrates that containment integrity is maintained.

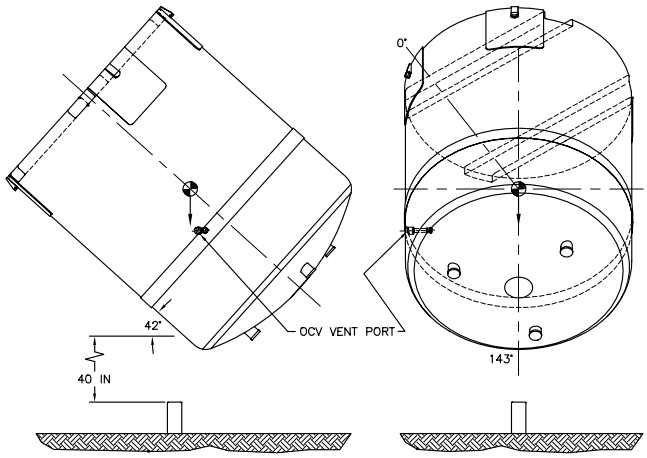

CTU-3 Puncture Drop No. 5 impacts directly onto the package bottom corner, adjacent to a forklift pocket. The puncture drop height is based on the requirements of 10 CFR §71.73(c)(3). The purpose of this test is to penetrate the 1/4 inch thick OCA flat bottom at a location where structural discontinuities will more easily induce tearing. Should tearing occur, this location could create a possible "chimney" for a subsequent HAC fire test. Alternating the axial impact direction also verifies the effectiveness of the wiper O-ring seal design by attempting to drive more debris into the ICV sealing region.

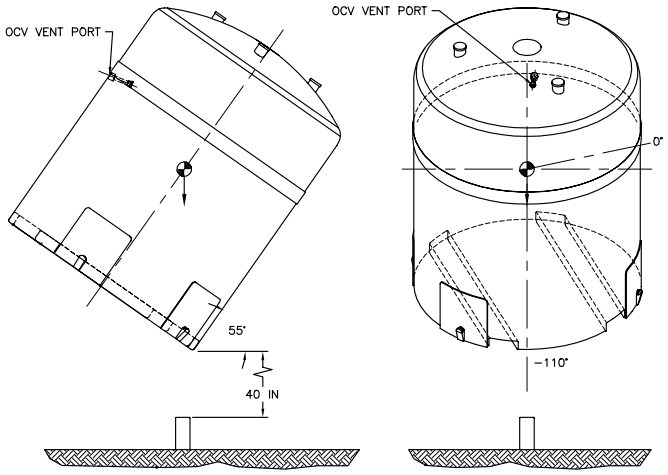

CTU-3 Puncture Drop No. 6 impacts directly onto the inverted package's OCA lid side, adjacent to the outer thermal shield. The puncture drop height is based on the requirements of 10 CFR §71.73(c)(3). The purpose of this test is to attempt a tearing dislocation of the outer thermal shield by getting the pin to "snag" the protruding sheet metal. Sufficient outer thermal shield damage could expose the closure joint gap to direct flame impingement during the HAC fire test. Alternating the axial impact direction also verifies the effectiveness of the wiper O-ring seal design by attempting to drive more debris into the ICV sealing region.

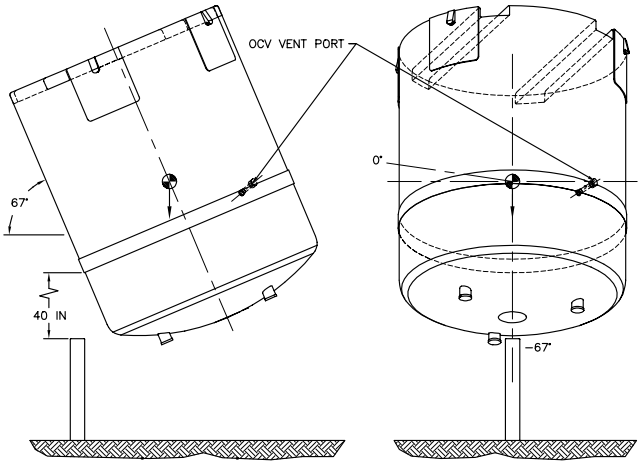

CTU-3 Puncture Drop No. 7 impacts directly onto the OCA body at the same elevation as the OCV vent port fitting. The puncture drop height is based on the requirements of 10 CFR §71.73(c)(3). The purpose of this test is to demonstrate that the 3/8 inch thick OCA body cylindrical shell adjacent to the closure will not deform inward to the extent that the HAC fire test damages the O-ring seal region.

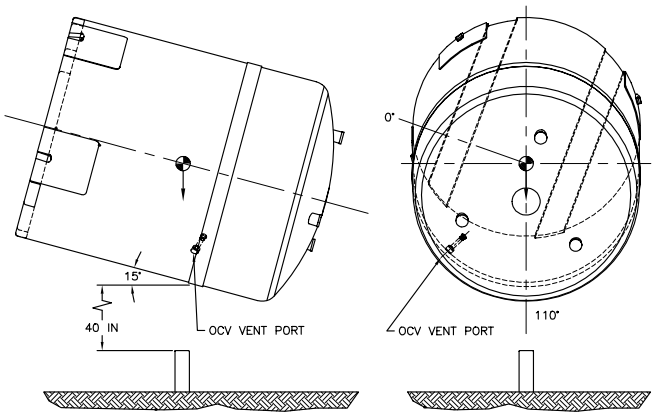

CTU-3 Puncture Drop No. 8 impacts directly onto the OCA body at the same elevation as the OCV seal test port fitting. The puncture drop height is based on the requirements of 10 CFR §71.73(c)(3). The purpose of this test is to demonstrate that the 3/8 inch thick OCA lid cylindrical shell adjacent to the closure will not deform inward to the extent that the HAC fire test damages the O-ring seal region.

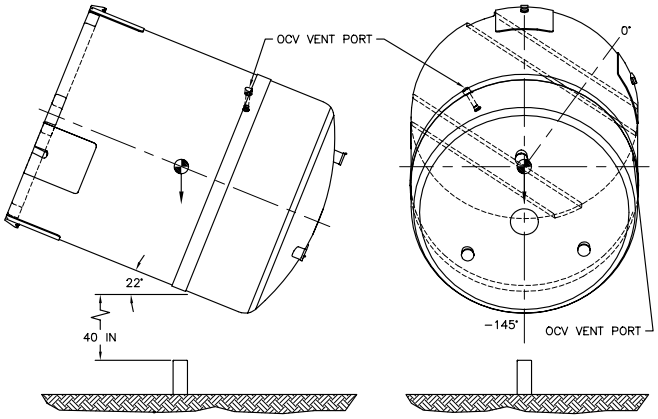

2.10.3.7 Test Results

The following sections report the results of free drop, puncture drop, and fire tests following the sequence provided in Section 2.10.3.6, *Test Sequence for Selected Free Drop, Puncture Drop, and Fire Tests*. Results are summarized in Table 2.10.3-2, Table 2.10.3-3, and Table 2.10.3-3, and correspondingly illustrated in Figure 2.10.3-4, Figure 2.10.3-5, and Figure 2.10.3-6 for CTU-1, CTU-2, and CTU-3, respectively.

Figure 2.10.3-26 through Figure 2.10.3-53 sequentially photo-document the certification testing process for the CTU-1, Figure 2.10.3-54 through Figure 2.10.3-79 sequentially photo-document the certification testing process for the CTU-2, and Figure 2.10.3-80 through Figure 2.10.3-99 sequentially photo-document the certification testing process for the CTU-3.

2.10.3.7.1 Test Results for CTU-1

2.10.3.7.1.1 CTU-1 Free Drop No. 1

Free Drop No. 1 was an NCT free drop from a height of 3 feet, impacting onto the OCA vent port. As shown in Figure 2.10.3-4, CTU-1 was oriented horizontal to the impact surface (axial angle (i.e., pitch) = 0º), and circumferentially aligned to impact onto the OCA vent port (110º from the forklift pocket reference). At the time of the test, the measured ICV and OCV temperatures were 58 ºF and 48 ºF, respectively. The test was conducted on 12/04/88.

The measured permanent deformations for CTU-1 were flats 18 inches wide at the top (OCA lid), and 18 inches wide at the bottom (OCA body), each corresponding to a crush depth of approximately 7/8 inches. The ICV and OCV internal pressures did not change.

2.10.3.7.1.2 CTU-1 Free Drop No. 2

Free Drop No. 2 was a HAC free drop from a height of 30 feet, impacting onto the OCA vent port. As shown in Figure 2.10.3-4, CTU-1 was oriented horizontal to the impact surface (axial angle (i.e., pitch) = 0º), and circumferentially aligned to impact onto the OCA vent port (110º from the forklift pocket reference). At the time of the test, the measured OCV temperature was 53 ºF. The test was conducted on 12/04/88.

The measured permanent deformations for CTU-1 were flats 37 inches wide at the top (OCA lid), and 35 inches wide at the bottom (OCA body), corresponding to a crush depth of approximately 3⅝ inches. The ICV and OCV internal pressures did not change.

2.10.3.7.1.3 CTU-1 Free Drop No. 3

Free Drop No. 3 was a HAC free drop from a height of 30 feet, impacting onto the CTU lid knuckle near an OCA lid lifting pocket. As shown in Figure 2.10.3-4, CTU-1 was oriented -47º from horizontal (axial angle (i.e., pitch) = 47º top down), and circumferentially aligned to impact nearly opposite the OCA vent port (-100º from the forklift pocket reference). At the time of the test, the measured OCV temperature was 50 ºF. The test was conducted on 12/05/88.

The measured permanent deformation for CTU-1 was a flat 30 inches wide and 53 inches long on the OCA lid, corresponding to a crush depth of approximately 3¾ inches. The ICV and OCV internal pressures were not measured due to test damage to the pressurization lines.

2.10.3.7.1.4 CTU-1 Free Drop No. 4

Free Drop No. 4 was a HAC free drop from a height of 30 feet, impacting vertically onto the CTU lid (i.e., top-down orientation), as shown in Figure 2.10.3-4. At the time of the test, the measured OCV temperature was 47 ºF. The test was conducted on 12/06/88.

The measured permanent deformation for CTU-1 was a 53 inch diameter flat on the OCA lid, corresponding to a crush depth of approximately 3⅞ inches. The ICV internal pressure did not change; however, the OCV internal pressure dropped 1.3 psig.

2.10.3.7.1.5 CTU-1 Puncture Drop No. 5

Puncture Drop No. 5 was a HAC puncture drop from a height of 40 inches, impacting onto the OCA vent port. As shown in Figure 2.10.3-4, CTU-1 was oriented -15º from horizontal (axial angle (i.e., pitch) = 15º top down) through the package's center of gravity, and circumferentially aligned to impact onto the OCA vent port (110º from the forklift pocket reference). At the time of the test, the measured OCV temperature was 32 ºF. The test was conducted on 12/07/88.

The measured permanent deformation for CTU-1 was a dent approximately 3 inches deep, and a 16 inch long tear at the shell-to-angle (Z-flange) interface. The ICV and OCV internal pressures did not change.

2.10.3.7.1.6 CTU-1 Puncture Drop No. 6

Puncture Drop No. 6 was a HAC puncture drop from a height of 40 inches, impacting onto the OCA body at the 1/4-to-3/8 inch thickness outer shell transition. As shown in Figure 2.10.3-4, CTU-1 was oriented -3º from horizontal (axial angle (i.e., pitch) = 3º top down) through the

package's center of gravity, and circumferentially aligned with the OCA vent port (110º from the forklift pocket reference). At the time of the test, the measured OCV temperature was 30 ºF. The test was conducted on 12/07/88.

The measured permanent deformation for CTU-1 was a dent approximately 3/4 inches deep. The ICV internal pressure did not change; however, the OCV internal pressure dropped 0.3 psig.

2.10.3.7.1.7 CTU-1 Puncture Drop No. 7

Puncture Drop No. 7 was a HAC puncture drop from a height of 40 inches, impacting onto the OCA body at a location 40 inches above the package bottom. As shown in Figure 2.10.3-4, CTU-1 was oriented 28º from horizontal (axial angle (i.e., pitch) = 28º top up) through the package's center of gravity, and circumferentially aligned with the OCA vent port (110º from the forklift pocket reference). At the time of the test, the measured OCV temperature was 25 ºF. The test was conducted on 12/08/88.

The measured permanent deformation for CTU-1 was an 8 inch wide, 11 inch long, and 8½ inch deep hole through the OCA outer shell. The ICV and OCV internal pressures did not change.

2.10.3.7.1.8 CTU-1 Puncture Drop No. 8

Puncture Drop No. 8 was a HAC puncture drop from a height of 40 inches, impacting onto the OCA lid's knuckle at the location of side drop damage from Free Drop Nos. 1 and 2. As shown in Figure 2.10.3-4, CTU-1 was oriented -54º from horizontal (axial angle (i.e., pitch) = 54º top down) through the package's center of gravity, and circumferentially aligned with the OCA vent port (110º from the forklift pocket reference). At the time of the test, the measured OCV temperature was 37 ºF. The test was conducted on 12/09/88.

The measured permanent deformation for CTU-1 was some additional denting of the OCA lid's knuckle. The ICV and OCV internal pressures did not change.

2.10.3.7.1.9 CTU-1 Puncture Drop No. 9

Puncture Drop No. 9 was a HAC puncture drop from a height of 40 inches, impacting onto the OCA seal test port. As shown in Figure 2.10.3-4, CTU-1 was oriented -24º from horizontal (axial angle (i.e., pitch) = 24º top down) through the package's center of gravity, and circumferentially aligned with the OCA seal test port (20º from the forklift pocket reference). At the time of the test, the measured OCV temperature was 36 ºF. The test was conducted on 12/10/88.

The measured permanent deformation for CTU-1 was a dent approximately 3 inches deep, and a 7 inch wide tear in the outer thermal shield. The ICV internal pressure did not change; however, the OCV internal pressure dropped 0.5 psig.

2.10.3.7.1.10 CTU-1 Fire No. 10

Fire No. 10 was performed to demonstrate packaging compliance with the requirements of 10 CFR §71.73(c)(4) and the guidelines set forth in IAEA Safety Series No. 37[5]. The following list summarizes the test parameters:

- CTU-1 was oriented on an insulated test stand with the most severe damage approximately 1½ meters above the fuel surface. With a circumferential orientation of 145º (see Figure 2.10.3-4), the most severe damage was determined to be from the cumulative effects of Free Drop Nos. 1 and 2, and Puncture Drop Nos. 5 and 7 located 1½ meters above the fuel surface.
- Consistent with 10 CFR §71.73(c)(4), CTU-1 was installed onto an insulated test stand at an elevation to place the lowest part of the package one meter above the fuel surface. CTU-1 was oriented horizontally on the test stand to maximize heat input.
- Consistent with 10 CFR §71.73(c)(4), requiring the test pool to extend 1 to 3 meters beyond the package edges, the test pool size extended approximately 1½ meters beyond each side of CTU-1.
- Consistent with Paragraph A-628.5 of IAEA Safety Series No. 37, requiring wind speeds not to exceed 2 m/s (4.5 mph), the average wind speed was measured to be 1.97 m/s (4.4 mph).
- Consistent with 10 CFR §71.73(c)(4), a JP4-type fuel was used for the fire test, and the amount of fuel was controlled to ensure the fire duration exceeded 30 minutes. The fuel was floated on a pool of water approximately 1/2 meter deep to ensure even distribution during burning. The fire test lasted approximately 32 minutes, and burning continued for approximately 64 minutes after the end of the fire.
- The test pool was instrumented to measure fire temperatures and heat fluxes at various locations around CTU-1. Temperatures were monitored before, during, and following the fire test until magnitudes stabilized back to ambient conditions. The average OCA surface temperature, based on thermocouple traces, was between 1,500 ºF and 1,750 ºF.
- The CTU-1 containment O-ring seals were leak tested following performance testing to verify containment integrity, as discussed in Section 2.10.3.7.1.12, *CTU-1 Post-Test Disassembly*.
- The average OCV thermocouple pre-heat temperature was 127 ºF at the time of the test (compared to the analytically determined HAC initial temperature of 120 ºF).
- The test was conducted on 12/14/88.

The maximum ICV seal flange temperature was 170 ºF (via temperature indicating labels), and the maximum OCV seal flange temperature was 260 ºF (via thermocouples; 250 ºF via temperature indicating labels). The temperature indicating label locations and results are provided in Table 2.10.3-4, and Figure 2.10.3-7 and Figure 2.10.3-8. The thermocouple locations are provided in Figure 2.10.3-10, and the results are provided in Figure 2.10.3-12, Figure 2.10.3-13, Figure 2.10.3-14, and Figure 2.10.3-15. The ICV internal pressure increased 1.9 psig, and the OCV internal pressure increased 1.6 psig (see Figure 2.10.3-24).

[5] IAEA Safety Series No. 37, *Advisory Material for the IAEA Regulations for the Safe Transport of Radioactive Material (1985 Edition)*, Third Edition (As Amended 1990), International Atomic Energy Agency, Vienna, 1990.

2.10.3.7.1.11 CTU-1 Testing Anomalies

As can be expected with any test program, a certain number of test-related anomalies occurred during CTU-1 testing. The following paragraphs summarize each anomaly and its significance.

- The secondary impact from Free Drop No. 3 resulted in the ICV and OCV pressurization lines being cut (however, pressure was maintained throughout the primary impact; post-test re-pressurization of the ICV and OCV demonstrated containment integrity was maintained.
- Pressure rise leak testing of the OCV was planned between each free drop and puncture test; shifting of the OCV relative to the seal leak test port, pump oil contamination (used to pump hot, pre-heat air into the ICV and OCV), and expediting testing were the reasons that pressure rise leak testing was not always performed.
- Puncture Drop No. 7 was not considered a valid test, and was repeated as Puncture Drop No. R on CTU-2; CTU-1 contacted the ground prior to expending all of its kinetic energy on the puncture bar.
- Pressure within the OCV was lost during post-fire test cool-down; the pressure loss was traced to a non-prototypic test gasket (see "FLAT GASKET" in Figure 2.10.3-2).
- During post-test helium leak testing of the ICV, the bottom port to be used for helium injection had frozen closed; a new port was drilled in the ICV lid's torispherical head (in an undamaged region on the crown).

2.10.3.7.1.12 CTU-1 Post-Test Disassembly

Post-test disassembly of CTU-1 was performed following Fire No. 10. Both abrasive cutting and gas plasma cutting methods were utilized, depending on their potential effect on subsequent post-test seal testing, to enable destructive disassembly of CTU-1.

Upon removal of the OCA lid and body outer shells, the presence of several inches of very light density foam char showed the intumescing behavior of the polyurethane foam. Except for the local area damaged by the puncture impact 40 inches above the bottom of the OCA body, a layer of unburned polyurethane foam remained around the entire OCV. The average thickness of the layer was approximately 5 to 6 inches along the cylindrical sides and bottom, and 10 inches on top.

Demonstration of containment vessel leaktightness was accomplished by performing helium mass spectrometer leakage rate testing on each containment vessel's main O-ring seal, vent port O-ring seal, and metallic boundary. The main and vent port O-ring seals were tested when cooled to an average measured temperature below -20 ºF; the metallic boundary was tested at ambient temperature. Results of successful mass spectrometer helium leakage rate testing are summarized in the following table:

Sealing Component	OCV	ICV
Main O-ring Seal	$<2.0 \times 10^{-8}$ cc/s, helium	3.0×10^{-8} cc/s, helium
Vent Port Plug O-ring Seal	$<2.0 \times 10^{-8}$ cc/s, helium	6.4×10^{-8} cc/s, helium
Metallic Boundary	2.0×10^{-8} cc/s, helium	7.0×10^{-8} cc/s, helium

When accounting for the conversion between air leakage (per ANSI N14.5) and helium leakage, a 2.6 factor applies for standard temperatures and pressures. Thus, a reported helium leakage rate of 1.3×10^{-7} cc/s, helium, is equivalently 5×10^{-8} cc/s, air, a magnitude well below the "leaktight" criterion of 1×10^{-7} cc/s, air, per ANSI N14.5.

In conclusion, the test series performed on CTU-1 demonstrates the TRUPACT-II package's ability to meet the normal conditions of transport and hypothetical accident conditions regulatory requirements as defined in 10 CFR §71.71 and §71.73, respectively.

2.10.3.7.2 Test Results for CTU-2

2.10.3.7.2.1 CTU-2 Free Drop No. 1

Free Drop No. 1 was a HAC free drop from a height of 30 feet. The primary impact for this slapdown drop occurred onto the OCA lid knuckle, with the secondary impact onto the OCA body's bottom edge, approximately midway between tie-down lugs. As shown in Figure 2.10.3-5, CTU-2 was oriented -20º from horizontal (axial angle (i.e., pitch) = 20º top down), and circumferentially aligned to impact the ICV and OCV locking ring pinned joints and coincident payload drums to produce maximum damage (-5º from the forklift pocket reference). At the time of the test, the measured OCV temperature was -26 ºF. The test was conducted on 01/14/89.

The measured permanent deformations for CTU-2 were flats 45 inches wide at the top (OCA lid), and 21 inches wide at the bottom (OCA body). The OCV internal pressure did not change; however, the ICV internal pressure dropped 0.5 psig, and was most likely due to disconnecting and reconnecting the pressure monitoring device.

2.10.3.7.2.2 CTU-2 Free Drop No. 2

Free Drop No. 2 was a HAC free drop from a height of 30 feet, impacting vertically onto the CTU bottom, as shown in Figure 2.10.3-5. At the time of the test, the measured OCV temperature was -26 ºF. The test was conducted on 01/16/89.

The permanent deformation for CTU-2 was negligible. The ICV and OCV internal pressures were lost due to damaged pressure test fittings from the free drop test. The maximum axial acceleration was 385 *g*s (filtered at 500 Hz; see Figure 2.10.3-18 and Figure 2.10.3-19).

2.10.3.7.2.3 CTU-2 Free Drop No. 3

Free Drop No. 3 was a HAC free drop from a height of 30 feet. The primary impact for this slapdown drop occurred onto a tie-down lug, with the secondary impact onto the OCA lid. As shown in Figure 2.10.3-5, CTU-2 was oriented 18º from horizontal (axial angle (i.e., pitch) = 18º top up), and circumferentially aligned with the tie-down lug (143º from the forklift pocket reference). The test was conducted on 01/17/89.

The measured permanent deformations for CTU-2 were flats 15 inches wide at the top (OCA lid), and 45 inches wide at the bottom (OCA body). The ICV and OCV internal pressures did not change. The maximum axial acceleration was 44 *g*s (filtered at 500 Hz; see Figure 2.10.3-20 and Figure 2.10.3-21.

2.10.3.7.2.4 CTU-2 Puncture Drop No. R

Puncture Drop No. R was a HAC puncture drop from a height of 40 inches, impacting onto the OCA body at a location 40 inches above the package bottom. As shown in Figure 2.10.3-5, CTU-2 was oriented 23º from horizontal (axial angle (i.e., pitch) = 23º top up) through the package's center of gravity, and circumferentially aligned with the tie-down lug (143º from the forklift pocket reference). The test was conducted on 01/17/89.

The measured permanent deformation for CTU-2 was a 10 inch wide, 11 inch long, and 9 inch deep hole through the OCA outer shell. The ICV and OCV internal pressures did not change.

2.10.3.7.2.5 CTU-2 Puncture Drop No. 4

Puncture Drop No. 4 was a HAC puncture drop from a height of 40 inches, impacting onto the OCA body at the 1/4-to-3/8 inch thickness outer shell transition. As shown in Figure 2.10.3-5, CTU-2 was oriented -42º from horizontal (axial angle (i.e., pitch) = 42º top down) through the package's center of gravity, and circumferentially aligned with the tie-down lug (143º from the forklift pocket reference). The test was conducted on 01/18/89.

The measured permanent deformation for CTU-2 was an 8 inch wide, 10 inch long, and 7 inch deep hole through the OCA outer shell. The ICV internal pressure did not change; however, the OCV internal pressure dropped 1.0 psig.

2.10.3.7.2.6 CTU-2 Puncture Drop No. 5

Puncture Drop No. 5 was a HAC puncture drop from a height of 40 inches, impacting onto the OCA bottom edge, adjacent to a forklift pocket. As shown in Figure 2.10.3-5, CTU-2 was oriented 55º from horizontal (axial angle (i.e., pitch) = 55º top up) through the package's center of gravity, and circumferentially -110º from the forklift pocket reference. The test was conducted on 01/19/89.

The measured permanent deformation for CTU-2 was a dent approximately 5 inches deep. The ICV and OCV internal pressures did not change.

2.10.3.7.2.7 CTU-2 Puncture Drop No. 6

Puncture Drop No. 6 was a HAC puncture drop from a height of 40 inches, impacting glancingly onto the OCA lid adjacent to the outer thermal shield. As shown in Figure 2.10.3-5, CTU-2 was oriented -67º from horizontal (axial angle (i.e., pitch) = 67º top down), and circumferentially -67º from the forklift pocket reference. The test was conducted on 01/20/89.

The measured permanent deformation for CTU-2 was a 24 inch long dent approximately 1 inch deep. The ICV and OCV internal pressures did not change.

2.10.3.7.2.8 CTU-2 Puncture Drop No. 7

Puncture Drop No. 7 was a HAC puncture drop from a height of 40 inches, impacting onto the OCA body at the closure joint. As shown in Figure 2.10.3-5, CTU-2 was oriented -15º from horizontal (axial angle (i.e., pitch) = 15º top down) through the package's center of gravity, and circumferentially 110º from the forklift pocket reference. The test was conducted on 01/20/89.

The measured permanent deformation for CTU-2 was a 4 inch deep dent and a 3 inch long tear in the outer shell-to-Z-flange angle interface. The ICV and OCV internal pressures did not change.

2.10.3.7.2.9 CTU-2 Puncture Drop No. 8

Puncture Drop No. 8 was a HAC puncture drop from a height of 40 inches, impacting onto the OCA lid at the closure joint. As shown in Figure 2.10.3-5, CTU-2 was oriented -22º from horizontal (axial angle (i.e., pitch) = 22º top down) through the package's center of gravity, and circumferentially -145º from the forklift pocket reference. The test was conducted on 01/21/89.

The measured permanent deformation for CTU-2 was a 4 inch deep dent. The ICV and OCV internal pressures did not change.

2.10.3.7.2.10 CTU-2 Fire No. 9

Fire No. 9 was performed to demonstrate packaging compliance with the requirements of 10 CFR §71.73(c)(4) and the guidelines set forth in IAEA Safety Series No. 37. The following list summarizes the test parameters:

- CTU-2 was oriented on an insulated test stand with the most severe damage approximately 1½ meters above the fuel surface. With a circumferential orientation of 200º (see Figure 2.10.3-5), the most severe damage was determined to be from the cumulative effects of Free Drop No. 3, and Puncture Drop Nos. R and 4 located 1½ meters above the fuel surface.
- Consistent with 10 CFR §71.73(c)(4), CTU-2 was installed onto an insulated test stand at an elevation to place the lowest part of the package one meter above the fuel surface. CTU-2 was oriented horizontally on the test stand to maximize heat input.
- Consistent with 10 CFR §71.73(c)(4), requiring the test pool to extend 1 to 3 meters beyond the package edges, the test pool size extended approximately 1½ meters beyond each side of CTU-2.
- Consistent with Paragraph A-628.5 of IAEA Safety Series No. 37, requiring wind speeds not to exceed 2 m/s (4.5 mph), the average wind speed was measured to be 1.9 m/s (4.2 mph).
- Consistent with 10 CFR §71.73(c)(4), a JP4-type fuel was used for the fire test, and the amount of fuel was controlled to ensure the fire duration exceeded 30 minutes. The fuel was floated on a pool of water approximately 1/2 meter deep to ensure even distribution during burning. The fire test lasted approximately 31 minutes, and burning continued for approximately 70 minutes after the end of the fire.
- The test pool was instrumented to measure fire temperatures and heat fluxes at various locations around CTU-2. Temperatures were monitored before, during, and following the fire test until magnitudes stabilized back to ambient conditions. The average OCA surface temperature, based on thermocouple traces, was between 1,500 ºF and 1,750 ºF.
- The CTU-2 containment O-ring seals were leakage rate tested following performance testing to verify containment integrity, as discussed in Section 2.10.3.7.2.12, *CTU-2 Post-Test Disassembly*.
- The average OCV thermocouple pre-heat temperature was 127 ºF at the time of the test (compared to the analytically determined HAC initial temperature of 120 ºF).
- The test was conducted on 01/30/89.

The maximum ICV seal flange temperature was 200 ºF (via temperature indicating labels), and the maximum OCV seal flange temperature was 253 ºF (via thermocouples; 250 ºF via temperature indicating labels). Temperature indicating label locations and results are provided in Table 2.10.3-5, and Figure 2.10.3-7 and Figure 2.10.3-9. Thermocouple locations are provided in Figure 2.10.3-11, and the results are provided in Figure 2.10.3-16 and Figure 2.10.3-17. The ICV internal pressure increased 2.6 psig, and the OCV internal pressure increased 4.6 psig (see Figure 2.10.3-25).

2.10.3.7.2.11 CTU-2 Testing Anomalies

As can be expected with any test program, a certain number of test-related anomalies occurred during CTU-2 testing. The following paragraphs summarize each anomaly and its significance.

- The impact from Free Drop No. 2 caused the neoprene weather seal to slide downward and break the OCV pressurization line, the break occurring just after the impact event and, therefore, not compromising the test; post-test re-pressurization of the OCV demonstrated containment integrity was maintained.
- Following impact from Puncture Drop No. 4, CTU-2 rolled off the puncture bar and damaged the OCV and ICV pressurization fittings; the 1.0 psig OCV pressure loss was attributed to this post-test condition.
- Pressure rise leak testing of the OCV was planned between each free drop and puncture test; shifting of the OCV relative to the seal leak test port and expediting testing were the reasons that pressure rise leak testing was not always performed.
- The ICV main O-ring seal could not be made to pass the post-test helium leakage rate test; however, the lower (non-containment) O-ring seal was leakage rate tested and shown to remain leaktight at -20 ºF. The cause of debris getting past the debris shield was determined to be water condensate from the concrete-filled payload drums collecting on the open-cell foam rubber and freezing, thereby loosing enough resiliency to prevent debris from getting into the main O-ring seal (see Figure 2.10.3-79). A wiper O-ring seal was added to the ICV design to prevent debris from contaminating the main O-ring seals for all temperature and moisture ranges.

2.10.3.7.2.12 CTU-2 Post-Test Disassembly

Post-test disassembly of CTU-2 was performed following Fire No. 9. Both abrasive cutting and gas plasma cutting methods were utilized, depending on their potential effect on subsequent post-test seal testing, to enable destructive disassembly of CTU-2.

As with CTU-1, upon removal of the OCA lid and body outer shells, the presence of several inches of very light density foam char showed the intumescing behavior of the polyurethane foam. Except for the local area damaged by the puncture impact 40 inches above the bottom of the OCA body and in the OCA lid, a layer of unburned polyurethane foam remained around the entire OCV. The average thickness of the layer was approximately 5 to 6 inches along the cylindrical sides and bottom, and 10 inches on top.

Demonstration of containment vessel leaktightness was accomplished by performing helium mass spectrometer leakage rate testing on each containment vessel's main O-ring seal, vent port O-ring seal, and metallic boundary. The main and vent port O-ring seals were tested when cooled to an average measured temperature below -20 ºF; the metallic boundary was tested at

ambient temperature. Results of successful mass spectrometer helium leakage rate testing for all components of each containment boundary, except the ICV main O-ring seal, are summarized in the following table:

Sealing Component	OCV	ICV
Main O-ring Seal	4.5×10^{-8} cc/s, helium	- - -
Vent Port Plug O-ring Seal	$<2.0 \times 10^{-8}$ cc/s, helium	$<2.0 \times 10^{-8}$ cc/s, helium
Metallic Boundary	6.0×10^{-8} cc/s, helium	$<2.0 \times 10^{-8}$ cc/s, helium

Subsequent testing of the main ICV non-containment O-ring seal showed it to be leaktight. When accounting for the conversion between air leakage (per ANSI N14.5) and helium leakage, a 2.6 factor applies for standard temperatures and pressures. Thus, a reported helium leakage rate of 1.3×10^{-7} cc/s, helium, is equivalently 5×10^{-8} cc/s, air, a magnitude well below the "leaktight" criterion of 1×10^{-7} cc/s, air, per ANSI N14.5.

2.10.3.7.3 Test Results for CTU-3

2.10.3.7.3.1 CTU-3 Free Drop No. 1

Free Drop No. 1 was a HAC free drop from a height of 30 feet. The primary impact for this slapdown drop occurred onto the OCA lid knuckle, with the secondary impact onto the OCA body's bottom edge, approximately midway between tie-down lugs. As shown in Figure 2.10.3-6, CTU-3 was oriented -20º from horizontal (axial angle (i.e., pitch) = 20º top down), and circumferentially aligned to impact the ICV and OCV locking ring pinned joints and coincident payload drums to produce maximum damage (-5º from the forklift pocket reference). At the time of the test, the measured OCV temperature was -26 ºF. The test was conducted on 04/19/89.

The measured permanent deformations for CTU-3 were flats 48 inches wide at the top (OCA lid), and 23 inches wide at the bottom (OCA body). The ICV and OCV internal pressures did not change.

2.10.3.7.3.2 CTU-3 Free Drop No. 2

Free Drop No. 2 was a HAC free drop from a height of 30 feet, impacting vertically onto the CTU bottom, as shown in Figure 2.10.3-6. At the time of the test, the measured OCV temperature was -22 ºF. The test was conducted on 04/19/89.

The permanent deformation for CTU-3 was negligible. The ICV internal pressure did not change; however, the OCV internal pressure dropped 0.5 psig. The maximum axial acceleration was 335 *g*s (filtered at 500 Hz; see Figure 2.10.3-22 and Figure 2.10.3-23).

2.10.3.7.3.3 CTU-3 Free Drop No. 3

Free Drop No. 3 was a HAC free drop from a height of 30 feet. The primary impact for this slapdown drop occurred onto a tie-down lug, with the secondary impact onto the OCA lid. As shown in Figure 2.10.3-6, CTU-3 was oriented 18º from horizontal (axial angle (i.e., pitch) = 18º

top up), and circumferentially aligned with the tie-down lug (143º from the forklift pocket reference). The test was conducted on 04/19/89.

The measured permanent deformations for CTU-3 were flats 13 inches wide at the top (OCA lid), and 40 inches wide at the bottom (OCA body). The ICV internal pressure did not change; however, the OCV internal pressure dropped 1.0 psig.

2.10.3.7.3.4 CTU-3 Puncture Drop No. 4

Puncture Drop No. 4 was a HAC puncture drop from a height of 40 inches, impacting onto the OCA body at the 1/4-to-3/8 inch thickness outer shell transition. As shown in Figure 2.10.3-6, CTU-3 was oriented -42º from horizontal (axial angle (i.e., pitch) = 42º top down) through the package's center of gravity, and circumferentially aligned with the tie-down lug (143º from the forklift pocket reference). The test was conducted on 04/19/89.

The measured permanent deformation for CTU-3 was an 8 inch wide, 10 inch long, and 8 inch deep hole through the OCA outer shell. The ICV internal pressure did not change; however, the OCV internal pressure dropped 0.5 psig.

2.10.3.7.3.5 CTU-3 Puncture Drop No. 5

Puncture Drop No. 5 was a HAC puncture drop from a height of 40 inches, impacting onto the OCA bottom edge, adjacent to a forklift pocket. As shown in Figure 2.10.3-6, CTU-3 was oriented 55º from horizontal (axial angle (i.e., pitch) = 55º top up) through the package's center of gravity, and circumferentially -110º from the forklift pocket reference. The test was conducted on 04/20/89.

The measured permanent deformation for CTU-3 was a hole approximately 8 inches deep. The ICV and OCV internal pressures did not change.

2.10.3.7.3.6 CTU-3 Puncture Drop No. 6

Puncture Drop No. 6 was a HAC puncture drop from a height of 40 inches, impacting glancingly onto the OCA lid adjacent to the outer thermal shield. As shown in Figure 2.10.3-6, CTU-3 was oriented -67º from horizontal (axial angle (i.e., pitch) = 67º top down), and circumferentially -67º from the forklift pocket reference. The test was conducted on 04/21/89.

The measured permanent deformation for CTU-3 was a dent approximately 2 inches deep. The ICV and OCV internal pressures did not change.

2.10.3.7.3.7 CTU-3 Puncture Drop No. 7

Puncture Drop No. 7 was a HAC puncture drop from a height of 40 inches, impacting onto the OCA body at the closure joint. As shown in Figure 2.10.3-6, CTU-3 was oriented -15º from horizontal (axial angle (i.e., pitch) = 15º top down) through the package's center of gravity, and circumferentially 110º from the forklift pocket reference. The test was conducted on 04/21/89.

The measured permanent deformation for CTU-3 was a 4 inch deep dent. The ICV and OCV internal pressures did not change.

2.10.3.7.3.8 CTU-3 Puncture Drop No. 8

Puncture Drop No. 8 was a HAC puncture drop from a height of 40 inches, impacting onto the OCA lid at the closure joint. As shown in Figure 2.10.3-6, CTU-3 was oriented -22º from horizontal (axial angle (i.e., pitch) = 22º top down) through the package's center of gravity, and circumferentially -145º from the forklift pocket reference. The test was conducted on 04/21/89.

The measured permanent deformation for CTU-3 was a 4 inch deep dent. The ICV and OCV internal pressures did not change.

2.10.3.7.3.9 CTU-3 Testing Anomalies

As can be expected with any test program, a certain number of test related anomalies occurred during CTU-3 testing. The following paragraphs summarize each anomaly and its significance.

- Pressure rise leak testing of the OCV was planned between each free drop and puncture test; shifting of the OCV relative to the seal leak test port and expediting testing were the reasons that pressure rise leak testing was not always performed.
- One of the four OCV seal region thermocouples failed early in testing; reported temperatures are the average of the remaining three thermocouples.
- Pressure drops in the OCV were noted for Free Drop Nos. 2 and 3, and Puncture Drop No. 4; a momentary increase in pressure occurred at the moment of CTU impact, followed by a reduction below the original value, was most likely due to the gauge "sticking" because of the pressure pulse.
- Because the ICV main O-ring seal could not be made to pass the post-test helium leakage rate test for CTU-2, a wiper O-ring seal was added to the ICV design for CTU-3 to prevent debris from contaminating the main O-ring seal for all temperature and moisture ranges. The wiper O-ring seal holder was fabricated from rolled sheet and attached via 114 drive screws. Of the 114 original drive screws, 16 were damaged (sheared head); nevertheless, the seal holder remained in position and prevented debris from contaminating the main O-ring seal.

2.10.3.7.3.10 CTU-3 Post-Test Disassembly

Post-test disassembly of CTU-3 was performed following Puncture Drop No. 8. Both abrasive cutting and gas plasma cutting methods were utilized, depending on their potential effect on subsequent post-test seal testing, to enable destructive disassembly of CTU-3.

Demonstration of containment vessel leaktightness was accomplished by performing helium mass spectrometer leakage rate testing on each containment vessel's main O-ring seal, vent port O-ring seal, and metallic boundary. The ICV main and ICV vent port O-ring seals were tested when cooled to an average measured temperature below -20 ºF; the metallic boundary was tested at ambient temperature. The OCV main and OCV vent port O-ring seals, and metallic boundary were tested at ambient temperature. Results of successful mass spectrometer helium leakage rate testing are summarized in the following table:

Sealing Component	OCV	ICV
Main O-ring Seal	$<2.0 \times 10^{-8}$ cc/s, helium	$<2.0 \times 10^{-8}$ cc/s, helium
Vent Port Plug O-ring Seal	$<2.0 \times 10^{-8}$ cc/s, helium	$<2.0 \times 10^{-8}$ cc/s, helium
Metallic Boundary	$<2.0 \times 10^{-8}$ cc/s, helium	$<9.2 \times 10^{-8}$ cc/s, helium

When accounting for the conversion between air leakage (per ANSI N14.5) and helium leakage, a 2.6 factor applies for standard temperatures and pressures. Thus, a reported helium leakage rate of 1.3×10^{-7} cc/s, helium, is equivalently 5×10^{-8} cc/s, air, a magnitude well below the "leaktight" criterion of 1×10^{-7} cc/s, air, per ANSI N14.5.

In conclusion, the test series performed on CTU-3 demonstrates the TRUPACT-II package's ability to meet the normal conditions of transport and hypothetical accident conditions regulatory requirements as defined in 10 CFR §71.71 and §71.73, respectively, and demonstrates that the wiper O-ring seal retrofit prevents debris from contaminating the ICV main O-ring seal.

Table 2.10.3-1 – Summary of CTU-1 Test Results in Sequential Order

Test No.	Test Description	Test Unit Angular Orientation		Pressure (psig)		CTU Temperature	Observations and Results
		Axial①	Circumferential②	ICV	OCV		
1	NCT, 3-foot side drop onto OCV vent port	0º	110º	50	50	Ambient	18" wide flat at top (OCA lid) × 18" wide flat at bottom (OCA body) × ~7/8" deep
2	HAC, 30-foot side drop onto OCV vent port	0º	110º	50	0	Ambient	37" wide flat at top (OCA lid) × 35" wide flat at bottom (OCA body) × ~3⅝" deep
3	HAC, 30-foot CG onto OCA lid knuckle near OCA lid lift pocket	-47º	-100º	50	50	Ambient	30" wide × 53" long flat at top (OCA lid) × ~3¾" deep
4	HAC, 30-foot top drop	-90º	N/A	50	50	Ambient	53" diameter flat at top (OCA lid) × ~3⅞" deep
5	HAC, puncture drop on OCA vent port fitting	-15º	110º	50	50	Ambient	16" long tear at shell-to-angle interface on OCA body at vent port × ~3" deep
6	HAC, puncture drop onto OCA body below 1/4-to-3/8 shell weld	-3º	110º	50	50	Ambient	~3/4" deep dent
7	HAC, puncture drop 40 inches above package bottom	28º	110º	50	0	Ambient	8" wide × 11" long × ~8½" deep hole through OCA outer shell; CTU-1 may have hit ground; repeated as CTU-2, Test No. R
8	HAC, puncture drop onto damaged OCA lid knuckle	-54º	110º	50	0	Ambient	Some additional denting; no penetration
9	HAC, puncture drop on OCA seal test port fitting	-24º	20º	50	50	Ambient	~3" deep dent; ~7" wide tear of outer thermal shield
10	HAC, fire test	0º	145º	50	50	At HAC pre-fire temperature	~32 minute fire; maximum 170 ºF and 260 ºF ICV and OCV seal flange temperature, and maximum 1.9 psig and 1.4 psig ICV and OCV pressure rise, respectively

Notes:

① Axial angle, θ, is relative to horizontal (i.e., side drop orientation).

② Circumferential angle, ϕ, is relative to the forklift pockets when parallel to the ground.

Table 2.10.3-2 – Summary of CTU-2 Test Results in Sequential Order

Test No.	Test Description	Test Unit Angular Orientation		Pressure (psig)		CTU Temperature	Observations and Results
		Axial①	Circumferential②	ICV	OCV		
1	HAC, 30-foot top slapdown drop; initial impact on OCA lid knuckle	-20º	-5º	33	0	-20 ºF	45" wide flat at top (OCA lid) × 21" wide flat at bottom (OCA body)
2	HAC, 30-foot bottom drop	90º	N/A	33	33	-20 ºF	negligible visible damage
3	HAC, 30-foot slapdown drop; initial impact on tie-down lug	18º	143º	50	50	Ambient	15" wide flat at top (OCA lid) × 45" wide flat at bottom (OCA body)
R	HAC, puncture drop 40 inches above package bottom	23º	143º	50	0	Ambient	10" wide × 11" long hole; ~9" deep hole; minor denting of OCV and ICV shells
4	HAC, puncture drop at the 1/4-to-3/8 lid shell interface	-42º	143º	50	50	Ambient	8" wide × 10" long hole; ~7" deep hole
5	HAC, puncture drop onto package bottom adjacent to forklift pocket	55º	-110º	50	0	Ambient	~5" deep dent
6	HAC, puncture drop onto outer thermal shield	-67º	-67º	0	0	Ambient	~24” long × ~1" deep dent
7	HAC, puncture drop onto OCA body at closure; 40º from OCA vent port fitting	-15º	110º	50	50	Ambient	3" long tear at shell-to-angle interface on OCA body × ~4" deep dent
8	HAC, puncture drop onto OCA lid at closure; 180º from OCA seal test port fitting	-22º	-145º	50	50	Ambient	~4" deep dent
9	HAC, fire test	0º	200º	50	50	At HAC pre-fire temperature	~31 minute fire; maximum 200 ºF and 250 ºF ICV and OCV seal flange temperature, and maximum 2.7 psig and 4.5 psig ICV and OCV pressure rise, respectively

Notes:

① Axial angle, θ, is relative to horizontal (i.e., side drop orientation).

② Circumferential angle, ϕ, is relative to the forklift pockets when parallel to the ground.

Table 2.10.3-3 – Summary of CTU-3 Test Results in Sequential Order

Test No.	Test Description	Test Unit Angular Orientation		Pressure (psig)		CTU Temperature	Observations and Results
		Axial①	Circumferential②	ICV	OCV		
1	HAC, 30-foot top slapdown drop; initial impact on OCA lid knuckle	-20º	-5º	33	0	-20 ºF	48" wide flat at top (OCA lid) × 23" wide flat at bottom (OCA body)
2	HAC, 30-foot bottom drop	90º	N/A	33	33	-20 ºF	negligible visible damage
3	HAC, 30-foot slapdown drop; initial impact on tie-down lug	18º	143º	50	50	Ambient	13" wide flat at top (OCA lid) × 40" wide flat at bottom (OCA body)
4	HAC, puncture drop at the 1/4-to-3/8 lid shell interface	-42º	143º	50	50	Ambient	8" wide × 10" long hole; ~8" deep hole
5	HAC, puncture drop onto package bottom adjacent to forklift pocket	55º	-110º	50	0	Ambient	~8" deep hole
6	HAC, puncture drop onto outer thermal shield	-67º	-67º	0	0	Ambient	~2" deep dent
7	HAC, puncture drop onto OCA body at closure; 40º from OCA vent port fitting	-15º	110º	50	50	Ambient	~4" deep dent
8	HAC, puncture drop onto OCA lid at closure; 180º from OCA seal test port fitting	-22º	-145º	50	50	Ambient	~4" deep dent

Notes:

① Axial angle, θ, is relative to horizontal (i.e., side drop orientation).

② Circumferential angle, ϕ, is relative to the forklift pockets when parallel to the ground.

This page intentionally left blank.

Table 2.10.3-4 – CTU-1 Temperature Indicating Label Locations and Results

Label Identifier	Location		Indicated Temperature	Remarks
	Y (in)	C (deg)		
TI-1	0.0	0.0	160 ºF	Payload pallet; top center
TI-2	19.0	85.0	130 ºF	Drum #1; side toward payload center
TI-3	19.0	12.0	140 ºF	Drum #4 (bottom center drum); side
TI-4	34.0	0.0	130 ºF	Drum #4 (bottom center drum); top center
TI-5	53.0	85.0	130 ºF	Drum #8; side toward payload center
TI-6	53.0	12.0	130 ºF	Drum #11 (top center drum); side
TI-7	69.0	0.0	130 ºF	Drum #11 (top center drum); top
TI-8	62.0	49.0	150 ºF	ICV body; inner lower seal flange surface
TI-9	62.0	13.5	170 ºF	ICV body; inner lower seal flange surface
TI-10	62.0	205.0	170 ºF	ICV body; inner lower seal flange surface
TI-11	62.0	166.0	150 ºF	ICV body; inner lower seal flange surface
TI-12	62.0	128.0	140 ºF	ICV body; inner lower seal flange surface
TI-13	62.0	88.5	150 ºF	ICV body; inner lower seal flange surface
TI-14	29.5	49.0	160 ºF	ICV body; inner shell surface
TI-15	29.5	13.5	170 ºF	ICV body; inner shell surface
TI-16	29.5	205.0	160 ºF	ICV body; inner shell surface
TI-17	29.5	166.0	140 ºF	ICV body; inner shell surface
TI-18	29.5	128.0	140 ºF	ICV body; inner shell surface
TI-19	29.5	88.5	160 ºF	ICV body; inner shell surface
TI-20	1.5	49.0	150 ºF	ICV body; shell-to-lower torispherical head weld
TI-21	1.5	13.5	170 ºF	ICV body; shell-to-lower torispherical head weld
TI-22	1.5	205.0	190 ºF	ICV body; shell-to-lower torispherical head weld
TI-23	1.5	166.0	140 ºF	ICV body; shell-to-lower torispherical head weld
TI-24	1.5	128.0	150 ºF	ICV body; shell-to-lower torispherical head weld
TI-25	1.5	88.5	180 ºF	ICV body; shell-to-lower torispherical head weld
TI-26	Bottom Center		270 ºF	ICV body; lower torispherical head
TI-27	1.5	90.0	160 ºF	ICV lid; shell-to-upper torispherical head weld
TI-28	1.5	210.0	160 ºF	ICV lid; shell-to-upper torispherical head weld
TI-29	1.5	330.0	130 ºF	ICV lid; shell-to-upper torispherical head weld
TI-30	Top Center		150 ºF	ICV lid; upper torispherical head
TI-31	Near TI-29		140 ºF	Upper aluminum honeycomb spacer; lower face
TI-32	57.5	30.0	220 ºF	OCV body; inner lower seal flange surface
TI-33	57.5	64.0	230 ºF	OCV body; inner lower seal flange surface
TI-34	57.5	74.0	250 ºF	OCV body; inner lower seal flange surface
TI-35	57.5	101.0	220 ºF	OCV body; inner lower seal flange surface
TI-36	57.5	138.0	190 ºF	OCV body; inner lower seal flange surface
TI-37	57.5	183.0	190 ºF	OCV body; inner lower seal flange surface
TI-38	57.5	201.0	210 ºF	OCV body; inner lower seal flange surface

Label Identifier	Location		Indicated Temperature	Remarks
	Y (in)	C (deg)		
TI-39	57.5	236.0	200 ºF	OCV body; inner lower seal flange surface
TI-40	50.5	30.0	190 ºF	OCV body; inner conical shell surface
TI-41	50.5	74.0	240 ºF	OCV body; inner conical shell surface
TI-42	50.5	101.0	180 ºF	OCV body; inner conical shell surface
TI-43	50.5	138.0	160 ºF	OCV body; inner conical shell surface
TI-44	50.5	183.0	170 ºF	OCV body; inner conical shell surface
TI-45	50.5	201.0	170 ºF	OCV body; inner conical shell surface
TI-46	50.5	236.0	170 ºF	OCV body; inner conical shell surface
TI-47	26.5	30.0	310 ºF	OCV body; inner shell surface near stiffening ring
TI-48	26.5	74.0	340 ºF	OCV body; inner shell surface near stiffening ring
TI-49	26.5	101.0	290 ºF	OCV body; inner shell surface near stiffening ring
TI-50	26.5	138.0	220 ºF	OCV body; inner shell surface near stiffening ring
TI-51	26.5	183.0	170 ºF	OCV body; inner shell surface near stiffening ring
TI-52	26.5	201.0	160 ºF	OCV body; inner shell surface near stiffening ring
TI-53	26.5	236.0	170 ºF	OCV body; inner shell surface near stiffening ring
TI-54	1.5	30.0	160 ºF	OCV body; shell-to-lower torispherical head weld
TI-55	1.5	74.0	340 ºF	OCV body; shell-to-lower torispherical head weld
TI-56	1.5	101.0	270 ºF	OCV body; shell-to-lower torispherical head weld
TI-57	1.5	138.0	170 ºF	OCV body; shell-to-lower torispherical head weld
TI-58	1.5	183.0	150 ºF	OCV body; shell-to-lower torispherical head weld
TI-59	1.5	201.0	170 ºF	OCV body; shell-to-lower torispherical head weld
TI-60	1.5	236.0	200 ºF	OCV body; shell-to-lower torispherical head weld
TI-61	-16.6	30.0	210 ºF	OCV body; lower torispherical head
TI-62	-16.6	74.0	200 ºF	OCV body; lower torispherical head
TI-63	-16.6	160.0	200 ºF	OCV body; lower torispherical head
TI-64	-16.6	201.0	230 ºF	OCV body; lower torispherical head
TI-65	1.0	90.5	220 ºF	OCV lid; shell-to-upper torispherical head weld
TI-66	1.0	131.5	220 ºF	OCV lid; shell-to-upper torispherical head weld
TI-67	1.0	171.5	230 ºF	OCV lid; shell-to-upper torispherical head weld
TI-68	1.0	211.5	190 ºF	OCV lid; shell-to-upper torispherical head weld
TI-69	1.0	251.5	200 ºF	OCV lid; shell-to-upper torispherical head weld
TI-70	1.0	291.5	210 ºF	OCV lid; shell-to-upper torispherical head weld
TI-71	18.0	90.5	160 ºF	OCV lid; upper torispherical head
TI-72	18.0	131.5	260 ºF	OCV lid; upper torispherical head
TI-73	18.0	171.5	300 ºF	OCV lid; upper torispherical head
TI-74	18.0	211.5	170 ºF	OCV lid; upper torispherical head
TI-75	18.0	251.5	340 ºF	OCV lid; upper torispherical head
TI-76	18.0	291.5	170 ºF	OCV lid; upper torispherical head
TI-77	Top Center		Damaged	OCV lid; upper torispherical head

Table 2.10.3-5 – CTU-2 Temperature Indicating Label Locations and Results

Label Identifier	Location		Indicated Temperature	Remarks
	Y (in)	C (deg)		
TI-1	Top Center		160 ºF	Payload pallet; top center
TI-2	19.0	27.0	140 ºF	Drum #1 (bottom center drum); side
TI-3	19.0	210.0	150 ºF	Drum #3; side
TI-4	Top Center		150 ºF	Drum #1 (bottom center drum); top center
TI-5	19.0	180.0	Damaged	Drum #3; side (outside edge of payload)
TI-6	19.0	250.0	150 ºF	Drum #5; side (outside edge of payload)
TI-7	19.0	120.0	170 ºF	Drum #7; side (outside edge of payload)
TI-8	54.0	90.0	160 ºF	Drum #8 (top center drum); side
TI-9	Top Center		150 ºF	Drum #8 (top center drum); top center
TI-10	56.0	120.0	150 ºF	Drum #10; side (outside edge of payload)
TI-11	6.0	0.0	Damaged	OCV lid; shell surface
TI-12	6.0	90.0	200 ºF	OCV lid; shell surface
TI-13	6.0	180.0	170 ºF	OCV lid; shell surface
TI-14	6.0	270.0	190 ºF	OCV lid; shell surface
TI-15	25.0	0.0	340 ºF	OCV lid; upper torispherical head
TI-16	25.0	90.0	250 ºF	OCV lid; upper torispherical head
TI-17	25.0	180.0	170 ºF	OCV lid; upper torispherical head
TI-18	25.0	270.0	220 ºF	OCV lid; upper torispherical head
TI-19	18.0	143.0	270 ºF	OCV lid; upper torispherical head
TI-20	Top Center		290 ºF	OCV lid; upper torispherical head
TI-21	6.0	135.0	220 ºF	OCV lid; upper torispherical head
TI-22	6.0	225.0	280 ºF	OCV lid; upper torispherical head
TI-23	57.0	0.0	250 ºF	OCV body; inner lower seal flange surface
TI-24	57.0	90.0	220 ºF	OCV body; inner lower seal flange surface
TI-25	57.0	180.0	220 ºF	OCV body; inner lower seal flange surface
TI-26	57.0	215.0	230 ºF	OCV body; inner lower seal flange surface
TI-27	57.0	270.0	200 ºF	OCV body; inner lower seal flange surface
TI-28	49.0	0.0	220 ºF	OCV body; inner conical shell surface
TI-29	49.0	90.0	190 ºF	OCV body; inner conical shell surface
TI-30	49.0	180.0	210 ºF	OCV body; inner conical shell surface
TI-31	49.0	215.0	170 ºF	OCV body; inner conical shell surface
TI-32	49.0	270.0	170 ºF	OCV body; inner conical shell surface
TI-33	26.0	0.0	Damaged	OCV body; inner shell surface near stiffening ring
TI-34	26.0	90.0	170 ºF	OCV body; inner shell surface near stiffening ring
TI-35	26.0	180.0	190 ºF	OCV body; inner shell surface near stiffening ring
TI-36	26.0	270.0	170 ºF	OCV body; inner shell surface near stiffening ring
TI-37	1.0	0.0	Damaged	OCV body; shell-to-lower torispherical head weld
TI-38	1.0	90.0	Damaged	OCV body; shell-to-lower torispherical head weld
TI-39	1.0	135.0	220 ºF	OCV body; shell-to-lower torispherical head weld

Label Identifier	Location		Indicated Temperature	Remarks
	Y (in)	C (deg)		
TI-40	1.0	180.0	Damaged	OCV body; shell-to-lower torispherical head weld
TI-41	1.0	225.0	190 ºF	OCV body; shell-to-lower torispherical head weld
TI-42	1.0	270.0	Damaged	OCV body; shell-to-lower torispherical head weld
TI-43	-18.0	0.0	350 ºF	OCV body; lower torispherical head
TI-44	-18.0	90.0	250 ºF	OCV body; lower torispherical head
TI-45	-18.0	180.0	250 ºF	OCV body; lower torispherical head
TI-46	-11.0	250.0	250 ºF	OCV body; lower torispherical head
TI-47	-18.0	270.0	260 ºF	OCV body; lower torispherical head
TI-48	66.5	0.0	200 ºF	ICV body; inner lower seal flange surface
TI-49	Seal Test Port		170 ºF	ICV body; inner lower seal flange surface
TI-50	Vent Port		170 ºF	ICV body; inner lower seal flange surface
TI-51	66.5	270.0	170 ºF	ICV body; inner lower seal flange surface
TI-52	66.5	180.0	170 ºF	ICV body; inner lower seal flange surface
TI-53	66.5	90.0	180 ºF	ICV body; inner lower seal flange surface
TI-54	45.5	0.0	200 ºF	ICV body; inner shell surface
TI-55	45.5	90.0	170 ºF	ICV body; inner shell surface
TI-56	45.5	180.0	Damaged	ICV body; inner shell surface
TI-57	45.5	270.0	160 ºF	ICV body; inner shell surface
TI-58	-14.5	270.0	190 ºF	ICV body; lower torispherical head
TI-59	21.5	0.0	210 ºF	ICV body; inner shell surface
TI-60	21.5	90.0	170 ºF	ICV body; inner shell surface
TI-61	21.5	180.0	180 ºF	ICV body; inner shell surface
TI-62	21.5	270.0	160 ºF	ICV body; inner shell surface
TI-63	3.5	0.0	220 ºF	ICV body; shell-to-lower torispherical head weld
TI-64	3.5	90.0	170 ºF	ICV body; shell-to-lower torispherical head weld
TI-65	3.5	180.0	Damaged	ICV body; shell-to-lower torispherical head weld
TI-66	3.5	270.0	180 ºF	ICV body; shell-to-lower torispherical head weld
TI-67	-14.5	0.0	Damaged	ICV body; lower torispherical head
TI-68	-14.5	90.0	200 ºF	ICV body; lower torispherical head
TI-69	-14.5	180.0	190 ºF	ICV body; lower torispherical head
TI-70	Near Test Ports		250 ºF	ICV body; lower torispherical head
TI-71	4.0	0.0	200 ºF	ICV lid; shell-to-upper torispherical head weld
TI-72	4.0	90.0	Damaged	ICV lid; shell-to-upper torispherical head weld
TI-73	4.0	180.0	210 ºF	ICV lid; shell-to-upper torispherical head weld
TI-74	4.0	270.0	180 ºF	ICV lid; shell-to-upper torispherical head weld
TI-75	24.0	0.0	190 ºF	ICV lid; upper torispherical head
TI-76	24.0	90.0	170 ºF	ICV lid; upper torispherical head
TI-77	24.0	180.0	200 ºF	ICV lid; upper torispherical head
TI-78	24.0	270.0	190 ºF	ICV lid; upper torispherical head
TI-79	N/A	120.0	180 ºF	ICV lid; inner lift pocket surface
TI-80	N/A	240.0	190 ºF	ICV lid; inner lift pocket surface

Figure Withheld Under 10 CFR 2.390

Figure 2.10.3-1 – Drop Pad at the Coyote Canyon Aerial Cable Facility

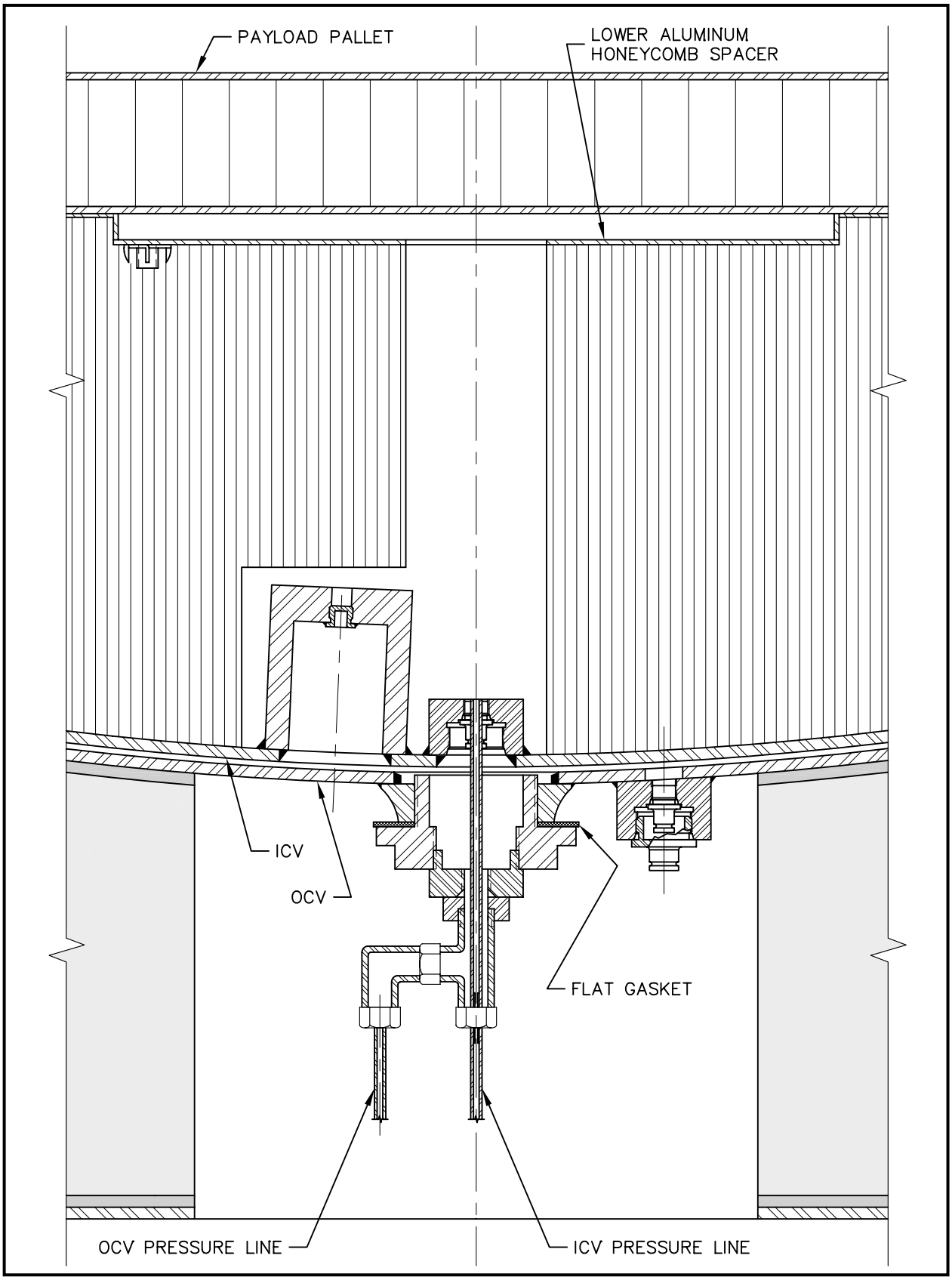

Figure 2.10.3-2 – CTU OCV and ICV Pressurization Port Detail

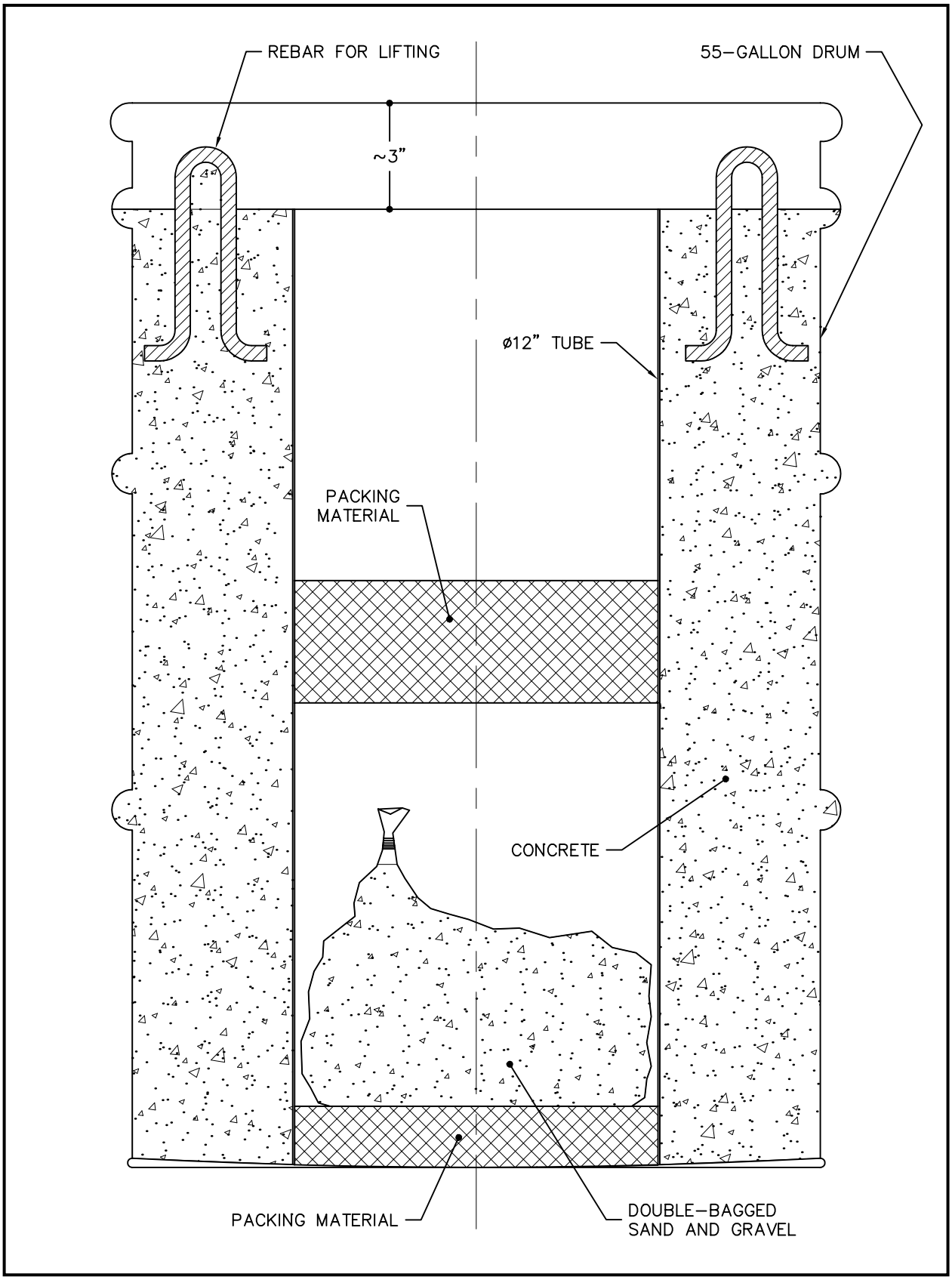

Figure 2.10.3-3 – CTU Payload Representation (Concrete-Filled 55-Gallon Drums)

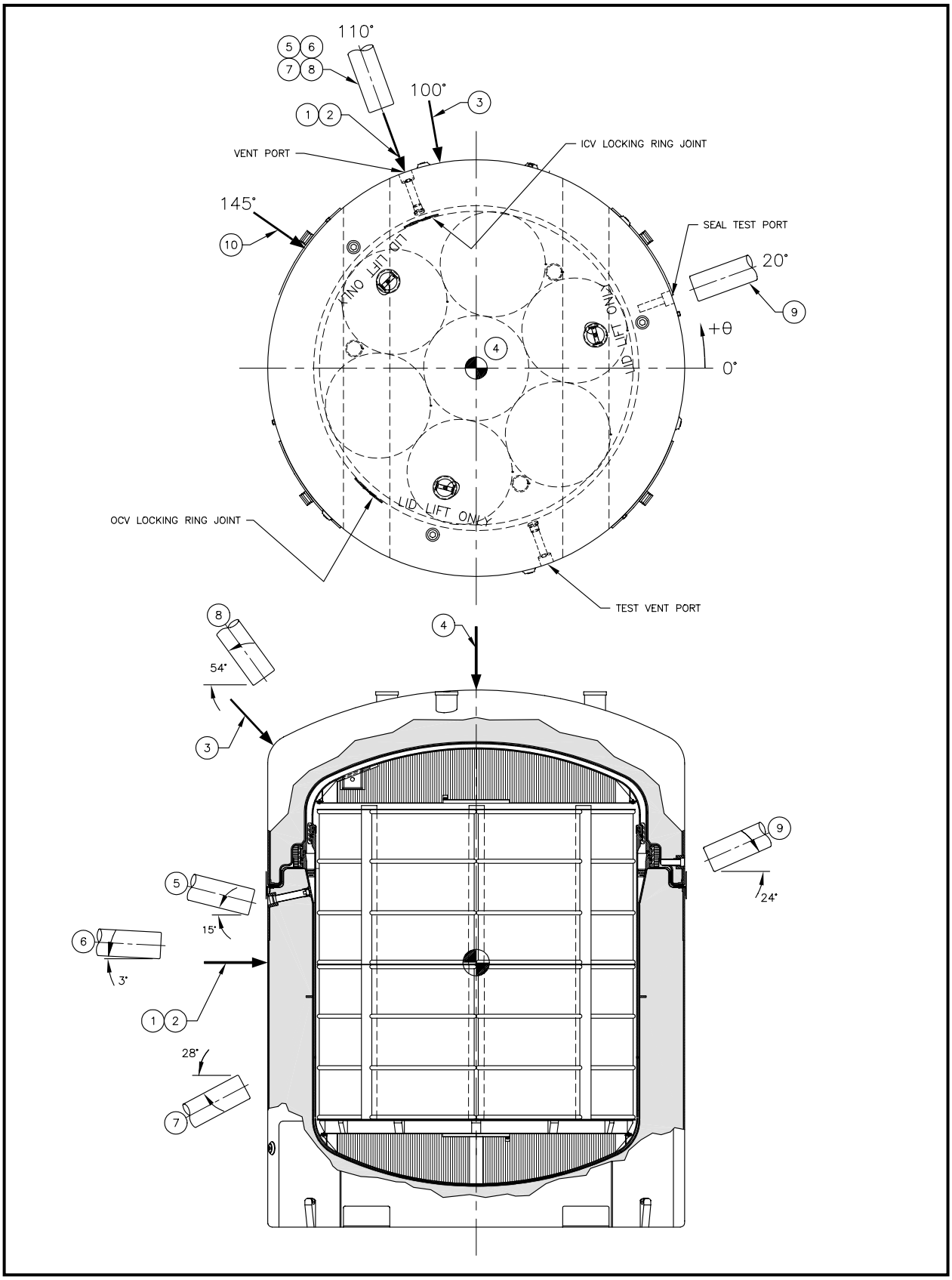

Figure 2.10.3-4 – Schematic of the CTU-1 Test Orientations

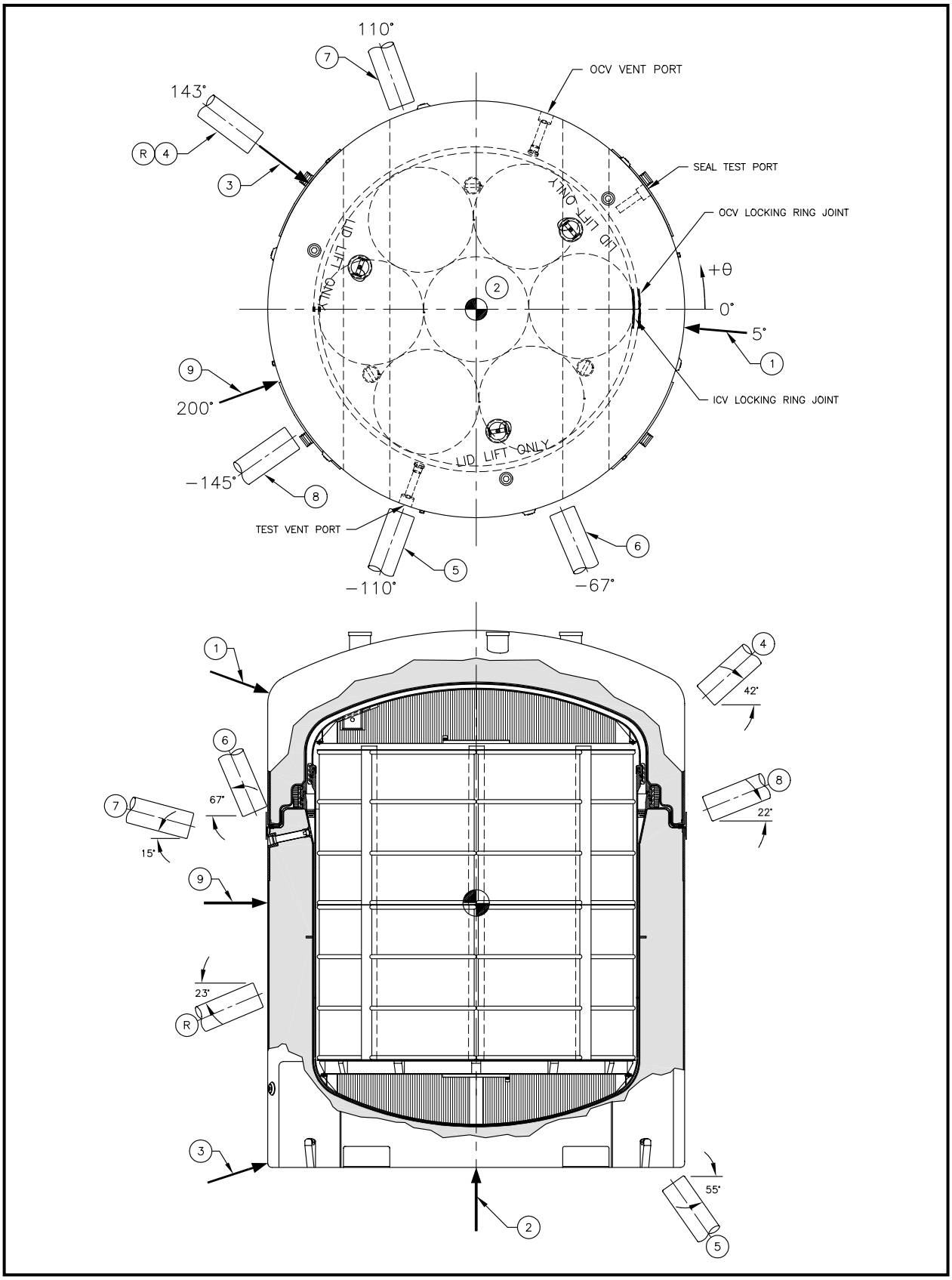

Figure 2.10.3-5 – Schematic of the CTU-2 Test Orientations

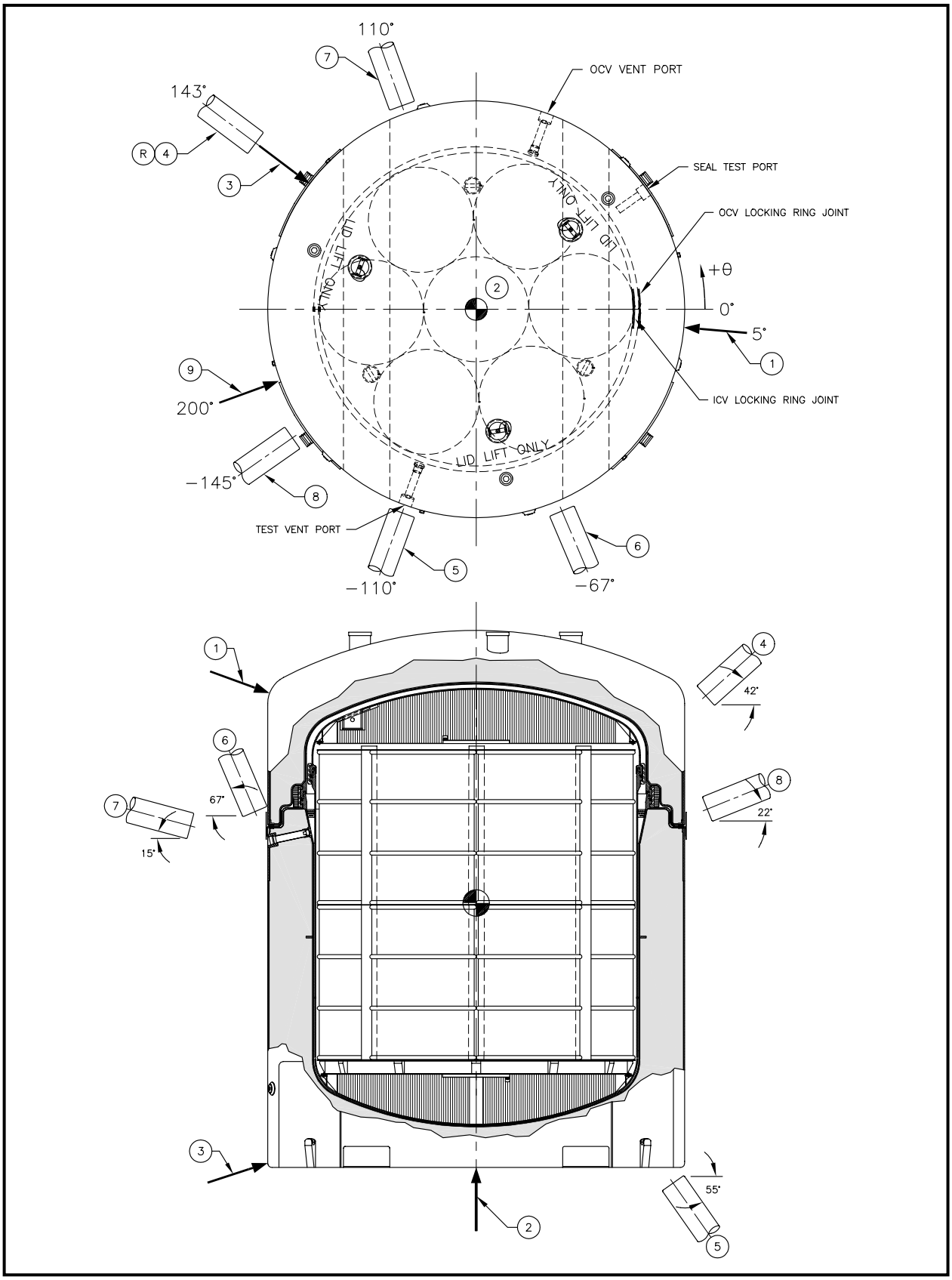

Figure 2.10.3-6 – Schematic of the CTU-3 Test Orientations

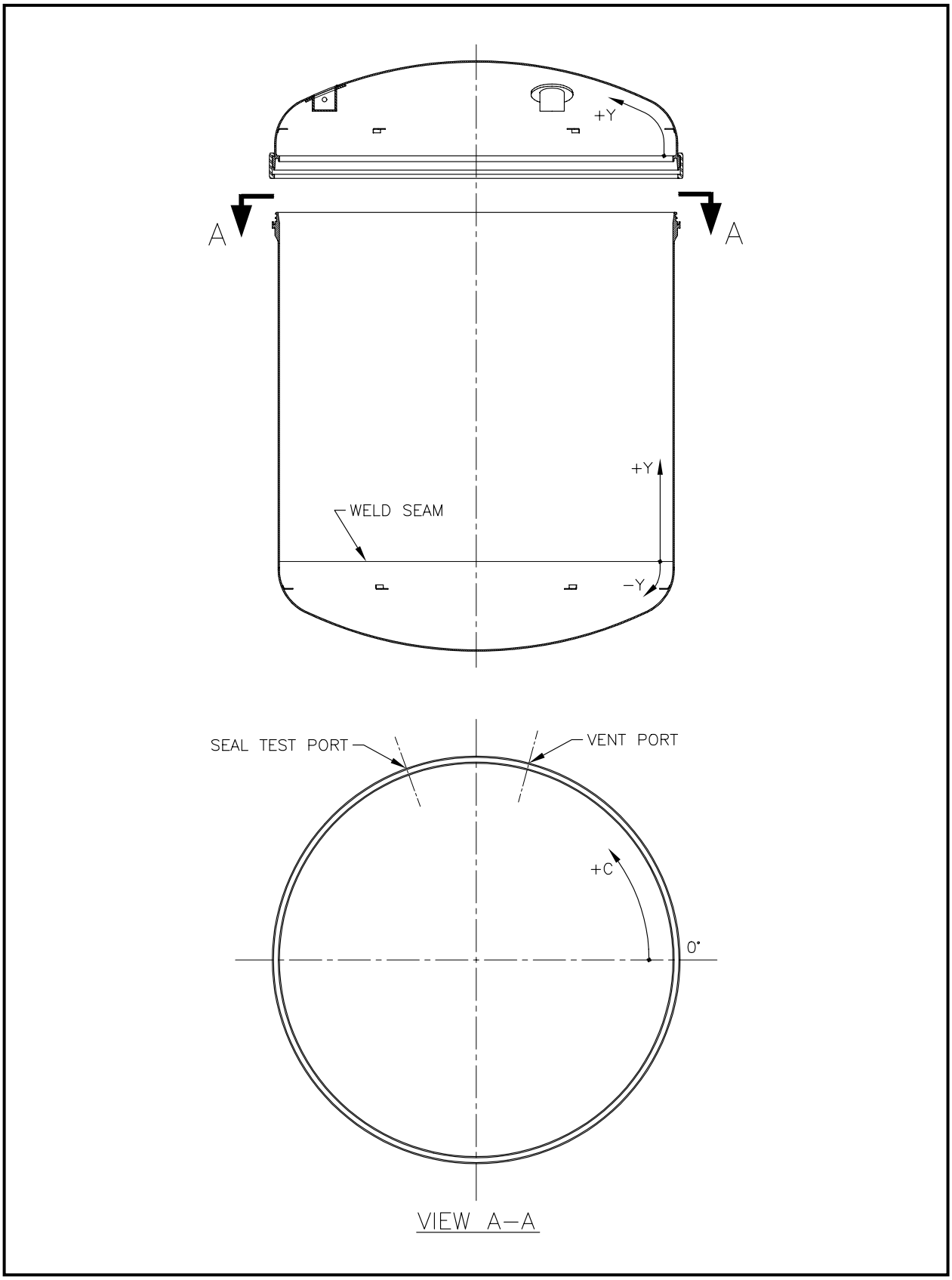

Figure 2.10.3-7 – CTU-1 and CTU-2 ICV Temperature Indicating Label Locations

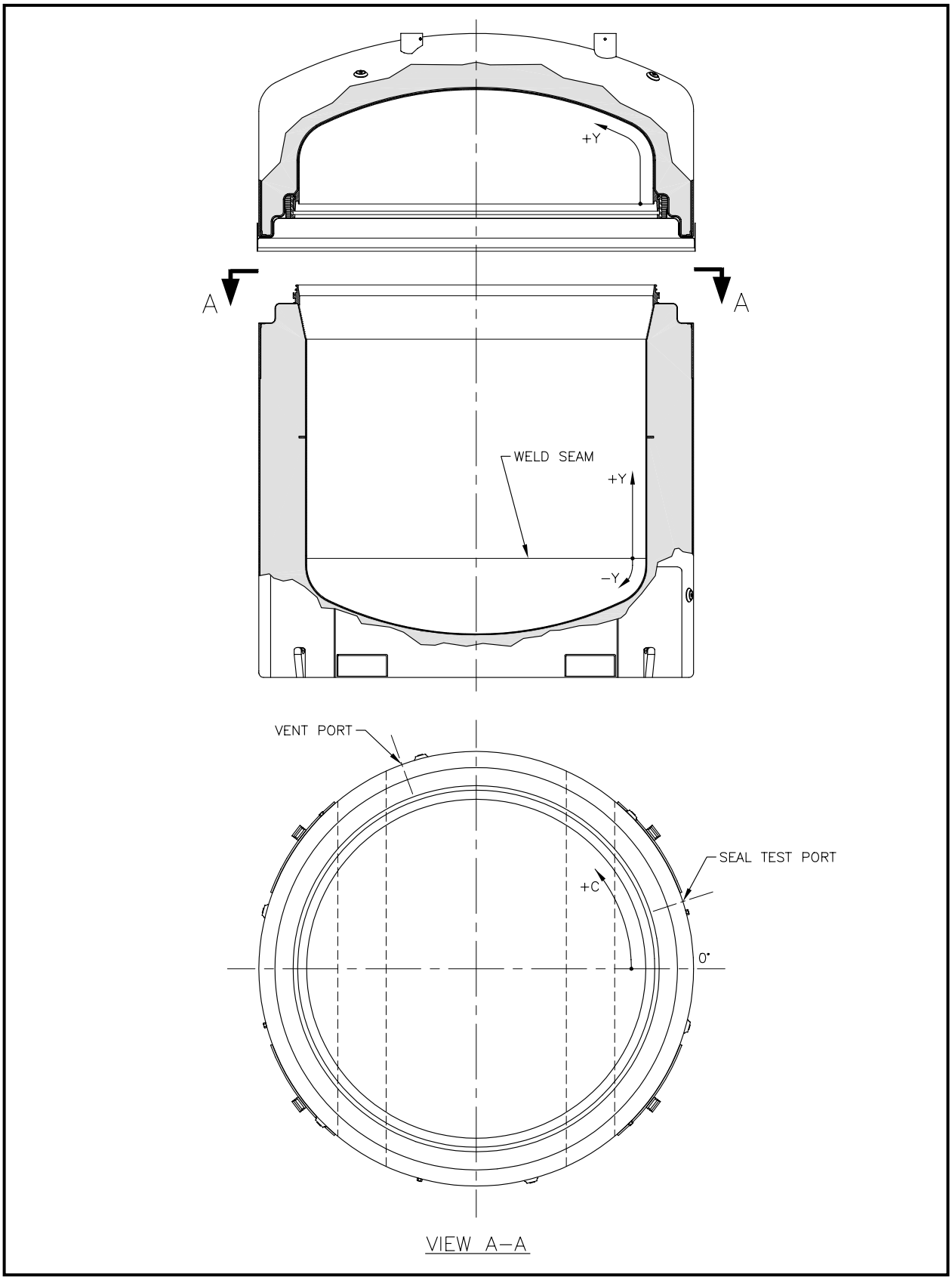

Figure 2.10.3-8 – CTU-1 OCV Temperature Indicating Label Locations

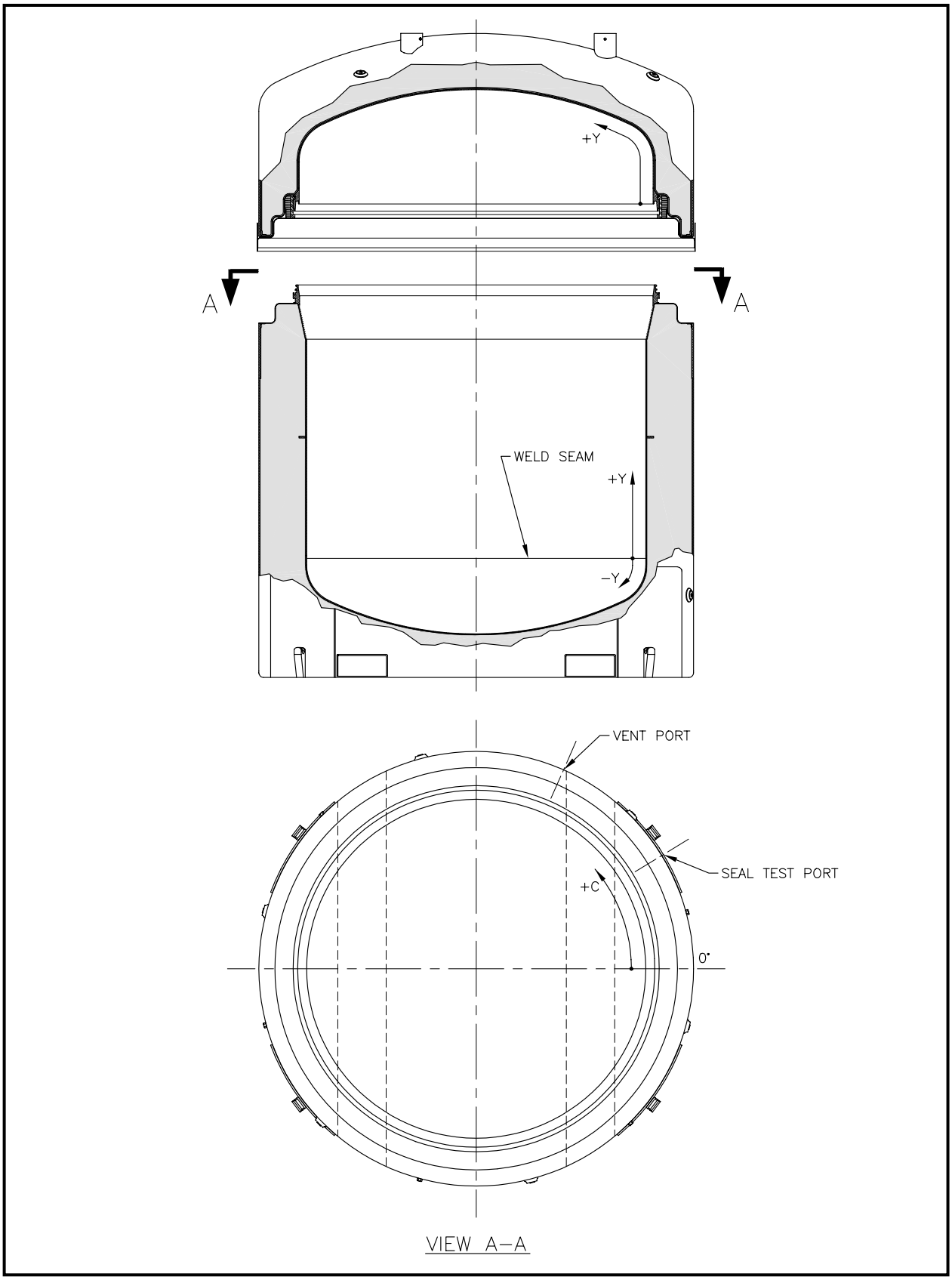

Figure 2.10.3-9 – CTU-2 OCV Temperature Indicating Label Locations

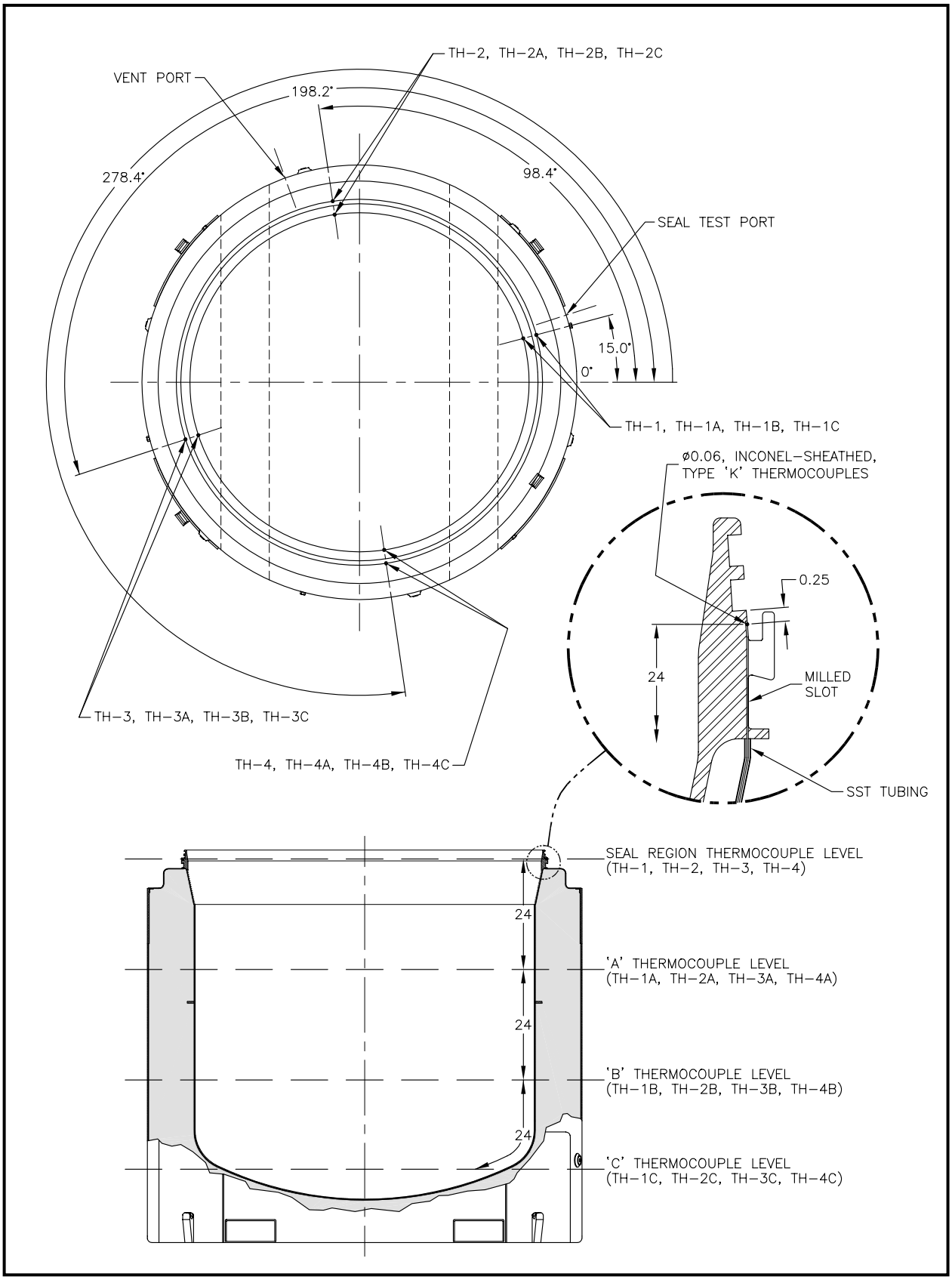

Figure 2.10.3-10 – CTU-1 OCV Thermocouple Locations

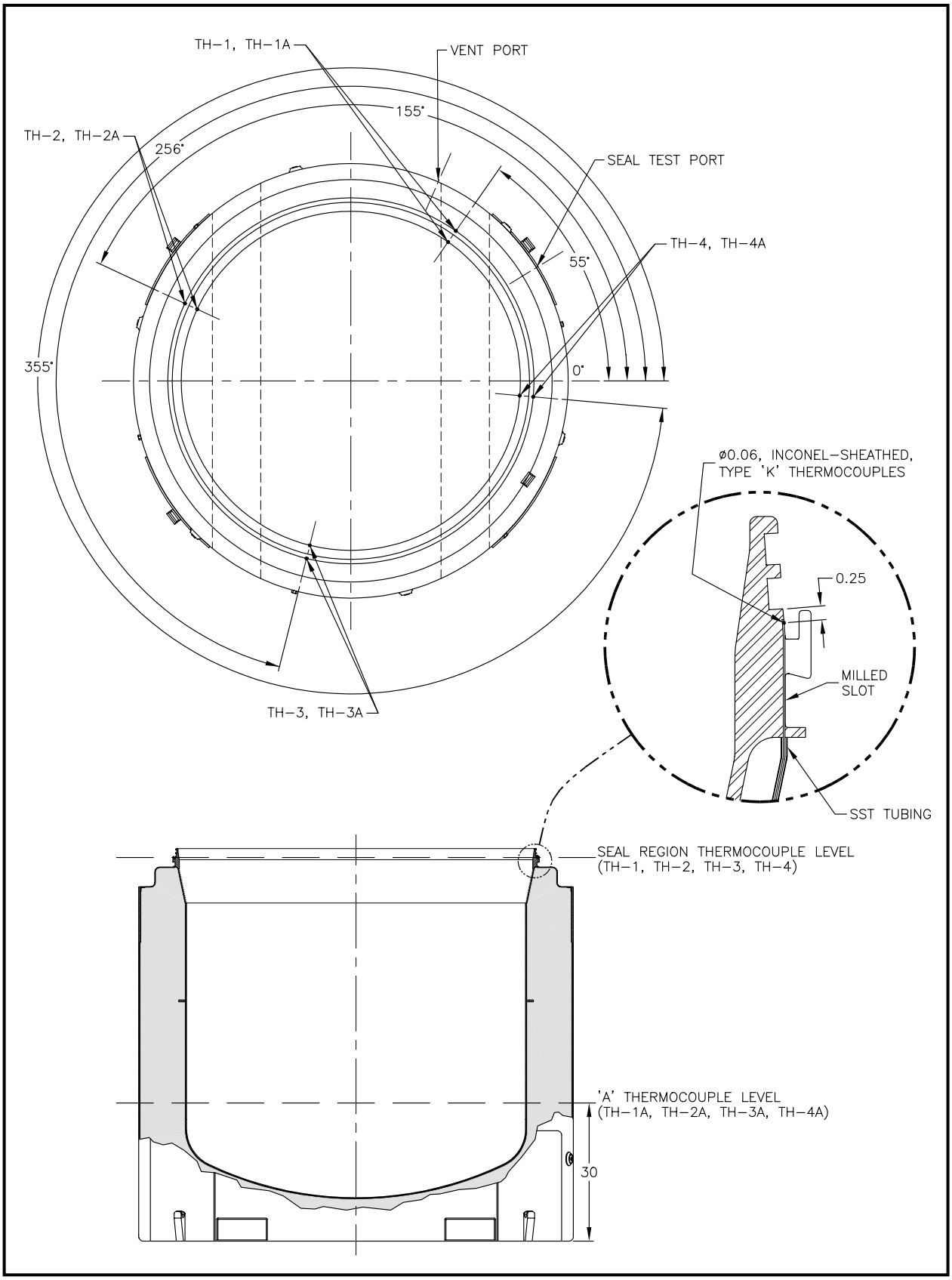

Figure 2.10.3-11 – CTU-2 OCV Thermocouple Locations

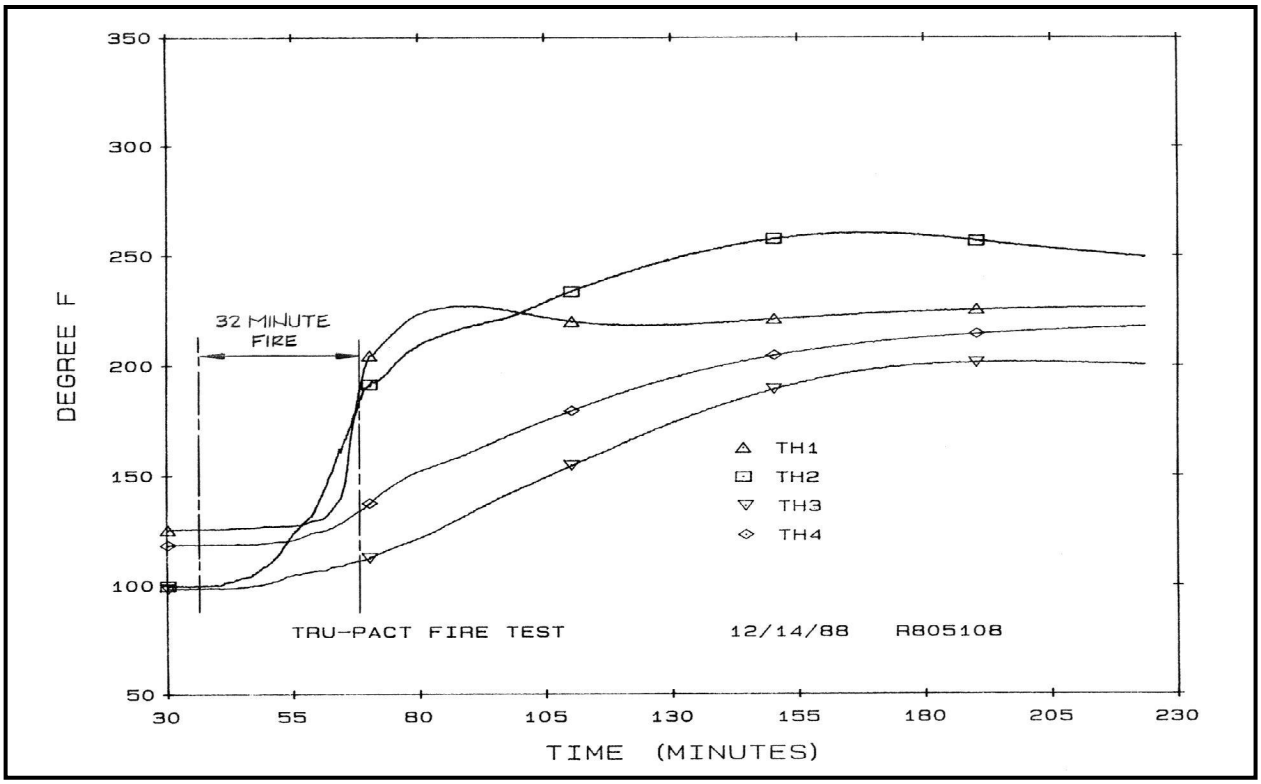

Figure 2.10.3-12 – CTU-1 OCV Thermocouple Data (TH-1, TH-2, TH-3, TH-4)

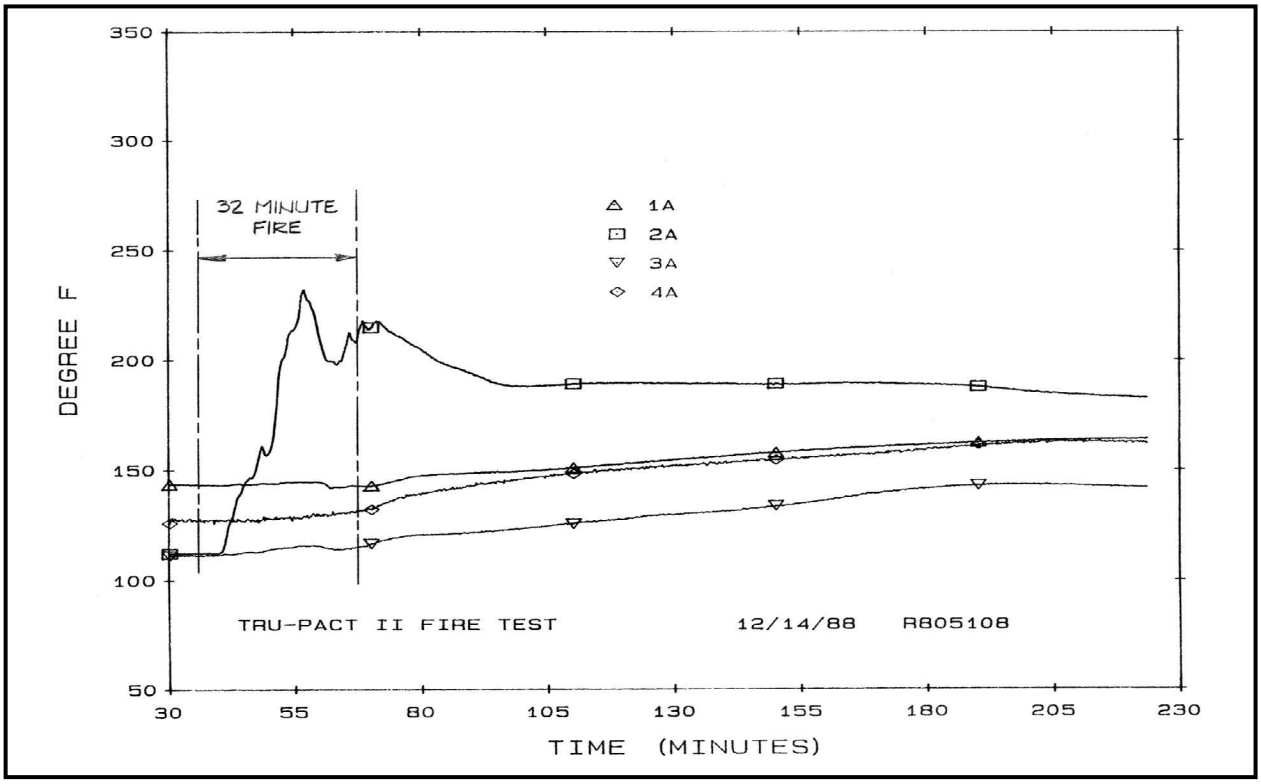

Figure 2.10.3-13 – CTU-1 OCV Thermocouple Data (TH-1A, TH-2A, TH-3A, TH-4A)

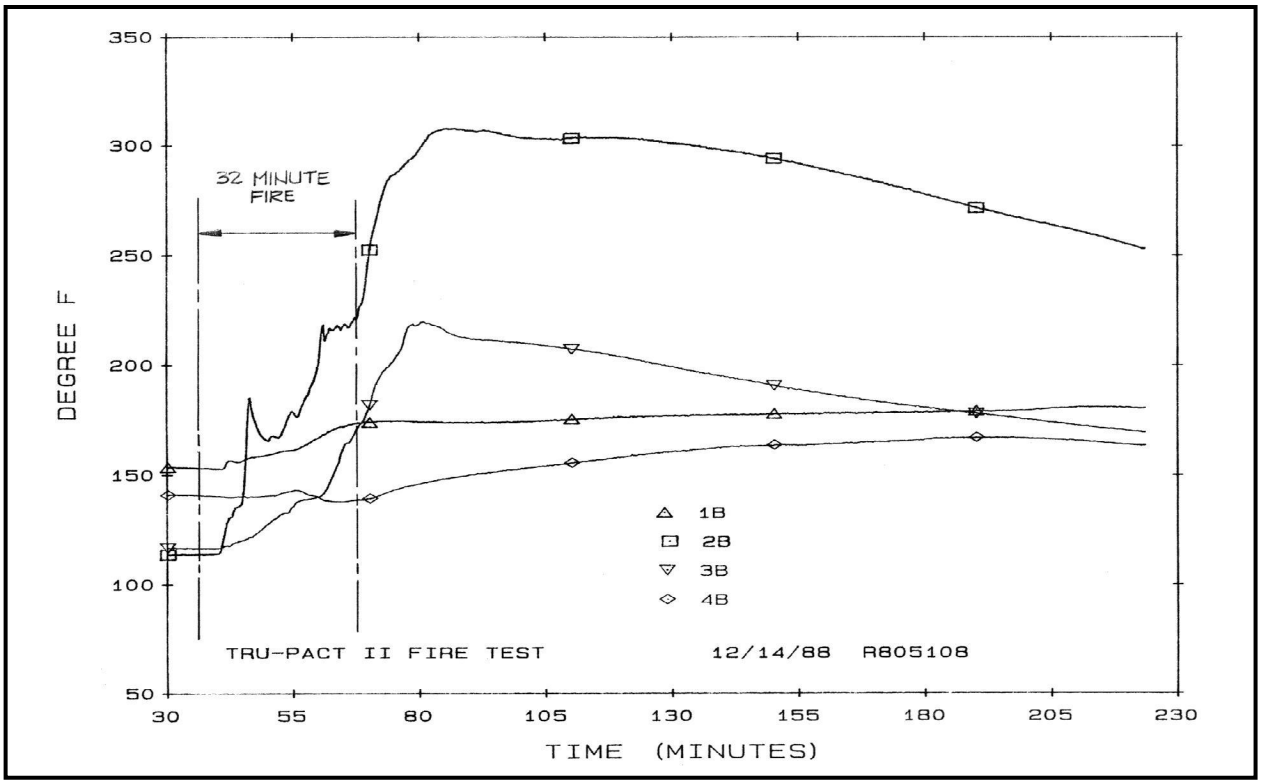

Figure 2.10.3-14 – CTU-1 OCV Thermocouple Data (TH-1C, TH-2C, TH-3C, TH-4C)

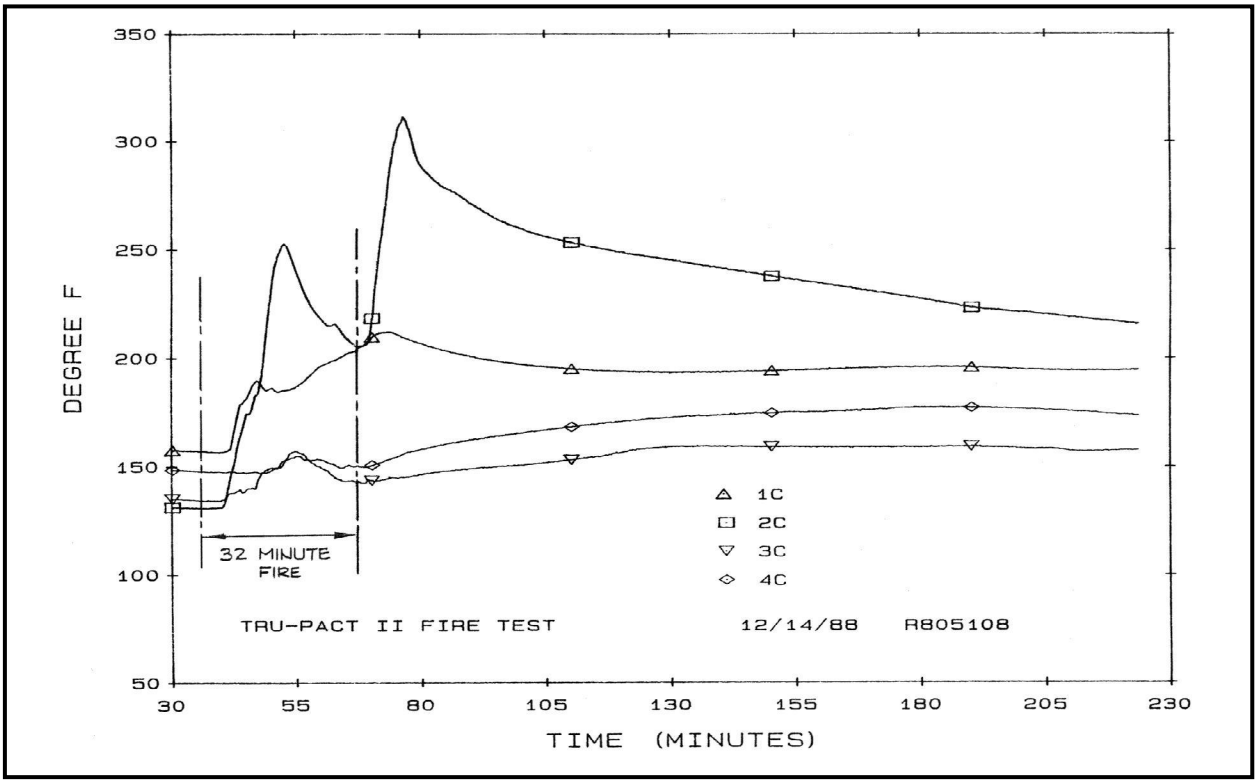

Figure 2.10.3-15 – CTU-1 OCV Thermocouple Data (TH-1D, TH-2D, TH-3D, TH-4D)

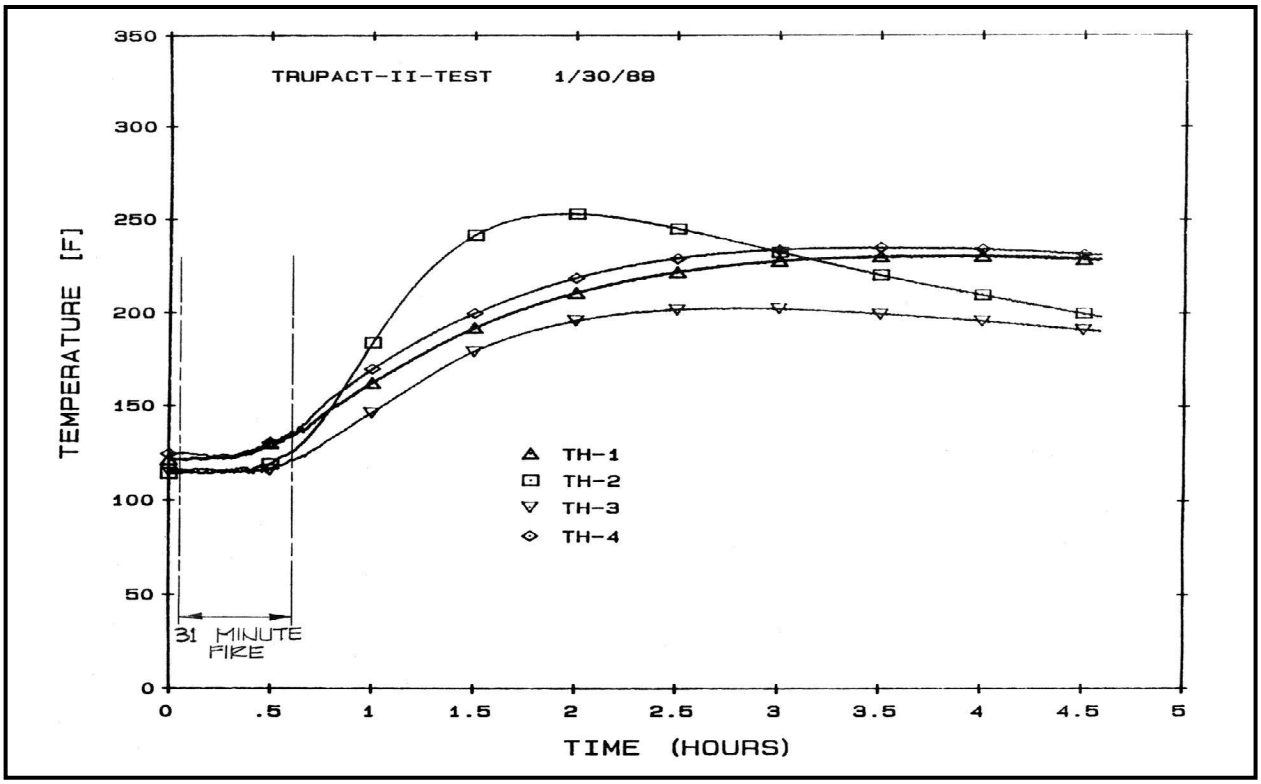

Figure 2.10.3-16 – CTU-2 OCV Thermocouple Data (TH-1, TH-2, TH-3, TH-4)

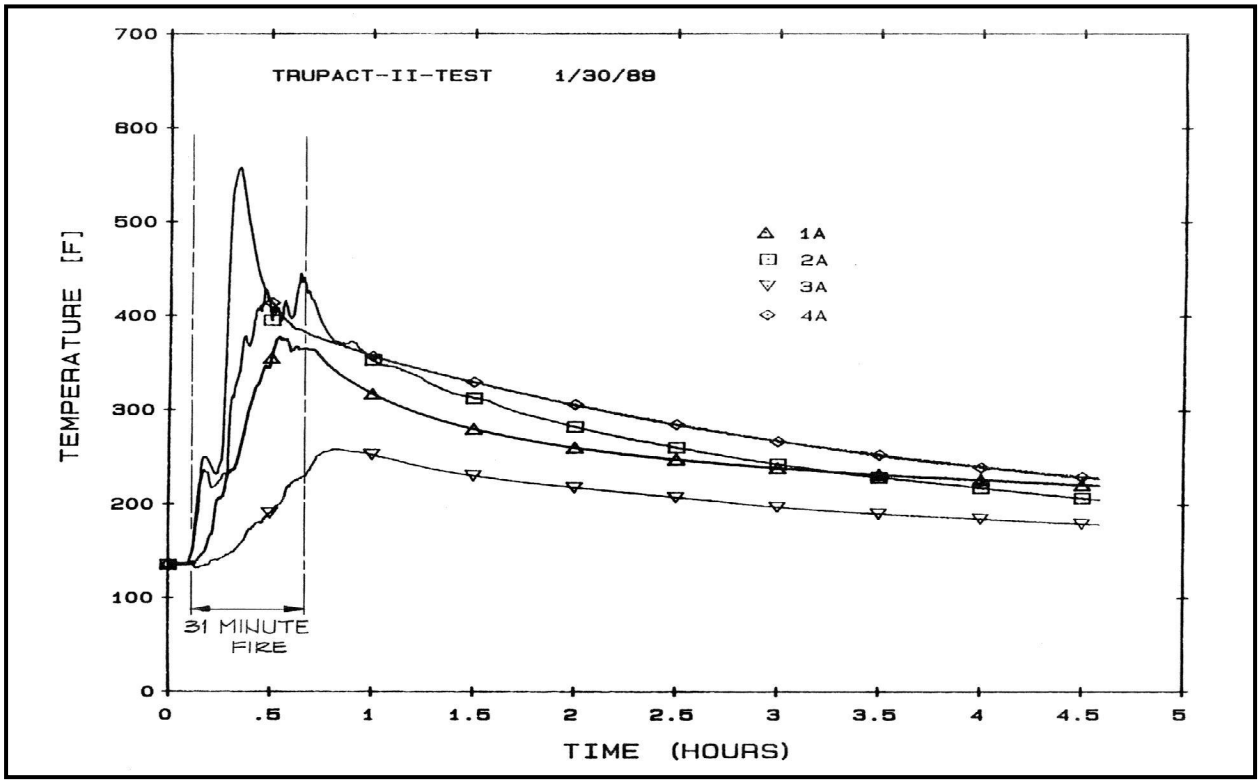

Figure 2.10.3-17 – CTU-2 OCV Thermocouple Data (TH-1A, TH-2A, TH-3A, TH-4A)

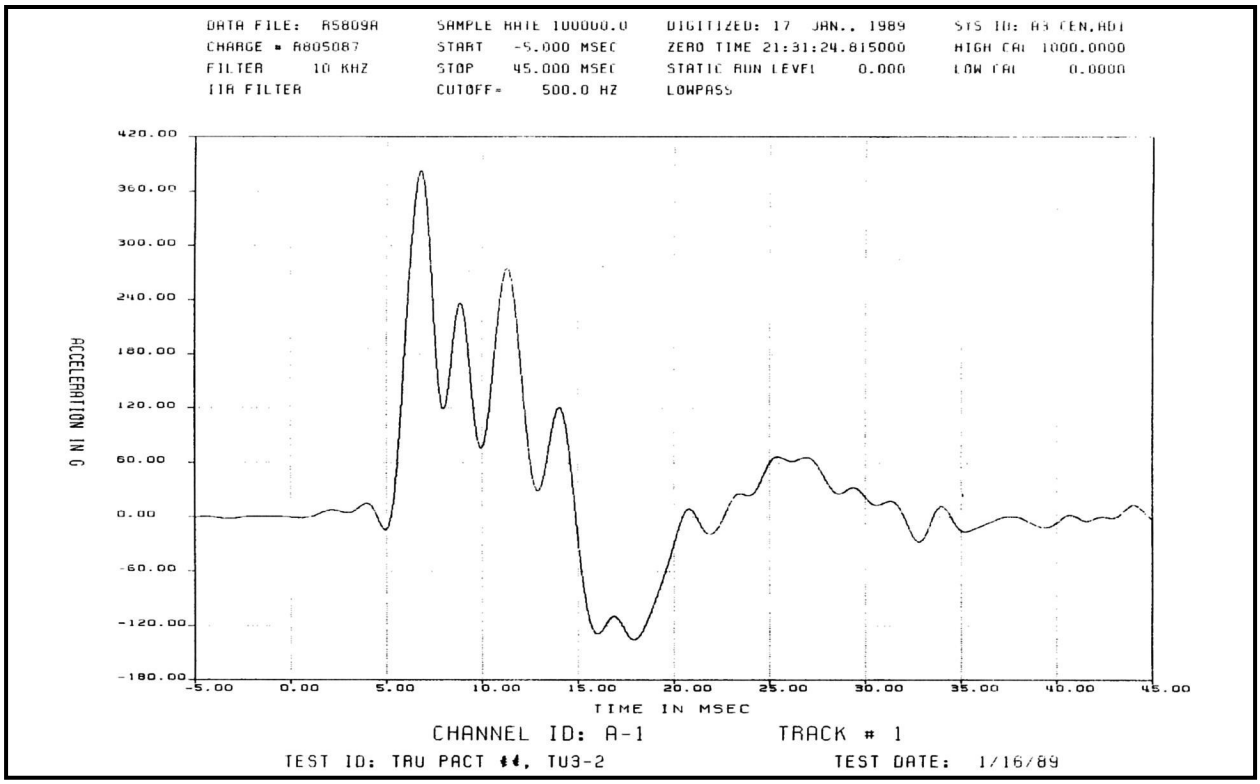

Figure 2.10.3-18 – CTU-2 Free Drop Test No. 2 Accelerometer Data (Gage 1)

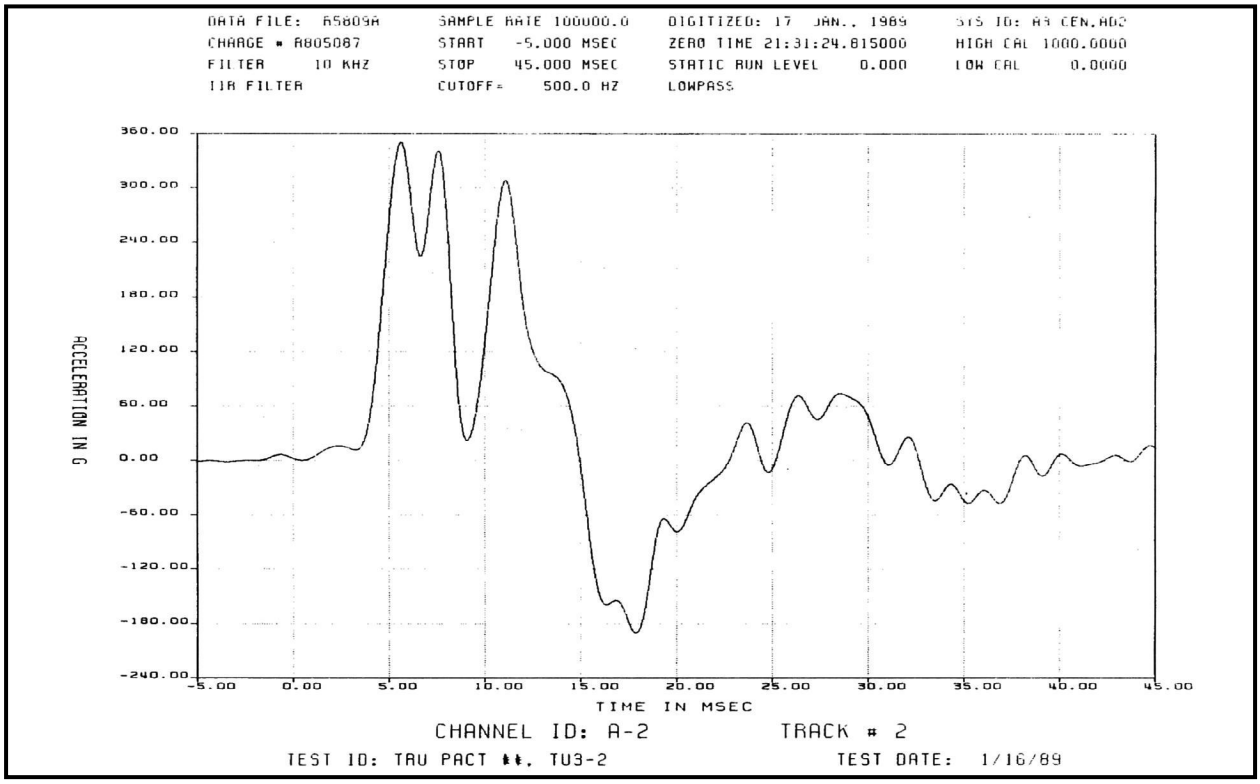

Figure 2.10.3-19 – CTU-2 Free Drop Test No. 2 Accelerometer Data (Gage 2)

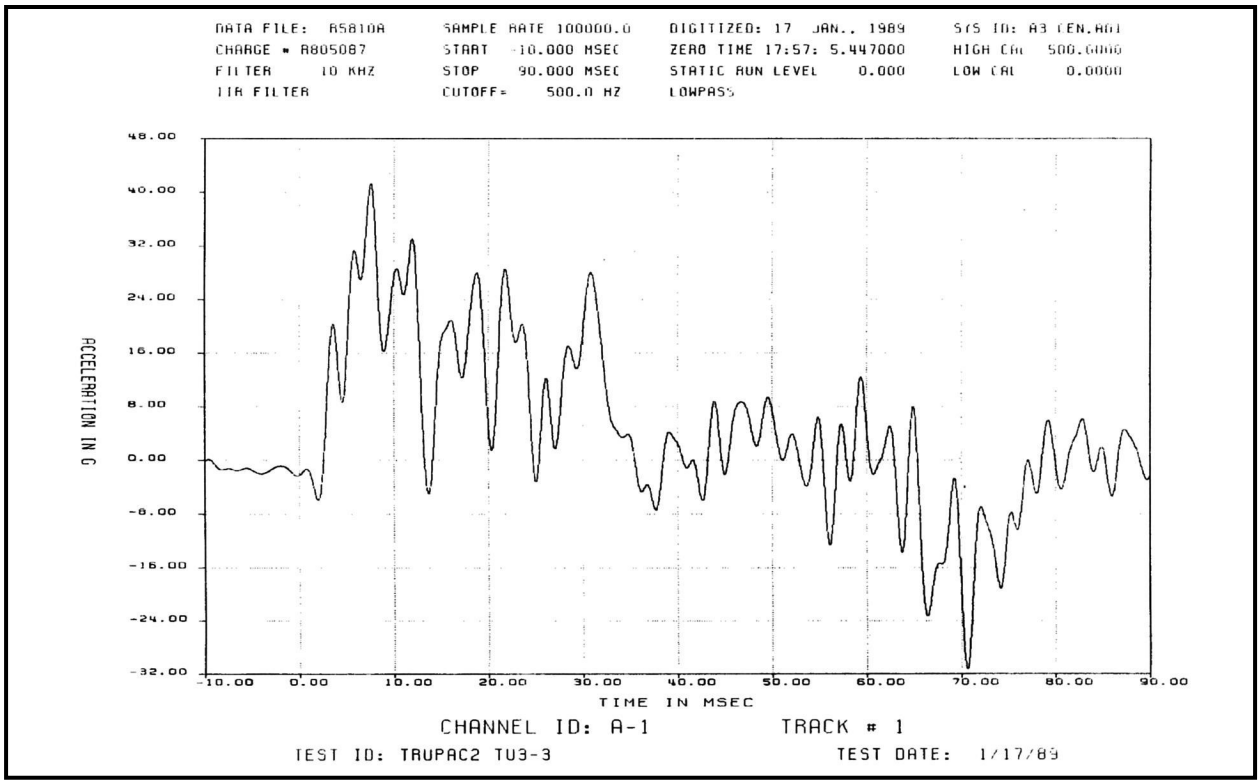

Figure 2.10.3-20 – CTU-2 Free Drop Test No. 3 Accelerometer Data (Gage 1)

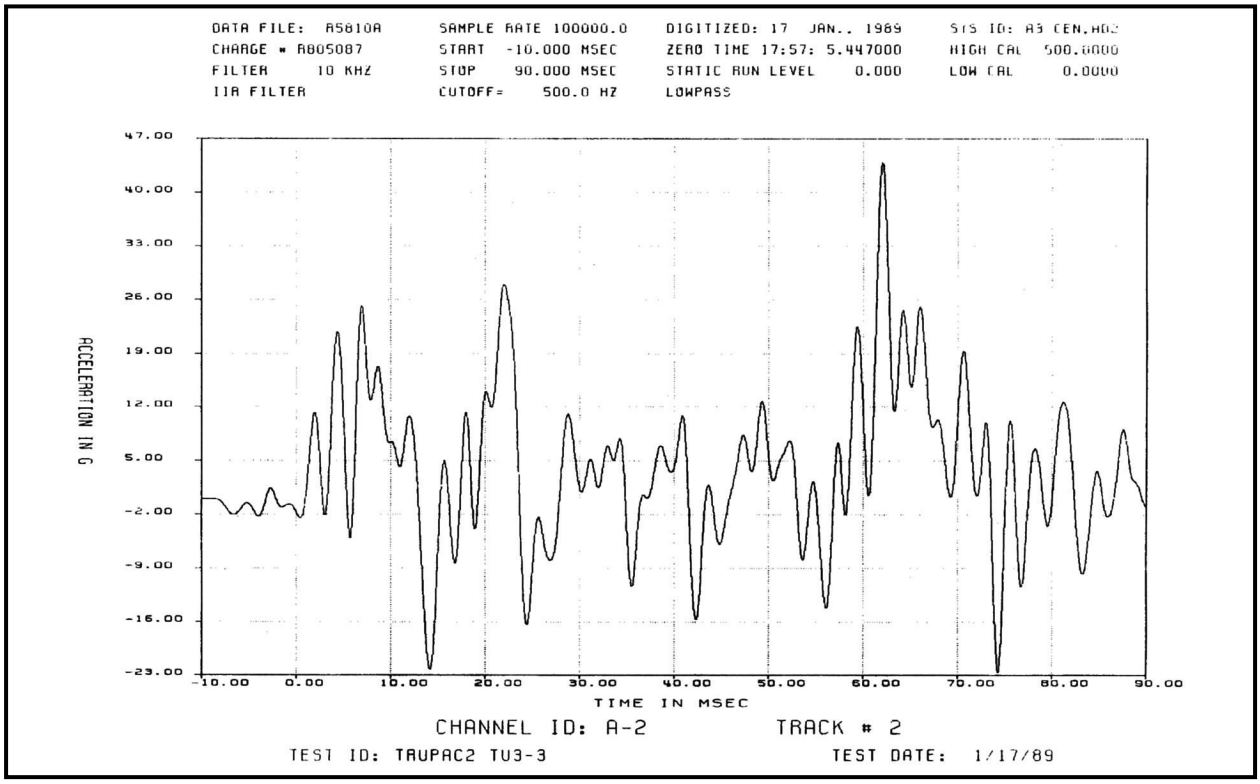

Figure 2.10.3-21 – CTU-2 Free Drop Test No. 3 Accelerometer Data (Gage 2)

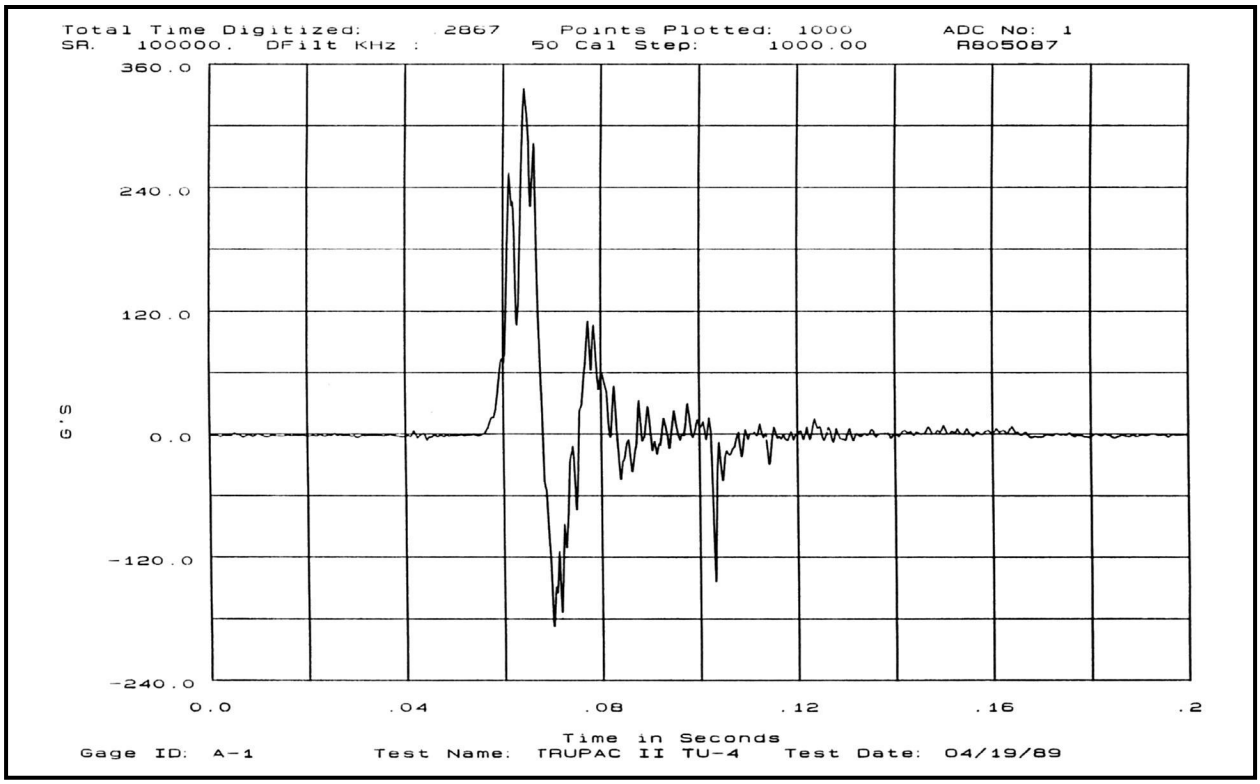

Figure 2.10.3-22 – CTU-3 Free Drop Test No. 2 Accelerometer Data (Gage 1)

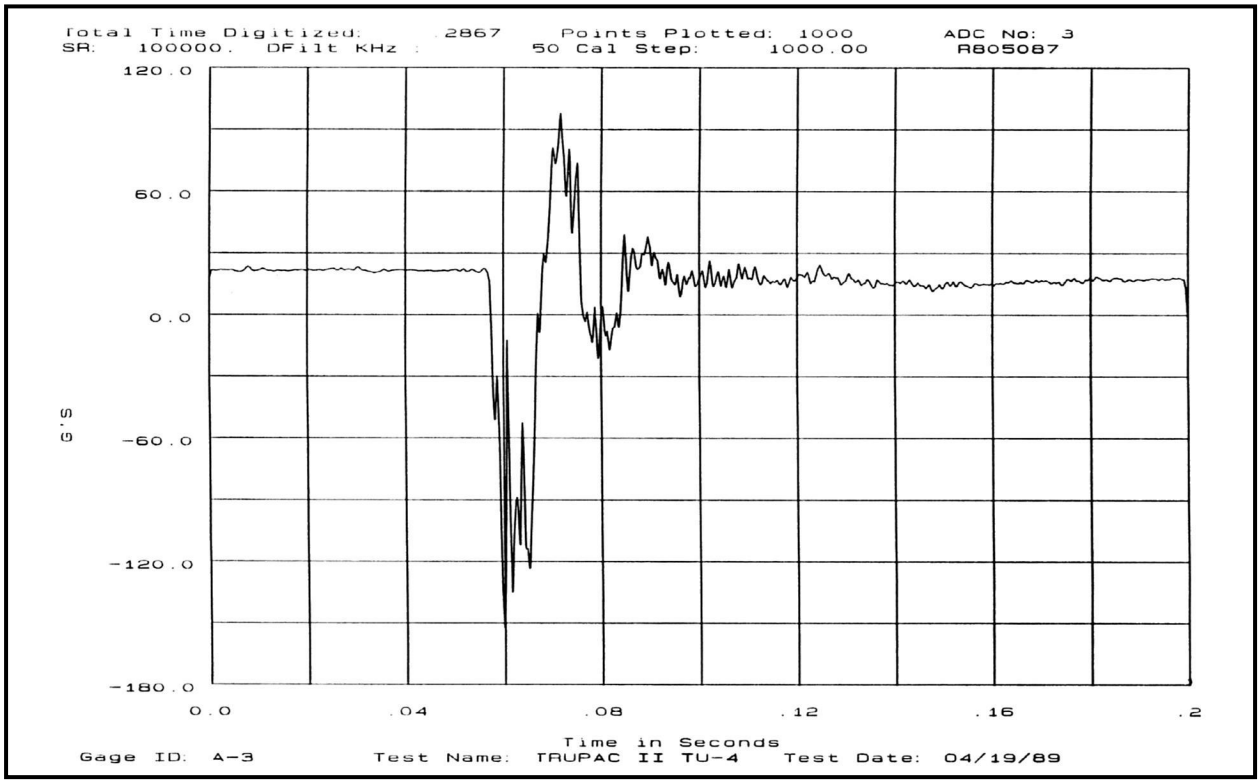

Figure 2.10.3-23 – CTU-3 Free Drop Test No. 2 Accelerometer Data (Gage 2)

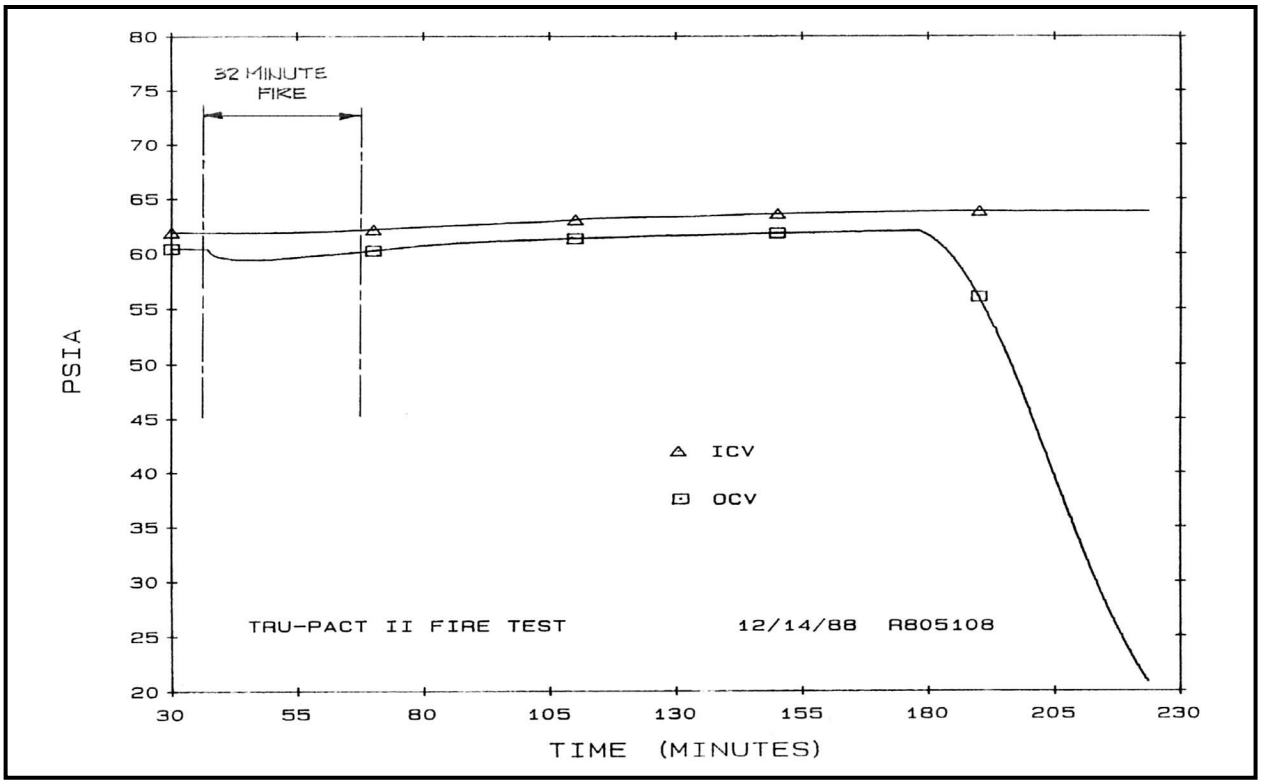

Figure 2.10.3-24 – CTU-1 Pressure Transducer Data During Fire Test No. 10

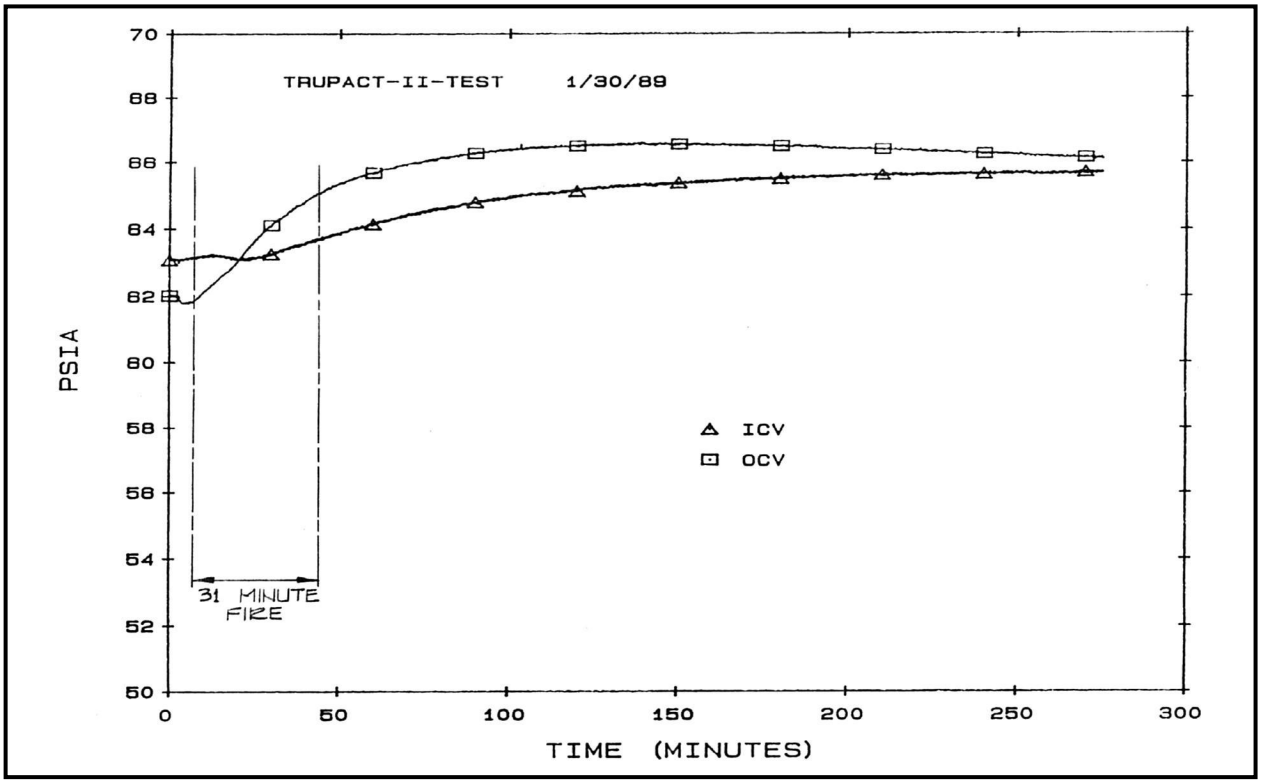

Figure 2.10.3-25 – CTU-2 Pressure Transducer Data During Fire Test No. 9

Figure 2.10.3-26 – CTU-1 Free Drop No. 1; Initial Preparation for Testing

Figure 2.10.3-27 – CTU-1 Free Drop No. 1; Pre-Drop Positioning

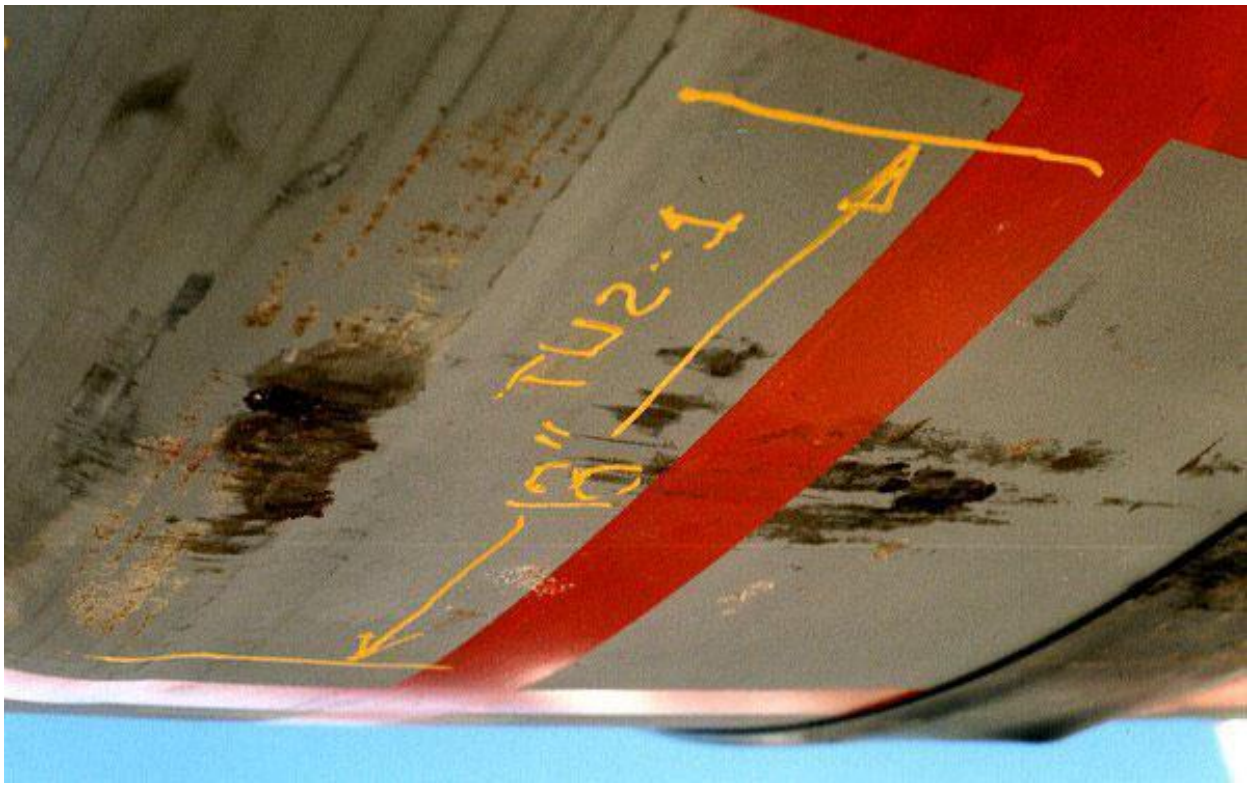

Figure 2.10.3-28 – CTU-1 Free Drop No. 1; Post-Drop Damage at Top (Lid)

Figure 2.10.3-29 – CTU-1 Free Drop No. 1; Post-Drop Damage at Bottom (Body)

Figure 2.10.3-30 – CTU-1 Free Drop No. 2; Pre-Drop Positioning

Figure 2.10.3-31 – CTU-1 Free Drop No. 2; Post-Drop Damage

Figure 2.10.3-32 – CTU-1 Free Drop No. 3; Pre-Drop Positioning

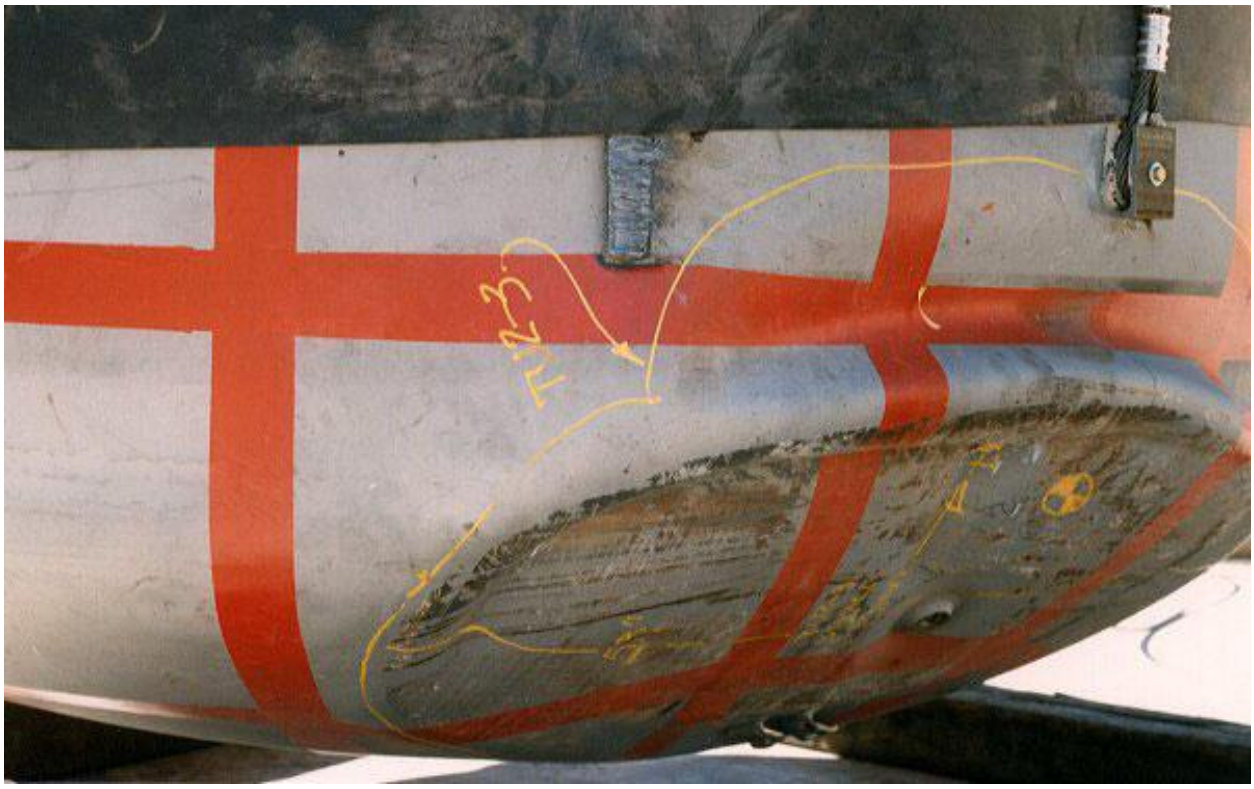

Figure 2.10.3-33 – CTU-1 Free Drop No. 3; Post-Drop Damage

Figure 2.10.3-34 – CTU-1 Free Drop No. 4; Pre-Drop Positioning

Figure 2.10.3-35 – CTU-1 Free Drop No. 4; Post-Drop Damage

Figure 2.10.3-36 – CTU-1 Puncture Drop No. 5; Pre-Drop Positioning

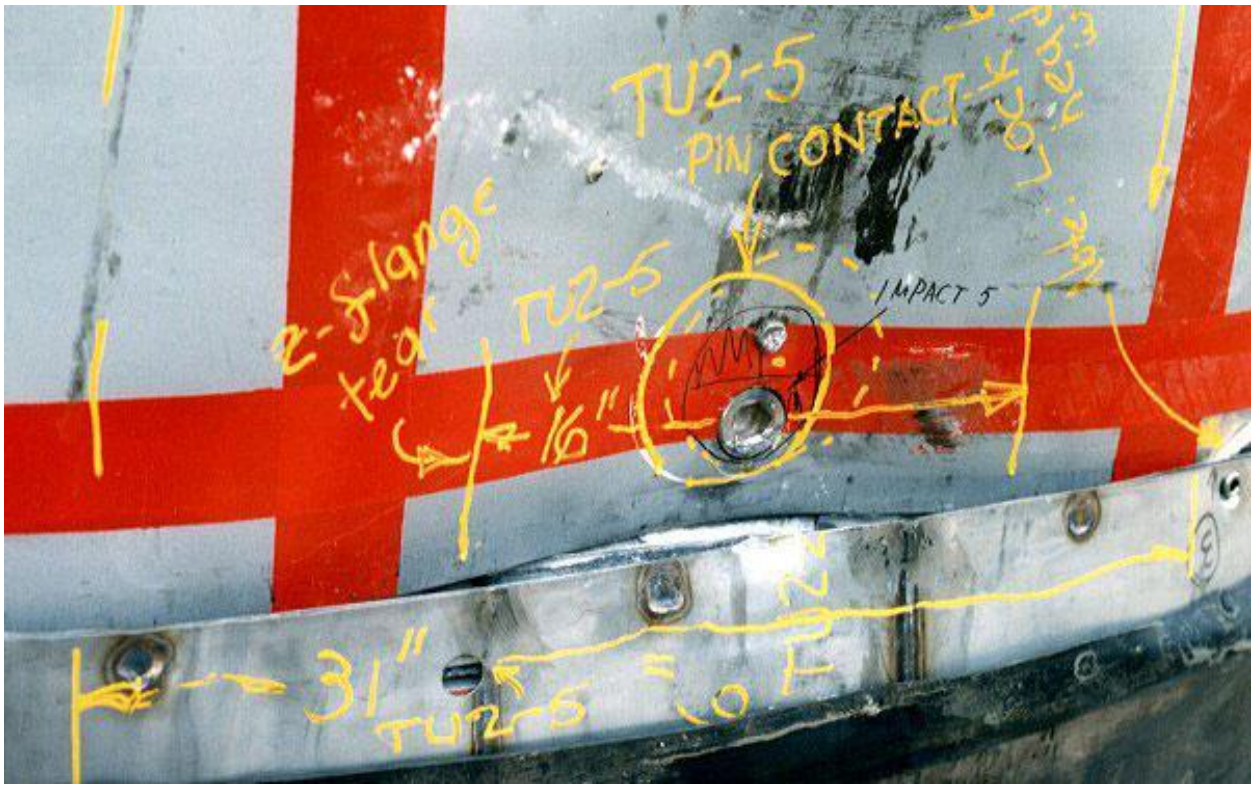

Figure 2.10.3-37 – CTU-1 Puncture Drop No. 5; Post-Drop Damage

Figure 2.10.3-38 – CTU-1 Puncture Drop No. 6; Pre-Drop Positioning

Figure 2.10.3-39 – CTU-1 Puncture Drop No. 6; Post-Drop Damage

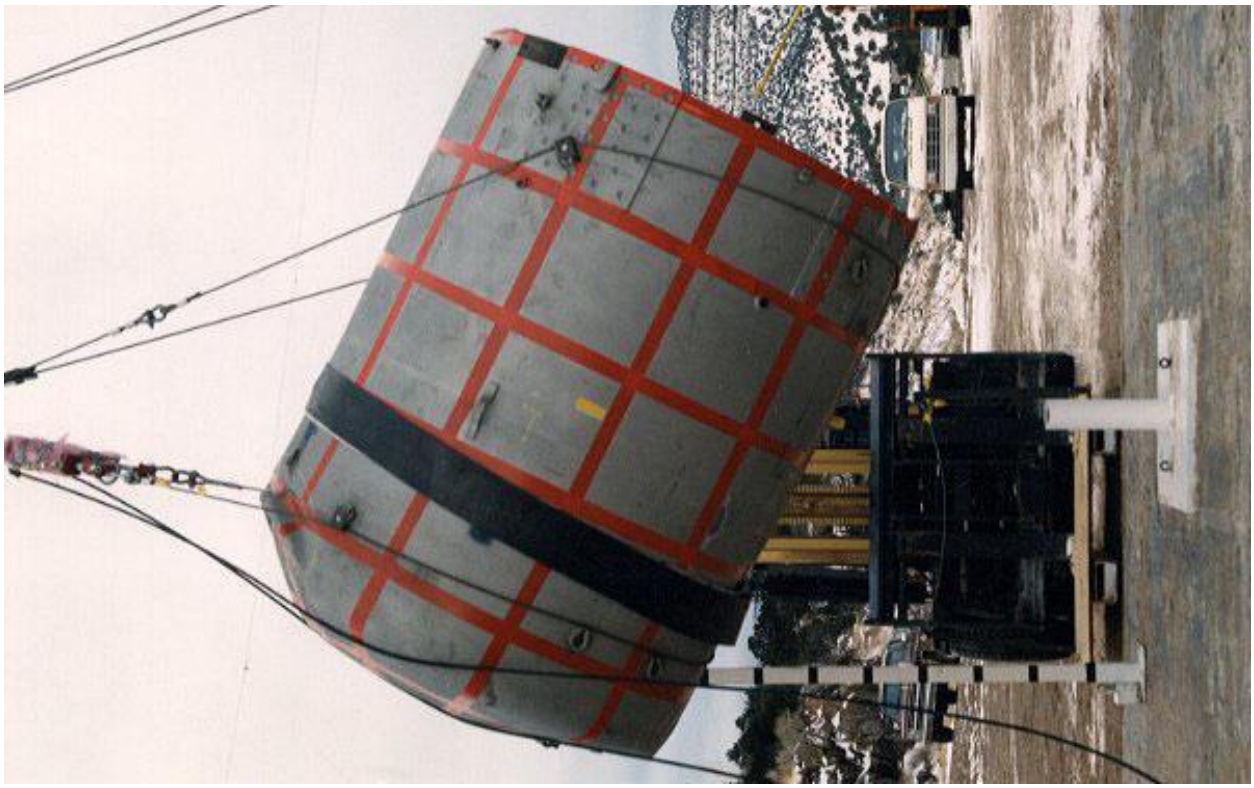

Figure 2.10.3-40 – CTU-1 Puncture Drop No. 7; Pre-Drop Positioning

Figure 2.10.3-41 – CTU-1 Puncture Drop No. 7; Post-Drop Damage

Figure 2.10.3-42 – CTU-1 Puncture Drop No. 8; Pre-Drop Positioning

Figure 2.10.3-43 – CTU-1 Puncture Drop No. 8; Moment of Impact

Figure 2.10.3-44 – CTU-1 Puncture Drop No. 9; Pre-Drop Positioning

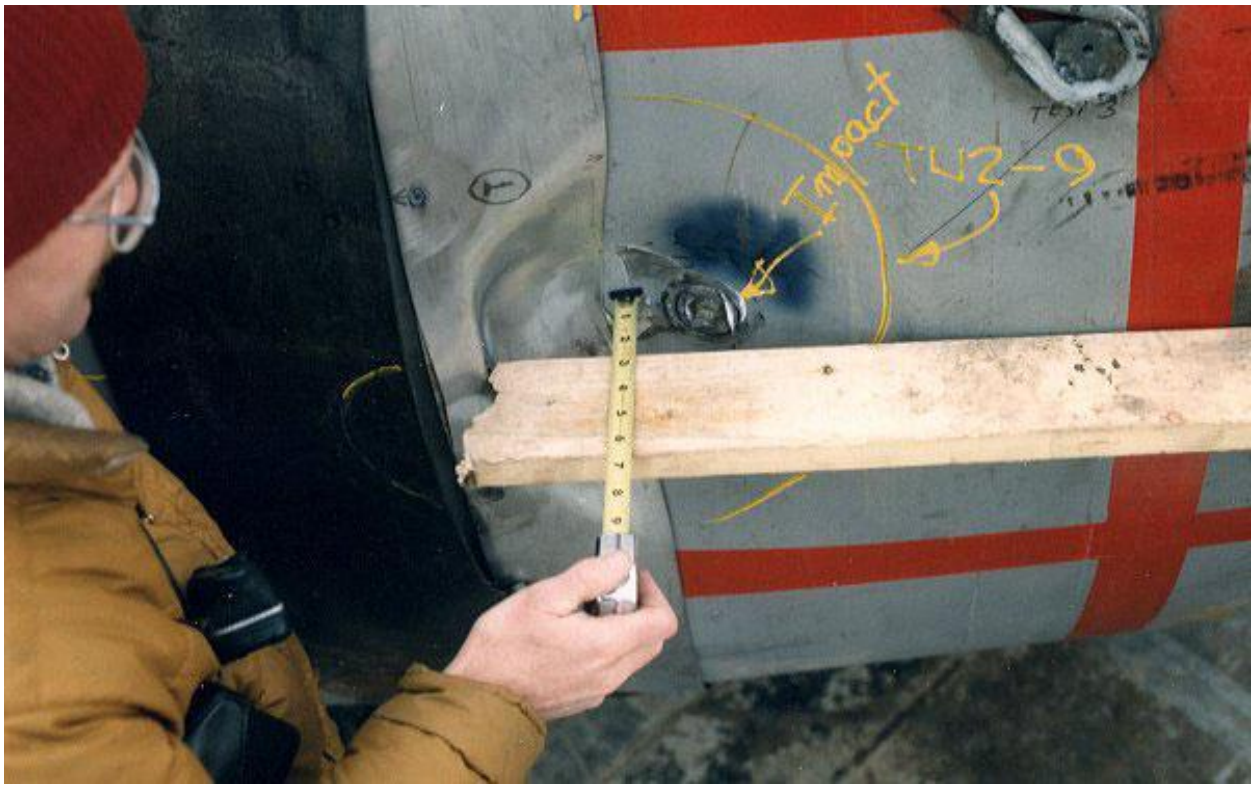

Figure 2.10.3-45 – CTU-1 Puncture Drop No. 9; Post-Drop Damage

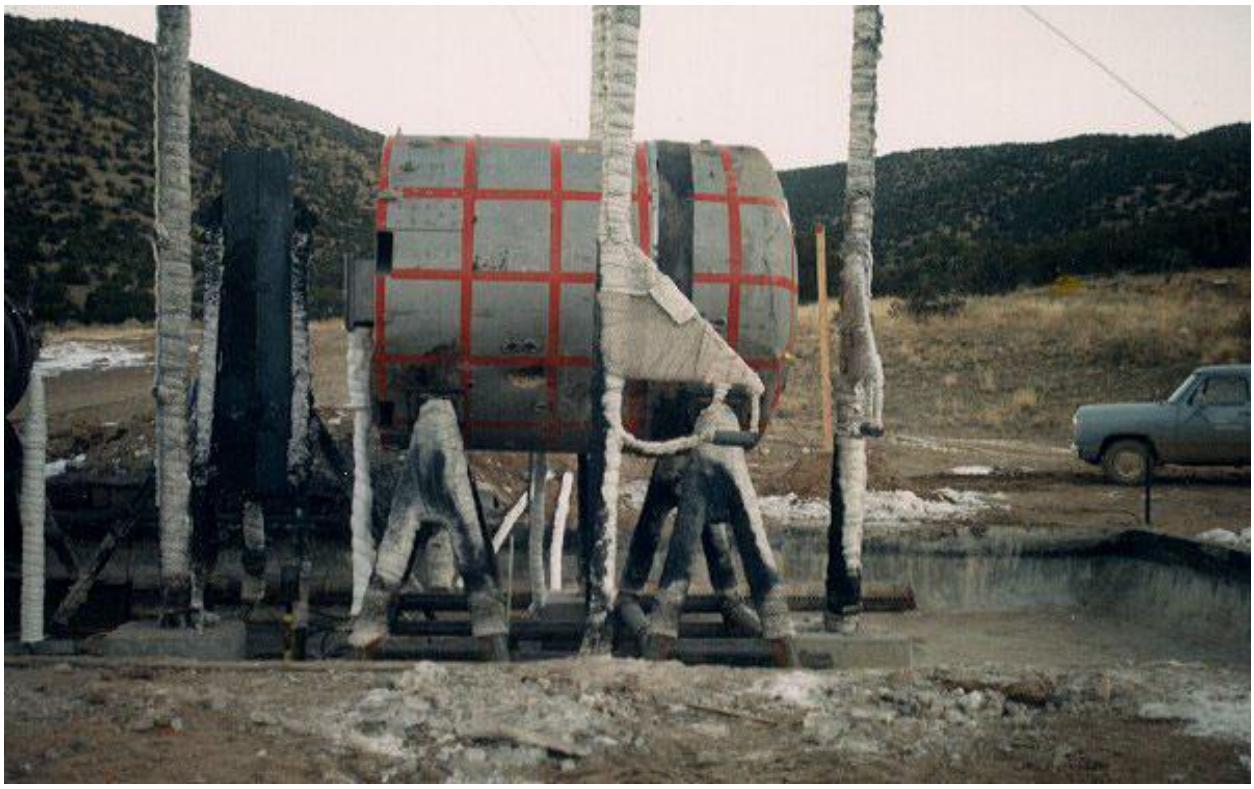

Figure 2.10.3-46 – CTU-1 Fire No. 10; Pre-Fire Positioning, Side View

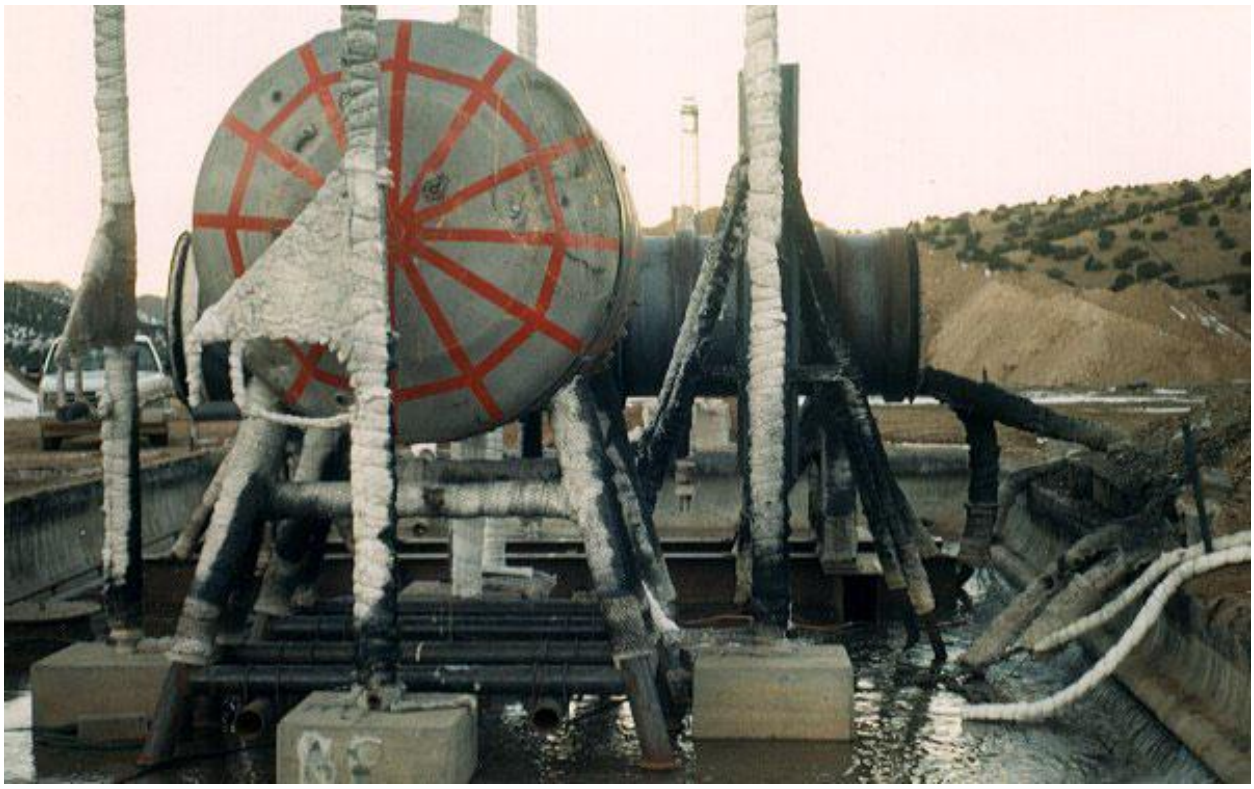

Figure 2.10.3-47 – CTU-1 Fire No. 10; Pre- Fire Positioning, Top End View

Figure 2.10.3-48 – CTU-1 Fire No. 10; Fully Engulfing Fire

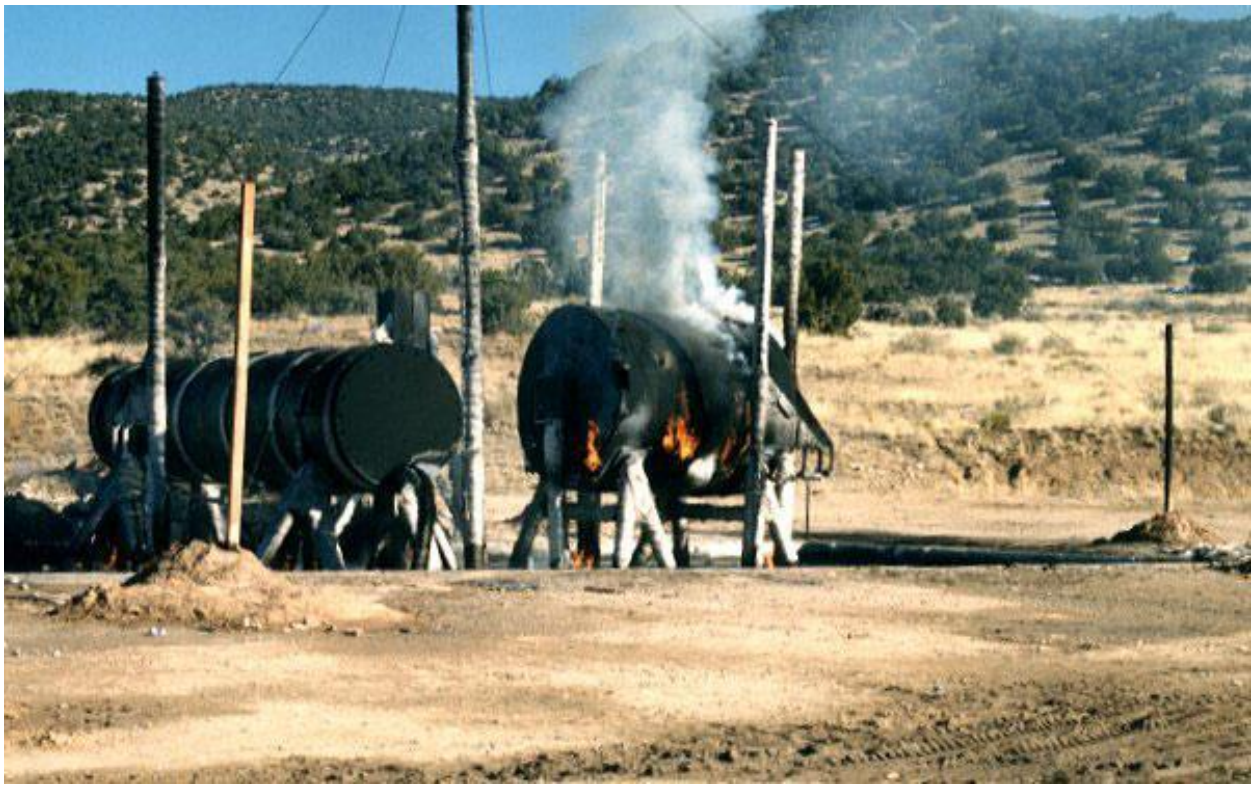

Figure 2.10.3-49 – CTU-1 Fire No. 10; Post-Fire Cool-Down

Figure 2.10.3-50 – CTU-1 Disassembly; OCA Lid Unburned Foam

Figure 2.10.3-51 – CTU-1 Disassembly; OCA Lid Unburned Foam Thickness

Figure 2.10.3-52 – CTU-1 Disassembly; Payload Drum Removal

Figure 2.10.3-53 – CTU-1 Disassembly; Loose Debris on Pallet in ICV Body

Figure 2.10.3-54 – CTU-2 Free Drop No. 1; Initial Preparation for Testing

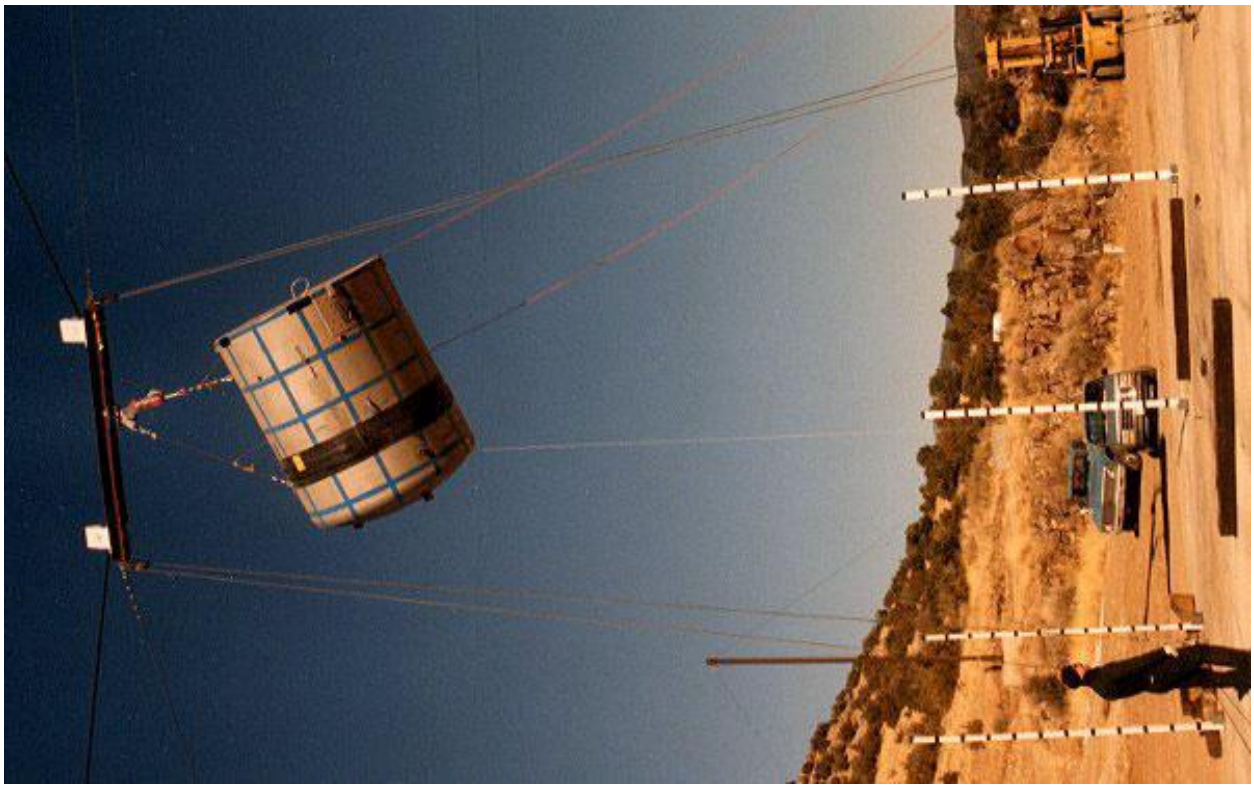

Figure 2.10.3-55 – CTU-2 Free Drop No. 1; Pre-Drop Positioning

Figure 2.10.3-56 – CTU-2 Free Drop No. 1; Post-Drop Damage

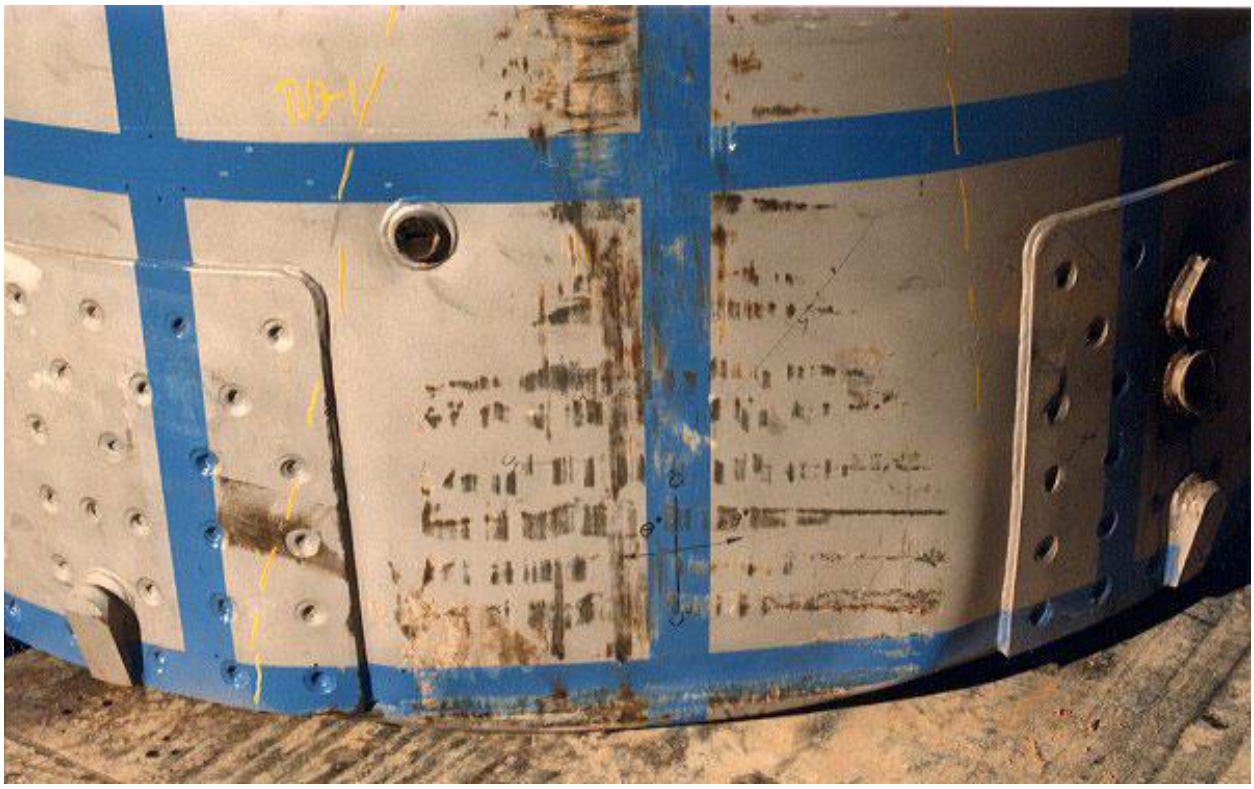

Figure 2.10.3-57 – CTU-2 Free Drop No. 1; Post-Drop Damage

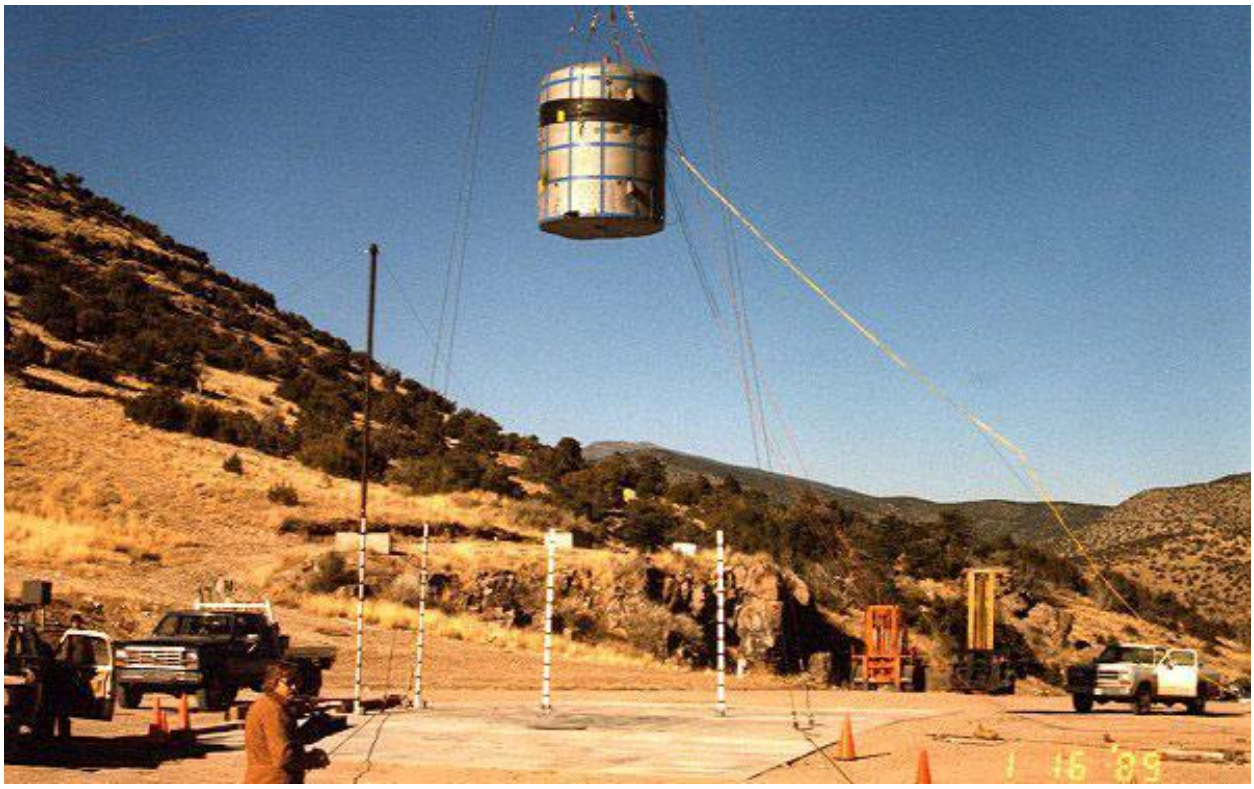

Figure 2.10.3-58 – CTU-2 Free Drop No. 2; Pre-Drop Positioning

Figure 2.10.3-59 – CTU-2 Free Drop No. 2; Post-Drop Damage

Figure 2.10.3-60 – CTU-2 Free Drop No. 3; Pre-Drop Positioning

Figure 2.10.3-61 – CTU-2 Free Drop No. 3; Post-Drop Damage

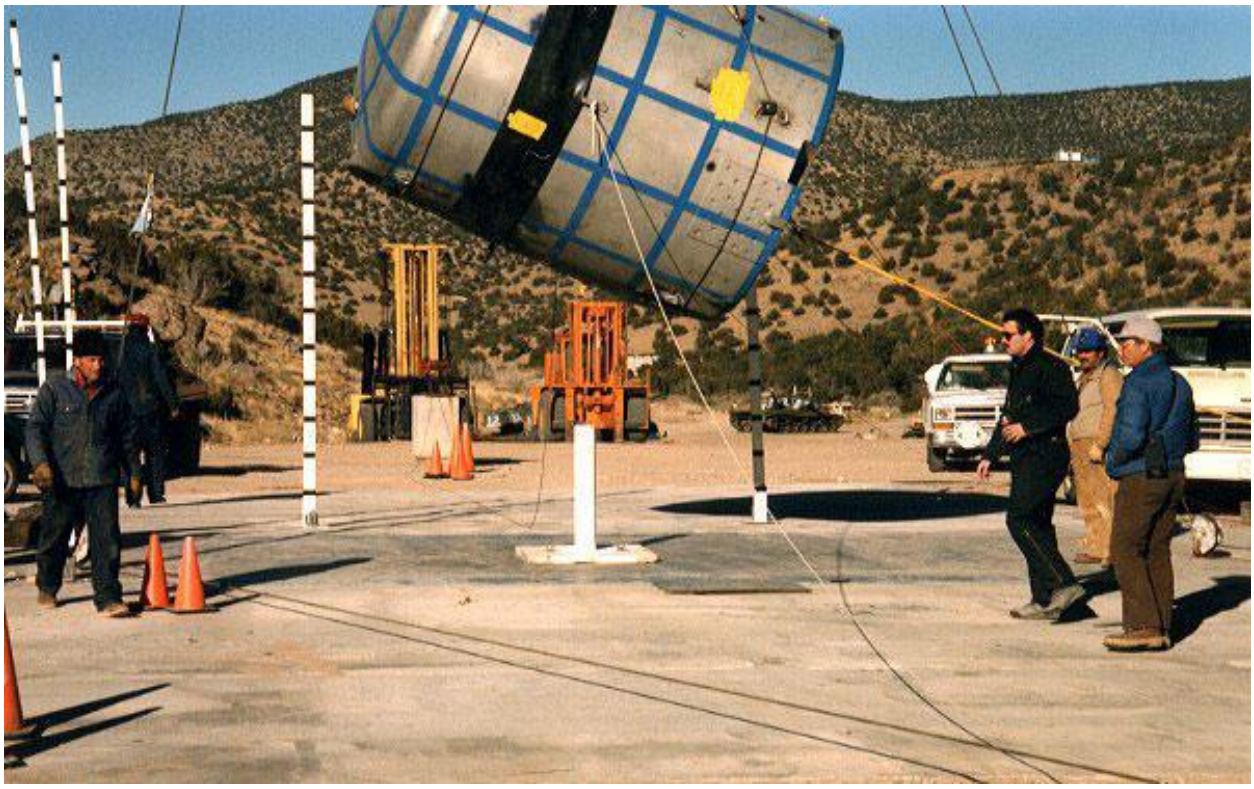

Figure 2.10.3-62 – CTU-2 Puncture Drop No. R; Pre-Drop Positioning

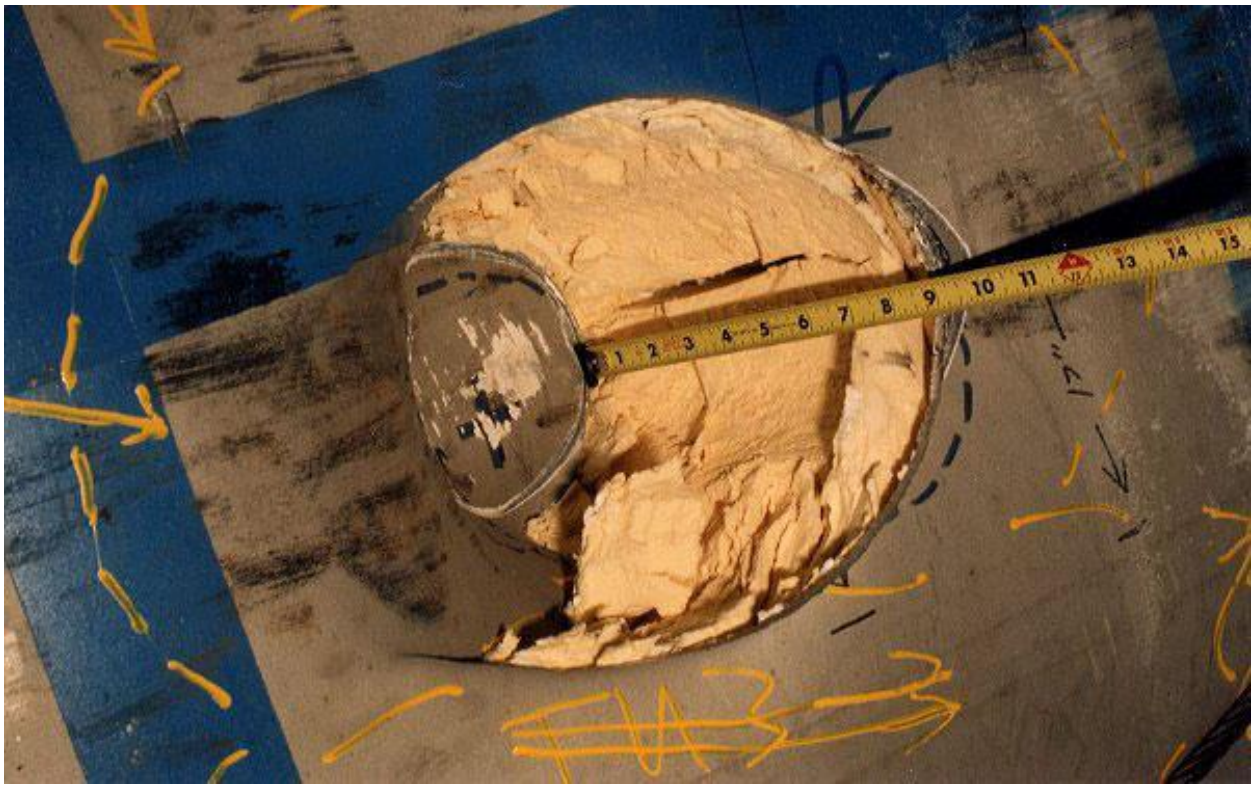

Figure 2.10.3-63 – CTU-2 Puncture Drop R; Post-Drop Damage

Figure 2.10.3-64 – CTU-2 Puncture Drop No. 4; Pre-Drop Positioning

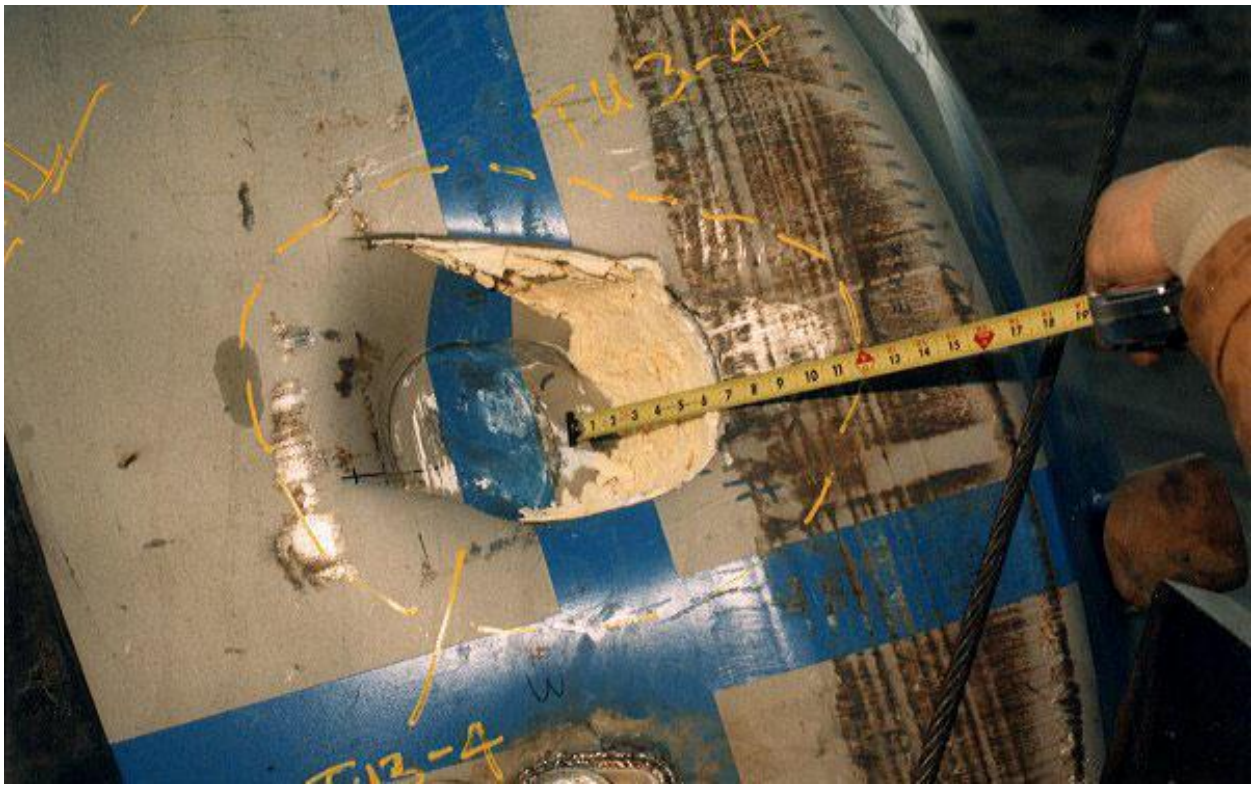

Figure 2.10.3-65 – CTU-2 Puncture Drop 4; Post-Drop Damage

Figure 2.10.3-66 – CTU-2 Puncture Drop No. 5; Pre-Drop Positioning

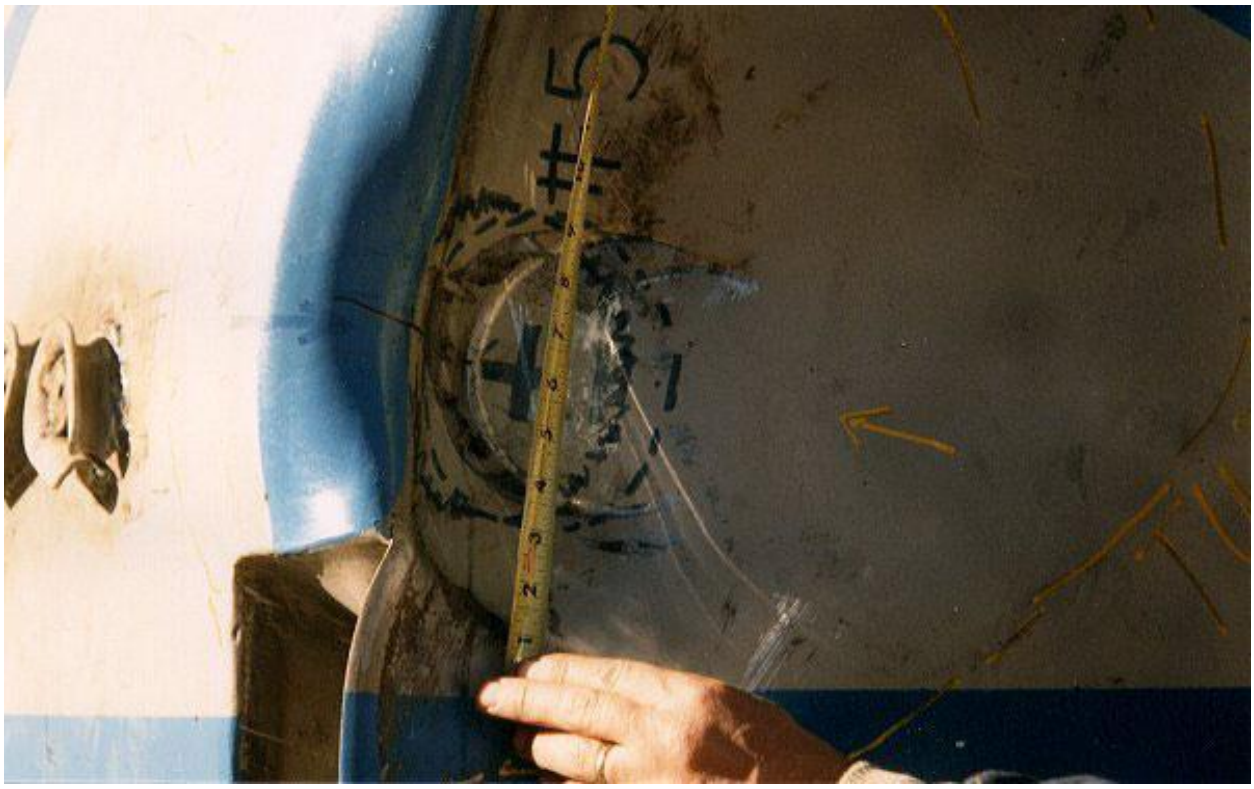

Figure 2.10.3-67 – CTU-2 Puncture Drop 5; Post-Drop Damage

Figure 2.10.3-68 – CTU-2 Puncture Drop No. 6; Pre-Drop Positioning

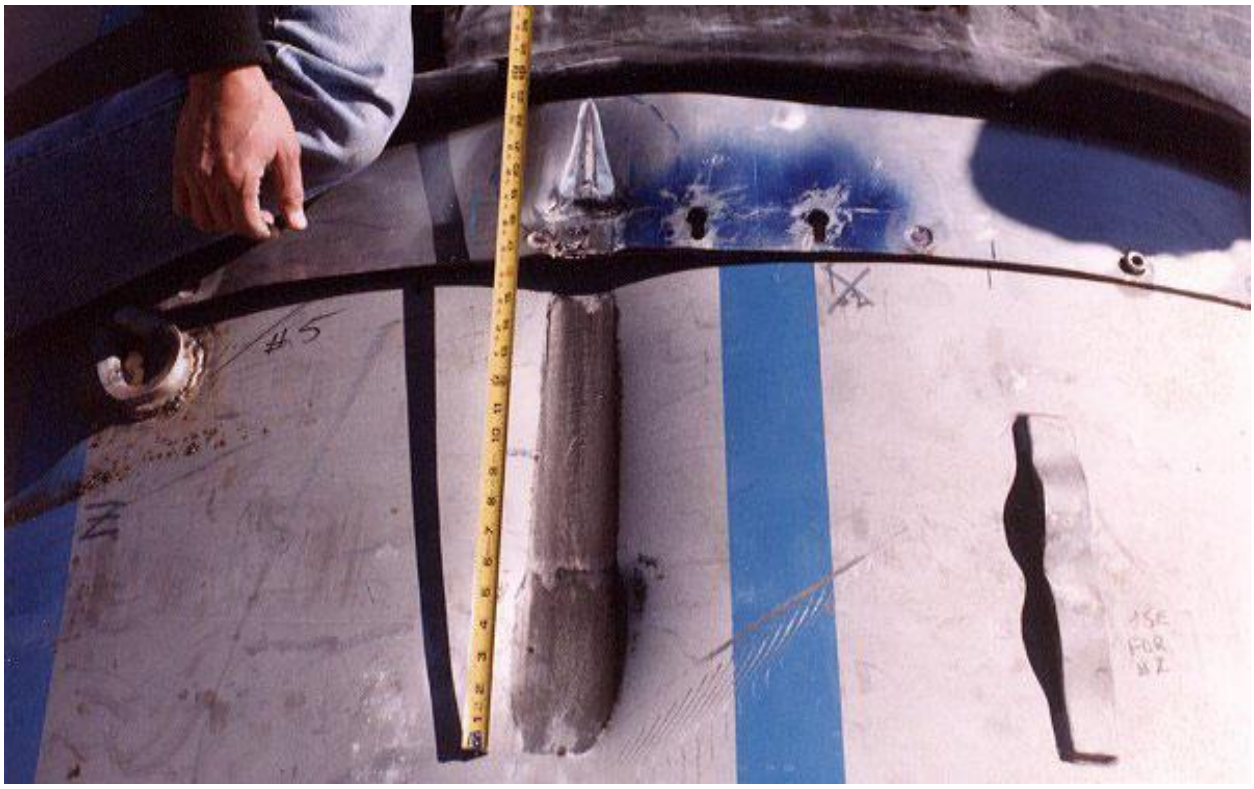

Figure 2.10.3-69 – CTU-2 Puncture Drop 6; Post-Drop Damage

Figure 2.10.3-70 – CTU-2 Puncture Drop No. 7; Pre-Drop Positioning

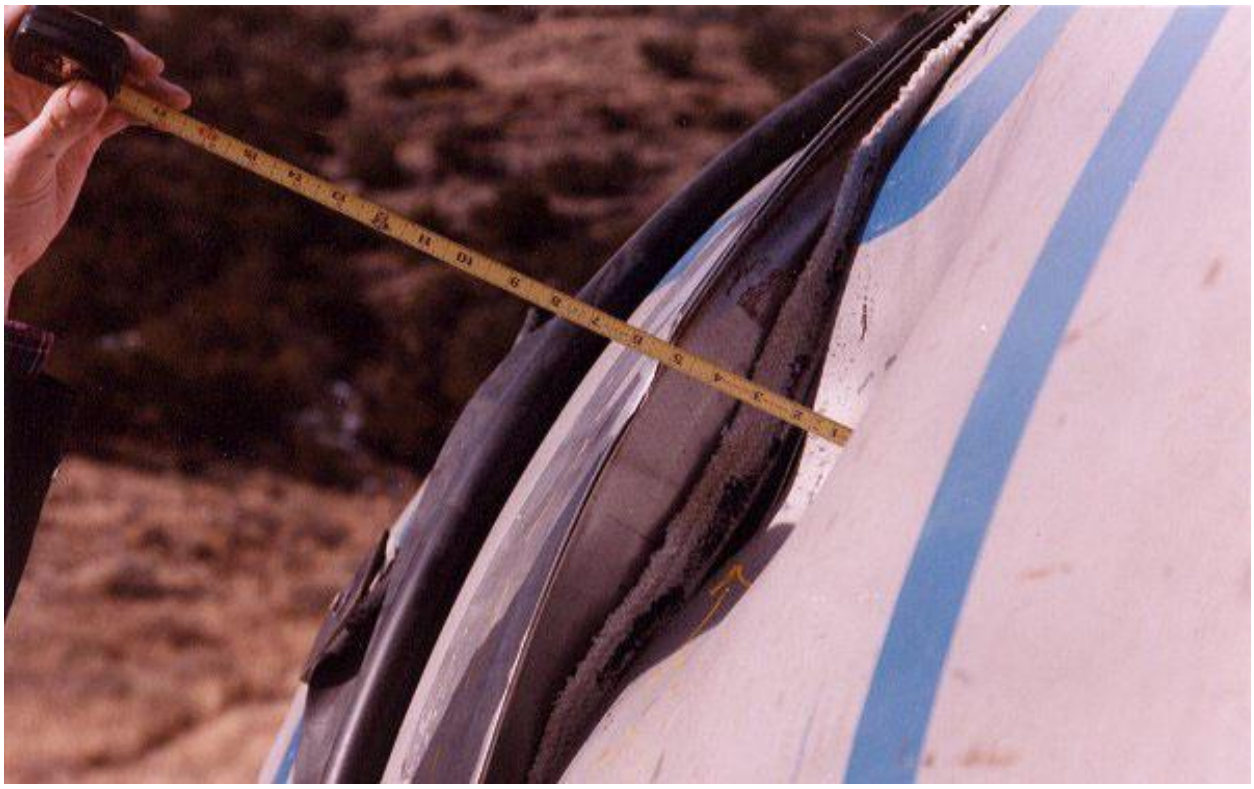

Figure 2.10.3-71 – CTU-2 Puncture Drop 7; Post-Drop Damage

Figure 2.10.3-72 – CTU-2 Puncture Drop No. 8; Pre-Drop Positioning

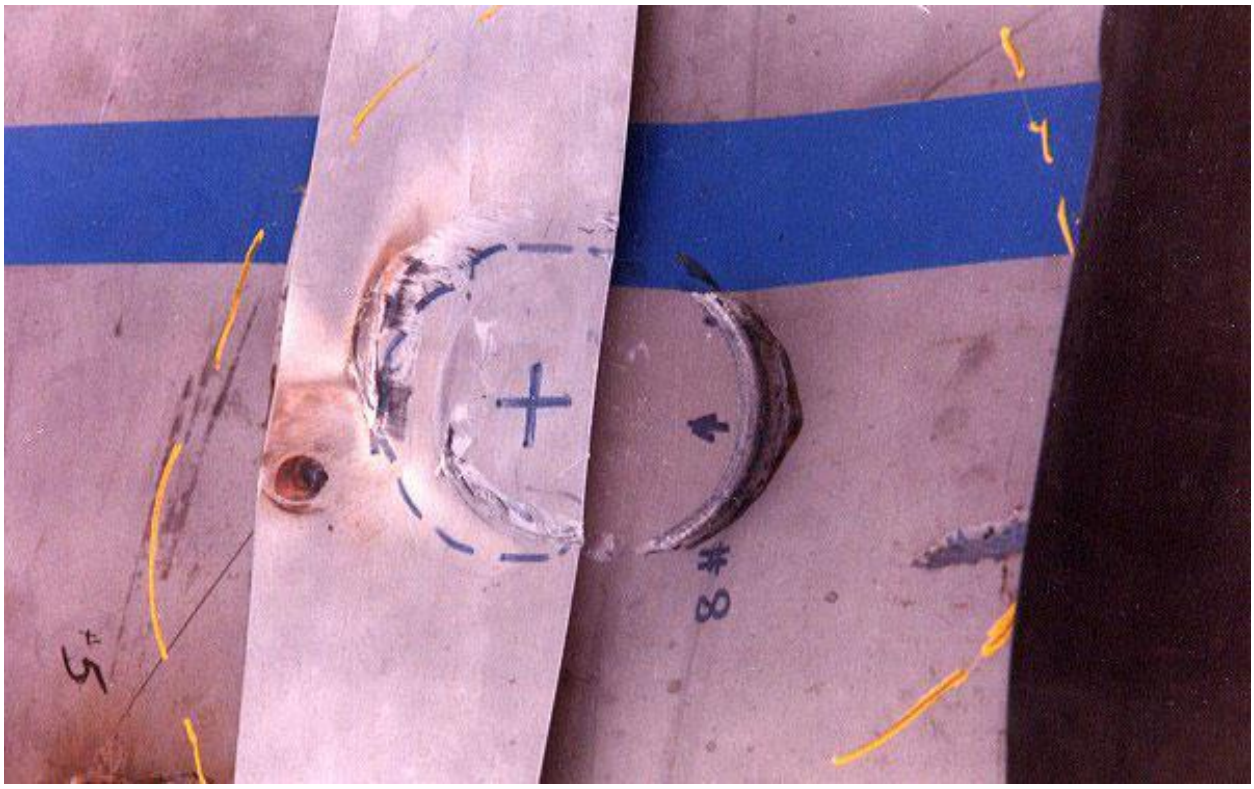

Figure 2.10.3-73 – CTU-2 Puncture Drop 8; Post-Drop Damage

Figure 2.10.3-74 – CTU-2 Fire No. 9; Pre-Fire Positioning

Figure 2.10.3-75 – CTU-2 Fire No. 9; Pre-Fire Positioning

Figure 2.10.3-76 – CTU-2 Fire No. 9; Starting Fire

Figure 2.10.3-77 – CTU-2 Fire No. 9; Post-Fire Cool-Down

Figure 2.10.3-78 – CTU-2 Disassembly; Loose Debris in ICV Lid

Figure 2.10.3-79 – CTU-2 Disassembly; Debris Contaminating the ICV Main O-ring Seals

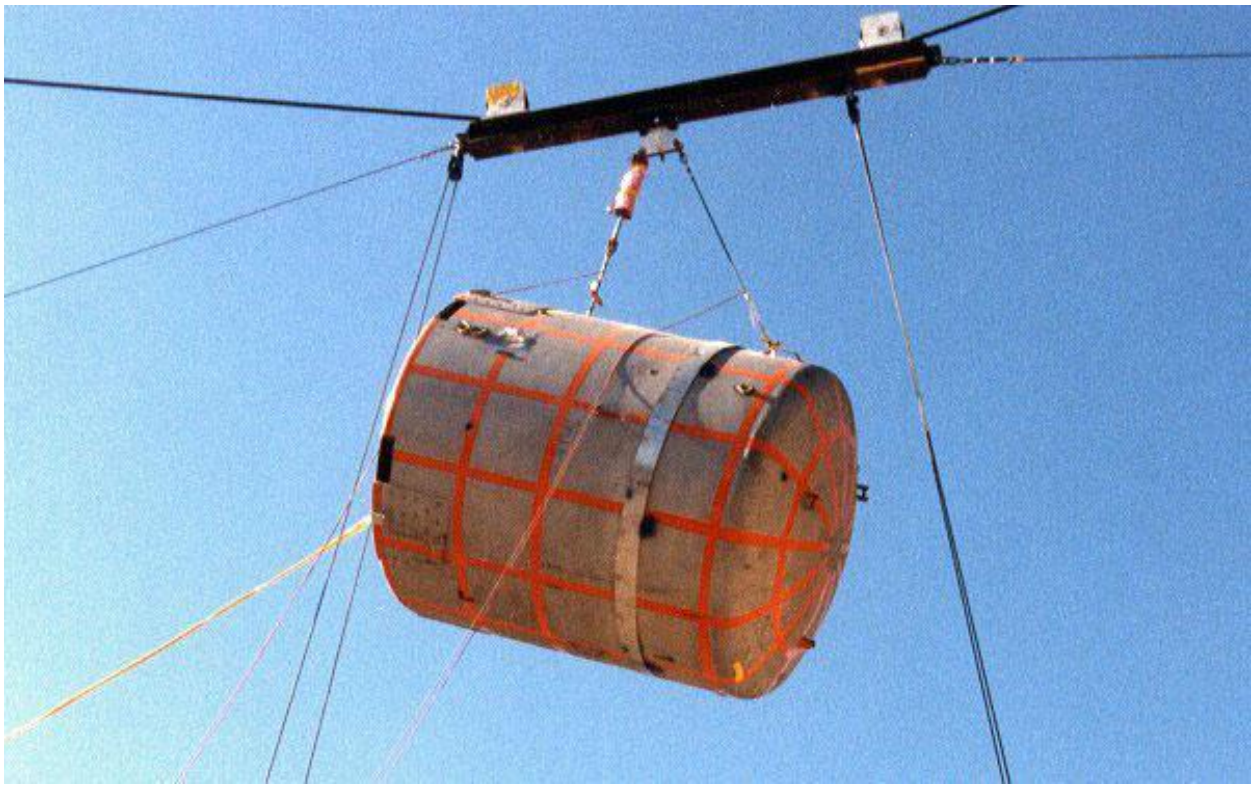

Figure 2.10.3-80 – CTU-3 Free Drop No. 1; Pre-Drop Positioning

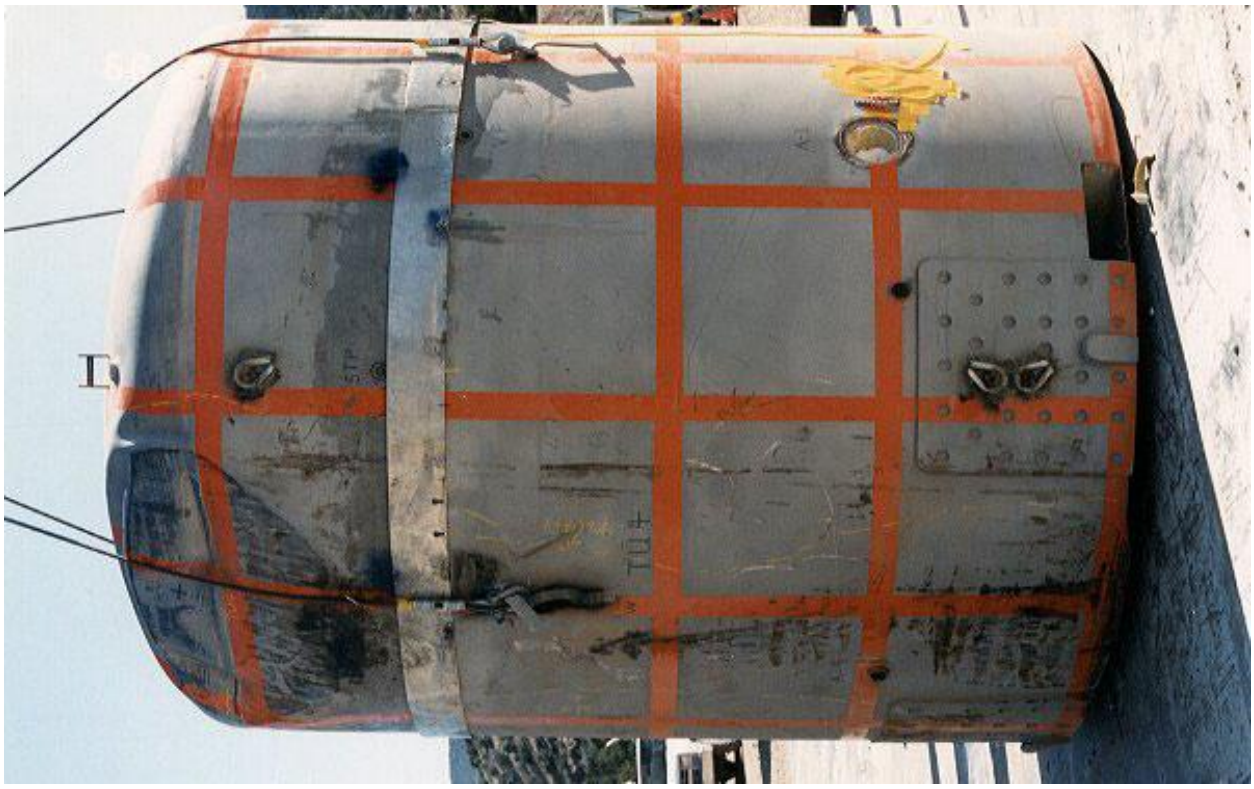

Figure 2.10.3-81 – CTU-3 Free Drop No. 1; Post-Drop Damage

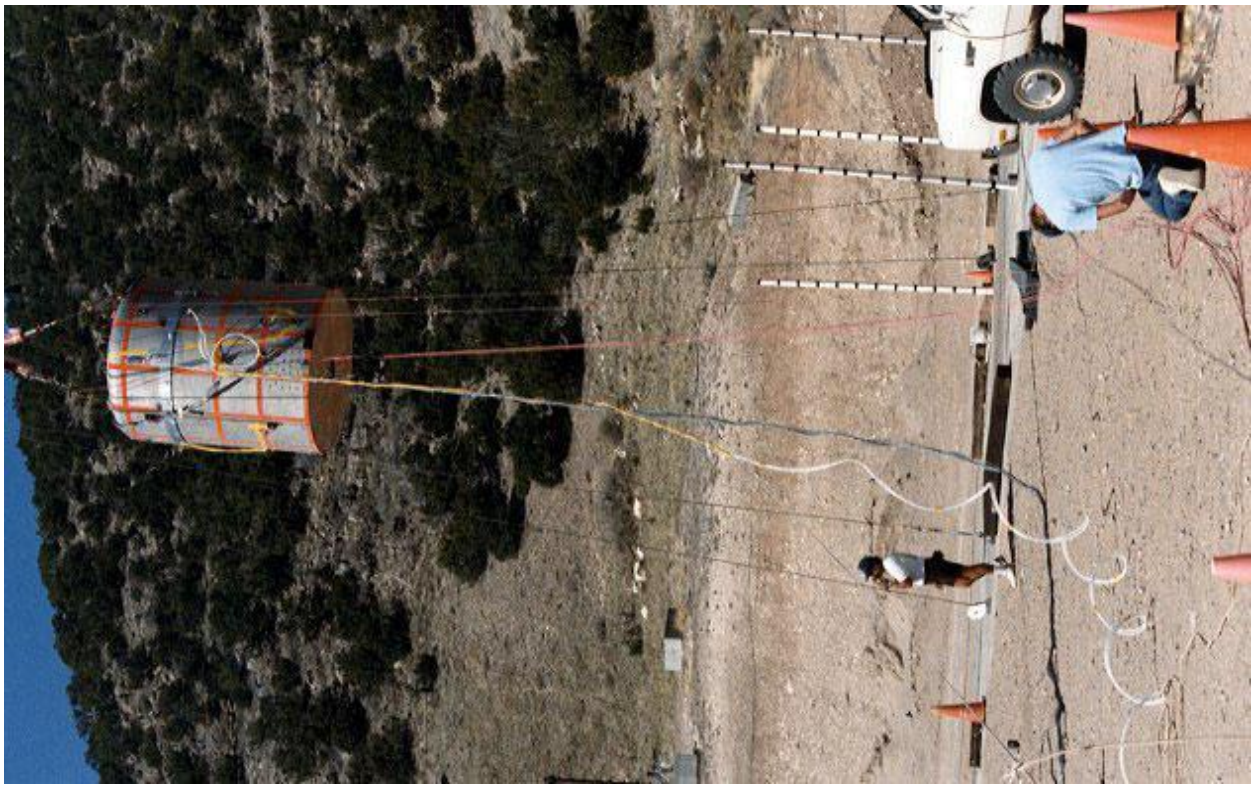

Figure 2.10.3-82 – CTU-3 Free Drop No. 2; Pre-Drop Positioning

Figure 2.10.3-83 – CTU-3 Free Drop No. 2; Post-Drop Damage

Figure 2.10.3-84 – CTU-3 Free Drop No. 3; Pre-Drop Positioning

Figure 2.10.3-85 – CTU-3 Free Drop No. 3; Post-Drop Damage

Figure 2.10.3-86 – CTU-3 Puncture Drop No. 4; Pre-Drop Positioning

Figure 2.10.3-87 – CTU-3 Puncture Drop 4; Post-Drop Damage

Figure 2.10.3-88 – CTU-3 Puncture Drop No. 5; Pre-Drop Positioning

Figure 2.10.3-89 – CTU-3 Puncture Drop 5; Post-Drop Damage

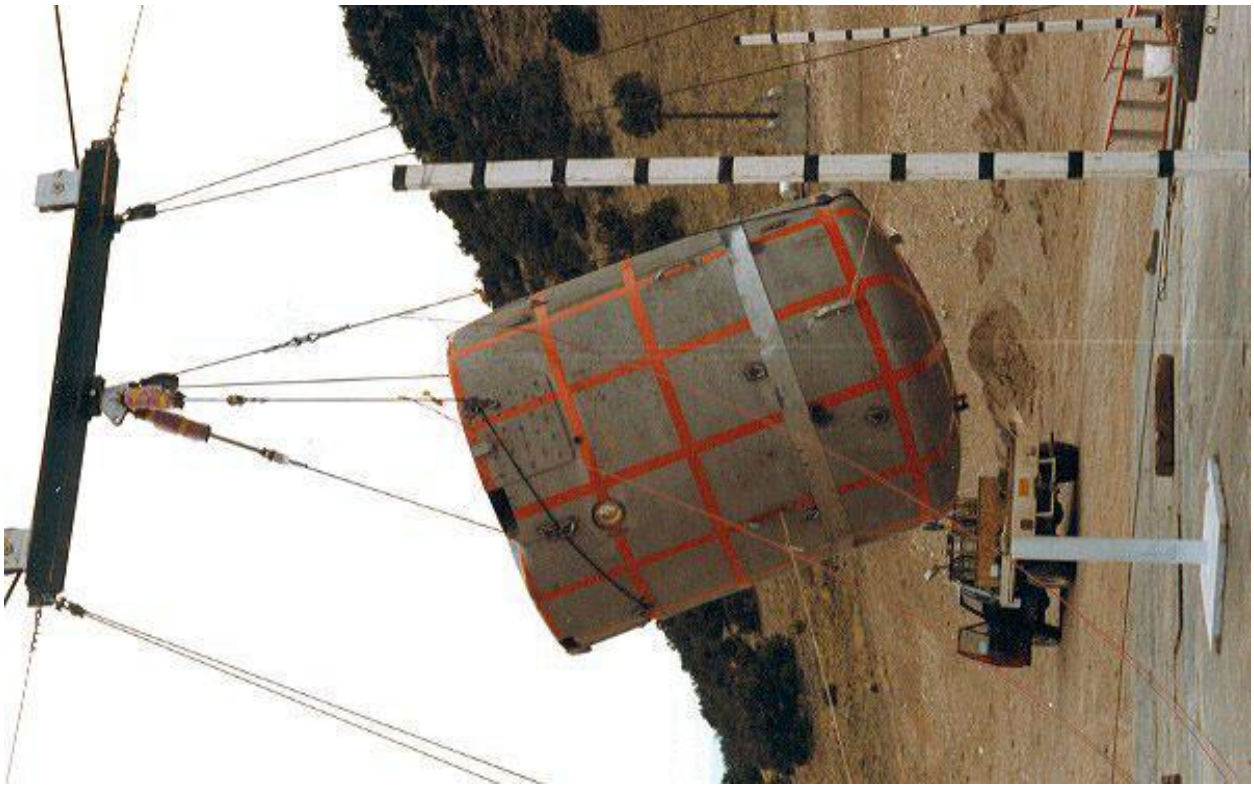

Figure 2.10.3-90 – CTU-3 Puncture Drop No. 6; Pre-Drop Positioning

Figure 2.10.3-91 – CTU-3 Puncture Drop 6; Post-Drop Damage

Figure 2.10.3-92 – CTU-3 Puncture Drop No. 7; Pre-Drop Positioning

Figure 2.10.3-93 – CTU-3 Puncture Drop 7; Post-Drop Damage

Figure 2.10.3-94 – CTU-3 Puncture Drop No. 8; Pre-Drop Positioning

Figure 2.10.3-95 – CTU-3 Puncture Drop 8; Post-Drop Damage

Figure 2.10.3-96 – CTU-3 Disassembly; OCA Lid

Figure 2.10.3-97 – CTU-3 Disassembly; OCA Body

Figure 2.10.3-98 – CTU-3 Disassembly; ICV Lid Removal

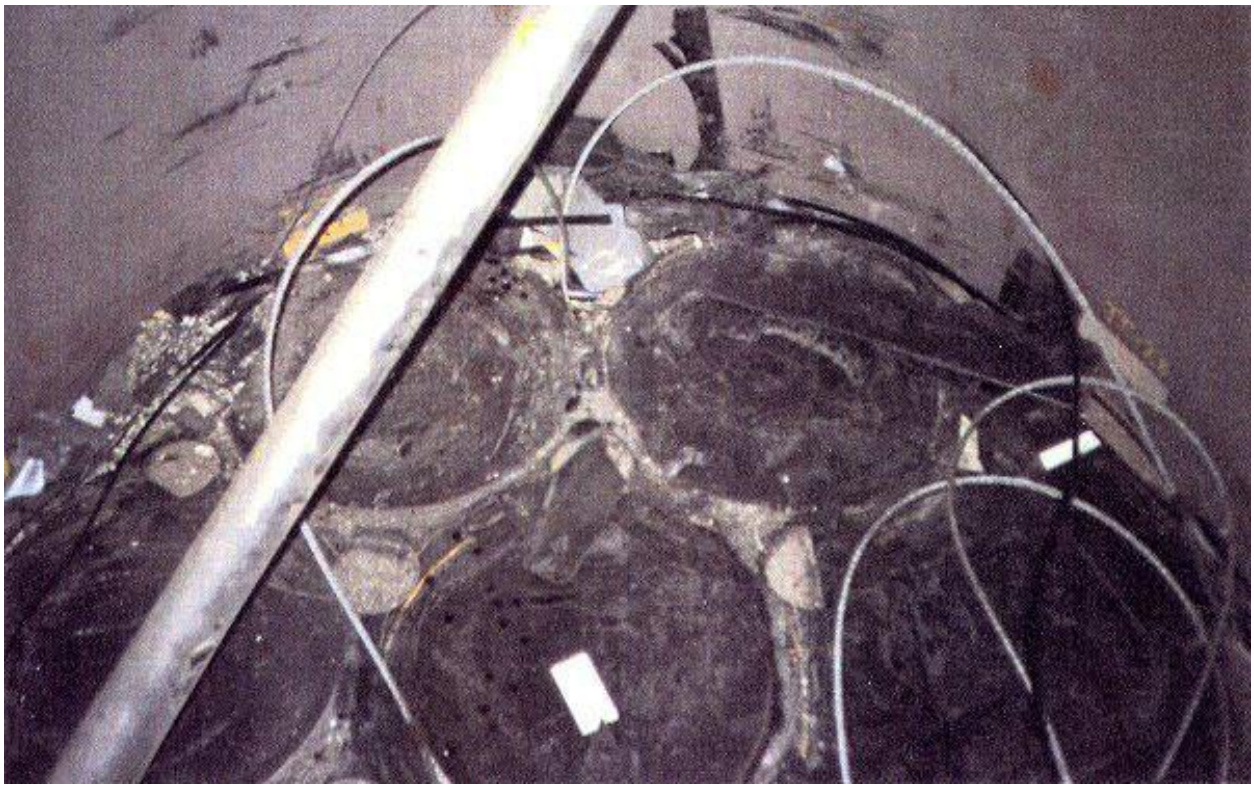

Figure 2.10.3-99 – CTU-3 Disassembly; Loose Debris on Pallet in ICV Body

This page intentionally left blank.

3.0 THERMAL EVALUATION

This chapter identifies and describes the principal thermal design aspects of the TRUPACT-II package. This chapter further demonstrates the thermal safety of the system and compliance with the thermal requirements of 10 CFR 71[1] when transporting a payload generating a maximum of 40 watts decay heat. Specifically, per 10 CFR §71.43(g), the maximum accessible package surface temperature is shown to be less than 122 ºF during normal conditions of transport (NCT). The bulk temperature of the impact absorbing, polyurethane foam is shown to be less than 160 ºF based on NCT maximum temperature conditions thereby retaining sufficient structural integrity to protect the payload during the subsequent hypothetical accident condition (HAC) drop scenarios described in Chapter 2.0, *Structural Evaluation*. Finally, the maximum HAC containment seal temperature of 260 ºF is sufficiently below the seal material limit to ensure containment integrity.

All details relating to payloads and payload preparation for shipment in a TRUPACT-II package are presented in the *Contact-Handled Transuranic Waste Authorized Methods for Payload Control* (CH-TRAMPAC)[2].

3.1 Discussion

3.1.1 Packaging

The TRUPACT-II packaging is designed with a totally passive thermal system. As illustrated in Figure 1.1-1 and Figure 1.1-2 from Section 1.1, *Introduction*, the principal thermal characteristic of the TRUPACT-II package is that it does not contain the relatively thick steel shells and lead shielding typical of other shipping packages. Instead, the TRUPACT-II packaging utilizes two relatively thin containment vessels with shell thicknesses of 3/16 and 1/4 inch. Use of thin shells means that the thermal response of the packaging shells to transient heat input is more rapid than for conventional, heavy walled packages. This characteristic is significantly offset by the unusually large, insulating capability of the polyurethane foam tending to isolate, or decouple, interior responses from temperature variations due to exterior transients. The outer surface of these shells may be painted. The analyses herein use unpainted surface (i.e., bare stainless steel) thermal properties. Since painted surfaces have higher emissivities that allow for better decay heat rejection than unpainted surfaces, the use of unpainted surface thermal properties is conservative.

Both the inner containment vessel (ICV) and the outer containment vessel (OCV) are constructed of Type 304 stainless steel. As discussed in Section 1.2, *Package Description*, the ICV has a 72⅝ inch inside diameter, and the OCV has a 73⅝ inch inside diameter and is completely encased in polyurethane foam with a density of approximately 8¼ lb/ft^3. The foam provides impact protection for the NCT and HAC drop events, and thermal protection during the subsequent HAC thermal event. The 1/4-to-3/8 inch thick outer shell of the outer containment

[1] Title 10, Code of Federal Regulations, Part 71 (10 CFR 71), *Packaging and Transportation of Radioactive Material*, 01-01-07 Edition.

[2] U.S. Department of Energy (DOE), *Contact-Handled Transuranic Waste Authorized Methods for Payload Control* (CH-TRAMPAC), U.S. Department of Energy, Carlsbad Field Office, Carlsbad, New Mexico.

assembly (OCA) is comprised of Type 304 stainless steel that serves to protect the polyurethane foam from damage encountered during normal handling and shipping operations.

3.1.2 Payload Configuration

As described in Section 1.1, *Introduction*, the TRUPACT-II packaging is designed to carry five different payload configurations. The first payload configuration consists of fourteen 55-gallon drums arranged on one pallet. The drums are arranged by placing six drums symmetrically around a seventh, center drum, in two layers of seven drums each. Figure 2.9-2 of the *Contact-Handled Transuranic Waste Authorized Methods for Payload Control* (CH-TRAMPAC)[3] illustrates the arrangement of the fourteen, 55-gallon drums. This fourteen drum configuration represents the bounding thermal case for the TRUPACT-II package due to the center drum being insulated from the package side wall by six peripheral drums, and due to their smaller relative size, a higher volumetric heat generation than the other payload configurations described below.

Four polyethylene sheets (a molded, bottom slip sheet, and a flat, top reinforcing plate for each set of seven drums) may be used for handling operations (as an option, the bottom slip sheets may be of cardboard). In addition, optional polyethylene plastic wrap may be used to provide greater stability for the payload drums once loaded on the pallet. Calculations show that as many as eighteen layers of the clear-to-translucent plastic wrap (each 0.002 inches thick) may be installed around the outside of the drums without having a significant thermal effect (see Appendix 3.6.2.2, *Polyethylene Plastic Wrap Transmittance Calculation*). The plastic wrap may also overlap the top of the drums by a few inches. As an option, steel banding straps may be used around the outside of the payload drums instead of the polyethylene stretch wrap to maintain drum stability.

The second payload configuration consists of two 37 inch tall standard waste boxes (SWBs) designed specifically for this type of packaging. Figure 2.9-17 of the CH-TRAMPAC illustrates the two SWB arrangement. This configuration does not represent a bounding thermal condition due to its relatively large size corresponding to a lower volumetric heat generation rate in comparison to the fourteen 55-gallon drum payload configuration; however, analyses for SWBs are included herein.

The third payload configuration consists of eight 85-gallon drums, which range in dimensions to yield 75 to 88 gallons. Figure 2.9-10 of the CH-TRAMPAC illustrates the arrangement of eight short 85-gallon drums. As with the 55-gallon drums, both top and bottom polyethylene sheets may be used for handling operations (as an option, the bottom slip sheet may be of cardboard). In addition, the 85-gallon drums may be banded together with either polyethylene plastic wrap or steel banding straps. Similarly, this configuration does not represent a bounding thermal condition since all of the drums are adjacent to the package side wall resulting in cooler payload drum temperatures. Thus, presentation of the 85-gallon drum payload evaluation is not explicitly included herein.

The fourth payload configuration consists of six 100-gallon drums. Figure 2.9-14 of the CH-TRAMPAC illustrates the arrangement of six 100-gallon drums. As with the 55-gallon drums, both top and bottom polyethylene sheets may be used for handling operations. In addition, the 100-gallon drums may be banded together with either polyethylene plastic wrap or steel banding straps.

[3] U.S. Department of Energy (DOE), *Contact-Handled Transuranic Waste Authorized Methods for Payload Control* (CH-TRAMPAC), U.S. Department of Energy, Carlsbad Field Office, Carlsbad, New Mexico.

Similarly, this configuration does not represent a bounding thermal condition since all of the drums are adjacent to the package side wall resulting in cooler payload drum temperatures. Thus, presentation of the 100-gallon drum payload evaluation is not explicitly included herein.

The fifth payload configuration consists of a ten drum overpack (TDOP). Figure 2.9-20 of the CH-TRAMPAC illustrates the arrangement of the TDOP. Similarly, this configuration does not represent a bounding thermal condition since the TDOP is adjacent to the package side wall resulting in cooler payload temperatures. Thus, presentation of the TDOP payload evaluation is not explicitly included herein.

Based on the wide variety of payloads for the TRUPACT-II, the analyses presented herein use a bounding thermal payload of 40 thermal watts per package[4] uniformly distributed in one or more payload container(s) combined with a conservatively low payload conductivity commensurate with that of loosely packed paper. Actual payload decay heat is typically far less than 40 watts. Additionally, high heat payloads typically have correspondingly higher thermal conductivities than loosely packed paper, so a combination of low conductivity with a uniform heat generation will lead to conservatively upper bounded temperature predictions. Five steady-state thermal analysis cases are presented based on decay heat distributions as follows:

1. Fourteen 55-gallon drums with all the decay heat distributed uniformly in all fourteen drums (Case 1),
2. Fourteen 55-gallon drums with all the decay heat distributed uniformly in the top and bottom center drums (Case 2),
3. Fourteen 55-gallon drums with all the decay heat distributed uniformly within the top center drum (Case 3),
4. Two SWBs with all the decay heat distributed uniformly in the top and bottom SWB (Case 4) and,
5. Two SWBs with all the decay heat distributed uniformly in the top SWB (Case 5).

3.1.3 Boundary Conditions

The heat transfer characteristics of the TRUPACT-II packaging are evaluated for the bounding payload configuration under three thermal boundary conditions. These conditions are:

A. Steady-state conditions at an ambient temperature of 100 ºF, with insolation as defined in 10 CFR §71.71(c)(1), and

B. Steady-state conditions at an ambient temperature of 100 ºF, without insolation as an initial condition to the hypothetical accident condition (HAC) thermal event. The basis for excluding insolation as an initial condition to the HAC thermal event is discussed further in Section 3.5, *Thermal Evaluation for Hypothetical Accident Conditions*.

C. Steady-state conditions at an ambient temperature of -40 ºF, without insolation as described in 10 CFR §71.71(c)(1).

[4] U.S. Department of Energy (DOE), *Contact-Handled Transuranic Waste Authorized Methods for Payload Control* (CH-TRAMPAC), U.S. Department of Energy, Carlsbad Field Office, Carlsbad, New Mexico, Section 5.0, *Gas Generation Requirements*.

Note that 10 CFR §71.43(g) stipulates that for non-exclusive use packages, maximum accessible surface temperatures must be less than 122 ºF for a package under 100 ºF ambient conditions without insolation. Package temperatures prior to the start of the HAC thermal event are based on this condition, and are presented in Table 3.5-1 from Section 3.5.3, *Package Temperatures*.

Maximum steady-state package temperatures with insolation are determined by using a combination of solar heating values. An analysis is made using the insolation values delineated in 10 CFR §71.71(c)(1), averaged over 24 hours. This action is intended to simulate the slow thermal response that the payload and internal package components have to a varying (i.e., cyclic) solar load. The relatively large thermal mass on the inside of the polyurethane foam insulation isolates (i.e., decouples) the "12 hour on / 12 hour off" solar step function cycle applied to the outside of the foam insulation. Thus, components on the inside of the polyurethane foam use the insolation values of 10 CFR §71.71(c)(1), averaged over 24 hours.

In contrast, the outer sections of the polyurethane foam and the OCA outer shell will respond much more quickly to varying external solar loads. As such, the maximum steady-state temperatures of the polyurethane foam and OCA outer shell are estimated using the 10 CFR §71.71(c)(1) insolation values averaged over 12 hours thereby resulting in a more accurate estimate of the maximum external temperature during the "12 hour on" solar cycle. Table 3.1-1 presents results from both analyses, depending on the packaging component being considered.

Package performance and resulting component temperatures, when subjected to the hypothetical accident thermal event as described in 10 CFR §71.73(c)(4), are determined via full scale fire testing of the TRUPACT-II packaging, and are discussed in Section 3.5, *Thermal Evaluation for Hypothetical Accident Conditions*.

3.1.4 Analysis Summary

The primary heat transfer mechanisms utilized in the thermal analyses are conduction and radiation from component to component within the TRUPACT-II packaging, and convection and radiation from the exterior of the packaging to the ambient. Due to the relatively close coupling of the bodies within the package, convective heat transfer within the payload cavity is conservatively neglected. As discussed in Section 3.2, *Summary of Thermal Properties of Materials*, the thermal conductivity of the material inside the drums is conservatively chosen to be that of still air, based on the assumption of loosely packed paper. The following sections present these analyses in greater detail.

In all cases, the steady-state heat transfer analyses are performed using the Martin Marietta Interactive Thermal Analysis System (MITAS-II) computer program[5].

Table 3.1-1 through Table 3.1-4 present a summary of the temperatures determined by the steady-state heat transfer analyses for the major components of the TRUPACT-II packaging for the five payload configurations with the maximum internal decay heat of 40 thermal watts. Temperatures denoted as "average" use volume-based weighting of the nodal temperatures to determine the average. Further details of these analyses are presented in Section 3.4, *Thermal Evaluation for Normal Conditions of Transport*.

[5] *Martin Marietta Interactive Thermal Analysis System (MITAS-II)*, Version 2.0, May 1976, Martin Marietta Corporation, Denver, Colorado, 80201.

Discussion of HAC fire testing is provided in Section 3.5, *Thermal Evaluation for Hypothetical Accident Conditions*. From the certification test results, the maximum containment seal temperatures are 260 ºF for the OCV seals and 200 ºF for the ICV seals. All seal temperatures are shown to be well below the 350 ºF temperature limit for short term exposure.

Table 3.1-1 – NCT Steady-State Temperatures with 40 Watts Decay Heat Load and Insolation; Fourteen 55-Gallon Drums

Location	Solar Loading	Temperature (ºF)			
		Case 1	Case 2	Case 3	Max Allowable
Center Drum Centerline					
• Maximum	24 hr avg	167	245	334	N/A
• Average	24 hr avg	163	240	239	N/A
Center Drum Wall					
• Maximum	24 hr avg	154	159	162	N/A
• Average	24 hr avg	150	154	153	N/A
Outer Drum Centerline					
• Maximum	24 hr avg	165	153	155	N/A
• Average	24 hr avg	162	150	149	N/A
Outer Drum Wall					
• Maximum	24 hr avg	154	157	160	N/A
• Average	24 hr avg	149	149	148	N/A
Average All Drums					
• Centerline	24 hr avg	162	163	162	N/A
• Wall	24 hr avg	149	150	149	N/A
ICV Wall					
• Maximum	24 hr avg	149	149	156	N/A
• Average	24 hr avg	146	146	145	N/A
• Minimum	24 hr avg	142	143	133	N/A
ICV Air					
• Average	24 hr avg	148	149	148	N/A
ICV Main O-ring Seal					
• Maximum	24 hr avg	146	146	150	225
OCV Wall					
• Maximum	24 hr avg	148	148	154	N/A
OCV Main O-ring Seal					
• Maximum	24 hr avg	143	143	145	225
Polyurethane Foam					
• Maximum	12 hr avg	155	155	155	N/A
OCA Outer Shell					
• Maximum	12 hr avg	155	155	155	N/A

Table 3.1-2 – NCT Steady-State Temperatures with 40 Watts Decay Heat Load and No Insolation; Fourteen 55-Gallon Drums

Location	Temperature (ºF)			
	Case 1	Case 2	Case 3	Max Allowable
Center Drum Centerline				
• Maximum	141	220	308	N/A
• Average	138	215	214	N/A
Center Drum Wall				
• Maximum	128	134	137	N/A
• Average	125	129	128	N/A
Outer Drum Centerline				
• Maximum	139	127	128	N/A
• Average	136	124	123	N/A
Outer Drum Wall				
• Maximum	128	131	133	N/A
• Average	124	124	123	N/A
Average All Drums				
• Centerline	137	137	136	N/A
• Wall	124	125	124	N/A
ICV Wall				
• Maximum	123	123	128	N/A
• Average	121	121	120	N/A
• Minimum	118	117	113	N/A
ICV Air				
• Average	123	123	122	N/A
ICV Main O-ring Seal				
• Maximum	118	117	122	225
OCV Wall				
• Maximum	122	122	126	N/A
OCV Main O-ring Seal				
• Maximum	114	114	117	225
Polyurethane Foam				
• Maximum	122	122	126	N/A
OCA Outer Shell				
• Maximum	102	102	102	N/A

Table 3.1-3 – NCT Steady-State Temperatures with 40 Watts Decay Heat Load and Insolation; Two Standard Waste Boxes

Location	Solar Loading	Temperature (ºF)		
		Case 4	Case 5	Max Allowable
SWB Centerline				
• Maximum	24 hr avg	239	328	N/A
• Average	24 hr avg	238	236	N/A
SWB Wall				
• Maximum	24 hr avg	150	154	N/A
• Average	24 hr avg	148	148	N/A
ICV Wall				
• Maximum	24 hr avg	148	153	N/A
• Average	24 hr avg	146	146	N/A
• Minimum	24 hr avg	144	138	N/A
ICV Air				
• Average	24 hr avg	148	147	N/A
ICV Main O-ring Seal				
• Maximum	24 hr avg	146	150	225
OCV Wall				
• Maximum	24 hr avg	148	152	N/A
OCV Main O-ring Seal				
• Maximum	24 hr avg	143	145	225
Polyurethane Foam				
• Maximum	12 hr avg	155	155	N/A
OCA Outer Shell				
• Maximum	12 hr avg	155	155	N/A

Table 3.1-4 – NCT Steady-State Temperatures with 40 Watts Decay Heat Load and No Insolation; Two Standard Waste Boxes

Location	Temperature (ºF)		
	Case 4	Case 5	Max Allowable
SWB Centerline			
• Maximum	213	300	N/A
• Average	212	210	N/A
SWB Wall			
• Maximum	124	126	N/A
• Average	123	122	N/A
ICV Wall			
• Maximum	122	125	N/A
• Average	120	120	N/A
• Minimum	118	115	N/A
ICV Air			
• Average	122	121	N/A
ICV Main O-ring Seal			
• Maximum	118	122	225
OCV Wall			
• Maximum	121	123	N/A
OCV Main O-ring Seal			
• Maximum	114	116	225
Polyurethane Foam			
• Maximum	121	123	N/A
OCA Outer Shell			
• Maximum	102	102	N/A

This page intentionally left blank.

3.2 Summary of Thermal Properties of Materials

The TRUPACT-II packaging is fabricated primarily of Type 304 stainless steel, 6061-T6 aluminum, polyurethane foam, and ceramic fiber paper insulation. The payload containers (i.e., the 55-gallon drums, 85-gallon drums, 100-gallon drums, SWBs, and a TDOP) are constructed of carbon steel, and may be painted or galvanized.

The payload is expected to consist of a combination of low decay heat, non-solidified organically-based material, and higher decay heat, solidified organic or inorganically-based material as described in Section 5.0 of the *Contact-Handled Transuranic Waste Authorized Methods for Payload Control* (CH-TRAMPAC)[1]. Analyses presented herein assume a thermally conservative (i.e., very low thermal conductivity; analyzed as still air) payload of loosely packed paper with a maximum total decay heat of 40 watts. This assumption combines the low conductivity of a paper-based payload with the highest decay heat load expected from an all-metallic payload to yield the highest and, therefore, the most conservative payload temperatures. For the purposes of the thermal model, the space between the payload containers is conservatively assumed to be still air.

Table 3.2-1 presents the thermal properties used in the heat transfer model and the references from which they are obtained. The thermal conductivity of the ceramic paper insulation used as a liner between the polyurethane foam and the outer containment assembly (OCA) inner and outer shell surfaces is 0.0333 - 0.0358 Btu/hr-ft-ºF. The thermal analysis model ignores the relatively small effect that the ceramic paper insulation would have on the overall conductivity through the package wall. This assumption is valid because the relatively small thickness of the ceramic fiber paper insulation (1/4 inch thick on both the inside and outside shell surfaces) coupled with a thermal conductivity comparable to polyurethane foam (i.e., 0.0333 - 0.0358 Btu/hr-ft-ºF versus 0.0193 Btu/hr-ft-ºF, respectively) tends to minimize the overall effect. Also, using the lower conductivity of the polyurethane foam bounds the temperatures in the NCT steady-state thermal analyses.

Table 3.2-2 presents the thermal conductivity of air. Because the thermal conductivity of air varies significantly with temperature, the computer model calculates the thermal conductivity across air spaces as a function of the mean film temperature. The void spaces within the ICV, and between the ICV and OCV are conservatively assumed filled with one atmosphere air.

Table 3.2-3 presents the important parameters in radiative heat transfer, emissivity (ε) for each radiating surface and solar absorptivity (α) value for the exterior surfaces. The outer shell of the containment assembly (OCA) conservatively uses the lower value of emissivity ($\varepsilon = 0.25$) for the NCT steady-state analyses lower bounding heat transmission in the outward direction thereby conservatively upper bounding the package internal temperatures. Optionally painting the OCA outer surface significantly increases the emissivity; therefore, use of the lower value of emissivity of $\varepsilon = 0.25$ is conservative[2]. Transmittance (τ) of the optional drum polyethylene plastic wrap is discussed in Appendix 3.6.2.2, *Polyethylene Plastic Wrap Transmittance Calculation*.

---

[1] U.S. Department of Energy (DOE), *Contact-Handled Transuranic Waste Authorized Methods for Payload Control* (CH-TRAMPAC), U.S. Department of Energy, Carlsbad Field Office, Carlsbad, New Mexico.

[2] Rohsenow, W. M. and J. P. Hartnett, *Handbook of Heat Transfer*, McGraw-Hill, New York, 1973, Section 15, Table 5. This provides an effective emissivity for painted surfaces from 0.81 for oil based paint on polished iron to 0.95 for enamel based paints. Per Table 3.2-3, the package surface emissivity used in this analysis is 0.25.

Table 3.2-1 – Thermal Properties of Materials

Material	Temperature (ºF)	Thermal Conductivity (Btu/hr-ft-°F)	Specific Heat (Btu/lb-°F)	Density (lb/ft^3)
Stainless Steel, Type 304①	212	9.6	0.11	500
Carbon Steel, A516, Gr. 70②	212	26	0.113	487
Aluminum, 6061-T6①	212	89.5	0.23	169
Polyurethane Foam③	75	0.0193	0.300	8.25
Fiberglass Insulation④	---	0.023	0.160	12.5
Payload①	---	0.02	40	0.2

Notes:

① General Electric Company, *Heat Transfer and Fluid Flow Data Books*, Genium Publishing Company, Schenectady, NY 12303.

② W. M. Rohsenow and J. P. Hartnett, *Handbook of Heat Transfer*, McGraw-Hill, New York, 1973, Chapter 2, Table 28.

③ Thermal conductivity and specific heat for 8¼ pcf polyurethane foam are documented in Section 8.1.4.1.2.1.5, *Thermal Conductivity*, and Section 8.1.4.1.2.1.6, *Specific Heat*.

④ W. M. Rohsenow and J. P. Hartnett, *Handbook of Heat Transfer*, McGraw-Hill, New York, 1973. Properties for glass wool were used.

Table 3.2-2 – Thermal Properties of Air

Temperature (ºF)	Thermal Conductivity①② (Btu/hr-ft-°F)	Specific Heat①② (Btu/lb-°F)	Density①② (lb/ft^3)
32	0.0140	---	---
100	0.0154	0.240	0.071
200	0.0174	---	---
300	0.0193	---	---
400	0.0212	---	---
500	0.0231	---	---
600	0.0250	---	---
700	0.0268	---	---
800	0.0286	---	---
1,000	0.0319	---	---
1,500	0.0400	---	---

Notes:

① W. M. Rohsenow and J. P. Hartnett, *Handbook of Heat Transfer*, McGraw-Hill, New York, 1973, Chapter 2, Tables 35 and 39, et. al.

② Frank Kreith, *Principles of Heat Transfer*, 3rd Edition, Intext Press, Inc., 1973, Table A-3.

Table 3.2-3 – Thermal Radiative Properties

Material	Emissivity	Absorptivity	Transmittance
Stainless Steel①	0.25	0.50	---
Painted Carbon Steel②	0.80	---	---
Aluminum Honeycomb③	0.30	---	---
Plastic Shrink Wrap④	---	---	0.75
Ambient Environment	1.00	---	---

Notes:

① Nuclear Packaging, Inc., *Emissivity of Metal Surfaces*, Report No. 2-2623-2-RF-C86-349, August 21, 1986.

② General Electric Company, *Heat Transfer and Fluid Flow Data Books, et. al.*, Genium Publishing Company, Schenectady, NY 12303. The emissivity for painted surfaces ranges from 0.53 to 0.98, depending on pigment color and surface temperature.

③ Ibid.

④ Y.S. Touloukian and C.Y. Ho, Editors, *Thermophysical Properties of Matter*, Thermophysical Properties Research Center (TPRC) Data Series, Purdue University, 1970, IFI/Plenum, New York.

This page intentionally left blank.

3.3 Technical Specifications of Components

The materials used in the TRUPACT-II packaging that are considered temperature sensitive are the butyl O-ring seals and the polyurethane foam.

The butyl rubber O-ring seals are fabricated of Rainier Rubber compound RR0405-70[1], or equivalent meeting the requirements of ASTM D2000 M4AA710 A13 B13 F17 F48 Z Trace Element. Butyl rubber sealing material has a working temperature range of -65 ºF to 225 ºF[2], and have a short duration (8 hours) temperature range of 400 ºF. Developmental O-ring seal testing, conducted as part of the TRUPACT-II packaging program and presented in Appendix 2.10.2, *Elastomer O-ring Seal Performance Tests*, discusses the butyl rubber O-ring seal's performance at reduced and elevated temperatures. Further developmental O-ring seal testing was conducted as part of the Radioisotope Thermoelectric Generator (RTG) Transportation System Packaging[3] design effort. This testing demonstrated that this specific butyl rubber compound has a peak temperature rating of 380 ºF, minimum, for durations of 24 hours or less. Operation at temperatures between 350 ºF and 380 ºF may be allowed for longer durations, decreasing as a function of increasing temperature.

The NCT temperature range for the polyurethane foam material is -40 ºF to 300 ºF, per the foam manufacturer's recommendations[4]. Polyurethane foam is not subject to degradation with age when encased within the stainless steel shells of the OCA. Foam strength sensitivity to temperatures is addressed in Section 2.5, *Lifting and Tie-down Standards for All Packages*, Section 2.6, *Normal Conditions of Transport*, and Section 2.7, *Hypothetical Accident Conditions*.

The ceramic fiber paper, comprised almost entirely (>99%) of Al_2O_3 and SiO_2 in approximately 50/50 proportions, has a maximum use temperature of 2,300 ºF and a melting point of 3,260 ºF. Like the polyurethane foam, this essentially inert material is not subject to degradation with age when encased within the stainless steel shells of the OCA.

The other primary packaging materials are stainless steel and aluminum. The melting point for each of these materials is 2,600 ºF and 1,100 ºF, respectively. Carbon steel used for the payload

---

[1] Rainier Rubber Company, Seattle, WA.

[2] Rainier Rubber Company, Company Standard Compounds, http://www.rainierrubber.com, Seattle, WA.

[3] DOE Docket No. 94-6-9904, *Radioisotope Thermoelectric Generator Transportation System Safety Analysis Report for Packaging*, WHC-SD-RTG-SARP-001, prepared for the U.S. Department of Energy Office of Nuclear Energy under Contract No. DE-AC06-87RL10930 by Westinghouse Hanford Company, Richland, WA. Per Appendix 2.10.6, elevated temperature tests were performed on Rainier Rubber Company butyl rubber compound No. RR-0405-70 O-ring seals with seal compressions as low as 10%. The specific time-temperature test parameters evaluated were 380 ºF for 24 hours followed by 350 ºF for 144 hours, for a total of 168 hours (1 week). At these temperatures, all elastomeric compounds are susceptible to relatively high helium permeability; thus, helium leakage rate testing was not performed. Instead, a hard vacuum of less than 0.0029 psia (20 Pa) was maintained on the test O-ring seals with no measurable pressure loss that would indicate leakage. At the end of the entire test sequence, the test O-ring seals were stabilized at -20 ºF and shown, via helium leakage rate testing, to be leaktight (i.e., a leakage rate less than 1×10^{-7} standard cubic centimeters per second (scc/s), air leakage).

[4] *LAST-A-FOAM FR-3700 for Crash and Fire Protection of Nuclear Material Shipping Containers,* General Plastics Manufacturing Company, P.O. Box 9097, Tacoma, WA.

containers has a melting temperature of approximately 2,750 ºF. Polyethylene plastic wrap has a melting temperature of approximately 250 ºF. Loss of the plastic wrap is of no consequence to the safety of the TRUPACT-II package since its effect on conductive and radiative heat transfer is negligible, as discussed in Appendix 3.6.2.2, *Polyethylene Plastic Wrap Transmittance Calculation*. Similarly, the loss of items such as foam rubber padding or plastic sheets have negligible impact on the package thermal performance.

3.4 Thermal Evaluation for Normal Conditions of Transport

This section presents the steady-state thermal analyses of the TRUPACT-II package for normal conditions of transport (NCT). Under NCT, the package is mounted in an upright position on its transport trailer or railcar. This establishes the orientation of the exterior surfaces of the package for determining the free convection heat transfer coefficients and insolation loading. In addition, the bottom of the dedicated transport trailer is open to free air. Thus, the bottom of the TRUPACT-II package would be exposed to ambient air instead of resting on the ground or some other semi-adiabatic, conducting surface.

The thermal conditions that are considered for NCT are those specified in 10 CFR §71.71(c)(1)[1]. Accordingly, a 100 ºF ambient temperature with the following insolation values are used for heat input to the exterior package surfaces. Note that the flat base of the package has no insolation; all other surfaces, since they are curved, have an insolation value of 400 gcal/cm^2 (1,475 Btu/ft^2).

Form and Location of Surface	Total Insolation for a 12-Hour Period	
	(gcal/cm^2)	(Btu/ft^2)
Flat surfaces transported horizontally:		
• Base	None	None
• Other surfaces	800	2,950
Flat surfaces not transported horizontally	200	737.5
Curved surfaces	400	1,475

3.4.1 Thermal Model

3.4.1.1 Analytical Model

Figure 3.4-1 through Figure 3.4-4 illustrate the location of the thermal nodes used in the analytical model of the TRUPACT-II package and its two alternative payload configurations. The location and the number of thermal nodes are chosen to achieve an accurate determination of the temperature distribution within the major package components.

The analysis model was constructed using Martin Marietta Interactive Thermal Analysis System (MITAS-II)[2], and utilizes the thermal properties presented in Section 3.2, *Summary of Thermal Properties of Materials*. For purposes of these analyses, constant values of thermal conductivity are used for the metals and the polyurethane foam because their change in conductivity with temperature is relatively small over the NCT temperature range of interest. However, the thermal conductivity for air is computed as a function of the mean film temperature since its conductivity variation is significant.

[1] Title 10, Code of Federal Regulations, Part 71 (10 CFR 71), *Packaging and Transportation of Radioactive Material*, 01-01-07 Edition.

[2] *Martin Marietta Interactive Thermal Analysis System (MITAS-II)*, Version 2.0, May 1976, Martin Marietta Corporation, Denver, Colorado, 80201.

The thermal model represents a two-dimensional axisymmetric model of the packaging and its payload. The two bounding payloads, described in Section 3.1.2, *Payload Configuration*, consist of a uniform payload of low conductivity and uniform heat distribution. Sensitivity studies have shown that, with a maximum total decay heat load of 40 watts, the placement of the payload within the TRUPACT-II packaging cavity has a negligible effect on component maximum temperatures.

As seen from Figure 3.4-1, a two-dimensional, axisymmetric model consisting of 154 nodes is used to represent the TRUPACT-II packaging. The model is spread over five (5) axial stations for the package and four (4) axial stations for the payload. In addition, a one-dimensional model is used to represent the polyurethane foam on each end of the package. Approximately 400 linear and non-linear conductors are used in constructing the thermal model. Increased resolution is utilized in the outer containment vessel (OCV) and inner containment vessel (ICV) sealing regions to enhance the accuracy of seal temperature predictions (refer to Figure 3.4-2).

Figure 3.4-3 and Figure 3.4-4 illustrate the thermal model used for the 55-gallon drum and SWB payload configurations, respectively. To account for the non-symmetric effects that occur within the drum-based payload configuration, a quasi-three-dimensional model (i.e., a three-dimensional model with symmetry planes along adiabatic boundaries) of the drums is used. Using the quasi-three-dimensional model with the drum-based payload configuration provides a simplified, yet accurate representation of the packaging as each analysis assumes the heat is either uniformly distributed in all fourteen drums, in both center drums, or in one center drum. Thus, with none of the outer drums loaded in an anti-symmetric configuration, the heat transfer out of the package is completely radial and axial in nature with no outer drum-to-outer drum heat transfer taking place. The drum configuration with all the decay heat in the center drum represents the bounding case. This is because this particular payload configuration has the highest heat concentration within a single drum and six surrounding drums adding an additional insulating barrier.

Heat transfer across air gaps is calculated using a combination of conduction and radiation heat transfer. Since any offset of the ICV within OCV would be relatively small, and would tend to decrease the net thermal resistance across the shells, the ICV and OCV are assumed to be concentric cylinders. Thus, the air gaps separating the side and top of these components are assumed to be uniform with no contacting surfaces. The bottom ICV/OCV interface is separated by a 1/8 inch thick rubber pad. To maximize the insulating properties of this interface, the pad is assumed to behave as a layer of still air without radiative heat transfer (air conduction only).

Both payload configurations are assumed loaded in the ICV cavity with uniform and symmetrical separation from the ICV walls. Again, any eccentricity in the placement of the payload in the package would result in reduced thermal resistance between the payload and cask. Due to the relatively low decay heat load and the narrowness of most gaps and the blockage provided by the pallets, stretch wrap, etc., the model also assumes that no significant internal natural convection paths exist. Free convection of decay heat and solar radiation from the exterior surfaces of the package is computed as a function of temperature and orientation of the surface using standard equations for free convection from vertical and horizontal surfaces. Methodology for calculating convection coefficients is presented in Appendix 3.6.2.1, *Convection Coefficient Calculation*.

The optional polyethylene plastic wrap around the payload drums has a small effect on the radiative heat transfer between the drums and the ICV wall. As discussed in Appendix 3.6.2.2, *Polyethylene*

Plastic Wrap Transmittance Calculation, the interaction of the plastic wrap with regard to the heat transfer process is determined to have a negligible effect and, therefore, is ignored.

3.4.1.2 Test Model

This section is not applicable since NCT thermal tests are not performed.

3.4.2 Maximum Temperatures

The maximum temperatures noted for normal conditions of transportation (i.e., 100 ºF ambient temperature and insolation) are presented in Table 3.4-1 through Table 3.4-5 for the major components of the TRUPACT-II packaging for the two payload configurations at different levels of internal decay heat. Average drum wall temperatures, ICV wall temperatures, and ICV air temperatures are determined using the area-weighted nodal temperatures. A complete listing of nodal temperatures for the evaluated cases is also provided in the Appendix 3.6.1, *Computer Analysis Results*.

3.4.3 Minimum Temperatures

The minimum temperature distribution for the TRUPACT-II package occurs with a zero decay heat load and an ambient air temperature of -40 ºF per 10 CFR §71.71(c)(2). Since the steady-state analysis of this condition represents a trivial case, no thermal calculations are performed. Instead, it is assumed that all package components achieve the -40 ºF temperature under steady-state conditions. As discussed in Section 3.3, *Technical Specifications of Components*, the -40 ºF temperature is within the allowable range of all TRUPACT-II packaging components. As a potential initial condition for all normal or accident events, a minimum uniform temperature of -20 ºF must be considered per 10 CFR §71.71(b) and §71.73(b). Detailed structural analyses considering the effects of minimum temperatures are presented in Section 2.6.2, *Cold*.

3.4.4 Maximum Internal Pressure

The evaluation of the maximum internal pressure for the TRUPACT-II package considers the factors that affect pressure to demonstrate that the pressure increases are below the allowable pressure for the package.

3.4.4.1 Design Pressure

The TRUPACT-II packaging has a design pressure of 50 psig. Chapter 2.0, *Structural Evaluation*, discusses the ability of the package to withstand 50 psig for both normal conditions of transport and hypothetical accident conditions. The ICV or both the OCV and ICV were pressurized to 50 psig in many of the full-scale tests for hypothetical accident conditions as described in Appendix 2.10.3, *Certification Tests*. The maximum normal operating pressure (MNOP) is discussed in Section 3.4.4.3, *Maximum Normal Operating Pressure*.

3.4.4.2 Maximum Pressure for Normal Conditions of Transport

The maximum pressure in the ICV under normal conditions of transport is less than the 50 psig design pressure, as shown by the following analysis. The major factors affecting the ICV internal pressure are radiolytic gas generation, thermal expansion of gases, and the vapor pressure of water within the ICV cavity. Barometric changes that affect the external pressure, and hence the gauge pressure of the TRUPACT-II packaging containment vessels, are bounded

by the regulatory condition of a 3.5 psia external pressure and considered in the use of the 50 psig pressure increase limit. ICV internal pressure would not increase significantly due to chemical reactions, biological gas generation, or thermal decomposition in the payload. For the payload shipping categories qualified for transport by gas generation testing, the maximum pressure increase allowed in the ICV for normal conditions is the 50 psig pressure increase limit.

The maximum pressure in the ICV for all categories is calculated for the maximum shipping period of 60 days. The use of a 60-day shipping period in the calculation of maximum normal operating pressure is consistent with 10 CFR 71.41(c). As specified by 10 CFR 71.41(c), this section shows that the "…controls proposed to be exercised by the shipper are demonstrated to be adequate to provide equivalent safety of the shipment." The use of this shipping period is consistent with the analysis presented in Appendix 3.4 of the *CH-TRU Payload Appendices*[3], which shows that the maximum normal shipping period will be less than 60 days by a large margin of safety. As described in Appendix 3.4 of the *CH-TRU Payload Appendices*, routine monitoring of shipments includes the use of the TRANSCOM system at the Waste Isolation Pilot Plant, which provides continuous tracking of shipments from the shipping site to its destination.

Calculation of maximum pressure in the ICV for all categories considers immediate release of gases from the innermost layer of confinement around the waste to the available void volume of the ICV cavity. The available void volume for accumulation of gas in the ICV is conservatively estimated. The available ICV void volume is the ICV void volume less the volume occupied by the payload assembly. The ICV void volume is the internal volume within the ICV containment boundary less the volume occupied by the materials of construction of the end spacers. Since the end spacers were purposely designed to use perforated aluminum honeycomb, each has a large void volume for gas accumulation.

The volume occupied by the payload assembly is the volume of the payload containers plus the volume occupied by the pallet, slipsheets, reinforcing plates, and guide tubes, if applicable. The estimate of the void volume of the ICV considers only the volume in the ICV outside of the payload containers with no credit for the void volume present within the payload containers except for SWBs overpacking four 55-gallon drums. Since drum payload containers have a significant void volume that has historically averaged over 50% of the internal volume, neglecting the void volume in the payload containers will overestimate the pressure increase in the ICV.

The void volume between the SWB and four overpacked 55-gallon drums is included in the ICV volume for pressure analyses because this SWB overpack configuration is not sealed and the internal void volume is quantifiable. The external volume of a single, steel 55-gallon drum can be calculated based on its internal dimensions, tare weight, and the density of steel as follows:

$$V_{drum} = \left(\frac{\pi}{4} \times D^2 \times H + \frac{W}{\rho} \right) \times \frac{0.01639 \text{ liters}}{\text{inches}^3}$$

[3] U.S. Department of Energy (DOE), *CH-TRU Payload Appendices*, U.S. Department of Energy, Carlsbad Field Office, Carlsbad, New Mexico.

where:

D = Internal diameter of a 55-gallon drum (cubic inches)

H = Internal height of a 55-gallon drum (cubic inches)

W = Tare weight (empty) of a 55-gallon drum (pounds)

ρ = Density of steel (pounds per cubic inch)

Therefore, the external volume of a 55-gallon drum is:

$$V_{drum} = \left(\frac{\pi}{4} \times 22.5^2 \times 33.25 + \frac{60}{0.285}\right) \times \frac{0.01639 \text{ liters}}{\text{inches}^3} = 220 \text{ liters}$$

As shown in Appendix 2.4 of the *CH-TRU Payload Appendices*, the internal void volume of an empty SWB is conservatively taken as 1,750 liters. Subtracting the volume of four overpacked 55-gallon drums from the empty SWB void volume results in an internal void volume of approximately 870 liters per SWB overpack.

The net void volume in the ICV is assumed filled with air at 70 ºF and 14.7 psia when the ICV is sealed for transport. Sufficient water is assumed present for saturated water vapor at any temperature. The pressure increase due to water vapor is obtained from the tabulated thermodynamic properties of saturated water and steam.

The maximum pressure increase analysis for TRUPACT-II payloads can be categorized as follows:

- Analytical category payloads have decay heat limits based on conservative theoretical analyses of flammable gas generation as shown in Section 5.0 of the *Contact-Handled Transuranic Waste Authorized Methods for Payload Control* (CH-TRAMPAC)[4]. These limits are lower than applicable limits for test category wastes and the pressure increase for all analytical category payloads is bound by the test category payloads.
- Test category payloads for which the MNOP can be shown to be below the design pressure by analysis. This analysis is presented in Section 3.4.4.2.1, *MNOP Determination by Analysis*.
- Test category payloads for which the MNOP is limited to the design pressure and compliance is shown by measurement. Derivation of gas generation rates for these cases in compliance with the pressure limit is presented in Section 3.4.4.2.2, *MNOP Determination by Measurement*.

In addition, the following conditions govern the pressure analysis for TRUPACT-II package payloads:

- Waste Material Types I.2, I.3, II.3, III.2, and III.3 have lower G values compared to Waste Material Types I.1, II.1, and III.1, respectively, and will therefore have lower pressure increases.
- The case of the decay heat uniformly distributed in all containers in a payload (versus all decay heat in one container) results in the lowest void volume and bounds the pressure increase calculations (Note that to meet flammable gas generation requirements, the decay heat in a TRUPACT-II with a single drum will be less than the decay heat in a TRUPACT-II package with 14 drums.)

[4] U.S. Department of Energy (DOE), *Contact-Handled Transuranic Waste Authorized Methods for Payload Control* (CH-TRAMPAC), U.S. Department of Energy, Carlsbad Field Office, Carlsbad, New Mexico.

- The evaluation of the thermal analysis for SWBs indicates that the temperatures needed for the pressure analysis for other container types are bounded by the SWB temperatures. Therefore, the use of the SWB temperature versus decay heat curves for payload containers other than 55-gallon drums is considered to be conservative.

3.4.4.2.1 MNOP Determination by Analysis

The method used to calculate the maximum ICV pressure is provided below for an example payload shipping category. The number of moles per second of total gas generated by radiolysis is calculated from the following equation:

$$n_{gen} = G_{eff(T)} \times W \times C$$

where n_{gen} is the rate of radiolytic gas generation (moles/sec), $G_{eff(T)}$ is the temperature-corrected effective G value (the total number of molecules of gas generated per 100 eV of energy emitted (molecules/100 eV) at the temperature of the target material), W is the total decay heat (watts), and the conversion constant for the units used is $C = 1.04(10)^{-5}$ (g-moles)(eV)/(molecule)(watt-sec).

The effective G values are provided in Appendix 3.2 of the *CH-TRU Payload Appendices* for the payload shipping categories. Pressure increase calculations are carried out for the waste material types up to a maximum of 40 watts. The maximum decay heat for each category determines the average contents temperature for that category. As discussed in Appendix 3.2 of the *CH-TRU Payload Appendices*, the effective G values provided at room temperature (RT) are a function of temperature based on the activation energy (E_a) for the material. The effective G values used in the calculation for pressure increase in the ICV are corrected to the average contents temperature for each category using the activation energy of the material in the category that is provided in Appendix 3.2 of the *CH-TRU Payload Appendices*.

For example, the effective G value (total gas) at room temperature for Waste Material Type I.1 is 2.4 (from Appendix 3.2 of the *CH-TRU Payload Appendices*). The temperature-corrected effective G value is calculated using the following equation:

$$G_{(Total,\,T)} = G_{(Total,\,RT)} e^{\left(\frac{E_a}{R}\right)\left(\frac{T - T_{RT}}{(T)(T_{RT})}\right)}$$

where $G_{(Total,\,RT)}$ is the effective G value at room temperature (the number of molecules of gas generated per 100 eV of energy (molecules/100 eV) for target material at room temperature), E_a is the activation energy for the target material, kcal/g-mole, the ideal gas constant $R = 1.99(10)^{-3}$ kcal/g-mole-K, T is the temperature of the target material (the average contents temperature), and the room temperature is T_{RT} = 25 ºC = 298 K.

The temperature-corrected effective G value for Waste Material Type I.1 is calculated at the average contents temperature based on the maximum decay heat for that waste material type. Table 3.4-1 through Table 3.4-5 provide the normal condition, steady state temperatures for decay heat values from 0 to 40 watts for package temperatures of interest including average contents temperatures. From Table 3.4-1, the average contents temperature for a payload of 14 drums with a total payload decay heat of 40 watts is 163.0 ºF. From Appendix 3.2 of the *CH-TRU Payload Appendices*, the activation energy is zero ($E_a = 0$) for water, which is the target material. The temperature corrected effective G-value is:

$$G_{(\text{eff},163.0^\circ\text{F})} = (2.4\ \text{molecules}/100\ \text{eV})e^{\left(\frac{0\ \text{kcal/g-mole}}{1.99(10)^{-3}\ \text{kcal/g-mole-K}}\right)\left(\frac{346\ \text{K}-298\ \text{K}}{(346\ \text{K})(298\ \text{K})}\right)}$$
$$= 2.4\ \text{molecules}/100\ \text{eV}$$

Using this temperature-corrected effective G value, the radiolytic gas generation rate, n_{gen}, is:

$$n_{gen} = (2.4\ \text{molecules}/100\ \text{eV})(40\ \text{watts})[1.04(10)^{-5}\ (\text{g - moles})(\text{eV})/(\text{molecule})(\text{watt - sec})]$$
$$= 9.98(10)^{-6}\ \text{moles/sec}$$

The total number of liters of radiolytic gases that is generated, V_R, when corrected from moles to liters at STP (32 ºF and 1 atmosphere pressure) after 60 days would be:

$$V_R = [n_{gen}](60\ \text{days})\{\text{conversion factors}\}$$
$$= [9.98(10)^{-6}](60)\{(86{,}400\ \text{sec/day})(22.4\ \text{liters/mole})\} = 1{,}158.89\ \text{liters @ STP}$$

The generated volume of radiolytic gases (corrected to STP) is heated to the average ICV gas temperature for normal conditions of transport. The average ICV gas temperature is also available from the TRUPACT-II package temperatures given in Table 3.4-1. For Waste Material Type I.1, the average gas temperature is 148.0 ºF. The radiolytic gas would occupy a volume, V_{rg} of:

$$V_{rg} = (1{,}158.89)\left(\frac{148\ ^\circ\text{F} + 460\ ^\circ\text{R}}{32\ ^\circ\text{F} + 460\ ^\circ\text{R}}\right) = 1{,}432.13\ \text{liters @ } 148\ ^\circ\text{F}$$

For a payload of fourteen 55-gallon drums and an available void volume in the ICV of 2,450 liters, this gas contributes a pressure, p_{rg}, of:

$$p_{rg} = \frac{1{,}432.13}{2{,}450} = 0.58\ \text{atm (8.53 psia) @ } 148\ ^\circ\text{F}$$

The initial volume of gas present in the ICV at 70 ºF and 14.7 psia is also heated to 148.0 ºF for a decay heat of 40 watts. The increased pressure associated with this heat-up, p_{hu}, is:

$$p_{hu} = (14.7\ \text{psia})\left(\frac{148\ ^\circ\text{F} + 460\ ^\circ\text{R}}{70\ ^\circ\text{F} + 460\ ^\circ\text{R}}\right) = 16.86\ \text{psia}$$

The water vapor pressure is based on the temperature of the coolest or condensing surface of the ICV. From Table 3.4-1, the minimum ICV wall temperature is 142 ºF for a decay heat of 40 watts. The corresponding water vapor pressure, p_{wv}, at this temperature is 3.04 psia.

The maximum ICV pressure after 60 days for Waste Material Type I.1, p_{max}, is the sum of the three pressure components less an assumed atmospheric pressure, p_a, of 14.7 psia, or:

$$p_{max} = p_{rg} + p_{hu} + p_{wv} - p_a = 8.53\ \text{psia} + 16.86\ \text{psia} + 3.04\ \text{psia} - 14.7\ \text{psia} = 13.73\ \text{psig}$$

After 60 days, the maximum ICV pressure would be 13.73 psig for a payload of fourteen 55-gallon drums of Waste Material Type I.1 with a total payload decay heat of 40 watts. Thus, the pressure increase for any such payload with a decay heat less than 40 watts is below the allowable pressure increase limit of 50 psig.

Waste Material Types I.2 and I.3 have lower G values and will therefore have lower total gas generation rates. This means that the pressure increase will be lower than that of Waste Material Type I.1. Hence, the pressure increase for Waste Material Type I.1 is the bounding value for Waste Type I. Similar logic applies for Waste Types II and III and hence Table 3.4-6 provides pressure increase values for Waste Material Types I.1, II.1 and III.1 only. In addition to the above-stated decay heat limit for a payload of fourteen 55-gallon drums for Waste Type I, compliance with the 50 psig pressure limit can be demonstrated for other container types and Waste Material Types as shown in Table 3.4-6 through Table 3.4-11. Maximum allowable decay heat limits for analytical shipping categories are below the associated test category values shown in Table 3.4-6 through Table 3.4-11, and will therefore have lower pressure increase values.

For all payloads satisfying the applicable container decay heat limits specified in Table 3.4-6 through Table 3.4-11, there is no need to perform total gas generation testing to determine compliance with the 50 psig pressure limit.

For cases where the wattage limits specified in Table 3.4-6 through Table 3.4-11 are exceeded but the packaging design limit of 40 watts per TRUPACT-II is met, compliance with the container flammable gas generation can be used to evaluate compliance with the total gas generation rate limit. Because the primary mechanism for gas generation for both flammable and total gas for Waste Types I, II, and III is radiolysis, compliance with the flammable gas generation rate limit implies actual G values (both flammable and total) that are much lower than those used to derive the limits in Table 3.4-6 through Table 3.4-11. Therefore, as described in Section 5.2.5.3.3 of the CH-TRAMPAC, compliance with the flammable gas generation rate limits will ensure compliance with the total gas generation rate limits for these cases (e.g., SWBs of Waste Type III greater than 23 watts). Note that, as shown below, Waste Type IV containers compliance with the total gas generation rate limit will be evaluated by measurement.

3.4.4.2.2 MNOP Determination by Measurement

For all containers of Waste Type IV, the total gas generation rate must be measured by testing and shown to comply with the applicable limits as described below. (Note: Payloads must also comply with the TRUPACT-II decay heat limit of 40 watts.)

For containers requiring total gas generation testing as specified above, the allowable number of moles per second of gases (excluding water vapor) released may not exceed a specified limit (see Table 5.2-11 in Section 5.2.5 of the CH-TRAMPAC). The calculation is based on the maximum decay heat for each test category. This decay heat provides the minimum ICV wall temperature for determining the vapor pressure of water, and the average ICV gas temperature for determining the pressure rise due to heating the gases initially present when the ICV is sealed. Assuming that atmospheric pressure is 14.7 psia, the allowable absolute pressure in the ICV, p_{abs}, is:

$$p_{abs} = 50 \text{ psig} + 14.7 \text{ psia} = 64.7 \text{ psia}$$

This absolute pressure is decreased by the water vapor pressure and the increased pressure of the gas initially present in the ICV.

The maximum gas release rate in moles/sec per payload container for containers subjected to total gas generation testing is provided in Section 5.2.5 of the CH-TRAMPAC. The method used to calculate the maximum gas release rate is provided below with an example for Waste Type IV.

The maximum decay heat for Waste Type IV in 55-gallon drums is 7 watts (see Section 5.2.5 of the CH-TRAMPAC). Interpolating from data in Table 3.4-1, the minimum ICV wall temperature is 124.5 ºF and the average ICV gas temperature is 130.2 ºF. The corresponding water vapor pressure at the ICV wall temperature is 1.92 psia. The increased pressure of the ICV gas initially present (assuming air at 70 ºF and 14.7 psia), p_{ini}, is then:

$$p_{ini} = (14.7\text{ psia})\left(\frac{130.2\,°\text{F} + 460\,°\text{R}}{70\,°\text{F} + 460\,°\text{R}}\right) = 16.4\text{ psia}$$

The allowable absolute pressure in the ICV available for accumulation of gas released from the payload containers, p_{all}, is:

$$p_{all} = 64.7\text{ psia} - 1.92\text{ psia} - 16.4\text{ psia} = 46.4\text{ psia (3.16 atm)}$$

For a payload of fourteen 55-gallon drums and an available void volume in the ICV of 2,450 liters, the amount of gas that may be released from the payload containers at 130.2 ºF, V_g, is:

$$V_g = (3.16\text{ atm})(2{,}450\text{ liters}) = 7{,}742\text{ liters @ } 130.2\,°\text{F and 1 atm pressure}$$

Thus, the number of moles per second at STP allowed for 60 days from all fourteen (14) 55-gallon drums for Waste Type IV, n_g, is:

$$n_g = (7{,}742\text{ liters})\left(\frac{32\,°\text{F} + 460\,°\text{R}}{130.2\,°\text{F} + 460\,°\text{R}}\right)\left(\frac{1\text{ mole}}{22.4\text{ liters}}\right)\left(\frac{1}{60\text{ days}}\right)\left(\frac{1\text{ day}}{86{,}400\text{ sec}}\right)$$

$$= 5.56(10)^{-5}\text{ moles/sec}$$

The number of moles/sec per 55-gallon drum, n_p, would be:

$$n_p = \frac{5.56(10)^{-5}\text{ moles/sec}}{14\text{ drums}} = 3.97(10)^{-6}\text{ moles/sec per drum}$$

The maximum allowable gas release rate for 60 days for 55-gallon drums from Waste Type IV is $3.97(10)^{-6}$ moles/sec per payload container. The limit for moles/sec per payload container for Waste Type IV is provided in Section 5.2.5 of the CH-TRAMPAC. Compliance with these limits will be evaluated for payload containers of Waste Type IV less than or equal to a decay heat of 7 watts per payload container and per TRUPACT-II. The maximum allowable gas release rates provided ensure that the maximum pressure increase in 60 days under normal conditions of transport will not exceed the 50 psig design limit.

The maximum allowable internal pressure in the OCV is also 50 psig. The OCV would only experience significant internal pressure if the ICV had such a pressure and the gases were free to communicate with the OCV. In this case, the maximum internal pressure is 50 psig in the ICV and the additional void volume in the OCV would result in a maximum pressure in the OCV of less than 50 psig.

3.4.4.3 Maximum Normal Operating Pressure

The TRUPACT-II package was designed to withstand 50 psig of internal pressure to accommodate the transport of payload materials with the potential to generate gases and increase pressure within the ICV. For the analytical payload shipping categories, the pressure

increase in 60 days is less than that for test category waste due to the decay heat limits imposed on analytical category waste. Therefore, the MNOP for the ICV for the analytical categories is not the limiting MNOP for the ICV since a higher value is established by the test payload shipping categories. As discussed in Section 3.4.4.2, *Maximum Pressure for Normal Conditions of Transport*, the maximum pressure increase in the ICV in 60 days for a test category is allowed to be 50 psig. Since the ICV pressure is allowed to increase to the design pressure of 50 psig, the MNOP for the ICV in the TRUPACT-II package is 50 psig.

The MNOP for the OCV is low and the pressure increase is due to the temperature increase of the air in the OCV cavity and the vapor pressure of water within the OCV cavity when the TRUPACT-II package reaches the maximum normal operating temperature. Per Table 3.4-1 through Table 3.4-5, the normal condition steady state temperature of the ICV and OCV walls with 40 watts of decay heat is less than 156 ºF. Conservatively assuming that the initial volume of gas present in the OCV at 70 ºF and 14.7 psia is heated to 156 ºF, the increased pressure associated with this heat-up, p_{hu}, is:

$$p_{hu} = (14.7\ \text{psia})\left(\frac{156\ °\text{F} + 460\ °\text{R}}{70\ °\text{F} + 460\ °\text{R}}\right) = 17.09\ \text{psia}$$

Also, conservatively assuming a condensing OCV surface temperature of 156 ºF, the water vapor pressure, p_{wv}, at this temperature is 4.31 psia.

Thus, for normal conditions of transport, the MNOP for the OCV is the sum of the two pressure components less an assumed atmospheric pressure, p_a, of 14.7 psia, or:

$$p_{max} = p_{hu} + p_{wv} - p_a = 17.09\ \text{psia} + 4.31\ \text{psia} - 14.7\ \text{psia} = 6.70\ \text{psig}$$

The design pressure for the OCV is the same as that for the ICV or 50 psig and ensures pressure retention by the OCV in a non-normal situation in which the ICV cavity communicates with the OCV cavity.

3.4.5 Maximum Thermal Stresses

Maximum thermal stresses for NCT are determined using the temperature results from Section 3.4.2, *Maximum Temperatures*, and Section 3.4.3, *Minimum Temperatures*. NCT thermal stresses are discussed in Section 2.6.1, *Heat*, and Section 2.6.2, *Cold*. Corresponding structural analyses utilize a minimum temperature of -40 ºF (-20 ºF when combined with any other load cases), and a maximum temperature of 160 ºF for any TRUPACT-II packaging component.

3.4.6 Evaluation of Package Performance for Normal Conditions of Transport

The component temperatures and internal decay heat distributions presented in Section 3.4.2, *Maximum Temperatures*, and Section 3.4.3, *Minimum Temperatures*, are all within the allowable limits for the materials of construction delineated in Section 3.3, *Technical Specifications of Components*.

Table 3.4-1 – NCT Steady-State Temperatures with Insolation, Payload Configuration 1 - Fourteen 55-Gallon Drums, Thermal Case 1

Location	Temperature (ºF) with Internal Decay Heat (watts)				
	0	10	20	30	40
Center Drum Centerline					
• Maximum	129	138	147	157	167
• Average	126	136	145	154	163
Center Drum Wall					
• Maximum	129	134	141	148	154
• Average	126	132	138	144	150
Outer Drum Centerline					
• Maximum	129	137	147	156	165
• Average	126	136	144	153	162
Outer Drum Wall					
• Maximum	129	134	141	148	154
• Average	126	132	138	144	149
Average All Drums					
• Centerline	126	136	144	153	162
• Wall	126	132	138	144	149
ICV Wall					
• Maximum	129	134	138	143	149
• Average	126	131	136	141	146
• Minimum	121	126	131	137	142
ICV Air					
• Average	126	132	137	143	148
ICV Main O-ring Seal					
• Maximum	129	133	138	142	146
OCV Wall					
• Maximum	129	133	138	143	148
OCV Main O-ring Seal					
• Maximum	129	133	136	139	143
Polyurethane Foam①					
• Maximum	155	155	155	155	155
OCA Outer Shell①					
• Maximum	155	155	155	155	155

Notes:

① Based on the Case 3 heat distribution; 40 watts internal decay heat and full solar heat load averaged over 12 hours.

Table 3.4-2 – NCT Steady-State Temperatures with Insolation, Payload Configuration 1 - Fourteen 55-Gallon Drums, Thermal Case 2

Location	Temperature (ºF) with Internal Decay Heat (watts)				
	0	10	20	30	40
Center Drum Centerline					
• Maximum	129	157	187	216	245
• Average	126	155	184	212	240
Center Drum Wall					
• Maximum	129	136	144	151	159
• Average	126	133	140	147	154
Outer Drum Centerline					
• Maximum	129	134	141	147	153
• Average	126	132	138	144	150
Outer Drum Wall					
• Maximum	129	135	142	150	157
• Average	126	132	138	144	149
Average All Drums					
• Centerline	126	136	145	154	163
• Wall	126	132	138	144	150
ICV Wall					
• Maximum	129	134	139	143	149
• Average	126	131	136	141	146
• Minimum	121	126	132	137	143
ICV Air					
• Average	126	132	138	143	149
ICV Main O-ring Seal					
• Maximum	129	133	137	141	146
OCV Wall					
• Maximum	129	134	138	143	148
OCV Main O-ring Seal					
• Maximum	129	133	136	139	143
Polyurethane Foam①					
• Maximum	155	155	155	155	155
OCA Outer Shell①					
• Maximum	155	155	155	155	155

Notes:

① Based on the Case 3 heat distribution; 40 watts internal decay heat and full solar heat load averaged over 12 hours.

Table 3.4-3 – NCT Steady-State Temperatures with Insolation, Payload Configuration 1 - Fourteen 55-Gallon Drums, Thermal Case 3

Location	Temperature (ºF) with Internal Decay Heat (watts)				
	0	10	20	30	40
Center Drum Centerline					
• Maximum	129	181	232	283	334
• Average	126	155	183	211	239
Center Drum Wall					
• Maximum	129	138	146	154	162
• Average	126	133	140	147	153
Outer Drum Centerline					
• Maximum	129	136	142	149	155
• Average	126	132	138	143	149
Outer Drum Wall					
• Maximum	129	137	145	152	160
• Average	126	132	138	143	148
Average All Drums					
• Centerline	126	135	144	153	162
• Wall	126	132	138	143	149
ICV Wall					
• Maximum	129	136	143	149	156
• Average	126	131	136	140	145
• Minimum	121	124	127	130	133
ICV Air					
• Average	126	132	137	142	148
ICV Main O-ring Seal					
• Maximum	129	134	140	145	150
OCV Wall					
• Maximum	129	136	142	148	154
OCV Main O-ring Seal					
• Maximum	129	133	137	141	145
Polyurethane Foam①					
• Maximum	155	155	155	155	155
OCA Outer Shell①					
• Maximum	155	155	155	155	155

Notes:

① Based on the Case 3 heat distribution; 40 watts internal decay heat and full solar heat load averaged over 12 hours.

Table 3.4-4 – NCT Steady-State Temperatures with Insolation, Payload Configuration 2 - Two Standard Waste Boxes, Thermal Case 4

Location	Temperature (ºF) with Internal Decay Heat (watts)				
	0	10	20	30	40
SWB Centerline					
• Maximum	128	158	186	212	239
• Average	126	157	184	210	238
SWB Wall					
• Maximum	128	134	140	144	150
• Average	126	132	138	143	148
ICV Wall					
• Maximum	128	134	139	143	148
• Average	126	132	137	141	146
• Minimum	122	128	134	138	144
ICV Air					
• Average	126	132	138	142	148
ICV Main O-ring Seal					
• Maximum	128	133	139	141	146
OCV Wall					
• Maximum	129	133	139	142	148
OCV Main O-ring Seal					
• Maximum	129	133	137	139	143
Polyurethane Foam①					
• Maximum	155	155	155	155	155
OCA Outer Shell①					
• Maximum	155	155	155	155	155

Notes:

① Based on the Case 4 heat distribution; 40 watts internal decay heat and full solar heat load averaged over 12 hours.

Table 3.4-5 – NCT Steady-State Temperatures with Insolation, Payload Configuration 2 - Two Standard Waste Boxes, Thermal Case 5

Location	Temperature (ºF) with Internal Decay Heat (watts)				
	0	10	20	30	40
SWB Centerline					
• Maximum	128	181	229	279	328
• Average	126	155	181	209	236
SWB Wall					
• Maximum	128	136	141	147	154
• Average	126	132	137	143	148
ICV Wall					
• Maximum	128	135	140	147	153
• Average	126	132	136	141	146
• Minimum	122	127	130	134	138
ICV Air					
• Average	126	132	136	142	147
ICV Main O-ring Seal					
• Maximum	128	135	139	145	150
OCV Wall					
• Maximum	129	135	140	146	152
OCV Main O-ring Seal					
• Maximum	129	133	137	141	145
Polyurethane Foam①					
• Maximum	155	155	155	155	155
OCA Outer Shell①					
• Maximum	155	155	155	155	155

Notes:

① Based on the Case 4 heat distribution; 40 watts internal decay heat and full solar heat load averaged over 12 hours.

Table 3.4-6 – TRUPACT-II Pressure Increase with a 14-Drum Payload, 60-Day Duration*

Waste Material Type	Decay Heat per Drum (watts)	Total Decay Heat per Package (watts)	Average Contents Temperature (°F)	Total Gas Value, G_{eff} (molecules/100eV)	Activation Energy (kcal/g-mole)	Temperature Correlation Value, G_{eff} (molecules/100eV)	Radiolytic Gas Generation Rate (moles/sec)	Radiolytic Gas Generation STP/60 days (liters)	Average ICV Gas Temperature (°F)	Radiolytic Gas Pressure Increase (psia)	Initial Gas Pressure Increase (psia)	Minimum ICV Wall Temperature (°F)	Water Vapor Pressure (psia)	Pressure Increase @ 60 days (psig)
I.1	2.8571	40.00	163.0	2.4	0	2.4	$9.98(10)^{-6}$	1158.89	148.0	8.53	16.86	142.0	3.04	13.73
II.1	2.8571	40.00	163.0	1.7	0.8	2.0	$8.53(10)^{-6}$	990.52	148.0	7.35	16.86	142.0	3.04	12.56
III.1	2.6429	37.00	160.3	8.4	2.1	13.5	$5.21(10)^{-5}$	6049.94	146.5	44.69	16.82	140.5	2.93	49.74

* void volume in the TRUPACT-II with 14 55-gallon drums is 2,450 liters

Table 3.4-7 – TRUPACT-II Pressure Increase with a 2 SWB Payload, 60-Day Duration*

Waste Material Type	Decay Heat per SWB (watts)	Total Decay Heat per Package (watts)	Average Contents Temperature (°F)	Total Gas Value, G_{eff} (molecules/100eV)	Activation Energy (kcal/g-mole)	Temperature Correlation Value, G_{eff} (molecules/100eV)	Radiolytic Gas Generation Rate (moles/sec)	Radiolytic Gas Generation STP/60 days (liters)	Average ICV Gas Temperature (°F)	Radiolytic Gas Pressure Increase (psia)	Initial Gas Pressure Increase (psia)	Minimum ICV Wall Temperature (°F)	Water Vapor Pressure (psia)	Pressure Increase @ 60 days (psig)
I.1	20.0000	40.00	238.0	2.4	0	2.4	$9.98(10)^{-6}$	1158.89	148.0	12.05	16.86	144.0	3.20	17.42
II.1	20.0000	40.00	238.0	1.7	0.8	2.3	$9.66(10)^{-6}$	1121.73	148.0	11.61	16.86	144.0	3.20	16.98
III.1	11.5000	23.00	191.8	8.4	2.1	15.7	$3.76(10)^{-5}$	4361.53	139.2	44.69	16.62	135.2	2.55	49.16

* void volume in the TRUPACT-II with two direct load SWBs is 1,750 liters

Table 3.4-8 – TRUPACT-II Pressure Increase with 8 Drums Overpacked in 2 SWBs, 60-Day Duration*

Waste Material Type	Decay Heat per Drum (watts)	Total Decay Heat per Package (watts)	Average Contents Temperature (°F)	Total Gas Value, G_{eff} (molecules/100eV)	Activation Energy (kcal/g-mole)	Temperature Correlation Value, G_{eff} (molecules/100eV)	Radiolytic Gas Generation Rate (moles/sec)	Radiolytic Gas Generation STP/60 days (liters)	Average ICV Gas Temperature (°F)	Radiolytic Gas Pressure Increase (psia)	Initial Gas Pressure Increase (psia)	Minimum ICV Wall Temperature (°F)	Water Vapor Pressure (psia)	Pressure Increase @ 60 days (psig)
I.1	5.0000	40.00	238.0	2.4	0	2.4	$9.98(10)^{-6}$	1158.89	148.0	6.03	16.86	144.0	3.20	11.39
II.1	5.0000	40.00	238.0	1.7	0.8	2.3	$9.66(10)^{-6}$	1121.73	148.0	5.88	16.86	144.0	3.20	11.25
III.1	4.7500	38.00	232.4	8.4	2.1	18.6	$7.36(10)^{-5}$	8550.03	146.8	44.39	16.83	142.8	3.11	49.63

* void volume in the TRUPACT-II with eight 55-gallon drums in two SWB overpacks is 3,490 liters

Table 3.4-9 – TRUPACT-II Pressure Increase with 8 85-Gallon Drums or 8 55-Gallon Drums Overpacked in 8 85-Gallon Drums, 60-Day Duration*

Waste Material Type	Decay Heat per Drum (watts)	Total Decay Heat per Package (watts)	Average Contents Temperature (°F)	Total Gas Value, G_{eff} (molecules/100eV)	Activation Energy (kcal/g-mole)	Temperature Correlation Value, G_{eff} (molecules/100eV)	Radiolytic Gas Generation Rate (moles/sec)	Radiolytic Gas Generation STP/60 days (liters)	Average ICV Gas Temperature (°F)	Radiolytic Gas Pressure Increase (psia)	Initial Gas Pressure Increase (psia)	Minimum ICV Wall Temperature (°F)	Water Vapor Pressure (psia)	Pressure Increase @ 60 days (psig)
I.1	5.0000	40.00	238.0	2.4	0	2.4	$9.98(10)^{-6}$	1158.89	148.0	10.14	16.86	144.0	3.20	15.51
II.1	5.0000	40.00	238.0	1.7	0.8	2.3	$9.66(10)^{-6}$	1121.73	148.0	9.70	16.86	144.0	3.20	15.07
III.1	3.2500	26.00	199.6	8.4	2.1	16.3	$4.40(10)^{-5}$	5103.54	140.4	43.81	16.65	136.4	2.63	48.39

* void volume in the TRUPACT-II with eight 85-gallon drums is 2,087 liters

Table 3.4-10 – TRUPACT-II Pressure Increase with 6 100-Gallon Drums, 60-Day Duration*

Waste Material Type	Decay Heat per Drum (watts)	Total Decay Heat per Package (watts)	Average Contents Temperature (°F)	Total Gas Value, G_{eff} (molecules/100eV)	Activation Energy (kcal/g-mole)	Temperature Correlation Value, G_{eff} (molecules/100eV)	Radiolytic Gas Generation Rate (moles/sec)	Radiolytic Gas Generation STP/60 days (liters)	Average ICV Gas Temperature (°F)	Radiolytic Gas Pressure Increase (psia)	Initial Gas Pressure Increase (psia)	Minimum ICV Wall Temperature (°F)	Water Vapor Pressure (psia)	Pressure Increase @ 60 days (psig)
I.1	6.6667	40.00	238.0	2.4	0	2.4	$9.98(10)^{-6}$	1158.89	148.0	7.79	16.86	144.0	3.20	13.16
II.1	6.6667	40.00	238.0	1.7	0.8	2.3	$9.66(10)^{-6}$	1121.73	148.0	7.50	16.86	144.0	3.20	12.86
III.1	5.3333	32.00	215.6	8.4	2.1	17.4	$5.79(10)^{-5}$	6724.60	143.2	44.69	16.73	139.2	2.83	49.55

* void volume in the TRUPACT-II with six 100-gallon drums is 2,715 liters

Table 3.4-11 – TRUPACT-II Pressure Increase with a 1 TDOP Payload, 60-Day Duration*

Waste Material Type	Decay Heat per TDOP (watts)	Total Decay Heat per Package (watts)	Average Contents Temperature (°F)	Total Gas Value, G_{eff} (molecules/100eV)	Activation Energy (kcal/g-mole)	Temperature Correlation Value, G_{eff} (molecules/100eV)	Radiolytic Gas Generation Rate (moles/sec)	Radiolytic Gas Generation STP/60 days (liters)	Average ICV Gas Temperature (°F)	Radiolytic Gas Pressure Increase (psia)	Initial Gas Pressure Increase (psia)	Minimum ICV Wall Temperature (°F)	Water Vapor Pressure (psia)	Pressure Increase @ 60 days (psig)
I.1	40.0000	40.00	238.0	2.4	0	2.4	$9.98(10)^{-6}$	1158.89	148.0	16.46	16.86	144.0	3.20	21.83
II.1	40.0000	40.00	238.0	1.7	0.8	2.3	$9.66(10)^{-6}$	1121.73	148.0	16.02	16.86	144.0	3.20	21.39
III.1	18.0000	18.00	178.6	8.4	2.1	14.8	$2.77(10)^{-5}$	3213.08	136.8	44.84	16.55	132.8	2.40	49.08

* void volume in the TRUPACT-II with one direct load TDOP is 1,277 liters

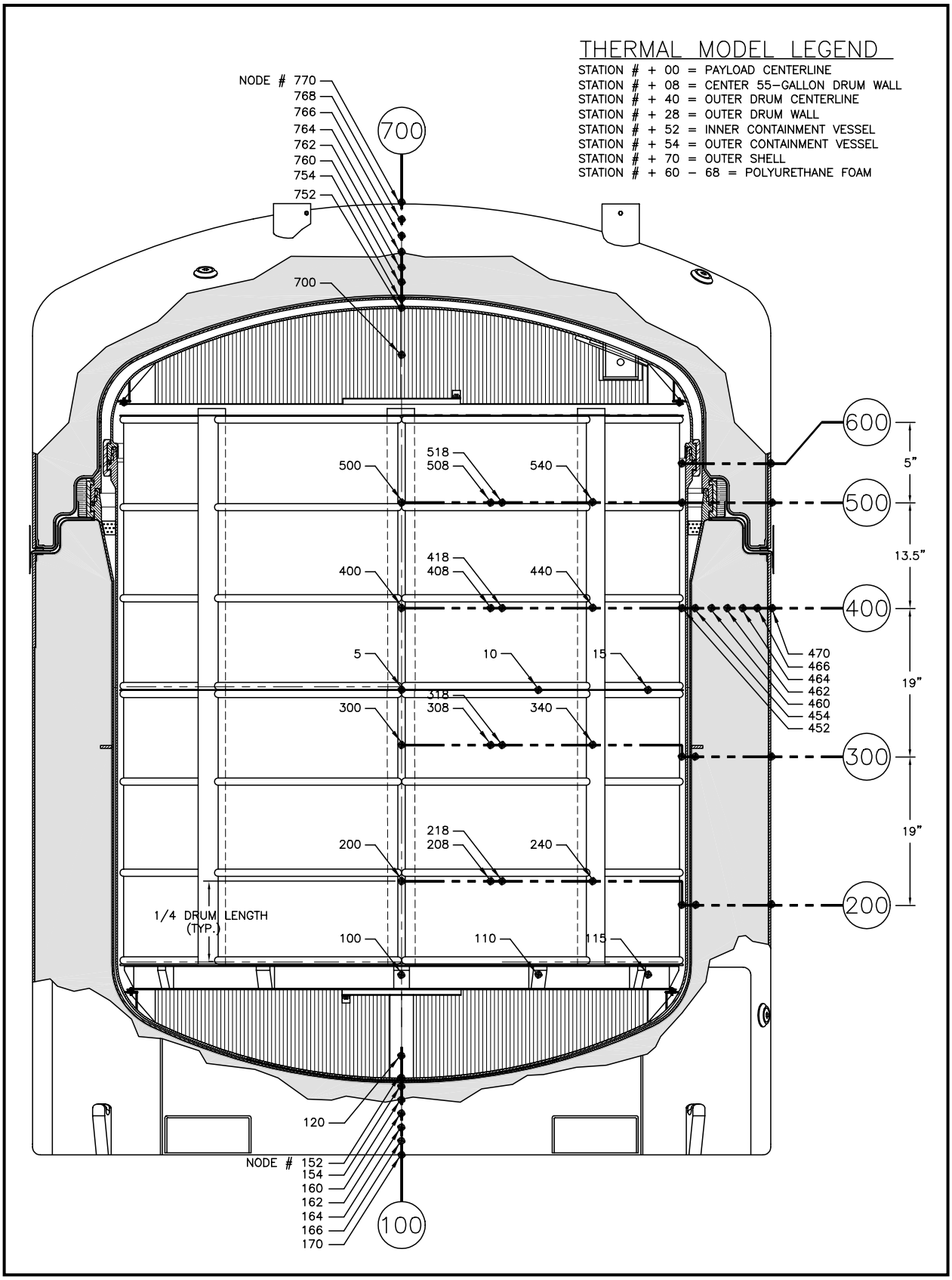

Figure 3.4-1 – TRUPACT-II Packaging Thermal Model Node Layout

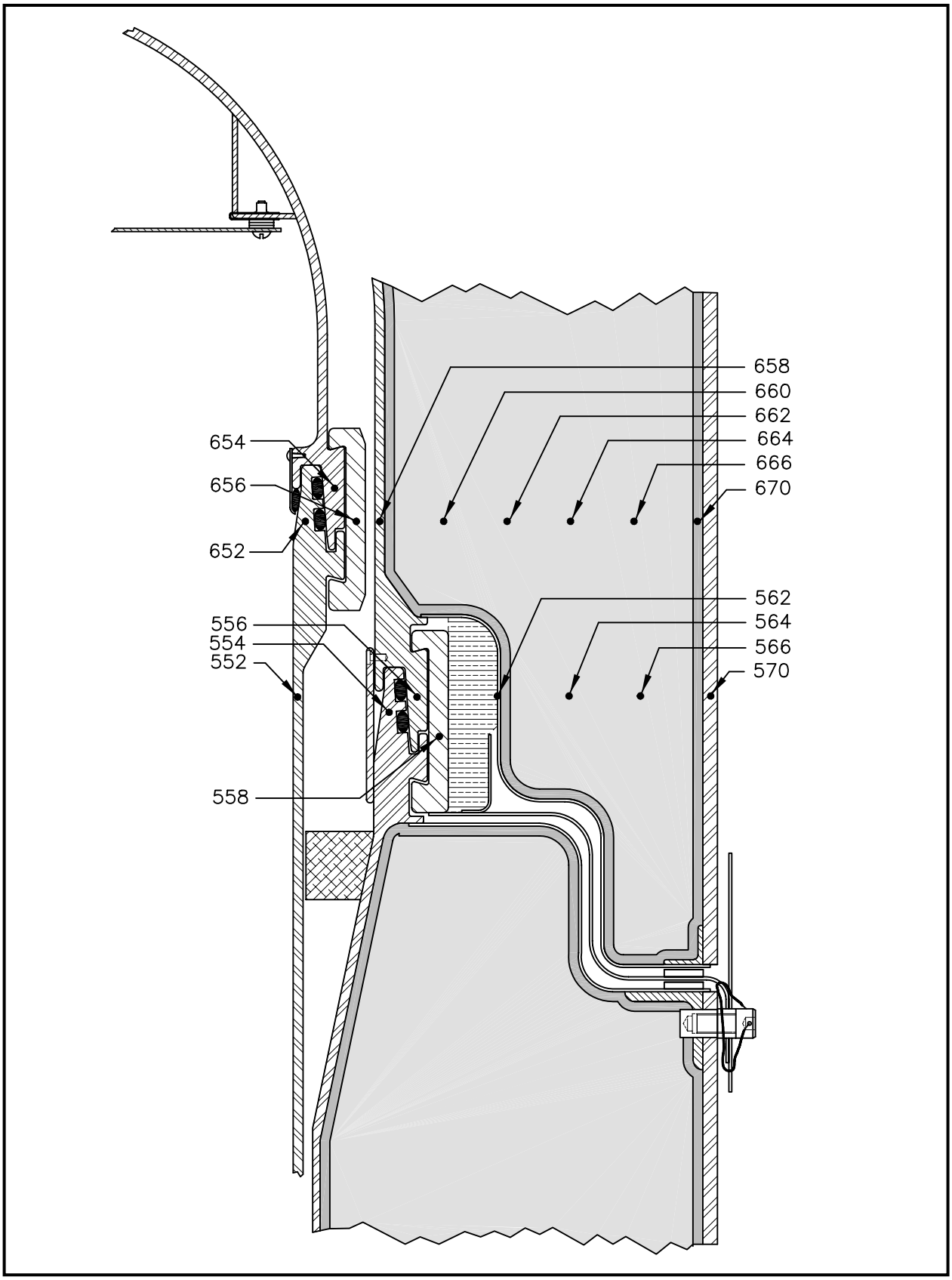

Figure 3.4-2 – Seal Region Thermal Model Node Layout

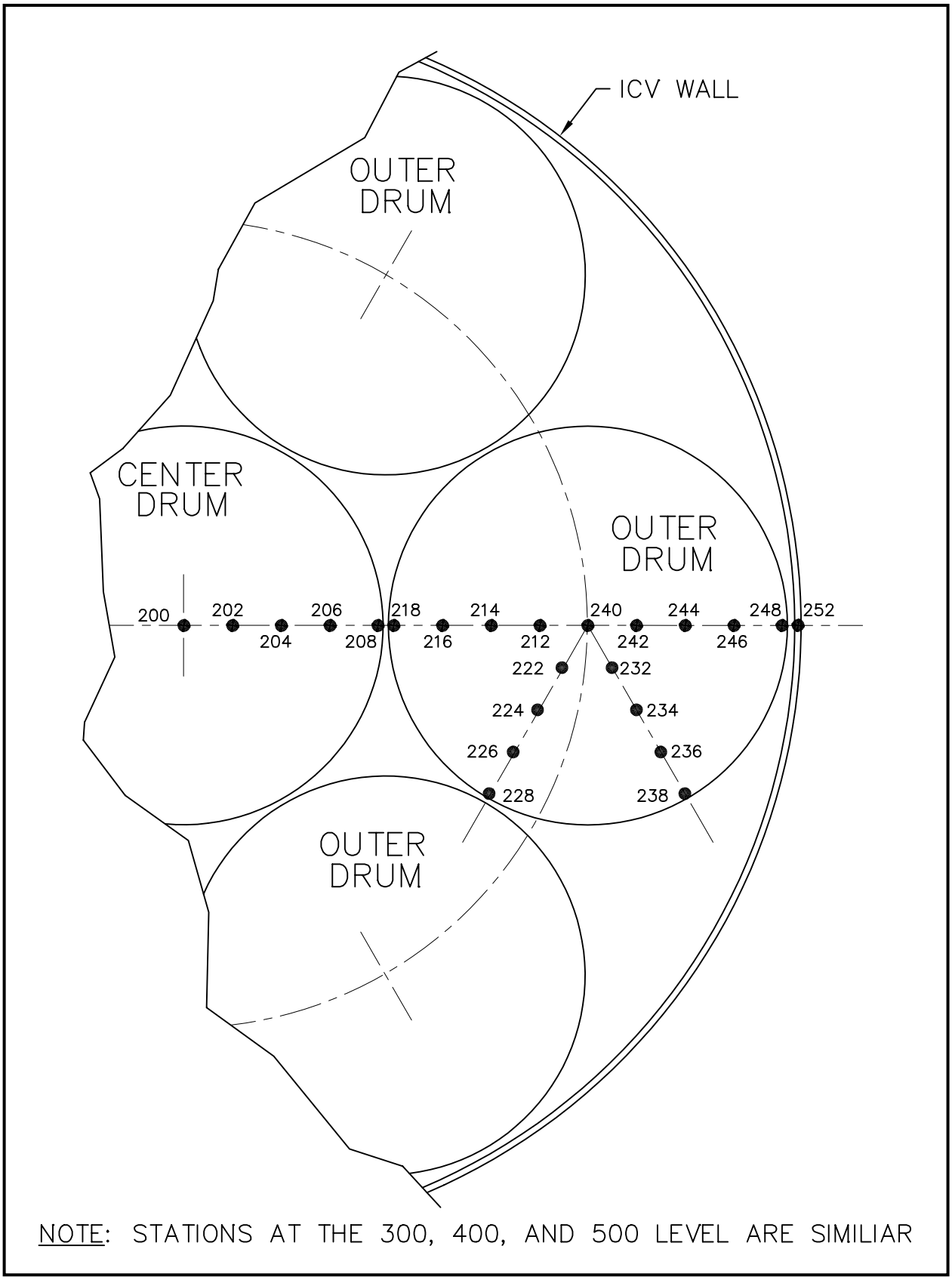

Figure 3.4-3 – Fourteen 55-Gallon Drum Payload Thermal Node Layout

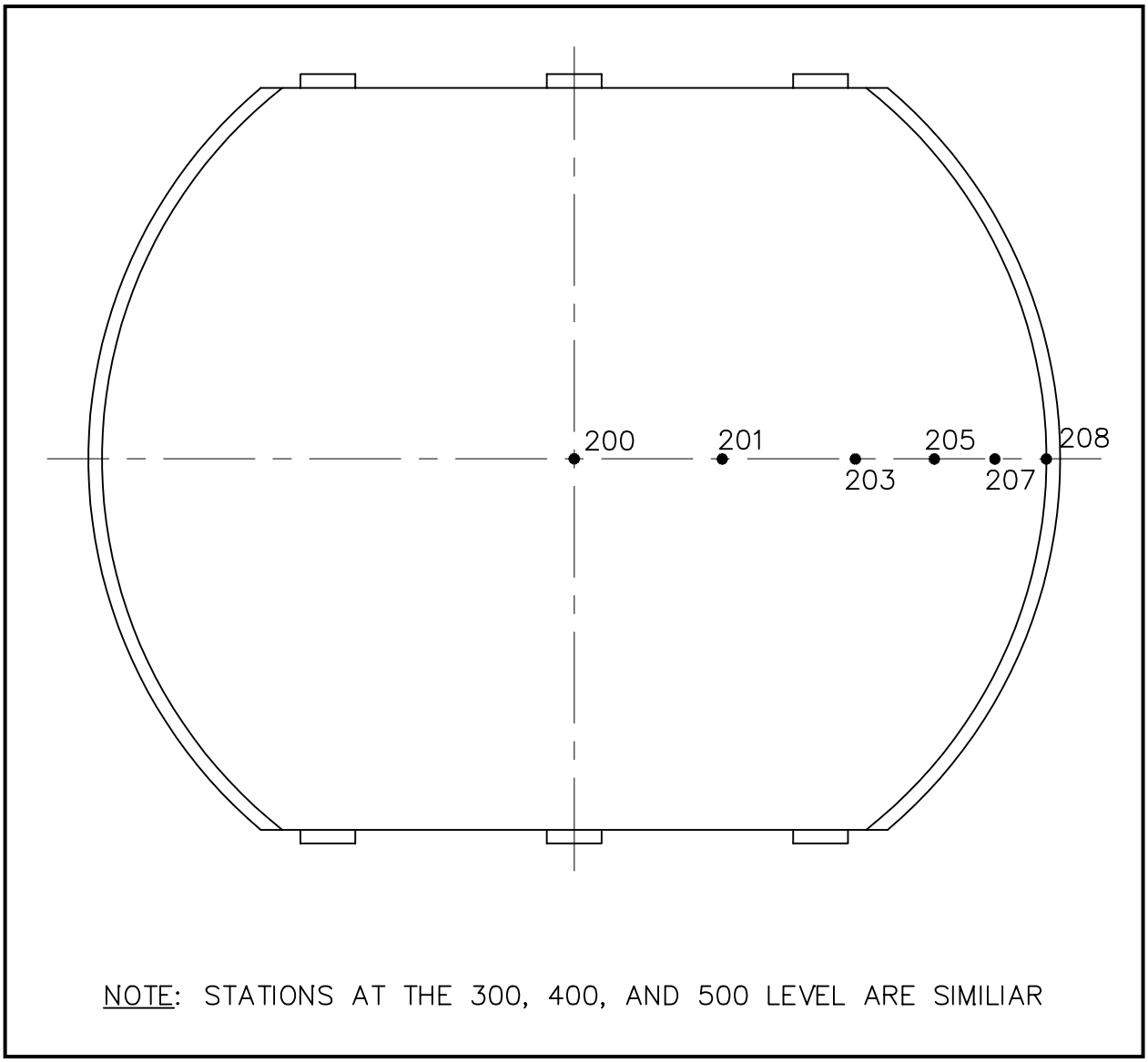

Figure 3.4-4 – Two Standard Waste Boxes Thermal Model Node Layout

3.5 Thermal Evaluation for Hypothetical Accident Conditions

This section presents the results of thermal testing of the TRUPACT-II package for the hypothetical accident condition (HAC) specified in 10 CFR §71.73(c)(4)[1].

3.5.1 Thermal Model

3.5.1.1 Analytical Model

Consistent with the *Summary and Resolution of Public Comments* relating to §71.73, "…the effects of solar radiation may be neglected before and during the thermal test…", the initial conditions for the HAC thermal event ignore insolation. Table 3.5-1 and Table 3.5-2 summarize component temperatures with the maximum decay heat load of 40 watts, but ignoring insolation. These analyses utilize the NCT model as described in Section 3.4.1, *Thermal Model*, and provide a basis for the worst-case HAC initial temperatures for the five thermal cases.

3.5.1.2 Test Model

HAC thermal event (fire) testing was performed on two prototypical TRUPACT-II packages, Certification Test Unit No. 1 and No. 2 (CTU-1 and CTU-2). A full description of the CTUs, the test facilities, the pre-fire damage, initial orientation in the fire, and the test results are presented in Appendix 2.10.3, *Certification Tests*. Both CTU-1 and CTU-2 utilized both active and passive temperature measuring instrumentation at various locations near each containment vessel's seal flanges (as well as many other locations) to record temperatures from the HAC fire test.

Seventy-seven (77) sets of passive temperature indicating labels were installed inside the CTU-1 OCV and ICV cavity, and eighty (80) sets of passive temperature indicating labels were installed inside the CTU-2 OCV and ICV cavity. Each set of temperature indicating labels covered the temperature range from 100 ºF to 550 ºF in 10 ºF increments. CTU-1 temperature indicating label locations and results are provided in Table 3.5-3, and Figure 3.5-1 and Figure 3.5-2, and CTU-2 temperature indicating label locations and results are provided in Table 3.5-4, and Figure 3.5-1 and Figure 3.5-3.

Sixteen (16) active thermocouples were installed on the exterior surface of the CTU-1 OCV, with ten (10) active thermocouples installed onto the CTU-1 OCA outer shell surface just prior to the beginning of the fire test; CTU-1 thermocouple locations are provided in Figure 3.5-4, and the results are provided in Figure 3.5-6, Figure 3.5-7, Figure 3.5-8, and Figure 3.5-9.

Eight (8) active thermocouples were installed on the exterior surface of the CTU-2 OCV, with eight (8) active thermocouples installed onto the CTU-2 OCA outer shell surface just prior to the beginning of the fire test; CTU-2 thermocouple locations are provided in Figure 3.5-5, and the results are provided in Figure 3.5-10 and Figure 3.5-11.

The "Y" and "C" locations in the aforementioned tables and figures refer to the axial and circumferential locations of the temperature indicating strips and thermocouples.

[1] Title 10, Code of Federal Regulations, Part 71 (10 CFR 71), *Packaging and Transportation of Radioactive Material*, 01-01-07 Edition.

3.5.2 Package Conditions and Environment

The exterior surfaces of CTU-1 and CTU-2 were not painted (other than painted reference grids), an option allowed on the drawings in Appendix 1.3.1, *Packaging General Arrangement Drawings*. If the paint were present on the OCA exterior surface, it would be conservative for the HAC fire test because of the relatively high emissivity of paint ($\varepsilon > 0.90$) compared to that of bare stainless steel ($\varepsilon = 0.25$). The higher emissivity results in higher heat flow into the CTU during the HAC fire test, but the net affect is small since the paint burns away shortly after the start of the fire.

As discussed further in Appendix 2.10.3, *Certification Tests*, CTU-1 and CTU-2 were supported horizontally on a test stand with the bottom of the package approximately two (2) meters above the fuel pool floor. The test stand was designed to minimize its effect on the package's thermal testing.

Within the pool, JP-4 jet fuel of sufficient quantity to sustain a fire for thirty (30) minutes was floated on a layer of water. Consistent with 10 CFR §71.73(c)(4), the surface of the fuel was adjusted to a level approximately one (1) meter from the bottom of each CTU. The maximum damage for each CTU was positioned at a level 1½ meters above the fuel surface (1/2 meter above the CTU bottom surface). These particular arrangements put the maximum drop damage in the hottest part of the fire[2].

Prior to beginning the hypothetical accident thermal event, both CTUs were elevated in temperature to achieve the initial condition requirement of approximately 120 ºF for the average ICV/OCV wall temperature. Very warm, dry air (approximately 330 ºF for CTU-1, and 350 ºF for CTU-2) was circulated through the ICV and OCV annulus to preheat each CTU.

3.5.2.1 CTU-1 Package Conditions and Environment

A total of nine (9) free and puncture drop events were performed on CTU-1 prior to the fire test, as presented in Figure 2.10.3-4 in Appendix 2.10.3, *Certification Tests*. With reference to Figure 2.10.3-4, CTU-1 was circumferentially oriented at an angle of 145º to position the damage from Free Drop Nos. 1 and 2, and Puncture Drop Nos. 5 and 7 at a distance 1/2 meter above the lowest part of the package on the stand (i.e., 1½ meters above the fuel).

The CTU-1 OCV seal region thermocouple readings at the start of the fire averaged 109 ºF. For purposes of comparison, all sixteen OCV thermocouples averaged 127 ºF, a temperature well above the hypothetical accident initial condition temperature of 120 ºF determined in Section 3.5.1.1, *Analytical Model*.

Per Appendix 2.10.3.7.1.10, *CTU-1 Fire No. 10*, the ICV and OCV internal pressures were set to 50.0 psig and 48.5 psig, respectively, at the start of the fire test, the ambient temperature was 36 ºF (2 ºC) at the start of the fire test, and the wind speed averaged 4.4 mph (1.97 meter/sec) during the fire test.

---

[2] M. E. Schneider and L. A. Kent, *Measurements of Gas Velocities and Temperatures in a Large Open Pool Fire*, Sandia National Laboratories (reprinted from *Heat and Mass Transfer in Fire*, A. K. Kulkarni and Y. Jaluria, Editors, HTD-Vol. 73 (Book No. H00392), American Society of Mechanical Engineers). Figure 3 shows that maximum temperatures occur at an elevation approximately 2.3 meters above the pool floor. The pool was initially filled with water and fuel to a level of 0.814 meters. The maximum temperatures therefore occur approximately 1½ meters above the level of the fuel, i.e., 1/2 meter above the lowest part of the package when set one meter above the fuel source per the requirements of 10 CFR §71.73(c)(4).

3.5.2.2 CTU-2 Package Conditions and Environment

A total of nine (9) free and puncture drop events were performed on CTU-2 prior to the fire test, as presented in Figure 2.10.3-5 in Appendix 2.10.3, *Certification Tests*. With reference to Figure 2.10.3-5, CTU-2 was circumferentially oriented at an angle of 200º to position the damage from Free Drop No. 3, and Puncture Drop Nos. R and 4 at a distance 1/2 meter above the lowest part of the package on the stand (i.e., 1½ meters above the fuel).

The CTU-2 OCV seal region thermocouple readings at the start of the fire averaged 119 ºF. For purposes of comparison, all eight OCV thermocouples averaged 127 ºF, a temperature well above the hypothetical accident initial condition temperature of 120 ºF determined in Section 3.5.1.1, *Analytical Model*.

Per Appendix 2.10.3.7.2.10, *CTU-2 Fire No. 9*, the ICV and OCV internal pressures were set to 51.1 psig and 50.0 psig, respectively, at the start of the fire test, the ambient temperature was 21 ºF (-6 ºC) at the start of the fire test, and the wind speed averaged 4.2 mph (1.88 meter/sec) during the fire test.

3.5.3 Package Temperatures

As stated in Section 3.5.1.1, *Analytical Model*, the maximum initial temperatures noted for the hypothetical accident initial conditions (40 thermal watts maximum internal decay heat, without insolation) are presented in Table 3.5-1 and Table 3.5-2 for the major components of the TRUPACT-II package for both of the payload configurations. As a result, a temperature of approximately 120 ºF for the average ICV/OCV shell temperature was utilized as the desired pre-fire condition of both CTU-1 and CTU-2.

The actual length of time of the fire tests was approximately 32 and 31 minutes for CTU-1 and CTU-2, respectively. In addition, the time-averaged temperature of the exterior of both test units exceeded the minimum requirement of 1,475 ºF per 10 CFR §71.73(c)(4).

A summary of the maximum temperatures attained in CTU-1 and CTU-2 during the hypothetical accident thermal event is presented in Table 3.5-5. On the average, the payload drums and ICV in CTU-1 averaged approximately 30 ºF cooler than the payload drums and ICV in CTU-2. Similarly, the OCV in CTU-1 averaged approximately 10 ºF cooler than the OCV in CTU-2. Maximum and average OCV seal area temperatures were very similar between the two CTUs. Additional details of the temperature results are presented in Appendix 2.10.3, *Certification Tests*.

3.5.4 Maximum Internal Pressure

Prior to initiating the CTU-1 fire test, the ICV and OCV were pressurized to 50.0 and 48.5 psig, respectively. The CTU-1 ICV internal pressure increased 1.9 psig, and the OCV internal pressure increased 1.6 psig (see Figure 3.5-12). The ICV pressure peaked at 51.9 psig, 154 minutes after the start of the fire test, then dropped slowly. The OCV pressure peaked at 50.1 psig, 136 minutes after the start of the fire test, then dropped rapidly to zero. Additional HAC fire testing details are available in Appendix 2.10.3.7.1.10, *CTU-1 Fire No. 10*. Thus, the maximum OCV pressure for CTU-1 is not available due to a test-related failure of the OCV pressure-measuring hardware. Further discussion of this anomaly is presented in Appendix 2.10.3.7.1.11, *CTU-1 Testing Anomalies*

Prior to initiating the CTU-2 fire test, the ICV and OCV were pressurized to 51.1 and 50 psig, respectively. The CTU-2 ICV internal pressure increased 2.6 psig, and the OCV internal pressure increased 4.6 psig (see Figure 3.5-13). The ICV pressure peaked at 53.7 psig, 230 minutes after the start of the fire test. The OCV pressure peaked at 54.6 psig, 185 minutes after the start of the fire test. Additional HAC fire testing details are available in Appendix 2.10.3.7.2.10, *CTU-2 Fire No. 9*.

3.5.5 Maximum Thermal Stresses

As shown for CTU-2 in Section 3.5.4, *Maximum Internal Pressure*, the internal pressure within the ICV increases 2.6 psig (+5%), and within the OCV increases 4.6 psig (+9%) due to the HAC fire test. Pressure stresses due to the HAC fire test correspondingly increase a maximum of 9%. With reference to Table 2.1-1 from Section 2.1.2.1.1, *Containment Structures*, the HAC allowable stress intensity for general primary membrane stresses (applicable to pressure loads) is 240% of the NCT allowable stress intensity. Therefore, a HAC pressure stress increase of 9% will not exceed the HAC allowable stresses. Further discussion regarding HAC thermal stresses is presented in Section 2.7.4, *Thermal*.

3.5.6 Evaluation of Package Performance for the Hypothetical Accident Thermal Conditions

The most temperature sensitive material in the TRUPACT-II package containment boundaries is the butyl rubber used for the containment O-ring seals. The certification test units (CTU-1 and CTU-2), when subjected to the rigors of the HAC free drops, puncture drops, and fire testing, were shown to be leaktight (i.e., demonstrating a leakage rate of 1×10^{-7} standard cubic centimeters per second (scc/s), air, or less) for both the ICV and OCV. Following testing, the maximum ICV and OCV O-ring seal region temperatures were recorded as 200 ºF and 260 ºF, respectively, temperatures well below the 400 ºF O-ring seal material limit for short durations (8 hours).

With regard to the criticality analyses of Chapter 6.0, *Criticality Evaluation*, the minimum remaining polyurethane foam for the CTU averaged approximately five inches. Sufficient polyurethane foam material remained to validate modeling assumptions used in the criticality analyses.

Table 3.5-1 – HAC Pre-Fire Steady-State Temperatures with 40 Watts Decay Heat Load and No Insolation; Fourteen 55-Gallon Drums

Location	Temperature (ºF)		
	Case 1	Case 2	Case 3
Center Drum Centerline			
• Maximum	141	220	308
• Average	138	215	214
Center Drum Wall			
• Maximum	128	134	137
• Average	125	129	128
Outer Drum Centerline			
• Maximum	139	127	128
• Average	136	124	123
Outer Drum Wall			
• Maximum	128	131	133
• Average	124	124	123
Average All Drums			
• Centerline	137	137	136
• Wall	124	125	124
ICV Wall			
• Maximum	123	123	128
• Average	121	121	120
• Minimum	118	117	113
ICV Air			
• Average	123	123	122
ICV Main O-ring Seal			
• Maximum	118	117	122
OCV Wall			
• Maximum	122	122	126
OCV Main O-ring Seal			
• Maximum	114	114	117
Polyurethane Foam			
• Maximum	122	122	126
OCA Outer Shell			
• Maximum	102	102	102

Table 3.5-2 – HAC Pre-Fire Steady-State Temperatures with 40 Watts Decay Heat Load and No Insolation; Two Standard Waste Boxes

Location	Temperature (ºF)	
	Case 4	Case 5
SWB Centerline		
• Maximum	213	300
• Average	212	210
SWB Wall		
• Maximum	124	126
• Average	123	122
ICV Wall		
• Maximum	122	125
• Average	120	120
• Minimum	118	115
ICV Air		
• Average	122	121
ICV Main O-ring Seal		
• Maximum	118	122
OCV Wall		
• Maximum	121	123
OCV Main O-ring Seal		
• Maximum	114	116
Polyurethane Foam		
• Maximum	121	123
OCA Outer Shell		
• Maximum	102	102

Table 3.5-3 – CTU-1 Temperature Indicating Label Locations and Results

Label Identifier	Location		Indicated Temperature	Remarks
	Y (in)	C (deg)		
TI-1	0.0	0.0	160 ºF	Payload pallet; top center
TI-2	19.0	85.0	130 ºF	Drum #1; side toward payload center
TI-3	19.0	12.0	140 ºF	Drum #4 (bottom center drum); side
TI-4	34.0	0.0	130 ºF	Drum #4 (bottom center drum); top center
TI-5	53.0	85.0	130 ºF	Drum #8; side toward payload center
TI-6	53.0	12.0	130 ºF	Drum #11 (top center drum); side
TI-7	69.0	0.0	130 ºF	Drum #11 (top center drum); top
TI-8	62.0	49.0	150 ºF	ICV body; inner lower seal flange surface
TI-9	62.0	13.5	170 ºF	ICV body; inner lower seal flange surface
TI-10	62.0	205.0	170 ºF	ICV body; inner lower seal flange surface
TI-11	62.0	166.0	150 ºF	ICV body; inner lower seal flange surface
TI-12	62.0	128.0	140 ºF	ICV body; inner lower seal flange surface
TI-13	62.0	88.5	150 ºF	ICV body; inner lower seal flange surface
TI-14	29.5	49.0	160 ºF	ICV body; inner shell surface
TI-15	29.5	13.5	170 ºF	ICV body; inner shell surface
TI-16	29.5	205.0	160 ºF	ICV body; inner shell surface
TI-17	29.5	166.0	140 ºF	ICV body; inner shell surface
TI-18	29.5	128.0	140 ºF	ICV body; inner shell surface
TI-19	29.5	88.5	160 ºF	ICV body; inner shell surface
TI-20	1.5	49.0	150 ºF	ICV body; shell-to-lower torispherical head weld
TI-21	1.5	13.5	170 ºF	ICV body; shell-to-lower torispherical head weld
TI-22	1.5	205.0	190 ºF	ICV body; shell-to-lower torispherical head weld
TI-23	1.5	166.0	140 ºF	ICV body; shell-to-lower torispherical head weld
TI-24	1.5	128.0	150 ºF	ICV body; shell-to-lower torispherical head weld
TI-25	1.5	88.5	180 ºF	ICV body; shell-to-lower torispherical head weld
TI-26	Bottom Center		270 ºF	ICV body; lower torispherical head
TI-27	1.5	90.0	160 ºF	ICV lid; shell-to-upper torispherical head weld
TI-28	1.5	210.0	160 ºF	ICV lid; shell-to-upper torispherical head weld
TI-29	1.5	330.0	130 ºF	ICV lid; shell-to-upper torispherical head weld
TI-30	Top Center		150 ºF	ICV lid; upper torispherical head
TI-31	Near TI-29		140 ºF	Upper aluminum honeycomb spacer; lower face
TI-32	57.5	30.0	220 ºF	OCV body; inner lower seal flange surface
TI-33	57.5	64.0	230 ºF	OCV body; inner lower seal flange surface
TI-34	57.5	74.0	250 ºF	OCV body; inner lower seal flange surface
TI-35	57.5	101.0	220 ºF	OCV body; inner lower seal flange surface
TI-36	57.5	138.0	190 ºF	OCV body; inner lower seal flange surface
TI-37	57.5	183.0	190 ºF	OCV body; inner lower seal flange surface
TI-38	57.5	201.0	210 ºF	OCV body; inner lower seal flange surface

Label Identifier	Location		Indicated Temperature	Remarks
	Y (in)	C (deg)		
TI-39	57.5	236.0	200 ºF	OCV body; inner lower seal flange surface
TI-40	50.5	30.0	190 ºF	OCV body; inner conical shell surface
TI-41	50.5	74.0	240 ºF	OCV body; inner conical shell surface
TI-42	50.5	101.0	180 ºF	OCV body; inner conical shell surface
TI-43	50.5	138.0	160 ºF	OCV body; inner conical shell surface
TI-44	50.5	183.0	170 ºF	OCV body; inner conical shell surface
TI-45	50.5	201.0	170 ºF	OCV body; inner conical shell surface
TI-46	50.5	236.0	170 ºF	OCV body; inner conical shell surface
TI-47	26.5	30.0	310 ºF	OCV body; inner shell surface near stiffening ring
TI-48	26.5	74.0	340 ºF	OCV body; inner shell surface near stiffening ring
TI-49	26.5	101.0	290 ºF	OCV body; inner shell surface near stiffening ring
TI-50	26.5	138.0	220 ºF	OCV body; inner shell surface near stiffening ring
TI-51	26.5	183.0	170 ºF	OCV body; inner shell surface near stiffening ring
TI-52	26.5	201.0	160 ºF	OCV body; inner shell surface near stiffening ring
TI-53	26.5	236.0	170 ºF	OCV body; inner shell surface near stiffening ring
TI-54	1.5	30.0	160 ºF	OCV body; shell-to-lower torispherical head weld
TI-55	1.5	74.0	340 ºF	OCV body; shell-to-lower torispherical head weld
TI-56	1.5	101.0	270 ºF	OCV body; shell-to-lower torispherical head weld
TI-57	1.5	138.0	170 ºF	OCV body; shell-to-lower torispherical head weld
TI-58	1.5	183.0	150 ºF	OCV body; shell-to-lower torispherical head weld
TI-59	1.5	201.0	170 ºF	OCV body; shell-to-lower torispherical head weld
TI-60	1.5	236.0	200 ºF	OCV body; shell-to-lower torispherical head weld
TI-61	-16.6	30.0	210 ºF	OCV body; lower torispherical head
TI-62	-16.6	74.0	200 ºF	OCV body; lower torispherical head
TI-63	-16.6	160.0	200 ºF	OCV body; lower torispherical head
TI-64	-16.6	201.0	230 ºF	OCV body; lower torispherical head
TI-65	1.0	90.5	220 ºF	OCV lid; shell-to-upper torispherical head weld
TI-66	1.0	131.5	220 ºF	OCV lid; shell-to-upper torispherical head weld
TI-67	1.0	171.5	230 ºF	OCV lid; shell-to-upper torispherical head weld
TI-68	1.0	211.5	190 ºF	OCV lid; shell-to-upper torispherical head weld
TI-69	1.0	251.5	200 ºF	OCV lid; shell-to-upper torispherical head weld
TI-70	1.0	291.5	210 ºF	OCV lid; shell-to-upper torispherical head weld
TI-71	18.0	90.5	160 ºF	OCV lid; upper torispherical head
TI-72	18.0	131.5	260 ºF	OCV lid; upper torispherical head
TI-73	18.0	171.5	300 ºF	OCV lid; upper torispherical head
TI-74	18.0	211.5	170 ºF	OCV lid; upper torispherical head
TI-75	18.0	251.5	340 ºF	OCV lid; upper torispherical head
TI-76	18.0	291.5	170 ºF	OCV lid; upper torispherical head
TI-77	Top Center		Damaged	OCV lid; upper torispherical head

Table 3.5-4 – CTU-2 Temperature Indicating Label Locations and Results

Label Identifier	Location		Indicated Temperature	Remarks
	Y (in)	C (deg)		
TI-1	Top Center		160 ºF	Payload pallet; top center
TI-2	19.0	27.0	140 ºF	Drum #1 (bottom center drum); side
TI-3	19.0	210.0	150 ºF	Drum #3; side
TI-4	Top Center		150 ºF	Drum #1 (bottom center drum); top center
TI-5	19.0	180.0	Damaged	Drum #3; side (outside edge of payload)
TI-6	19.0	250.0	150 ºF	Drum #5; side (outside edge of payload)
TI-7	19.0	120.0	170 ºF	Drum #7; side (outside edge of payload)
TI-8	54.0	90.0	160 ºF	Drum #8 (top center drum); side
TI-9	Top Center		150 ºF	Drum #8 (top center drum); top center
TI-10	56.0	120.0	150 ºF	Drum #10; side (outside edge of payload)
TI-11	6.0	0.0	Damaged	OCV lid; shell surface
TI-12	6.0	90.0	200 ºF	OCV lid; shell surface
TI-13	6.0	180.0	170 ºF	OCV lid; shell surface
TI-14	6.0	270.0	190 ºF	OCV lid; shell surface
TI-15	25.0	0.0	340 ºF	OCV lid; upper torispherical head
TI-16	25.0	90.0	250 ºF	OCV lid; upper torispherical head
TI-17	25.0	180.0	170 ºF	OCV lid; upper torispherical head
TI-18	25.0	270.0	220 ºF	OCV lid; upper torispherical head
TI-19	18.0	143.0	270 ºF	OCV lid; upper torispherical head
TI-20	Top Center		290 ºF	OCV lid; upper torispherical head
TI-21	6.0	135.0	220 ºF	OCV lid; upper torispherical head
TI-22	6.0	225.0	280 ºF	OCV lid; upper torispherical head
TI-23	57.0	0.0	250 ºF	OCV body; inner lower seal flange surface
TI-24	57.0	90.0	220 ºF	OCV body; inner lower seal flange surface
TI-25	57.0	180.0	220 ºF	OCV body; inner lower seal flange surface
TI-26	57.0	215.0	230 ºF	OCV body; inner lower seal flange surface
TI-27	57.0	270.0	200 ºF	OCV body; inner lower seal flange surface
TI-28	49.0	0.0	220 ºF	OCV body; inner conical shell surface
TI-29	49.0	90.0	190 ºF	OCV body; inner conical shell surface
TI-30	49.0	180.0	210 ºF	OCV body; inner conical shell surface
TI-31	49.0	215.0	170 ºF	OCV body; inner conical shell surface
TI-32	49.0	270.0	170 ºF	OCV body; inner conical shell surface
TI-33	26.0	0.0	Damaged	OCV body; inner shell surface near stiffening ring
TI-34	26.0	90.0	170 ºF	OCV body; inner shell surface near stiffening ring
TI-35	26.0	180.0	190 ºF	OCV body; inner shell surface near stiffening ring
TI-36	26.0	270.0	170 ºF	OCV body; inner shell surface near stiffening ring
TI-37	1.0	0.0	Damaged	OCV body; shell-to-lower torispherical head weld
TI-38	1.0	90.0	Damaged	OCV body; shell-to-lower torispherical head weld
TI-39	1.0	135.0	220 ºF	OCV body; shell-to-lower torispherical head weld

Label Identifier	Location		Indicated Temperature	Remarks
	Y (in)	C (deg)		
TI-40	1.0	180.0	Damaged	OCV body; shell-to-lower torispherical head weld
TI-41	1.0	225.0	190 ºF	OCV body; shell-to-lower torispherical head weld
TI-42	1.0	270.0	Damaged	OCV body; shell-to-lower torispherical head weld
TI-43	-18.0	0.0	350 ºF	OCV body; lower torispherical head
TI-44	-18.0	90.0	250 ºF	OCV body; lower torispherical head
TI-45	-18.0	180.0	250 ºF	OCV body; lower torispherical head
TI-46	-11.0	250.0	250 ºF	OCV body; lower torispherical head
TI-47	-18.0	270.0	260 ºF	OCV body; lower torispherical head
TI-48	66.5	0.0	200 ºF	ICV body; inner lower seal flange surface
TI-49	Seal Test Port		170 ºF	ICV body; inner lower seal flange surface
TI-50	Vent Port		170 ºF	ICV body; inner lower seal flange surface
TI-51	66.5	270.0	170 ºF	ICV body; inner lower seal flange surface
TI-52	66.5	180.0	170 ºF	ICV body; inner lower seal flange surface
TI-53	66.5	90.0	180 ºF	ICV body; inner lower seal flange surface
TI-54	45.5	0.0	200 ºF	ICV body; inner shell surface
TI-55	45.5	90.0	170 ºF	ICV body; inner shell surface
TI-56	45.5	180.0	Damaged	ICV body; inner shell surface
TI-57	45.5	270.0	160 ºF	ICV body; inner shell surface
TI-58	-14.5	270.0	190 ºF	ICV body; lower torispherical head
TI-59	21.5	0.0	210 ºF	ICV body; inner shell surface
TI-60	21.5	90.0	170 ºF	ICV body; inner shell surface
TI-61	21.5	180.0	180 ºF	ICV body; inner shell surface
TI-62	21.5	270.0	160 ºF	ICV body; inner shell surface
TI-63	3.5	0.0	220 ºF	ICV body; shell-to-lower torispherical head weld
TI-64	3.5	90.0	170 ºF	ICV body; shell-to-lower torispherical head weld
TI-65	3.5	180.0	Damaged	ICV body; shell-to-lower torispherical head weld
TI-66	3.5	270.0	180 ºF	ICV body; shell-to-lower torispherical head weld
TI-67	-14.5	0.0	Damaged	ICV body; lower torispherical head
TI-68	-14.5	90.0	200 ºF	ICV body; lower torispherical head
TI-69	-14.5	180.0	190 ºF	ICV body; lower torispherical head
TI-70	Near Test Ports		250 ºF	ICV body; lower torispherical head
TI-71	4.0	0.0	200 ºF	ICV lid; shell-to-upper torispherical head weld
TI-72	4.0	90.0	Damaged	ICV lid; shell-to-upper torispherical head weld
TI-73	4.0	180.0	210 ºF	ICV lid; shell-to-upper torispherical head weld
TI-74	4.0	270.0	180 ºF	ICV lid; shell-to-upper torispherical head weld
TI-75	24.0	0.0	190 ºF	ICV lid; upper torispherical head
TI-76	24.0	90.0	170 ºF	ICV lid; upper torispherical head
TI-77	24.0	180.0	200 ºF	ICV lid; upper torispherical head
TI-78	24.0	270.0	190 ºF	ICV lid; upper torispherical head
TI-79	N/A	120.0	180 ºF	ICV lid; inner lift pocket surface
TI-80	N/A	240.0	190 ºF	ICV lid; inner lift pocket surface

Table 3.5-5 – HAC Fire Temperature Readings; Fourteen 55-Gallon Drums

Location	Measured Temperature (ºF)		
	CTU-1	CTU-2	Max Allowable
Center Drum Wall			
• Maximum	140	160	N/A
• Average	135	150	N/A
Outer Drum Wall			
• Maximum	130	170	N/A
• Average	130	155	N/A
Average All Drums			
• Wall	132	153	N/A
ICV Wall			
• Maximum	190①	220②	N/A
• Average	161	187	N/A
ICV Air			
• Average	155	179	N/A
ICV Main O-ring Seal			
• Maximum	170	200	400
• Average	155	177	400
OCV Wall, Maximum			
• Thermocouples	312	439	N/A
• Temperature Indicating Labels	340	350	N/A
OCV Wall, Average			
• Thermocouples③	206	284	N/A
• Temperature Indicating Labels	214	225	N/A
OCV Main O-ring Seal, Maximum			
• Thermocouples	260	253	400
• Temperature Indicating Labels	250	250	400
OCV Main O-ring Seal, Average			
• Thermocouples	229	230	400
• Temperature Indicating Labels	215	224	400

Notes:

① Maximum passive temperature indicating label reading of 270 ºF at a location (TI-26) near the inlet where 350 ºF pre-heat air was injected; this temperature is test-induced and not real.

② Maximum passive temperature indicating label reading of 250 ºF at a location (TI-70) near the inlet where 350 ºF pre-heat air was injected; this temperature is test-induced and not real.

③ Conservatively taken as the average of the absolute maximum temperature, a conservative estimate because maximum temperatures do not occur at the same time. Thus, the actual average at any time would be less (see Figure 3.5-6 through Figure 3.5-11).

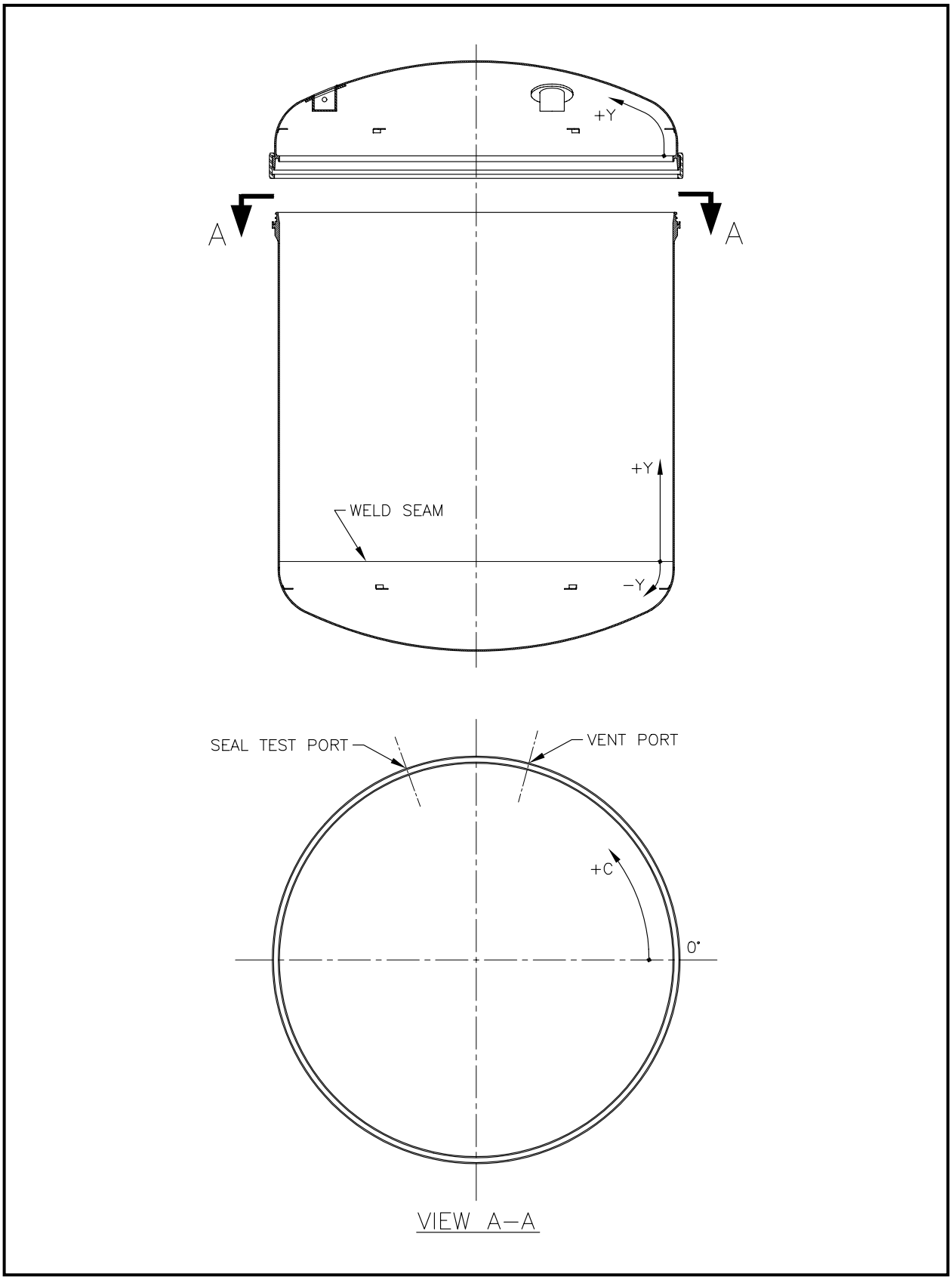

Figure 3.5-1 – CTU-1 and CTU-2 ICV Temperature Indicating Label Locations

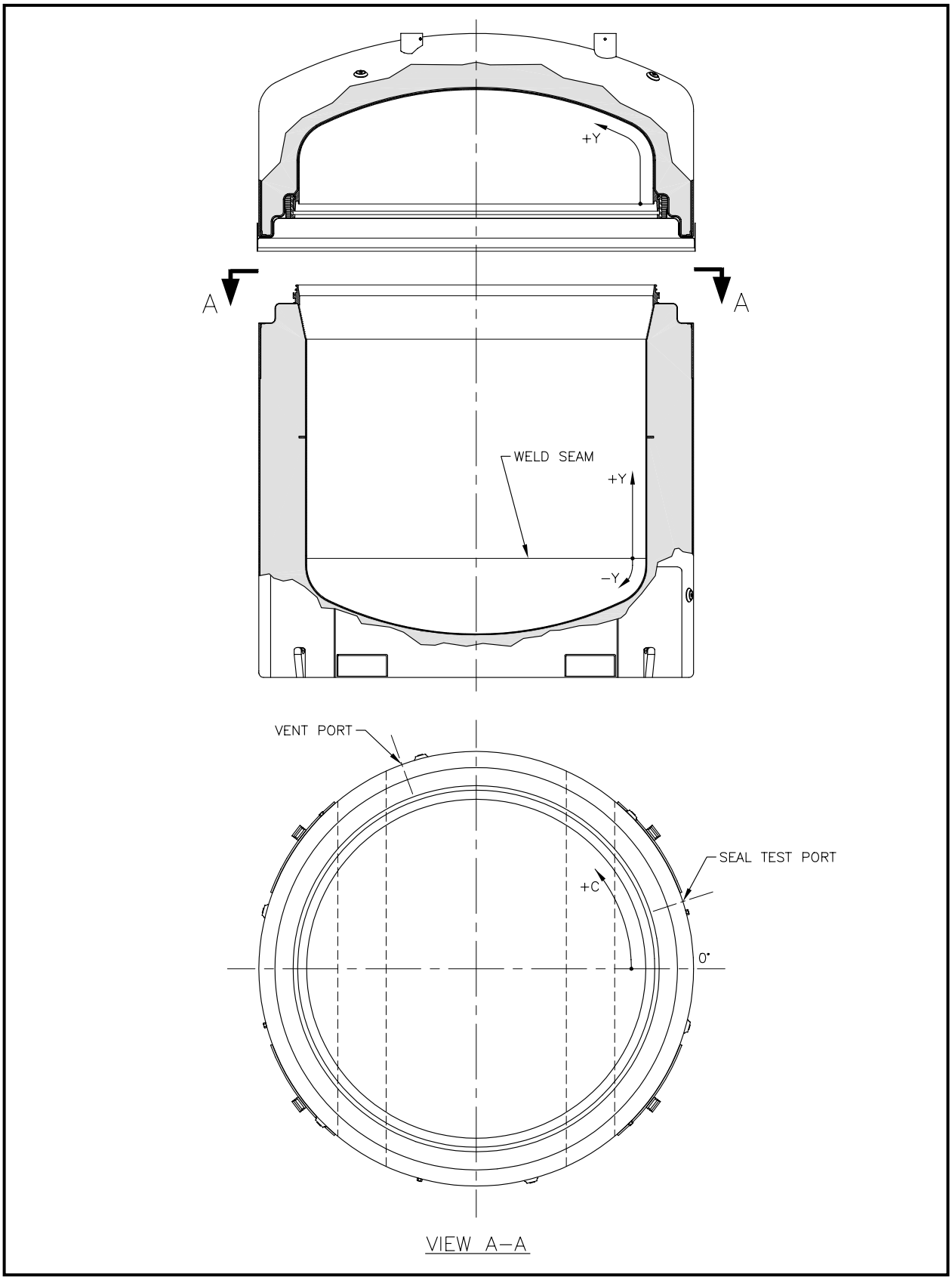

Figure 3.5-2 – CTU-1 OCV Temperature Indicating Label Locations

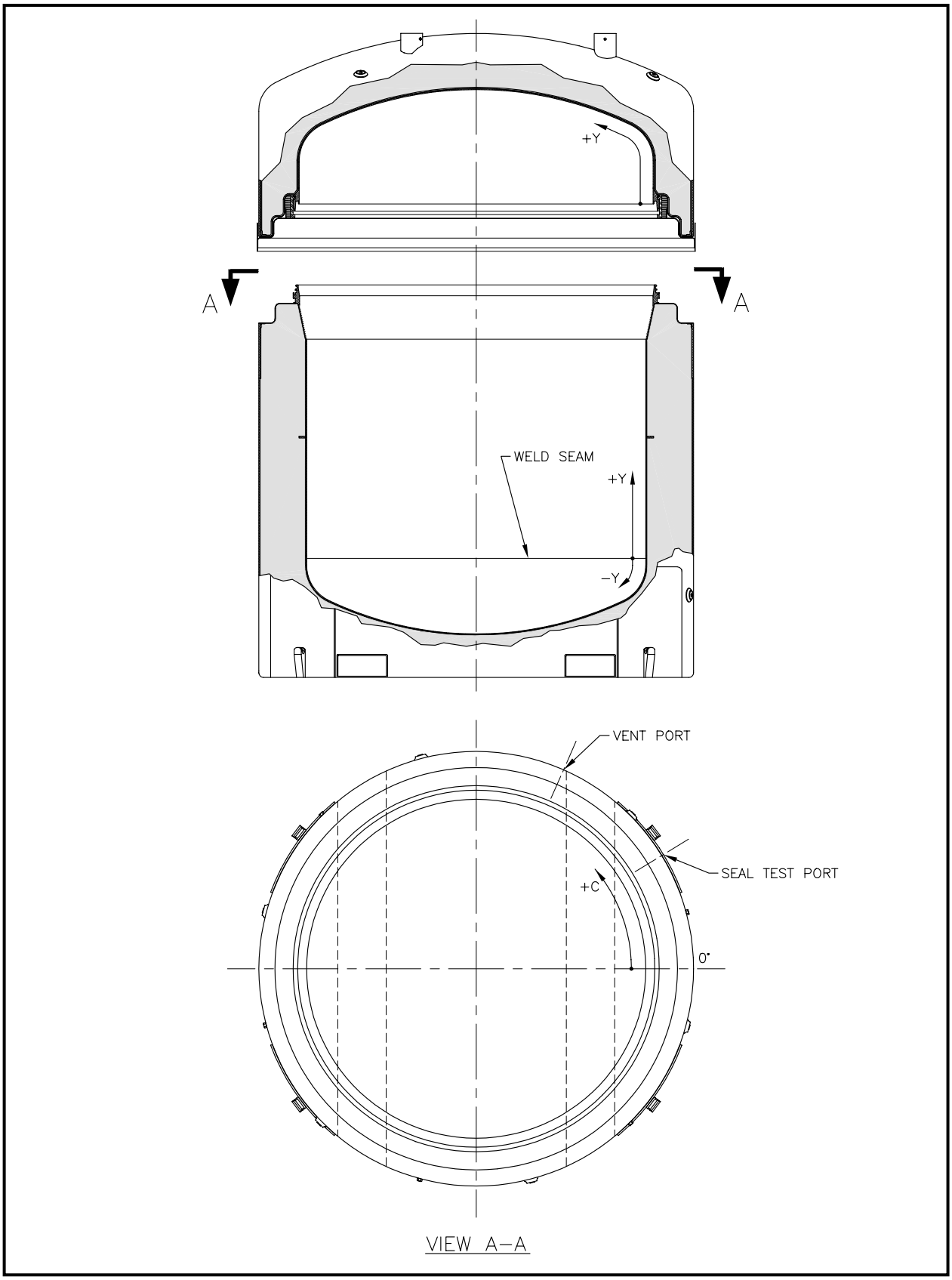

Figure 3.5-3 – CTU-2 OCV Temperature Indicating Label Locations

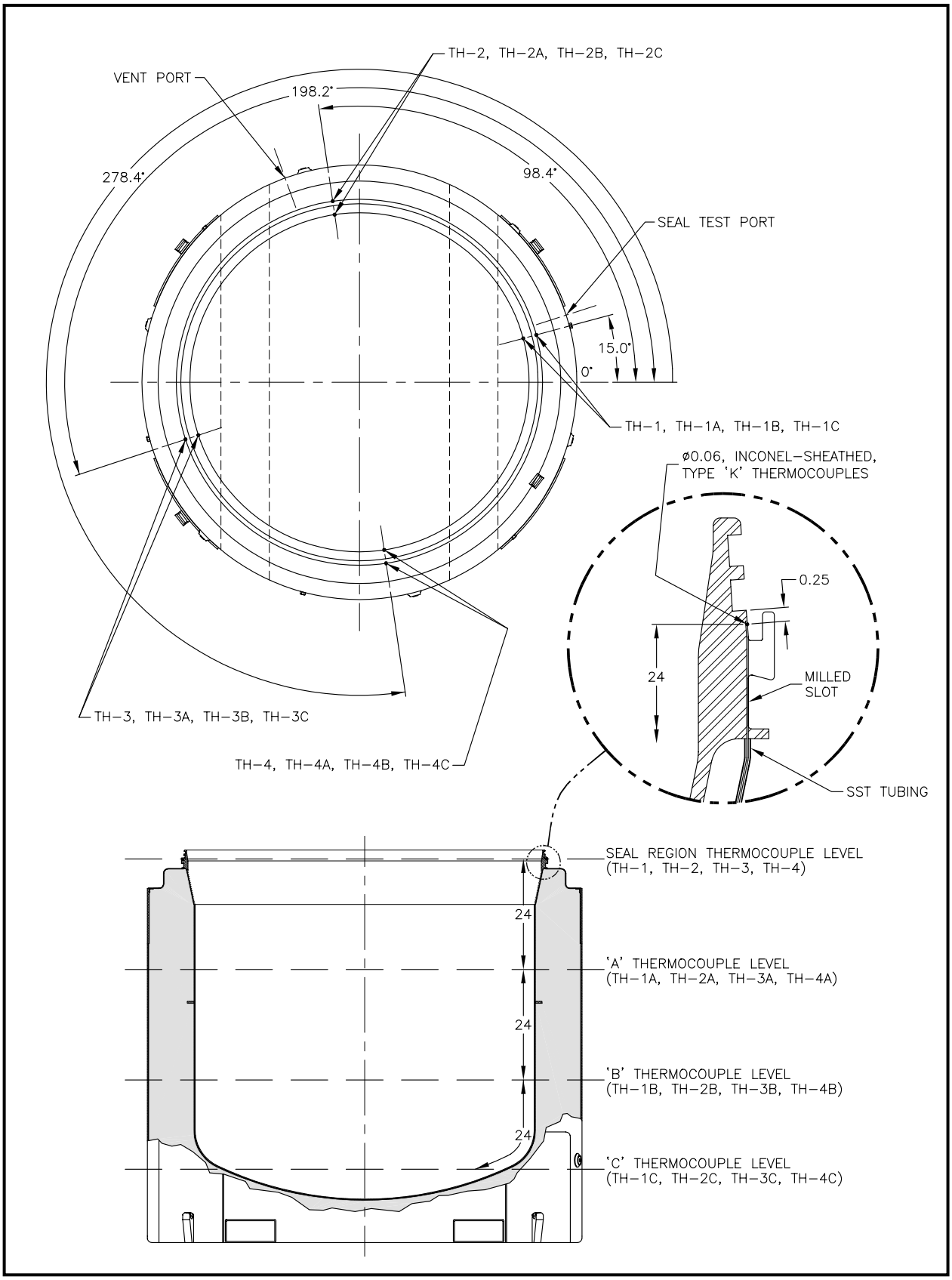

Figure 3.5-4 – CTU-1 OCV Thermocouple Locations

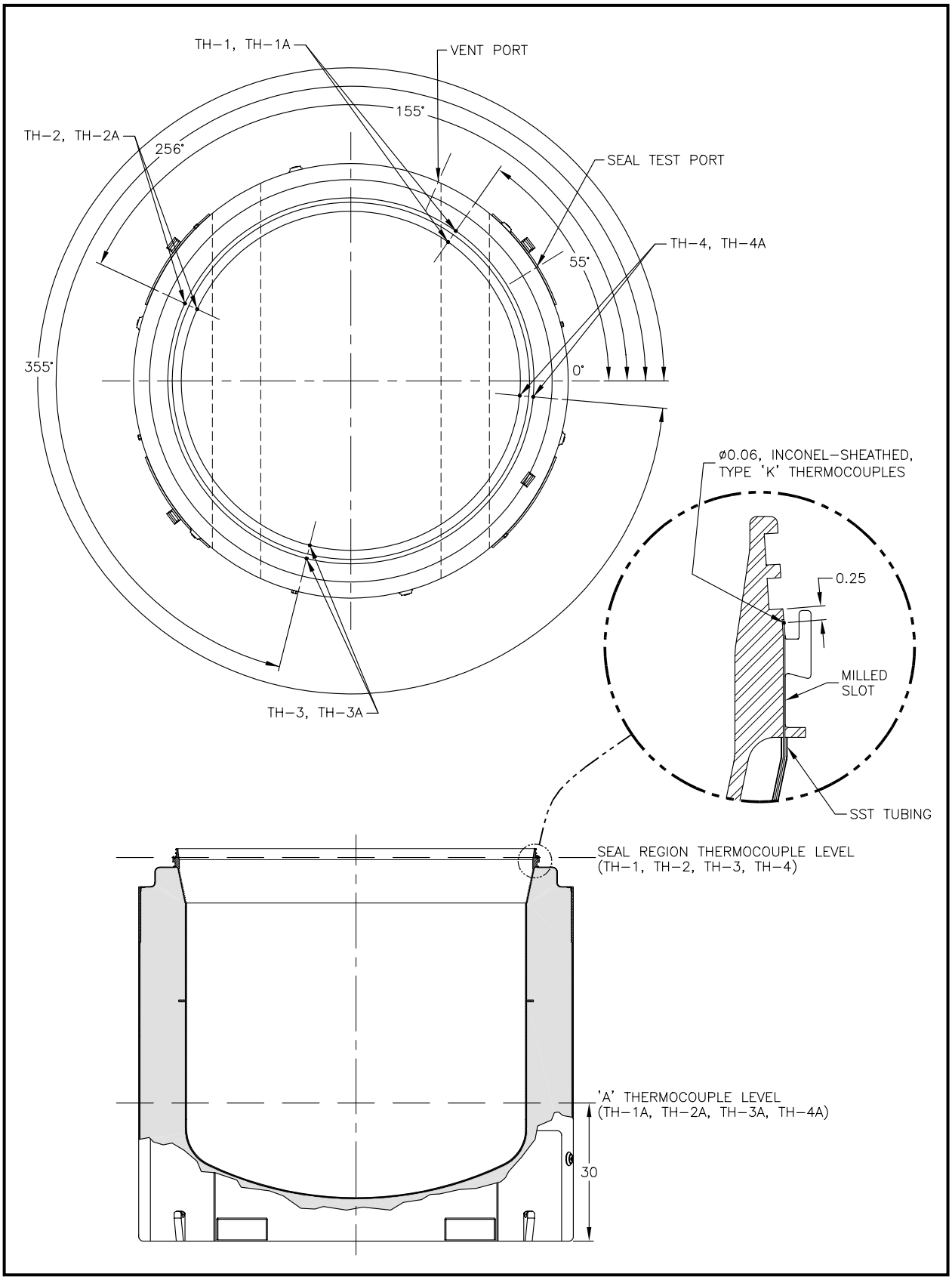

Figure 3.5-5 – CTU-2 OCV Thermocouple Locations

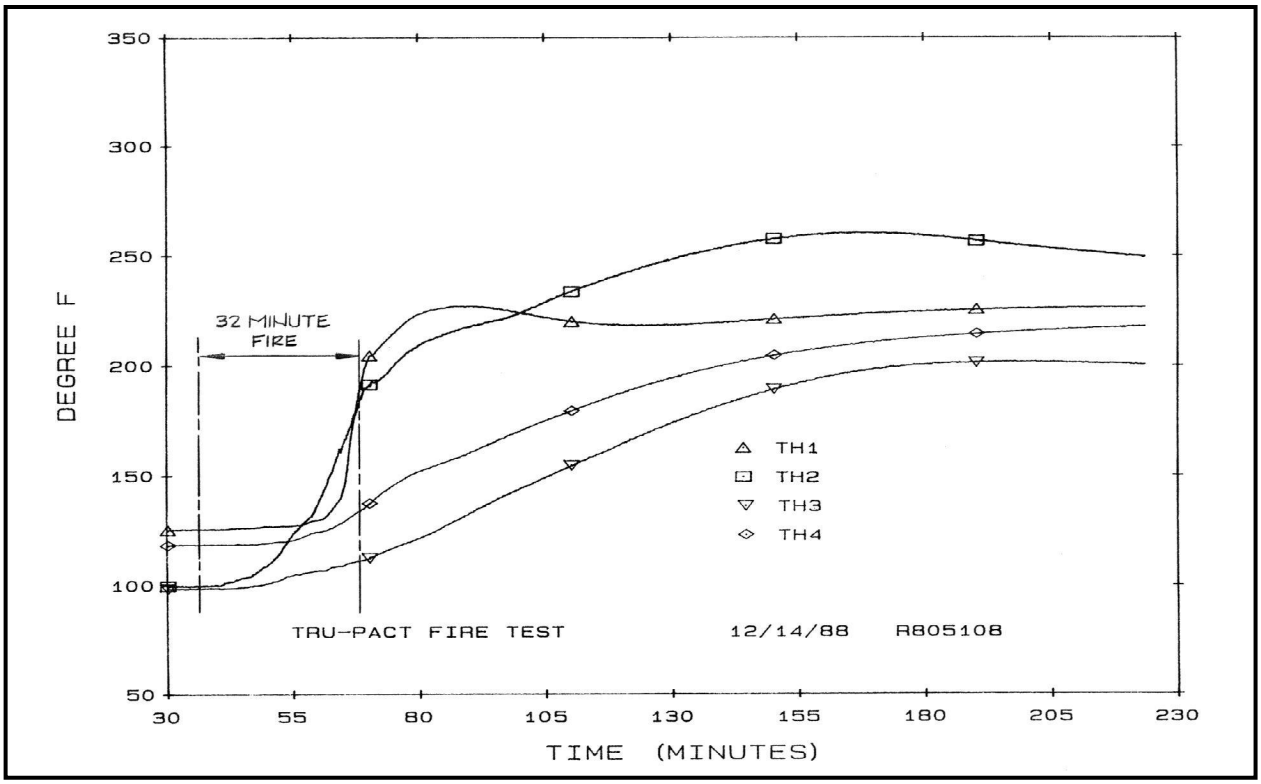

Figure 3.5-6 – CTU-1 OCV Thermocouple Data (TH-1, TH-2, TH-3, TH-4)

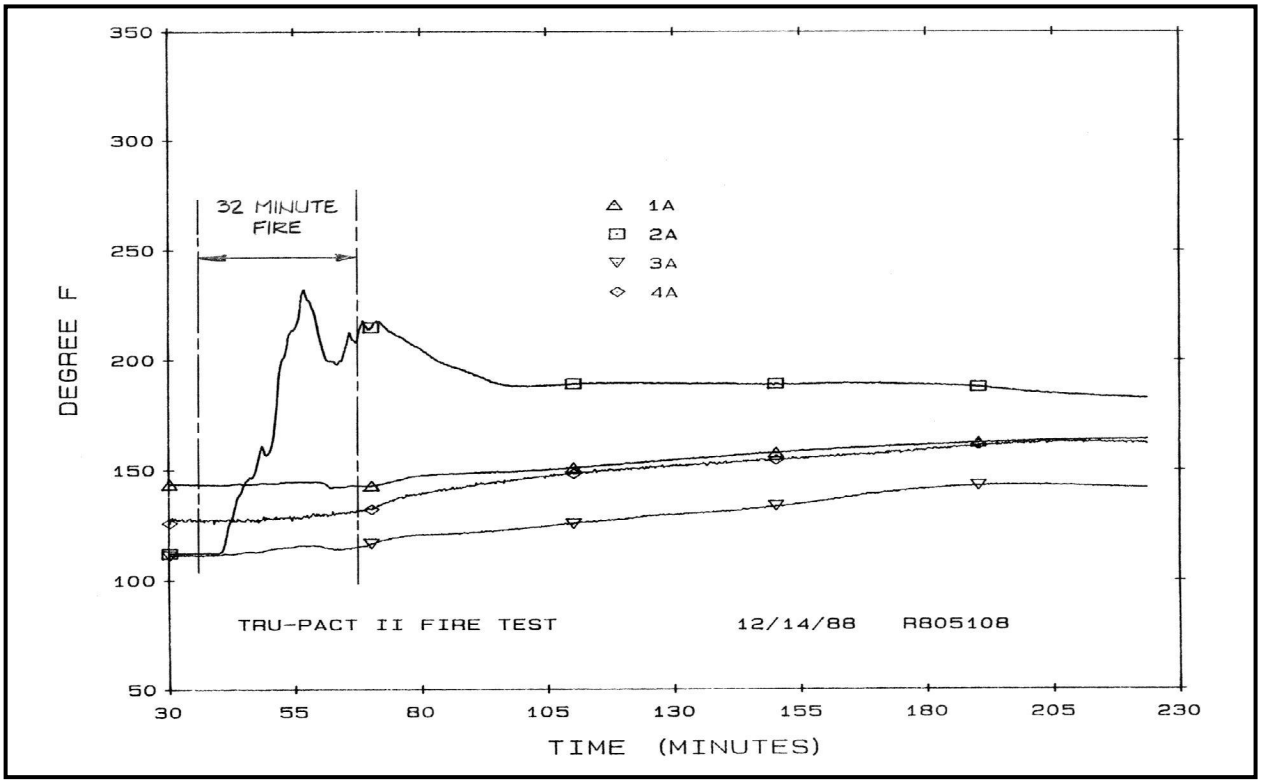

Figure 3.5-7 – CTU-1 OCV Thermocouple Data (TH-1A, TH-2A, TH-3A, TH-4A)

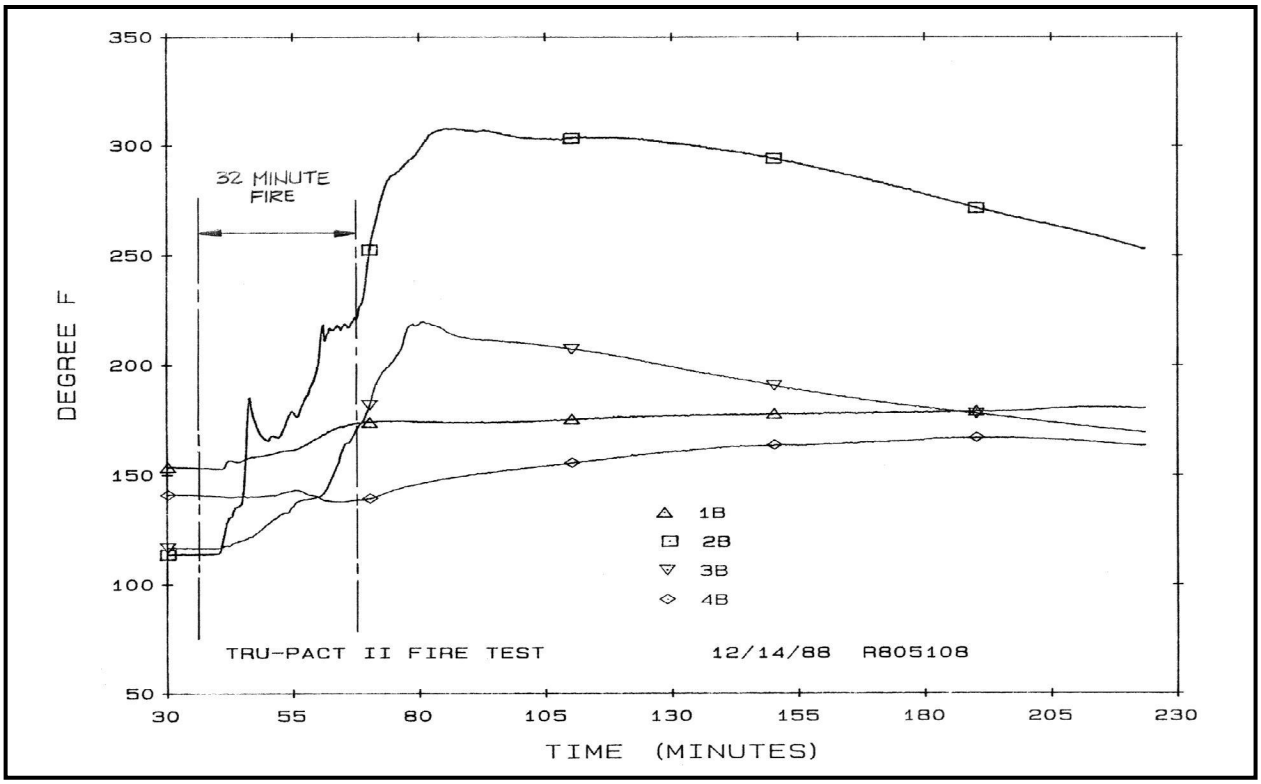

Figure 3.5-8 – CTU-1 OCV Thermocouple Data (TH-1B, TH-2B, TH-3B, TH-4B)

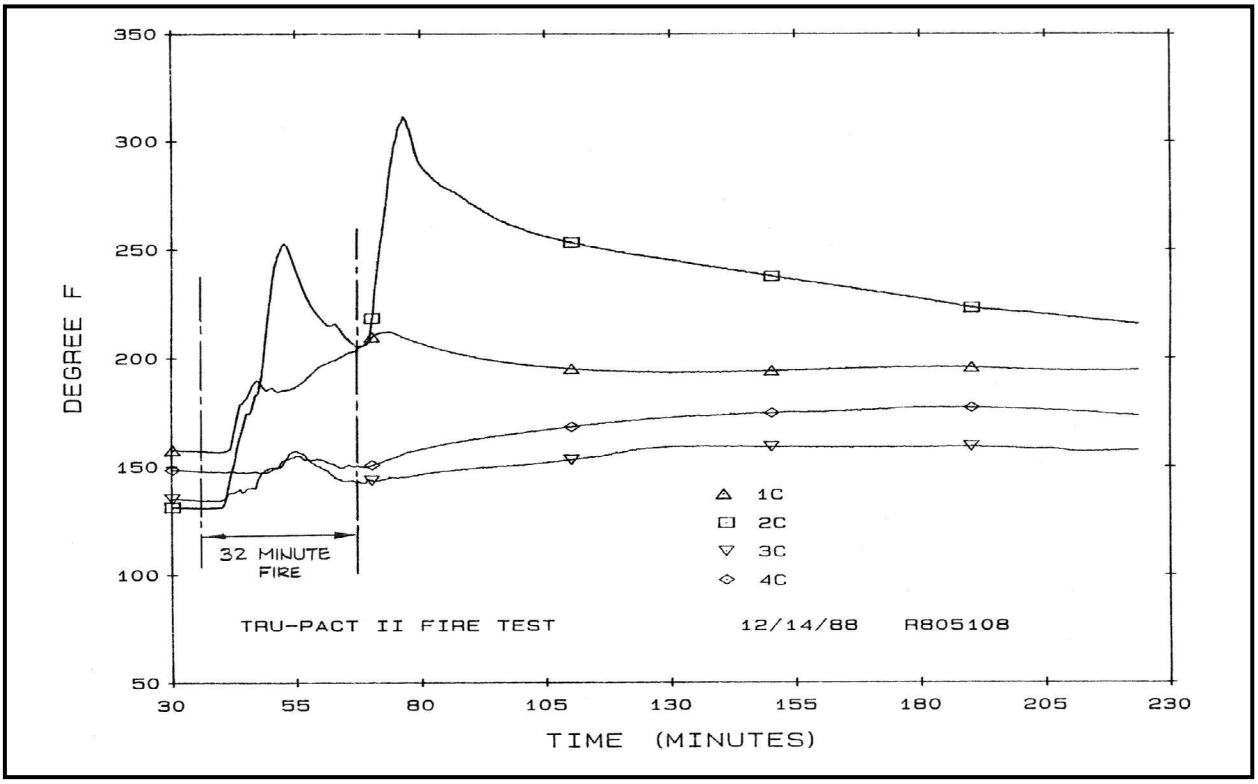

Figure 3.5-9 – CTU-1 OCV Thermocouple Data (TH-1C, TH-2C, TH-3C, TH-4C)

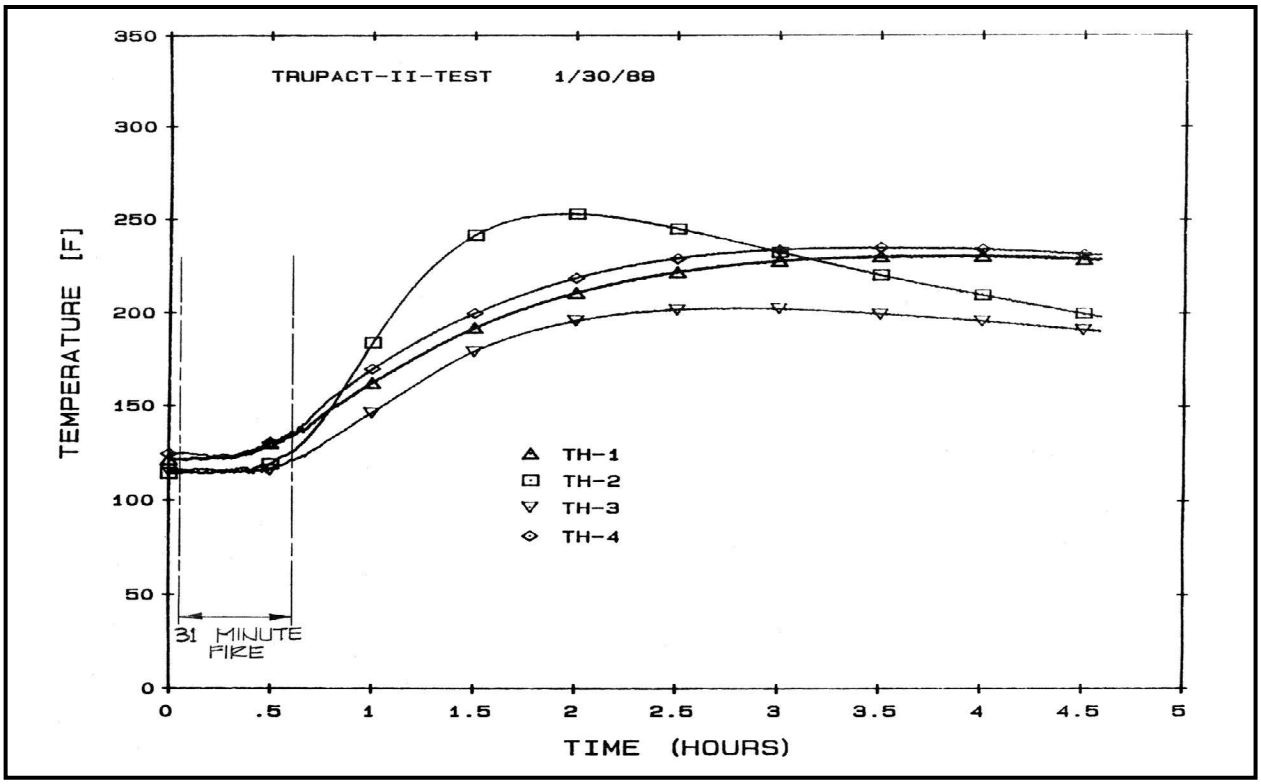

Figure 3.5-10 – CTU-2 OCV Thermocouple Data (TH-1, TH-2, TH-3, TH-4)

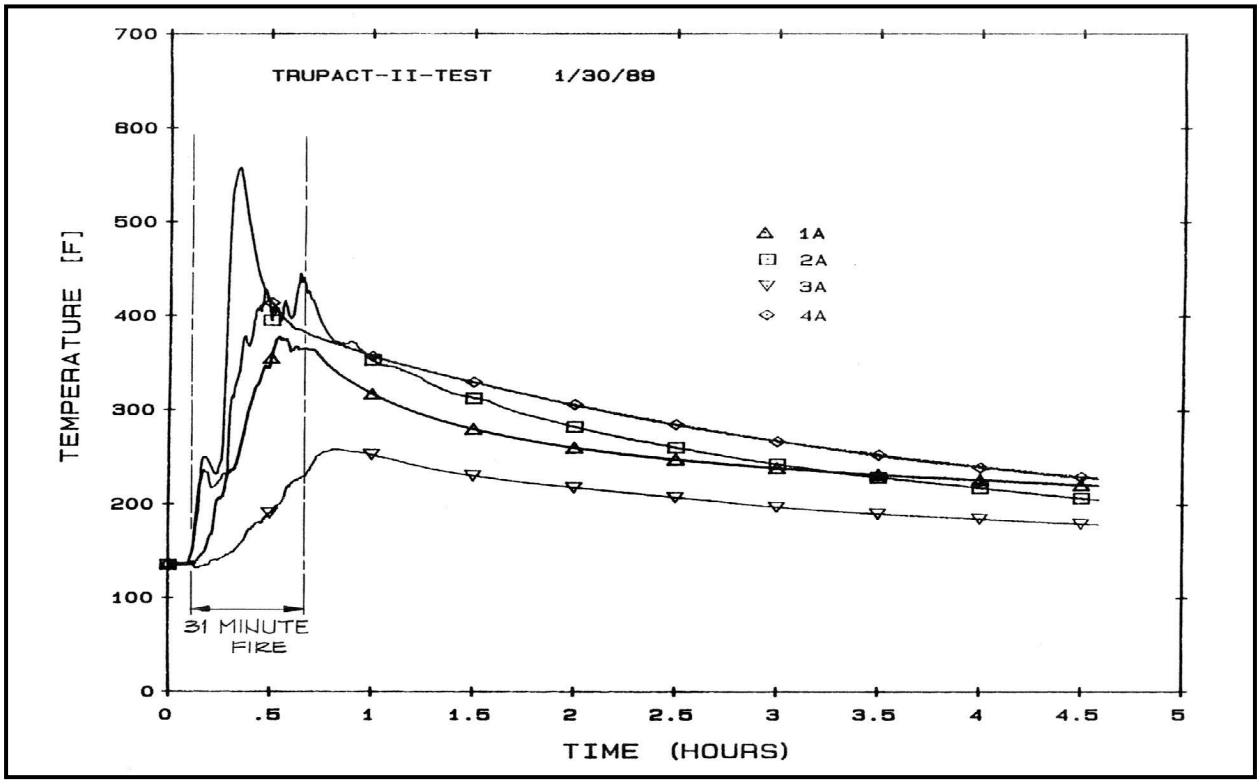

Figure 3.5-11 – CTU-2 OCV Thermocouple Data (TH-1A, TH-2A, TH-3A, TH-4A)

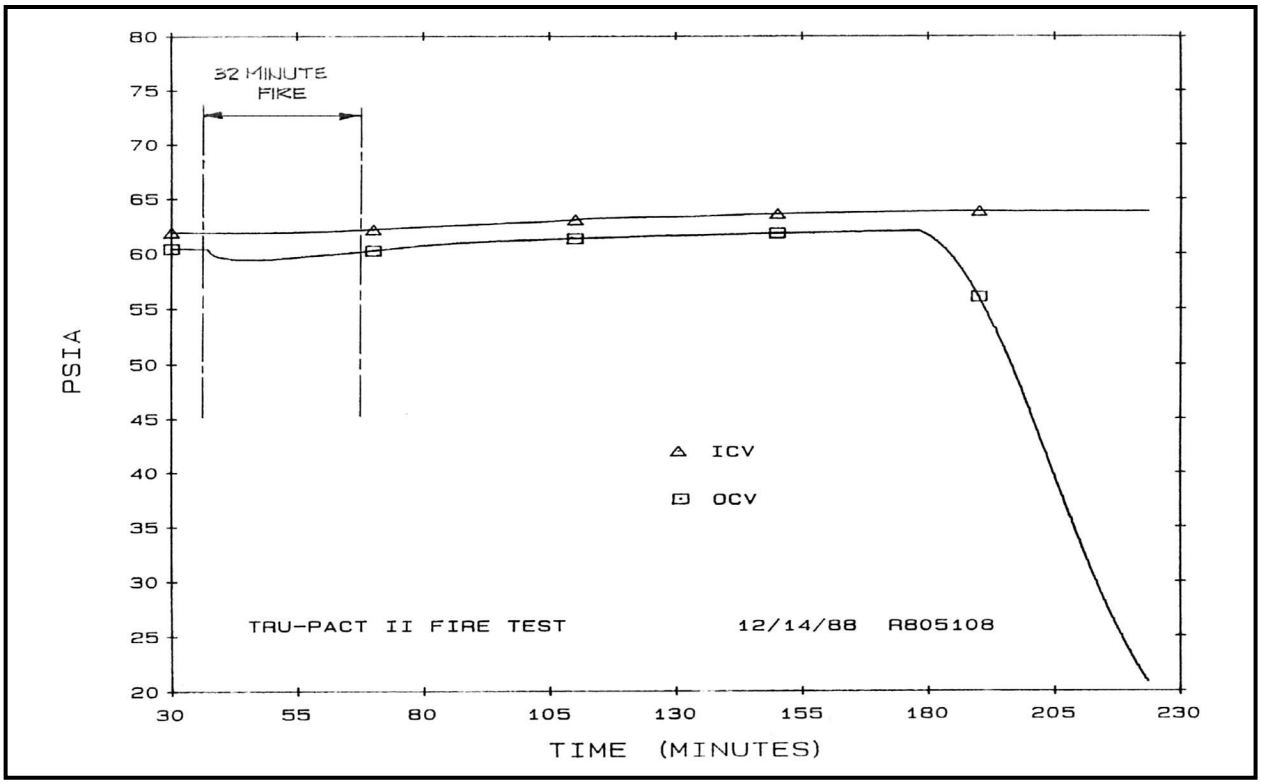

Figure 3.5-12 – CTU-1 Pressure Transducer Data During Fire Test No. 10

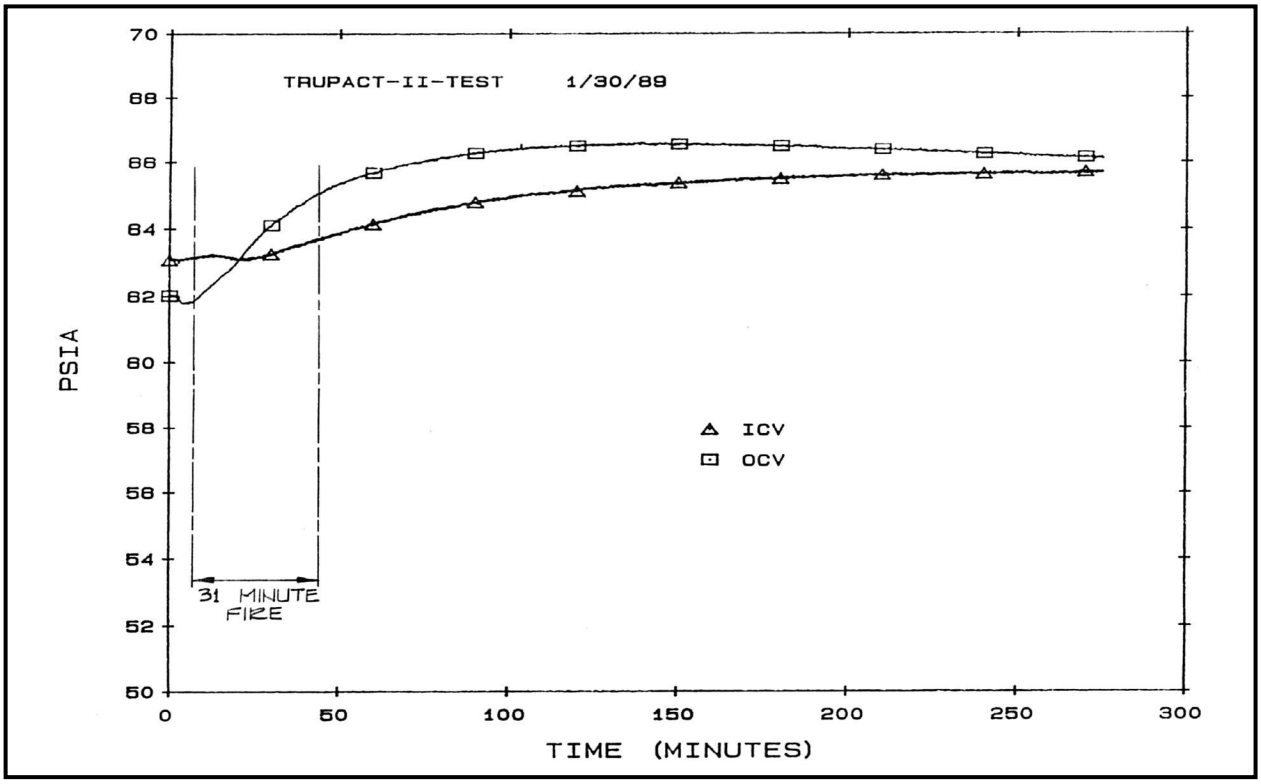

Figure 3.5-13 – CTU-2 Pressure Transducer Data During Fire Test No. 9

3.6 Appendices

3.6.1 *Computer Analysis Results*

3.6.2 *Thermal Model Details*

This page intentionally left blank.

3.6.1 Computer Analysis Results

3.6.1.1 Fourteen 55-Gallon Drum Payload with 100 ºF Ambient and Full Solar, Uniformly Distributed Decay Heat Load in All Drums (Case 1)

CASE 1 - ALL DECAY HEAT EQUALLY IN ALL DRUMS (FULL SOLAR LOAD)

Location	Decay Heat (watts) 0	10	20	30	40
Maximum Center Drum Centerline:	129.21	137.74	147.49	157.19	166.85
Average Center Drum Centerline:	126.22	135.76	144.77	153.78	162.68
Maximum Center Drum Wall:	129.21	134.23	140.92	147.57	154.17
Average Center Drum Wall:	126.22	132.25	138.20	144.15	150.00
Maximum Outer Drum Centerline:	129.17	137.37	146.65	155.91	165.07
Average Outer Drum Centerline:	126.38	135.57	144.30	153.03	161.67
Maximum Outer Drum Wall:	129.20	134.22	140.89	147.52	154.12
Average Outer Drum Wall:	126.43	132.18	137.87	143.56	149.15
Average Drum Centerline:	126.35	135.59	144.37	153.14	161.82
Average Drum Wall:	126.40	132.19	137.92	143.64	149.27
Maximum ICV Wall:	129.23	133.63	138.31	143.45	149.01
Average ICV Wall:	126.20	131.22	136.21	141.23	146.17
Minimum ICV Wall:	120.58	125.99	131.34	136.73	142.07
Average ICV Air:	126.33	131.85	137.32	142.79	148.18
Maximum ICV O-ring Seal:	129.17	133.36	137.53	141.72	145.83
Maximum OCV Wall:	129.34	133.45	137.90	142.91	148.30
Maximum OCV O-ring Seal:	129.34	132.72	136.10	139.49	142.85
Maximum Polyurethane Foam:	154.95	154.95	154.95	154.95	154.95
Maximum OCA Outer Shell:	154.95	154.95	154.95	154.95	154.95

Area of Each Node (ft^2)

Center Drum (Node)	(Area)	Outer Drums (Node)	(Area)	ICV Wall (Node)	(Area)
208:	11.35145	218:	11.35145	152:	28.96573
308:	11.35145	228:	22.70291	252:	27.42553
408:	11.35145	238:	22.70291	352:	30.20783
508:	11.35145	248:	11.35145	452:	25.83564
		318:	11.35145	552:	14.70644
Total:	45.40583	328:	22.70291	652:	16.29633
		338:	22.70291	752:	28.96573
		348:	11.35145	Total:	172.4032
		418:	11.35145		
		428:	22.70291		
		438:	22.70291		
		448:	11.35145		
		518:	11.35145		
		528:	22.70291		
		538:	22.70291		
		548:	11.35145		
		Total:	272.4349		

NOTE: Average temperatures are "area-weighted" based on the above nodal areas

CASE 1 - ALL DECAY HEAT EQUALLY IN ALL DRUMS (FULL SOLAR LOAD)

DECAY HEAT = 0 WATTS

202	120.963	302	127.253	402	127.446	502	129.205	204	120.962	304	127.253
404	127.446	504	129.205	206	120.962	306	127.253	406	127.446	506	129.205
208	120.962	308	127.253	408	127.446	508	129.205	212	121.58	312	127.084
412	127.603	512	129.176	222	121.653	322	127.064	422	127.622	522	129.172
232	121.838	332	127.019	432	127.669	532	129.166	242	121.925	342	126.998
442	127.691	542	129.162	214	121.324	314	127.152	414	127.538	514	129.186
224	121.465	324	127.105	424	127.574	524	129.179	234	122.06	334	126.964
434	127.725	534	129.157	244	122.3	344	126.906	444	127.787	544	129.149
216	121.132	316	127.209	416	127.488	516	129.196	226	121.261	326	127.185
426	127.522	526	129.19	236	122.339	336	126.895	436	127.797	536	129.147
246	122.706	346	126.805	446	127.89	546	129.133	218	121.046	318	127.232
418	127.467	518	129.2	228	121.126	328	127.212	428	127.487	528	129.194
238	122.486	338	126.863	438	127.834	538	129.142	248	122.9	348	126.757
448	127.939	548	129.126	5	127.35	10	127.35	15	127.35	260	124.769
360	127.244	262	126.712	362	128.397	264	128.511	364	129.493	266	130.175
366	130.524	460	128.686	462	129.382	464	130.054	466	130.69	562	129.694
564	130.188	566	130.792	660	129.425	662	129.833	664	130.382	666	130.835
160	117.554	162	112.417	164	107.444	166	103.576	760	129.328	762	129.46
764	129.589	766	129.714	768	129.835	170	102.14	172	130.858	270	130.963
370	131.015	470	130.994	570	130.97	670	131.038	77O	129.883	100	120.585
110	120.585	115	120.585	120	120.584	700	129.229	152	120.583	154	120.165
752	129.23	754	129.26	252	123.466	352	126.616	452	128.079	552	128.998
254	123.727	354	126.648	454	128.196	554	129.338	556	129.339	558	129.338
652	129.168	654	129.168	656	129.169	658	129.292				
200	120.963	300	127.253	400	127.446	500	129.205	240	121.653	340	127.064
440	127.622	540	129.172								

CASE 1 - ALL DECAY HEAT EQUALLY IN ALL DRUMS (FULL SOLAR LOAD)

DECAY HEAT = 10 WATTS

202	129.84	302	137.242	402	137.371	502	137.107	204	129.126	304	136.529
404	136.658	504	136.393	206	127.832	306	135.235	406	135.364	506	135.099
208	126.697	308	134.099	408	134.228	508	133.964	212	130.332	312	136.594
412	137.022	512	136.85	222	130.402	322	136.541	422	136.999	522	136.836
232	130.586	332	136.463	432	136.949	532	136.84	242	130.673	342	136.421
442	136.926	542	136.837	214	129.431	314	136.122	414	136.453	514	136.244
224	129.528	324	135.886	424	136.36	524	136.11	234	130.152	334	135.716
434	136.235	534	136.194	244	130.393	344	135.58	444	136.175	544	136.162
216	128.009	316	135.079	416	135.286	516	135.081	226	128.022	326	134.86
426	135.107	526	134.944	236	129.178	336	134.36	436	134.908	536	134.962
246	129.536	346	134.096	446	134.809	546	134.858	218	126.825	318	134.062
418	134.22	518	134.01	228	126.735	328	133.805	428	133.987	528	133.845
238	128.209	338	133.118	438	133.754	538	133.779	248	128.604	348	132.857
448	133.635	548	133.705	5	134.164	10	133.896	15	133.896	260	129.299
360	131.922	262	129.869	362	131.652	264	130.376	364	131.416	266	130.831
366	131.208	460	132.773	462	132.27	464	131.808	466	131.382	562	132.392
564	131.942	566	131.381	660	132.956	662	132.491	664	131.864	666	131.353
160	122.089	162	115.51	164	109.141	166	104.187	760	133.067	762	132.319
764	131.594	766	130.891	768	130.209	170	102.349	172	130.866	270	131.044
370	131.11	470	131.182	570	131.215	670	131.125	770	129.94	100	125.994
110	125.994	115	125.994	120	125.993	700	133.629	152	125.991	154	125.433
752	133.628	754	133.448	252	128.848	352	132.243	452	133.205	552	133.294
254	128.977	354	132.08	454	133.056	554	132.718	556	132.718	558	132.718
652	133.356	654	133.356	656	133.356	658	133.108				
200	130.21	300	137.613	400	137.742	500	137.477	240	130.772	340	136.912
440	137.37	540	137.207								

CASE 1 - ALL DECAY HEAT EQUALLY IN ALL DRUMS (FULL SOLAR LOAD)

DECAY HEAT = 20 WATTS

202	138.562	302	147.049	402	147.116	502	144.883	204	137.19	304	145.678
404	145.744	504	143.511	206	134.626	306	143.114	406	143.18	506	140.947
208	132.363	308	140.851	408	140.917	508	138.684	212	139.003	312	146.008
412	146.35	512	144.475	222	139.069	322	145.921	422	146.283	522	144.447
232	139.258	332	145.817	432	146.144	532	144.469	242	139.347	342	145.757
442	146.078	542	144.467	214	137.467	314	145.003	414	145.281	514	143.26
224	137.521	324	144.582	424	145.062	524	143.001	234	138.178	334	144.387
434	144.668	534	143.193	244	138.419	344	144.176	444	144.49	544	143.138
216	134.818	316	142.861	416	142.998	516	140.928	226	134.717	326	142.451
426	142.611	526	140.662	236	135.953	336	141.748	436	141.948	536	140.743
246	136.304	346	141.316	446	141.663	546	140.549	218	132.538	318	140.804
418	140.886	518	138.783	228	132.28	328	140.315	428	140.407	528	138.462
238	133.87	338	139.299	438	139.604	538	138.384	248	134.248	348	138.889
448	139.268	548	138.251	5	140.884	10	140.361	15	140.361	260	133.797
360	136.577	262	133.004	362	134.89	264	132.227	364	133.33	266	131.483
366	131.888	460	136.848	462	135.15	464	133.557	466	132.073	562	135.086
564	133.694	566	131.968	660	136.482	662	135.146	664	133.343	666	131.87
160	126.577	162	118.571	164	110.819	166	104.79	760	136.792	762	135.165
764	133.59	766	132.064	768	130.582	170	102.554	172	130.874	270	131.126
370	131.205	470	131.369	570	131.459	670	131.212	770	129.997	100	131.346
110	131.345	115	131.345	120	131.343	700	138.004	152	131.341	154	130.647
752	138.004	754	137.619	252	134.188	352	137.836	452	138.31	552	137.57
254	134.189	354	137.485	454	137.9	554	136.095	556	136.094	558	136.094
652	137.532	654	137.531	656	137.531	658	136.92				
200	138.932	300	147.42	400	147.486	500	145.253	240	139.439	340	146.291
440	146.653	540	144.818								

CASE 1 - ALL DECAY HEAT EQUALLY IN ALL DRUMS (FULL SOLAR LOAD)

DECAY HEAT = 30 WATTS

202	147.31	302	156.817	402	156.821	502	152.675.	204	145.28	304	154.787
404	154.792	504	150.645	206	141.446	306	150.953	406	150.958	506	146.811
208	138.056	308	147.563	408	147.567	508	143.42	212	147.7	312	155.396
412	155.649	512	152.111	222	147.761	322	155.275	422	155.539	522	152.07
232	147.954	332	155.147	432	155.312	532	152.107	242	148.045	342	155.07
442	155.205	542	152.106	214	145.528	314	153.854	414	154.08	514	150.289
224	145.54	324	153.25	424	153.737	524	149.904	234	146.225	334	153.037
434	153.076	534	150.199	244	146.467	344	152.753	444	152.784	544	150.12
216	141.653	316	150.611	416	150.677	516	146.788	226	141.44	326	150.013
426	150.087	526	146.395	236	142.749	336	149.117	436	148.965	536	146.53
246	143.09	346	148.52	446	148.499	546	146.243	218	138.276	318	147.511
418	147.519	518	143.569	228	137.854	328	146.796	428	146.797	528	143.095
238	139.552	338	145.461	438	145.432	538	142.993	248	139.908	348	144.908
448	144.885	548	142.8	5	147.565	10	146.797	15	146.797	260	138.323
360	141.251	262	136.159	362	138.141	264	134.09	364	135.252	266	132.138
366	132.571	460	140.944	462	138.044	464	135.315	466	132.766	562	137.799
564	135.457	566	132.559	660	140.028	662	137.816	664	134.831	666	132.389
160	131.099	162	121.653	164	112.509	166	105.396	760	140.548	762	138.036
764	135.604	766	133.246	768	130.959	170	102.758	172	130.882	270	131.207
370	131.3	470	131.558	570	131.704	670	131.3	770	130.054	100	136.734
110	136.733	115	136.733	120	136.73	700	142.412	152	136.728	154	135.9
752	142.411	754	141.825	252	139.559	352	143.449	452	143.432	552	141.86
254	139.434	354	142.912	454	142.768	554	139.494	556	139.492	558	139.492
652	141.722	654	141.722	656	141.72	658	140.753				
200	147.68	300	157.187	400	157.192	500	153.045	240	148.131	340	155.646
440	155.91	540	152.44								

CASE 1 - ALL DECAY HEAT EQUALLY IN ALL DRUMS (FULL SOLAR LOAD)

DECAY HEAT = 40 WATTS

202	156.003	302	166.48	402	166.422	502	160.34	204	153.315	304	163.793
404	163.734	504	157.653	206	148.211	306	158.688	406	158.63	506	152.548
208	143.693	308	154.171	408	154.112	508	148.031	212	156.343	312	164.692
412	164.854	512	159.631	222	156.399	322	164.539	422	164.702	522	159.576
232	156.597	332	164.389	432	164.389	532	159.631	242	156.688	342	164.294
442	164.241	542	159.632	214	153.536	314	162.611	414	162.782	514	157.198
224	153.506	324	161.827	424	162.317	524	156.69	234	154.219	334	161.599
434	161.393	534	157.094	244	154.46	344	161.245	444	160.988	544	156.993
216	148.433	316	158.262	416	158.258	516	152.525	226	148.11	326	157.481
426	157.468	526	152.008	236	149.491	336	156.401	436	155.892	536	152.207
246	149.821	346	155.644	446	155.248	546	151.832	218	143.958	318	154.118
418	154.052	518	148.231	228	143.376	328	153.182	428	153.093	528	147.606
238	145.178	338	151.539	438	151.17	538	147.493	248	145.514	348	150.848
448	150.418	548	147.245	5	154.141	10	153.137	15	153.137	260	142.817
360	145.889	262	139.291	362	141.368	264	135.939	364	137.158	266	132.788
366	133.248	460	144.999	462	140.909	464	137.055	466	133.453	562	140.477
564	137.197	566	133.142	660	143.51	662	140.437	664	136.292	666	132.9
160	135.584	162	124.71	164	114.183	166	105.995	760	144.208	762	140.833
764	137.566	766	134.398	768	131.325	170	102.958	172	130.89	270	131.288
370	131.394	470	131.744	570	131.946	670	131.386	770	130.11	100	142.076
110	142.075	115	142.074	120	142.072	700	146.701	152	142.069	154	141.111
752	146.699	754	145.923	252	144.89	352	149.013	452	148.503	552	146.07
254	144.641	354	148.296	454	147.59	554	142.851	556	142.847	558	142.848
652	145.825	654	145.824	656	145.822	658	144.517				
200	156.373	300	166.851	400	166.792	500	160.711	240	156.769	340	164.909
440	165.072	540	159.946								

3.6.1.2 Fourteen 55-Gallon Drum Payload with 100 ºF Ambient and Full Solar, Uniformly Distributed Decay Heat Load in Two Center Drums (Case 2)

CASE 2 - ALL DECAY HEAT EQUALLY IN TOP AND BOTTOM CENTER DRUMS (FULL SOLAR LOAD)

Location	Decay Heat (watts) 0	10	20	30	40
Maximum Center Drum Centerline:	129.21	157.42	186.77	215.99	245.14
Average Center Drum Centerline:	126.22	155.21	183.62	211.93	240.15
Maximum Center Drum Wall:	129.21	135.58	143.54	151.36	159.13
Average Center Drum Wall:	126.22	133.37	140.38	147.3	154.14
Maximum Outer Drum Centerline:	129.17	134.15	140.60	146.98	153.34
Average Outer Drum Centerline:	126.38	132.30	138.14	143.94	149.71
Maximum Outer Drum Wall:	129.20	135.01	142.43	149.78	157.13
Average Outer Drum Wall:	126.43	132.27	138.04	143.77	149.46
Average Drum Centerline:	126.35	135.57	144.64	153.65	162.63
Average Drum Wall:	126.40	132.43	138.37	144.27	150.12
Maximum ICV Wall:	129.23	133.89	138.54	143.21	148.69
Average ICV Wall:	126.20	131.26	136.27	141.27	146.26
Minimum ICV Wall:	120.58	126.23	131.78	137.33	142.84
Average ICV Air:	126.33	132.02	137.64	143.21	148.76
Maximum ICV O-ring Seal:	129.17	133.29	137.40	141.47	145.56
Maximum OCV Wall:	129.34	133.68	138.09	142.66	147.98
Maximum OCV O-ring Seal:	129.34	132.67	136.00	139.32	142.65
Maximum Polyurethane Foam:	154.95	154.95	154.95	154.95	154.95
Maximum OCA Outer Shell:	154.95	154.95	154.95	154.95	154.95

Area of Each Node (ft^2)

Center Drum (Node)	(Area)	Outer Drums (Node)	(Area)	ICV Wall (Node)	(Area)
208:	11.35145	218:	11.35145	152:	28.96573
308:	11.35145	228:	22.70291	252:	27.42553
408:	11.35145	238:	22.70291	352:	30.20783
508:	11.35145	248:	11.35145	452:	25.83564
Total:	45.40583	318:	11.35145	552:	14.70644
		328:	22.70291	652:	16.29633
		338:	22.70291	752:	28.96573
		348:	11.35145	Total:	172.4032
		418:	11.35145		
		428:	22.70291		
		438:	22.70291		
		448:	11.35145		
		518:	11.35145		
		528:	22.70291		
		538:	22.70291		
		548:	11.35145		
		Total:	272.4349		

NOTE: Average temperatures are "area-weighted" based on the above nodal areas

CASE 2 - ALL DECAY HEAT EQUALLY IN TOP AND BOTTOM CENTER DRUMS (FULL SOLAR LOAD)

DECAY HEAT = 0 WATTS

202	120.963	302	127.253	402	127.446	502¶	29.205	204	120.962	304	127.253
404	127.446	504	129.205	206	120.962	306	127.253	406	127.446	506	129.205
208	120.962	308	127.253	408	127.446	508	129.205	212	121.58	312	127.084
412	127.603	512	129.176	222	121.653	322	127.064	422	127.622	522	129.172
232	121.838	332	127.019	432	127.669	532	129.166	242	121.925	342	126.998
442	127.691	542	129.162	214	121.324	314	127.152	414	127.538	514	129.186
224	121.465	324	127.105	424	127.574	524	129.179	234	122.06	334	126.964
434	127.725	534	129.157	244	122.3	344	126.906	444	127.787	544	129.149
216	121.132	316	127.209	416	127.488	516	129.196	226	121.261	326	127.185
426	127.522	526	129.19	236	122.339	336	126.895	436	127.797	536	129.147
246	122.706	346	126.805	446	127.89	546	129.133	218	121.046	313	127.232
418	127.467	518	129.2	228	121.126	328	127.212	428	127.487	528	129.194
238	122.486	338	126.863	438	127.834	538	129.142	248	122.9	348	126.797
443	127.939	548	129.126	5	127.35	10	127.35	15	127.35	260	124.769
360	127.244	262	126.712	362	128.397	264	128.511	364	129.493	266	130.175
366	130.524	460	128.636	462	129.382	464	130.054	466	130.69	562	129.694
564	130.188	566	130.792	660	129.425	662	129.833	664	130.382	666	130.835
160	117.554	162	112.417	164	107.444	166	103.576	760	129.328	762	129.46
764	129.589	766	129.714	768	129.835	170	102.14	172	130.858	270	130.963
370	131.015	470	130.994	570	130.97	670	131.038	770	129.883	100	120.585
110	120.585	115	120.585	120	120.584	700	129.229	152	120.583	154	120.165
752	129.23	754	129.26	252	123.466	352	126.616	452	128.079	552	128.998
254	123.727	354	126.648	454	128.196	554	129.338	556	129.339	558	129.338
652	129.168	654	129.168	656	129.169	658	129.292				
200	120.963	300	127.253	400	127.446	500	129.205	240	121.653	340	127.064
440	127.622	540	129.172								

CASE 2 - ALL DECAY HEAT EQUALLY IN TOP AND BOTTOM CENTER DRUMS (FULL SOLAR LOAD)

DECAY HEAT = 10 WATTS

202	149.064	302	156.925	402	157.052	502	156.335	204	144.402	304	152.263
404	152.39	504	151.673	206	135.487	306	143.348	406	143.475	506	142.758
208	127.588	308	135.448	408	135.575	508	134.858	212	127.365	312	133.849
412	134.229	512	133.945	222	127.398	322	133.746	422	134.154	522	133.894
232	127.526	332	133.568	432	134.031	532	133.818	242	127.589	342	133.488
442	133.976	542	133.784	214	127.262	314	134.229	414	134.511	514	134.134
224	127.24	324	133.868	424	134.239	524	133.937	234	127.681	334	133.353
434	133.883	534	133.726	244	127.865	344	133.15	444	133.751	544	133.645
216	127.254	316	134.635	416	134.824	516	134.353	226	127.046	326	134.097
426	134.299	526	134.015	236	127.887	336	133.099	436	133.714	536	133.621
246	128.176	346	132.796	446	133.524	546	133.503	218	127.278	318	134.851
418	135.006	518	134.476	228	126.907	328	134.143	428	134.324	528	134.02
238	127.997	338	132.978	438	133.627	538	133.571	248	128.325	348	132.629
448	133.418	548	133.437	5	135.512	10	134.233	15	134.233	260	129.235
360	131.865	262	129.825	362	131.612	264	130.349	364	131.393	266	130.822
366	131.199	460	132.723	462	132.235	464	131.786	466	131.374	562	132.356
564	131.919	566	131.373	660	132.921	662	132.465	664	131.849	666	131.348
160	122.281	162	115.641	164	109.213	166	104.213	760	133.278	762	132.48
764	131.707	766	130.957	768	130.23	170	102.358	172	130.866	270	131.043
370	131.109	470	131.179	570	131.212	670	131.124	770	129.943	100	126.234
110	126.232	115	126.231	120	126.23	700	133.894	152	126.229	154	125.656
752	133.894	754	133.684	252	128.761	352	132.175	452	133.144	552	133.214
254	128.903	354	132.014	454	132.997	554	132.673	556	132.673	558	132.673
652	133.289	654	133.289	656	133.289	658	133.07				
200	149.434	300	157.295	400	157.422	500	156.705	240	127.398	340	133.746
440	134.154	540	133.894								

CASE 2 - ALL DECAY HEAT EQUALLY IN TOP AND BOTTOM CENTER DRUMS (FULL SOLAR LOAD)

DECAY HEAT = 20 WATTS

202	176.941	302	186.336	402	186.401	502	183.31	204	167.673	304	177.068
404	177.132	504	174.042	206	149.867	306	159.262	406	159.326	506	156.236
208	134.077	308	143.472	408	143.536	508	140.445	212	133.054	312	140.519
412	140.765	512	138.682	222	133.048	322	140.334	422	140.599	522	138.585
232	133.122	332	140.027	432	140.308	532	138.44	242	133.162	342	139.89
442	140.179	542	138.377	214	133.101	314	141.203	414	141.386	514	139.048
224	132.919	324	140.536	424	140.813	524	138.664	234	133.212	334	139.654
434	139.96	534	138.265	244	133.344	344	139.31	444	139.64	544	138.112
216	133.272	316	141.951	416	142.053	516	139.472	226	132.734	326	140.911
426	140.983	526	138.807	236	133.348	336	139.22	436	139.554	536	138.067
246	133.564	346	138.71	446	139.091	546	137.846	218	133.405	318	142.356
418	142.434	518	139.712	228	132.591	328	140.976	428	141.067	528	138.814
238	133.423	338	139.011	438	139.346	538	137.972	248	133.671	348	138.429
448	138.833	548	137.721	5	143.504	10	141.022	15	141.022	260	133.65
360	136.452	262	132.902	362	134.803	264	132.167	364	133.279	266	131.461
366	131.869	460	136.743	462	135.075	464	133.512	466	132.055	562	135.012
564	133.646	566	131.952	660	136.41	662	135.091	664	133.313	666	131.859
160	126.929	162	118.811	164	110.951	166	104.838	760	137.215	762	135.489
764	133.817	766	132.197	768	130.625	170	102.57	172	130.874	270	131.123
370	131.202	470	131.364	570	131.452	670	131.21	770	130.003	100	131.784
110	131.78	115	131.78	120	131.778	700	138.537	152	131.776	154	131.055
752	138.536	754	138.093	252	133.99	352	137.689	452	138.181	552	137.409
254	134.017	354	137.34	454	137.777	554	136.002	556	136	558	136
652	137.397	654	137.397	656	137.396	658	136.842				
200	177.312	300	186.707	400	186.771	500	183.681	240	133.048	340	140.334
440	140.599	540	138.585								

CASE 2 - ALL DECAY HEAT EQUALLY IN TOP AND BOTTOM CENTER DRUMS (FULL SOLAR LOAD)

DECAY HEAT = 30 WATTS

202	204.782	302	215.616	402	215.617	502	210.21	204	190.907	304	201.742
404	201.743	504	196.336	206	164.21	306	175.044	406	175.045	506	169.638
208	140.528	308	151.362	408	151.363	508	145.957	212	138.739	312	147.128
412	147.237	512	143.375	222	138.694	322	146.864	422	146.981	522	143.231
232	138.713	332	146.43	432	146.525	532	143.018	242	138.73	342	146.237
442	146.323	542	142.925	214	138.934	314	148.108	414	148.191	514	143.915
224	138.593	324	147.143	424	147.323	524	143.348	234	138.739	334	145.903
434	145.98	534	142.76	244	138.819	344	145.424	444	145.476	544	142.538
216	139.283	316	149.189	416	149.205	516	144.542	226	138.418	326	147.66
426	147.601	526	143.556	236	138.805	336	145.292	436	145.341	536	142.471
246	138.948	346	144.584	446	144.611	546	142.148	218	139.523	318	149.779
418	149.78	518	144.897	228	138.272	328	147.744	428	147.744	528	143.565
238	138.844	338	144.998	438	145.011	538	142.331	248	139.013	348	144.191
448	144.204	548	141.966	5	151.363	10	147.744	15	147.744	260	138.068
360	141.036	262	135.981	362	137.991	264	133.985	364	135.163	266	132.101
366	132.539	460	140.756	462	137.911	464	135.234	466	132.734	562	137.66
564	135.368	566	132.529	660	139.879	662	137.703	664	134.768	666	132.367
160	131.581	162	121.982	164	112.689	166	105.461	760	141.129	762	138.48
764	135.915	766	133.429	768	131.016	170	102.779	172	130.882	270	131.203
370	131.295	470	131.549	570	131.692	670	131.296	770	130.063	100	137.337
110	137.331	115	137.331	120	137.329	700	143.145	152	137.326	154	136.46
752	143.144	754	142.475	252	139.221	352	143.194	452	143.206	552	141.575
254	139.136	354	142.662	454	142.549	554	139.32	556	139.318	558	139.318
652	141.472	654	141.471	656	141.47	658	140.592				
200	205.152	300	215.987	400	215.987	500	210.58	240	138.694	340	146.864
440	146.981	540	143.231								

CASE 2 - ALL DECAY HEAT EQUALLY IN TOP AND BOTTOM CENTER DRUMS (FULL SOLAR LOAD)

DECAY HEAT = 40 WATTS

202	232.554	302	244.774	402	244.713	502	237.073	204	214.073	304	226.293
404	226.233	504	218.592	206	178.484	306	190.704	406	190.644	506	183.003
208	146.912	308	159.132	408	159.071	508	151.431	212	144.389	312	153.679
412	153.654	512	148.062	222	144.306	322	153.337	422	153.31	522	147.873
232	144.271	332	152.75	432	152.693	532	147.593	242	144.266	342	152.533
442	152.419	542	147.471	214	144.729	314	154.95	414	154.934	514	148.773
224	144.233	324	153.692	424	153.778	524	148.025	234	144.234	334	152.102
434	151.953	534	147.254	244	144.263	344	151.491	444	151.271	544	146.963
216	145.253	316	156.357	416	156.288	516	149.6	226	144.066	326	154.35
426	154.163	526	148.299	236	144.231	336	151.318	436	151.085	536	146.573
246	144.303	346	150.419	446	150.097	546	146.451	218	145.598	318	157.126
418	157.054	518	150.069	228	143.917	328	154.451	428	154.363	528	148.309
238	144.235	338	150.94	438	150.636	538	146.688	248	144.327	348	149.917
448	149.546	548	146.212	5	159.102	10	154.407	15	154.407	260	142.473
360	145.614	262	139.051	362	141.176	264	135.798	364	137.045	266	132.739
366	133.208	460	144.775	462	140.75	464	136.958	466	133.415	562	140.318
564	137.095	566	133.108	660	143.364	662	140.327	664	136.23	666	132.878
160	136.208	162	125.136	164	114.416	166	106.079	760	145.049	762	141.476
764	138.016	766	134.663	768	131.409	170	102.985	172	130.89	270	131.282
370	131.388	470	131.733	570	131.932	670	131.382	770	130.123	100	142.857
110	142.849	115	142.848	120	142.846	700	147.754	152	142.843	154	141.836
752	147.753	754	146.865	252	144.435	352	148.688	452	148.23	552	145.747
254	144.24	354	147.978	454	147.321	554	142.65	556	142.647	558	142.647
652	145.561	654	145.56	656	145.558	658	144.359				
200	232.924	300	245.144	400	245.084	500	237.443	240	144.306	340	153.337
440	153.31	540	147.873								

3.6.1.3 Fourteen 55-Gallon Drum Payload with 100 ºF Ambient and Full Solar, Uniformly Distributed Decay Heat Load in Top Center Drum (Case 3)

CASE 3 - ALL DECAY HEAT IN TOP CENTER DRUM (FULL SOLAR LOAD)

Location	Decay Heat (watts) 0	10	20	30	40
Maximum Center Drum Centerline:	129.21	180.98	232.13	283.09	333.98
Average Center Drum Centerline:	126.22	154.71	182.87	210.90	238.85
Maximum Center Drum Wall:	129.21	137.74	146.12	154.31	162.41
Average Center Drum Wall:	126.22	133.09	139.86	146.50	153.07
Maximum Outer Drum Centerline:	129.17	135.76	142.30	148.73	155.18
Average Outer Drum Centerline:	126.38	132.02	137.62	143.15	148.66
Maximum Outer Drum Wall:	129.20	136.98	144.68	152.26	159.81
Average Outer Drum Wall:	126.43	132.00	137.52	142.98	148.42
Average Drum Centerline:	126.35	135.26	144.08	152.82	161.54
Average Drum Wall:	126.40	132.15	137.86	143.48	149.08
Maximum ICV Wall:	129.23	135.89	142.50	149.04	155.60
Average ICV Wall:	126.20	130.98	135.75	140.48	145.22
Minimum ICV Wall:	120.58	123.65	126.71	129.74	132.78
Average ICV Air:	126.33	131.74	137.12	142.42	147.73
Maximum ICV O-ring Seal:	129.17	134.47	139.77	145.01	150.30
Maximum OCV Wall:	129.34	135.54	141.79	147.98	154.21
Maximum OCV O-ring Seal:	129.34	133.25	137.19	141.10	145.05
Maximum Polyurethane Foam:	154.95	154.95	154.95	154.95	154.95
Maximum OCA Outer Shell:	154.95	154.95	154.95	154.95	154.95

Area of Each Node (ft^2)

Center Drum (Node)	(Area)	Outer Drums (Node)	(Area)	ICV Wall (Node)	(Area)
208:	11.35145	218:	11.35145	152:	28.96573
308:	11.35145	228:	22.70291	252:	27.42553
408:	11.35145	238:	22.70291	352:	30.20783
508:	11.35145	248:	11.35145	452:	25.83564
Total:	45.40583	318:	11.35145	552:	14.70644
		328:	22.70291	652:	16.29633
		338:	22.70291	752:	28.96573
		348:	11.35145	Total:	172.4032
		418:	11.35145		
		428:	22.70291		
		438:	22.70291		
		448:	11.35145		
		518:	11.35145		
		528:	22.70291		
		538:	22.70291		
		548:	11.35145		
		Total:	272.4349		

NOTE: Average temperatures are "area-weighted" based on the above nodal areas

CASE 3 - ALL DECAY HEAT IN TOP CENTER DRUM (FULL SOLAR LOAD)

DECAY HEAT = 0 WATTS

202	920.963	302	127.253	402	127.446	502	129.205	204	120.962	304	127.253
404	127.446	504	129.205	206	120.962	306	127.253	406	127.446	506	129.205
208	120.962	308	127.253	408	127.446	508	129.205	212	121.58	312	127.084
412	127.603	512	129.176	222	121.653	322	127.064	422	127.622	522	129.172
232	121.838	332	127.019	432	127.669	532	129.166	242	121.925	342	126.998
442	127.691	542	129.162	214	121.324	314	127.152	414	127.538	514	129.186
224	121.465	324	127.105	424	127.574	524	129.179	234	122.06	334	126.964
434	127.725	534	129.157	244	122.3	344	126.906	444	127.787	544	129.149
216	121.132	316	127.209	416	127.488	516	129.196	226	121.261	326	127.185
426	127.522	526	129.19	236	122.339	336	126.895	436	127.797	536	129.147
246	122.706	346	126.805	446	127.89	546	129.133	218	121.046	318	127.232
418	127.467	518	129.2	228	121.126	328	127.212	428	127.487	528	129.194
238	122.486	338	126.863	438	127.834	538	129.142	248	122.9	348	126.757
448	127.939	548	129.126	5	127.35	10	127.35	15	127.35	260	124.769
360	127.244	262	126.712	362	128.397	264	128.511	364	129.493	266	130.175
366	130.524	460	128.686	462	129.382	464	130.054	466	130.69	562	129.694
564	130.188	566	130.792	660	129.425	662	129.833	664	130.382	666	130.835
160	117.554	162	112.417	164	107.444	166	103.576	760	129.328	762	129.46
764	129.589	766	129.714	768	129.835	170	102.14	172	130.858	270	130.963
370	131.015	470	130.994	570	130.97	670	131.038	770	129.883	100	120.585
110	120.585	115	120.585	120	120.584	700	129.229	152	120.583	154	120.165
752	129.23	754	129.26	252	123.466	352	126.616	452	128.079	552	128.998
254	123.727	354	126.648	454	128.196	554	129.338	556	129.339	558	129.338
652	129.168	654	129.168	656	129.169	658	129.292				
200	120.963	300	127.253	400	127.446	500	129.205	240	121.653	340	127.064
440	127.622	540	129.172								

CASE 3 - ALL DECAY HEAT IN TOP CENTER DRUM (FULL SOLAR LOAD)

DECAY HEAT = 10 WATTS

202	124.083	302	134.157	402	179.255	502	180.606	204	124.083	304	134.157
404	169.987	504	171.337	206	124.083	306	134.157	406	152.181	506	153.531
208	124.083	308	134.157	408	136.39	508	137.741	212	124.798	312	133.215
412	134.389	512	135.869	222	124.882	322	133.133	422	134.294	522	135.762
232	125.096	332	132.964	432	134.162	532	135.595	242	125.198	342	132.885
442	134.106	542	135.522	214	124.501	314	133.509	414	134.757	514	136.27
224	124.665	324	133.275	424	134.36	524	135.861	234	125.354	334	132.756
434	134.005	534	135.393	244	125.632	344	132.546	444	133.88	544	135.213
216	124.277	316	133.783	416	135.203	516	136.725	226	124.428	326	133.548
426	134.377	526	136.041	236	125.678	336	132.503	436	133.835	536	135.163
246	126.103	346	132.182	446	133.664	546	134.898	218	124.178	318	133.911
418	135.472	518	136.979	228	124.27	328	133.63	428	134.364	528	136.059
238	125.848	338	132.382	438	133.75	538	135.052	248	126.327	348	132.009
448	133.564	548	134.751	5	135.275	10	133.997	15	133.997	260	127.775
360	131.303	262	128.818	362	131.219	264	129.758	364	131.161	266	130.613
366	131.118	460	132.933	462	132.378	464	131.876	466	131.418	562	132.821
564	132.23	566	131.478	660	133.867	662	133.174	664	132.239	666	131.481
160	120.133	162	114.176	164	108.409	166	103.924	760	134.933	762	133.744
764	132.593	766	131.478	768	130.396	170	102.26	172	130.863	270	131.015
370	131.099	470	131.204	570	131.255	670	131.144	770	129.968	100	123.647
110	123.648	115	123.647	120	123.646	700	135.885	152	123.645	154	123.161
752	135.885	754	135.537	252	126.968	352	131.522	452	133.321	552	134.174
254	127.197	354	131.364	454	133.171	554	133.254	556	133.254	558	133.254
652	134.471	654	134.471	656	134.47	658	134.095				
200	124.083	300	134.157	400	179.625	500	180.976	240	124.882	340	133.133
440	134.294	540	135.762								

CASE 3 - ALL DECAY HEAT IN TOP CENTER DRUM (FULL SOLAR LOAD)

DECAY HEAT = 20 WATTS

202	127.208	302	140.977	402	230.792	502	231.758	204	127.208	304	140.977
404	212.311	504	213.277	206	127.208	306	140.977	406	176.722	506	177.688
208	127.208	308	140.977	408	145.15	508	146.116	212	128.02	312	139.299
412	141.113	512	142.504	222	128.116	322	139.155	422	140.905	522	142.295
232	128.36	332	138.863	432	140.598	532	141.971	242	128.475	342	138.729
442	140.466	542	141.829	214	127.682	314	139.813	414	141.905	514	143.287
224	127.869	324	139.396	424	141.083	524	142.485	234	128.653	334	138.507
434	140.232	534	141.579	244	128.968	344	138.148	444	139.927	544	141.232
216	127.428	316	140.298	416	142.835	516	144.178	226	127.599	326	139.859
426	141.168	526	142.832	236	129.022	336	138.071	436	139.825	536	141.132
246	129.503	346	137.526	446	139.4	546	140.623	218	127.315	318	140.529
418	143.388	518	144.675	228	127.42	328	139.995	428	141.177	528	142.866
238	129.216	338	137.864	438	139.62	538	140.916	248	129.758	348	137.232
448	139.155	548	140.339	5	143.067	10	140.586	15	140.587	260	130.783
360	135.365	262	130.925	362	134.043	264	131.006	364	132.329	266	131.052
366	131.712	460	137.187	462	135.379	464	133.701	466	132.148	562	135.962
564	134.28	566	132.167	660	138.317	662	136.521	664	134.098	666	132.129
160	122.717	162	115.939	164	109.376	166	104.272	760	140.516	762	138.012
764	135.587	766	133.236	768	130.955	170	102.378	172	130.868	270	131.068
370	131.183	470	131.414	570	131.541	670	131.251	770	130.053	400	126.715
110	126.716	115	126.715	120	126.714	700	142.5	152	126.713	154	126.163
752	142.498	754	141.79	252	130.471	352	136.427	452	138.562	552	139.343
254	130.668	354	136.083	454	138.152	554	137.188	556	137.187	558	137.187
652	139.768	654	139.769	656	139.767	658	138.905				
200	127.208	300	140.977	400	231.162	500	232.128	240	128.116	340	139.155
440	140.905	540	142.295								

CASE 3 - ALL DECAY HEAT IN TOP CENTER DRUM (FULL SOLAR LOAD)

DECAY HEAT = 30 WATTS

202	130.298	302	147.69	402	282.129	502	282.724	204	130.298	304	147.69
404	254.436	504	255.031	206	130.298	306	147.69	406	201.064	506	201.659
208	130.298	308	147.69	408	153.71	508	154.305	212	131.207	312	145.306
412	147.747	512	149.044	222	131.315	322	145.103	422	147.43	522	148.734
232	131.588	332	144.691	432	146.95	532	148.256	242	131.717	342	144.502
442	146.744	542	148.046	214	130.828	314	146.036	414	148.954	514	150.201
224	131.037	324	145.441	424	147.716	524	149.015	234	131.918	334	144.188
434	146.378	534	147.675	244	132.271	344	143.685	444	145.898	544	147.165
216	130.543	316	146.727	416	150.358	516	151.519	226	130.735	326	146.091
426	147.868	526	149.527	236	132.332	336	143.573	436	145.739	536	147.014
246	132.87	346	142.811	446	145.066	546	146.268	218	130.415	318	147.059
418	151.19	518	152.255	228	130.534	328	146.281	428	147.898	528	149.578
238	132.55	338	143.28	438	145.414	538	146.695	248	133.155	348	142.397
448	144.68	545	145.849	5	150.708	10	147.09	15	147.09	260	133.761
360	139.403	262	133.012	362	136.85	264	132.242	364	134.488	266	131.456
366	132.303	460	141.418	462	138.363	464	135.516	466	132.874	562	139.085
564	136.318	566	132.852	660	142.733	662	139.843	664	135.943	666	132.771
160	125.272	162	117.681	164	110.331	166	104.615	760	146.048	762	142.239
764	138.551	766	134.977	768	131.508	170	102.495	172	130.873	270	131.12
370	131.267	470	131.623	570	131.825	670	131.357	770	130.137	100	129.747
110	129.748	115	129.748	120	129.746	700	149.038	152	129.744	154	129.13
752	149.036	754	147.984	252	133.939	352	141.301	452	143.769	552	144.464
254	134.105	354	140.774	454	143.105	554	141.099	556	141.098	558	141.098
652	145.013	654	145.014	656	145.011	658	143.68				
200	130.298	300	147.69	400	282.5	500	283.094	240	131.315	340	145.103
440	147.43	540	148.734								

CASE 3 - ALL DECAY HEAT IN TOP CENTER DRUM (FULL SOLAR LOAD)

DECAY HEAT = 40 WATTS

202	133.39	302	154.348	402	333.326	502	333.607	204	133.39	304	154.348
404	296.42	504	296.701	206	133.39	306	154.347	406	225.266	506	225.547
208	133.39	308	154.347	408	162.129	508	162.411	212	134.397	312	151.287
412	154.343	512	155.583	222	134.517	322	151.025	422	153.918	522	155.175
232	134.82	332	150.495	432	153.271	532	154.543	242	134.964	342	150.252
442	152.992	542	154.266	214	133.976	314	152.228	414	155.955	514	157.108
224	134.209	324	151.458	424	154.311	524	155.546	234	135.186	334	149.847
434	152.498	534	153.776	244	135.578	344	149.203	444	151.848	544	153.104
216	133.66	316	153.122	416	157.823	516	158.845	226	133.873	326	152.294
426	154.528	526	156.224	236	135.647	336	149.055	436	151.631	536	152.902
246	136.242	346	148.082	446	150.72	546	151.923	218	133.518	318	153.551
418	158.928	518	159.814	228	133.65	328	152.537	428	154.579	528	156.291
238	135.89	338	148.677	438	151.189	538	152.479	248	136.558	348	147.552
448	150.196	548	151.371	5	158.252	10	153.559	15	153.559	260	136.743
360	143.455	262	135.101	362	139.667	264	133.48	364	136.153	266	131.921
366	132.895	460	145.673	462	141.365	464	137.342	466	133.604	562	142.239
564	138.376	566	133.542	660	147.191	662	143.196	664	137.806	666	133.419
160	127.828	162	119.424	164	111.287	166	104.958	760	151.61	762	146.49
764	141.533	766	136.727	768	132.065	170	102.61	172	130.878	270	131.173
370	131.35	470	131.834	570	132.111	670	131.464	770	130.222	100	132.782
110	132.782	115	132.782	120	132.78	700	155.599	152	132.778	154	132.101
752	155.596	754	154.212	252	137.409	352	146.189	452	148.996	552	149.614
254	137.546	354	145.482	454	148.084	554	145.05	556	145.048	558	145.048
652	150.298	654	150.298	656	150.294	658	148.5				
200	133.39	300	154.348	400	333.696	500	333.978	240	134.517	340	151.025
440	153.918	540	155.175								

3.6.1.4 Two Standard Waste Box Payload with 100 ºF Ambient and Full Solar, Uniformly Distributed Decay Heat Load in Both SWBs (Case 4)

CASE 4 - ALL DECAY HEAT EQUALLY IN BOTH STANDARD WASTE BOXES (FULL SOLAR LOAD)

Location	Decay Heat (watts) 0	10	20	30	40
Maximum Standard Waste Box Centerline:	128.10	158.11	185.59	211.54	238.95
Average Standard Waste Box Centerline:	126.22	156.67	184.36	210.21	237.51
Maximum Standard Waste Box Wall:	128.34	133.72	139.62	144.31	150.37
Average Standard Waste Box Wall:	126.22	132.19	138.35	142.69	148.47
Maximum ICV Wall:	128.47	133.60	139.14	142.54	148.18
Average ICV Wall:	126.18	131.62	137.29	141.09	146.40
Minimum ICV Wall:	122.28	128.04	133.90	138.33	143.91
Average ICV Air:	126.20	131.92	137.86	141.96	147.52
Maximum ICV O-ring Seal:	128.47	133.38	138.64	141.30	146.04
Maximum OCV Wall:	128.77	133.42	138.70	142.08	147.55
Maximum OCV O-ring Seal:	128.77	132.56	136.73	139.00	142.79
Maximum Polyurethane Foam:	154.93	154.93	154.93	154.93	154.93
Maximum OCA Outer Shell:	154.93	154.93	154.93	154.93	154.93

Area of Each Node (ft^2)

Standard Waste Box (Node)	(Area)	ICV Wall (Node)	(Area)
208:	50.80244	152:	28.96573
308:	50.80244	252:	27.42553
408:	50.80244	352:	30.20783
508:	50.80244	452:	25.83564
Total:	203.2097	552:	14.70644
		652:	16.29633
		752:	28.96573
		Total:	172.4032

NOTE: Average temperatures are "area-weighted" based on the above nodal areas

CASE 4 - ALL DECAY HEAT EQUALLY IN BOTH STANDARD WASTE BOXES (FULL SOLAR LOAD)

DECAY HEAT = 0 WATTS

201	123.572	301	126.011	401	127.2	501	128.098	203	123.498	303	126.084
403	127.173	503	128.125	205	123.405	305	126.178	405	127.138	505	128.159
207	123.277	307	126.307	407	121.09	507	128.207	208	122.907	308	126.677
408	126.953	508	128.344	260	125.17	360	127.127	262	126.986	362	128.317
264	128.671	364	129.445	266	130.232	366	130.506	460	128.167	462	129.019
464	129.833	466	130.599	562	129.237	564	129.891	566	130.692	660	128.829
662	129.384	664	130.132	666	130.748	160	118.947	162	113.367	164	107.965
166	103.764	760	128.613	762	128.914	764	129.207	766	129.489	768	129.763
170	102.205	172	130.86	270	130.971	370	131.012	470	130.964	570	130.929
670	131.023	770	129.872	120	122.279	700	128.382	152	122.278	154	121.784
752	128.382	754	128.46	252	123.95	352	126.466	452	127.44	552	128.313
254	124.2	354	126.511	454	127.602	554	128.766	556	128.767	558	128.767
652	128.471	654	128.471	656	128.472	658	128.647				
200	123.572	300	126.011	400	127.2	500	128.098				

CASE 4 - ALL DECAY HEAT EQUALLY IN BOTH STANDARD WASTE BOXES (FULL SOLAR LOAD)

DECAY HEAT = 10 WATTS

201	151.183	301	153.838	401	154.871	501	155.22	203	148.256	303	151.071
403	152.014	503	152.384	205	144.827	305	147.846	405	148.673	505	149.069
207	140.443	307	143.744	407	144.412	507	144.844	208	128.863	308	132.974
408	133.184	508	133.721	260	129.896	360	131.923	262	130.278	362	131.656
264	130.615	364	131.421	266	130.916	366	131.209	460	132.537	462	132.107
464	131.71	466	131.344	562	132.265	564	131.863	566	131.355	660	132.932
662	132.472	664	131.851	666	131.347	160	123.776	162	116.661	164	109.772
166	104.414	760	133.046	762	132.303	764	131.582	766	130.884	768	130.207
170	102.426	172	130.868	270	131.056	370	131.11	470	131.172	570	131.204
670	131.123	770	129.939	120	128.039	700	133.604	152	128.037	154	127.392
752	133.604	754	133.424	252	129.567	352	132.212	452	132.872	552	133.203
254	129.677	354	132.076	454	132.764	554	132.559	556	132.559	558	132.559
652	133.384	654	133.384	656	133.384	658	133.082				
200	154.072	300	156.727	400	157.76	500	158.109				

CASE 4 - ALL DECAY HEAT EQUALLY IN BOTH STANDARD WASTE BOXES (FULL SOLAR LOAD)

DECAY HEAT = 20 WATTS

201	178.84	301	181.775	401	182.697	501	182.558	203	173.099	303	176.211
403	177.049	503	176.902	205	166.344	305	169.682	405	170.412	505	170.254
207	157.71	307	161.358	407	161.94	507	161.768	208	134.923	308	139.465
408	139.622	508	139.407	260	134.737	360	136.899	262	133.652	362	135.122
264	132.607	364	133.471	266	131.617	366	131.939	460	137.167	462	135.379
464	133.701	466	132.137	562	135.594	564	134.029	566	132.081	660	137.349
662	135.797	664	133.702	666	131.994	160	128.692	162	120.012	164	111.609
166	105.074	760	137.757	762	135.903	764	134.108	766	132.367	768	130.679
170	102.649	172	130.877	270	131.143	370	131.213	470	131.396	570	131.506
670	131.232	770	130.012	120	133.902	700	139.142	152	133.899	154	133.104
752	139.141	754	138.7	252	135.314	352	138.166	452	138.568	552	138.416
254	135.287	354	137.848	454	138.2	554	136.729	556	136.728	558	136.728
652	138.635	654	138.634	656	138.633	658	137.158				
200	181.729	300	184.664	400	185.586	500	185.447				

CASE 4 - ALL DECAY HEAT EQUALLY IN BOTH STANDARD WASTE BOXES (FULL SOLAR LOAD)

DECAY HEAT = 30 WATTS

201	205.01	301	208.058	401	208.648	501	207.562	203	196.461	303	199.693
403	200.223	503	199.072	205	186.388	305	189.853	405	190.308	505	189.074
207	173.513	307	177.3	407	177.652	507	176.303	208	139.545	308	144.26
408	144.313	508	142.633	260	138.394	360	140.541	262	136.199	362	137.655
264	134.111	364	134.968	266	132.145	366	132.471	460	140.234	462	137.544
464	135.013	466	132.649	562	137.403	564	135.203	566	132.474	660	139.643
662	137.524	664	134.666	666	132.331	160	132.408	162	122.546	164	112.998
166	105.571	760	140.354	762	137.888	764	135.5	766	133.185	768	130.939
170	102.816	172	130.883	270	131.21	370	131.286	470	131.528	570	131.669
670	131.289	770	130.051	120	138.331	700	142.2	152	138.328	154	137.422
752	142.198	754	141.607	252	139.663	352	142.537	452	142.5	552	141.353
254	139.526	354	142.077	454	141.902	554	138.998	556	138.996	558	138.996
652	141.295	654	141.295	656	141.293	658	140.337				
200	207.9	300	210.947	400	211.537	500	210.452				

CASE 4 - ALL DECAY HEAT EQUALLY IN BOTH STANDARD WASTE BOXES (FULL SOLAR LOAD)

DECAY HEAT = 40 WATTS

201	232.357	301	235.628	401	236.064	501	234.426	203	220.995	303	224.464
403	224.851	503	223.114	205	207.599	305	211.319	405	211.643	505	209.78
207	190.475	307	194.541	407	194.779	507	192.744	208	145.308	308	150.37
408	150.359	508	147.825	260	143.011	360	145.26	262	139.417	362	140.941
264	136.011	364	136.911	266	132.814	366	133.162	460	144.565	462	140.604
464	136.873	466	133.388	562	140.432	564	137.173	566	133.135	660	143.652
662	140.543	664	136.348	666	132.918	160	137.091	162	125.738	164	114.746
166	106.196	760	144.667	762	141.185	764	137.812	766	134.543	768	131.371
170	103.025	172	130.891	270	131.293	370	131.383	470	131.734	570	131.943
670	131.388	770	130.117	120	143.909	700	147.258	152	143.906	154	142.863
752	147.257	754	146.436	252	145.142	352	148.179	452	147.855	552	146.114
254	144.878	354	147.552	454	147.01	554	142.792	556	142.789	558	142.789
652	146.037	654	146.036	656	146.034	658	144.671				
200	235.246	300	238.517	400	238.953	500	237.316				

3.6.1.5 Two Standard Waste Box Payload with 100 ºF Ambient and Full Solar, Uniformly Distributed Decay Heat Load in Top SWB (Case 5)

CASE 5 - ALL DECAY HEAT IN TOP STANDARD WASTE BOX (FULL SOLAR LOAD)

Location	Decay Heat (watts) 0	10	20	30	40
Maximum Standard Waste Box Centerline:	128.10	181.19	229.28	278.88	328.25
Average Standard Waste Box Centerline:	126.22	155.34	181.39	208.59	235.74
Maximum Standard Waste Box Wall:	128.34	135.53	140.58	147.22	153.60
Average Standard Waste Box Wall:	126.22	132.34	136.87	142.55	148.18
Maximum ICV Wall:	128.47	135.33	140.17	146.61	152.83
Average ICV Wall:	126.18	131.78	135.78	140.97	146.14
Minimum ICV Wall:	122.28	126.58	129.68	133.64	137.91
Average ICV Air:	126.20	132.08	136.37	141.82	147.24
Maximum ICV O-ring Seal:	128.47	134.90	139.00	144.87	150.44
Maximum OCV Wall:	128.77	135.06	139.64	145.77	151.70
Maximum OCV O-ring Seal:	128.77	133.49	136.54	140.85	144.85
Maximum Polyurethane Foam:	154.93	154.93	154.93	154.93	154.93
Maximum OCA Outer Shell:	154.93	154.93	154.93	154.93	154.93

Area of Each Node (ft^2)

Standard Waste Box (Node)	(Area)	ICV Wall (Node)	(Area)
208:	50.80244	152:	28.96573
308:	50.80244	252:	27.42553
408:	50.80244	352:	30.20783
508:	50.80244	452:	25.83564
Total:	203.2097	552:	14.70644
		652:	16.29633
		752:	28.96573
		Total:	172.4032

NOTE: Average temperatures are "area-weighted" based on the above nodal areas

CASE 5 - ALL DECAY HEAT IN TOP STANDARD WASTE BOX (FULL SOLAR LOAD)

DECAY HEAT = 0 WATTS

201	123.572	301	126.011	401	127.2	501	128.098	203	123.498	303	126.084
403	127.173	503	128.125	205	123.405	305	126.178	405	127.138	505	128.159
207	123.277	307	126.307	407	127.09	507	128.207	208	122.907	308	126.677
408	126.953	508	128.344	260	125.17	360	127.127	262	126.986	362	128.317
264	128.671	364	129.445	266	130.232	366	130.506	460	128.167	462	129.019
464	129.833	466	130.599	562	129.237	564	129.891	566	130.692	660	128.829
662	129.384	664	130.132	666	130.748	160	118.947	162	113.367	164	107.965
166	103.764	760	128.613	762	128.914	764	129.207	766	129.489	768	129.763
170	102.205	172	130.86	270	130.971	370	131.012	470	130.964	570	130.929
670	131.023	770	129.872	120	122.279	700	128.382	152	122.278	154	121.784
752	128.382	754	128.46	252	123.95	352	126.466	452	127.44	552	128.313
254	124.2	354	126.511	454	127.602	554	128.766	556	128.767	558	128.767
652	128.471	654	128.471	656	128.472	658	128.647				
200	123.572	300	126.011	400	127.2	500	128.098				

CASE 5 - ALL DECAY HEAT IN TOP STANDARD WASTE BOX (FULL SOLAR LOAD)

DECAY HEAT = 10 WATTS

201	128.311	301	131.937	401	177.031	501	178.295	203	128.201	303	132.046
403	171.341	503	172.682	205	128.062	305	132.185	405	164.651	505	166.088
207	127.87	307	132.376	407	156.105	507	157.676	208	127.318	308	132.927
408	133.572	508	135.528	260	128.973	360	131.782	262	129.644	362	131.557
264	130.243	364	131.363	266	130.785	366	131.19	460	133.045	462	132.463
464	131.93	466	131.443	562	133.01	564	132.354	566	131.52	660	134.145
662	133.383	664	132.354	666	131.522	160	122.557	162	115.829	164	109.316
166	104.25	760	134.503	762	133.416	764	132.364	766	131.343	768	130.353
170	102.371	172	130.866	270	131.038	370	131.109	470	131.213	570	131.273
670	131.151	770	129.962	120	126.577	700	135.329	152	126.575	154	125.976
752	135.329	754	135.056	252	128.409	352	132.061	452	133.372	552	134.483
254	128.596	354	131.914	454	133.267	554	133.491	556	133.492	558	133.491
652	134.897	654	134.897	656	134.896	658	134.394				
200	128.311	300	131.937	400	179.921	500	181.185				

CASE 5 - ALL DECAY HEAT IN TOP STANDARD WASTE BOX (FULL SOLAR LOAD)

DECAY HEAT = 20 WATTS

201	131.8	301	136.438	401	225.155	501	226.392	203	131.661	303	136.577
403	213.855	503	215.167	205	131.483	305	136.755	405	200.537	505	201.944
207	131.237	307	137	407	183.521	507	185.059	208	130.531	308	137.705
408	138.664	508	140.578	260	131.774	360	135.293	262	131.603	362	133.998
264	131.403	364	132.805	266	131.192	366	131.703	460	136.555	462	134.939
464	133.434	466	132.04	562	135.441	564	133.94	566	132.053	660	137.574
662	135.962	664	133.788	666	132.02	160	125.168	162	117.61	164	110.293
166	104.601	760	138.595	762	136.543	764	134.557	766	132.631	768	130.763
170	102.49	172	130.871	270	131.088	370	131.181	470	131.38	570	131.494
670	131.233	770	130.024	120	129.684	700	140.167	152	129.681	154	129.01
752	140.166	754	139.638	252	131.687	352	136.295	452	137.762	552	138.641
254	131.832	354	135.992	454	137.419	554	136.537	556	136.536	558	136.536
652	139	654	139	656	138.999	658	138.102				
200	131.8	300	136.438	400	228.044	500	229.281				

CASE 5 - ALL DECAY HEAT IN TOP STANDARD WASTE BOX (FULL SOLAR LOAD)

DECAY HEAT = 20 WATTS

201	136.179	301	141.954	401	274.449	501	275.989	203	136.004	303	142.128
403	257.529	503	259.162	205	135.782	305	142.35	405	237.571	505	239.321
207	135.478	307	142.654	407	212.068	507	213.98	208	134.599	308	143.533
408	144.835	508	147.215	260	135.297	360	139.657	262	134.067	362	137.035
264	132.861	364	134.601	266	131.704	366	132.343	460	141.095	462	138.143
464	135.385	466	132.821	562	138.882	564	136.186	566	132.807	660	142.451
662	139.63	664	135.825	666	132.729	160	128.493	162	119.877	164	111.535
166	105.047	760	144.011	762	140.728	764	137.492	766	134.355	768	131.311
170	102.64	172	130.877	270	131.15	370	131.272	470	131.608	570	131.807
670	131.35	770	130.108	120	133.64	700	146.608	152	133.638	154	132.873
752	146.606	754	145.769	252	135.814	352	141.54	452	143.304	552	144.319
254	135.904	354	141.058	454	142.709	554	140.846	556	140.845	958	140.844
652	144.872	654	144.871	656	144.869	658	143.375				
200	136.179	300	141.954	400	277.338	500	278.878				

CASE 5 - ALL DECAY HEAT IN TOP STANDARD WASTE BOX (FULL SOLAR LOAD)

DECAY HEAT = 20 WATTS

201	140.767	301	147.462	401	323.611	501	325.357	203	140.565	303	147.664
403	301.075	503	302.926	205	140.307	305	147.921	405	274.48	505	276.465
207	139.953	307	143.274	407	240.495	507	242.664	208	138.933	308	149.292
408	150.9	508	153.601	260	138.98	360	144.019	262	136.641	362	140.071
264	134.382	364	136.396	266	132.239	366	132.982	460	145.493	462	141.246
464	137.272	466	133.574	562	142.076	564	138.273	566	133.505	660	147.07
662	143.104	664	137.753	666	133.4	160	132.079	162	122.322	164	112.875
166	105.527	760	149.366	762	144.775	764	140.33	766	136.021	768	131.841
170	102.802	172	130.883	270	131.215	370	131.362	470	131.823	570	132.097
670	131.46	770	130.188	120	137.909	700	152.832	152	137.907	154	137.039
752	152.83	754	151.699	252	140.139	352	146.774	452	148.723	552	149.738
254	140.164	354	146.121	454	147.87	554	144.846	556	144.844	558	144.844
652	150.438	654	150.438	656	150.434	658	148.37				
200	140.767	300	147.462	400	326.501	500	328.247				

3.6.1.6 Fourteen 55-Gallon Drum Payload with 100 ºF Ambient and No Solar, 40 Watts Uniform Decay Heat Load

40 WATTS DECAY HEAT (NO SOLAR LOAD)

Location	All Drums (Case 1)	Two Center Drums (Case 2)	Top Center Drums (Case 3)
Maximum Center Drum Centerline:	140.90	219.64	308.36
Average Center Drum Centerline:	137.55	215.37	214.15
Maximum Center Drum Wall:	128.22	133.63	136.79
Average Center Drum Wall:	124.87	129.35	128.37
Maximum Outer Drum Centerline:	139.03	127.48	127.63
Average Outer Drum Centerline:	136.32	124.35	123.36
Maximum Outer Drum Wall:	128.14	131.27	132.99
Average Outer Drum Wall:	123.74	124.04	123.06
Average Drum Centerline:	136.50	137.35	136.33
Average Drum Wall:	123.90	124.80	123.82
Maximum ICV Wall:	123.14	122.84	127.60
Average ICV Wall:	120.72	120.79	119.81
Minimum ICV Wall:	117.52	117.20	112.57
Average ICV Air:	122.78	123.39	122.41
Maximum ICV O-ring Seal:	117.52	117.20	122.11
Maximum OCV Wall:	122.35	122.20	126.03
Maximum OCV O-ring Seal:	114.25	114.02	116.50
Maximum Polyurethane Foam:	122.35	122.20	126.03
Maximum OCA Outer Shell:	101.96	101.93	102.26

Area of Each Node (ft^2)

Center Drum (Node)	Center Drum (Area)	Outer Drums (Node)	Outer Drums (Area)	ICV Wall (Node)	ICV Wall (Area)
208:	11.35145	218:	11.35145	152:	28.96573
308:	11.35145	228:	22.70291	252:	27.42553
408:	11.35145	238:	22.70291	352:	30.20783
508:	11.35145	248:	11.35145	452:	25.83564
		318:	11.35145	552:	14.70644
Total:	45.40583	328:	22.70291	652:	16.29633
		338:	22.70291	752:	28.96573
		348:	11.35145		
		418:	11.35145	Total:	172.4032
		428:	22.70291		
		438:	22.70291		
		448:	11.35145		
		518:	11.35145		
		528:	22.70291		
		538:	22.70291		
		548:	11.35145		
		Total:	272.4349		

NOTE: Average temperatures are "area-weighted" based on the above nodal areas

40 WATTS DECAY HEAT (NO SOLAR LOAD)

CASE 1 - ALL DECAY HEAT EQUALLY IN ALL DRUMS

202	135.663	302	140.53	402	140.292	502	132.215	204	132.976	304	137.843
404	137.604	504	129.527	206	127.871	306	132.738	406	132.5	506	124.423
208	123.354	308	128.221	408	127.982	508	119.906	212	135.4	312	138.796
412	138.473	512	131.524	222	135.384	322	138.655	422	138.296	522	131.472
232	135.403	332	138.535	432	137.926	532	131.536	242	135.411	342	138.454
442	137.75	542	131.541	214	132.844	314	136.675	414	136.485	514	129.083
224	132.671	324	135.913	424	135.967	524	128.576	234	132.81	334	135.784
434	134.865	534	129.011	244	132.822	344	135.464	444	134.379	544	128.92
216	127.934	316	132.297	416	132.03	516	124.408	226	127.47	326	131.507
426	131.176	526	123.874	236	121.811	336	130.637	436	129.283	536	124.14
246	127.796	346	129.926	446	128.509	546	123.779	218	123.548	318	128.144
418	127.858	518	120.114	228	122.865	328	127.186	428	126.839	528	119.464
238	123.355	338	125.801	438	124.521	538	119.434	248	123.304	348	125.159
448	123.615	548	119.2	5	128.102	10	127.012	15	127.012	260	118.656
360	119.323	262	113.14	362	113.615	264	107.945	364	108.276	266	103.086
366	103.303	460	117.061	462	112.3	464	107.801	466	103.59	562	111.573
564	107.858	566	103.293	660	114.836	662	111.337	664	106.614	666	102.741
160	118.491	162	112.692	164	107.078	166	102.711	760	115.653	762	112.066
764	108.592	766	105.226	768	101.959	170	101.091	172	100.139	270	100.777
370	100.941	470	101.592	570	101.955	670	101.009	770	100.668	100	122.027
110	122.026	115	122.025	120	122.024	700	118.373	152	122.022	154	121.438
752	118.372	754	117.476	252	122.074	352	123.137	452	121.213	552	117.971
254	121.544	354	122.345	454	120.131	554	114.25	556	114.246	558	114.247
652	117.521	654	117.519	656	117.517	658	115.984				
200	136.034	300	140.901	400	140.662	500	132.585	240	135.755	340	139.025
440	138.667	540	131.842								

40 WATTS DECAY HEAT (NO SOLAR LOAD)

CASE 2 - ALL DECAY HEAT IN TOP AND BOTTOM CENTER DRUMS

202	212.445	302	219.271	402	219.031	502	209.232	204	193.965	304	200.79
404	200.551	504	190.752	206	158.376	306	165.201	406	164.962	506	155.163
208	126.803	308	133.629	408	133.39	508	123.59	212	123.453	312	127.817
412	127.305	512	119.891	222	123.295	322	127.479	422	126.929	522	119.699
232	123.075	332	126.94	432	126.242	532	119.418	242	122.981	342	126.701
442	125.933	542	119.296	214	124.059	314	129.078	414	128.701	514	120.616
224	123.408	324	127.811	424	127.462	524	119.846	234	122.813	334	126.288
434	125.421	534	119.081	244	122.602	344	125.694	444	124.64	544	118.788
216	124.79	316	130.491	416	130.159	516	121.467	226	123.443	326	128.42
426	127.911	526	120.108	236	122.529	336	125.541	436	124.456	536	118.705
246	122.236	346	124.661	446	123.307	546	118.276	218	125.23	318	131.271
418	130.978	518	121.951	228	123.426	328	128.499	428	128.151	528	120.111
238	122.386	338	125.182	438	123.959	538	118.523	248	122.067	348	124.174
448	122.679	548	118.036	5	133.509	10	128.325	15	128.325	260	118.315
360	119.036	262	112.901	362	113.412	264	107.801	364	108.153	266	103.031
366	103.254	460	116.811	462	112.12	464	107.687	466	103.537	562	111.385
564	107.734	566	103.243	660	114.653	662	111.197	664	106.532	666	102.708
160	119.148	162	113.142	164	107.328	166	102.806	760	116.468	762	112.693
764	109.038	766	105.494	768	102.057	170	101.128	172	100.139	270	100.764
370	100.928	470	101.569	570	101.927	670	100.997	770	100.698	100	122.849
110	122.841	115	122.841	120	122.84	700	119.404	152	122.837	154	122.201
752	119.402	754	118.387	252	121.623	352	122.799	452	120.912	552	117.599
254	121.15	354	122.013	454	119.842	554	114.019	556	114.014	558	114.015
652	117.203	654	117.202	656	117.2	658	115.787				
200	212.816	300	219.641	400	219.402	500	209.603	240	123.295	340	127.479
440	126.929	540	119.699								

40 WATTS DECAY HEAT (NO SOLAR LOAD)

CASE 3 - ALL DECAY HEAT IN TOP CENTER DRUM

202	112.826	302	128.552	402	307.986	502	306.5	204	112.826	304	128.552
404	271.08	504	269.594	206	112.826	306	128.552	406	199.926	506	198.44
208	112.826	308	128.552	408	136.789	508	135.304	212	113.241	312	125.392
412	128.085	512	127.82	222	113.29	322	125.138	422	127.625	522	127.401
232	113.414	332	124.632	432	126.902	532	126.759	242	113.472	342	124.397
442	126.588	542	126.476	214	113.07	314	126.307	414	129.829	514	129.389
224	113.164	324	125.548	424	128.084	524	127.772	234	113.562	334	124.015
434	126.043	534	125.983	244	113.724	344	123.391	444	125.292	544	125.292
216	112.941	316	127.186	416	131.821	516	131.185	226	113.028	326	126.334
426	128.363	526	128.444	236	113.749	336	123.266	436	125.074	536	125.105
246	113.997	346	122.313	446	124.001	546	124.086	218	112.884	318	127.613
418	132.992	518	132.191	228	112.937	328	126.558	428	128.452	528	128.501
238	113.846	338	122.91	438	124.58	538	124.681	248	114.127	348	121.802
448	123.397	548	123.52	5	132.686	10	127.506	15	127.506	260	112.524
360	116.855	262	108.879	362	111.878	264	105.4	364	107.233	266	102.121
366	102.908	460	117.787	462	112.811	464	108.147	466	103.805	562	113.402
564	109.134	566	103.824	660	118.609	662	114.192	664	108.233	666	103.372
160	110.605	162	107.285	164	104.07	166	101.57	760	123.309	762	117.958
764	112.776	766	107.753	768	102.88	170	100.643	172	100.096	270	100.557
370	100.854	470	101.75	570	102.262	670	101.201	770	100.954	100	112.574
110	112.574	115	112.574	120	112.573	700	127.601	152	112.572	154	112.292
752	127.598	754	126.029	252	114.529	352	120.275	452	121.765	552	121.605
254	114.398	354	119.497	454	120.678	554	116.498	556	116.495	558	116.495
652	122.113	654	122.113	656	122.109	658	120.057				
200	112.826	300	128.552	400	308.356	500	306.871	240	113.29	340	125.138
440	127.625	540	127.401								

3.6.1.7 Two Standard Waste Box Payload with 100 ºF Ambient and No Solar, 40 Watts Uniform Decay Heat Load

40 WATTS DECAY HEAT (NO SOLAR LOAD)

Location	Both SWBs (Case 4)	Top SWB (Case 5)
Maximum Standard Waste Box Centerline:	212.98	300.43
Average Standard Waste Box Centerline:	211.70	209.63
Maximum Standard Waste Box Wall:	124.20	125.52
Average Standard Waste Box Wall:	122.66	122.07
Maximum ICV Wall:	121.97	124.59
Average ICV Wall:	120.45	119.87
Minimum ICV Wall:	117.70	115.14
Average ICV Air:	121.64	121.06
Maximum ICV O-ring Seal:	117.70	121.88
Maximum OCV Wall:	121.28	123.30
Maximum OCV O-ring Seal:	114.14	116.32
Maximum Polyurethane Foam:	121.28	123.30
Maximum OCA Outer Shell:	101.94	102.24

Area of Each Node (ft^2)

Standard Waste Box (Node)	(Area)	ICV Wall (Node)	(Area)
208:	50.80244	152:	28.96573
308:	50.80244	252:	27.42553
408:	50.80244	352:	30.20783
508:	50.80244	452:	25.83564
		552:	14.70644
Total:	203.2097	652:	16.29633
		752:	28.96573
		Total:	172.4032

NOTE: Average temperatures are "area-weighted" based on the above nodal areas

40 WATTS DECAY HEAT (NO SOLAR LOAD)

CASE 4 - ALL DECAY HEAT EQUALLY IN BOTH STANDARD WASTE BOXES

201	209.134	301	210.09	401	209.337	501	206.667	203	197.843	303	198.857
403	198.155	503	195.324	205	184.536	305	185.623	405	184.986	505	181.951
207	167.536	307	168.724	407	168.177	507	164.86	208	122.722	308	124.2
408	123.914	508	119.785	260	118.133	360	118.406	262	112.768	362	112.981
264	107.719	364	107.899	266	102.999	366	103.159	460	116.635	462	111.993
464	107.611	466	103.513	562	111.48	564	107.803	566	103.273	660	114.95
662	111.42	664	106.657	666	102.754	160	118.352	162	112.597	164	107.025
166	102.691	760	116.235	762	112.514	764	108.911	766	105.418	768	102.029
170	101.083	172	100.136	270	100.756	370	100.907	470	101.569	570	101.944
670	101.009	770	100.69	120	121.871	700	119.091	152	121.869	154	121.277
752	119.089	754	118.127	252	121.476	352	121.971	452	120.628	552	118.005
254	120.947	354	121.271	454	119.581	554	114.135	556	114.131	558	114.131
652	117.697	654	117.696	656	117.693	658	116.107				
200	212.024	300	212.98	400	212.226	500	209.556				

40 WATTS DECAY HEAT (NO SOLAR LOAD)

CASE 5 - ALL DECAY HEAT IN TOP STANDARD WASTE BOX

201	116.913	301	121.566	401	296.737	501	297.538	203	116.773	303	121.707
403	274.229	503	275.079	205	116.594	305	121.886	405	247.671	505	248.582
207	116.349	307	122.131	407	213.735	507	214.731	208	115.641	308	122.839
408	124.285	508	125.523	260	113.676	360	116.904	262	109.674	362	111.922
264	105.873	364	107.264	266	102.3	366	102.922	460	117.52	462	112.625
464	108.032	466	103.755	562	113.261	564	109.033	566	103.781	660	118.255
662	113.925	664	108.081	666	103.312	160	112.735	162	108.746	164	104.884
166	101.88	760	120.863	762	116.076	764	111.441	766	106.948	768	102.589
170	100.765	172	100.106	270	100.597	370	100.859	470	101.73	570	102.237
670	101.182	770	100.865	120	115.145	700	124.589	152	115.143	154	114.763
752	124.587	754	123.295	252	115.959	352	120.259	452	121.381	552	121.507
254	115.748	354	119.541	454	120.347	554	116.324	556	116.322	558	116.321
652	121.881	654	121.88	656	121.877	658	119.675				
200	116.913	300	121.566	400	299.627	500	300.427				

3.6.2 Thermal Model Details

3.6.2.1 Convection Coefficient Calculation

Heat transfer coefficients from the OCA outer surface are calculated as follows. From *Principles of Heat Transfer*[1], the convective heat transfer coefficient, h, is:

$$h = Nu\frac{k}{L} \text{ Btu/hr-in}^2\text{-°F}$$

where k is the conductivity of gas at film temperature (Btu/hr-in-°F) and L is the effective length of the vertical surface or cylinder diameter for the horizontal surface.

The Nusselt number, Nu, for horizontally heated surfaces facing upward is:

$$Nu = 0.54(Gr\,Pr)^{1/4} \qquad \text{for } 10^5 < GrPr < 2\times10^7$$

$$Nu = 0.14(Gr\,Pr)^{1/3} \qquad \text{for } 2\times10^7 < GrPr < 3\times10^{10}$$

and, for horizontally heated surfaces facing downward:

$$Nu = 0.27(Gr\,Pr)^{1/4} \qquad \text{for } 3\times10^5 < GrPr < 3\times10^{10}$$

The Nusselt number, Nu, for vertically heated surfaces is:

$$Nu = 0.555(Gr\,Pr)^{1/4} \qquad \text{for } 10 < GrPr < 10^9$$

For both horizontally and vertically heated surfaces, the Grashof number, Gr, is:

$$Gr = \frac{g\beta\Delta TL^3}{\nu^2}$$

where g is the gravitational acceleration constant (in/s^2), β is the gas coefficient of thermal expansion (ºF^{-1}), where $\beta = (T_{abs})^{-1}$ for an ideal gas, ΔT is the differential temperature (ºF), where $\Delta T = |T_{wall} - T_\infty|$, ν is the kinematic viscosity of gas at the film temperature (in^2/s), and Pr is the Prandtl number. Note that k, Gr, and Pr are each a function of air temperature as taken from Table A-3 of *Principles of Heat Transfer*[1].

[1] Frank Kreith, *Principles of Heat Transfer*, InText Press, Inc., New York, 1973, pp396-398.

3.6.2.2 Polyethylene Plastic Wrap Transmittance Calculation

As many as 18 layers of the optional, 0.002 inch thick, polyethylene plastic wrap is used to restrain the payload drums during transport. Data on the transmittance of polyethylene is available from Figure 659 of *Thermophysical Properties of Matter*[2]. Assuming a plastic wrap temperature of 200 ºF to 250 ºF, Curve 1 through Curve 4 from Figure 659 of *Thermophysical Properties of Matter* are applicable. Wien's displacement law states:

$$\lambda_{max} T = 5215.6\,\mu\text{m-}^{\circ}\text{R}$$

Thus, at 250 ºF, the wavelength of maximum intensity is:

$$\lambda_{max} = \frac{5215.6}{(250+460)} = 7.436\ \mu\text{m}$$

The number of wraps is of secondary importance to the overall transmittance, since the first few layers perform essentially all of the filtering. The maximum monochromatic radiation is near 10 μm, and since the low end of the transmittance curves is near $\tau = 0.75$, an overall transmittance of 0.75 is applicable.

[2] Y.S. Touloukian and C.Y. Ho, Editors, *Thermophysical Properties of Matter*, Thermophysical Properties Research Center (TPRC) Data Series, Purdue University, 1970, IFI/Plenum, New York.

4.0 CONTAINMENT

4.1 Containment Boundary

4.1.1 Containment Vessel

Two independent levels of containment are established within the TRUPACT-II package. In general, each containment vessel is constructed primarily of ASTM A240, Type 304, austenitic stainless steel. The exceptions to the use of ASTM A240, Type 304, stainless steel are so noted in the following detailed descriptions.

4.1.1.1 Outer Containment Assembly (Primary Level of Containment)

The containment boundary of the Outer Containment Vessel (OCV), provided as part of the Outer Containment Assembly (OCA), consists of the inner stainless steel vessel comprised of a mating lid and body, plus the uppermost (innermost) of two main O-ring seals between them. In addition, the containment boundary includes an ASTM B16, Alloy 360, brass OCV vent port plug with a mating butyl O-ring seal. A more detailed description of the OCV containment boundary is provided in Section 1.2.1.1.1, *Outer Containment Assembly (OCA)*, and in Appendix 1.3.1, *Packaging General Arrangement Drawings*.

The non-stainless steel components utilized in the OCV containment boundary are the upper (inner) butyl O-ring seal, the brass vent port plug, and the butyl O-ring seal on the vent port plug.

4.1.1.2 Inner Containment Vessel (Secondary Level of Containment)

The containment boundary of the Inner Containment Vessel (ICV) consists of a stainless steel vessel comprised of a mating lid and body, plus the uppermost (innermost) of the two main O-ring seals between them. In addition, the containment boundary includes an ASTM B16, Alloy 360, brass ICV outer vent port plug with a mating butyl O-ring seal. A more detailed description of the ICV containment boundary is provided in Section 1.2.1.1.2, *Inner Containment Vessel (ICV) Assembly*, and in Appendix 1.3.1, *Packaging General Arrangement Drawings*.

The non-stainless steel components utilized in the ICV containment boundary are the upper (inner) butyl O-ring seal, the brass outer vent port plug, and the butyl O-ring seal on the vent port plug.

4.1.2 Containment Penetrations

The only containment boundary penetrations into each of the two containment vessels (OCV and ICV) are the lids themselves, and the corresponding vent ports. Each penetration is designed to demonstrate "leaktight" sealing integrity, i.e., a leakage rate not to exceed 1×10^{-7} standard cubic centimeters per second (scc/sec), air, as defined in ANSI N14.5[1].

[1] ANSI N14.5-1997, *American National Standard for Radioactive Materials – Leakage Tests on Packages for Shipment,* American National Standards Institute, Inc. (ANSI).

4.1.3 Seals and Welds

4.1.3.1 Seals

Seals affecting containment are described above. A summary of seal testing prior to first use, during routine maintenance, and upon assembly for transportation is as follows.

4.1.3.1.1 Fabrication Leakage Rate Tests

During fabrication and following the pressure testing per Section 8.1.2.2, *Containment Vessel Pressure Testing*, both the OCV and ICV (primary and secondary containment, respectively) shall be individually leakage rate tested as delineated in Section 8.1.3, *Fabrication Leakage Rate Tests*. The fabrication leakage rate tests are consistent with the guidelines of Section 7.3 of ANSI N14.5. This leakage rate test verifies the containment integrity of the TRUPACT-II package's OCV and ICV to a leakage rate not to exceed 1×10^{-7} scc/sec, air.

4.1.3.1.2 Maintenance/Periodic Leakage Rate Tests

Annually, or at the time of damaged containment seal replacement or sealing surface repair, the OCV and/or ICV O-ring seals shall be leakage rate tested as delineated in Section 8.2.2, *Maintenance/Periodic Leakage Rate Tests*. The maintenance/periodic leakage rate tests are consistent with the guidelines of Section 7.4 of ANSI N14.5. This test verifies the sealing integrity of the TRUPACT-II package's ICV and OCV lid and vent port containment seals to a leakage rate not to exceed 1×10^{-7} scc/sec, air.

4.1.3.1.3 Preshipment Leakage Rate Tests

Prior to shipment of the loaded TRUPACT-II package, the main O-ring seal and vent port plug O-ring seal for both the OCV and ICV shall be leakage rate tested per Section 7.4, *Preshipment Leakage Rate Test*. The preshipment leakage rate tests are consistent with the guidelines of Section 7.6 of ANSI N14.5. This test verifies the sealing integrity of the TRUPACT-II package's OCV and ICV lid and vent port containment seals to a leakage rate sensitivity of 1×10^{-3} scc/sec, air, or less.

As an option, the maintenance/periodic leakage rate tests, delineated in Section 8.2.2, *Maintenance/Periodic Leakage Rate Tests*, may be performed in lieu of the preshipment leakage rate tests.

4.1.3.2 Welds

All containment vessel body welds are full penetration welds that have been radiographed to ensure structural and containment integrity. Non-radiographed, safety related welds such as those that attach the OCV vent port coupling and the ICV vent port insert to their respective containment shells are examined using liquid penetrant testing on the final pass or both the root and final passes, as applicable. All containment boundary welds are confirmed to be leaktight as delineated in Section 8.1.3, *Fabrication Leakage Rate Tests*.

4.1.4 Closure

4.1.4.1 Outer Containment Assembly (OCA) Closure

With reference to Figure 1.1-1 and Figure 1.1-2 from Section 1.1, *Introduction*, the OCA lid is secured to the OCA body via an OCV locking ring assembly located at the outer diameter of the OCV upper (lid) and lower (body) seal flanges. The upper end of the OCV locking ring is a continuous ring that mates with the OCV upper seal flange (also a continuous ring). The lower end of the OCV locking ring is comprised of 18 tabs that mate with a corresponding set of 18 tabs on the OCV lower seal flange. The OCV locking ring and OCV upper seal flange are an assembly that normally does not disassemble.

Figure 1.2-1 from Section 1.2*, Package Description*, illustrates OCA lid installation in five steps:

1. As an option, lightly lubricate the main O-ring seals with vacuum grease; install the main O-ring seals into the O-ring seal grooves located in the OCV lower seal flange.
2. Using external alignment stripes as a guide, align the OCA lid's OCV locking ring tabs with the OCV lower seal flange tab spaces.
3. Install the OCA lid; if necessary, evacuate the OCV cavity through the OCV vent port to fully seat the OCA lid and allow free movement of the OCV locking ring.
4. Rotate the OCV locking ring to the "locked" position, again using external alignment stripes as a guide. The locked position aligns the OCV locking ring's tabs with the OCV lower seal flange's tabs. A locking "Z-flange" is bolted to the bottom end of the OCV locking ring and extends radially outward to the exterior of the TRUPACT-II package. The exterior flange of the locking Z-flange is attached to an outer thermal shield. This Z-flange/thermal shield assembly allows external operation of the OCV locking ring.
5. Install six 1/2 inch diameter lock bolts (socket head cap screws) through the outer thermal shield and into the exterior surface of the OCA to secure the OCV locking ring assembly in the locked position.

4.1.4.2 Inner Containment Vessel (ICV) Closure

With the exception of the locking Z-flange/outer thermal shield assembly, and the use of three rather than six locking ring lock bolts, ICV lid installation is identical to OCA lid installation as described in Section 4.1.4.1, *Outer Containment Assembly (OCA) Closure*.

This page intentionally left blank.

4.2 Containment Requirements for Normal Conditions of Transport

4.2.1 Containment of Radioactive Material

The results of the normal conditions of transport (NCT) structural and thermal evaluations performed in Section 2.6, *Normal Conditions of Transport*, and Section 3.4, *Thermal Evaluation for Normal Conditions of Transport*, respectively, and the results of the full-scale, structural testing presented in Appendix 2.10.3, *Certification Tests*, verify that there will be no release of radioactive materials per the "leaktight" definition of ANSI N14.5[1] under any of the NCT tests described in 10 CFR §71.71[2].

4.2.2 Pressurization of Containment Vessel

The maximum normal operating pressure (MNOP) of both the OCV and ICV is 50 psig per Section 3.4.4, *Maximum Internal Pressure*. The design pressure of both the OCV and ICV is 50 psig. Based on the structural evaluations performed in Chapter 2.0, *Structural Evaluation*, pressure increases to 50 psig will not reduce the effectiveness of the TRUPACT-II package to maintain containment integrity per Section 4.2.1, *Containment of Radioactive Material*.

4.2.3 Containment Criterion

At the completion of fabrication, both the OCV and ICV shall be leakage rate tested as described in Section 4.1.3.1.1, *Fabrication Leakage Rate Tests*. For annual maintenance, both the OCV and ICV shall be leakage rate tested as described in Section 4.1.3.1.2, *Maintenance/Periodic Leakage Rate Tests*. In addition, at the time of seal replacement if other than during routine maintenance (e.g., if damage during assembly necessitates seal replacement), maintenance/ periodic leakage rate testing shall be performed for that seal. For verification of proper assembly prior to shipment, both the OCV and ICV shall be leakage rate tested as described in Section 4.1.3.1.3, *Preshipment Leakage Rate Tests*.

[1] ANSI N14.5-1997, *American National Standard for Radioactive Materials – Leakage Tests on Packages for Shipment,* American National Standards Institute, Inc. (ANSI).

[2] Title 10, Code of Federal Regulations, Part 71 (10 CFR 71), *Packaging and Transportation of Radioactive Material*, 01-01-07 Edition.

This page intentionally left blank.

4.3 Containment Requirements for Hypothetical Accident Conditions

4.3.1 Fission Gas Products

There are no fission gas products in the TRUPACT-II package payload.

4.3.2 Containment of Radioactive Material

The results of the hypothetical accident condition (HAC) structural and thermal evaluations performed in Section 2.7, *Hypothetical Accident Conditions*, and Section 3.5, *Thermal Evaluation for Hypothetical Accident Conditions*, respectively, and the results of the full-scale, structural and thermal testing presented in Appendix 2.10.3, *Certification Tests*, verify that there will be no release of radioactive materials per the "leaktight" definition of ANSI N14.5[1] under any of the HAC tests described in 10 CFR §71.73[2].

4.3.3 Containment Criterion

The TRUPACT-II package has been designed, and has been verified by leakage rate testing both prior to and following structural and thermal certification testing as presented in Appendix 2.10.3, *Certification Tests*, to meet the "leaktight" definition of ANSI N14.5.

[1] ANSI N14.5-1997, *American National Standard for Radioactive Materials – Leakage Tests on Packages for Shipment,* American National Standards Institute, Inc. (ANSI).

[2] Title 10, Code of Federal Regulations, Part 71 (10 CFR 71), *Packaging and Transportation of Radioactive Material*, 01-01-07 Edition.

This page intentionally left blank.

4.4 Special Requirements

4.4.1 Plutonium Shipments

The TRUPACT-II package is designed and has been structurally and thermally tested as a Type B(U), double containment package meeting the requirements of 10 CFR §71.63[1] for plutonium shipments. Both containment vessels (i.e., the OCV and ICV) are shown on the drawings in Appendix 1.3.1, *Packaging General Arrangement Drawings*, and described in Section 4.1.1.1, *Outer Containment Assembly (Primary Level of Containment)*, and Section 4.1.1.2, *Inner Containment Vessel (Secondary Level of Containment)*. Further, the TRUPACT-II package has been designed, and has been verified by leakage rate testing both prior to and following structural and thermal certification testing as presented in Appendix 2.10.3, *Certification Tests*, to meet the "leaktight" definition of ANSI N14.5[2].

4.4.2 Interchangeability

The TRUPACT-II package is designed and fabricated so that both the OCV lid assembly and the ICV lid assembly are interchangeable between OCV body assemblies and ICV body assemblies, respectively. Each combination of a particular lid assembly and body assembly becomes a containment system that shall be maintained in accordance with Section 4.1.3.1.2, *Maintenance/Periodic Leakage Rate Tests*, and used in accordance with Section 4.1.3.1.3, *Preshipment Leakage Rate Tests*. When the interchangeability option has been exercised, newly combining a lid and a body, measure the axial play per the requirements of Section 8.2.3.3.2.3, *Axial Play*, to determine acceptability.

[1] Title 10, Code of Federal Regulations, Part 71 (10 CFR 71), *Packaging and Transportation of Radioactive Material*, 01-01-07 Edition.

[2] ANSI N14.5-1997, *American National Standard for Radioactive Materials – Leakage Tests on Packages for Shipment,* American National Standards Institute, Inc. (ANSI).

This page intentionally left blank.

5.0 SHIELDING EVALUATION

The compliance evaluations of the TRUPACT-II packaging with respect to the dose rate limits established by 10 CFR §71.47(a)[1] for normal conditions of transport (NCT) or 10 CFR §71.51(a)(2) for hypothetical accident conditions (HAC) are based on two categories. The first category does not permit the use of shielding materials to meet the NCT or HAC dose rate limits and is evaluated for compliance in this section. The second category permits the use of shielding materials in the standard, S100, S200, and S300 pipe overpack payload containers as evaluated in Appendices 4.1 through 4.4 of the *CH-TRU Payload Appendices*[2].

Each contact-handled transuranic (CH-TRU) waste payload container (i.e., 55-gallon drum, 85-gallon drum, 100-gallon drum, standard waste box (SWB), or ten drum overpack (TDOP)), as prepared for transport in a TRUPACT-II package, is limited such that the external radiation field, both gamma and neutron, shall be less than or equal to 200 millirem per hour (mrem/hr) at the package surface. This dose rate limit is for payload containers prior to addition of any lead, steel or other shielding material to the payload containers for *as-low-as-reasonably-achievable* (ALARA) dose reduction purposes during non-transport handling operations.

The TRUPACT-II packaging is not designed to provide significant gamma or neutron shielding. Three shells, the inner containment vessel (ICV), outer containment vessel (OCV), and outer containment assembly (OCA) outer shell are composed of stainless steel having minimum thicknesses of 1/4 inch, 3/16 inch, and 1/4 inch, respectively. Approximately ten inches of polyurethane foam occupies the annular cavity between the OCV and OCA outer shell.

Prior to transport, the TRUPACT-II package shall be monitored on the semi-trailer or railcar for both gamma and neutron radiation to demonstrate compliance with 10 CFR §71.47. Since the TRUPACT-II package is not significantly deformed under NCT, the package will meet the dose rate limits for NCT if the measurements demonstrate compliance with the allowable dose rate levels in 10 CFR §71.47. The shielding Transport Index (TI), as defined in 10 CFR §71.4, will be determined by measuring the dose rate a distance of one meter from the package surface per the requirements of 49 CFR §173.403[3].

Shielding materials are not specifically provided by the TRUPACT-II packaging, and none are permitted in the payload containers to meet the dose rate limits of 10 CFR §71.47 for NCT. Therefore, shielding provided by the stainless steel shells and polyurethane foam of the packaging is not needed to meet the higher dose rate limits after the HAC tests delineated in 10 CFR §71.73. This ensures that the post-HAC, allowable dose rate of one rem per hour (rem/hr) a distance of one meter from the package surface per 10 CFR §71.51(a)(2) will be met.

Even if payload material is released from a payload container during a HAC event, the post-HAC dose rate limit of one rem/hr at one meter from the package surface will always be met.

---

[1] Title 10, Code of Federal Regulations, Part 71 (10 CFR 71), *Packaging and Transportation of Radioactive Material*, 01-01-07 Edition.

[2] U.S. Department of Energy (DOE), *CH-TRU Payload Appendices*, current revision, U.S. Department of Energy, Carlsbad Field Office, Carlsbad, New Mexico.

[3] Title 49, Code of Federal Regulations, Part 173 (49 CFR 173), *Shippers – General Requirements for Shipments and Packagings*, 10-01-06 Edition.

This is because each CH-TRU waste payload container must have a dose rate less than or equal to 200 mrem/hr on contact prior to the addition of any ALARA dose reduction shielding for non-transport handling operations prior to being loaded into the TRUPACT-II packaging. Since shielding within the payload containers is not permitted to meet the transportation dose rate limits for NCT, release of the materials from the payload containers during a HAC event will not increase the dose rate significantly or cause it to exceed the dose rate limit for the HAC.

6.0 CRITICALITY EVALUATION

The following analyses demonstrate that the TRUPACT-II package complies with the requirements of 10 CFR §71.55[1] and §71.59. The analyses show that the criticality requirements are satisfied when limiting the payload containers and the TRUPACT-II package to fissile gram equivalent (FGE) of Pu-239 limits given in Table 6.1-1 and Table 6.1-2, respectively for the payloads described in the *Contact-Handled Transuranic Waste Authorized Methods for Payload Control* (CH-TRAMPAC)[2]. In summary, Case A is applicable to waste that is not machine compacted and contains less than or equal to 1% by weight quantities of special reflector materials and Case B is applicable to waste that is not machine compacted and contains greater than 1% by weight quantities of special reflector materials. For Case A, package limits were calculated for various Pu-240 contents in the package. Case C is applicable to machine compacted waste that contains less than or equal to 1% by weight quantities of special reflector materials. Case D is specifically applicable to machine compacted waste in the form of "puck" drums overpacked in 55-, 85-, or 100-gallon drums with less than or equal to 1% by weight quantities of special reflector materials. Case E is applicable to waste that is not machine compacted in the standard, S100, S200, and S300 pipe overpacks with less than or equal to 1% by weight quantities of special reflector materials and Case F is applicable to waste that is not machine compacted in the standard, S100, S200, and S300 pipe overpacks with greater than 1% by weight quantities of special reflector materials. However, if the quantity of special reflector material in the payload is greater than 1% by weight but the form of the payload is such that the thickness and/or packing fraction of the special reflector material is less than the reference poly/water reflector or the special reflector material (excluding beryllium in non-pipe overpack configurations) is mechanically or chemically bound to the fissile material, then Case A and Case E limits apply in lieu of Case B and Case F limits, respectively. Similarly, Case C and Case D limits are applicable to machine compacted waste with greater than 1% by weight quantities of special reflectors in the above stated forms.

The criticality evaluations for Cases E and F are presented in Appendices 4.1, 4.2, 4.3, and 4.4 in the *CH-TRU Payload Appendices*[3] whereas the analyses for Cases A through D are presented in this chapter. Based on an unlimited array of undamaged or damaged TRUPACT-II packages, the Criticality Safety Index (CSI), per 10 CFR §71.59, is 0.0.

6.1 Discussion and Results

The criticality analyses presented herein are identical to the analyses presented in Chapter 6.0, *Criticality Evaluation*, of the *HalfPACT Shipping Package Safety Analysis Report*[4]. Since the

[1] Title 10, Code of Federal Regulations, Part 71 (10 CFR 71), *Packaging and Transportation of Radioactive Material*, 01-01-07 Edition.

[2] U.S. Department of Energy (DOE), *Contact-Handled Transuranic Waste Authorized Methods for Payload Control* (CH-TRAMPAC), U.S. Department of Energy, Carlsbad Field Office, Carlsbad, New Mexico.

[3] U.S. Department of Energy (DOE), *CH-TRU Payload Appendices*, current revision, U.S. Department of Energy, Carlsbad Field Office, Carlsbad, New Mexico.

[4] U.S. Department of Energy (DOE), *HalfPACT Shipping Package Safety Analysis Report*, USNRC Certificate of Compliance 71-9279, U.S. Department of Energy, Carlsbad Area Office, Carlsbad, New Mexico.

height of a HalfPACT package is 30 inches shorter than a TRUPACT-II package, resulting in a closer axial packaging in the infinite arrays, the criticality analyses utilizing the HalfPACT package geometry are considered conservative for Cases A through D. A comprehensive description of the TRUPACT-II packaging is provided in Section 1.2, *Package Description*, and in the packaging drawings in Appendix 1.3.1, *Packaging General Arrangement Drawings*.

For the contents of the TRUPACT-II package specified in Section 6.2, *Package Contents*, no special features are required to maintain criticality safety for any number of TRUPACT-II packages for both normal conditions of transport (NCT) and hypothetical accident conditions (HAC). The presence and location of the stainless steel, inner and outer containment vessel shells (ICV and OCV, respectively) and outer containment assembly (OCA) outer shell are all that are required to maintain criticality safety.

The criteria for ensuring that a package (or package array) is safely subcritical is:

$$k_s = k_{eff} + 2\sigma < USL$$

where the quantity k_s is the multiplication factor computed for a given configuration plus twice the uncertainty in the computed result, σ. This quantity is computed and reported in order to permit a direct comparison of results against the upper subcriticality limit, USL, determined in Section 6.5, *Critical Benchmark Experiments*. The USL is determined on the basis of a benchmark analysis and incorporates the combined effects of code computational bias, the uncertainty in the bias based on both experimental and computational uncertainties, and an administrative margin. Further discussion regarding the USL is provided in Chapter 4, *Determination of Bias and Subcritical Limits*, of NUREG/CR-6361[5].

The results of the criticality calculations are summarized in Table 6.1-3. Calculations performed for Case A for a TRUPACT-II single unit and infinite arrays of damaged TRUPACT-II packages indicate that the maximum reactivity of the package arrays are essentially the same as that of the NCT single-unit to within the calculated uncertainty of the Monte Carlo analysis. This occurs because:

- When the ICV and OCA regions are filled with reflecting material, the size of these regions allows the presence of enough material to isolate the fissile material region of each TRUPACT-II packages from each other, and
- When the fissile material region of each damaged or undamaged TRUPACT-II package is unreflected, interaction among TRUPACT-II packages is maximized. However, interactive effects are not as great as the effect of full reflection.

As discussed below, all k_s values are less than the USL of 0.9382. For all cases, the modeled conditions are considered to be extremely conservative, nevertheless, they provide an upper limit on k_s. Therefore, the requirements of 10 CFR §71.55 are met when the contents of a single TRUPACT-II package are limited in accordance with Table 6.1-1 and Table 6.1-2. The

[5] J. J. Lichtenwalter, S. M. Bowman, M. D. DeHart, C. M. Hopper, *Criticality Benchmark Guide for Light-Water-Reactor Fuel in Transportation and Storage Packages*, NUREG/CR-6361, ORNL/TM-13211, March 1997.

application of these limits to the TRUPACT-II payload described in the CH-TRAMPAC[6] is discussed, in summary, in Section 6.4.3.5, *Applicable Criticality Limits for CH-TRU Waste*.

Infinite arrays of both damaged and undamaged TRUPACT-II packages, as defined in Section 6.3.4, *Array Models*, are also safely subcritical (k_s < USL). The post-accident geometry used in the model of the damaged TRUPACT-II packages conservatively bounds the damage experienced from certification testing described in Appendix 2.10.3, *Certification Tests*. Based on the results of the HAC 30 foot drops, the criticality model conservatively assumes that the OCA outer shell is deformed inward on the side, top, and bottom to a distance of 5 inches from the OCV. Further, the criticality model conservatively models the region between the ICV and the OCA as containing a mixture of 25% polyethylene, 74% water and 1% beryllium in all bounding cases to bound the presence of polyurethane foam in this region. After the HAC thermal event (fire), actual post-test measurements show 3 inches of foam, minimum, remains in impact regions, and 5 inches, minimum, remains elsewhere.

For an infinite array of damaged TRUPACT-II packages, the maximum calculated k_s values for each case occurred for optimal internal moderation and maximum reflection within the ICV, OCA and interspersed regions. Of all calculations performed and summarized in Table 6.1-3, the maximum neutron multiplication factor, adjusted for code bias and uncertainty, of k_s = 0.9359 occurs in Case A at the 360 FGE limit with 15 g of Pu-240 for an infinite array of HAC packages when optimally moderated and reflected. All results are detailed in Section 6.4.3, *Criticality Results*. As with the single-unit cases, the calculations contain conservatism in the geometry and material assumptions (as identified in Section 6.2, *Package Contents*, and Section 6.4.2, *Fuel Loading or Other Contents Loading Optimization*). At maximum reflection, the packages in the array are isolated from each other. An investigation of array reactivity when array interaction effects become significant as a result of decreased reflector volume fraction is provided in Section 6.4.3.2, *Criticality Results for Infinite Arrays of TRUPACT-II Packages*. Therefore, the requirements of 10 CFR §71.59 are met as arrays of TRUPACT-II packages will remain subcritical when the contents of a single TRUPACT-II package is limited as indicated in Table 6.1-1 and Table 6.1-2. Furthermore, a CSI of zero (0.0) is justified.

[6] U.S. Department of Energy (DOE), *Contact-Handled Transuranic Waste Authorized Methods for Payload Control* (CH-TRAMPAC), U.S. Department of Energy, Carlsbad Field Office, Carlsbad, New Mexico.

Table 6.1-1 – Fissile Material Limit per Payload Container

Payload Configuration	Fissile Material Limit per Payload Container (Pu-239 FGE)					
	Case A①	Case B	Case C	Case D	Case E	Case F
55-gallon drums	200	100	200	200	-	-
Pipe overpacks	-	-	-	-	200	140
SWB or TDOP	325	100	250	-	-	-
85-gallon drums	200	100	200	200	-	-
100-gallon drums	200	100	200	200	-	-

Note:

① The FGE limit given applies to the payload container regardless of Pu-240 content in the package.

Table 6.1-2 – Fissile Material Limit per TRUPACT-II Package

Minimum Pu-240 Content in Package	Fissile Material Limit per TRUPACT-II Package (Pu-239 FGE)					
	Case A	Case B	Case C	Case D	Case E	Case F
0 g	325	100	250	325	2800	1960
5 g	340	-	-	-	-	-
15 g	360	-	-	-	-	-
25 g	380	-	-	-	-	-

Table 6.1-3 – Summary of Criticality Analysis Results

	Case A	Case B	Case C	Case D
Normal Conditions of Transport (NCT)				
Number of undamaged packages calculated to be subcritical	∞	∞	∞	∞
Single Unit Maximum k_s	0.9339	Same as HAC Infinite Array k_s		
Infinite Array Maximum k_s	Same as HAC Infinite Array k_s			
Hypothetical Accident Conditions (HAC)				
Number of damaged packages calculated to be subcritical	∞	∞	∞	∞
Single Unit Maximum k_s (0 g Pu-240)	0.9331	Same as HAC Infinite Array k_s		
Infinite Array Maximum k_s (0 g Pu-240)	0.9331	0.9184	0.9345	0.9349
Infinite Array Maximum k_s (with Pu-240)	0.9359	-	-	-
Upper Subcriticality Limit (USL)	0.9382			

This page intentionally left blank.

6.2 Package Contents

The payload cavity of a TRUPACT-II package can accommodate fourteen 55-gallon drums, eight 85-gallon drums, six 100-gallon drums, two standard waste boxes (SWB), or a single ten drum overpack (TDOP). Different fissile gram equivalent (FGE) limits are available depending on the contents of the shipment as described in the subsections below.

The quantities of all fissile isotopes other than Pu-239 present in the CH-TRU waste material and other authorized payloads may be converted to a FGE using the conversion factors outlined in the CH-TRAMPAC[1]. For modeling purposes, the package is assumed to contain Pu-239 at the FGE limit. The fissile composition of the payload will typically be as follows:

Nuclide	Weight-Percent
Pu-238	Trace
Pu-239	93.0
Pu-240	5.8
Pu-241	0.4
Pu-242	Trace
Am-241	Trace
All other fissile isotopes	0.7

Except for Cases A and D, no credit is taken for parasitic neutron absorption in CH-TRU waste materials and other authorized payloads, dunnage, or package contents. The entire contents of a TRUPACT-II package are conservatively modeled as an optimally moderated sphere of Pu-239 as determined by varying the H/Pu atom ratio. The size of the sphere is calculated based on the H/Pu ratio and the Pu mass. Case A takes credit for the presence of varying amounts of Pu-240 in the package, see Table 6.1-2. Case D is applicable to a very specific case where drums and their contents are machine compacted and then overpacked in 55-, 85-, or 100-gallon drums. Due to the machine compaction, a higher polyethylene packing fraction is achieved and the fissile material is in a more reactive state within the pucks than if it reconfigured outside of the pucks and homogenized at a lower polyethylene packing fraction within the inner containment vessel (ICV). Thus, in this case, some of structural materials are credited and a cylindrical fissile region is modeled as discussed in Section 6.3.1.4, *Case D Contents Model*. The TRUPACT-II package meets the criticality safety requirements as specified in 10 CFR §71.55[2] and §71.59, provided the limits specified in Table 6.1-1 and Table 6.1-2 are not exceeded.

[1] U.S. Department of Energy (DOE), *Contact-Handled Transuranic Waste Authorized Methods for Payload Control* (CH-TRAMPAC), U.S. Department of Energy, Carlsbad Field Office, Carlsbad, New Mexico.

[2] Title 10, Code of Federal Regulations, Part 71 (10 CFR 71), *Packaging and Transportation of Radioactive Material*, 01-01-07 Edition.

6.2.1 Applicability of Case A Limit

The Case A limit is applicable provided the contents are manually compacted (i.e., not machine compacted) and contain less than or equal to 1% by weight quantities of special reflector materials. These requirements drive the assumptions regarding the appropriately bounding moderator and reflector materials that are utilized in the analyses to bound the presence of all materials that are authorized for shipment under the Case A FGE limits. The contents model assumptions are provided in Section 6.3.1.1, *Case A Contents Model*.

The utilization of polyethylene as the bounding hydrogenous moderating material is justified by the SAIC-1322-001[3] study which concludes that polyethylene is the most reactive moderator that could credibly moderate CH-TRU waste in a pure form. A 25% volumetric packing fraction for polyethylene is used as a conservative value which is based on physical testing that bounds the packing fraction of polyethylene in manually compacted CH-TRU waste of 13.36%[4].

Materials that can credibly provide better than 25% polyethylene/75% water equivalent reflection are termed "special reflectors" and not authorized for shipment under Case A in quantities that exceed 1% by weight except in specific configurations discussed below. Based on the results from SAIC-1322-001[3], Be, BeO, C, D_2O, MgO and depleted U (≥0.3% ^{235}U) are the only materials that can provide reflection equivalent to a 2 ft thickness of 25% polyethylene and 75% water mixture under any of the following conditions and are therefore the only materials considered as special reflectors:

- Less than 5/8 inch thick at 100% of theoretical density[5] in the form of large solids
- Less than 11/16 inch thick at 70% of theoretical density in the form of tightly-packed particulate solids
- Less than 20% packing fraction at 24 inches thick in the form of randomly dispersed particulate solids

The utilization of 1% by volume beryllium in the reflector material filling the ICV bounds the presence of up to 1% by weight quantities of special reflectors that are randomly dispersed in the payload containers based on the volume of the ICV and the maximum allowed weight of the payload containers in the package. SAIC-1322-001 found that beryllium is the bounding special reflector as it provides the best reflection of the system resulting in the highest reactivity.

If the fissile material is bound to the special reflector material, these materials will provide moderation of the fissile material but will not be available to reflect the fissile region. The reference study, SAIC-1322-001, found that adding special reflector materials, with the exception of beryllium, to the fissile region reduced the reactivity of a single 325 FGE 25% polyethylene/75% water reflected sphere. The moderating effect of heavy water was not studied,

---

[3] Neeley, G. W., D. L. Newell, S. L. Larson, and R. J. Green, *Reactivity Effects of Moderator and Reflector Materials on a Finite Plutonium System*, SAIC-1322-001, Revision 1, Science Applications International Corporation, Oak Ridge, Tennessee, May 2004.

[4] WP 08-PT.09, *Test Plan to Determine the TRU Waste Polyethylene Packing Fraction*, Washington TRU Solutions, LLC., Revision 0, June 2003.

[5] Theoretical densities used in the study are 1.85 g/cm^3 for Be, 2.69 g/cm^3 for BeO, 2.1 g/cm^3 for C, 1.1054 g/cm^3 for D_2O, 3.22 g/cm^3 for MgO, and 19.05 g/cm^3 for U.

but the quantity of liquid allowed in the TRUPACT-II is limited such that heavy water would not be present in greater than 1% by weight quantities. Thus, if the special reflector, excluding beryllium, is chemically or mechanically bound to the fissile material, Case A limits apply even in the presence of greater than 1% by weight quantities of the special reflector. Chemically bound means that the special reflector materials are chemically reacted with the fissile material such that the reflector materials and the fissile materials are chemically interacted and are stable. Mechanically bound means the fissile material is mechanically bound to the reflector such that the reflector material will not disengage from the fissile material because it is topographically imbedded, topographically interlocked, or surface contaminated. A summary discussion of special reflectors is provided in Section 6.4.3.3.

6.2.2 Applicability of Case B Limit

The Case B limit is applicable for contents containing greater than 1% by weight quantities of special reflector materials provided the contents are manually compacted (i.e., not machine compacted). These requirements drive the assumptions regarding the appropriately bounding moderator and reflector materials that are utilized in the analyses to bound the presence of all materials that are authorized for shipment under the Case B FGE limits. However, if the special reflector materials can be demonstrated to be in thicknesses and/or packing fractions that are less than the 25% polyethylene/ 75% water equivalent parameters given in Table 6.2-1, then Case A limits can be used. Note that equivalent thicknesses for Be and BeO are not given as, for thin reflectors of these materials, 100% packing fraction does not result in the highest reactivity and the equivalent thickness increases inversely with the packing fraction; thus, only a packing fraction comparison can be used for Be and BeO. The contents model assumptions are provided in Section 6.3.1.2, *Case B Contents Model*.

The utilization of polyethylene as the bounding hydrogenous moderating material at a 25% packing fraction is consistent with the justification provided in Section 6.2.1, *Applicability of Case A Limit*. However, the fissile sphere is moderated with varying volume fractions of beryllium as beryllium was also found in SAIC-1322-001 to increase reactivity when significant quantities are included in the moderator. The use of a 100% dense thick Be reflector in the model bounds the presence of other special reflector materials.

6.2.3 Applicability of Case C Limit

The Case C limit is applicable provided the contents are machine compacted and contain less than or equal to 1% by weight quantities of special reflector materials. These requirements drive the assumptions regarding the appropriately bounding moderator and reflector materials that are utilized in the analyses to bound the presence of all materials that are authorized for shipment under the Case C FGE limits. The contents model assumptions are provided in Section 6.3.1.3, *Case C Contents Model*.

The utilization of polyethylene as the bounding hydrogenous moderating material at a 100% packing fraction is consistent with the justification provided in Section 6.2.1, *Applicability of Case A Limit*. Additionally, SAIC-1322-001 concluded no material, that could credibly moderate a fissile sphere in a pure form, resulted in a higher reactivity than the 100% polyethylene moderated system. Thus, compared to Case A, the packing fraction of the moderator is the dominant factor that results in an increase in reactivity. The only inorganic

material that increased reactivity when added to the fissile mixture was beryllium. The effect of more than 1% by weight quantities of beryllium in the moderator is studied under Case B as beryllium is also the leading special reflector. The use of 99% polythylene and 1% beryllium (by volume) in the reflector region is an appropriately bounding reflector material as it is consistent with the moderator assumption and accounts for the less than or equal to 1% by weight quantities of special reflector materials allowed in the package.

Again, if the special reflector material, excluding beryllium, is chemically or mechanically bound to the fissile material or if the special reflector materials can be demonstrated to be in thicknesses and/or packing fractions that are less than the 25% polyethylene/ 75% water equivalent parameters given in Table 6.2-1, then Case C limits apply even in the presence of greater than 1% by weight quantities of the special reflector.

6.2.4 Applicability of Case D Limit

The Case D limit is specifically applicable provided the contents are machine compacted in the form of "puck" drums overpacked in 55-, 85-, or 100-gallon drums with less than or equal to 1% by weight quantities of special reflector materials and either of the following two controls: a) the packing fraction of polyethylene in the pucks is not greater than 70% or b) the separation between pucks in two axially adjacent overpack drums is maintained at greater than or equal to 0.50 inch through the use of a compacted puck drum spacer placed in the bottom of each overpack drum. These requirements drive the assumptions regarding the appropriately bounding moderator and reflector materials that are utilized in the analyses to bound the presence of all materials that are authorized for shipment under the Case D FGE limits. The contents model assumptions are provided in Section 6.3.1.4, *Case D Contents Model*.

The utilization of polyethylene as the bounding hydrogenous moderating material is consistent with the justification provided in Section 6.2.1, *Applicability of Case A Limit*. The use of a 70% packing fraction is applicable provided that controls are implemented to ensure the packing fraction is limited during machine compaction. The use of 70% polyethylene, 29% water and 1% beryllium (by volume) in the reflector region is an appropriately bounding reflector material as it is consistent with the moderator assumption, again provided that controls are implemented to ensure the packing fraction is limited during machine compaction, and accounts for the less than or equal to 1% by weight quantities of special reflector materials allowed in the package. Otherwise, the use of 99% polyethylene and 1% beryllium (by volume) in the reflector region is an appropriately bounding reflector material as it is consistent with the moderator assumption and accounts for the less than or equal to 1% by weight quantities of special reflector materials allowed in the package.

The compacted puck drum spacers have been demonstrated to maintain the minimum required axial spacing between pucks in axially adjacent overpack drums under Hypothetical Accident Conditions (HAC) and are described in Appendix 1.3.1, *Packaging General Arrangement Drawings*[6].

[6] Packaging Technology, Inc., *Test Report for Compacted Drums*, TR-017, Revision 0, Packaging Technology, Inc., Tacoma, Washington, March 2004.

Again, if the special reflector material, excluding beryllium, is chemically or mechanically bound to the fissile material or if the special reflector materials can be demonstrated to be in thicknesses and/or packing fractions that are less than the 25% polyethylene/ 75% water equivalent parameters given in Table 6.2-1, then Case D limits apply even in the presence of greater than 1% by weight quantities of the special reflector.

6.2.5 Applicability of Case E Limit

The Case E limit is specifically applicable provided the contents are manually compacted and shipped in the standard, S100, S200, or S300 pipe overpacks with less than or equal to 1% by weight quantities of special reflector materials. Following the logic presented in Section 6.2.1, *Applicability of Case A Limit*, the presence of greater than 1% by weight quantities of special reflectors may be authorized for shipment under the Case E FGE limits if the fissile material is chemically and/or mechanically bound to the special reflector material. Due to the fact that beryllium was also specifically evaluated as a moderator in the pipe overpacks, this applies to all special reflector materials except heavy water, which is restricted based on the free liquid requirements for the package. The contents model assumptions and analysis results are provided in Appendices 4.1, 4.2, 4.3, and 4.4 in the *CH-TRU Payload Appendices*.

6.2.6 Applicability of Case F Limit

The Case F limit is specifically applicable provided the contents are manually compacted and shipped in the standard, S100, S200, or S300 pipe overpacks with greater than 1% by weight quantities of special reflector materials. However, if the special reflector materials can be demonstrated to be in thicknesses and/or packing fractions that are less than the 25% polyethylene/ 75% water equivalent parameters given in Table 6.2-1, then Case E limits can be used. The contents model assumptions and analysis results are provided in Appendices 4.1, 4.2, 4.3, and 4.4 in the *CH-TRU Payload Appendices*.

Table 6.2-1 – Special Reflector Material Parameters that Achieve the Reactivity of a 25%/75% Polyethylene/Water Mixture Reflector

Special Reflector Material	Equivalent Thickness at 100% of Theoretical Density (inch)	Equivalent Thickness at 70% of Theoretical Density (inch)	Equivalent Packing Fraction at 24 in. Thickness (%)
Be	N/A	N/A	7
BeO	N/A	N/A	7
C	0.18	0.25	9
D_2O	0.24	0.27	14
MgO	0.26	0.33	15
U(Natural)	0.08	0.10	1
U(0.6% ^{235}U)	0.14	0.18	1
U(0.5% ^{235}U)	0.18	0.28	2
U(0.4% ^{235}U)	0.33	0.51	3
U(0.3% ^{235}U)	0.56	0.73	5

6.3 Model Specification

Criticality calculations for the TRUPACT-II package are performed using the three-dimensional Monte Carlo computer code KENO-V.a[1], executed as part of the SCALE-PC v4.4a system[2] using the CSAS25 driver utility[3]. Descriptions of the calculational models are given in Section 6.3.1, *Contents Model*, Section 6.3.2, *Packaging Model*, Section 6.3.3, *Single-Unit Models*, and Section 6.3.4, *Array Models* for all cases except Cases E and F, which are discussed in Appendices 4.1, 4.2, 4.3, and 4.4 in the *CH-TRU Payload Appendices*[4]. A summary of materials and atom densities that are used in the evaluation of the TRUPACT-II package is given in Section 6.3.5, *Package Regional Densities*.

The limiting mass of fissile material that may be transported in a single TRUPACT-II package is shown to provide adequate subcritical margin based on detailed KENO-V.a analyses. These calculations are performed for an optimally moderated single-unit model and an infinite array model of TRUPACT-II packages under both normal conditions of transport (NCT) and hypothetical accident conditions (HAC).

In all cases, the computational model consists of a contents model and a packaging model. The contents model conservatively represents the package contents, including all payload material, dunnage, fissile and moderating material. The packaging model represents the remaining structural materials comprising the TRUPACT-II packaging. The amount of moderating and reflecting material assumed to be present in the packaging model is varied to maximize reactivity.

6.3.1 Contents Model

6.3.1.1 Case A Contents Model

The Case A contents are represented as an optimally moderated homogeneous sphere of Pu-239 and a 25% polyethylene and 75% water mixture (by volume). The radius of the model sphere is determined based on the modeled mass of plutonium and a specified H/Pu ratio. In each case, the H/Pu ratio is varied until the most reactive configuration is identified. FGE limits with 0 g, 5 g, 15 g, and 25 g Pu-240 present are calculated. When Pu-240 is present, the H/Pu ratio specified represents the H/Pu-239 atom ratio.

The remainder of the inner containment vessel (ICV) around the fissile sphere is filled with a 25% polyethylene, 74% water and 1% beryllium mixture (by volume). (Henceforward, unless otherwise specified, any reference to a polyethylene/water/beryllium mixture implies this particular

---

[1] L. M. Petrie and N. F. Landers, *KENO-V.a: An Improved Monte Carlo Criticality Program with Supergrouping*, ORNL/NUREG/CSD-2/V2/R6, Volume 2, Section F11, March 2000.

[2] Oak Ridge National Laboratory (ORNL), *SCALE 4.4a: Modular Code System for Performing Standardized Computer Analyses for Licensing Evaluation for Workstations and Personal Computers*, ORNL/NUREG/CSD-2/R6, March 2000.

[3] N. F. Landers and L. M. Petrie, *CSAS: Control Module for Enhanced Criticality Safety Analysis Sequences*, ORNL/NUREG/CSD-2/V1/R6, Volume 1, Section C4, March 2000.

[4] U.S. Department of Energy (DOE), *CH-TRU Payload Appendices*, current revision, U.S. Department of Energy, Carlsbad Field Office, Carlsbad, New Mexico.

25% polyethylene, 74% water and 1% beryllium reflector composition.) The beryllium is added to represent less than or equal to 1% by weight quantities of special reflectors that are allowed under the Case A loading limits. Based on the volume of the ICV and the maximum allowed weight of the payload containers in the package, modeling 1% beryllium by volume bounds the limit of 1% by weight. The reactivity effect of the addition of the 1% beryllium is shown to be very slight but positive. The KENO-V.a representation of the Case A single-unit contents model is illustrated in Figure 6.3-1.

The fissile sphere is nominally positioned in the center of the packaging model. In the array analyses, the effect of displacing the contents model within the packaging model in directions likely to increase reactivity is investigated. These array models are further described in Section 6.3.4, *Array Models*.

6.3.1.2 Case B Contents Model

The fissile sphere composition in the Case B model is identical to the Case A fissile sphere composition. Unlimited quantities of beryllium in the fissile sphere are also studied but shown to reduce reactivity with the beryllium reflector. The difference in the Case A and B model lies in the reflector material filling the ICV. In the Case B model, the ICV is filled with beryllium and the volume fraction is varied from 10% to 100% to determine the point of maximum reactivity. The KENO-V.a representation of the Case B single-unit contents model is illustrated in Figure 6.3-2.

6.3.1.3 Case C Contents Model

The fissile sphere composition in the Case C model is moderated with 100% polyethylene and the reflector material filling the ICV is 99% polyethylene and 1% beryllium (by volume). The 1% beryllium in the ICV accounts for the reactivity increase provided by less than or equal to 1% by weight quantities of special reflector materials allowed in the package. The KENO-V.a representation of the Case C single-unit contents model is illustrated in Figure 6.3-3.

6.3.1.4 Case D Contents Model

The Case D model is an extension of Case C applied to compacted “puck” drums overpacked in 55-, 85-, or 100-gallon drums where either the packing fraction of the contents is limited to 70% through the use of process controls implemented during machine compaction or the separation between pucks in two axially adjacent overpack drums is maintained at greater than or equal to 0.50 inch through the use of a compacted puck drum spacer placed in the bottom of each overpack drum. The HalfPACT package can accommodate only a single tier of overpack drums whereas two tiers of overpack drums can be loaded into a TRUPACT-II package. Reconfiguration of the fissile material from within each compacted puck is bounded by the Case A analysis since the reconfiguration would reduce the polyethylene packing fraction to below 25% as the material with the ICV is homogenized. Because of the axial separation between the overpack drums in a single tier and the 200 FGE limit per overpack drum, the most reactive scenario occurs in the TRUPACT-II package instead of in the HalfPACT package.

The most reactive, credible scenario consists of 325 FGE in two overpack drums that are stacked on top of one another. The fissile material will be separated by the steel of the compacted puck and overpack drum (or steel of the compacted puck drum spacer) and the polyethylene slip-sheet

and reinforcing plate placed between the layers of overpack drums in the package. Thus, the contents model includes two cylinders of fissile material with 0.06 inch (0.1524 cm) thick steel representing a conservative lower bound of the thickness of the steel in the lid of the lower puck and overpack drum (or steel in the compacted puck drum spacer), 0.15 inch (0.3810 cm) thick polyethylene representing 50% of the thickness of the slip-sheet and reinforcing plate, and another 0.06 inch (0.1524 cm) thick layer of steel representing a conservative lower bound of the thickness of steel in the bottom of the upper puck and overpack drum (or steel in the compacted puck drum spacer). Where applicable due to the use of a compacted puck drum spacer, the contents model includes an additional 0.50 inch of separation between the pucks, modeled filled with polyethylene or water to determine which is most reactive.

A 325 FGE fissile cylinder is modeled with an optimum height to diameter ratio of 0.924 to maximize reactivity and then split in two to represent the material in each overpack drum. The bottom half of the cylinder contains 200 FGE to represent the FGE limit in an overpack payload container and the top half of the cylinder contains 125 FGE. Modeling of the polyethylene in the slip-sheet and reinforcing plate is more reactive than modeling a water gap. The moderator is modeled either as 70% polyethylene and 30% water by volume or as 100% polyethylene. The material filling the ICV is either 70% polyethylene, 29% water and 1% beryllium or 99% polyethylene and 1% beryllium. The 1% beryllium is included to account for less than or equal to 1% by weight quantities of special reflector materials. Filling the ICV with this material is conservative as the void space around the overpack drums is filled with the better reflecting polyethylene/water/beryllium or polyethylene/beryllium mixture. The results of calculations performed for Case A as discussed in Section 6.4.3.1.1, *Case A Single Unit Results*, showed that including 1% beryllium in the ICV region but not in the moderator was the most reactive placement and thus this configuration was modeled in the Case D calculations.

Even though only the TRUPACT-II package would allow the stacked drum configuration modeled, the packaging model representing the HalfPACT configuration is used to increase interaction between packages as discussed in the following section. The KENO-V.a representation of the Case D single-unit contents model is illustrated in Figure 6.3-4.

6.3.2 Packaging Model

The criticality analyses presented herein are identical to the analyses presented in Chapter 6.0, *Criticality Evaluation*, of the *HalfPACT Shipping Package Safety Analysis Report*[5]. With the exception of removing 30 inches from the package's height, all other post-test aspects (i.e., the package's configuration following free drop, puncture, and fire testing) between the HalfPACT and TRUPACT-II packages are essentially identical, especially with regard to the amount of remaining polyurethane foam. Also, the ICV region of the HalfPACT is large enough to provide full reflection of the fissile contents by the material contained therein. Therefore, due to the closer axial packaging in the infinite arrays, the criticality analyses utilizing the HalfPACT package geometry are considered conservative.

The packaging model represents the package structural materials, including the stainless steel shells and polyurethane foam. The model consists of nested, right circular cylindrical shells of

[5] U.S. Department of Energy (DOE), *HalfPACT Shipping Package Safety Analysis Report*, USNRC Certificate of Compliance 71-9279, U.S. Department of Energy, Carlsbad Area Office, Carlsbad, New Mexico.

Type 304 stainless steel (SS304). The right cylindrical geometry of the model conservatively neglects the torispherical shape of the inner and outer containment vessel ends. The model's inner shell represents the combined ICV and outer containment vessel (OCV) components of the actual package. The narrow gap between the ICV and OCV shells is neglected, and the two components are modeled as a single shell of thickness ¼ + 3⁄16 = 7⁄16 inches thick (1.1113 cm) on the side, and ¼ + ¼ = ½ inches thick (1.2700 cm) on the top and bottom. The outside radius of the cylindrical shell representing the combined ICV and OCV components is 38 21⁄32 inches (98.1869 cm), preserving the outer radius of OCV lid shell. The height of the cylinder, 44 15⁄16 inches (114.1413 cm), preserves the distance between the upper and lower aluminum honeycomb spacer assemblies within the ICV.

The second, outermost, cylindrical shell is ¼ inches (0.6350 cm) thick, also of Type 304 stainless steel, and represents the outer containment assembly (OCA) outer shell. The ⅜ inch thick portion of the OCA outer shell is conservatively ignored. Under NCT, the inside radius and inside height of the OCA outer shell are 46 15⁄16 inches (119.2213 cm) and 70 inches (177.8000 cm), respectively and the outer radius and height are 47 3⁄16 inches (119.8563 cm) and 70½ inches (179.0700 cm), respectively. Under HAC, the inner radius and height of the OCA outer shell are based on the observed maximum deformation of the OCA following certification testing. At the conclusion of testing, approximately 5 inches of foam remained in the certification test units, except for local areas damaged by puncture bar drops. Hence, the inside of the OCA outer shell is set a distance of 5 inches (12.7000 cm) from the outside of the combined ICV and OCV shell and the ¼ inches (0.6350 cm) thick OCA shell is modeled. Under both NCT and HAC, no credit is taken for parasitic neutron absorption properties of the polyurethane foam. Instead, the foam is replaced with the 25% polyethylene/ 74% water/1% beryllium mixture used in Case A as a bounding reflecting material at a volume fraction that maximizes reactivity. Consideration is made for the structural properties of the foam by assuming that the inner cylindrical shell is maintained in its central position subsequent to all HAC tests. The KENO-V.a representation of single-unit undamaged and damaged TRUPACT-II packages are illustrated in Figure 6.3-5 and Figure 6.3-6, respectively.

The following simplifying assumptions tend to decrease the amount of structural material represented in the calculational model and decrease the center-to-center separation between TRUPACT-II packages in the array analyses and are, therefore, conservative.

- The domed surfaces of the torispherical heads are represented as flat surfaces and are positioned such that the overall height of the TRUPACT-II packaging is reduced.
- Under HAC, the thickness of the polyurethane foam region is reduced to 5 inches (12.7000 cm) throughout the entire OCA. In all cases, polyurethane foam is ignored and replaced with a polyethylene/water/beryllium mixture that fills the space at a volume fraction that optimizes reactivity.

6.3.3 Single-Unit Models

Compliance with the requirements of 10 CFR §71.55[6] is demonstrated by analyzing optimally moderated damaged and undamaged, single-unit TRUPACT-II packages. In the NCT single-unit model, the packaging and contents models described above are employed, and water is conservatively assumed to leak into the containment vessel to an extent that optimizes reactivity. In Case A, the ICV is filled with the same polyethylene/water/beryllium mixture employed in the contents model. In Case B, the ICV is filled with beryllium to represent the bounding special reflector material and in Case C, the ICV is filled with 99% polyethylene and 1% beryllium to represent machine compacted waste with no limitations on compaction. In Case D, the ICV is filled with either a mixture of 70% polyethylene, 29% water and 1% beryllium to represent machine compacted waste that is controlled to a 70% packing fraction or 99% polyethylene and 1% beryllium to represent machine compacted waste without packing fraction controls. In all cases, the area between the ICV/OCV shells and the OCA outer shell, simply termed the OCA, is filled with the 25% polyethylene/ 74% water/1% beryllium mixture employed in the ICV of Case A. This material is a bounding reflector for the low density foam normally present and the water that could leak into this area. These reflectors are assumed to occupy all void space within the packaging model at full theoretical density to maximize reflection of the fissile material and thus maximize reactivity. In addition, a 30 cm thick, close-fitting water reflector is placed around the outside of the packaging model to ensure full reflection is achieved.

The single-unit, HAC model is identical to the single-unit, NCT model, except the HAC packaging model assumes the model's outer shell is displaced to within 5 inches (12.7000 cm) of the model's inner shell.

6.3.4 Array Models

Calculations are performed for an infinite array of damaged TRUPACT-II packages in a close-packed, square-pitch configuration. Triangular-pitched array configurations are not considered because the square-pitch array analyses demonstrate that array interaction effects are of minor consequence. A specularly reflective boundary condition is applied to all six faces of the unit cell defining the array configuration in order to represent an infinite array of TRUPACT-II packages. Displacement of the contents models within the ICV/OCV shell is considered in a manner that maximizes interaction of the fissile material between packages. Table 6.3-1 describes the configurations considered, with reference to KENO-generated plots that graphically illustrate each variation.

In the HAC array analysis, reflection of the fissile sphere by a 25% polyethylene/74% water/1% beryllium mixture filling the ICV is considered in Case A. Case B considers beryllium filling the ICV as the bounding special reflector material and Case C considers full density polyethylene in the ICV to represent machine compacted waste. Case D is specific to machine compacted waste compacted in puck drums and then placed in 55-, 85-, or 100-gallon overpack drums with either a 70% packing fraction or puck separation controls modeled with either 70% polyethylene/29% water/1% beryllium or 99% polyethylene/1% beryllium reflection filling the ICV, respectively. In all cases, water is considered between the packages in addition to a 25%

[6] Title 10, Code of Federal Regulations, Part 71 (10 CFR 71), *Packaging and Transportation of Radioactive Material*, 01-01-07 Edition.

polyethylene/74% water/1% beryllium mixture in the OCA region. The volume fraction of all of these materials is varied to ensure the most reactive conditions are analyzed.

As a result of the explicit optimization of reactivity against interspersed moderator volume fraction, and because of the closer spacing between packages achieved in the accident geometry, the result of the HAC array calculations bound the NCT array cases.

6.3.5 Package Regional Densities

A summary of all material compositions used in the TRUPACT-II package contents models is given in Table 6.3-2 for various H/Pu ratios. The parameters are computed based on SCALE Standard Composition Library[7] values of a plutonium density of 19.84 g/cm^3, a polyethylene density of 0.923 g/cm^3 and a water density of 0.9982 g/cm^3. The material used to represent the TRUPACT-II package is Type 304 stainless steel (SS304) with a density of 7.94 g/cm^3 and carbon steel, with a density of 7.82 g/cm^3, was used to represent the drum lid/bottom modeled in Case D. Number densities of the SS304 and carbon steel constituent nuclides are also based on the SCALE Standard Composition Library composition as presented in Table 6.3-3. The number densities for the various polyethylene, water and beryllium reflector mixtures are given in Table 6.3-4. The SCALE standard composition identifier "BEBOUND", nuclide identifier 4309, was used to model the beryllium reflector. The theoretical density of this material is 1.85 g/cm^3 and the number density is 1.23621E-01 a/b-cm. The cross-section for BEBOUND is based on a beryllium metal whereas the cross-section for standard material BE is based on a free gas representation. BEBOUND is also used to model beryllium in the benchmark cases discussed in Section 6.5, *Critical Benchmark Experiments*.

Table 6.3-1 – Description of Contents Displacement in Array Models

Variation	Replicated Array Size	Description	Reference
0	1×1×1	Contents centered in packaging model	Figure 6.3-7
1	2×2×2	All contents models displaced toward center	Figure 6.3-8

[7] L.M. Petrie, P.B. Fox and K. Lucius, *Standard Composition Librar*y, ORNL/NUREG/CSD-2/V3/R6, Volume 3, Section M8, March 2000.

Table 6.3-2 – Fissile Contents Model Properties for Various H/Pu Ratios

		Number Density			
		Pu (a/b-cm)	H (a/b-cm)	O (a/b-cm)	C (a/b-cm)
25% Polyethylene/75% Water Moderator used in Cases A and B					
500	55.32	1.39374E-04	6.96904E-02	2.49700E-02	9.88730E-03
600	46.12	1.16199E-04	6.97198E-02	2.49802E-02	9.89131E-03
700	39.55	9.96359E-05	6.97470E-02	2.49901E-02	9.89517E-03
800	34.61	8.71898E-05	6.97634E-02	2.49958E-02	9.89720E-03
900	30.77	7.75285E-05	6.97805E-02	2.50019E-02	9.89996E-03
1,000	27.70	6.97733E-05	6.97894E-02	2.50040E-02	9.90030E-03
1,100	25.19	6.34398E-05	6.97967E-02	2.50067E-02	9.90185E-03
1,200	23.09	5.81675E-05	6.98011E-02	2.50093E-02	9.90271E-03
1,300	21.31	5.36925E-05	6.98150E-02	2.50137E-02	9.90445E-03
1,400	19.79	4.98652E-05	6.98177E-02	2.50142E-02	9.90461E-03
1,500	18.48	4.65401E-05	6.98231E-02	2.50171E-02	9.90571E-03
100% Polyethylene Moderator used in Cases C and D					
500	62.76	1.58107E-04	7.90648E-02	---	3.95315E-02
600	52.33	1.31834E-04	7.91113E-02	---	3.95542E-02
700	44.87	1.13038E-04	7.91400E-02	---	3.95699E-02
800	39.27	9.89296E-05	7.91566E-02	---	3.95785E-02
900	34.92	8.79796E-05	7.91787E-02	---	3.95891E-02
1,000	31.43	7.91773E-05	7.91959E-02	---	3.95974E-02
1,100	28.58	7.20029E-05	7.92017E-02	---	3.95998E-02
1,200	26.20	6.60091E-05	7.92166E-02	---	3.96070E-02
1,300	24.19	6.09431E-05	7.92274E-02	---	3.96122E-02
70% Polyethylene/30% Water Moderator used in Case D					
500	59.79	1.50619E-04	7.53181E-02	9.98572E-03	2.76775E-02
600	49.85	1.25577E-04	7.53520E-02	9.99020E-03	2.76903E-02
700	42.75	1.07685E-04	7.53858E-02	9.99448E-03	2.77024E-02
800	37.41	9.42500E-05	7.54065E-02	9.99712E-03	2.77094E-02
900	33.26	8.37973E-05	7.54144E-02	9.99869E-03	2.77136E-02
1,000	29.94	7.54335E-05	7.54312E-02	1.00011E-02	2.77201E-02
1,100	27.22	6.85754E-05	7.54447E-02	1.00022E-02	2.77236E-02
1,200	24.96	6.28771E-05	7.54476E-02	1.00029E-02	2.77255E-02

Table 6.3-3 – Composition of Modeled Steels

Component	SCALE Nuclide ID	Number Density (a/b-cm)
Type 304 Stainless Steel for TRUPACT-II Package		
Cr	24304	1.74726E-02
Mn	25055	1.74071E-03
Fe	26304	5.85446E-02
Ni	28304	7.74020E-03
P	15031	6.94680E-05
Si	14000	1.70252E-03
C	6012	3.18772E-04
Carbon Steel used in Case D		
Fe	26000	8.34982E-02
C	6012	3.92503E-03

Table 6.3-4 – Composition of the Polyethylene/Water/Beryllium Reflector

Component	SCALE Nuclide ID	Number Density (a/b-cm)
25% Polyethylene/ 74% Water/ 1% Beryllium Reflector used in Case A		
C	6012	9.91472E-03
H	1001	6.92387E-02
O	8016	2.47046E-02
Be	4309	1.23621E-03
99% Polyethylene/ 1% Beryllium used in Cases C and D		
C	6012	3.92623E-02
H	1001	7.85246E-02
Be	4309	1.23621E-03
70% Polyethylene/ 29% Water/ 1% Beryllium used in Case D		
C	6012	2.77612E-02
H	1001	7.48855E-02
O	8016	9.68153E-03
Be	4309	1.23621E-03

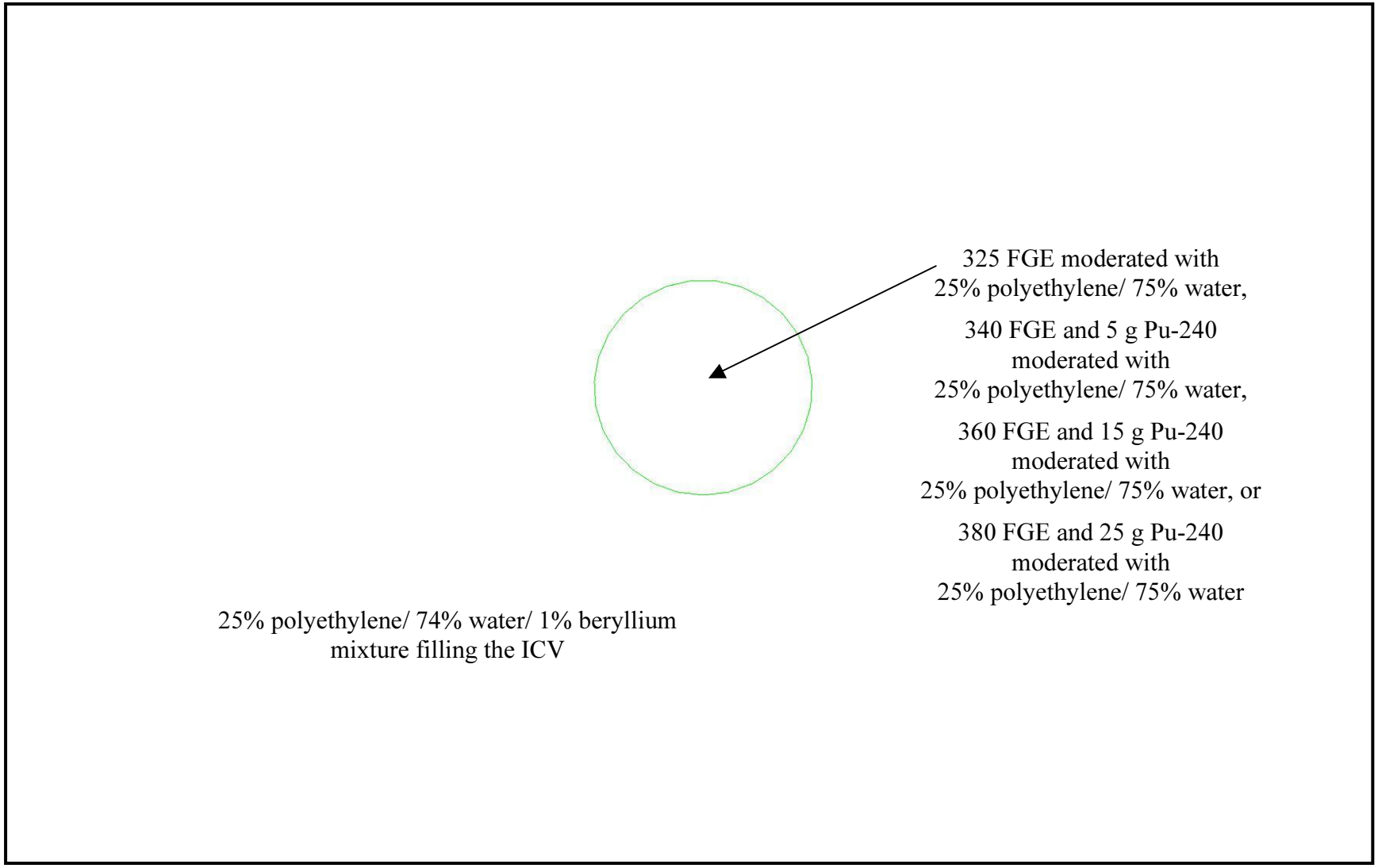

Figure 6.3-1 – Case A Contents Model

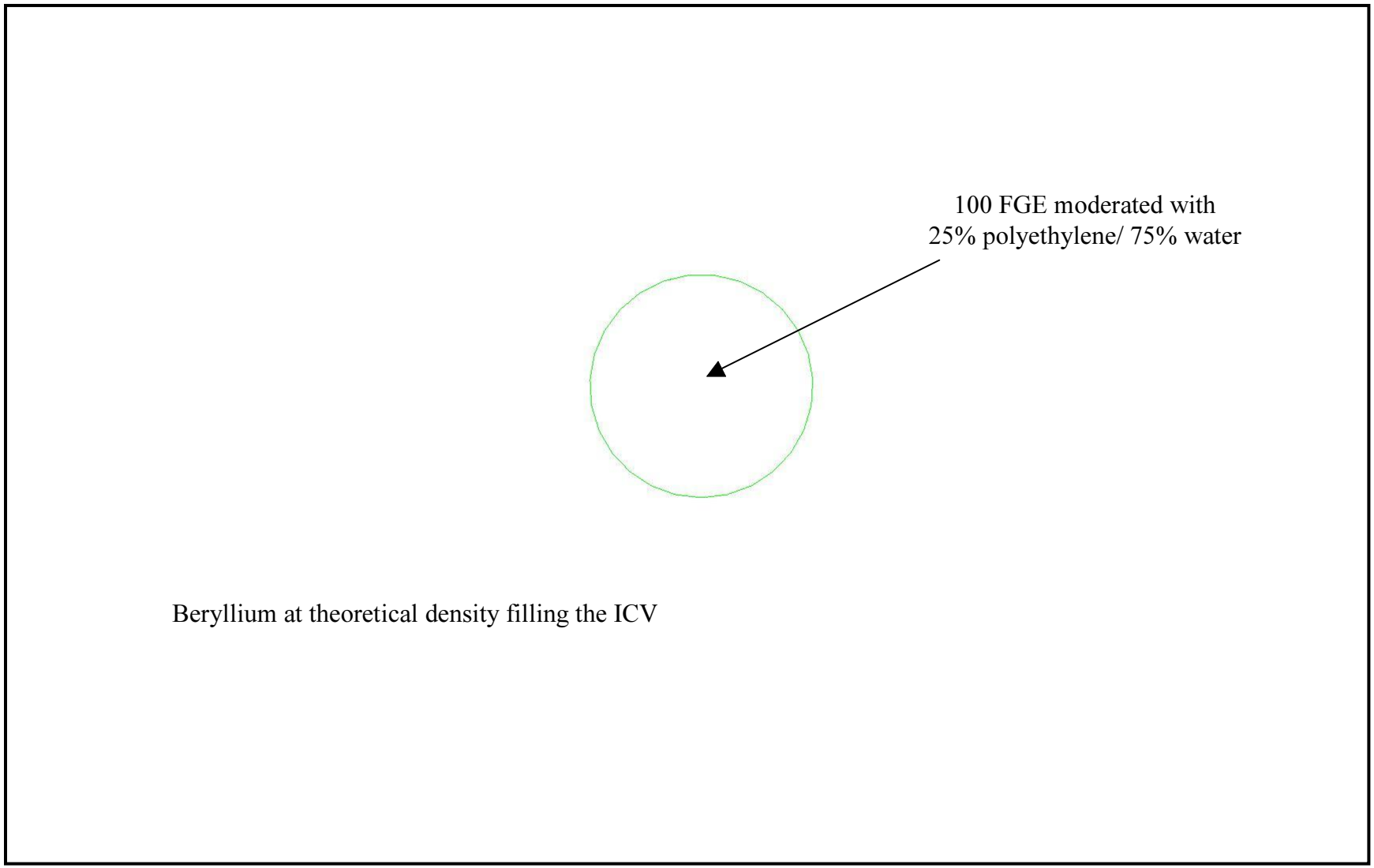

Figure 6.3-2 – Case B Contents Model

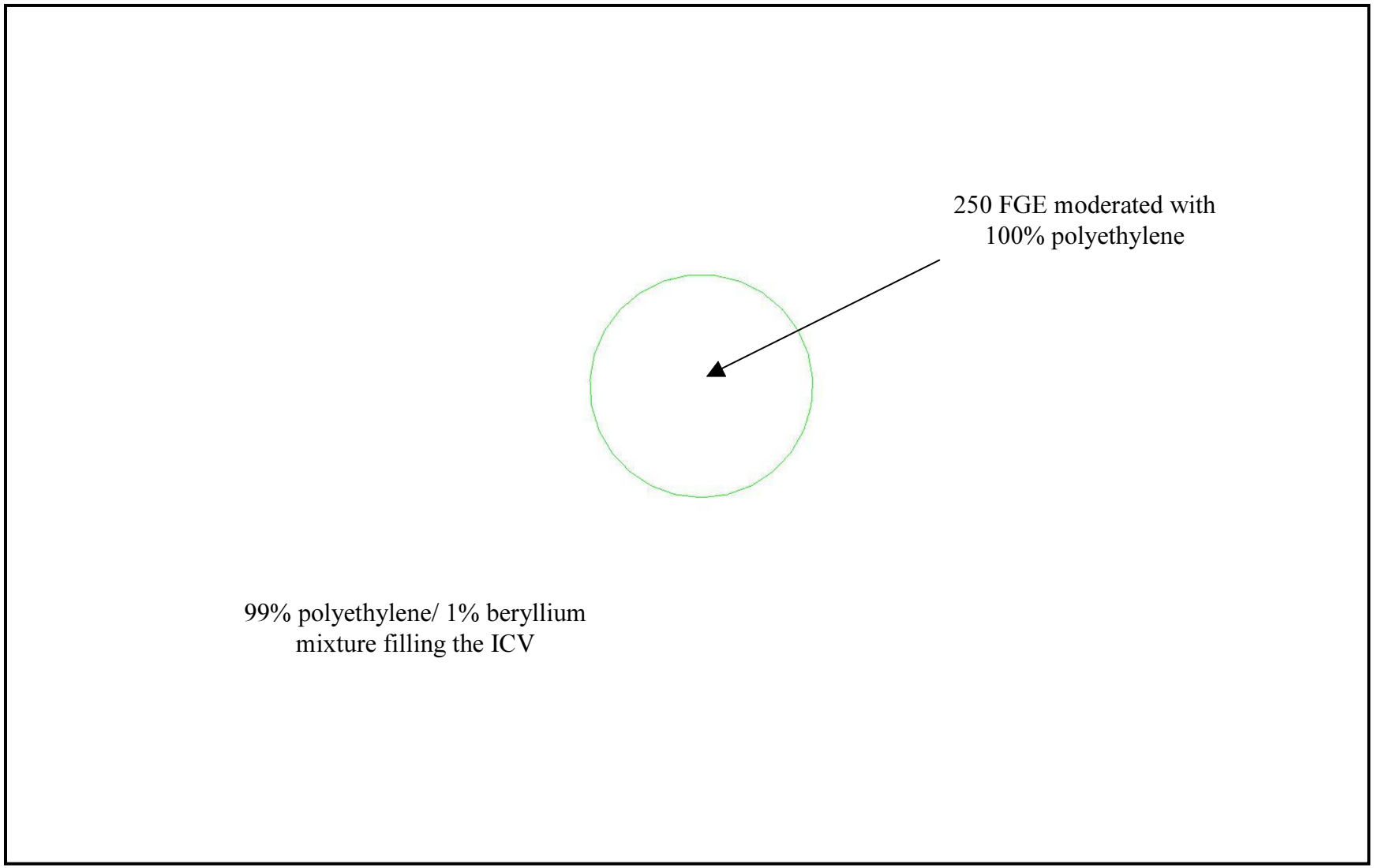

Figure 6.3-3 – Case C Contents Model

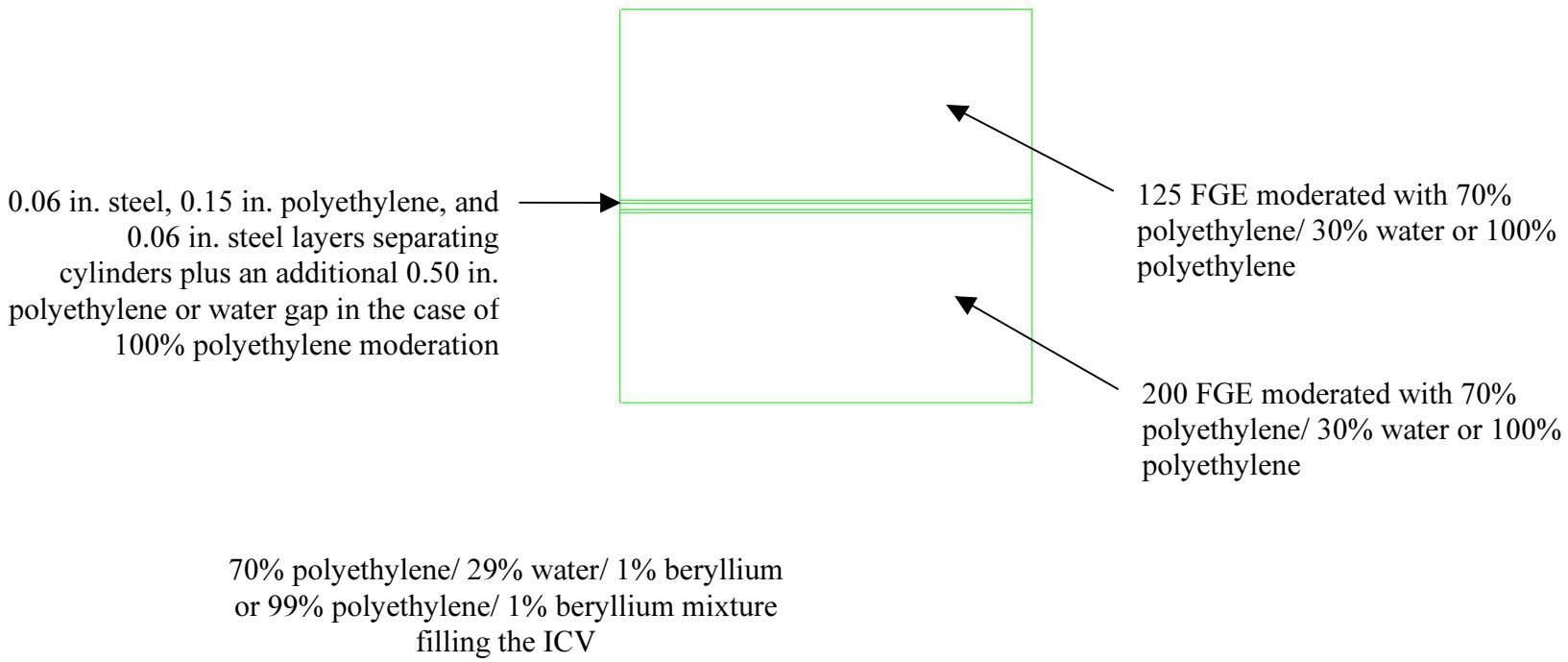

Figure 6.3-4 – Case D Contents Model

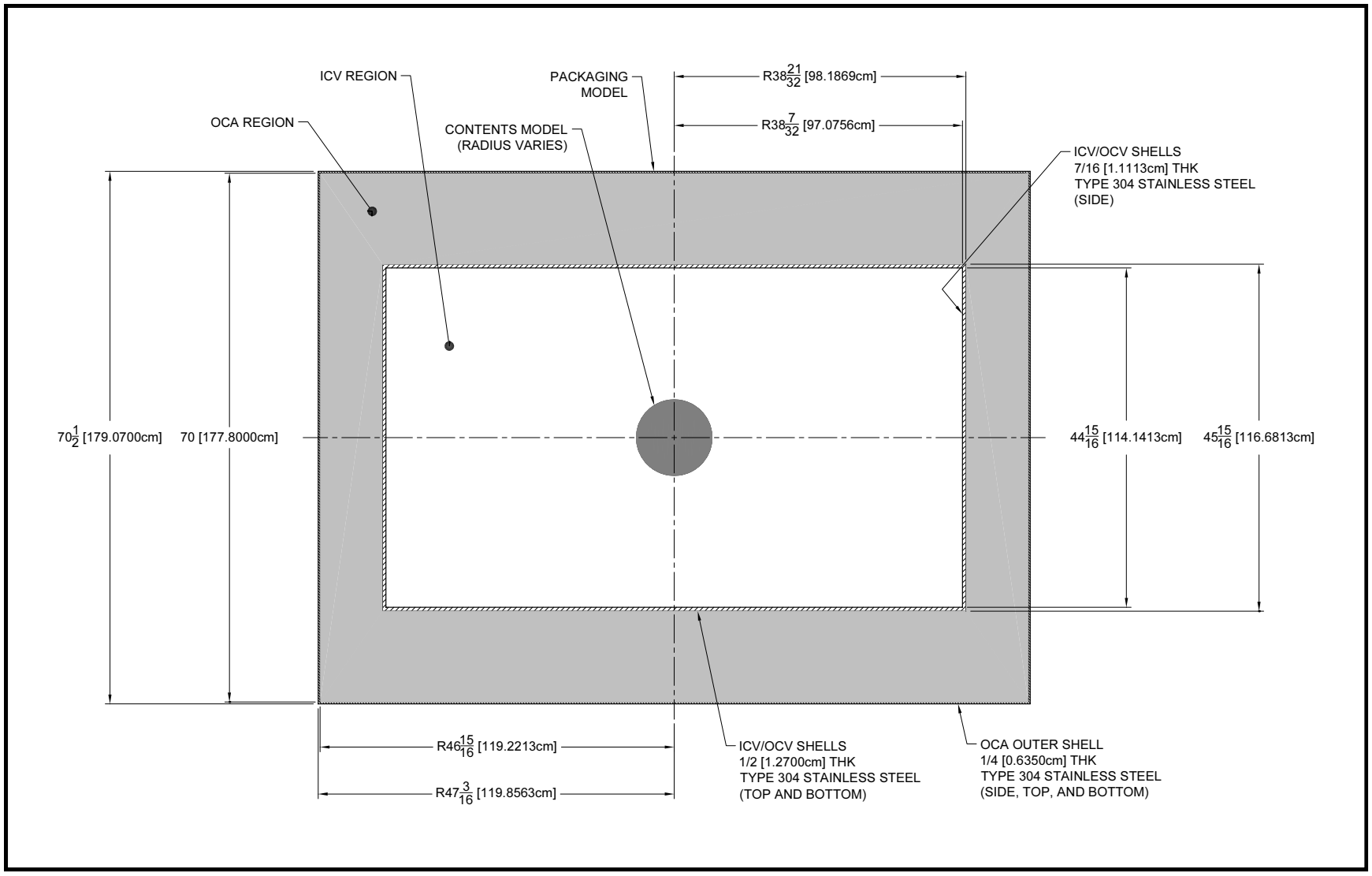

Figure 6.3-5 – NCT, Single-Unit Model; R-Z Slice

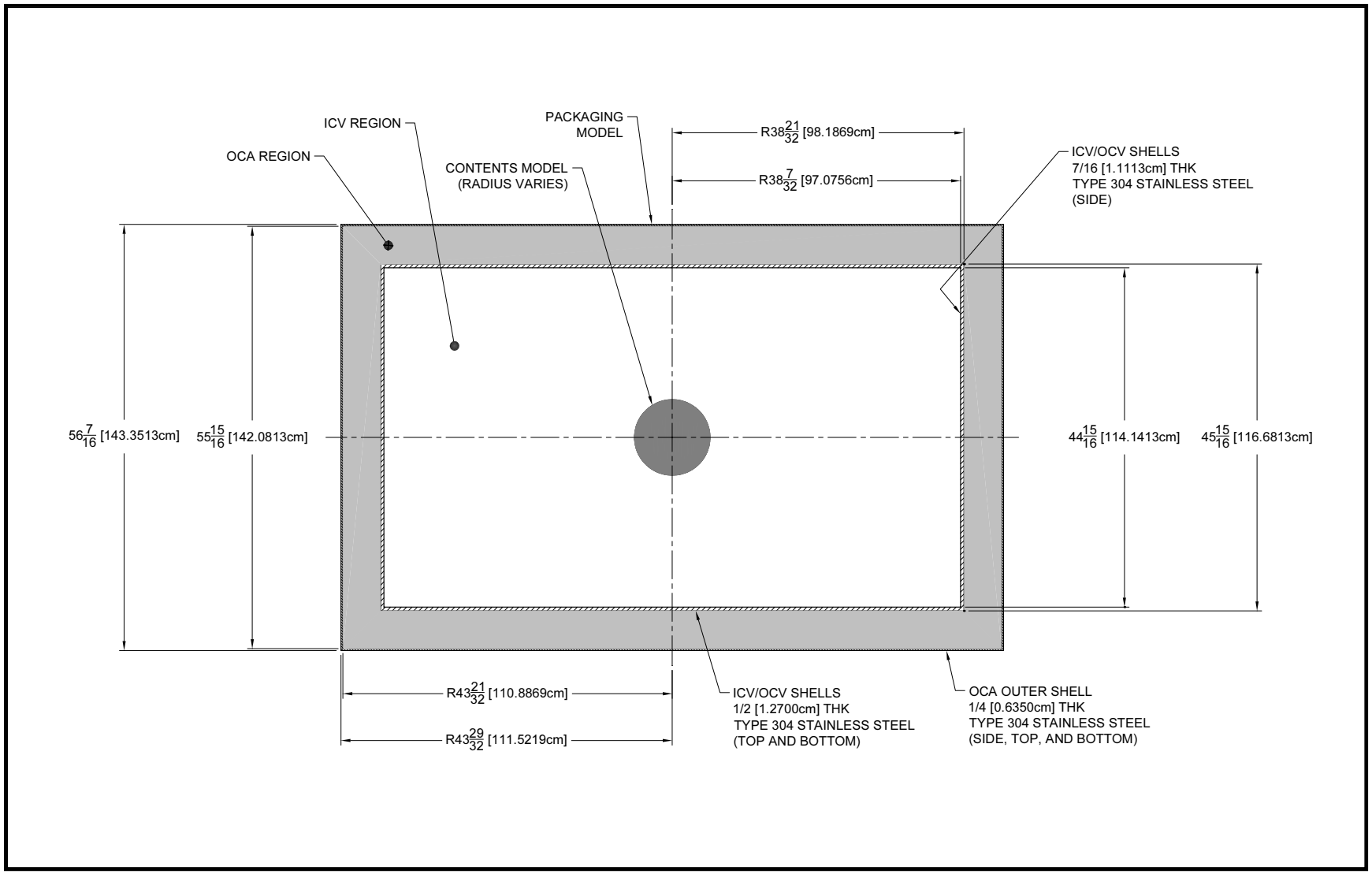

Figure 6.3-6 – HAC, Single-Unit Model; R-Z Slice

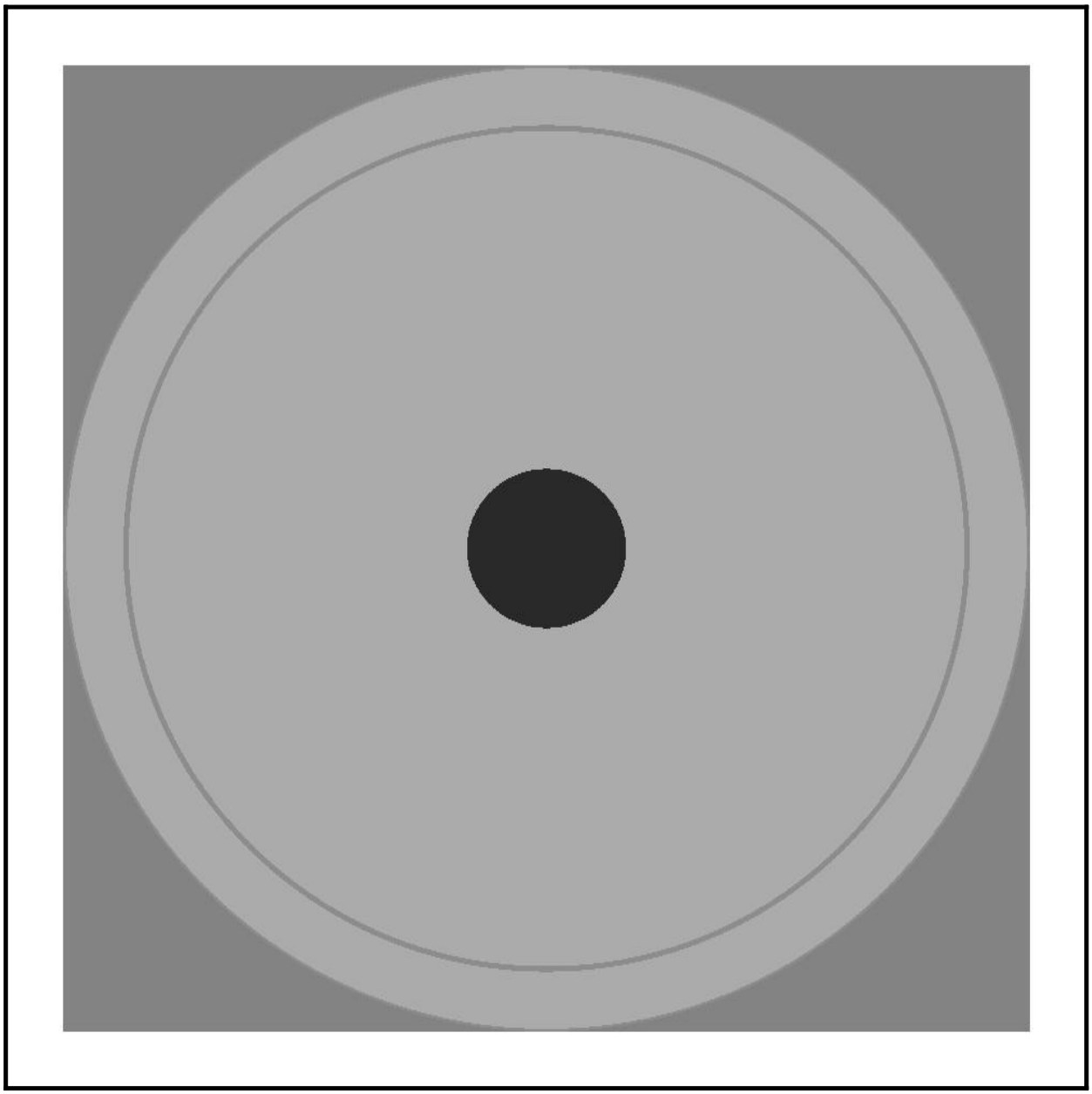

Figure 6.3-7 – Array Model Variation 0 (Reflective Boundary Conditions Imposed)

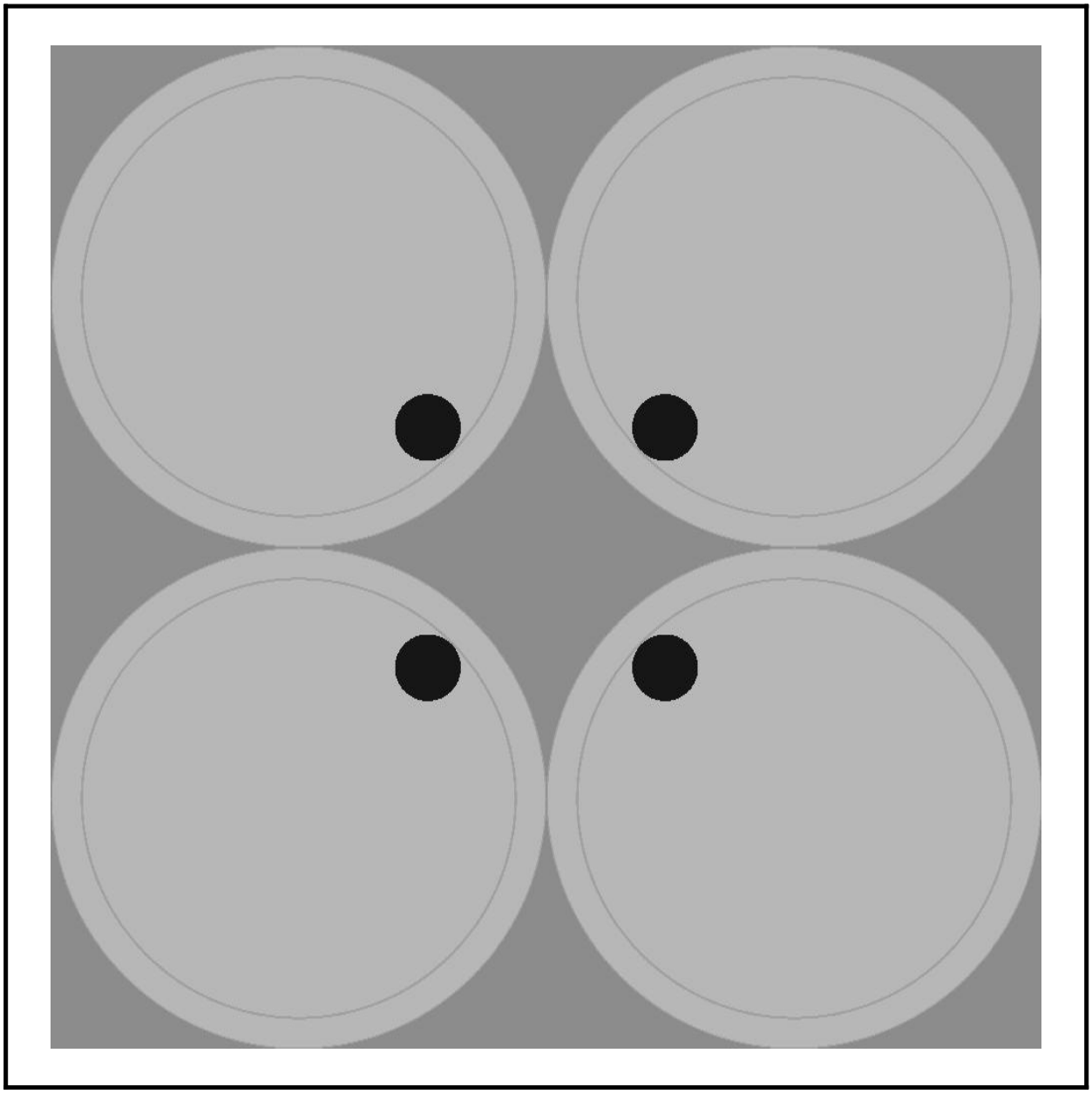

Figure 6.3-8 – Array Model Variation 1; X-Y Slice Through Top Axial Layer

6.4 Criticality Calculations

A description of the criticality calculations performed for the TRUPACT-II package is presented in this section. The calculational methodology is discussed in Section 6.4.1, *Calculational or Experimental Method*. The optimization of the payload model is discussed in Section 6.4.2, *Fuel Loading or Other Contents Loading Optimization*. The results of all calculations are presented in Section 6.4.3, *Criticality Results*.

The intent of the analysis is to demonstrate that the TRUPACT-II package is safely subcritical under normal conditions of transport (NCT) and hypothetical accident conditions (HAC).

6.4.1 Calculational or Experimental Method

Calculations for the TRUPACT-II package are performed with the three-dimensional Monte Carlo transport theory code, KENO-V.a[1]. The SCALE-PC v4.4a[2], CSAS25 utility[3] is used as a driver for the KENO code. In this role, CSAS25 determines nuclide number densities, performs resonance processing, and automatically prepares the necessary input for the KENO code based on a simplified input description. The 238 energy-group (238GROUPNDF5), cross-section library based on ENDF/B-V cross-section data[4] is used as the nuclear data library for the KENO-V.a code.

The KENO code has been used extensively in the criticality safety industry. KENO-V.a is an extension of earlier versions of the KENO code and includes many versatile geometry capabilities and screen plots to facilitate geometry verification. The KENO-V.a code and the associated 238GROUPNDF5 cross-section data set are validated for proper operation on the PC platform by performing criticality analyses of a number of relevant benchmark criticality experiments. A description of these benchmark calculations, along with justification for the computed bias in the code and library for the relevant region of applicability, is provided in Section 6.5, *Critical Benchmark Experiments*.

6.4.2 Fuel Loading or Other Contents Loading Optimization

The allowable fuel loading for a single TRUPACT-II package is based on the FGE package fissile loading limit established in the CH-TRAMPAC[5]. The analysis demonstrates that the TRUPACT-II package is safely subcritical under NCT and HAC. Calculations are based on the following conservative assumptions:

---

[1] L. M. Petrie and N. F. Landers, *KENO-V.a: An Improved Monte Carlo Criticality Program with Supergrouping*, ORNL/NUREG/CSD-2/V2/R6, Volume 2, Section F11, March 2000.

[2] Oak Ridge National Laboratory (ORNL), *SCALE 4.4a: Modular Code System for Performing Standardized Computer Analyses for Licensing Evaluation for Workstations and Personal Computers*, ORNL/NUREG/CSD-2/R6, March 2000.

[3] N. F. Landers and L. M. Petrie, *CSAS: Control Module For Enhanced Criticality Safety Analysis Sequences*, ORNL/NUREG/CSD-2/V1/R6, Volume 1, Section C4, March 2000.

[4] W. C. Jordan and S. M. Bowman, *Scale Cross-Section Libraries*, ORNL/NUREG/CSD-2/V3/R6, Volume 3, Section M4, March 2000.

[5] U.S. Department of Energy (DOE), *Contact-Handled Transuranic Waste Authorized Methods for Payload Control* (CH-TRAMPAC), U.S. Department of Energy, Carlsbad Field Office, Carlsbad, New Mexico.

1. Pu-239 is present at the fissile gram equivalent (FGE) limit. FGE limits with 0 g, 5 g, 15 g, and 25 g Pu-240 are calculated for Case A. FGE limits ignoring Pu-240 are calculated for Cases B, C and D.
2. All Pu is assumed to be optimally moderated and reflected with the optimal degree of moderation determined in each case for the applicable moderator. Studies indicate that the presence of voids in the optimal spherical contents model significantly reduces k_{eff}. The presence of less than or equal to 1% by weight beryllium in the moderator was also shown to have a small effect on k_{eff}, and at larger quantities, k_{eff} is reduced.
3. The reflector material is tight fitting around the fissile geometry and assumed to fill the inner containment vessel (ICV) at up to 100% of theoretical density. Especially in Case B with a beryllium reflector, results in Section 6.4.3, *Criticality Results* show that the presence of voids in the reflector reduces k_{eff}.

The two additional conservative assumptions below are applicable to Cases A, B and C but not to Case D. As discussed is Section 6.3.1.4, *Case D Contents Model*, Case D is applicable to a very specific scenario and thus details of the specific configuration are credited.

4. The fissile material is represented in a spherical geometry. Calculations performed for other geometries, such as cylinders and cubes, indicate a reduction in k_{eff} for these other geometries
5. All structural material comprising the payload drums and material within the payload drums, other than Pu-239 and hydrogenous material (represented as a polyethylene/water/beryllium mixture), are conservatively neglected.

The same conservative assumptions that are used to analyze the single-unit TRUPACT-II package are used for the infinite array calculations. However, the presence of reflector in the ICV and outer containment assembly (OCA) region and water around the package tends to isolate the replicated fissile regions from each other. In order to identify the limiting case, the volume fraction of the materials in these regions are varied in order to maximize reactivity of the configuration. Additional conservative assumptions used to model the TRUPACT-II package are delineated in Section 6.2, *Package Contents*.

6.4.3 Criticality Results

The results of the calculations for the TRUPACT-II package criticality evaluation are divided into two sections. Results for a single TRUPACT-II package are presented in Section 6.4.3.1, *Criticality Results for a Single TRUPACT-II Package*, and results for arrays of TRUPACT-II packages are presented in Section 6.4.3.2, *Criticality Results for Infinite Arrays of TRUPACT-II Packages*. Reported multiplication factors represent the computed k_{eff} values plus twice the standard deviation in the result calculated for each case, as follows:

$$k_s = k_{eff} + 2\sigma$$

This quantity is then compared with the upper subcriticality limit (USL) in order to demonstrate an adequate margin of subcriticality. Generally, the Monte Carlo calculations reported here are performed with sufficient histories to bring the computed relative standard deviation in the result to

approximately 0.1%. Typical KENO parameters required to obtain this level of uncertainty are 1000 generations of 1000 histories per generation, with the initial 50 generations skipped.

6.4.3.1 Criticality Results for a Single TRUPACT-II Package

With the model described in Section 6.3.3, *Single-Unit Models*, subcriticality of the TRUPACT-II package under both NCT and HAC is demonstrated for each case.

6.4.3.1.1 Case A Single Unit Results

The results of studies that identify optimal model parameters for NCT calculations are summarized in Table 6.4-1 and Table 6.4-2. Although tabulated values of both k_s and the reported Monte-Carlo standard deviation, σ, are provided, recall that k_s includes the 2σ uncertainty in the result. Calculations were performed for the single-unit TRUPACT-II package model to demonstrate the reactivity effect of adding less than or equal to 1% by weight quantities of beryllium to the package under NCT and HAC. First, the reactivity of a 325 FGE sphere of ^{239}Pu, polyethylene and water with a polyethylene/water mixture filling the ICV and OCA (25% by volume polyethylene and 75% by volume water in both the moderator and reflector) was calculated. Optimal moderation of the contents model is determined by parametrically varying the H/Pu ratio in the fissile sphere. Then, two different compositions for the fissile moderator were considered, namely one in which the moderator consisted only of ^{239}Pu, polyethylene and water and the other in which the moderator contained less than or equal to 1% by weight quantities of beryllium resulting in a conservative mixture of ^{239}Pu and 25% polyethylene, 74% water and 1% by volume beryllium. In both cases, the ICV and OCA regions were filled with a 25% polyethylene, 74% water and 1% by volume beryllium. The results of these calculations are shown in Table 6.4-1. The difference in reactivity for the cases with beryllium in the moderator and those without is statistically insignificant. However, the maximum reactivity occurs when beryllium is not included in the moderator but is included in the reflector. Thus, a polyethylene/water moderator and polyethylene/water/beryllium reflector were modeled in the remainder of the calculations.

Table 6.4-2 shows that the reactivity of the NCT single-unit model decreases as the volume fraction of the reflector material is decreased. As expected for a single unit, the full density reflector case is limiting, with a k_s value of 0.9339.

Thus, optimal reactivity parameters for the single-unit, NCT model with a 25% polyethylene and 75% water moderator are H/Pu(900) at maximum reflection conditions with a 25% polyethylene, 74% water, and 1% beryllium reflector composition.

For HAC conditions, variation of k_s with H/Pu ratio at maximum reflection conditions is shown in Table 6.4-3. The maximum k_s value (0.9331) for the single-unit, HAC occurs at H/Pu(1000). Note that the maximum reactivity of the NCT single unit model (0.9339) is statistically the same as the maximum reactivity for the HAC single unit model. This is expected because of the similarity of the models and the fact that maximum reflection increases the reactivity of a single unit. Although the OCA region is thinner under HAC vs. NCT, the single-unit package model contains a 30 cm external water reflector to ensure that the package is infinitely reflected under both HAC and NCT.

6.4.3.1.2 Case B Single Unit Results

Section 6.4.3.2.1, *Case A Infinite Array Results*, found that the maximum reactivity of a single-unit TRUPACT-II package under NCT or HAC conditions is statistically equivalent to that of an infinite array of HAC packages under maximum reflection conditions. Thus the analysis given in Section 6.4.3.2.2, *Case B Infinite Array Results* is bounding for the Case B single unit.

6.4.3.1.3 Case C Single Unit Results

Section 6.4.3.2.1, *Case A Infinite Array Results*, found that the maximum reactivity of a single-unit TRUPACT-II package under NCT or HAC conditions is statistically equivalent to that of an infinite array of HAC packages under maximum reflection conditions. Thus the analysis given in Section 6.4.3.2.3, *Case C Infinite Array Results* is bounding for the Case C single unit.

6.4.3.1.4 Case D Single Unit Results

Section 6.4.3.2.1, *Case A Infinite Array Results*, found that the maximum reactivity of a single-unit TRUPACT-II package under NCT or HAC conditions is statistically equivalent to that of an infinite array of HAC packages under maximum reflection conditions. Thus the analysis given in Section 6.4.3.2.4, *Case D Infinite Array Results* is bounding for the Case D single unit.

6.4.3.1.5 Conclusions from Single Unit Calculations

Based on optimum moderation of the fissile contents and the maximum reflection conditions modeled by filling the ICV and OCA regions with full density materials appropriate for each case and surrounding the package by an additional 30 cm of water, all single unit results are less than the USL. Thus, a single TRUPACT-II package will remain subcritical under both NCT and HAC conditions.

6.4.3.2 Criticality Results for Infinite Arrays of TRUPACT-II Packages

The infinite array model studies the interaction between the fissile contents in adjacent TRUPACT-II packages. The models described in Section 6.3, *Model Specification* provide the basis for the KENO-V.a calculations. The only difference in the NCT and HAC models is that the thickness of the OCA area is reduced to 5 inches (12.7000 cm) in the HAC model. Thus, the interaction between HAC packages will be greater compared to NCT packages as the spacing between fissile regions is smaller. Also, the results shown below indicate that the reactivity effects of array interaction are less than those of close, full reflection of the package contents. Thus, the infinite array calculations based on the HAC model performed in the following subsections demonstrate that an infinite array of TRUPACT-II packages is safely subcritical under both NCT and HAC conditions.

In addition, the infinite array calculations assume the presence of interspersed water between the damaged packages. The volume fraction of water in the array interstitial space, abbreviated Int in the tables, is varied to determine the most reactive condition.

6.4.3.2.1 Case A Infinite Array Results

As in the single unit calculations for Case A, additional moderation of the spheres of fissile contents is assumed by in-leakage of water into the ICV. The maximum polyethylene density in the cavity is 25% and 1% by volume beryllium is present. The fissile material is assumed to mix homogeneously

with a 25% polyethylene/75% water moderator (by volume). The ICV and OCA areas are filled with a 25% polyethylene/74% water/1% beryllium composition (by volume) reflector. The moderator does not contain 1% by volume beryllium based on the slight reduction in k_s obtained from the single-unit model when beryllium was added to the moderator as discussed in Section 6.4.3.1.1, *Case A Single Unit Results*. The optimum H/Pu ratio for the HAC infinite array model is determined to be 1000 from the results in Table 6.4-4.

Results for an infinite number of TRUPACT-II packages arranged in a close-packed, square-pitched array with contents models centered in each package (model variation 0) and various reflector volume fractions are shown in Table 6.4-5. These results indicate that the reactivity effect of tight reflection of the fissile contents by the full density 25% polyethylene/74% water/1% beryllium mixture is greater than that of array interaction. With the reflector removed and the ICV, OCA and exterior regions of the package voided, the array interaction effect is maximized. However, in this case the computed reactivity is less than that at full moderator density in which the packages are effectively isolated from one another.

These results also indicate that the HAC infinite array maximum reactivity (0.9331) achieved with maximum reflection is statistically equivalent to the HAC single-unit maximum reactivity (0.9331) and the NCT single-unit maximum reactivity (0.9339). Thus, the HAC infinite array model with maximum reflection is equivalent to the single-unit model and is used in the remainder of the calculations.

The reactivity results for the fissile contents displacement Variation 1 described in Section 6.3.4, *Array Models*, are shown in Table 6.4-6 as a function of H/Pu for the case with only the ICV filled with the polyethylene/water/beryllium reflector mixture and the case with the entire interior and exterior of the package voided. The case with maximum array interaction resulted in a lower k_s compared to the case with the ICV region filled with the polyethylene/water/beryllium mixture. Both model Variation 1 cases, however, were less reactive than the Variation 0 model with the spheres centered in the package surrounded by the full density reflector mixture.

The addition of Pu-240 to the fissile sphere was also studied and FGE limits calculated based on the Pu-240 gram content in the package. As shown in Table 6.4-7, a package containing 5 g Pu-240 is subcritical at a FGE limit of 340, a package containing 15 g Pu-240 is subcritical at a FGE limit of 360 and a package containing 25 g Pu-240 is subcritical at a FGE limit of 380. The fissile sphere was modeled centered in the package with the polyethylene/water/beryllium mixture filling the ICV and OCA regions and water in the interstitial region between packages as these parameters were found to result in the most reactive configuration for the cases without Pu-240. These limits are based on the grams of Pu-240 present, not wt% Pu-240 in order to allow the limits to apply to packages containing both U and Pu fissile isotopes. Calculations were performed based on the 340 FGE limit with 5 g Pu-240 with varying mixtures of U-235 and Pu-239 to verify applicability of this limit to mixed fissile systems. The conversion factor of 0.643 g U-235 per FGE given in the CH-TRAMPAC[6] was used. The results shown in Table 6.4-8 verify that mixed fissile systems will remain subcritical under this limit. In fact, the most reactive scenario occurs with 100% Pu-239. The case with 100% U-235 and 5 g Pu-240 is obviously unrealistic but shown for comparison purposes.

[6] U.S. Department of Energy (DOE), *Contact-Handled Transuranic Waste Authorized Methods for Payload Control* (CH-TRAMPAC), U.S. Department of Energy, Carlsbad Field Office, Carlsbad, New Mexico.

All infinite array results are less than the USL. Thus, an infinite array of TRUPACT-II packages containing 325 FGE per package (with 0 g Pu-240), 340 FGE per package (with ≥5 g Pu-240), 360 FGE per package (with ≥15 g Pu-240), and 380 FGE per package (with ≥25 g Pu-240) under the limitations imposed for Case A is subcritical.

6.4.3.2.2 Case B Infinite Array Results

The results for the Case B beryllium reflected cases are consistent with the results for Case A in that the maximum reactivity occurs at maximum reflection conditions. The maximum reactivity (0.9184) occurs at an H/Pu ratio of 800 for the 100 FGE beryllium reflected, polyethylene/water moderated scenario as shown in Table 6.4-9. The addition of beryllium to the fissile sphere was also studied as beryllium was found to increase reactivity when added to a polyethylene/water moderator in a water reflected system per SAIC-1322-001[7]. Volume fractions in the fissile sphere from 1 to 60% beryllium were modeled and the results shown in Table 6.4-10 indicate that k_s is reduced as more beryllium is added to this beryllium reflected system. The results in Table 6.4-11 indicate that the reactivity is reduced as the volume fraction of the reflectors in the ICV, OCA and interstitial regions are reduced. As expected from the Case A results, array Variation 1 with the fissile spheres moved off-center in the ICV to minimize distance between spheres in adjacent packages is significantly less reactive than the Variation 0 base model. These results are shown in Table 6.4-12. Overall, these calculations indicate that an infinite array of TRUPACT-II packages is subcritical with 100 FGE and an unlimited mass of special reflectors.

6.4.3.2.3 Case C Infinite Array Results

The Case C results support the 250 FGE package limit for mechanically compacted waste that does not meet the Case D specifications. As shown in Table 6.4-13, the reactivity is increased when 1% beryllium is added to the polyethyelene reflector in the ICV and the maximum reactivity (0.9345) occurs at an H/Pu ratio of 900. The results in Table 6.4-14 indicate that the reactivity is lower as the volume fraction of the reflector materials in the ICV, OCA and interstitial regions are reduced. Again, moving the fissile spheres off-center in the ICV reduces reactivity based on the results tabulated in Table 6.4-15. Thus, again the maximum reactivity occurs at maximum reflection conditions with the fissile spheres centered in the packages and remains below the USL. Thus, an infinite array of TRUPACT-II packages containing machine compacted waste is subcritical at 250 FGE per package.

6.4.3.2.4 Case D Infinite Array Results

The results of the Case D calculations show that at a maximum packing fraction of 70%, machine compacted pucks are subcritical when each overpack drum is limited to 200 FGE and the package is limited to 325 FGE or if the packing fraction is not limited, when a minimum gap of 0.50 inches exists between the puck drums. The results shown in Table 6.4-16 indicate that the highest reactivity for the modeled configuration at 70% packing fraction (0.9325) occurs at an H/Pu ratio of 800 and the highest reactivity at 100% packing fraction (0.9349) also occurs at

[7] Neeley, G. W., D. L. Newell, S. L. Larson, and R. J. Green, *Reactivity Effects of Moderator and Reflector Materials on a Finite Plutonium System*, SAIC-1322-001, Revision 1, Science Applications International Corporation, Oak Ridge, Tennessee, May 2004.

an H/Pu ratio of 800. At 100% packing fraction, the required separation distance between the puck drums, in addition to the ½ thickness of the the drum steel and the ½ thickness of the slip sheet/ reinforcing plate thicknesses modeled, is 0.50 inches. The reactivity resulting from filling the gap with polyethylene versus water is statistically equivalent. As in the other cases, the results in Table 6.4-17 show that reducing the volume fraction of reflector material in the ICV, OCA and interstitial regions reduces reactivity as does placing the fissile material off-center in the package (i.e., infinite array variation 1) as shown in Table 6.4-18. The cases in these tables were only calculated at the 70% packing fraction, but the results are obviously also applicable to the 100% packing fraction case. Thus, an infinite array of TRUPACT-II packages containing machine compacted waste under the specific restrictions applied to Case D is subcritical at 325 FGE per package.

6.4.3.2.5 Conclusions from Infinite Array Calculations

The calculations reported in this section are performed with conservative representations of arrays of damaged TRUPACT-II packages. The HAC model used gives a smaller center-to-center spacing between packages compared to the NCT model. In addition, the results indicate that the reactivity effects of array interaction are less than those of close, full reflection of the package contents. Hence, maximum reactivity results for arrays of TRUPACT-II packages under NCT are essentially the same as those under HAC at optimal moderation conditions. Therefore, infinite arrays of TRUPACT-II packages are safely subcritical under both NCT and HAC, and the requirements of 10 CFR §71.59[8] are satisfied. Furthermore, a CSI of zero (0.0) is justified.

6.4.3.3 Special Reflectors in CH-TRU Waste

As described previously, the only "special reflectors" credibly applicable to CH-TRU waste criticality analysis are: beryllium (Be), beryllium oxide (BeO), carbon (C), deuterium (D_2O), magnesium oxide (MgO), and depleted uranium (≥0.3% ^{235}U) when present in quantities greater than 1 weight percent. Each special reflector with regard to its possible presence in CH-TRU waste is discussed below:

<u>Beryllium and Beryllium Oxide</u> – Be, and/or BeO, may be present in CH-TRU waste in quantities greater than 1% by weight. The limits for payload containers other than pipe overpacks are found in Table 6.1-1 and Table 6.1-2 under Case B. As described in Section 6.2.1, beryllium is the limiting special reflector for CH-TRU waste. For pipe overpack configurations, beryllium may be present in neutron sources and other source materials where the beryllium is completely bound to the fissile material in the source. Therefore, for pipe overpack configurations, Case E limits in Table 6.1-1 and Table 6.1-2 apply.

<u>Carbon</u> – Carbon is present as a constituent in CH-TRU waste but not in forms that can credibly reconfigure as a reflector. For example: (1) Carbon may be present as graphite molds or crucibles. In these forms the carbon will be chemically and irreversibly bound to the plutonium or other fissile material and cannot be separated. (2) Carbon may be present in filter media as spent or activated carbon. The plutonium or other fissile material would then be attached to the carbon filter media and would not be easily separated. (3) Granular activated carbon (GAC)

[8] Title 10, Code of Federal Regulations, Part 71 (10 CFR 71), *Packaging and Transportation of Radioactive Material*, 01-01-07 Edition.

pads may also be present in an enclosed bag for the purpose of absorbing volatile organic compounds. Once the GAC pad is placed inside the payload container, there is no credible method for the carbon to fully-surround the fissile material and reconfigure as a reflector. (4) Carbon may also be present in alloys, which are by definition chemically and/or mechanically bound. In summary, there is no identified mechanism that could cause the carbon in CH-TRU waste to be separated from the fissile material and/or to be reconfigured as a reflector.

Deuterium – The presence of liquid waste in the payload containers, except for residual amounts in well-drained containers, is prohibited. As specified by the CH-TRAMPAC, the total volume of residual liquid in a payload container shall be less than 1 percent (volume) of the payload container. This limitation on the authorized contents is such that D_2O will not be present in greater than 1% by weight.

Magnesium Oxide – Magnesium oxide crucibles used in high temperature-controlled applications, such as reduction processes, may be present in solid inorganic waste forms such as glass, metal, and pyrochemical salts. If present, MgO will be bound to the fissile material and would not be easily separated. MgO used for neutralization in solidified material cannot be separated out as it is chemically reacted in the waste generation process. There is no identified mechanism that could cause the magnesium oxide in CH-TRU waste to be reconfigured as a reflector.

Depleted Uranium (≥0.3% ^{235}U) – Depleted uranium may be present in CH-TRU waste, but it will be chemically and/or mechanically bound to the plutonium or physically inseparable because the densities of U and Pu are similar. Separation by mechanical means or by leaching is extremely difficult and is considered highly unlikely in CH-TRU waste. Depleted uranium in CH-TRU waste will, therefore, not be separated from the fissile material and/or reconfigured as a reflector.

6.4.3.4 Machine Compacted CH-TRU Waste

Two criticality cases were analyzed for machine compacted CH-TRU waste:

Case C assumes all the machine compacted waste reconfigures into a single sphere during the hypothetical accident conditions and is applicable to machine compacted waste in a 55-gallon drum, 85-gallon drum, 100-gallon drum, SWB, or TDOP. As shown in Table 6.1-1 and Table 6.1-2, the limits for Case C are 200 FGE per drum, 250 FGE per SWB or TDOP, and 250 FGE per package.

Case D assumes either a maximum 70% packing fraction or a minimum vertical spacing of at least 0.50 inches is maintained between two cylinders during the hypothetical accident conditions (in addition to credit for the steel and slipsheets as described in Section 6.3.1.4). Case D is applicable to machine compacted waste in the form of compacted pucks in a 55-gallon drum, 85-gallon drum, or 100-gallon drum. As shown in Table 6.1-1 and Table 6.1-2, the limits for Case D are 200 FGE per payload container and 325 FGE per package.

6.4.3.5 Applicable Criticality Limits for CH-TRU Waste

In conclusion, the only special reflector in CH-TRU waste requiring special controls is Be/BeO. The criticality analyses for CH-TRU waste with greater than 1% by weight Be/BeO in any form is bounded by Case B. Non-machine compacted CH-TRU waste payloads are covered by Cases A and E. Machine compacted CH-TRU waste payloads are covered by Cases C and D. The applicable FGE limits are specified by case in Table 6.1-1 and Table 6.1-2. Considering machine compaction and special reflectors in CH-TRU waste, as discussed in Sections 6.4.3.3 and 6.4.3.4, the applicable FGE limits are summarized below.

FGE Limits Considering Machine Compaction and Special Reflectors

Contents	Payload Container	Fissile Limit per Payload Container (Pu-239 FGE)	Fissile Limit per Package (Pu-239 FGE)	Applicable Analysis Case
Not machine compacted with ≤ 1% by weight Be/BeO①	Drum	200	325	A
	Pipe Overpack	200	2,800	E
	SWB	325	325	A
	TDOP	325	325	A
Not machine compacted with > 1% by weight Be/BeO①	Drum	100	100	B
	Pipe Overpack	200	2,800	E②
	SWB	100	100	B
	TDOP	100	100	B
Machine compacted with ≤ 1% by weight Be/BeO①	Drum	200	250	C
	Pipe Overpack	Unauthorized	Unauthorized	N/A
	SWB	250	250	C
	TDOP	250	250	C
Machine compacted with controls③ and ≤ 1% by weight Be/BeO①	Drum	200	325	D
	Pipe Overpack	Unauthorized	Unauthorized	N/A
	SWB	Unauthorized	Unauthorized	N/A
	TDOP	Unauthorized	Unauthorized	N/A
Machine compacted with > 1% by weight Be/BeO①	Drum	Unauthorized	Unauthorized	N/A
	Pipe Overpack	Unauthorized	Unauthorized	N/A
	SWB	Unauthorized	Unauthorized	N/A
	TDOP	Unauthorized	Unauthorized	N/A

Notes:

① Special reflectors other than Be/BeO in greater than 1% by weight quantities are exempted by the evaluation given in Section 6.4.3.3.

② Case E is applicable in lieu of Case F because Be/BeO is always mechanically or chemically bound to fissile material in pipe overpack payloads (see Section 6.4.3.3).

③ The contents shall be machine compacted waste in the form of "puck" drums with the payload controls specified in Sections 6.2.4 and 6.3.1.4.

Table 6.4-1 – Single-Unit, NCT, Case A, 325 FGE; ks vs. H/Pu Ratio with Different Moderator and Reflector Compositions

Case	H/Pu	Composition	k_{eff}	σ	k_s
NPWPW5	500	Moderator and Reflector in ICV and OCA = 25% poly/ 75% water	0.8981	0.0011	0.9003
NPWPW6	600		0.9141	0.0010	0.9161
NPWPW7	700		0.9242	0.0010	0.9262
NPWPW8	800		0.9280	0.0010	0.9300
NPWPW9	900		0.9299	0.0010	0.9319
NPWPW10	1,000		0.9288	0.0009	0.9306
NPWPW11	1,100		0.9247	0.0010	0.9267
NPWPW12	1,200		0.9216	0.0010	0.9236
NPWPW13	1,300		0.9155	0.0009	0.9173
NPWPWB5	500	Moderator = 25% poly/75% water Reflector in ICV and OCA = 25% poly/ 74% water/ 1% beryllium	0.9000	0.0009	0.9018
NPWPWB6	600		0.9149	0.0011	0.9171
NPWPWB7	700		0.9259	0.0010	0.9279
NPWPWB8	800		0.9297	0.0009	0.9315
NPWPWB9	900		0.9319	0.0010	0.9339
NPWPWB10	1,000		0.9308	0.0009	0.9326
NPWPWB11	1,100		0.9281	0.0009	0.9299
NPWPWB12	1,200		0.9211	0.0009	0.9229
NPWPWB13	1,300		0.9169	0.0009	0.9187
N2PWB5	500	Moderator and Reflector in ICV and OCA = 25% poly/ 74% water/ 1% beryllium	0.9015	0.0011	0.9037
N2PWB6	600		0.9155	0.0010	0.9175
N2PWB7	700		0.9265	0.0010	0.9285
N2PWB8	800		0.9302	0.0010	0.9322
N2PWB9	900		0.9318	0.0010	0.9338
N2PWB10	1,000		0.9302	0.0010	0.9322
N2PWB11	1,100		0.9277	0.0008	0.9293
N2PWB12	1,200		0.9224	0.0009	0.9242
N2PWB13	1,300		0.9173	0.0010	0.9193

Table 6.4-2 – Single Unit, NCT, Case A, 325 FGE; Variation of Reflector Volume Fraction (VF) at Near-Optimal H/Pu Ratio

Case	H/Pu	Reflector	VF	k_{eff}	σ	k_s
NPWPWB9	900	ICV = OCA = 25% poly/ 74% water/ 1% Be at VF given Int = water at VF given	1.00	0.9319	0.0010	0.9339
NWCVOL95			0.95	0.9283	0.0010	0.9303
NWCVOL90			0.90	0.9256	0.0009	0.9274
NWCVOL75			0.75	0.9157	0.0010	0.9177
NWCVOL50			0.50	0.8888	0.0009	0.8906
NWCVOL25			0.25	0.8434	0.0010	0.8454
NWCVOL10			0.10	0.7963	0.0011	0.7985
NWCVOL00			0	0.7583	0.0010	0.7603

Table 6.4-3 – Single-Unit, HAC, Case A, 325 FGE; k_s vs. H/Pu at Maximum Reflection Conditions

Case	H/Pu	Reflector	k_{eff}	σ	k_s
HPWPWB5	500	ICV = OCA = 25% poly/ 74% water/ 1% Be at VF=1.0 Int = water at VF=1.0	0.8996	0.0010	0.9016
HPWPWB6	600		0.9149	0.0011	0.9171
HPWPWB7	700		0.9234	0.0009	0.9252
HPWPWB8	800		0.9296	0.0010	0.9316
HPWPWB9	900		0.9295	0.0009	0.9313
HPWPWB10	1,000		0.9311	0.0010	0.9331
HPWPWB11	1,100		0.9273	0.0009	0.9291
HPWPWB12	1,200		0.9219	0.0009	0.9237
HPWPWB13	1,300		0.9170	0.0009	0.9188

Table 6.4-4 – Infinite Array Variation 0, HAC, Case A, 325 FGE; k_s vs. H/Pu at Extremes of Reflection Conditions

Case	H/Pu	Reflector	k_{eff}	σ	k_s
HINFAR5	500	ICV = OCA = 25% poly/ 74% water/ 1% Be at VF=1.0 Int = water at VF=1.0	0.8997	0.0012	0.9021
HINFAR6	600		0.9163	0.0010	0.9183
HINFAR7	700		0.9275	0.0009	0.9293
HINFAR8	800		0.9291	0.0010	0.9311
HINFAR9	900		0.9307	0.0009	0.9325
HINFAR10	1,000		0.9311	0.0010	0.9331
HINFAR11	1,100		0.9266	0.0010	0.9286
HINFAR12	1,200		0.9224	0.0008	0.9240
HINFAR13	1,300		0.9161	0.0008	0.9177
HVINAR8	800	ICV = Void OCA = Void Int = Void	0.8677	0.0010	0.8697
HVINAR9	900		0.8759	0.0009	0.8777
HVINAR10	1,000		0.8832	0.0010	0.8852
HVINAR11	1,100		0.8859	0.0008	0.8875
HVINAR12	1,200		0.8878	0.0009	0.8896
HVINAR13	1,300		0.8860	0.0008	0.8876
HVINAR14	1,400		0.8840	0.0009	0.8858
HVINAR15	1,500		0.8814	0.0008	0.8830

Table 6.4-5 – Infinite Array Variation 0, HAC, Case A, 325 FGE; Variation of Reflector Volume Fraction at Near-Optimal H/Pu Ratios

Case	H/Pu	Reflector	VF	k_{eff}	σ	k_s
HINFAR10	1000	ICV = OCA = 25% poly/ 74% water/ 1% Be at VF given Int = water at VF given	1.00	0.9311	0.0010	0.9331
HWC10VOL95			0.95	0.9266	0.0009	0.9284
HWC10VOL90			0.90	0.9244	0.0011	0.9266
HWC10VOL75			0.75	0.9159	0.0010	0.9179
HWC10VOL50			0.50	0.8915	0.0010	0.8935
HWC10VOL25			0.25	0.8483	0.0010	0.8503
HWC10VOL10			0.10	0.8047	0.0009	0.8065
HWC10VOL1			0.01	0.7888	0.0009	0.7906
HWC10VOL01			0.001	0.8439	0.0009	0.8457
HVINAR10			0	0.8832	0.0010	0.8852
HINFAR12	1,200	ICV = OCA = 25% poly/ 74% water/ 1% Be at VF given Int = water at VF given	1.00	0.9224	0.0008	0.9240
HWC12VOL90			0.95	0.9190	0.0009	0.9208
HWC12VOL95			0.90	0.9201	0.0009	0.9219
HWC12VOL75			0.75	0.9098	0.0009	0.9116
HWC12VOL50			0.50	0.8888	0.0010	0.8908
HWC12VOL25			0.25	0.8543	0.0010	0.8563
HWC12VOL10			0.10	0.8129	0.0009	0.8147
HWC12VOL1			0.01	0.7972	0.0010	0.7992
HWC12VOL01			0.001	0.8014	0.0010	0.8034
HVINAR12			0	0.8878	0.0009	0.8896

Table 6.4-6 – Infinite Array Variation 1, HAC, Case A, 325 FGE; Variation of H/Pu Ratio at Extremes of Reflection Conditions

					σ	
HINFAROFF9		900	ICV = 25% poly/74% water/1% Be at VF=1.0 OCA = Int = Void	0.9226	0.0009	0.9244
HINFAROFF10		1,000		0.9239	0.0010	0.9259
HINFAROFF11		1,100		0.9209	0.0010	0.9229
HINFAROFF12		1,200		0.9188	0.0010	0.9208
HVINAROFF9		900		0.8948	0.0010	0.8968
HVINAROFF10		1,000		0.9006	0.0009	0.9024
HVINAROFF11		1,100		0.9027	0.0010	0.9047
HVINAROFF12		1,200		0.9022	0.0009	0.9040
HVINAROFF13		1,300		0.8997	0.0009	0.9015

Table 6.4-7 – Infinite Array Variation 0, HAC, Case A; Variation of H/Pu Ratio for Various Gram Quantities of Pu-240 at Maximum Reflection Conditions

	Pu-240 (g)	Pu-239 (g)					
5PU340H6			600		0.9144	0.0011	0.9166
5PU340H7			700		0.9237	0.0022	0.9281
5PU340H8			800		0.9313	0.0009	0.9331
5PU340H9			900		0.9316	0.0010	0.9336
5PU340H10			1,000		0.9304	0.0009	0.9322
5PU340H11			1,100		0.9278	0.0009	0.9296
5PU340H12			1,200		0.9248	0.0011	0.9270
5PU340H13			1,300		0.9196	0.0010	0.9216
15PU360H6			600		0.9136	0.0009	0.9154
15PU360H7			700		0.9233	0.0008	0.9249
15PU360H8			800		0.9307	0.0009	0.9325
15PU360H9			900		0.9337	0.0011	0.9359
15PU360H10			1,000		0.9302	0.0009	0.9320
15PU360H11			1,100		0.9308	0.0008	0.9324
15PU360H12			1,200		0.9254	0.0010	0.9274
15PU360H13			1,300		0.9197	0.0008	0.9213
25PU380H6			600		0.9121	0.0009	0.9139
25PU380H7			700		0.9246	0.0010	0.9266
25PU380H8			800		0.9299	0.0009	0.9317
25PU380H9			900		0.9316	0.0010	0.9336
25PU380H10			1,000		0.9339	0.0009	0.9357
25PU380H11			1,100		0.9298	0.0010	0.9318
25PU380H12			1,200		0.9268	0.0009	0.9286
25PU380H13			1.300		0.9206	0.0008	0.9222

Table 6.4-8 – Infinite Array Variation 0, HAC, Case A, 5 g Pu-240, 340 FGE; k_s vs. H/Pu for Various Combinations of U-235 and Pu-239 under Maximum Reflection Conditions

Case	Fissile Material	H/X	k_{eff}	σ	k_s
U100H3	FGE = 100% U-235① = 528.7 g U-235	300	0.9000	0.0011	0.9022
U100H4		400	0.9198	0.0009	0.9216
U100H5		500	0.9261	0.0009	0.9279
U100H6		600	0.9214	0.0009	0.9232
U100H7		700	0.9131	0.0010	0.9151
U75H4	FGE = 75% U-235/ 25% Pu-239 = 396.6 g U-235/ 85.0 g Pu-239	400	0.9141	0.0010	0.9161
U75H5		500	0.9245	0.0009	0.9263
U75H6		600	0.9272	0.0010	0.9292
U75H7		700	0.9224	0.0010	0.9244
U75H8		800	0.9162	0.0008	0.9178
U50H5	FGE = 50% U-235/ 50% Pu-239 = 264.4 g U-235/ 170.0 g Pu-239	500	0.9188	0.0009	0.9206
U50H6		600	0.9272	0.0009	0.9290
U50H7		700	0.9275	0.0010	0.9295
U50H8		800	0.9240	0.0008	0.9256
U50H9		900	0.9194	0.0010	0.9214
U25H5	FGE = 25% U-235/ 75% Pu-239 = 132.2 g U-235/ 255 g Pu-239	500	0.9152	0.0010	0.9172
U25H6		600	0.9253	0.0011	0.9275
U25H7		700	0.9310	0.0010	0.9330
U25H8		800	0.9295	0.0010	0.9315
U25H9		900	0.9289	0.0010	0.9309
5PU340H7	FGE = 100% Pu-239 = 340 g Pu-239	700	0.9237	0.0022	0.9281
5PU340H8		800	0.9313	0.0009	0.9331
5PU340H9		900	0.9316	0.0010	0.9336
5PU340H10		1,000	0.9304	0.0009	0.9322
5PU340H11		1,100	0.9278	0.0009	0.9296

Note:

① 1 g U-235 = 0.643 FGE

Table 6.4-9 – Infinite Array Variation 0, HAC, Case B, 100 FGE; k_s vs. H/Pu at Maximum Reflection Conditions

Case	H/Pu	Reflector	k_{eff}	σ	k_s
HINFAR5B	500	ICV = Be at VF=1.0	0.8892	0.0009	0.8910
HINFAR6B	600		0.9041	0.0009	0.9059
HINFAR7B	700	OCA = 25% poly/ 74% water/ 1% Be at VF =1.0	0.9127	0.0008	0.9143
HINFAR8B	800		0.9168	0.0008	0.9184
HINFAR9B	900		0.9127	0.0009	0.9145
HINFAR10B	1,000		0.9095	0.0008	0.9111
HINFAR11B	1,100	Int = water at VF=1.0	0.9042	0.0008	0.9058
HINFAR12B	1,200		0.8988	0.0008	0.9004

Table 6.4-10 – Infinite Array Variation 0, HAC, Case B, 100 FGE; k_s vs. H/Pu for Various Moderator Volume Fractions of Beryllium under Maximum Reflection Conditions

Case	VF Beryllium in Moderator	H/Pu	k_{eff}	σ	k_s
B01H6	1	600	0.9027	0.0008	0.9043
B01H7		700	0.9102	0.0009	0.9120
B01H8		800	0.9144	0.0010	0.9164
B01H9		900	0.9129	0.0009	0.9147
B01H10		1,000	0.9101	0.0008	0.9117
B10H6	10	600	0.9027	0.0009	0.9045
B10H7		700	0.9102	0.0009	0.9120
B10H8		800	0.9125	0.0008	0.9141
B10H9		900	0.9104	0.0009	0.9122
B10H10		1,000	0.9075	0.0009	0.9093
B20H6	20	600	0.9001	0.0010	0.9021
B20H7		700	0.9081	0.0009	0.9099
B20H8		800	0.9093	0.0009	0.9111
B20H9		900	0.9094	0.0009	0.9112
B20H10		1,000	0.9042	0.0008	0.9058
B40H6	40	600	0.8972	0.0010	0.8992
B40H7		700	0.9012	0.0009	0.9030
B40H8		800	0.9022	0.0009	0.9040
B40H9		900	0.9010	0.0009	0.9028
B40H10		1,000	0.8960	0.0008	0.8976
B60H6	60	600	0.8822	0.0009	0.8840
B60H7		700	0.8859	0.0008	0.8875
B60H8		800	0.8846	0.0009	0.8864
B60H9		900	0.8815	0.0008	0.8831
B60H10		1,000	0.8771	0.0008	0.8787

Table 6.4-11 – Infinite Array Variation 0, HAC, Case B, 100 FGE; Variation of Reflector Volume Fraction at Near-Optimal H/Pu Ratio

Case	H/Pu	Reflector	VF	k_{eff}	σ	k_s
HINFAR8B	800	ICV = Be at VF given OCA = 25% poly/ 74% water/ 1% Be at VF given Int = water at VF given	1.00	0.9168	0.0008	0.9184
HINFAR8B95			0.95	0.8973	0.0009	0.8991
HINFAR8B90			0.90	0.8838	0.0009	0.8856
HINFAR8B75			0.75	0.8320	0.0008	0.8336
HINFAR8B50			0.50	0.7188	0.0009	0.7206
HINFAR8B25			0.25	0.5671	0.0008	0.5687
HINFAR8B10			0.10	0.4678	0.0009	0.4696
HINFAR8B00			0	0.5013	0.0008	0.5029

Table 6.4-12 – Infinite Array Variation 1, HAC, Case B, 100 FGE; Variation of H/Pu Ratio at Reflector Volume Fraction to Maximize Interaction while Maintaining Beryllium Reflection

					σ	
HINFAR8BOFF		800		0.7680	0.0010	0.7700
HINFAR9BOFF		900		0.7752	0.0009	0.7770
HINFAR10BOFF		1,000		0.7795	0.0009	0.7813
HINFAR11BOFF		1,100		0.7798	0.0009	0.7816
HINFAR12BOFF		1,200		0.7800	0.0008	0.7816
HINFAR13BOFF		1,300		0.7782	0.0007	0.7796

Table 6.4-13 – Infinite Array Variation 0, HAC, Case C, 250 FGE; k_s vs. H/Pu at Maximum Reflection Conditions

Case	H/Pu	Reflector	k_{eff}	σ	k_s
C0B250H6	600	ICV = 100% poly	0.9152	0.0010	0.9172
C0B250H7	700		0.9248	0.0010	0.9268
C0B250H8	800	OCA = 25% poly/ 74% water/ 1% Be	0.9287	0.0010	0.9307
C0B250H9	900		0.9320	0.0010	0.9340
C0B250H10	1,000		0.9305	0.0009	0.9323
C0B250H11	1,100	Int = water	0.9274	0.0009	0.9292
C0B250H12	1,200	All at VF=1.0	0.9223	0.0010	0.9243
C0B250H13	1,300		0.9148	0.0008	0.9164
C1B250H5	500	ICV = 99% poly/ 1% Be	0.8969	0.0010	0.8989
C1B250H6	600		0.9148	0.0009	0.9166
C1B250H7	700		0.9250	0.0009	0.9268
C1B250H8	800	OCA = 25% poly/ 74% water/ 1% Be	0.9309	0.0011	0.9331
C1B250H9	900		0.9325	0.0010	0.9345
C1B250H10	1,000		0.9296	0.0010	0.9316
C1B250H11	1,100	Int = water	0.9271	0.0009	0.9289
C1B250H12	1,200	All at VF=1.0	0.9237	0.0008	0.9253
C1B250H13	1,300		0.9188	0.0009	0.9206

Table 6.4-14 – Infinite Array Variation 0, HAC, Case C, 250 FGE; Variation of Reflector Volume Fraction at Near-Optimal H/Pu Ratio

Case	H/Pu	Reflector	VF	k_{eff}	σ	k_s
C1B250H9	900	ICV = 99% poly/1% Be at VF given	1.00	0.9325	0.0010	0.9345
C1B250H9V95			0.95	0.9295	0.0009	0.9313
C1B250H9V90		OCA = 25% poly/ 74% water/ 1% Be at VF given	0.90	0.9269	0.0010	0.9289
C1B250H9V75			0.75	0.9149	0.0010	0.9169
C1B250H9V50			0.50	0.8880	0.0009	0.8898
C1B250H9V25			0.25	0.8460	0.0010	0.8480
C1B250H9V10		Int = water at VF given	0.10	0.7974	0.0010	0.7994
C1B250H9V00			0	0.8560	0.0009	0.8578

Table 6.4-15 – Infinite Array Variation 1, HAC, Case C, 250 FGE; Variation of H/Pu Ratio at Reflector Volume Fraction to Maximize Interaction while Maintaining Reflection

					σ	
C1BOFF7		700		0.9134	0.0010	0.9154
C1BOFF8		800		0.9202	0.0009	0.9220
C1BOFF9		900		0.9218	0.0011	0.9240
C1BOFF10		1,000		0.9224	0.0009	0.9242
C1BOFF11		1,100		0.9185	0.0009	0.9203

Table 6.4-16 – Infinite Array Variation 0, HAC, Case D, 325 FGE; k_s vs. H/Pu at Maximum Reflection Conditions

Case	H/Pu	Reflector	k_{eff}	σ	k_s
70% Polyethylene/ 30% Water Moderator and No Separation Between Pucks					
CASED70H5	500	ICV = 70% poly/ 29% water/ 1% Be	0.9123	0.0010	0.9143
CASED70H6	600		0.9245	0.0010	0.9265
CASED70H7	700		0.9298	0.0010	0.9318
CASED70H8	800	OCA = 25% poly/ 74% water/ 1% Be	0.9307	0.0009	0.9325
CASED70H9	900		0.9292	0.0010	0.9312
CASED70H10	1,000		0.9257	0.0010	0.9277
CASED70H11	1,100		0.9183	0.0008	0.9199
CASED70H12	1,200	Int = water All VF=1.0	0.9144	0.0009	0.9162
100% Polyethylene Moderator and 0.50 in. Separation Between Pucks Filled with Water					
CASED100H5	500	ICV = 99% poly/ 1% Be	0.9154	0.0010	0.9174
CASED100H6	600		0.9258	0.0009	0.9276
CASED100H7	700		0.9319	0.0009	0.9337
CASED100H8	800	OCA = 25% poly/ 74% water/ 1% Be	0.9320	0.0008	0.9336
CASED100H9	900		0.9310	0.0009	0.9328
CASED100H10	1,000		0.9263	0.0009	0.9281
CASED100H11	1,100	Int = water	0.9233	0.0010	0.9253
CASED100H12	1,200	All VF=1.0	0.9147	0.0009	0.9165
100% Polyethylene Moderator and 0.50 in. Separation Between Pucks Filled with Polyethylene					
CASED100H5P	500	ICV = 99% poly/ 1% Be	0.9159	0.0010	0.9179
CASED100H6P	600		0.9261	0.0009	0.9279
CASED100H7P	700		0.9319	0.0010	0.9339
CASED100H8P	800	OCA = 25% poly/ 74% water/ 1% Be	0.9329	0.0010	0.9349
CASED100H9P	900		0.9308	0.0009	0.9326
CASED100H10P	1,000		0.9260	0.0009	0.9278
CASED100H11P	1,100	Int = water	0.9210	0.0009	0.9228
CASED100H12P	1,200	All VF=1.0	0.9136	0.0009	0.9154

Table 6.4-17 – Infinite Array Variation 0, HAC, Case D, 325 FGE; Variation of Reflector Volume Fraction at Near-Optimal H/Pu Ratio

Case	H/Pu	Reflector	VF	k_{eff}	σ	k_s
CASED70H8	800	ICV = 70% poly/29% water/1% Be at VF given OCA = 25% poly/74% water/1% Be at VF given Int = water at VF given	1.00	0.9307	0.0009	0.9325
CASED70H8V95			0.95	0.9292	0.0009	0.9310
CASED70H8V90			0.90	0.9252	0.0009	0.9270
CASED70H8V75			0.75	0.9143	0.0009	0.9161
CASED70H8V50			0.50	0.8893	0.0009	0.8911
CASED70H8V25			0.25	0.8382	0.0011	0.8404
CASED70H8V10			0.10	0.7828	0.0010	0.7848
CASED70H8V00			0	0.8501	0.0010	0.8521

Table 6.4-18 – Infinite Array Variation 1, HAC, Case D, 325 FGE; Variation of H/Pu Ratio at Reflector Volume Fraction to Maximize Interaction while Maintaining Reflection

					σ	
D1BOFF70H6		600	ICV = 70% poly/29% water/1% Be at VF=1.0 OCA = Int = Void	0.9037	0.0010	0.9057
D1BOFF70H7		700		0.9125	0.0011	0.9147
D1BOFF70H8		800		0.9144	0.0008	0.9160
D1BOFF70H9		900		0.9153	0.0009	0.9171

This page intentionally left blank.

6.5 Critical Benchmark Experiments

The KENO-V.a Monte Carlo criticality code[1] has been used extensively in criticality evaluations. The 238 energy-group, ENDF-B/V cross-section library[2] employed here has been selected based on its relatively fine neutron energy group structure. This section justifies the validity of this computation tool and data library combination for application to the TRUPACT-II package criticality analysis.

The ORNL USLSTATS code, described in Appendix C, *User's Manual for USLSTATS V1.0*, of NUREG/CR-6361[3], is used to establish an upper subcriticality limit, USL, for the analysis. Computed multiplication factors, k_{eff}, for the TRUPACT-II package are deemed to be adequately subcritical if the computed value of k_{eff} plus two standard deviations is below the USL as follows:

$$k_s = k_{eff} + 2\sigma < USL$$

The USL includes the combined effects of code bias, uncertainty in the benchmark experiments, uncertainty in the computational evaluation of the benchmark experiments, and an administrative margin of subcriticality. The USL is determined using the confidence band with administrative margin technique (USLSTATS Method 1).

The result of the statistical analysis of the benchmark experiments is a USL of 0.9382. Due to the significant positive bias exhibited by the code and library for the benchmark experiments, the USL is constant with respect to the various parameters selected for the benchmark analysis.

6.5.1 Benchmark Experiments and Applicability

A total of 196 benchmark experiments of water-reflected solutions of plutonium nitrate are evaluated using the KENO-V.a Monte Carlo criticality code with the SCALE-PC v4.4a[4], 238 energy-group, ENDF-B/V cross-section library. The benchmark cases are evaluated with respect to three independent parameters: 1) the H/Pu ratio, 2) the average fission energy group (AEG), and 3) the ratio of Pu-240 to total Pu.

Detailed descriptions of the benchmark experiments are obtained from the OECD Nuclear Energy Agency's *International Handbook of Evaluated Criticality Safety Benchmark Experiments*[5]. The critical experiments selected for this analysis are presented in Table 6.5-1. Experiments with beryllium and Pu as the fissile component are not available. The only experiments with beryllium in the thermal energy range identified from the OECD Handbook

---

[1] L. M. Petrie and N. F. Landers, *KENO-V.a: An Improved Monte Carlo Criticality Program with Supergrouping*, ORNL/NUREG/CSD-2/V2/R6, Volume 2, Section F11, March 2000.

[2] W. C. Jordan and S. M. Bowman, *Scale Cross-Section Libraries*, ORNL/NUREG/CSD-2/V3/R6, Volume 3, Section M4, March 2000.

[3] J. J. Lichtenwalter, S. M. Bowman, M. D. DeHart, C. M. Hopper, *Criticality Benchmark Guide for Light-Water-Reactor Fuel in Transportation and Storage Packages*, NUREG/CR-6361, ORNL/TM-13211, March 1997.

[4] Oak Ridge National Laboratory (ORNL), *SCALE 4.4a: Modular Code System for Performing Standardized Computer Analyses for Licensing Evaluation for Workstations and Personal Computers*, ORNL/NUREG/CSD-2/R6, March 2000.

[5] OECD Nuclear Energy Agency, *International Handbook of Evaluated Criticality Safety Benchmark Experiments*, NEA/NSC/DOC(95)03, September 2002.

contained U-233 as the fissile isotope. Thus, 31 benchmarks with U-233 and beryllium in the thermal energy range and 15 benchmarks with U-233 and no beryllium also in the thermal energy range were evaluated. With respect to validation of polyethylene, CH_2, in the models, some of the U-233 benchmarks contained polyethylene and some of the plutonium experiments contained Plexiglas, which also contains carbon. All criticality models of the TRUPACT-II package fall within the range of applicability of the benchmark experiments for the H/Pu ratio and AEG trending parameters as follows:

Range of Applicability for Trending Parameters
$45 \leq$ H/Pu Ratio $\leq 2{,}730$
$173 \leq$ AEG ≤ 220
$4.95 \times 10^{-3} \leq$ Pu-240/Pu Ratio $\leq 2.32 \times 10^{-1}$

The intent of using the Pu-240/Pu ratio is to demonstrate the validity of an extension of the range of applicability of this parameter to the TRUPACT-II package criticality models. The Case A models include a Pu-240/Pu Ratio of up to 6.6×10^{-2}, which is within the range of applicability.

Only thermal benchmark experiments are analyzed. Criticality analysis of the TRUPACT-II package and package arrays demonstrate that multiplication factors are insignificant when the package contents are unmoderated.

6.5.2 Details of Benchmark Calculations

A total of 196 experimental benchmarks with Pu in the thermal energy range were evaluated with the KENO-V.a code with the SCALE-PC v4.4a, 238 group, ENDF-B/V cross-section library. Detailed descriptions of these experiments are found in the OECD Handbook. A summary of the experiment titles is provided in Table 6.5-1. The benchmark results were evaluated using the USLSTATS program as discussed in the next section.

6.5.3 Results of Benchmark Calculations

Table 6.5-2 summarizes the trending parameter values, computed k_{eff} values, and uncertainties for each case. The uncertainty value, σ_c, assigned to each case is a combination of the experimental uncertainty for each experiment, σ_{exp}, and the Monte Carlo uncertainty associated with the particular computational evaluation of the case, σ_{comp}, or:

$$\sigma_c = (\sigma_{exp}^2 + \sigma_{comp}^2)^{1/2}$$

These values were input into the USLSTATS program in addition to the following parameters:

- P, proportion of population falling above lower tolerance level = 0.995
- $1-\gamma$, confidence on fit = 0.95
- α, confidence on proportion P = 0.95
- x_{min}, minimum value of AEG for which USL correlation are computed = N/A, minimum of supplied data used by code

- x_{max}, maximum value of AEG for which USL correlation are computed = N/A, maximum of supplied data used by code
- σ_{eff}, estimate in average standard deviation of all input values of k_{eff} = -1.0, use supplied values
- Δk_m, administrative margin used to ensure subcriticality = 0.05.

This data is followed by triplets of trending parameter value, computed k_{eff}, and uncertainty for each case. The USL Method 1 result was chosen which performs a confidence band analysis on the data for the trending parameter.

Three trending parameters are identified for determination of the bias. First, the AEG is used in order to characterize any code bias with respect to neutron spectral effects. The USL is calculated vs. AEG separately for the Pu experiments, U-233 experiments with beryllium and U-233 experiments without beryllium in addition to the combined results of the Pu and U-233 with beryllium experiments. Because the U-233 fissile isotope introduces a component that is not relative to the calculations performed for the TRUPACT-II and may have a distinct bias of its own, comparison of the USL for the U-233 experiments with beryllium to the USL for those without beryllium allows the effect of the beryllium reflector to be separated from the effect of the U-233 isotope. Next, the H/Pu ratio of each experimental case containing Pu is used in order to characterize the material and geometric properties of each sphere. Finally, since all the Pu experiments include Pu-240 to some extent and the TRUPACT-II models contain varying amount of Pu-240, a trending analysis of the results of the Pu experiments with respect to Pu-240/Pu ratio is performed. The U-233 results are not considered in the trending with respect to H/Pu as the optimum H/Pu range will be significantly different for a U-233 system vs. a Pu system. For obvious reasons, the U-233 results are also not considered in the trending with respect to the Pu-240/Pu ratio.

The USLs calculated using USLSTATS Method 1 for the benchmark combinations discussed above are tabulated in Table 6.5-3. The USL calculated based on the combined results of the U-233 with beryllium and Pu experiments of 0.9382 is chosen as the USL for this analysis. This USL value is ~0.001 below that of the Pu experiments alone. The ^{233}U benchmarks without Be result in a lower USL (0.0032) than calculated from the U-233 benchmark results with beryllium. This difference is greater than the experimental uncertainty of each benchmark case (~0.001). Both of the U-233 USL values are lower than the Pu experiment USL values indicating that the U-233 isotope in the experiments has a more significant effect on the USL than the beryllium. Thus, the USL based on the combined results of the U-233 with beryllium and Pu experiments chosen adequately accounts for any bias attributable to beryllium. In addition, the USLs calculated for the Pu experiments using either H/X or the Pu-240/Pu ratio as the trending parameter do not differ significantly from the Pu USL vs. AEG and are bounded by the chosen USL value of 0.9382. USLSTATS calculated constant USL values with respect to H/Pu and Pu-240/Pu ratio indicating no appreciable trend with respect to these parameters.

Table 6.5-1 – Benchmark Experiment Description with Experimental Uncertainties

Series	Title
PU-SOL-THERM-001	Water-reflected 11.5 inch diameter spheres of plutonium nitrate solutions
PU-SOL-THERM-002	Water-reflected 12 inch diameter spheres of plutonium nitrate solutions
PU-SOL-THERM-003	Water-reflected 13 inch diameter spheres of plutonium nitrate solutions
PU-SOL-THERM-004	Water-reflected 14 inch diameter spheres of plutonium nitrate solutions 0.54% to 3.43% Pu-240
PU-SOL-THERM-005	Water-reflected 14 inch diameter spheres of plutonium nitrate solutions 4.05% and 4.40% Pu-240
PU-SOL-THERM-006	Water-reflected 15 inch diameter spheres of plutonium nitrate solutions
PU-SOL-THERM-007	Water-reflected 11.5 inch diameter spheres partly filled with plutonium nitrate solutions
PU-SOL-THERM-009	Unreflected 48 inch-diameter sphere of plutonium nitrate solution
PU-SOL-THERM-010	Water-reflected 9-, 10-, 11-, and 12 inch-diameter cylinders of plutonium nitrate solutions
PU-SOL-THERM-011	Bare 16- and 18 inch-diameter spheres of plutonium nitrate solutions
PU-SOL-THERM-014	Interacting cylinders of 300-mm diameter with plutonium nitrate solution (115.1gPu/l) in air
PU-SOL-THERM-015	Interacting cylinders of 300-mm diameter with plutonium nitrate solution (152.5gPu/l) in air
PU-SOL-THERM-016	Interacting cylinders of 300-mm and 256-mm diameters with plutonium nitrate solution (152.5 and 115.1gPu/l) and nitric acid (2n) in air
PU-SOL-THERM-017	Interacting cylinders of 256-mm and 300-mm diameters with plutonium nitrate solution (115.1gPu/l) in air
PU-SOL-THERM-020	Water-reflected and water-cadmium reflected 14-inch diameter spheres of plutonium nitrate solutions
PU-SOL-THERM-021	Water-reflected and bare 15.2-inch-diameter spheres of plutonium nitrate solutions
PU-SOL-THERM-024	Slabs of plutonium nitrate solutions reflected by 1-inch-thick Plexiglas
U233-SOL-THERM-001	Unreflected spheres of ^{233}U nitrate solutions
U233-SOL-THERM-003	Paraffin-reflected 5-, 5.4-, 6-, 6.6-, 7.5- 8-, 8.5-, 9- and 12-inch-diameter cylinders of ^{233}U uranyl fluoride solutions
U233-SOL-THERM-015	Uranyl-fluoride (^{233}U) solutions in spherical stainless steel vessels with reflectors of Be, CH_2, and Be-CH_2 composites

Table 6.5-2 – Benchmark Case Parameters and Computed Results

Case Name	k_{eff}	σ_{comp}	AEG	H/X①	Pu-240/ Pu Ratio	Experiment Uncertainty σ_{exp}
PUST001_CASE_1	1.0080	0.0010	212.494	352.9	0.04650	0.0050
PUST001_CASE_2	1.0100	0.0010	209.961	258.1	0.04650	0.0050
PUST001_CASE_3	1.0133	0.0010	207.777	204.1	0.04650	0.0050
PUST001_CASE_4	1.0073	0.0010	206.439	181	0.04650	0.0050
PUST001_CASE_5	1.0111	0.0011	205.757	171.2	0.04650	0.0050
PUST001_CASE_6	1.0089	0.0010	195.766	86.7	0.04650	0.0050
PUST002_CASE_1	1.0074	0.0010	214.693	508	0.03110	0.0047
PUST002_CASE_2	1.0088	0.0011	214.457	489.2	0.03110	0.0047
PUST002_CASE_3	1.0074	0.0010	213.798	437.3	0.03110	0.0047
PUST002_CASE_4	1.0103	0.0010	213.343	407.5	0.03110	0.0047
PUST002_CASE_5	1.0125	0.0011	212.898	380.6	0.03110	0.0047
PUST002_CASE_6	1.0099	0.0010	211.974	333.5	0.03110	0.0047
PUST002_CASE_7	1.0101	0.0010	211.146	299.3	0.03110	0.0047
PUST003_CASE_1	1.0089	0.0010	216.630	774.1	0.01750	0.0047
PUST003_CASE_2	1.0076	0.0011	216.438	742.7	0.01750	0.0047
PUST003_CASE_3	1.0103	0.0010	216.055	677.2	0.03110	0.0047
PUST003_CASE_4	1.0094	0.0010	215.948	660.5	0.03110	0.0047
PUST003_CASE_5	1.0097	0.0010	215.535	607.2	0.03110	0.0047
PUST003_CASE_6	1.0099	0.0011	214.960	545.3	0.03110	0.0047
PUST003_CASE_7	1.0121	0.0009	216.482	714.8	0.03110	0.0047
PUST003_CASE_8	1.0091	0.0011	216.321	692.1	0.03110	0.0047
PUST004_CASE_1	1.0080	0.0010	217.470	981.7	0.00538	0.0047
PUST004_CASE_2	1.0032	0.0009	217.408	898.6	0.04180	0.0047
PUST004_CASE_3	1.0059	0.0008	217.241	864	0.04500	0.0047
PUST004_CASE_4	1.0033	0.0009	217.034	842	0.03260	0.0047
PUST004_CASE_5	1.0043	0.0010	217.257	780.2	0.03630	0.0047
PUST004_CASE_6	1.0074	0.0009	217.195	668	0.00495	0.0047
PUST004_CASE_7	1.0104	0.0010	217.030	573.3	0.00495	0.0047
PUST004_CASE_8	1.0040	0.0009	216.917	865	0.00504	0.0047
PUST004_CASE_9	1.0041	0.0009	216.580	872.2	0.01530	0.0047

Case Name	k_{eff}	σ_{comp}	AEG	H/X①	Pu-240/ Pu Ratio	Experiment Uncertainty σ_{exp}
PUST004_CASE_10	1.0078	0.0009	215.881	971.6	0.02510	0.0047
PUST004_CASE_11	1.0041	0.0010	215.106	929.6	0.02330	0.0047
PUST004_CASE_12	1.0094	0.0009	217.031	884.1	0.03160	0.0047
PUST004_CASE_13	1.0042	0.0009	217.074	925.5	0.03350	0.0047
PUST005_CASE_1	1.0072	0.0010	217.069	866.4	0.04030	0.0047
PUST005_CASE_2	1.0084	0.0009	216.909	832.7	0.04030	0.0047
PUST005_CASE_3	1.0092	0.0009	216.749	800.7	0.04030	0.0047
PUST005_CASE_4	1.0091	0.0010	216.360	734.4	0.04030	0.0047
PUST005_CASE_5	1.0102	0.0010	215.906	666.1	0.04030	0.0047
PUST005_CASE_6	1.0112	0.0010	215.451	607.9	0.04030	0.0047
PUST005_CASE_7	1.0099	0.0010	215.004	557.2	0.04030	0.0047
PUST005_CASE_8	1.0024	0.0010	216.903	830.6	0.04030	0.0047
PUST005_CASE_9	1.0078	0.0010	216.687	788.9	0.04030	0.0047
PUST006_CASE_1	1.0059	0.0008	217.615	1028.2	0.03110	0.0035
PUST006_CASE_2	1.0079	0.0009	217.459	986.2	0.03110	0.0035
PUST006_CASE_3	1.0072	0.0010	217.147	910.9	0.03110	0.0035
PUST007_CASE_2	1.0090	0.0011	198.911	102.6	0.04570	0.0047
PUST007_CASE_3	1.0024	0.0010	199.553	110.11	0.04570	0.0047
PUST007_CASE_5	1.0099	0.0010	209.885	253.3	0.04570	0.0047
PUST007_CASE_6	1.0054	0.0011	209.689	247.3	0.04570	0.0047
PUST007_CASE_7	1.0072	0.0010	209.816	250.5	0.04570	0.0047
PUST007_CASE_8	1.0007	0.0012	209.577	246.5	0.04570	0.0047
PUST007_CASE_9	0.9996	0.0011	209.628	246.5	0.04570	0.0047
PUST007_CASE_10	1.0009	0.0011	210.426	275.5	0.04570	0.0047
PUST009_CASE_1	1.0202	0.0007	219.730	2579.3	0.02510	0.0033
PUST009_CASE_2	1.0242	0.0005	219.819	2706.5	0.02510	0.0033
PUST009_CASE_3	1.0232	0.0006	219.830	2729.8	0.02510	0.0033
PUST010_CASE_1.11	1.0158	0.0011	219.830	471.3	0.02840	0.0048
PUST010_CASE_1.12	1.0125	0.0009	214.122	527.7	0.02890	0.0048
PUST010_CASE_1.9	1.0183	0.0012	214.895	259.3	0.02840	0.0048
PUST010_CASE_2.11	1.0124	0.0011	210.075	542.3	0.02840	0.0048

Case Name	k_{eff}	σ_{comp}	AEG	H/X①	Pu-240/ Pu Ratio	Experiment Uncertainty σ_{exp}
PUST010_CASE_2.12	1.0136	0.0010	214.882	600.5	0.02890	0.0048
PUST010_CASE_2.9	1.0140	0.0011	215.514	346.8	0.02840	0.0048
PUST010_CASE_3.11	1.0128	0.0011	212.361	542.3	0.02840	0.0048
PUST010_CASE_3.12	1.0208	0.0009	215.036	707	0.02890	0.0048
PUST010_CASE_3.9	1.0120	0.0010	216.250	470.4	0.02840	0.0048
PUST010_CASE_4.11	1.0055	0.0011	214.300	588.7	0.02840	0.0048
PUST010_CASE_4.12	1.0142	0.0009	215.366	825.1	0.02890	0.0048
PUST010_CASE_5.11	1.0068	0.0010	216.852	646.5	0.02840	0.0048
PUST010_CASE_6.11	1.0176	0.0012	215.739	402.3	0.02890	0.0048
PUST010_CASE_7.11	1.0065	0.0010	213.340	519.8	0.02890	0.0048
PUST011_CASE_1.16	1.0135	0.0010	214.790	733	0.04150	0.0052
PUST011_CASE_1.18	1.0001	0.0009	215.818	1157.3	0.04180	0.0052
PUST011_CASE_2.16	1.0196	0.0010	217.686	705.5	0.04150	0.0052
PUST011_CASE_2.18	1.0065	0.0011	215.633	1103.2	0.04180	0.0052
PUST011_CASE_3.16	1.0213	0.0010	217.509	662.8	0.04150	0.0052
PUST011_CASE_3.18	1.0027	0.0010	215.281	1109.8	0.04180	0.0052
PUST011_CASE_4.16	1.0139	0.0011	217.525	653.4	0.04150	0.0052
PUST011_CASE_4.18	0.9991	0.0011	215.196	1053.7	0.04180	0.0052
PUST011_CASE_5.16	1.0113	0.0010	217.313	550.7	0.04150	0.0052
PUST011_CASE_5.18	1.0099	0.0010	214.156	995.4	0.04180	0.0052
PUST011_CASE_6.18	1.0068	0.0010	217.071	870.4	0.04180	0.0052
PUST011_CASE_7.18	1.0050	0.0010	216.471	1056.4	0.04180	0.0052
PUST014_CASE_1	1.0068	0.0012	205.455	210.2	0.04230	0.0032
PUST014_CASE_3	1.0065	0.0010	205.477	210.2	0.04230	0.0032
PUST014_CASE_4	1.0079	0.0011	205.504	210.2	0.04230	0.0032
PUST014_CASE_5	1.0065	0.0011	205.510	210.2	0.04230	0.0032
PUST014_CASE_6	1.0073	0.0013	205.516	210.2	0.04230	0.0032
PUST014_CASE_7	1.0082	0.0012	205.434	210.2	0.04230	0.0043
PUST014_CASE_8	1.0051	0.0012	205.462	210.2	0.04230	0.0032
PUST014_CASE_9	1.0068	0.0012	205.477	210.2	0.04230	0.0032
PUST014_CASE_10	1.0060	0.0011	205.499	210.2	0.04230	0.0032

Case Name	k_{eff}	σ_{comp}	AEG	H/X①	Pu-240/ Pu Ratio	Experiment Uncertainty σ_{exp}
PUST014_CASE_11	1.0046	0.0010	205.526	210.2	0.04230	0.0032
PUST014_CASE_12	1.0076	0.0010	205.522	210.2	0.04230	0.0032
PUST014_CASE_13	1.0080	0.0011	205.420	210.2	0.04230	0.0043
PUST014_CASE_14	1.0062	0.0011	205.458	210.2	0.04230	0.0043
PUST014_CASE_15	1.0067	0.0011	205.507	210.2	0.04230	0.0043
PUST014_CASE_16	1.0057	0.0011	205.512	210.2	0.04230	0.0043
PUST014_CASE_17	1.0033	0.0011	205.506	210.2	0.04230	0.0043
PUST014_CASE_18	1.0070	0.0011	205.430	210.2	0.04230	0.0043
PUST014_CASE_19	1.0045	0.0011	205.469	210.2	0.04230	0.0043
PUST014_CASE_20	1.0061	0.0011	205.487	210.2	0.04230	0.0043
PUST014_CASE_21	1.0066	0.0012	205.514	210.2	0.04230	0.0043
PUST014_CASE_22	1.0060	0.0012	205.527	210.2	0.04230	0.0043
PUST014_CASE_23	1.0048	0.0012	205.530	210.2	0.04230	0.0043
PUST014_CASE_24	1.0080	0.0012	205.393	210.2	0.04230	0.0043
PUST014_CASE_25	1.0042	0.0011	205.445	210.2	0.04230	0.0043
PUST014_CASE_26	1.0066	0.0011	205.490	210.2	0.04230	0.0043
PUST014_CASE_27	1.0044	0.0011	205.504	210.2	0.04230	0.0043
PUST014_CASE_28	1.0052	0.0011	205.534	210.2	0.04230	0.0043
PUST014_CASE_29	1.0050	0.0011	205.525	210.2	0.04230	0.0043
PUST014_CASE_30	1.0060	0.0010	205.416	210.2	0.04230	0.0043
PUST014_CASE_31	1.0046	0.0011	205.444	210.2	0.04230	0.0043
PUST014_CASE_33	1.0021	0.0011	205.446	210.2	0.04230	0.0043
PUST014_CASE_34	1.0045	0.0011	205.480	210.2	0.04230	0.0043
PUST015_CASE_1	1.0065	0.0010	201.243	155.3	0.04230	0.0038
PUST015_CASE_2	1.0069	0.0011	201.272	155.3	0.04230	0.0038
PUST015_CASE_3	1.0060	0.0011	201.289	155.3	0.04230	0.0038
PUST015_CASE_4	1.0056	0.0012	201.324	155.3	0.04230	0.0038
PUST015_CASE_5	1.0072	0.0011	201.311	155.3	0.04230	0.0038
PUST015_CASE_6	1.0078	0.0012	201.327	155.3	0.04230	0.0038
PUST015_CASE_7	1.0078	0.0011	201.209	155.3	0.04230	0.0047
PUST015_CASE_8	1.0056	0.0011	201.255	155.3	0.04230	0.0047

Case Name	k_{eff}	σ_{comp}	AEG	H/X①	Pu-240/ Pu Ratio	Experiment Uncertainty σ_{exp}
PUST015_CASE_9	1.0062	0.0012	201.292	155.3	0.04230	0.0047
PUST015_CASE_10	1.0060	0.0011	201.333	155.3	0.04230	0.0047
PUST015_CASE_11	1.0012	0.0010	201.196	155.3	0.04230	0.0047
PUST015_CASE_12	1.0053	0.0011	201.280	155.3	0.04230	0.0047
PUST015_CASE_13	1.0084	0.0010	201.307	155.3	0.04230	0.0047
PUST015_CASE_14	1.0065	0.0012	201.335	155.3	0.04230	0.0047
PUST015_CASE_15	1.0082	0.0013	201.196	155.3	0.04230	0.0047
PUST015_CASE_16	1.0064	0.0010	201.222	155.3	0.04230	0.0047
PUST015_CASE_17	1.0067	0.0010	201.299	155.3	0.04230	0.0047
PUST016_CASE_1	1.0077	0.0011	201.225	155.3	0.04230	0.0043
PUST016_CASE_2	1.0048	0.0011	201.265	155.3	0.04230	0.0043
PUST016_CASE_3	1.0072	0.0011	201.295	155.3	0.04230	0.0043
PUST016_CASE_4	1.0075	0.0011	201.318	155.3	0.04230	0.0043
PUST016_CASE_5	1.0054	0.0012	205.463	210.2	0.04230	0.0038
PUST016_CASE_6	1.0047	0.0011	205.476	210.2	0.04230	0.0038
PUST016_CASE_7	1.0093	0.0013	205.511	210.2	0.04230	0.0038
PUST016_CASE_8	1.0072	0.0011	205.508	210.2	0.04230	0.0038
PUST016_CASE_9	1.0070	0.0012	205.607	210.2	0.04230	0.0033
PUST016_CASE_10	1.0065	0.0012	205.556	210.2	0.04230	0.0033
PUST016_CASE_11	1.0063	0.0011	205.516	210.2	0.04230	0.0033
PUST017_CASE_1	1.0076	0.0011	205.535	210.2	0.04230	0.0038
PUST017_CASE_2	1.0050	0.0011	205.488	210.2	0.04230	0.0038
PUST017_CASE_3	1.0041	0.0011	205.492	210.2	0.04230	0.0038
PUST017_CASE_4	1.0054	0.0012	205.482	210.2	0.04230	0.0038
PUST017_CASE_5	1.0066	0.0012	205.488	210.2	0.04230	0.0038
PUST017_CASE_6	1.0056	0.0011	205.479	210.2	0.04230	0.0038
PUST017_CASE_7	1.0069	0.0011	205.485	210.2	0.04230	0.0038
PUST017_CASE_8	1.0051	0.0011	205.497	210.2	0.04230	0.0038
PUST017_CASE_9	1.0071	0.0012	205.525	210.2	0.04230	0.0038
PUST017_CASE_10	1.0060	0.0011	205.500	210.2	0.04230	0.0038
PUST017_CASE_11	1.0050	0.0011	205.531	210.2	0.04230	0.0038

Case Name	k_{eff}	σ_{comp}	AEG	H/X①	Pu-240/ Pu Ratio	Experiment Uncertainty σ_{exp}
PUST017_CASE_12	1.0057	0.0011	205.509	210.2	0.04230	0.0038
PUST017_CASE_13	1.0047	0.0011	205.490	210.2	0.04230	0.0038
PUST017_CASE_14	1.0049	0.0013	205.487	210.2	0.04230	0.0038
PUST017_CASE_15	1.0072	0.0012	205.533	210.2	0.04230	0.0038
PUST017_CASE_16	1.0075	0.0010	205.522	210.2	0.04230	0.0038
PUST017_CASE_17	1.0068	0.0012	205.519	210.2	0.04230	0.0038
PUST017_CASE_18	1.0056	0.0010	205.487	210.2	0.04230	0.0038
PUST020_CASE_1	1.0075	0.0010	215.482	596.5	0.04570	0.0059
PUST020_CASE_2	1.0117	0.0010	215.622	615.6	0.04570	0.0059
PUST020_CASE_3	1.0049	0.0009	216.499	743.8	0.04570	0.0059
PUST020_CASE_5	1.0074	0.0010	213.992	462.9	0.04570	0.0059
PUST020_CASE_6	1.0078	0.0009	213.637	450.5	0.04570	0.0059
PUST020_CASE_7	1.0022	0.0009	216.277	722.9	0.04570	0.0059
PUST020_CASE_8	1.0066	0.0011	210.650	341.1	0.04570	0.0059
PUST020_CASE_9	1.0004	0.0010	214.048	543.2	0.04570	0.0059
PUST021_CASE_7	1.0109	0.0011	215.405	662	0.04570	0.0032
PUST021_CASE_8	1.0044	0.0010	197.712	125	0.04570	0.0065
PUST021_CASE_9	1.0117	0.0010	215.136	634	0.04570	0.0032
PUST021_CASE_10	1.0123	0.0008	218.033	1107	0.04570	0.0025
PUST024_CASE_1	1.0018	0.0010	191.676	87.5	0.18400	0.0062
PUST024_CASE_2	0.9999	0.0009	191.828	87.5	0.18400	0.0062
PUST024_CASE_3	1.0002	0.0011	191.933	87.5	0.18400	0.0062
PUST024_CASE_4	1.0020	0.0010	192.026	87.5	0.18400	0.0062
PUST024_CASE_5	0.9986	0.0011	192.017	87.5	0.18400	0.0062
PUST024_CASE_6	0.9988	0.0009	173.477	44.9	0.18400	0.0077
PUST024_CASE_7	1.0072	0.0010	201.097	143.9	0.18400	0.0053
PUST024_CASE_8	1.0073	0.0010	201.200	143.9	0.18400	0.0053
PUST024_CASE_9	1.0068	0.0010	201.253	143.9	0.18400	0.0053
PUST024_CASE_10	1.0090	0.0010	201.353	143.9	0.18400	0.0053
PUST024_CASE_11	1.0065	0.0011	201.418	143.9	0.18400	0.0053
PUST024_CASE_12	1.0069	0.0010	201.452	143.9	0.18400	0.0053

Case Name	k_{eff}	σ_{comp}	AEG	H/X①	Pu-240/ Pu Ratio	Experiment Uncertainty σ_{exp}
PUST024_CASE_13	1.0066	0.0010	201.493	143.9	0.18400	0.0053
PUST024_CASE_14	1.0019	0.0011	197.708	115.8	0.23200	0.0053
PUST024_CASE_15	1.0033	0.0012	197.781	115.8	0.23200	0.0053
PUST024_CASE_16	1.0017	0.0009	197.845	115.8	0.23200	0.0053
PUST024_CASE_17	1.0026	0.0010	197.990	115.8	0.23200	0.0053
PUST024_CASE_18	1.0085	0.0010	212.039	367.3	0.18400	0.0051
PUST024_CASE_19	1.0079	0.0009	212.057	367.3	0.18400	0.0051
PUST024_CASE_20	1.0100	0.0010	212.074	367.3	0.18400	0.0051
PUST024_CASE_21	1.0075	0.0010	212.106	367.3	0.18400	0.0051
PUST024_CASE_22	1.0054	0.0010	212.142	367.3	0.18400	0.0051
PUST024_CASE_23	1.0068	0.0011	212.166	367.3	0.18400	0.0051
233ST001CASE_1	0.9975	0.0008	218.415	1531.5	N/A	0.0031
233ST001CASE_2	0.9959	0.0008	218.224	1471.7	N/A	0.0033
233ST001CASE_3	0.9955	0.0007	218.055	1420.1	N/A	0.0033
233ST001CASE_4	0.9970	0.0007	217.875	1369.7	N/A	0.0033
233ST001CASE_5	0.9956	0.0008	217.697	1325.4	N/A	0.0033
233ST003CASE_40	1.0029	0.0011	192.780	74.1	N/A	0.0087
233ST003CASE_41	1.0164	0.0011	191.195	74.1	N/A	0.0151
233ST003CASE_42	1.0002	0.0013	191.824	74.1	N/A	0.0087
233ST003CASE_45	1.0040	0.0013	180.246	45.9	N/A	0.0126
233ST003CASE_55	1.0102	0.0011	176.271	39.4	N/A	0.0122
233ST003CASE_57	1.0196	0.0012	204.026	154	N/A	0.0087
233ST003CASE_58	1.0119	0.0012	209.393	250	N/A	0.0087
233ST003CASE_61	1.0056	0.0011	211.723	329	N/A	0.0087
233ST003CASE_62	1.0079	0.0012	213.031	396	N/A	0.0087
233ST003CASE_65	1.0039	0.0010	216.519	775	N/A	0.0087
233ST015_CASE_1	0.9928	0.0012	175.241	51.58	N/A	0.0075
233ST015_CASE_2	0.9869	0.0013	173.581	51.58	N/A	0.0070
233ST015_CASE_3	0.9863	0.0012	181.133	51.58	N/A	0.0068
233ST015_CASE_4	0.9863	0.0012	181.133	51.58	N/A	0.0041
233ST015_CASE_5	0.9844	0.0012	172.140	51.58	N/A	0.0055

Case Name	k_{eff}	σ_{comp}	AEG	H/X①	Pu-240/ Pu Ratio	Experiment Uncertainty σ_{exp}
233ST015_CASE_6	0.9750	0.0012	171.626	51.58	N/A	0.0099
233ST015_CASE_7	0.9807	0.0012	179.879	51.58	N/A	0.0070
233ST015_CASE_8	0.9719	0.0012	171.311	51.58	N/A	0.0067
233ST015_CASE_9	0.9664	0.0013	171.019	51.58	N/A	0.0050
233ST015_CASE_10	0.9841	0.0012	174.951	51.58	N/A	0.0051
233ST015_CASE_11	0.9937	0.0012	181.620	64.23	N/A	0.0075
233ST015_CASE_12	0.9942	0.0012	180.243	64.23	N/A	0.0069
233ST015_CASE_13	0.9924	0.0011	179.562	64.23	N/A	0.0069
233ST015_CASE_14	0.9930	0.0011	187.157	64.23	N/A	0.0036
233ST015_CASE_15	0.9881	0.0012	178.911	64.23	N/A	0.0060
233ST015_CASE_16	0.9877	0.0013	178.599	64.23	N/A	0.0043
233ST015_CASE_17	0.9924	0.0012	186.084	64.23	N/A	0.0029
233ST015_CASE_18	0.9727	0.0014	178.045	64.23	N/A	0.0056
233ST015_CASE_19	0.9728	0.0012	177.964	64.23	N/A	0.0052
233ST015_CASE_20	0.9969	0.0011	193.458	102.54	N/A	0.0079
233ST015_CASE_21	0.9992	0.0012	192.290	102.54	N/A	0.0070
233ST015_CASE_22	0.9966	0.0011	191.669	102.54	N/A	0.0062
233ST015_CASE_23	0.9949	0.0011	191.140	102.54	N/A	0.0055
233ST015_CASE_24	0.9901	0.0013	190.850	102.54	N/A	0.0051
233ST015_CASE_25	0.9917	0.0012	196.919	102.54	N/A	0.0023
233ST015_CASE_26	0.9964	0.0011	204.143	199.4	N/A	0.0066
233ST015_CASE_27	0.9982	0.0011	203.709	199.4	N/A	0.0063
233ST015_CASE_28	0.9948	0.0010	203.459	199.4	N/A	0.0058
233ST015_CASE_29	0.9928	0.0012	203.220	199.4	N/A	0.0051
233ST015_CASE_30	0.9940	0.0011	203.118	199.4	N/A	0.0048
233ST015_CASE_31	0.9946	0.0012	203.041	199.4	N/A	0.0055

① X refers to Pu or U-233 as applicable for the benchmark cases

All cases were run with 1000 neutrons per generation for 1000 generations with the initial 50 generations skipped.

Table 6.5-3 – Calculation of USL

Benchmark Set	Number of Cases	USL vs. AEG	USL vs. H/X	USL vs. Pu-240/Pu
U-233 without Be	15	0.9270	N/A	N/A
U-233 with Be	31	0.9302 (204.14)①	N/A	N/A
Pu	196	0.9395	0.9393	0.9395
Pu + U-233 with Be	227	0.9382②	N/A	N/A

① Calculated at maximum AEG of the set 204.14. USL increases with AEG such that this is conservative for the AEG of the calculations (~217)

② Range of applicability is 195.928 < AEG < 219.83

This page intentionally left blank.

7.0 OPERATING PROCEDURES

7.1 Procedures for Loading the Package

This section delineates the procedures for loading a payload into the TRUPACT-II packaging, and leakage rate testing both the outer containment vessel (OCV) and the inner containment vessel (ICV). Hereafter, reference to specific TRUPACT-II packaging components may be found in Appendix 1.3.1, *Packaging General Arrangement Drawings*.

The loading operation shall be performed in a dry environment. In the event of precipitation during outdoor loading operations, precautions, such as covering the OCV and ICV cavities shall be implemented to prevent water or precipitation from entering the cavities. If precipitation enters the cavities, the free-standing water shall be removed prior to loading the payload.

Based on the current configuration of the TRUPACT-II packaging when preparing for loading, begin at the section applicable to the following criteria:

- If the TRUPACT-II package will be loaded while on the transport trailer or railcar, proceed directly to Section 7.1.2, *Outer Containment Assembly (OCA) Lid Removal*.
- If the outer containment assembly (OCA) lid has already been removed, proceed directly to Section 7.1.3, *Inner Containment Vessel (ICV) Lid Removal*.
- If both the outer containment assembly and inner containment vessel (ICV) lids have already been removed, proceed directly to Section 7.1.4, *Loading the Payload into the TRUPACT-II Package*.

7.1.1 Removal of the TRUPACT-II Package from the Transport Trailer/Railcar

1. Uncover the forklift pockets located at the base of the OCA body.
2. Disengage each of the four (4) tie-down devices on the transport trailer or railcar from the corresponding tie-down lugs on the package.

   CAUTION: Failure to disengage the tie-down devices may cause damage to the packaging and/or transport trailer/railcar.

3. Using a forklift of appropriate size, position the forklift's forks inside the forklift pockets.
4. Lift the package from the transport trailer or railcar and move the package to the loading station.
5. Place the package in the loading station and remove the forklift.

7.1.2 Outer Containment Assembly (OCA) Lid Removal

1. If necessary, clean the surfaces around the joint between the OCA lid and body as required.
2. Remove the OCV seal test port access plug, OCV seal test port thermal plug, and OCV seal test port plug.
3. Remove the OCV vent port access plug, OCV vent port thermal plug, and OCV vent port cover.
4. Remove the OCV vent port plug to vent the OCV cavity to ambient atmospheric pressure.

5. Remove the six 1/2 inch lock bolts (socket head cap screws) from the exterior of the OCA thermal shield.
6. Install a vacuum pump to the OCV vent port and evacuate the OCV cavity sufficiently to allow the OCV locking ring to freely rotate. Rotate the OCV locking ring approximately 10º counterclockwise until the exterior alignment mark indicates the unlocked position. Disconnect the vacuum system and equalize pressure to the OCV cavity.
7. Rig an overhead crane, or equivalent, with an appropriate lift fixture capable of handling the OCA lid. Engage the lift fixture and remove the OCA lid from the OCA body. Store the OCA lid in a manner such that potential damage to the OCA lid's sealing region is minimized.

7.1.3 Inner Containment Vessel (ICV) Lid Removal

1. Remove the ICV vent port cover, the ICV outer vent port plug, and ICV inner vent port plug to vent the ICV cavity to ambient atmospheric pressure.
2. Remove the ICV seal test port plug.
3. Remove the three 1/2 inch lock bolts (socket head cap screws) from the exterior of the ICV locking ring.
4. Install a vacuum pump to the ICV vent port and evacuate the ICV cavity sufficiently to allow the ICV locking ring to freely rotate. Rotate the ICV locking ring approximately 10º counterclockwise until the exterior alignment mark indicates the unlocked position. Disconnect the vacuum system and equalize pressure to the ICV cavity.
5. Rig an overhead crane, or equivalent, with an appropriate lift fixture capable of handling the ICV lid. Engage the lift fixture and remove the ICV lid from the ICV body. Store the ICV lid in a manner such that potential damage to the ICV lid's sealing region and ICV upper aluminum honeycomb spacer assembly is minimized.

7.1.4 Loading the Payload into the TRUPACT-II Package

The following loading sequence requires that a payload configuration has been properly prepared per the requirements of the *Contact-Handled Transuranic Waste Authorized Methods for Payload Control* (CH-TRAMPAC)[1].

1. Verify the presence of an ICV upper aluminum honeycomb spacer assembly in the ICV lid, and an ICV lower aluminum honeycomb spacer assembly in the ICV body.
2. Utilizing the 3-inch diameter hole in the ICV lower aluminum honeycomb spacer assembly, inspect the ICV lower head for the presence of water. Remove all freestanding water prior to loading the payload assembly into the ICV cavity.
3. Connect an appropriate lifting device to the payload assembly.
4. Balance the payload assembly to ensure the payload does not damage either the ICV or the OCV sealing regions during the loading operation.

[1] U.S. Department of Energy (DOE), *Contact-Handled Transuranic Waste Authorized Methods for Payload Control* (CH-TRAMPAC), U.S. Department of Energy, Carlsbad Field Office, Carlsbad, New Mexico.

5. Lower the payload assembly into the ICV cavity; disconnect and remove the lifting device.

7.1.5 Inner Containment Vessel (ICV) Lid Installation

1. Visually inspect each of the following ICV components for wear or damage that could impair their function and, if necessary, replace or repair per the requirements of the drawings in Appendix 1.3.1, *Packaging General Arrangement Drawings*.
   - **a.** ICV debris shield
   - **b.** ICV wiper O-ring seal and wiper O-ring holder
   - **c.** ICV seal test port plug and accompanying O-ring seal
   - **d.** ICV inner vent port plug and accompanying O-ring seal
   - **e.** ICV vent port cover and accompanying seal (O-ring or gasket)
   - **f.** Lock bolts
2. Visually inspect both ICV main O-ring seals. If necessary, remove the O-ring seal(s) and clean the seal(s) and sealing surface(s) on the ICV lid and body to remove contamination. If, during the visual examination, it is determined that damage to the O-ring seal(s) and/or sealing surface(s) is sufficient to impair ICV containment integrity, replace the damaged seal(s) and/or repair the damaged sealing surface(s) per Section 8.2.3.3.1, *Seal Area Routine Inspection and Repair.*
3. Visually inspect the O-ring seal on the ICV outer vent port plug. If necessary, remove the O-ring seal and clean the seal and sealing surfaces on the ICV outer vent port plug and in the ICV vent port to remove contamination. If, during the visual examination, it is determined that damage to the O-ring seal and/or sealing surface(s) is sufficient to impair ICV containment integrity, replace the damaged seal and/or repair the damaged sealing surface(s) per Section 8.2.3.3.1, *Seal Area Routine Inspection and Repair*.
4. As an option, sparingly apply vacuum grease to the O-ring seals and install into the appropriate O-ring seal grooves in the ICV body, ICV seal test port and vent port plugs.
5. Rig an overhead crane, or equivalent, with an appropriate lift fixture capable of handling the ICV lid. Engage the lift fixture and install the ICV lid onto the ICV body. Remove the lift fixture.
6. Install a vacuum pump to the ICV vent port and evacuate the ICV cavity sufficiently to allow the ICV locking ring to freely rotate. Rotate the ICV locking ring approximately 10º clockwise until the exterior alignment mark indicates the <u>locked</u> position. After rotating the ICV locking ring, disconnect the vacuum system and equalize pressure to the ICV cavity.
7. Install the three 1/2 inch lock bolts (socket head cap screws) through the cutouts in the ICV locking ring to secure the ICV locking ring in the locked position. Tighten the lock bolts to 28 - 32 lb-ft torque, lubricated.
8. Leakage rate testing of the ICV main O-ring seal shall be performed based on the following criteria:

a. If the ICV upper main O-ring seal (containment) is replaced, or the corresponding sealing surface(s) was repaired, then perform the maintenance/periodic leakage rate test per Section 8.2.2.2, *Helium Leakage Rate Testing the ICV Main O-ring Seal*.

b. If there are no changes to the ICV upper main O-ring seal (containment) and no repairs made to the corresponding sealing surfaces, then perform preshipment leakage rate testing per Section 7.4, *Preshipment Leakage Rate Test*, or per Section 8.2.2.2, *Helium Leakage Rate Testing the ICV Main O-ring Seal*.

9. Install the ICV seal test port plug; tighten to 55 - 65 lb-in torque.

10. Install the ICV outer vent port plug; tighten to 55 - 65 lb-in torque.

11. Leakage rate testing of the ICV outer vent port plug O-ring seal shall be performed based on the following criteria:

a. If the ICV outer vent port plug O-ring seal is replaced, or the corresponding ICV vent port sealing surface was repaired, then perform the maintenance/periodic leakage rate test per Section 8.2.2.3, *Helium Leakage Rate Testing the ICV Outer Vent Port Plug O-ring Seal*.

b. If the ICV outer vent port plug and accompanying O-ring seal are the same as previously removed, and no repairs made to the corresponding sealing surfaces, then perform preshipment leakage rate testing per Section 7.4, *Preshipment Leakage Rate Test*, or per Section 8.2.2.3, *Helium Leakage Rate Testing the ICV Outer Vent Port Plug O-ring Seal*.

12. Install the ICV vent port cover; tighten to 55 - 65 lb-in torque.

7.1.6 Outer Containment Assembly (OCA) Lid Installation

1. Visually inspect each of the following OCA components for wear or damage that could impair their function and, if necessary, replace or repair per the requirements of the drawings in Appendix 1.3.1, *Packaging General Arrangement Drawings*.

a. OCV seal test port plug and accompanying O-ring seal

b. OCV vent port cover and accompanying O-ring seal

c. Lock bolts

2. Visually inspect both OCV main O-ring seals. If necessary, remove the O-ring seal(s) and clean the seal(s) and sealing surface(s) on the OCA lid and body to remove contamination. If, during the visual examination, it is determined that damage to the O-ring seal(s) and/or sealing surface(s) is sufficient to impair OCV containment integrity, replace the damaged seal(s) and/or repair the damaged sealing surface(s) per Section 8.2.3.3.1, *Seal Area Routine Inspection and Repair*.

3. Visually inspect the O-ring seal on the OCV vent port plug. If necessary, remove the O-ring seal and clean the seal and sealing surfaces on the OCV vent port plug and in the OCV vent port to remove contamination. If, during the visual examination, it is determined that damage to the O-ring seal and/or sealing surface(s) is sufficient to impair OCV containment integrity, replace the damaged seal and/or repair the damaged sealing surface(s) per Section 8.2.3.3.1, *Seal Area Routine Inspection and Repair*.

4. As an option, sparingly apply vacuum grease to the O-ring seals and install into the appropriate O-ring seal grooves in the OCV body, OCV seal test port plug, and OCV vent port plug.
5. Rig an overhead crane, or equivalent, with an appropriate lift fixture capable of handling the OCA lid. Engage the lift fixture and install the OCA lid onto the OCA body. Remove the lift fixture.
6. Install a vacuum pump to the OCV vent port and evacuate the OCV cavity sufficiently to allow the OCV locking ring to freely rotate. Rotate the OCV locking ring approximately 10º clockwise until the alignment mark indicates the locked position. After rotating the OCV locking ring, disconnect the vacuum system and equalize pressure to the OCV cavity.
7. Install the six 1/2 inch lock bolts (socket head cap screws) through the cutouts in the OCA outer thermal shield to secure the OCV locking ring in the locked position. Tighten the lock bolts to 28 - 32 lb-ft torque, lubricated.
8. Leakage rate testing of the OCV main O-ring seal shall be performed based on the following criteria:
   - **a.** If the OCV upper main O-ring seal (containment) is replaced, or the corresponding sealing surface(s) was repaired, then perform the maintenance/periodic leakage rate test per Section 8.1.3.6, *Helium Leakage Rate Testing the OCV Main O-ring Seal Integrity*.
   - **b.** If there are no changes to the OCV upper main O-ring seal (containment) and no repairs made to the corresponding sealing surfaces, then perform preshipment leakage rate testing per Section 7.4, *Preshipment Leakage Rate Test*, or per Section 8.1.3.6, *Helium Leakage Rate Testing the OCV Main O-ring Seal Integrity*.
9. Install the OCV seal test port plug; tighten to 55 - 65 lb-in torque. Install the OCV seal test port thermal plug and the OCV seal test port access plug; tighten to 28 - 32 lb-ft torque.
10. Install the OCV vent port plug; tighten to 55 - 65 lb-in torque.
11. Leakage rate testing of the OCV vent port plug O-ring seal shall be performed based on the following criteria:
    - **a.** If the OCV vent port plug O-ring seal is replaced, or the corresponding OCV vent port sealing surface was repaired, then perform the maintenance/periodic leakage rate test per Section 8.1.3.7, *Helium Leakage Rate Testing the OCV Vent Port Plug O-ring Seal Integrity*.
    - **b.** If the OCV vent port plug and accompanying O-ring seal are the same as previously removed, and no repairs made to the corresponding sealing surfaces, then perform preshipment leakage rate testing per Section 7.4, *Preshipment Leakage Rate Test*, or per Section 8.1.3.7, *Helium Leakage Rate Testing the OCV Vent Port Plug O-ring Seal Integrity*.
12. Install the OCV vent port cover; tighten to 55 - 65 lb-in torque.
13. Install the OCV vent port thermal plug and the OCV vent port access plug; tighten to 28 - 32 lb-ft torque.

7.1.7 Final Package Preparations for Transport (Loaded)

1. Install the two tamper-indicating devices (security seals). One security seal is located at the OCA vent port access plug; the second is located at an OCA lock bolt.

2. If the TRUPACT-II package is not already loaded onto the transport trailer or railcar, perform the following steps:

- **a.** Using a forklift of appropriate size, position the forklift's forks inside the forklift pockets.
- **b.** Lift the loaded TRUPACT-II package, aligning the packaging over the tie-down points on the transport trailer or railcar.
- **c.** Secure the loaded TRUPACT-II package to the transport trailer or railcar using the appropriate tie-down devices.
- **d.** Load as many as three TRUPACT-II packages per transport trailer or up to seven TRUPACT-II packages per railcar.
- **e.** Install forklift pocket covers over the four forklift pockets located at the base of the OCA body.

3. Monitor external radiation for each loaded TRUPACT-II package per the guidelines of 49 CFR §173.441[2].

4. Determine that surface contamination levels for each loaded TRUPACT-II package are per the guidelines of 49 CFR §173.443.

5. Determine the shielding Transport Index (TI) for each loaded TRUPACT-II package per the guidelines of 49 CFR §173.403.

6. Complete all necessary shipping papers in accordance with Subpart C of 49 CFR 172[3].

7. TRUPACT-II package marking shall be in accordance with 10 CFR §71.85(c)[4] and Subpart D of 49 CFR 172. Package labeling shall be in accordance with Subpart E of 49 CFR 172. Package placarding shall be in accordance with Subpart F of 49 CFR 172.

---

[2] Title 49, Code of Federal Regulations, Part 173 (49 CFR 173), *Shippers–General Requirements for Shipments and Packagings*, 10-01-06 Edition.

[3] Title 49, Code of Federal Regulations, Part 172 (49 CFR 172), *Hazardous Materials Tables and Hazardous Communications Regulations*, 10-01-06 Edition.

[4] Title 10, Code of Federal Regulations, Part 71 (10 CFR 71), *Packaging and Transportation of Radioactive Material*, 01-01-07 Edition.

7.2 Procedures for Unloading the Package

This section delineates the procedures for unloading a payload from the TRUPACT-II packaging. Hereafter, reference to specific TRUPACT-II packaging components may be found in Appendix 1.3.1, *Packaging General Arrangement Drawings*.

The unloading operation shall be performed in a dry environment. In the event of precipitation during outdoor unloading operations, precautions, such as covering the outer containment vessel (OCV) and inner containment vessel (ICV) cavities shall be implemented to prevent water or precipitation from entering the cavities. If precipitation enters the cavities, the free-standing water shall be removed prior to installing the lids.

- If the TRUPACT-II package will be unloaded while on the transport trailer or railcar, proceed directly to Section 7.2.2, *Outer Containment Assembly (OCA) Lid Removal*.

7.2.1 Removal of the TRUPACT-II Package from the Transport Trailer/Railcar

1. Uncover the forklift pockets located at the base of the OCA body.
2. Disengage each of the four (4) tie-down devices on the transport trailer or railcar from the corresponding tie-down lugs on the package.

   CAUTION: Failure to disengage the tie-down devices may cause damage to the packaging and/or transport trailer/railcar.

3. Using a forklift of appropriate size, position the forklift's forks inside the forklift pockets.
4. Lift the package from the transport trailer or railcar and move the package to the loading station.
5. Place the package in the loading station and remove the forklift.

7.2.2 Outer Containment Assembly (OCA) Lid Removal

1. If necessary, clean the surfaces around the joint between the OCA lid and body as required.
2. Remove the OCV seal test port access plug, OCV seal test port thermal plug, and OCV seal test port plug.
3. Remove the OCV vent port access plug, OCV vent port thermal plug, and OCV vent port cover.
4. Remove the OCV vent port plug to vent the OCV cavity to ambient atmospheric pressure.
5. Remove the six 1/2 inch lock bolts (socket head cap screws) from the exterior of the OCA thermal shield.
6. Install a vacuum pump to the OCV vent port and evacuate the OCV cavity sufficiently to allow the OCV locking ring to freely rotate. Rotate the OCV locking ring approximately 10º counterclockwise until the exterior alignment mark indicates the unlocked position. Disconnect the vacuum system and equalize pressure to the OCV cavity.

7. Rig an overhead crane, or equivalent, with an appropriate lift fixture capable of handling the OCA lid. Engage the lift fixture and remove the OCA lid from the OCA body. Store the OCA lid in a manner such that potential damage to the OCA lid's sealing region is minimized.

7.2.3 Inner Containment Vessel (ICV) Lid Removal

1. Remove the ICV vent port cover, the ICV outer vent port plug, and ICV inner vent port plug to vent the ICV cavity to ambient atmospheric pressure.
2. Remove the ICV seal test port plug.
3. Remove the three 1/2 inch lock bolts (socket head cap screws) from the exterior of the ICV locking ring.
4. Install a vacuum pump to the ICV vent port and evacuate the ICV cavity sufficiently to allow the ICV locking ring to freely rotate. Rotate the ICV locking ring approximately 10º counterclockwise until the alignment mark indicates the unlocked position. Disconnect the vacuum system and equalize pressure to the ICV cavity.
5. Rig an overhead crane, or equivalent, with an appropriate lift fixture capable of handling the ICV lid. Engage the lift fixture and remove the ICV lid from the ICV body. Store the ICV lid in a manner such that potential damage to the ICV lid's sealing region and ICV upper aluminum honeycomb spacer assembly is minimized.

7.2.4 Unloading the Payload from the TRUPACT-II Package

1. Connect an appropriate lifting device to the payload assembly.
2. Balance the payload assembly sufficiently to ensure the payload does not damage either the ICV or the OCV sealing regions during the unloading operation.
3. Remove the payload assembly from the ICV cavity; disconnect and remove the lifting device.

7.2.5 Inner Containment Vessel (ICV) Lid Installation

1. Visually inspect each of the following ICV components for wear or damage that could impair their function and, if necessary, replace or repair per the requirements of the drawings in Appendix 1.3.1, *Packaging General Arrangement Drawings*.
   - **a.** ICV debris shield
   - **b.** ICV wiper O-ring seal and wiper O-ring holder
   - **c.** ICV main O-ring seals and sealing surfaces
   - **d.** ICV seal test port plug and accompanying O-ring seal
   - **e.** ICV inner and outer vent port plugs and accompanying O-ring seals
   - **f.** ICV vent port cover and accompanying seal (O-ring or gasket)
   - **g.** Lock bolts
2. As an option, sparingly apply vacuum grease to the O-ring seals and install into the appropriate O-ring seal grooves in the ICV body, ICV seal test port and vent port plugs.

3. Rig an overhead crane, or equivalent, with an appropriate lift fixture capable of handling the ICV lid. Engage the lift fixture and install the ICV lid onto the ICV body. Remove the lift fixture.
4. Install a vacuum pump to the ICV vent port and evacuate the ICV cavity sufficiently to allow the ICV locking ring to freely rotate. Rotate the ICV locking ring approximately 10º clockwise until the alignment mark indicates the locked position. After rotating the ICV locking ring, disconnect the vacuum system and equalize pressure to the ICV cavity.
5. Install the three 1/2 inch lock bolts (socket head cap screws) through the cutouts in the ICV locking ring to secure the ICV locking ring in the locked position. Tighten the lock bolts to 28 - 32 lb-ft torque, lubricated.
6. Install the ICV seal test port plug; tighten to 55 - 65 lb-in torque.
7. Install the ICV inner and outer vent port plugs, followed by the ICV vent port cover; tighten each to 55 - 65 lb-in torque.

7.2.6 Outer Containment Assembly (OCA) Lid Installation

1. Visually inspect each of the following OCA components for wear or damage that could impair their function and, if necessary, replace or repair per the requirements of the drawings in Appendix 1.3.1, *Packaging General Arrangement Drawings*.
   - **a.** OCV main O-ring seals and sealing surfaces
   - **b.** OCV seal test port plug and accompanying O-ring seal
   - **c.** OCV vent port plug and accompanying O-ring seal
   - **d.** OCV vent port cover and accompanying O-ring seal
   - **e.** Lock bolts
2. As an option, sparingly apply vacuum grease to the O-ring seals and install into the appropriate O-ring seal grooves in the OCV body, OCV seal test port and vent port plugs.
3. Rig an overhead crane, or equivalent, with an appropriate lift fixture capable of handling the OCA lid. Engage the lift fixture and install the OCA lid onto the OCA body. Remove the lift fixture.
4. Install a vacuum pump to the OCV vent port and evacuate the OCV cavity sufficiently to allow the OCV locking ring to freely rotate. Rotate the OCV locking ring approximately 10º clockwise until the alignment mark indicates the locked position. After rotating the OCV locking ring, disconnect the vacuum system and equalize pressure to the OCV cavity.
5. Install the six 1/2 inch lock bolts (socket head cap screws) through the cutouts in the OCA outer thermal shield to secure the OCV locking ring in the locked position. Tighten the lock bolts to 28 - 32 lb-ft torque, lubricated.
6. Install the OCV seal test port plug; tighten to 55 - 65 lb-in torque. Install the OCV seal test port thermal plug and the OCV seal test port access plug; tighten to 28 - 32 lb-ft torque.
7. Install the OCV vent port plug and OCV vent port cover; tighten each to 55 - 65 lb-in torque. Install the OCV vent port thermal plug and the OCV vent port access plug; tighten to 28 - 32 lb-ft torque.

7.2.7 Final Package Preparations for Transport (Unloaded)

1. If the TRUPACT-II package is not already loaded onto the transport trailer or railcar, perform the following steps:

a. Using a forklift of appropriate size, position the forklift's forks inside the forklift pockets.

b. Lift the TRUPACT-II package, aligning the packaging over the tie-down points on the transport trailer or railcar.

c. Secure the TRUPACT-II package to the transport trailer or railcar using the appropriate tie-down devices.

d. Load as many as three TRUPACT-II packages per transport trailer or up to seven TRUPACT-II packages per railcar.

e. Install forklift pocket covers over the four forklift pockets located at the base of the OCA body.

2. Transport the TRUPACT-II package in accordance with Section 7.3, *Preparation of an Empty Package for Transport*.

7.3 Preparation of an Empty Package for Transport

Previously used and empty TRUPACT-II packagings shall be prepared and transported per the requirements of 49 CFR §173.428[1].

[1] Title 49, Code of Federal Regulations, Part 173 (49 CFR 173), *Shippers–General Requirements for Shipments and Packagings*, 10-01-06 Edition.

This page intentionally left blank.

7.4 Preshipment Leakage Rate Test

After the TRUPACT-II package is assembled and prior to shipment, leakage rate testing shall be performed to confirm proper assembly of the package following the guidelines of Section 7.6, *Preshipment Leakage Rate Test*, and Appendix A.5.2, *Gas Pressure Rise*, of ANSI N14.5[1].

7.4.1 Gas Pressure Rise Leakage Rate Test Acceptance Criteria

In order to demonstrate containment integrity in preparation for shipment, no leakage shall be detected when tested to a sensitivity of 1×10^{-3} reference cubic centimeters per second (scc/s) air, or less, per Section 7.6, *Preshipment Leakage Rate Test*, of ANSI N14.5.

7.4.2 Determining the Test Volume and Test Time

1. Assemble a leakage rate test apparatus that consists of, at a minimum, the components illustrated in Figure 7.4-1, using a calibrated volume with a range of 100 - 500 cubic centimeters, and a calibrated pressure transducer with a minimum sensitivity of 100 millitorr. Connect the test apparatus to the test volume (i.e., the OCV or ICV seal test port, or OCV or ICV vent port, as appropriate).
2. Set the indicated sensitivity on the digital readout of the calibrated pressure transducer, ΔP, to, at a minimum, the resolution (i.e., sensitivity) of the calibrated pressure transducer (e.g, ΔP = 1, 10, or 100 millitorr for a pressure transducer with a 1 millitorr sensitivity).
3. Open all valves (i.e., the vent valve, calibration valve, and vacuum pump isolation valve), and record ambient atmospheric pressure, P_{atm}.
4. Isolate the calibrated volume by closing the vent and calibration valves.
5. Evacuate the test volume to a pressure less than the indicated sensitivity on the digital readout of the calibrated pressure transducer or 0.76 torr, whichever is less.
6. Isolate the vacuum pump from the test volume by closing the vacuum pump isolation valve. Allow the test volume pressure to stabilize and record the test volume pressure, P_{test} (e.g., P_{test} < 1 millitorr for an indicated sensitivity of 1 millitorr).
7. Open the calibration valve and, after allowing the system to stabilize, record the total volume pressure, P_{total}.
8. Knowing the calibrated volume, V_c, calculate and record the test volume, V_t, using the following equation:

$$V_t = V_c \left(\frac{P_{atm} - P_{total}}{P_{total} - P_{test}} \right)$$

9. Knowing the indicated sensitivity on the digital readout of the calibrated pressure transducer, ΔP, calculate and record the test time, t, using the following equation:

$$t = \Delta P(1.32)V_t$$

[1] ANSI N14.5-1997, *American National Standard for Radioactive Materials - Leakage Tests on Packages for Shipment,* American National Standards Institute, Inc. (ANSI).

7.4.3 Performing the Gas Pressure Rise Leakage Rate Test

1. Isolate the calibrated volume by closing the calibration valve.
2. Open the vacuum pump isolation valve and evacuate the test volume to a pressure less than the test volume pressure, P_{test}, determined in step 6 of Section 7.4.2, *Determining the Test Volume and Test Time*.
3. Isolate the vacuum pump from the test volume by closing the vacuum pump isolation valve. Allow the test volume pressure to stabilize and record the beginning test pressure, P_1. After a period of time equal to "t" seconds, determined in step 9 of Section 7.4.2, *Determining the Test Volume and Test Time*, record the ending test pressure, P_2. To be acceptable, there shall be no difference between the final and initial pressures such that the requirements of Section 7.4.1, *Gas Pressure Rise Leakage Rate Test Acceptance Criteria*, are met.
4. If, after repeated attempts, the O-ring seal fails to pass the leakage rate test, replace the damaged seal and/or repair the damaged sealing surfaces per Section 8.2.3.3.1, *Seal Area Routine Inspection and Repair*. Perform verification leakage rate test per the applicable procedure delineated in Section 8.2.2, *Maintenance/Periodic Leakage Rate Tests*.

7.4.4 Optional Preshipment Leakage Rate Test

As an option to Section 7.4.3, *Performing the Gas Pressure Rise Leakage Rate Test*, Section 8.2.2, *Maintenance/Periodic Leakage Rate Tests*, may be performed.

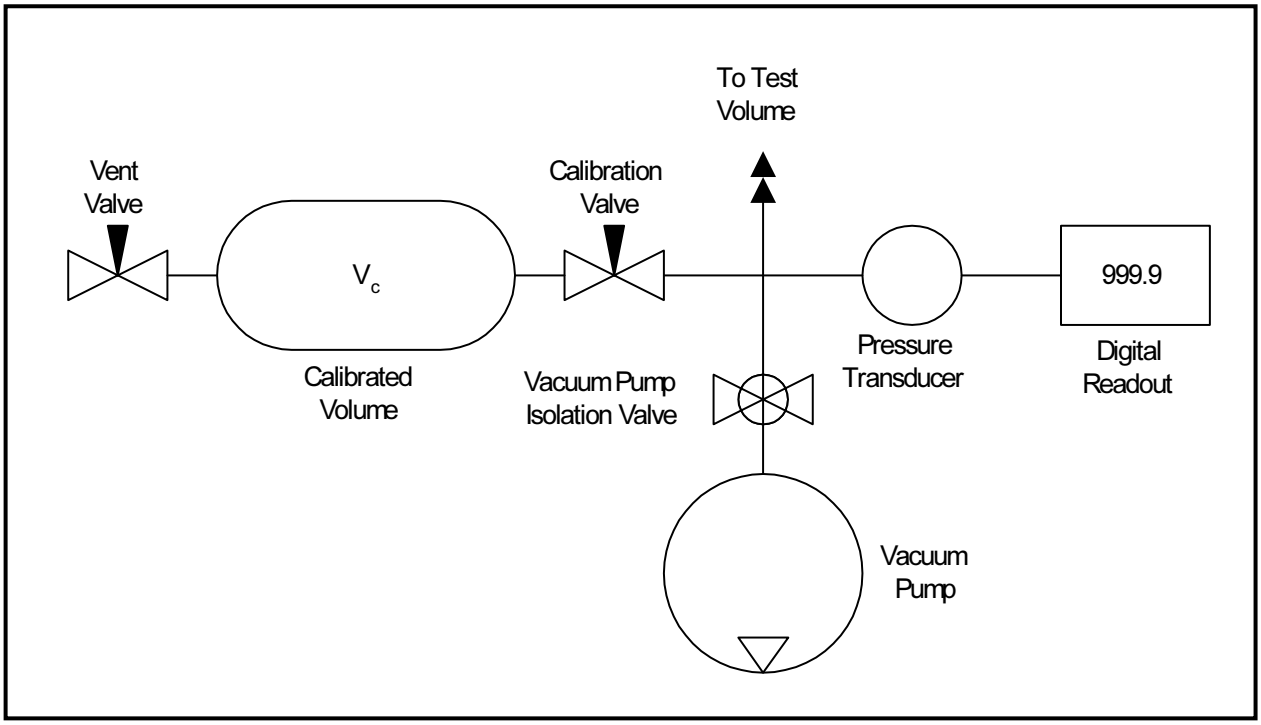

Figure 7.4-1 – Pressure Rise Leakage Rate Test Schematic

8.0 ACCEPTANCE TESTS AND MAINTENANCE PROGRAM

8.1 Acceptance Tests

Per the requirements of 10 CFR §71.85[1], this section discusses the inspections and tests to be performed prior to first use of the TRUPACT-II packaging.

8.1.1 Visual Inspection

All TRUPACT-II packaging materials of construction and welds shall be examined in accordance with requirements delineated on the drawings in Appendix 1.3.1, *Packaging General Arrangement Drawings*, per the requirements of 10 CFR §71.85(a). Furthermore, the inspections and tests of Section 8.2.3.3, *Seal Areas and Grooves*, shall be performed prior to pressure and leakage rate testing.

8.1.2 Structural and Pressure Tests

8.1.2.1 Lifting Device Load Testing

The bounding design load of the OCA lid lifting devices is 7,500 pounds total, or 2,500 pounds per lifting point. Load test each set of OCA lid lifting devices to 150% of their bounding design load, 11,250 pounds total, or 3,750 pounds per lifting point. Perform load testing of the OCA lid lifting devices prior to polyurethane foam installation.

The bounding design load of the ICV lifting sockets is 5,000 pounds total, or 1,667 pounds per lifting socket. Load test each set of ICV lifting sockets to 150% of their bounding design load, 7,500 pounds total, or 2,500 pounds per lifting socket.

Following load testing, all accessible base material and welds and adjacent base metal (minimum 1/2 inch on each side of the weld) directly related to load testing shall be visually inspected for plastic deformation or cracking, and liquid penetrant inspected per ASME Boiler and Pressure Vessel Code, Section V[2], Article 6, and ASME Boiler and Pressure Vessel Code, Section III[3], Division 1, Subsection NB, Article NB-5000. Indications of cracking or distortion shall be recorded on a nonconformance report and dispositioned prior to final acceptance in accordance with the cognizant quality assurance program.

8.1.2.2 Containment Vessel Pressure Testing

Per the requirements of 10 CFR §71.85(b), the outer containment vessel (OCV) and inner containment vessel (ICV) shall be pressure tested to 150% of the maximum normal operating pressure (MNOP) to

[1] Title 10, Code of Federal Regulations, Part 71 (10 CFR 71), *Packaging and Transportation of Radioactive Material*, 01-01-07 Edition.

[2] American Society of Mechanical Engineers (ASME) Boiler and Pressure Vessel Code, Section V, *Nondestructive Examination*, 1986 Edition.

[3] American Society of Mechanical Engineers (ASME) Boiler and Pressure Vessel Code, Section III, *Rules for Construction of Nuclear Power Plant Components*, 1986 Edition.

verify structural integrity. The MNOP of the OCV and ICV is equal to the 50 psig design pressure. Thus, each containment vessel shall be pressure tested to 50 × 1.5 = 75 psig.

Following containment vessel pressure testing, all accessible welds and adjacent base metal (minimum 1/2 inch on each side of the weld) directly related to the pressure testing of the containment vessels shall be visually inspected for plastic deformation or cracking, and liquid penetrant inspected per ASME Boiler and Pressure Vessel Code, Section V, Article 6, and ASME Boiler and Pressure Vessel Code, Section III, Division 1, Subsection NB, Article NB-5000, as delineated on the drawings in Appendix 1.3.1, *Packaging General Arrangement Drawings*. Indications of cracking or distortion shall be recorded on a nonconformance report and dispositioned prior to final acceptance in accordance with the cognizant quality assurance program.

Leakage rate testing per Section 8.1.3, *Fabrication Leakage Rate Tests*, shall be performed after completion of pressure testing to verify package configuration and performance to design criteria.

8.1.3 Fabrication Leakage Rate Tests

This section provides the generalized procedure for fabrication leakage rate testing of the containment vessel boundaries and penetrations following the completion of fabrication. Fabrication leakage rate testing shall follow the guidelines of Section 7.3, *Fabrication Leakage Rate Test*, of ANSI N14.5[4].

Prior to leakage rate testing, internal components such as the payload and spacer pallets, ICV aluminum honeycomb spacer assemblies, etc., shall be removed. For ease of leakage rate testing, each containment vessel should be thoroughly cleaned.

Fabrication leakage rate testing shall be performed on the inner containment vessel (ICV) and outer containment vessel (OCV). Six separate tests comprise the series with three on each containment vessel. Each test shall meet the acceptance criteria delineated in Section 8.1.3.1, *Fabrication Leakage Rate Test Acceptance Criteria*.

8.1.3.1 Fabrication Leakage Rate Test Acceptance Criteria

1. To be acceptable, each leakage rate test shall demonstrate a "leaktight" leakage rate of 1×10^{-7} reference cubic centimeters per second (scc/s), air, or less, per Section 6.3, *Application of Referenced Air Leakage Rate (L_R)*, of ANSI N14.5.
2. In order to demonstrate a leaktight leakage rate, the sensitivity of the leakage rate test procedure shall be 5×10^{-8} scc/s, air, or less, per Section 8.4, *Sensitivity*, of ANSI N14.5.

8.1.3.2 Helium Leakage Rate Testing the ICV Structure Integrity

1. The fabrication leakage rate test of the ICV structure shall be performed following the guidelines of Section A.5.4, *Evacuated Envelope – Gas Detector*, of ANSI N14.5.

[4] ANSI N14.5-1997, *American National Standard for Radioactive Materials – Leakage Tests on Packages for Shipment,* American National Standards Institute, Inc. (ANSI).

2. The ICV shall be assembled with both main O-ring seals installed into the ICV lower seal flange. Assembly is as shown in Appendix 1.3.1, *Packaging General Arrangement Drawings*.
3. Install the assembled ICV into a functional OCV body.
4. Remove the ICV vent port cover, ICV outer vent port plug, and ICV inner vent port plug.
5. Connect a vacuum pump to the ICV vent port and evacuate the ICV cavity to 90% vacuum or better (i.e., ≤10% ambient atmospheric pressure).
6. Provide a helium atmosphere inside the ICV cavity by backfilling with helium gas to a pressure slightly greater than atmospheric pressure (+1 psi, -0 psi).
7. Install the ICV outer vent port plug, followed by the ICV vent port cover; tighten each to 55 – 65 lb-in torque.
8. Ensure the OCV vent port access plug, OCV vent port thermal plug, OCV vent port cover, and OCV vent port plug have been removed from the OCV body.
9. With both main O-ring seals installed into the OCV lower seal flange, install the OCV lid. Assembly is as shown in Appendix 1.3.1, *Packaging General Arrangement Drawings*.
10. Install a helium mass spectrometer leak detector to the OCV vent port. Evacuate through the OCV vent port until the vacuum is sufficient to operate the helium mass spectrometer leak detector.
11. Perform the helium leakage rate test to the requirements of Section 8.1.3.1, *Fabrication Leakage Rate Test Acceptance Criteria*. If, after repeated attempts, the ICV structure fails to pass the leakage rate test, isolate the leak path and, prior to repairing the leak path and repeating the leakage rate test, record on a nonconformance report and disposition prior to final acceptance in accordance with the cognizant quality assurance program.

8.1.3.3 Helium Leakage Rate Testing the ICV Main O-ring Seal

1. The fabrication leakage rate test of the ICV main O-ring seal shall be performed following the guidelines of Section A.5.4, *Evacuated Envelope – Gas Detector*, of ANSI N14.5.
2. The ICV shall be assembled with both main O-ring seals installed into the ICV lower seal flange. Assembly is as shown in Appendix 1.3.1, *Packaging General Arrangement Drawings*.
3. Remove the ICV vent port cover, outer vent port plug, and inner vent port plug.
4. Connect a vacuum pump to the ICV vent port and evacuate the ICV cavity to 90% vacuum or better (i.e., ≤10% ambient atmospheric pressure).
5. Remove the ICV seal test port plug and install a helium mass spectrometer leak detector to the ICV seal test port. Evacuate through the ICV seal test port until the vacuum is sufficient to operate the helium mass spectrometer leak detector.
6. Provide a helium atmosphere inside the ICV cavity by backfilling with helium gas to a pressure slightly greater than atmospheric pressure (+1 psi, -0 psi).

7. Perform the helium leakage rate test to the requirements of Section 8.1.3.1, *Fabrication Leakage Rate Test Acceptance Criteria*. If, after repeated attempts, the ICV main O-ring seal fails to pass the leakage rate test, isolate the leak path and, prior to repairing the leak path and repeating the leakage rate test, record on a nonconformance report and disposition prior to final acceptance in accordance with the cognizant quality assurance program.

8.1.3.4 Helium Leakage Rate Testing the ICV Outer Vent Port Plug O-ring Seal

1. The fabrication leakage rate test of the ICV outer vent port plug O-ring seal shall be performed following the guidelines of Section A.5.4, *Evacuated Envelope – Gas Detector*, of ANSI N14.5.
2. The ICV shall be assembled with both main O-ring seals installed into the ICV lower seal flange. Assembly is as shown in Appendix 1.3.1, *Packaging General Arrangement Drawings*.
3. Remove the ICV vent port cover, ICV outer vent port plug, and the ICV inner vent port plug.
4. Connect a vacuum pump to the ICV vent port and evacuate the ICV cavity to 90% vacuum or better (i.e., ≤10% ambient atmospheric pressure).
5. Provide a helium atmosphere inside the ICV cavity by backfilling with helium gas to a pressure slightly greater than atmospheric pressure (+1 psi, -0 psi).
6. Install the ICV outer vent port plug; tighten to 55 - 65 lb-in torque.
7. Install a helium mass spectrometer leak detector to the ICV vent port. Evacuate through the ICV vent port until the vacuum is sufficient to operate the helium mass spectrometer leak detector.
8. Perform the helium leakage rate test to the requirements of Section 8.1.3.1, *Fabrication Leakage Rate Test Acceptance Criteria*. If, after repeated attempts, the ICV outer vent port plug O-ring seal fails to pass the leakage rate test, isolate the leak path and, prior to repairing the leak path and repeating the leakage rate test, record on a nonconformance report and disposition prior to final acceptance in accordance with the cognizant quality assurance program.

8.1.3.5 Helium Leakage Rate Testing the OCV Structure Integrity

1. The fabrication leakage rate test of the OCV structure shall be performed following the guidelines of Section A.5.3, *Gas Filled Envelope – Gas Detector*, of ANSI N14.5.
2. Remove the OCV vent port access plug, OCV vent port thermal plug, OCV vent port cover, and OCV vent port plug.
3. Install the OCV lid with both main O-ring seals installed into the OCV lower seal flange. As an option, an assembled ICV may be placed within the OCV cavity for volume reduction. Assembly is as shown in Appendix 1.3.1, *Packaging General Arrangement Drawings*.
4. Install a helium mass spectrometer leak detector to the OCV vent port. Evacuate through the OCV vent port until the vacuum is sufficient to operate the helium mass spectrometer leak detector.

5. Surround the assembled OCV with an envelope filled with helium.
6. Perform the helium leakage rate test to the requirements of Section 8.1.3.1, *Fabrication Leakage Rate Test Acceptance Criteria*. If, after repeated attempts, the OCV structure fails to pass the leakage rate test, isolate the leak path and, prior to repairing the leak path and repeating the leakage rate test, record on a nonconformance report and disposition prior to final acceptance in accordance with the cognizant quality assurance program.

8.1.3.6 Helium Leakage Rate Testing the OCV Main O-ring Seal Integrity

1. The fabrication leakage rate test of the OCV main O-ring seal shall be performed following the guidelines of Section A.5.4, *Evacuated Envelope – Gas Detector*, of ANSI N14.5.
2. The OCA shall be assembled with both main O-ring seals installed into the OCV lower seal flange. Assembly is as shown in Appendix 1.3.1, *Packaging General Arrangement Drawings*.
3. Remove the OCV vent port access plug, OCV vent port thermal plug, OCV vent port cover, and OCV vent port plug.
4. Connect a vacuum pump to the OCV vent port and evacuate the OCV cavity to 90% vacuum or better (i.e., ≤10% ambient atmospheric pressure).
5. Remove the OCV seal test port access plug, OCV seal test port thermal plug, and OCV seal test port plug and install a helium mass spectrometer leak detector to the OCV seal test port. Evacuate through the OCV seal test port until the vacuum is sufficient to operate the helium mass spectrometer leak detector.
6. Provide a helium atmosphere inside the OCV cavity by backfilling with helium gas to a pressure slightly greater than atmospheric pressure (+1 psi, -0 psi).
7. Perform the helium leakage rate test to the requirements of Section 8.1.3.1, *Fabrication Leakage Rate Test Acceptance Criteria*. If, after repeated attempts, the OCV main O-ring seal fails to pass the leakage rate test, isolate the leak path and, prior to repairing the leak path and repeating the leakage rate test, record on a nonconformance report and disposition prior to final acceptance in accordance with the cognizant quality assurance program.

8.1.3.7 Helium Leakage Rate Testing the OCV Vent Port Plug O-ring Seal Integrity

1. The fabrication leakage rate test of the OCV vent port plug O-ring seal shall be performed following the guidelines of Section A.5.4, *Evacuated Envelope – Gas Detector*, of ANSI N14.5.
2. The OCV shall be assembled with both main O-ring seals installed into the OCV lower seal flange. Assembly is as shown in Appendix 1.3.1, *Packaging General Arrangement Drawings*.
3. Remove the OCV vent port access plug, OCV vent port thermal plug, OCV vent port cover, and OCV vent port plug.
4. Connect a vacuum pump to the OCV vent port and evacuate the OCV cavity to 90% vacuum or better (i.e., ≤10% ambient atmospheric pressure).

5. Provide a helium atmosphere inside the OCV cavity by backfilling with helium gas to a pressure slightly greater than atmospheric pressure (+1 psi, -0 psi).
6. Install the OCV vent port plug; tighten to 55 - 65 lb-in torque.
7. Install a helium mass spectrometer leak detector to the OCV vent port. Evacuate through the OCV vent port until the vacuum is sufficient to operate the helium mass spectrometer leak detector.
8. Perform the helium leakage rate test to the requirements of Section 8.1.3.1, *Fabrication Leakage Rate Test Acceptance Criteria*. If, after repeated attempts, the OCV vent port plug O-ring seal fails to pass the leakage rate test, isolate the leak path and, prior to repairing the leak path and repeating the leakage rate test, record on a nonconformance report and disposition prior to final acceptance in accordance with the cognizant quality assurance program.

8.1.4 Component Tests

8.1.4.1 Polyurethane Foam

This section establishes the requirements and acceptance criteria for installation, inspection, and testing of rigid, closed-cell, polyurethane foam utilized within the TRUPACT-II packaging.

8.1.4.1.1 Introduction and General Requirements

The polyurethane foam used within the TRUPACT-II packaging is comprised of a specific "formulation" of foam constituents that, when properly apportioned, mixed, and reacted, produce a polyurethane foam material with physical characteristics consistent with the requirements given in this section. In practice, the chemical constituents are batched into multiple parts (e.g., parts A and B) for later mixing in accordance with a formulation. Therefore, a foam "batch" is considered to be a specific grouping and apportionment of chemical constituents into separate and controlled vats or bins for each foam formulation part. Portions from each batch part are combined in accordance with the foam formulation requirements to produce the liquid foam material for pouring into a component. Thus, a foam "pour" is defined as apportioning and mixing the batch parts into a desired quantity for subsequent installation (pouring).

The following sections describe the general requirements for chemical composition, constituent storage, foamed component preparation, foam material installation, and foam pour and test data records.

8.1.4.1.1.1 Polyurethane Foam Chemical Composition

The foam supplier shall certify that the chemical composition of the polyurethane foam is as delineated below, with the chemical component weight percents falling within the specified ranges. In addition, the foam supplier shall certify that the finished (cured) polyurethane foam does not contain halogen-type flame retardants or trichloromonofluoromethane (Freon 11).

Carbon	50% – 70%	Phosphorus	0% – 2%
Oxygen	14% – 34%	Silicon	< 1%
Nitrogen	4% – 12%	Chlorine	< 1%
Hydrogen	4% – 10%	Other	< 1%

8.1.4.1.1.2 Polyurethane Foam Constituent Storage

The foam supplier shall certify that the polyurethane foam constituents have been properly stored prior to use, and that the polyurethane foam constituents have been used within their shelf life.

8.1.4.1.1.3 Foamed Component Preparation

Prior to polyurethane foam installation, the foam supplier shall visually verify to the extent possible (i.e., looking through the foam fill ports) that the ceramic fiber insulation is still attached to the component shell interior surfaces. In addition, due to the internal pressures generated during the foam pouring/curing process, the foam supplier shall visually verify that adequate bracing/shoring of the component shells is provided to maintain the dimensional configuration throughout the foam pouring/curing process.

8.1.4.1.1.4 Polyurethane Foam Installation

As illustrated in the accompanying illustration, the direction of foam rise shall be vertically aligned with the shell component axis.

The surrounding walls of the component shell where the liquid foam material is to be installed shall be between 55 ºF and 95 ºF prior to foam installation. Measure and record the component shell temperature to an accuracy of ±2 ºF prior to foam installation.

In the case of multiple pours into a single foamed component, the cured level of each pour shall be measured and recorded to an accuracy of ±1 inch.

Measure and record the weight of liquid foam material installed during each pour to an accuracy of ±10 pounds.

All test samples shall be poured into disposable containers at the same time as the actual pour it represents, clearly marking the test sample container with the pour date and a unique pour identification number. All test samples shall be cut from a larger block to obtain freshly cut faces. Prior to physical testing, each test sample shall be cleaned of superfluous foam dust.

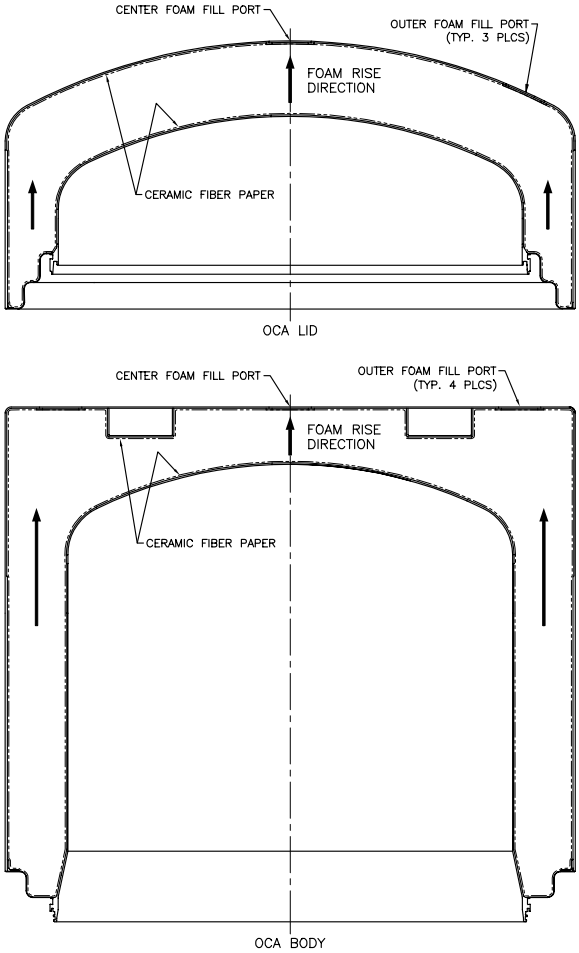

8.1.4.1.1.5 Polyurethane Foam Pour and Test Data Records

A production pour and testing record shall be compiled by the foam supplier during the foam pouring operation and subsequent physical testing. Upon completion of production and testing, the foam supplier shall issue certification referencing the production record data and test data pertaining to each foamed component. At a minimum, relevant pour and test data shall include:

- formulation, batch, and pour numbers, with foam material traceability, and pour date,
- foamed component description, part number, and serial number,
- instrumentation description, serial number, and calibration due date,
- pour and test data (e.g., date, temperature, dimensional, and/or weight measurements, compressive modulus, thermal conductivity, compressive stress, etc., as applicable), and
- technician and Quality Assurance/Quality Control (QA/QC) sign-off.

8.1.4.1.2 Physical Characteristics

The following subsections define the required physical characteristics of the polyurethane foam material used for the TRUPACT-II packaging design.

Testing for the various polyurethane foam physical characteristics is based on a "formulation," "batch," or "pour," as appropriate, as defined in Section 8.1.4.1.1, *Introduction and General Requirements*. The physical characteristics determined for a specific foam formulation are relatively insensitive to small variations in chemical constituents and/or environmental conditions, and therefore include physical testing for compressive modulus, Poisson's ratio, thermal expansion coefficient, thermal conductivity, and specific heat. Similarly, the physical characteristics determined for a batch are only slightly sensitive to small changes in formulation and/or environmental conditions during batch mixing, and therefore include physical testing for flame retardancy, intumescence, and leachable chlorides. Finally, the physical characteristics determined for a pour are also only slightly sensitive to small changes in formulation and slightly more sensitive to variations in environmental conditions during pour mixing, and therefore include physical testing for density and compressive stress.

8.1.4.1.2.1 Physical Characteristics Determined for a Foam Formulation

Foam material physical characteristics for the following parameters shall be determined once for a particular foam formulation. If multiple components are to be foamed utilizing a specific foam formulation, then additional physical testing, as defined below, need not be performed.

8.1.4.1.2.1.1 Parallel-to-Rise Compressive Modulus

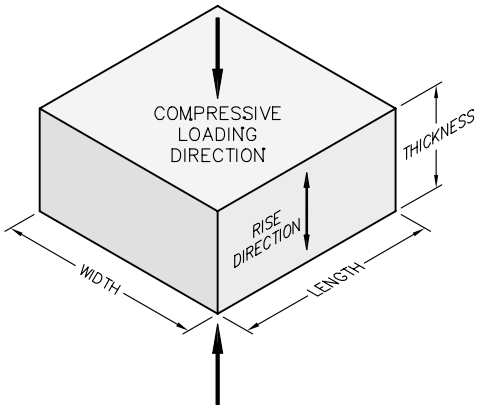

1. Three (3) test samples shall be taken from the sample pour. Each test sample shall be a rectangular prism with nominal dimensions of 1.0 inch thick (T) × 2.0 inches wide (W) × 2.0 inches long (L). The thickness dimension shall be in the parallel-to-rise direction.
2. Place the test samples in a room (ambient) temperature environment (i.e., 65ºF to 85ºF) for sufficient time to thermally stabilize the test samples. Measure and record the room temperature to an accuracy of ±2 ºF.
3. Measure and record the thickness, width, and length of each test sample to an accuracy of ±0.001 inches.
4. Compute and record the surface area of each test sample by multiplying the width by the length (i.e., W × L).
5. Place a test sample in a Universal Testing Machine. Lower the machine's crosshead until it touches the test sample. Set the machine's parameters for the thickness of the test sample.

6. Apply a compressive load to each test sample at a rate of 0.10 ±0.05 inches/minute until the compressive stress somewhat exceeds the elastic range of the foam material (i.e., the elastic range is typically 0% – 6% strain). Plot the compressive stress versus strain for each test sample.
7. Determine and record the parallel-to-rise compressive modulus, E, of each test sample by computing the slope in the linear region of the elastic range of the stress-strain curve, where ε_i and ε_j, and σ_i and σ_j are the strain and compressive stress at two selected points i and j, respectively, in the linear region of the stress-strain curve (see example curve to right) as follows:

$$E = \frac{\sigma_j - \sigma_i}{\varepsilon_j - \varepsilon_i}, \text{ psi}$$

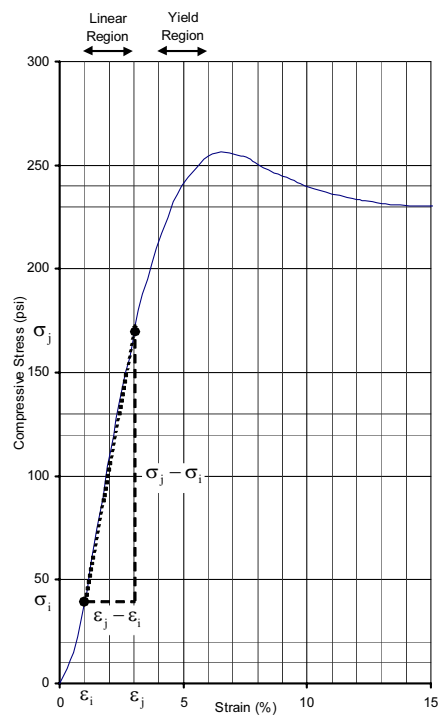

8. Determine and record the average parallel-to-rise compressive modulus of the three test samples. The numerically averaged, parallel-to-rise compressive modulus of the three test samples shall be 6,810 psi ±20% (i.e., within the range of 5,448 to 8,172 psi).

8.1.4.1.2.1.2 Perpendicular-to-Rise Compressive Modulus

1. Three (3) test samples shall be taken from the sample pour. Each test sample shall be a rectangular prism with nominal dimensions of 1.0 inch thick (T) × 2.0 inches wide (W) × 2.0 inches long (L). The thickness dimension shall be in the perpendicular-to-rise direction.

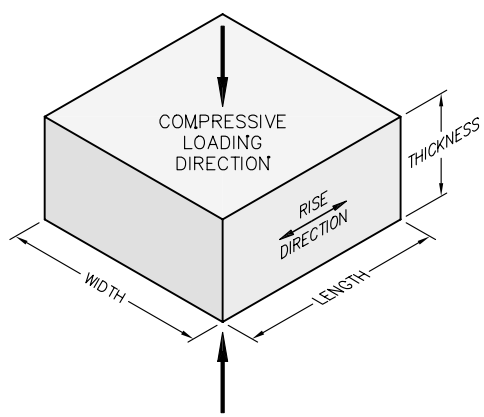

2. Place the test samples in a room (ambient) temperature environment (i.e., 65 ºF to 85 ºF) for sufficient time to thermally stabilize the test samples. Measure and record the room temperature to an accuracy of ±2 ºF.
3. Measure and record the thickness, width, and length of each test sample to an accuracy of ±0.001 inches.
4. Compute and record the surface area of each test sample by multiplying the width by the length (i.e., W × L).
5. Place a test sample in a Universal Testing Machine. Lower the machine's crosshead until it touches the test sample. Set the machine's parameters for the thickness of the test sample.
6. Apply a compressive load to each test sample at a rate of 0.10 ±0.05 inches/minute until the compressive stress somewhat exceeds the elastic range of the foam material (i.e., the elastic range is typically 0% – 6% strain). Plot the compressive stress versus strain for each test sample.

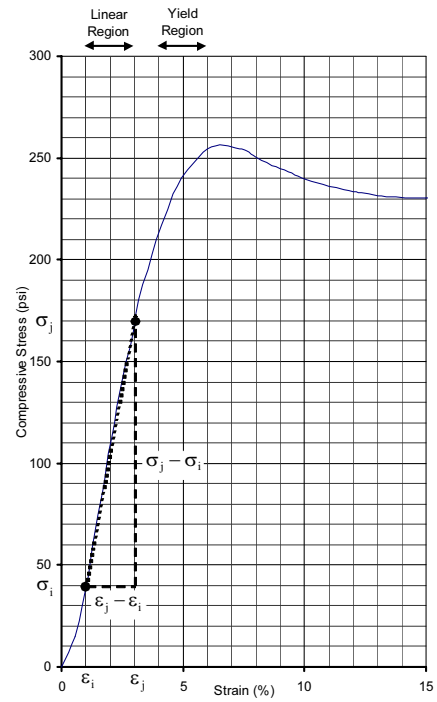

7. Determine and record the perpendicular-to-rise compressive modulus, E, of each test sample by computing the slope in the linear region of the elastic range of the stress-strain curve, where ε_i and ε_j, and σ_i and σ_j are the strain and compressive stress at two selected points i and j, respectively, in the linear region of the stress-strain curve (see example curve to right) as follows:

$$E = \frac{\sigma_j - \sigma_i}{\varepsilon_j - \varepsilon_i}, \text{ psi}$$

8. Determine and record the average perpendicular-to-rise compressive modulus of the three test samples. The numerically averaged, perpendicular-to-rise compressive modulus of the three test samples shall be 4,773 psi ±20% (i.e., within the range of 3,818 to 5,728 psi).

8.1.4.1.2.1.3 Poisson's Ratio

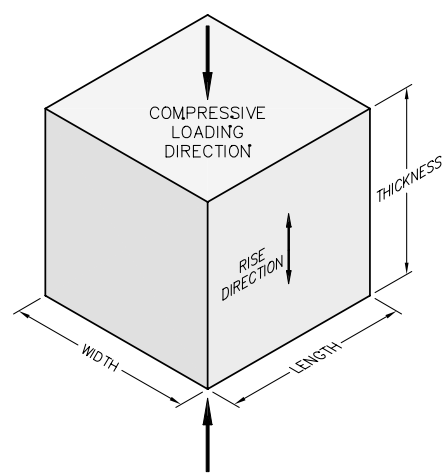

1. Three (3) test samples shall be taken from the sample pour. Each test sample shall be a rectangular prism with nominal dimensions of 2.0 inches thick (T) × 2.0 inches wide (W) × 2.0 inches long (L). The thickness dimension shall be in the parallel-to-rise direction.
2. Place the test samples in a room (ambient) temperature environment (i.e., 65 ºF to 85 ºF) for sufficient time to thermally stabilize the test samples. Measure and record the room temperature to an accuracy of ±2 ºF.
3. Measure and record the thickness, width, and length of each test sample to an accuracy of ±0.001 inches.
4. Place a test sample in a Universal Testing Machine. Lower the machine's crosshead until it touches the test sample. Set the machine's parameters for the thickness of the test sample.
5. As illustrated below, place two orthogonally oriented dial indicators at the mid-plane of one width face and one length face of the test sample to record the lateral deflections. The dial indicators shall be capable of measuring to an accuracy of ±0.001 inches.
6. Apply a compressive load to each test sample so that the strain remains within the elastic range of the material, as determined in Section 8.1.4.1.2.1.1, *Parallel-to-Rise Compressive Modulus*. Record the axial crosshead displacement (δ_T) and both dial indicator displacements (δ_W and δ_L) at one strain point within the elastic range for each test sample.

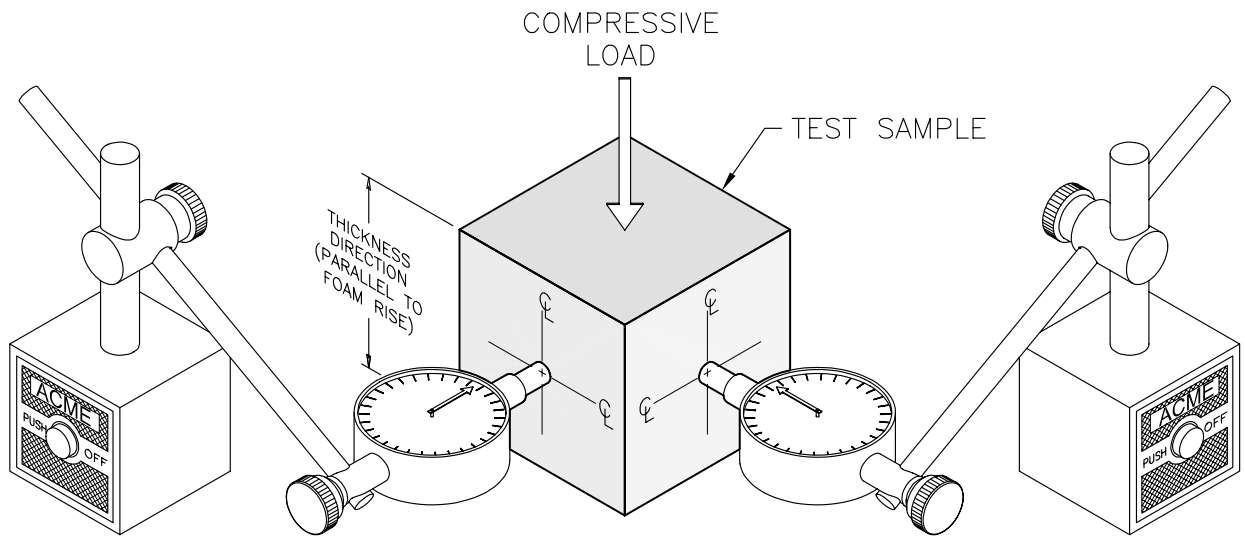

7. Determine and record Poisson's ratio of each test sample as follows:

$$\mu = \frac{\delta_W / W + \delta_L / L}{\delta_T / T}$$

8. Determine and record the average Poisson's ratio of the three test samples. The numerically averaged Poisson's ratio of the three test samples shall be 0.33 ±20% (i.e., within the range of 0.26 to 0.40).

8.1.4.1.2.1.4 Thermal Expansion Coefficient

1. Three (3) test samples shall be taken from the sample pour. Each test sample shall be a rectangular prism with a nominal cross-section of 1.0 inch square and a nominal length of 6.0 inches.

2. Place the test samples in a room (ambient) temperature environment (i.e., 65 ºF to 85 ºF) for sufficient time to thermally stabilize the test samples. Measure and record the room temperature (T_{RT}) to an accuracy of ±2 ºF.

3. Measure and record the room temperature length (L_{RT}) of each test sample to an accuracy of ±0.001 inches.

4. Place the test samples in a -40 ºF to -60 ºF cold environment for a minimum of three hours. Measure and record the cold environment temperature (T_C) to an accuracy of ±2 ºF.

5. Measure and record the cold environment length (L_C) of each test sample to an accuracy of ±0.001 inches.

6. Determine and record the cold environment thermal expansion coefficient for each test sample as follows:

$$\alpha_C = \frac{(L_C - L_{RT})}{(L_{RT})(T_C - T_{RT})}, \text{in/in/°F}$$

7. Place the test samples in a 180 ºF to 200 ºF hot environment for a minimum of three hours. Measure and record the hot environment temperature (T_H) to an accuracy of ±2 ºF.
8. Measure and record the hot environment length (L_H) of each test sample to an accuracy of ±0.001 inches.
9. Determine and record the hot environment thermal expansion coefficient for each test sample as follows:

$$\alpha_H = \frac{(L_H - L_{RT})}{(L_{RT})(T_H - T_{RT})}, \text{in/in/°F}$$

10. Determine and record the average thermal expansion coefficient of each test sample as follows:

$$\alpha = \frac{\alpha_C + \alpha_H}{2}, \text{in/in/°F}$$

11. Determine and record the average thermal expansion coefficient of the three test samples. The numerically averaged thermal expansion coefficient of the three test samples shall be 3.5×10^{-5} in/in/ºF ±20% (i.e., within the range of 2.8×10^{-5} to 4.2×10^{-5} in/in/ºF).

8.1.4.1.2.1.5 Thermal Conductivity

1. The thermal conductivity test shall be performed using a heat flux meter (HFM) apparatus. The HFM establishes steady state unidirectional heat flux through a test specimen between two parallel plates at constant but different temperatures. By measurement of the plate temperatures and plate separation, Fourier's law of heat conduction is used by the HFM to automatically calculate thermal conductivity. Description of a typical HFM is provided in ASTM C518[5]. The HFM shall be calibrated against a traceable reference specimen per the HFM manufacturer's operating instructions.
2. Three (3) test samples shall be taken from the sample pour. Each test sample shall be of sufficient size to enable testing per the HFM manufacturer's operating instructions.
3. Measure and record the necessary test sample parameters as input data to the HFM per the HFM manufacturer's operating instructions.
4. Perform thermal conductivity testing and record the measured thermal conductivity for each test sample following the HFM manufacturer's operating instructions.
5. Determine and record the average thermal conductivity of the three test samples. The numerically averaged thermal conductivity of the three test samples shall be 0.230 Btu-in/hr-ft^2-ºF ±20% (i.e., within the range of 0.184 to 0.276 Btu-in/hr-ft^2-ºF).

8.1.4.1.2.1.6 Specific Heat

1. The specific heat test shall be performed using a differential scanning calorimeter (DSC) apparatus. The DSC establishes a constant heating rate and measures the differential heat flow into both a test specimen and a reference specimen. Description of a typical DSC is

[5] ASTM C518, *Standard Test Method for Steady-State Heat Flux Measurements and Thermal Transmission Properties by Means of the Heat Flux Meter Apparatus*, American Society of Testing and Materials (ASTM).

provided in ASTM E1269[6]. The DSC shall be calibrated against a traceable reference specimen per the DSC manufacturer's operating instructions.

2. Three (3) test samples shall be taken from the sample pour. Each test sample shall be of sufficient size to enable testing per the DSC manufacturer's operating instructions.
3. Measure and record the necessary test sample parameters as input data to the DSC per the DSC manufacturer's operating instructions.
4. Perform specific heat testing and record the measured specific heat for each test sample following the DSC manufacturer's operating instructions.
5. Determine and record the average specific heat of the three test specimens. The numerically averaged specific heat at 77 ºF of the three test samples shall be 0.30 Btu/lb-ºF ±20% (i.e., within the range of 0.24 to 0.36 Btu/lb-ºF).

8.1.4.1.2.2 Physical Characteristics Determined for a Foam Batch

Foam material physical characteristics for the following parameters shall be determined once for a particular foam batch based on the batch definition from Section 8.1.4.1.1, *Introduction and General Requirements*. If a single or multiple components are to be poured utilizing multiple pours from a single foam batch, then additional physical testing, as defined below, need not be performed for each foam pour.

8.1.4.1.2.2.1 Flame Retardancy

1. Three (3) test samples shall be taken from a pour from each foam batch. Each test sample shall be a rectangular prism with nominal dimensions of 0.5 inches thick, 3.0 inches wide, and a minimum length of 6.0 inches. In addition, individual sample lengths must not be less than the total burn length observed for the sample when tested.
2. Place the test samples in a room (ambient) temperature environment (i.e., 65 ºF to 85 ºF) for sufficient time to thermally stabilize the test samples. Measure and record the room temperature to an accuracy of ±2 ºF.
3. Measure and record the length of each test sample to an accuracy of ±0.1 inches.
4. Install a Ø3/8 inches (10 mm), or larger, Bunsen or Tirrill burner inside an enclosure of sufficient size to perform flame retardancy testing. Adjust the burner flame height to 1½ ±1/8 inches. Verify that the burner flame temperature is 1,550 ºF, minimum.

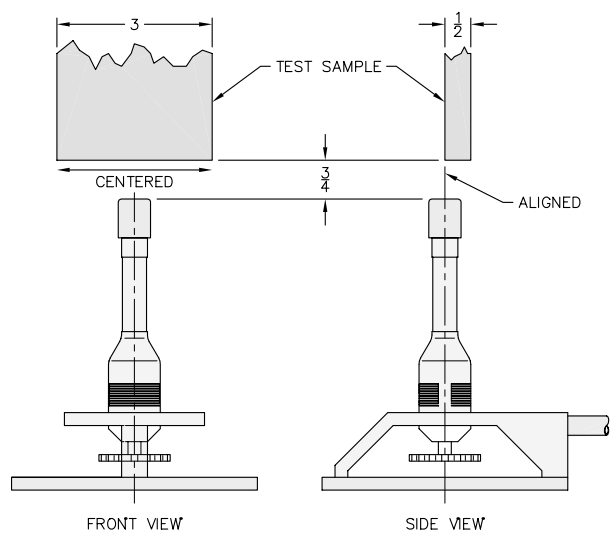

[6] ASTM E1269, *Standard Test Method for Determining Specific Heat Capacity by Differential Scanning Calorimetry*, American Society of Testing and Materials (ASTM).

5. Support the test sample with the long axis oriented vertically within the enclosure such that the test sample's bottom edge will be 3/4 ±1/16 inches above the top edge of the burner.
6. Move the burner flame under the test sample for an elapsed time of 60 ±2 seconds. As illustrated, align the burner flame with the front edge of the test sample thickness and the center of the test sample width.
7. Immediately after removal of the test sample from the burner flame, measure and record the following data:
   - **a.** Measure and record, to the nearest second, the elapsed time until flames from the test sample extinguish.
   - **b.** Measure and record, to the nearest second, the elapsed time from the occurrence of drips, if any, until drips from the test sample extinguish.
   - **c.** Measure and record, to the nearest 0.1 inches, the burn length following cessation of all visible burning and smoking.
8. Flame retardancy testing acceptance is based on the following criteria:
   - **a.** The numerically averaged flame extinguishment time of the three test samples shall not exceed fifteen (15) seconds.
   - **b.** The numerically averaged flame extinguishment time of drips from the three test samples shall not exceed three (3) seconds.
   - **c.** The numerically averaged burn length of the three test samples shall not exceed six (6) inches.

8.1.4.1.2.2.2 Intumescence

1. Three (3) test samples shall be taken from a pour from each foam batch. Each test sample shall be a cube with nominal dimensions of 2.0 inches.
2. Place the test samples in a room (ambient) temperature environment (i.e., 65 ºF to 85 ºF) for sufficient time to thermally stabilize the test samples. Measure and record the room temperature to an accuracy of ±2 ºF.
3. Preheat a furnace to 1,475 ºF ±18 ºF.
4. Identify two opposite faces on each test sample as the thickness direction. The thickness dimension shall be in the parallel-to-rise direction. Measure and record the initial thickness (t_i) of each test sample to an accuracy of ±0.01 inches.
5. Mount a test sample onto a fire resistant fiberboard, with one face of the thickness direction contacting to the board. As illustrated above, the test samples may be mounted by installing onto a 12 to 16 gauge wire (Ø0.105 to Ø0.063 inches, respectively) of sufficient length, oriented perpendicular to the fiberboard face. The test samples may be pre-drilled with an undersized hole to allow installation onto the wire.

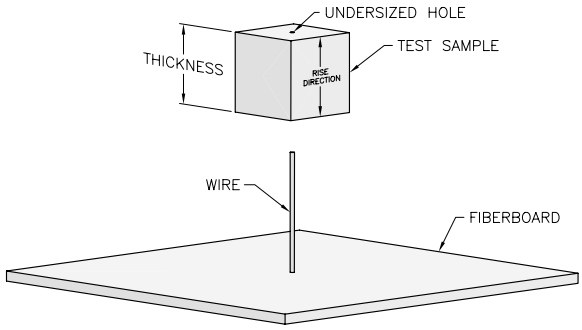

6. Locate the test sample/fiberboard assembly over the opening of the pre-heated furnace for a 90 ±3 second duration. After removal of the test sample/fiberboard assembly from the furnace, gently extinguish any remaining flames and allow the test sample to cool.
7. Measure and record the final thickness (t_f) of the test sample to an accuracy of ±0.1 inches.
8. For each sample tested, determine and record the intumescence, I, as a percentage of the original sample length as follows:

$$I = \left(\frac{t_f - t_i}{t_i} \right) \times 100$$

9. Determine and record the average intumescence of the three test samples. The numerically averaged intumescence of the three test samples shall be a minimum of 50%.

8.1.4.1.2.2.3 Leachable Chlorides

1. The leachable chlorides test shall be performed using an ion chromatograph (IC) apparatus. The IC measures inorganic anions of interest (i.e., chlorides) in water. Description of a typical IC is provided in EPA Method 300.0[7]. The IC shall be calibrated against a traceable reference specimen per the IC manufacturer's operating instructions.
2. One (1) test sample shall be taken from the sample pour. The test sample shall be a cube with dimensions of 2.00 ±0.03 inches.
3. Place the test sample in a room (ambient) temperature environment (i.e., 65 ºF to 85 ºF) for sufficient time to thermally stabilize the test sample. Measure and record the room temperature to an accuracy of ±2 ºF.
4. Measure and record the thickness, width, and length of each test sample to an accuracy of ±0.001 inches.
5. Obtain a minimum of 550 ml of distilled or de-ionized water for testing. The test water shall be from a single source to ensure consistent anionic properties for testing control.
6. Obtain a 400 ml, or larger, contaminant free container that is capable of being sealed. Fill the container with 262 ±3 ml of test water. Fully immerse the test sample inside the container for a duration of 72 ±3 hours. If necessary, use an inert standoff to ensure the test sample is completely immersed for the full test duration. Seal the container prior to the 72 hour duration.
7. Obtain a second, identical container to use as a "control". Fill the control container with 262 ±3 ml of the same test water. Seal the control container for a 72 ±3 hour duration.
8. At the end of the test period, measure and record the leachable chlorides in the test water per the IC manufacturer's operating instructions. The leachable chlorides in the test water shall not exceed one part per million (1 ppm).

[7] EPA Method 300.0, *Determination of Inorganic Anions in Water by Ion Chromatography*, U.S. Environmental Protection Agency.

9. Should leachable chlorides in the test water exceed 1 ppm, measure and record the leachable chlorides in the test water from the "control" container. The difference in leachable chlorides from the test water and "control" water sample shall not exceed 1 ppm.

8.1.4.1.2.3 Physical Characteristics Determined for a Foam Pour

Foam material physical characteristics for the following parameters shall be determined for each foam pour based on the pour definition from Section 8.1.4.1.1, *Introduction and General Requirements*.

8.1.4.1.2.3.1 Density

1. Three (3) test samples shall be taken from the foam pour. Each test sample shall be a rectangular prism with nominal dimensions of 1.0 inch thick (T) × 2.0 inches wide (W) × 2.0 inches long (L).
2. Place the test samples in a room (ambient) temperature environment (i.e., 65 ºF to 85 ºF) for sufficient time to thermally stabilize the test samples. Measure and record the room temperature to an accuracy of ±2 ºF.
3. Measure and record the weight of each test sample to an accuracy of ±0.01 grams.
4. Measure and record the thickness, width, and length of each test sample to an accuracy of ±0.001 inches.
5. Determine and record the room temperature density of each test sample utilizing the following formula:

$$\rho_{foam} = \frac{\text{Weight, g}}{453.6\ \text{g/lb}} \times \frac{1{,}728\ \text{in}^3/\text{ft}^3}{\text{T} \times \text{W} \times \text{L in}^3}\text{, pcf}$$

6. Determine and record the average density of the three test samples. The numerically averaged density of the three test samples shall be 8¼ pcf ±15% (i.e., within the range of 7 to 9½ pcf).

8.1.4.1.2.3.2 Parallel-to-Rise Compressive Stress

1. Three (3) test samples shall be taken from the foam pour. Each test sample shall be a rectangular prism with nominal dimensions of 1.0 inch thick (T) × 2.0 inches wide (W) × 2.0 inches long (L). The thickness dimension shall be the parallel-to-rise direction.
2. Place the test samples in a room (ambient) temperature environment (i.e., 65 ºF to 85 ºF) for sufficient time to thermally stabilize the test samples. Measure and record the room temperature to an accuracy of ±2 ºF.
3. Measure and record the thickness, width, and length of each test sample to an accuracy of ±0.001 inches.
4. Compute and record the surface area of each test sample by multiplying the width by the length (i.e., W × L).

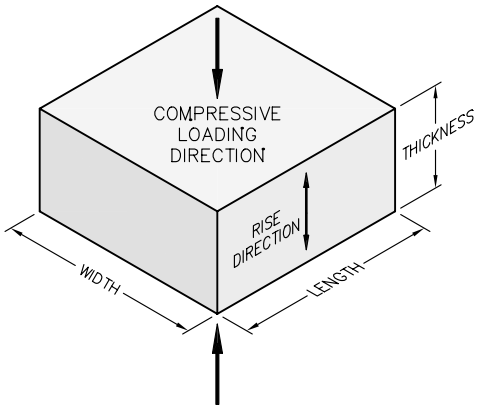

5. Place a test sample in a Universal Testing Machine. Lower the machine's crosshead until it touches the test sample. Set the machine's parameters for the thickness of the test sample.
6. Apply a compressive load to each test sample at a rate of 0.10 ±0.05 inches/minute until a strain of 70%, or greater, is achieved. For each test sample, plot the compressive stress versus strain and record the compressive stress at strains of 10%, 40%, and 70%.
7. Determine and record the average parallel-to-rise compressive stress of the three test samples from each pour. As delineated in Table 8.1-1, the average parallel-to-rise compressive stress for each pour shall be the nominal compressive stress ±20% at strains of 10%, 40%, and 70%.
8. Determine and record the average parallel-to-rise compressive stress of all test samples from each foamed component. As delineated in Table 8.1-1, the average parallel-to-rise compressive stress for a foamed component shall be the nominal compressive stress ±15% at strains of 10%, 40%, and 70%.

8.1.4.1.2.3.3 Perpendicular-to-Rise Compressive Stress

1. Three (3) test samples shall be taken from the foam pour. Each test sample shall be a rectangular prism with nominal dimensions of 1.0 inch thick (T) × 2.0 inches wide (W) × 2.0 inches long (L). The thickness dimension shall be the perpendicular-to-rise direction.
2. Place the test samples in a room (ambient) temperature environment (i.e., 65 ºF to 85 ºF) for sufficient time to thermally stabilize the test samples. Measure and record the room temperature to an accuracy of ±2 ºF.
3. Measure and record the thickness, width, and length of each test sample to an accuracy of ±0.001 inches.
4. Compute and record the surface area of each test sample by multiplying the width by the length (i.e., W × L).

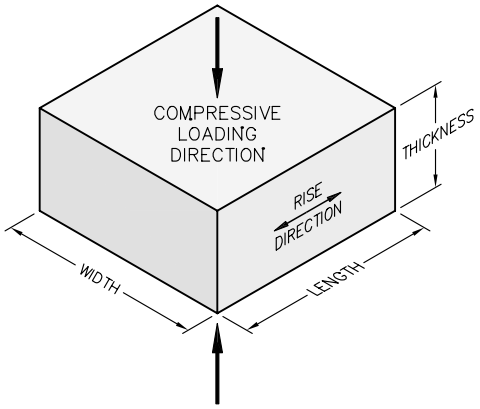

5. Place a test sample in a Universal Testing Machine. Lower the machine's crosshead until it touches the test sample. Set the machine's parameters for the thickness of the test sample.
6. Apply a compressive load to each test sample at a rate of 0.10 ±0.05 inches/minute until a strain of 70%, or greater, is achieved. For each test sample, plot the compressive stress versus strain and record the compressive stress at strains of 10%, 40%, and 70%.

7. Determine and record the average perpendicular-to-rise compressive stress of the three test samples from each pour. As delineated in Table 8.1-1, the average perpendicular-to-rise compressive stress for each pour shall be the nominal compressive stress ±20% at strains of 10%, 40%, and 70%.
8. Determine and record the average perpendicular-to-rise compressive stress of all test samples from each foamed component. As delineated in Table 8.1-1, the average perpendicular-to-rise compressive stress for a foamed component shall be the nominal compressive stress ±15% at strains of 10%, 40%, and 70%.

8.1.5 Tests for Shielding Integrity

The TRUPACT-II packaging does not contain any biological shielding.

8.1.6 Thermal Acceptance Test

Material properties utilized in Chapter 3.0, *Thermal Evaluation*, are consistently conservative for the normal conditions of transport (NCT) and hypothetical accident condition (HAC) thermal analyses performed. In addition, HAC fire certification testing of the TRUPACT-II package (see Appendix 2.10.3, *Certification Tests*) served to verify material performance in the HAC thermal environment. As such, with the exception of the tests required for polyurethane foam, as shown in Section 8.1.4, *Component Tests*, specific acceptance tests for material thermal properties are not performed.

Table 8.1-1 – Acceptable Compressive Stress Ranges for Foam (psi)

Sample Range	Parallel-to-Rise at Strain, $\varepsilon_{//}$			Perpendicular-to-Rise at Strain, $\varepsilon_{\perp}$		
	ε=10%	ε=40%	ε=70%	ε=10%	ε=40%	ε=70%
Nominal –20%	188	216	544	156	188	536
Nominal –15%	200	230	578	166	200	570
Nominal	235	270	680	195	235	670
Nominal +15%	270	311	782	224	270	771
Nominal +20%	282	324	816	234	282	804

This page intentionally left blank.

8.2 Maintenance Program

This section describes the maintenance program used to ensure continued performance of the TRUPACT-II package.

8.2.1 Structural and Pressure Tests

8.2.1.1 Containment Vessel Pressure Testing

Perform structural pressure testing on both the inner containment vessel (ICV) and the outer containment vessel (OCV) per the requirements of Section 8.1.2.2, *Containment Vessel Pressure Testing*, once every five years. Upon completing the structural pressure test, perform leakage rate testing per the requirements of Section 8.1.3, *Fabrication Leakage Rate Tests*.

8.2.1.2 ICV Interior Surfaces Inspection

Annual inspection shall be performed of the accessible interior surfaces of the ICV for evidence of chemically induced stress corrosion. After removal of the ICV spacer assemblies, perform a visual inspection for indications of ICV interior surface corrosion. Should evidence of corrosion exist, a liquid penetrant inspection of the ICV interior surfaces, including accessible shell, head, flange, and weld surfaces, shall be performed per ASME Boiler and Pressure Vessel Code, Section V[1], Article 6, and ASME Boiler and Pressure Vessel Code, Section III[2], Division 1, Subsection NB, Article NB-5000, as delineated on the drawings in Appendix 1.3.1, *Packaging General Arrangement Drawings*. Indications of cracking or distortion shall be recorded on a nonconformance report and dispositioned prior to corrective actions.

Once the packaging is put into service, at a maximum interval of five (5) years, an examination shall be performed on the accessible interior surfaces of the ICV for evidence of chemically induced stress corrosion. This examination shall consist of a liquid penetrant inspection of the entire ICV interior surfaces, including the accessible shell, head, flange, and weld surfaces, and shall be performed per ASME Boiler and Pressure Vessel Code, Section V, Article 6, and ASME Boiler and Pressure Vessel Code, Section III, Division 1, Subsection NB, Article NB-5000, as delineated on the drawings in Appendix 1.3.1, *Packaging General Arrangement Drawings*. Indications of cracking or distortion shall be recorded on a nonconformance report and dispositioned prior to corrective actions.

8.2.2 Maintenance/Periodic Leakage Rate Tests

This section provides the generalized procedure for maintenance and periodic leakage rate testing of the containment vessel penetrations during routine maintenance, or at the time of seal replacement or seal area repair. Maintenance/periodic leakage rate testing shall follow the guidelines of Section 7.4, *Maintenance Leakage Rate Test*, and Section 7.5, *Periodic Leakage Rate Test*, of ANSI N14.5[3].

---

[1] American Society of Mechanical Engineers (ASME) Boiler and Pressure Vessel Code, Section V, *Nondestructive Examination*, 1986 Edition.

[2] American Society of Mechanical Engineers (ASME) Boiler and Pressure Vessel Code, Section III, *Rules for Construction of Nuclear Power Plant Components*, 1986 Edition.

[3] ANSI N14.5-1997, *American National Standard for Radioactive Materials – Leakage Tests on Packages for Shipment,* American National Standards Institute, Inc. (ANSI).

Maintenance/periodic leakage rate testing shall be performed on the main O-ring seal and vent port plug seal for the inner containment vessel (ICV) in accordance with Section 8.2.2.2, *Helium Leakage Rate Testing the ICV Main O-ring Seal*, and Section 8.2.2.3, *Helium Leakage Rate Testing the ICV Outer Vent Port Plug O-ring Seal*. Leakage rate testing of the outer containment vessel (OCV) main O-ring seal and OCV vent port plug shall be performed in accordance with Section 8.1.3.6, *Helium Leakage Rate Testing the OCV Main O-ring Seal Integrity*, and Section 8.1.3.7, *Helium Leakage Rate Testing the OCV Vent Port Plug O-ring Seal Integrity*. Each leakage rate test shall meet the acceptance criteria delineated in Section 8.2.2.1, *Maintenance/Periodic Leakage Rate Test Acceptance Criteria*.

8.2.2.1 Maintenance/Periodic Leakage Rate Test Acceptance Criteria

Maintenance/periodic leakage rate test acceptance criteria are identical to the criteria delineated in Section 8.1.3.1, *Fabrication Leakage Rate Test Acceptance Criteria*.

8.2.2.2 Helium Leakage Rate Testing the ICV Main O-ring Seal

1. The maintenance/periodic leakage rate test of the ICV main O-ring seal shall be performed following the guidelines of A.5.4, *Evacuated Envelope – Gas Detector*, of ANSI N14.5.
2. The ICV shall be assembled with both main O-ring seals installed into the ICV lower seal flange and the wiper O-ring installed into the holder. Assembly is as shown in Appendix 1.3.1, *Packaging General Arrangement Drawings*.
3. Verify that the ICV vent port cover and ICV outer vent port plug have been removed. Verify that the ICV inner vent port plug is installed and tighten to 55 - 65 lb-in torque.
4. Connect a vacuum pump to the ICV vent port and evacuate the ICV vent port cavity to 90% vacuum or better (i.e., ≤10% ambient atmospheric pressure). If the ICV vent port cavity cannot be evacuated to the required vacuum, remove the ICV lid and inspect the ICV wiper O-ring seal, the ICV upper main O-ring seal, and sealing surfaces for damage. Replace any damaged O-ring seals and repair any damaged sealing surfaces prior to re-performing the ICV main O-ring seal test.
5. Remove the ICV seal test port plug and install a helium mass spectrometer leak detector to the ICV seal test port. Evacuate the ICV seal test port cavity until the vacuum is sufficient to operate the helium mass spectrometer leak detector.
6. Provide a helium atmosphere inside the ICV vent port cavity by backfilling with helium gas to a pressure slightly greater than atmospheric pressure (+1 psi, -0 psi).
7. Perform the helium leakage rate test to the requirements of Section 8.2.2.1, *Maintenance/Periodic Leakage Rate Test Acceptance Criteria*. If, after repeated attempts, the ICV main O-ring seal fails to pass the leakage rate test, isolate the leak path and, prior to repairing the leak path and repeating the leakage rate test, record on a nonconformance report and disposition prior to final acceptance in accordance with the cognizant quality assurance program.

8.2.2.3 Helium Leakage Rate Testing the ICV Outer Vent Port Plug O-ring Seal

1. The maintenance/periodic leakage rate test of the ICV outer vent port plug O-ring seal shall be performed following the guidelines of A.5.4, *Evacuated Envelope – Gas Detector*, of ANSI N14.5.

2. The ICV shall be assembled with both main O-ring seals installed into the ICV lower seal flange and the wiper O-ring installed into the holder. Assembly is as shown in Appendix 1.3.1, *Packaging General Arrangement Drawings*.
3. Verify that the ICV vent port cover and ICV outer vent port plug have been removed. Verify that the ICV inner vent port plug is installed and tighten to 55 - 65 lb-in torque.
4. Connect a vacuum pump to the ICV vent port and evacuate the ICV vent port cavity to 90% vacuum or better (i.e., ≤10% ambient atmospheric pressure). If the ICV vent port cavity cannot be evacuated to the required vacuum, remove the ICV lid and inspect the ICV wiper O-ring seal, the ICV upper main O-ring seal, and sealing surfaces for damage. Replace any damaged O-ring seals and repair any damaged sealing surfaces prior to re-performing the ICV main O-ring seal test.
5. Provide a helium atmosphere inside the ICV vent port cavity by backfilling with helium gas to a pressure slightly greater than atmospheric pressure (+1 psi, -0 psi).
6. Install the ICV outer vent port plug and tighten to 55 - 65 lb-in torque.
7. Install a helium mass spectrometer leak detector to the ICV vent port. Evacuate the ICV vent port cavity until the vacuum is sufficient to operate the helium mass spectrometer leak detector.
8. Perform the helium leakage rate test to the requirements of Section 8.2.2.1, *Maintenance/Periodic Leakage Rate Test Acceptance Criteria*. If, after repeated attempts, the ICV outer vent port plug O-ring seal fails to pass the leakage rate test, isolate the leak path and, prior to repairing the leak path and repeating the leakage rate test, record on a nonconformance report and disposition prior to final acceptance in accordance with the cognizant quality assurance program.

8.2.3 Subsystems Maintenance

8.2.3.1 Fasteners

All threaded components shall be inspected annually for deformed or stripped threads. Damaged components shall be repaired or replaced prior to further use. The threaded components to be visually inspected include the lock bolts, the OCV and ICV seal test port and vent port plugs, the OCV and ICV vent port covers, and OCV access plugs.

8.2.3.2 Locking Rings

Before each use, inspect the OCV and ICV locking ring assemblies for restrained motion. Any motion-impairing components shall be corrected prior to further use.

8.2.3.3 Seal Areas and Grooves

8.2.3.3.1 Seal Area Routine Inspection and Repair

Before each use and at the time of seal replacement, the OCV and ICV sealing surfaces shall be visually inspected for damage that could impair the sealing capabilities of the TRUPACT-II packaging. Damage shall be corrected prior to further use (e.g., using emery cloth restore sealing surfaces) to the surface finish specified in Section 8.2.3.3.2.4, *Surface Finish of Sealing Areas*.

Upon completion of containment seal area repairs, verify depth of O-ring groove does not exceed the value in Table 8.2-1 when repairs are in the O-ring groove; perform leakage rate test per the applicable section of Section 8.2.2, *Maintenance/Periodic Leakage Rate Tests*.

8.2.3.3.2 Annual Seal Area Dimensional Inspection

In order to demonstrate compliance of the OCV and ICV main O-ring seal regions, annual inspection of sealing area dimensions and surface finishes shall be performed as defined in Section 8.2.3.3.2.1, *Groove Widths*, through Section 8.2.3.3.2.5, *O-ring Groove Depth*.

Allowable measurements for these dimensions are based on a minimum O-ring compression of 12.5%, which will ensure "leaktight" seals are maintained (see calculation in Table 8.2-1).

Table 8.2-1 – Calculation of Minimum O-ring Compression

Calculation	Value
G = Maximum allowed upper seal flange groove width, in①	0.560
T = Minimum allowed lower seal flange tab width, in②	0.494
R = Maximum allowed radial gap due to axial play, in③	0.010
D = Maximum allowed O-ring groove depth, in④	0.253
M = Maximum gap that O-ring must fill, in⑤	0.329
W = Minimum O-ring cross section diameter, in⑥	0.376
C = Minimum O-ring compression, %⑦	12.5%

Notes: Refer to Appendix 1.3.1, *Packaging General Arrangement Drawings*, Sheet 7 of 11 and Sheet 1 of 11, Note 42, for key dimensions:

① Measured 0.250 inches from bottom of groove, G = 0.543 + 0.25(tan 3.95°)

② Measured 0.250 inches from top of tab, T = 0.477 + 0.25(tan 3.85°)

③ Derived from axial play measurements, R = 0.153(tan 3.90°)

④ Measured at center of groove

⑤ M = (G – T) + R + D

⑥ Minimum production O-ring cross section diameter including the effects of maximum stretch = 0.376 in

⑦ C = [1 – (M / W)] × 100

All measurement results shall be recorded and retained as part of the overall inspection record for the TRUPACT-II package. Measurements not in compliance with the following dimensional requirements require repairs. Upon completion of repairs, perform a maintenance/periodic leakage rate test per the applicable section of Section 8.2.2, *Maintenance/Periodic Leakage Rate Tests*.

8.2.3.3.2.1 Groove Widths

The method of measuring the OCV and ICV upper (lid) seal flange groove width is illustrated in Figure 8.2-1. Remove the ICV debris shield to measure the ICV upper seal flange groove width. As an option, the lid may be inverted to facilitate the measurement process. The measuring

equipment includes a Ø0.560 ±0.001 inch pin gauge of any convenient length, and a Ø0.250 ±0.001 inch ball. With reference to Figure 8.2-1, the pin gauge is aligned parallel with the inner lip of the upper seal flange. Acceptability is based on the following conditions:

- Having contact at location ①-① and a gap at location ②-② is a NO-GO condition indicating that the upper seal flange groove width is acceptable.
- Having contact or a gap at location ①-① and contact at location ②-② is a GO condition indicating that the upper seal flange groove width is unacceptable.

The method of measuring the OCV and ICV lower (body) seal flange groove width is illustrated in Figure 8.2-2. The measuring equipment includes a Ø0.273 ±0.001 inch pin gauge of any convenient length, and a Ø0.250 ±0.001 inch ball. With reference to Figure 8.2-2, the pin gauge is aligned parallel with the outer lip of the lower seal flange. Acceptability is based on the following conditions:

- Having contact at location ①-① and a gap at location ②-② is a NO-GO condition indicating that the lower seal flange groove width is acceptable.
- Having contact or a gap at location ①-① and contact at location ②-② is a GO condition indicating that the lower seal flange groove width is unacceptable.

Groove width measurements shall be taken and recorded at six equally spaced locations around the circumference of the seal flanges.

8.2.3.3.2.2 Tab Widths

The method of measuring the OCV and ICV upper (lid) seal flange tab width is illustrated in Figure 8.2-3. As an option, the lid may be inverted to facilitate the measurement process. The measuring device is a tab width gauge of any convenient size, with a 0.234 ±0.001 inch inside width × 0.428 ±0.001 inch inside height × 0.375 ±0.005 inch thickness. With reference to Figure 8.2-3, the tab width gauge is aligned parallel with the lowermost lip of the upper seal flange. Acceptability is based on the following conditions:

- Having contact at location ①-① and a gap at location ②-② is a NO-GO condition indicating that the upper seal flange tab width is acceptable.
- Having contact or a gap at location ①-① and contact at location ②-② is a GO condition indicating that the upper seal flange tab width is unacceptable.

The method of measuring the OCV and ICV lower (body) seal flange tab width is illustrated in Figure 8.2-4. The measuring device is a 0.494 ±0.001 inch inside width × 0.250 ±0.001 inch inside height × 0.375 ±0.005 inch thick tab width gauge of any convenient size. With reference to Figure 8.2-4, the tab width gauge is aligned parallel with the uppermost lip of the lower seal flange. Acceptability is based on the following conditions:

- Having contact at location ①-① and a gap at location ②-② is a NO-GO condition indicating that the lower seal flange tab width is acceptable.
- Having contact or a gap at location ①-① and contact at location ②-② is a GO condition indicating that the lower seal flange tab width is unacceptable.

Tab width measurements shall be taken and recorded at six equally spaced locations around the circumference of the seal flanges.

8.2.3.3.2.3 Axial Play

Measurement of axial play shall be performed to ensure that O-ring compression is sufficient to maintain package configuration and performance to design criteria. Axial play is the maximum axial distance that a lid can move relative to a body. Because the seal flange sealing surfaces are tapered, any axial movement where the lid moves *away* from the body results in a separation of the sealing surfaces and a slight reduction in O-ring compression. The procedure for measuring OCV and ICV axial play is as follows:

1. Remove the vent port access plug (OCV only), vent port thermal plug (OCV only), vent port cover, and vent port plug(s). Remove the ICV debris seal (ICV only).
2. Assemble the lid onto the body.
3. Locate a minimum of six equally spaced locations around the exterior circumference of the lid and body. At each location, place vertically aligned temporary reference marks on the lid and body.
4. Install a vacuum pump to the vent port and evacuate the containment vessel sufficiently to fully compress the upper seal flange to the lower seal flange.
5. At each location, scribe a horizontal mark that intersects both the lid and the body vertical marks.
6. Install a source of pressure to the vent port and pressurize the containment vessel sufficiently to fully separate the upper seal flange from the lower seal flange.
7. At each location, scribe a second horizontal mark that intersects either the lid or the body vertical mark (select either the lid or body mark as a base point).
8. Measure and record the difference between the initial and final horizontal marks at each location. The maximum acceptable axial play at any location is 0.153 inch.
9. Other measuring devices, such as dial indicators, digital calipers, etc., may be used in lieu of the reference marking method, provided that the axial play is measured at a minimum of six equally spaced locations.

8.2.3.3.2.4 Surface Finish of Sealing Areas

The surface finish in the main O-ring sealing regions shall be a 125 micro inch finish, or better, to maintain package configuration and performance to design criteria. Perform surface finish inspections for the bottom of the grooves on the lower seal flange and the mating sealing surfaces on the upper seal flange. If the surface condition is determined to exceed 125 micro inch, repair the surface per the requirements of Section 8.2.3.3.1, *Seal Area Routine Inspection and Repair*.

8.2.3.3.2.5 O-ring Groove Depth

Verify the OCV and ICV O-ring groove depth to be less than 0.253 inches at six equally spaced locations around the circumference of the seal flanges.

8.2.4 Valves, Rupture Discs, and Gaskets on the Containment Vessel

8.2.4.1 Valves

The TRUPACT-II packaging does not contain any valves.

8.2.4.2 Rupture Discs

The TRUPACT-II packaging does not contain any rupture discs.

8.2.4.3 Gaskets

Containment boundary O-ring seals shall be replaced within the 12-month period prior to shipment or when damaged (whichever is sooner), per the size and material requirements delineated on the drawings in Appendix 1.3.1, *Packaging General Arrangement Drawings*. Following containment O-ring seal replacement and prior to a loaded shipment, the new seals shall be leakage rate tested to the requirements of Section 8.2.2, *Maintenance/Periodic Leakage Rate Tests*.

The Inner Containment Vessel debris shield and wiper O-ring seal shall be replaced within the 12-month period prior to shipment or when damaged (whichever is sooner), per the size and material requirements delineated on the drawings in Appendix 1.3.1, *Packaging General Arrangement Drawings*.

8.2.5 Shielding

The TRUPACT-II packaging does not contain any biological shielding.

8.2.6 Thermal

No thermal tests are necessary to ensure continued performance of the TRUPACT-II packaging.

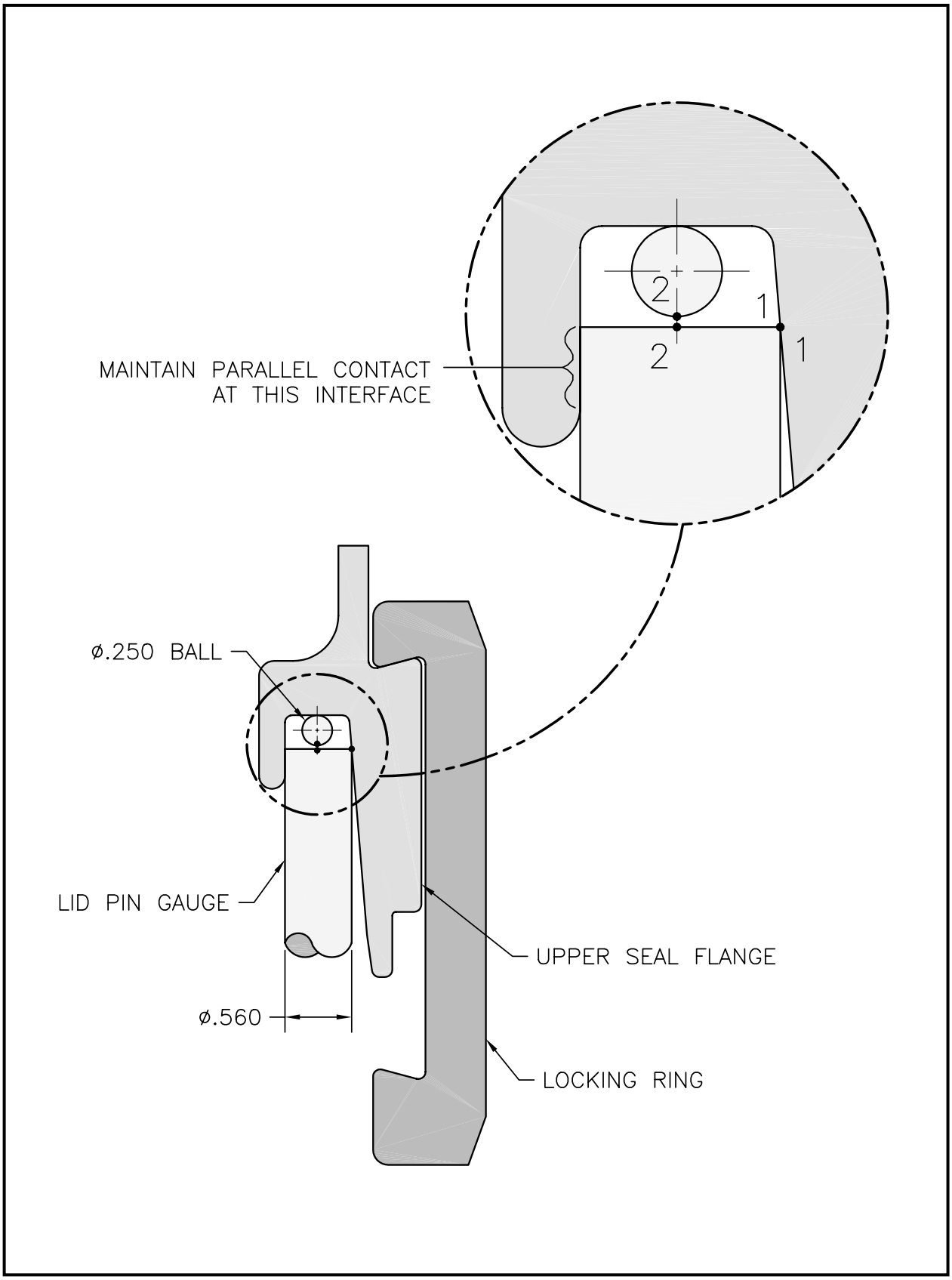

Figure 8.2-1 – Method of Measuring Upper Seal Flange Groove Widths

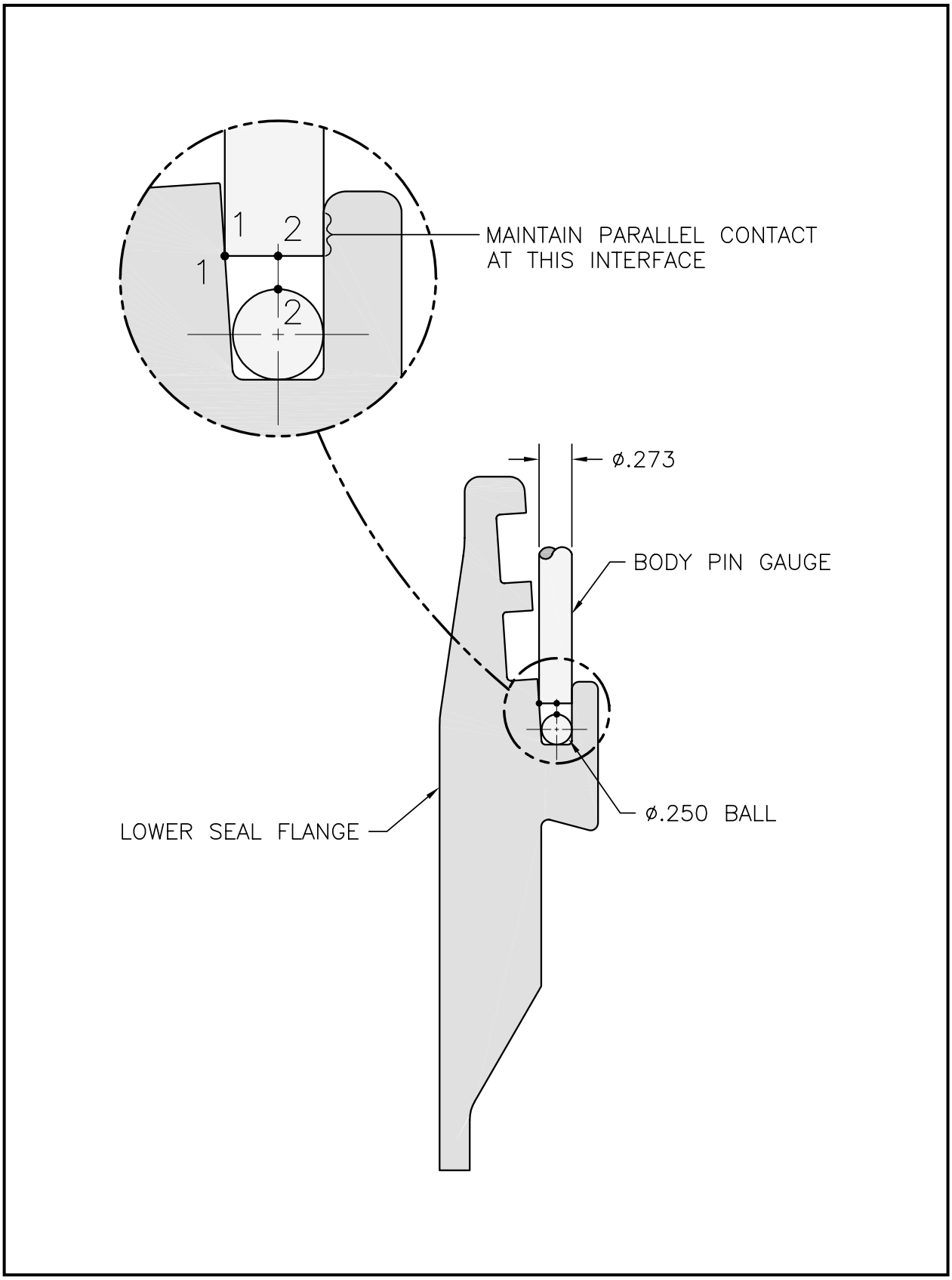

Figure 8.2-2 – Method of Measuring Lower Seal Flange Groove Widths

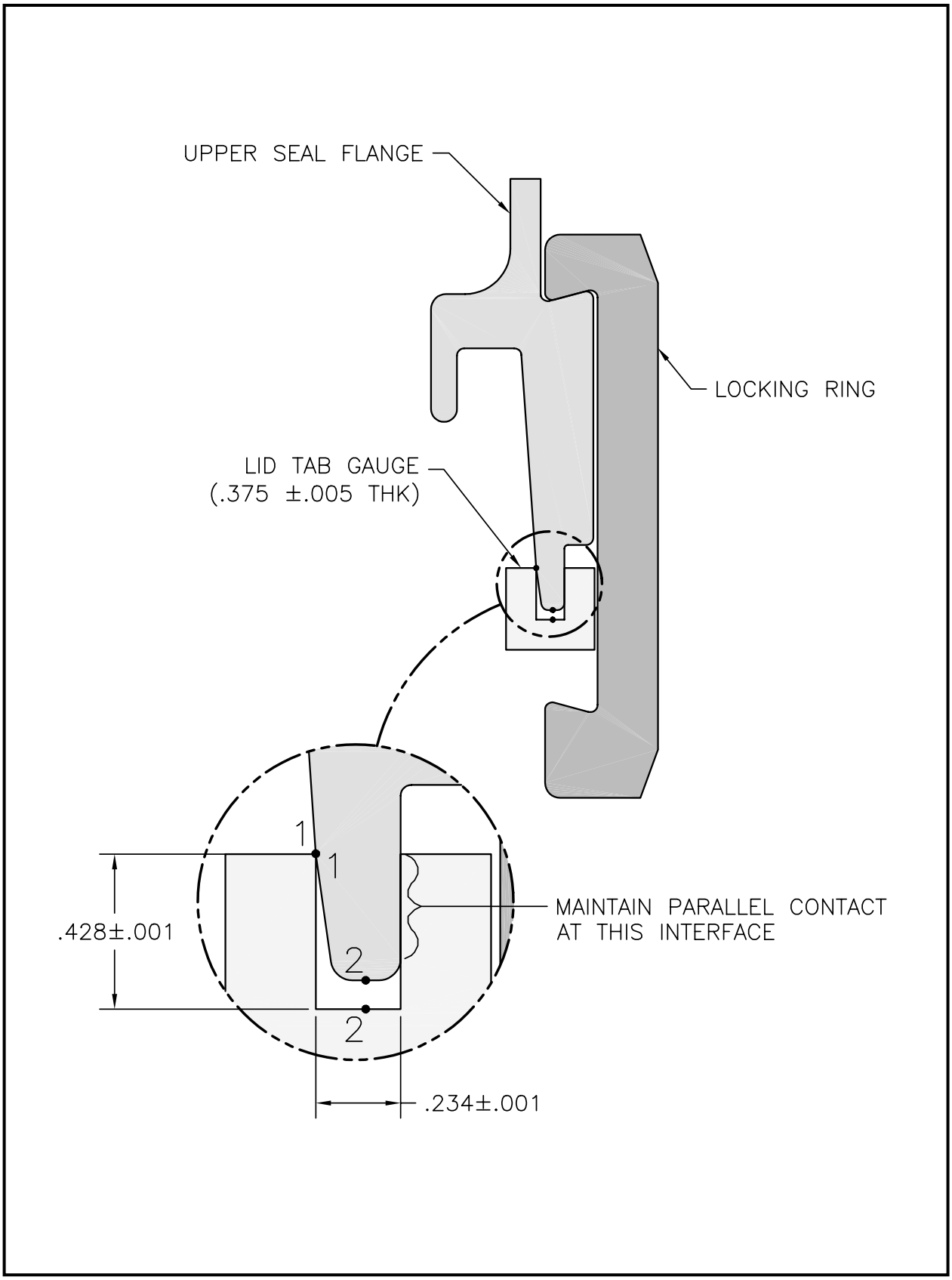

Figure 8.2-3 – Method of Measuring Upper Seal Flange Tab Widths

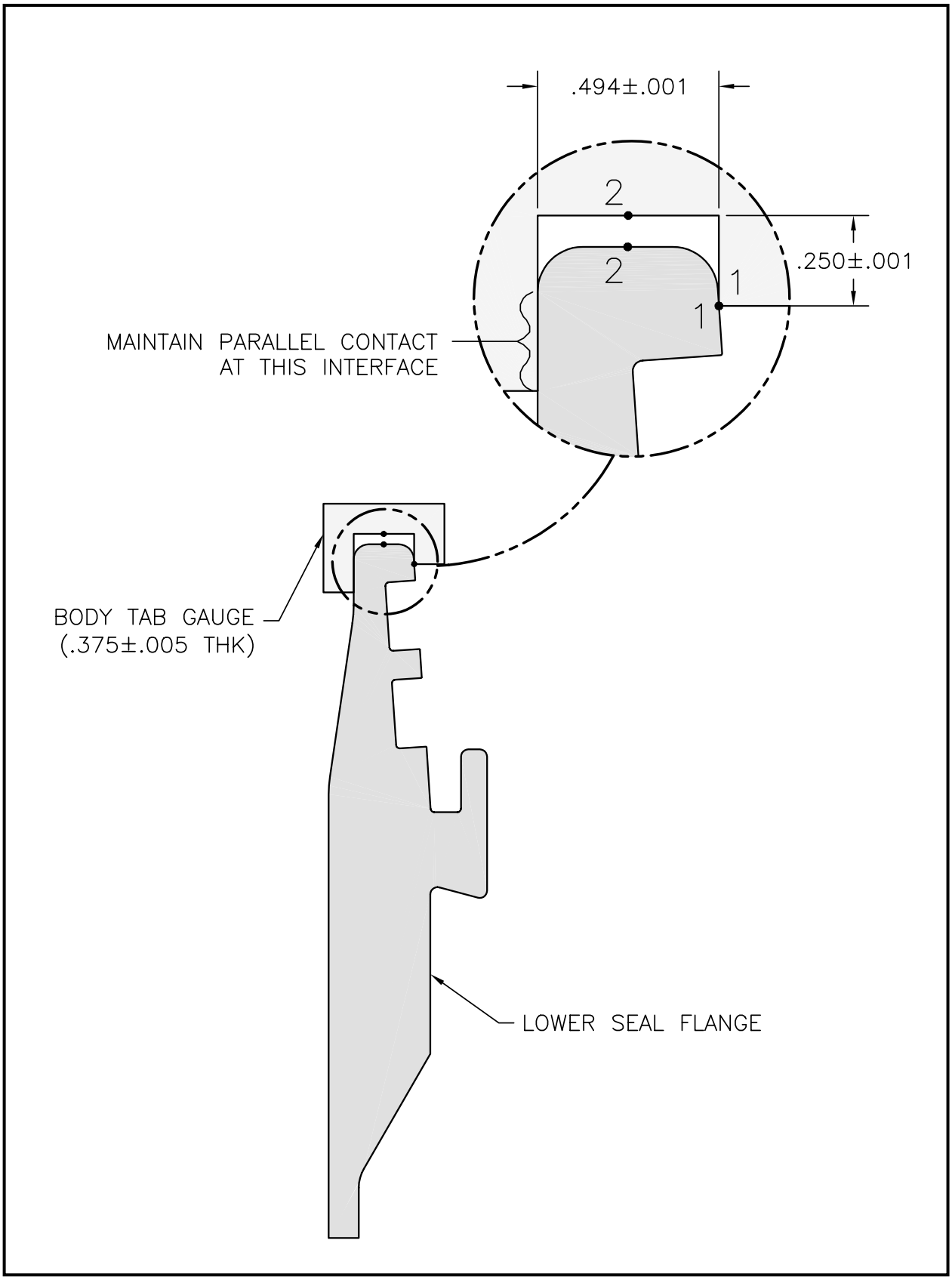

Figure 8.2-4 – Method of Measuring Lower Seal Flange Tab Widths

This page intentionally left blank.

9.0 QUALITY ASSURANCE

This section describes the quality assurance (QA) requirements and methods of compliance applicable to the TRUPACT-II package.

9.1 Introduction

The TRUPACT-II package is designed and shall be built for the U.S. Department of Energy (DOE), and must be approved by the U.S. Nuclear Regulatory Commission (NRC) for the shipment of radioactive material in accordance with the applicable provisions of the U.S. Department of Transportation, described in Subpart I of 49 CFR Part 173[1]. Procurement, design, fabrication, assembly, testing, maintenance, repair, modification, and use of the TRUPACT-II package are all done under QA programs that meet all applicable NRC and DOE QA requirements. QA requirements for payloads to be transported in the TRUPACT-II package are discussed in the *Contact-Handled Transuranic Waste Authorized Methods for Payload Control* (CH-TRAMPAC)[2].

[1] Title 49, Code of Federal Regulations, Part 173 (49 CFR 173), *Shippers–General Requirements for Shipments and Packagings*, 10-01-06 Edition.

[2] U.S. Department of Energy (DOE), *Contact-Handled Transuranic Waste Authorized Methods for Payload Control* (CH-TRAMPAC), U.S. Department of Energy, Carlsbad Field Office, Carlsbad, New Mexico.

This page intentionally left blank.

9.2 Quality Assurance Requirements

9.2.1 U.S. Nuclear Regulatory Commission

The QA requirements for packaging established by the NRC are described in Subpart H of 10 CFR 71[1]. Subpart H is an 18 criteria QA program based on ANSI/ASME NQA-1[2]. Guidance for QA programs for packaging is provided in Regulatory Guide 7.10[3].

9.2.2 U.S. Department of Energy

The QA requirements of DOE for the use of NRC certified packaging are described in Chapter 4 of DOE Order 460.1[4]. According to Chapter 4.(4)(b), the DOE and its contractors may use NRC certified Type B packaging only under the conditions specified in the certificate of compliance.

9.2.3 Transportation to or from WIPP

Public Law 102-579, enacted by the 102nd Congress, reads as follows:

SEC. 16. TRANSPORTATION.

(a) SHIPPING CONTAINERS. - No transuranic waste may be transported by or for the Secretary [of Energy] to or from WIPP, except in packages -

(1) the design of which has been certified by the Nuclear Regulatory Commission; and

(2) that have been determined by the Nuclear Regulatory Commission to satisfy its quality assurance requirements.

The determination under paragraph (2) shall not be subject to rulemaking or judicial review.

[1] Title 10, Code of Federal Regulations, Part 71 (10 CFR 71), *Packaging and Transportation of Radioactive Material*, 01-01-07 Edition.

[2] ANSI/ASME NQA-1, *Quality Assurance Requirements of Nuclear Power Plants*, American National Standards Institute.

[3] U.S. Nuclear Regulatory Commission, Regulatory Guide 7.10, *Establishing Quality Assurance Programs for Packaging Used in the Transport of Radioactive Material,* Revision 1, June 1986.

[4] U.S. Department of Energy Order 460.1, *Packaging and Transportation Safety,* September 1995.

This page intentionally left blank.

9.3 Quality Assurance Program

9.3.1 NRC Regulatory Guide 7.10

Guidance for QA programs applicable to design, fabrication, assembly, and testing of packaging used in transport of radioactive material is covered in Annex 1 of the NRC's Regulatory Guide 7.10[1]; procurement, use, maintenance and repair are covered in Annex 2.

9.3.2 Design

The TRUPACT-II package was designed under a QA program approved by the NRC for packaging design. Requests for modification or changes to the design will be submitted to the NRC for approval prior to modification of the TRUPACT-II packaging. Any future design changes shall be made under an appropriate NRC approved QA program.

9.3.3 Fabrication, Assembly, and Testing

Fabrication, assembly, and testing of each TRUPACT-II packaging are performed under a QA program approved by the NRC for these activities.

9.3.4 Procurement

Procurement of each TRUPACT-II packaging is performed under a QA program that meets the applicable QA requirements of the NRC.

9.3.5 Use

The TRUPACT-II package will be used primarily by the DOE for shipments of authorized contents to the WIPP site. However, it may also be used between DOE sites other than WIPP (inter-site), and for DOE on-site shipments within site boundaries (intra-site). The DOE is registered with the NRC as a user of the TRUPACT-II package under the general license provisions of 49 CFR §173.471[2]. The TRUPACT-II package may also be used for non-DOE shipments as authorized by the NRC.

9.3.5.1 DOE Shipments: To/From WIPP

Use of the TRUPACT-II packaging for shipments to or from the WIPP site shall be made under a QA program that meets the QA requirements of the NRC. The appropriate DOE Field Office(s) shall inspect and approve the QA programs of the DOE contractors that make shipments to or from WIPP in the TRUPACT-II package. DOE or the DOE managing and operating contractor for the WIPP shall perform surveillances of the TRUPACT-II package users' QA programs to ensure that the package is used in accordance with the requirements of the certificate of compliance.

---

[1] U.S. Nuclear Regulatory Commission, Regulatory Guide 7.10, *Establishing Quality Assurance Programs for Packaging Used in the Transport of Radioactive Material,* Revision 1, June 1986.

[2] Title 49, Code of Federal Regulations, Part 173 (49 CFR 173), *Shippers–General Requirements for Shipments and Packagings*, 10-01-06 Edition.

9.3.5.2 Other DOE Shipments: Non-WIPP

The appropriate DOE Field Office(s) shall inspect and approve the shippers' and receivers' QA programs for equivalency to the NRC's QA program requirements in Subpart H of 10 CFR 71. For example, a contractor working under an 18 criteria QA program per ANSI/ASME NQA-1[3] could be deemed acceptable if the program is applicable to packaging. DOE or the DOE managing and operating contractor for the WIPP shall perform surveillances of the TRUPACT-II package users' QA programs to ensure that the package is used in accordance with the requirements of the certificate of compliance.

9.3.5.3 Non-DOE Users of TRUPACT-II

Non-DOE users of the TRUPACT-II package shall have QA programs approved by the NRC.

9.3.6 Maintenance and Repair

Minor maintenance, such as changing seals or fasteners, may be performed under the user's QA program. Major maintenance, such as cutting or welding a containment boundary, shall be performed under an appropriate QA program that has been approved by the NRC.

[3] ANSI/ASME NQA-1, *Quality Assurance Requirements of Nuclear Power Plants*, American National Standards Institute.